

ENERGY DELIVERY OF SOLAR FARMS WITH REFERENCE TO SHADNG

By

MICHAEL JEFFREY

A thesis submitted in partial fulfilment of the requirements of Edinburgh Napier
University, for the award of

Doctor of Philosophy

School of Engineering and the Built Environment

May 2019

Contents

Abstract	ix
Declaration	x
Acknowledgements	xi
Publications List	xii
List of Figures	xiii
List of Tables	xvii
Chapter 1 Introduction.....	1
1.1 Chapter Summary	1
1.1.2 Research Question.....	1
1.1.2 Aims and objectives.....	1
1.1.3 Research Site and Further Education Context.....	2
1.2 Economic Arguments for Renewables & Solar	5
1.3 Drivers for Uptake of Solar in the UK	6
1.4 Existing Medium-Large Scale Solar Installations in UK	8
1.5 Existing Large-Scale Solar Installations in the UK	9
1.5.1 Cornwall Solar Parks.....	9
1.5.2 Other UK Installations.....	10
1.5.3 Errol Estate Solar Farm.....	10
1.6 Further Education Colleges Overview	12
1.6.1 Scottish FE college regionalisation.....	12
1.6.2 Expectations of FE colleges and the Scottish Governments STEM agenda.....	13
1.6.3 Learner Demographics.....	14
1.6.4 DYW.....	15
1.6.5 FE in the Future.....	15
1.6.6 College Innovation.....	16
1.7 Further Education Estate targets	16
1.7.1 Overview of Scotland College Estate.....	17
1.7.2 Funding options.....	18
1.7.3 College Surveys.....	19
1.7.4 Scotland’s Energy Efficiency Programme (SEEP).....	20
1.7.5 Aims of SEEP.....	20
1.7.6 Pathfinder Fund.....	20
1.7.6 College sector activity.....	21
1.7.7 College Energy Efficiency Partnership (CEEP).....	24
1.8 Edinburgh College Electricity Consumption	25
1.9 Edinburgh College Travel Costs	26
1.9.1 Scottish Government decarbonisation of the road transport sector.....	26

1.9.2 Edinburgh College green fleet – research project	26
1.10 Edinburgh College eCar research	26
1.10.1 Edinburgh College BEV - early adopters	26
1.10.2 Edinburgh College travel	27
1.10.3 College commuting requirements	28
1.10.4 Edinburgh College and staff mobility	28
1.11 Future developments	29
Chapter 2 – Literature Review, review of worldwide trends in solar photovoltaic technologies	30
2.0 Chapter Summary	30
2.0.1 Existing Literature and previous works.....	30
2.0.2 Previous works relevant to this research	31
2.1 Worldwide countries leading PV development and installation.....	31
2.2 China	33
2.2.1 Key policy drivers.....	33
2.2.2 Photo Voltaic Research & Development activities and associated funding.....	35
2.3 Japan.....	36
2.3.1 Key Policy Drivers.....	36
2.3.2 Photo Voltaic Research & Development activities and associated funding.....	37
2.4 USA.....	38
2.4.1 Key Policy Drivers.....	38
2.4.2 Photo Voltaic Research &Development activities and associated funding.....	40
2.5 Germany	40
2.5.1 Policy Drivers.....	40
2.5.2 Photo Voltaic Research & Development activities and associated funding.....	41
2.6 U.K	42
2.6.1 Policy Drivers.....	42
2.6.2 PV Research & Development activities and associated funding.....	44
2.7 PV electricity production in leading countries.....	45
2.8 PV cost analysis	46
2.9 Discussion and recommendations	51
2.9.1 Policy recommendations – Change is required.....	53
2.9.2 Incentive and framework.....	53
2.9.3 Market transformation	54
2.9.4 Development of technology and Research & Development	55
2.9.5 International expansion and collaborations	56
2.10 Scotland’s Key policy drivers	56
2.10.1 Kyoto Protocol.....	56
2.10.3 Climate Change (Scotland) act 2009.....	57

2.10.4 Low Carbon Scotland.....	58
2.10.5 Scottish Government Climate Change Plan (2018)	59
2.10.6 Political Background.....	62
2.11 Solar PV Technologies	64
2.12 Solar PV Materials	64
2.13 Photovoltaic module material and associated efficiencies	65
2.14 Crystalline Silicon (c-Si)	69
2.14.1 Mono crystalline	69
2.14.2 Multi crystalline or Poly crystalline	70
2.15 Thin film technology	71
2.15.1 Amorphous Silicon (a-Si).....	71
2.15.2 Cadmium Telluride (CdTe) / Cadmium Sulphide (CdS)	72
2.15.3 Copper Indium Gallium Selenide (CIGS) / Copper Indium (Di) Selenide (CIS).....	72
2.15.4 Gallium Arsenide (GaAs).....	73
2.16 New emerging technologies	74
2.16.1 Hybrid cell	74
2.16.2 Carbon Nanotube (CNT) cells	74
2.16.3 Dye Sensitized Solar Cells (DSSC)	74
2.16.4 Tandem cells / Multi Junction solar cell.....	75
2.17 Conclusion	75
2.18 Thesis Outline	77
Chapter 3 – Evaluation of Solar Modelling Techniques Edinburgh College – Midlothian campus, Scotland	78
3.1 Chapter Summary	78
3.2 Introduction	78
3.3 Summary of Analysis Process	80
3.3.1 Methodology	80
3.3.2 Solar Geometry Calculations to be utilised in this research.....	81
3.3.3 Solar Data Recording	83
3.3.4 Effects of Shading on String Output.....	85
3.3.5 Data Presentation	86
3.3.6 Horizontal to Slope Irradiation Conversion.....	86
3.3.7 Thermal Model for Cell Temperature.....	87
3.3.8 Alternative Thermal Model.....	87
3.4 Edinburgh College Solar Meadow Technology	88
3.4.1 Purpose and Investors	88
3.5 The Solar Meadow Farm	88
3.6 Specifics of Location and Site	90
3.8 Shading Analysis	101

3.8.1 Site Survey and Triangulation	102
3.8.2 Shading Charts	104
3.9 Experimental Setup	105
3.9.1 Position on Site	105
3.9.2 Sensor Specifications	105
3.9.3 Pyranometer Setup	106
3.9.4 Flux Sensor and Thermocouple Setup	109
3.9.5 Data-Loggers	111
3.10 Experimental Measurements at Solar Meadow Farm	112
3.11 Calculation Process	115
3.11.1 Slope Irradiation	115
3.11.2 Cell Temperature	117
3.11.3 Cell Efficiency	119
3.12 Results & Discussion	120
3.12.1 Slope Irradiation	120
3.12.2 Cell Temperature	121
3.12.3 Cell Efficiency	123
3.13 Experimental Results	124
3.13.1 Overview	124
3.13.2 Sensor Readings	125
3.14 Manual Readings	132
3.14.1 Inverter Power Output	132
3.14.2 Inverter kWh output	135
3.14.2 Overall System Output	137
3.15 Derived Quantities	139
3.15.1 Module Power Output	139
3.15.2 Energy Balance	142
3.15.3 Measuring Correlation	143
3.15.4 The Slope Irradiation	143
3.15.5 Results	144
3.15.6 Model Comparison	145
3.15.7 The Cell Temperature	145
3.15.8 The Cell Efficiency	148
3.15.9 Daily Variability	149
3.15.10 Averaged Values	150
3.16 Shading Analysis	152
3.17 Software	156
3.17.1 Workbook Structure	156

3.17.2 Excel-Only Implementation	158
3.18 Use and Adaptation of solar analysis Software	159
3.18 Implementation of Thermal Model	160
3.19 Cell Efficiency Calculations	161
3.20 Graphical Display Interface	162
3.21 Problems Encountered.....	163
3.22 Conclusions	164
Chapter 4 – Analysis of Energy Delivery of the Edinburgh College solar PV meadow: Effects of Shading	167
4.1 Chapter Summary	167
4.2 Introduction	167
4.3 PV modules in shade	169
4.4 Problems caused by shading	171
4.4.1 Establishing critical points of shade within the Solar Meadow at Edinburgh College	172
4.5 Modelling Approaches.....	175
4.5.1 Sun-Earth Geometry description	175
4.5.2 Day number description	176
4.5.3 Solar Declination description.....	176
4.5.4 Equation of Time description.....	177
4.5.5 Solar Altitude and Azimuth description.....	177
4.5.6 Sun Inclination description	178
4.5.7 Extra-terrestrial spectrum description	178
4.5.8 Solar radiation description	179
4.5.9 Hourly global slope irradiance description	180
4.6 3 Shading algorithms considered:	182
4.6.1 Budin shading algorithm	182
4.6.2 Horn shading algorithm.....	183
4.6.3 Geographic Information system packages	183
4.7 Algorithm selected – Sky View Factor (SVF)	185
4.7.1 Sky view factor	185
4.8 Calculation Process	187
4.8.1 Energy delivery from the solar meadow – the three approaches utilised	187
4.8.2 Calculating Energy Output with relation to shading.....	188
4.9 Results	191
4.9.1 The three approaches in results	191
4.9.2 Linear plots	192
4.9.3 Radar plots.....	194
4.10 Energy output of the Solar Farm	196
4.10.1 Scenario one	196

4.10.2 Scenario 2.....	198
4.11 Conclusions	199
Chapter 5 Future plans: Implementation of a solar charging station for e-cars at Edinburgh College	201
5.0 Chapter Summary	201
5.1 Calculation process: Slope irradiation, cell temperature and cell efficiency	203
5.1.1 Slope irradiation	203
5.1.2 Cell temperature.....	204
5.1.3 Cell efficiency	205
5.1.4 Design of the solar charging station: First phase.....	205
5.1.5 Design 1: South orientation.....	205
5.1.6 Design 2: East-west orientation.....	206
5.1.7 Design 3: East-West orientation.....	208
5.1.8 Design summary	210
5.1.9 Design of the solar carport: Second phase.....	210
5.1.10 Design 4: South orientation.....	211
5.1.11 Design 5: East-west orientation.....	214
6.1.12 Design 6: East-west orientation.....	215
5.2 Summary of results by design shape for the first and second phase.....	218
5.2.1 Design Review	218
5.2.2 Characteristics of the chosen design.....	218
5.2.3 Design of the PV system	220
5.2.4 Selection of the inverter	220
5.2.4 Selection of the PV module.....	224
5.2.5 Selection of the charging station	224
5.2.6 Layout.....	226
5.2.7 Driving behaviour	227
5.2.8 Number of vehicles to be charged during a day by the solar carport.....	230
5.3 Energy production and energy consumption by the carport.....	231
5.4 Load profile.....	231
5.5 Financial analysis	233
5.6 Scenario 1	233
5.7 Scenario 2	236
5.8 Scenario 3.....	238
5.9 Financial assumptions	238
5.10 Environmental analysis.....	240
5.11 Life cycle assessment (LCA) of the project.....	240
5.12 Life cycle assessment of the balance of system (BOS) and system mounting.....	243
5.12.1 Energy payback time (EPBT) and global warming potential (GWP) summary.....	244

5.12.2 CO2 emissions saved	245
5.13 Conclusions	245
Solar charging station at Edinburgh College.....	245
Chapter 6 – Conclusion	248
6.1 Introduction	248
6.2 Site identification	248
6.3 Site specific data.....	248
6.4 Site survey	249
6.5 Site monitoring	249
6.6 Site Modelling	250
6.7 Data Analysis.....	251
6.8 Comparison of solar output	251
6.9 Pedagogical impact on the College	252
6.10 Lessons learned.....	252
6.11 Recommendations for future study.....	253
References.....	255
Appendices	268
Appendix A: Data Tables	268
Appendix B: Datasheets	275
Inverters	277
Pyranometer specifications	279
Sensor Calibration Certificates	280
Data-Loggers.....	282
Appendix C: VBA Code Transcripts	283
Appendix D: SSE System Documents.....	293
Appendix E – Solar Farm Blockage Data	296
Appendix F: MATLAB codes.....	298
Reading data from excel primary data.....	298
Yallop’s algorithm to calculate sun declination and equation of time.....	298
Greenwich hour angle	298
Solar geometry	299
Hourly horizontal global irradiation.....	299
Hourly global slop irradiation.....	299
Block dedication for specific azimuths (Block first row-left).....	300
Blocks modification	300
Sky view factor	301
Global slop irradiation with consideration to shade	301
Mean global horizontal irradiation (December)	301

Appendix G – Linear Shading plots	302
Appendix H– Radar Shading plots.....	307
Appendix I - Edinburgh College Midlothian Campus electricity consumption 2013-2017	312
Appendix J – Edinburgh College Solar Array Cashflow only (SSE)	314

Abstract

This study has been undertaken to research the impact of shading on a large scale solar PV site at 56° latitude north, this is the first site in the UK at this latitude, consisting of 2500 solar panels across a 5 acres. As solar altitude decreases obstacles and blockages become more of a hindrance and careful planning is required to ensure the amount of shading on the panel surface is kept to a minimum. The impacts of shading on the Edinburgh College Solar Meadow, from obstacles along the Southern and Eastern edges have been investigated.

The accuracy and applicability of existing methods of solar resource modelling and solar photovoltaic (PV) module performance are investigated in the case of the ground array installation. The principal derived quantities consist of slope irradiation, cell temperature and cell efficiency. Experimental data was collected on site through both automated and manual measurements for comparison with the calculated quantities for both triangulation and quality assurance. The impact of shading has been analysed and the effect on energy delivery captured throughout the year. The research undertook detailed modelling in order to compare and evaluate the data obtained with further comparisons made between a number of modelling tools and other forms of output associated with the solar farm directly.

The site was expected to generate 560,000 kWh across the year with no impact from shading, based on the installers assumptions. Results indicate that the models used to compare and contrast slope irradiation, cell temperature and cell efficiency are accurate and within the expected range as per manufacturer specifications. The results also show that shading impacts the energy generation with a significant reduction in the winter months with respect to the available energy at the site by as much as 50%. Being the first study of its kind, at high latitude in the UK, to show the importance of accurate shade modelling at higher latitudes the findings show greater consideration is required at concept stages when taking account of solar obstacles. Shading has reduced the overall output, of this particular array, by 136,859 kWh across the year studied.

Declaration

I hereby declare that the contents of this thesis are original and have been submitted solely to Edinburgh Napier University for consideration in fulfilling the requirements for the degree of Doctor of Philosophy (PhD).

M Jeffrey

Signed:

Dated:

Acknowledgements

First and foremost, I would like to thank my Supervisors Prof Tariq Muneer at Edinburgh Napier University and Prof Stephen Tinsley formerly at Edinburgh College who made this research work possible. Without your encouragement and support I would never have considered this research into Energy deliver of solar farms with particular reference to shading a possibility.

Throughout the research I have had close cooperation with SSE and the Engineering staff at Edinburgh College Scotland. In addition, Iain Kelly and Vahid Rimahni aided with the data collection and supported the capture of specific issues within the solar farm and Edinburgh College.

I would like dedicate this work to my son Logan and Daughter Freya.

I would also like to thank my wife Janie Jeffrey for her full support and encouragement and my parents for their ability to keep me grounded...

And finally, the financial and continual support from Edinburgh College and Edinburgh Napier University is greatly appreciated their help and support has assisted throughout so as to allow me to complete this work.

Michael Jeffrey

Scottish Borders, Scotland, UK

May 2019

Publications List

Articles

Jeffery, M., Kelly, I., Muneer, T., Smith, I. (2015) **Evaluation of solar modelling techniques through experiment on a 627kWp photovoltaic solar power plant at Edinburgh College – Midlothian Campus**, Scotland Journal of Renewable and Sustainable Energy &, 033128 (2015)

Gary Husband & Michael Jeffrey (2016) **Advanced and higher vocational education in Scotland: recontextualising the provision of HE in FE**, Research in Post-Compulsory Education, 21:1-2, 66-72, DOI: 10.1080/13596748.2015.1125670

Submitted for publication with Renewable Energy Journal – Currently in review

Jeffrey, M. Muneer, T. Rahmani, V (2018) **Analysis of Energy Delivery of the Edinburgh College solar PV meadow: Effects of Shading**

Chapters within Books

Garcia, I., Jeffrey, M. (2017) **Recharging of electric cars by solar photovoltaics** in: T.Muneer, M. Kohle and A. Doyle (Eds) Electric Vehicles Prospects and Challenges (Elsevierinc.) pp. 415 - 487

List of Figures

Figure 1 Proposed solar meadow at Edinburgh College	4
Figure 2 UK Solar Resource, Source: PVGIS in (Rugg, 2012)	8
Figure 3 5MW Trenouth Solar PV Farm, Source: (Rugg, 2012)	9
Figure 4 Errol Estate Solar Farm (Source: ROAVR 2016)	11
Figure 5 Map of Scotland (SFC, 2013).....	13
Figure 6 Battery electric vehicle usage 2011-2016 (Edinburgh College, 2016).....	27
Figure 7 Percentages of travel distance (Edinburgh College, 2016)	28
Figure 8 Correlations between measured and calculated Slope Irradiation and Cell Temperature, Source: Aldali et al.(2013)	31
Figure 9 PV installation in the year 2017 for leading countries (Statista.com).....	33
Figure 10 Cumulative installation capacity of the leading countries for 2017 (Statista.com).....	33
Figure 11 Largest solar photovoltaic power plants worldwide by capacity (MW) (Statista.com)	45
Figure 12 - Solar PV cells price trend (Cost of Solar, 2013; Feldman.....	46
Figure 13 - BOS price trend for 10MW fixed-tilt blended c-Si projects in USA (Aboudi, 2011; Media, 2013).....	47
Figure 29 Solar Position Relative to a Plane, Source: Thomas Markvart in(Grassie, 2012)	81
Figure 30 Solstice Sun Chart for Dalkeith, Source: (UO Solar Radiation Monitoring Laboratory, 2007)	83
Figure 31 Diffuse, and Global (with N,S,E,W detectors) Pyranometers, Source: (Muneer, 2012)	84
Figure 32 Power Dissipation as a function of shaded cells, Source: (Ramabadran, R; Mathur, 2009)85	85
Figure 14 Midlothian Solar Meadow Farm.....	88
Figure 15 Site Plan of the Meadow	89
Figure 16 Google Maps Satellite Image of Site	91
Figure 17 Initial Site Layout and Design, Source: (Archial, 2013)	92
Figure 18 Computer-Generated Image of Completed Site, Source: (SSE, 2013).....	93
Figure 19 View from SW of Site towards College.....	94
Figure 20 View from W of site (front of panels).....	94
Figure 21 View from W of Site (back of panels).....	95
Figure 22 -View from NE, showing Classroom and Plant Room.....	96
Figure 23 View from NE across Site	96
Figure 24 Inverter and AC Distribution Box Setup.....	97
Figure 25 Front View of Inverter and Detail of Display Screen.....	98
Figure 26 View along Central Trench	98
Figure 27 Site String Plan, Source: (Archial, 2013)	99
Figure 28 Solar Module Mounting Initial Design, Source: (SSE, 2013).	100
Figure 33 Shading Reference Points, Adapted from (SSE, 2013).....	101
Figure 34 Theodolite	102
Figure 35 Determination of Tree Distance and Height (Angles/Lengths not to Scale)	102
Figure 36 Triangulation	103
Figure 37 Tree Line Triangulation, detail from (SSE, 2013)	104
Figure 38 Location of Experimental Setup, Adapted from (Archial, 2013)	105
Figure 39 Pyranometer Setup (Front and Back).....	106
Figure 40 Detail of Horizontal and Upper Slope Pyranometers (p1 & p2).....	107
Figure 41 Detail of Lower Slope Pyranometer (p3)	107
Figure 42 Alignment of Upper Slope Pyranometer (without cover)	108
Figure 43 Alignment of Lower Slope Pyranometer (with cover)	108
Figure 44 Placement of Flux & Temperature Sensors.....	109
Figure 45 Detail of Thermocouple.....	109
Figure 46 Detail of Flux Sensor	110

Figure 47 Data-Logger Housing	111
Figure 48 Data-Loggers, Source: (Grant Instruments, 2011)	112
Figure 49 Position of Pyranometers	113
Figure 50 Position of Flux Sensors	114
Figure 51 Calculation Flow Chart.....	115
Figure 52 Solar Geometry and Slope Irradiation	116
Figure 53 Heat Transmission from a Solar Module, Source: (Aldali et.al. 2013).....	118
Figure 54 Slope Irradiation Results.....	120
Figure 55 Cell Temperature Results.....	122
Figure 56 - Clear-Day Efficiency and Cloudy day efficiency	123
Figure 57 - Cell Efficiency: measured and computed values (note y-axis is the frequency count)	124
Figure 58 - Example Slope Irradiation Measurements (29th May) (W/m ²)	127
Figure 59 - Slope Irradiation Shading (30th May) (W/m ²)	127
Figure 60 Slope and Horizontal Measurements (6th June) (W/m ²)	129
Figure 61 - Thermocouple Temperature Readings (6th June) (°C).....	130
Figure 62 – Erroneous readings in t3 (3rd June) (°C).....	131
Figure 63 - Example Heat Flux Readings (1st June) (W/m ²)	131
Figure 64 - Change of Sensor Flux4 (30th May) (W/m ²)	132
Figure 65 - Inverter 16 Power Readings (4th June)	134
Figure 66 - Inverter 16 Power Readings (5th June)	135
Figure 67 daily energy production chart for the month of November	136
Figure 68 daily energy production chart for the month of January.....	137
Figure 69 Inverter 15 Output, Instant vs. Averaged (4th June) (kW).....	140
Figure 70 Instant vs Averaged Inverter Power Output (4th June).....	140
Figure 71 - Inverter 15 Output, Instant vs. Averaged (3rd June) (kW)	141
Figure 72 - Instant vs Averaged Inverter Power Output (3rd June)	141
Figure 73 -Time Series of 5 Different Measures of Cell Efficiency (3rd June)	142
Figure 74 - Time Series of 5 Different Measures of Cell Efficiency (4th June)	142
Figure 75 - Time Series of 5 Different Measures of Cell Efficiency (5th June)	143
Figure 76 Summer Model vs. Measured Irradiation (W/m ²).....	144
Figure 77 Measured vs. NOCT-Calculated Cell Temperature during Period 1 (°C)	146
Figure 78 Measured vs. NOCT-Calculated Cell Temperature during Period 2 (°C)	146
Figure 79 Measured vs. Homer-Calculated Cell Temperature during Period 2 (°C).....	147
Figure 80 Measured vs. Thermal-Model-Calculated Cell Temperature during Period 2 (°C).....	147
Figure 81 Correlations between Pavg (left) and Pinstant (right) Cell Efficiency against Cell Temperature Cell Efficiencies for 3rd June.....	149
Figure 82 Correlations between Pavg (left) and Pinstant (right) Cell Efficiency against Cell Temperature Cell Efficiencies for 4th June.....	149
Figure 83 Hourly-Averaged Efficiencies (3rd, 4th and 5th June)	150
Figure 84 3-Day Hourly Results for Pavg and Pinstant against Cell Temperature-Cell Efficiency	151
Figure 85 Morning/Afternoon-Averaged Cell Efficiencies.....	152
Figure 86 -Shading Acquisition, based on (SSE, 2013)	152
Figure 87 - Monthly Average Shading Chart, Point 1	154
Figure 88 -Monthly Average Shading Chart, Point 2.....	154
Figure 89 - Monthly Average Shading Chart, Point 3	155
Figure 90 - Monthly Average Shading Chart, Point 4	155
Figure 91 - Monthly Average Shading Chart, Point 5	156
Figure 92 Flow chart for the computer model. Source:(Aldali et. al. 2011)	161
Figure 93 - Graphical Display Screen (Time Series Plot).....	162
Figure 94 - Graphical Display Screen (correlation graph).....	163
Figure 95 - Setting Manual Calculation Mode	164
Figure 96 - Solar Meadow layout and markup (SSE, 2013)	168

Figure 97 - Shading along the southern edge.....	169
Figure 98 - SP, BL and TCT connections for 20*3 array (Ishaque, 2011).....	170
Figure 99 - (a) Module in normal condition and (b) bypass operation as the module is in shade (Ishaque, 2011).....	171
Figure 100 - Theodolite.....	174
Figure 101 - Position of critical points of shading (Burns 2015).....	174
Figure 102 - View of Solar Meadow from southern obstacles.....	175
Figure 103 - Solar declination in different seasons.....	176
Figure 104 - Sun geometry in a tilted surface (Team, 2008).....	178
Figure 105- Final scene construction and irradiance modelling for this algorithm (Nguyen and Pearce, 2012).....	184
Figure 106 - ASHRAE for diurnal temperature changing (Gago et al. 2010).....	189
Figure 107 - Shading analysis of the three approaches.....	191
Figure 108 - July shading analysis.....	192
Figure 109 - December shading analysis.....	193
Figure 110 - July Radar Plot.....	195
Figure 111 - December Radar Plot.....	195
Figure 112 - Energy Output - Scenario 1.....	197
Figure 113 - Energy output - scenario two.....	198
Figure 114 - Monthly-average hourly k-kt plot for UK (locations arranged in an increasing order of latitude). (Muneer et.al. 2014).....	203
Figure 115 - South facing design. Based on Formfonts, 2016.....	206
Figure 116 – East - West facing design. Based on Formfonts, 2016.....	207
Figure 117 – East - West facing curved design. Based on Formfonts, 2016.....	208
Figure 118 - Design 3A—Orientation of PV modules on the roof.....	208
Figure 119 - Design 3B—Orientation of PV modules on the roof.....	209
Figure 120 - Edinburgh college—Midlothian Campus. From Google maps.....	211
Figure 121 - Area selected for designs 4A & 4B, from Google maps.....	211
Figure 122 - Area to place the designs 4A. Modified from Google maps.....	212
Figure 123 - Area to place the design number 4B. Modified from Google maps.....	213
Figure 124 - Area to place the design number 4C, Modified from Google maps.....	213
Figure 125 – Diagram of design 5.....	214
Figure 126 - Area to place the design 5 Modified from Google maps.....	215
Figure 127 - Area to place the designs 6. Modified from Google maps.....	215
Figure 128 - Design 6AA—Orientation of PV modules on the roof.....	216
Figure 129 – representation of design 6A.....	217
Figure 130 - Design 6AB—Orientation of PV modules on the roof.....	217
Figure 131 - Horizontal positions of the PV modules.....	219
Figure 132 - Solar carport, rear view.....	219
Figure 133 - Solar carport, front view.....	220
Figure 134 - Full view of the solar carport.....	220
Figure 135 - Rapid charger CHAdeMO at Napier University. (Plugshare 2016).....	225
Figure 136 - Typical grid-connected PV system without battery storage From Narayan, N. (2013). Solar charging station for light electric vehicles. A design and feasibility study. Master of Science Thesis. Delft University of Technology.....	226
Figure 137 - Schematic circuit diagram of the 80kWp facility.....	226
Figure 138 - Trips by time of day and day of week. From Department for Transport (2015). (National travel survey 2014).....	227
Figure 139 - Trips in progress by start time and purpose, Monday to Friday.(National travel survey 2014).....	228
Figure 140 - Driving episodes in Edinburgh City (Walsh, J., Muneer, T., & Celik, 2011).....	230
Figure 141 - Energy production vs. Energy consumption.....	231

Figure 142 - Consumed and generated energy in March. 232

Figure 143 - Consumed and generated energy in May. 232

Figure 144 - Main costs distribution 234

Figure 145 - Balance of System costs distribution. 235

Figure 146 - PV system costs in 2015 combining minimum and maximum assumptions. (Kleiner, 2015)..... 237

Figure 147 - The product life-cycle (Granta, 2016) 240

Figure 148 - Monocrystalline solar cell structure Mohammad Bagher (2015). 241

Figure 149 - Energy and CO2 footprint details of a single module. Data from CES Edupack, 2016. 242

List of Tables

Table 1 College Building expenditure (SFC, 2017).....	17
Table 2 Electricity consumption (kWh) of the Midlothian Campus.....	25
Table 3 Size and cost of PV projects (D. C, 2011; I, 2011; S. C, 2011; T, 2011; Tech, 2014; Lieberose Photovoltaic Park, 2015; Lopburi Solar Farm, 2015; Bank, 2015; Energy, 2015; Ranch, 2015; Station, 2015) (over)	48
Table 4 Comparison and comments on all PV materials and their development (Fthenakis et.al. 1999; Razykov et.al. 2009; Razykov et.al. 2011)	52
Table 5 List of companies based on relevant countries and their reference numbers (Frankl and Tanaka, 2014)	66
Table 6 Efficiency of mono crystalline PV modules ((NREL), 2015).....	70
Table 7 Efficiency of multi crystalline PV modules ((NREL), 2015)	70
Table 8 Efficiency of a-Si PV modules ((NREL), 2015)	72
Table 9 Efficiency of CIS/CIGS PV modules ((NREL), 2015).....	73
Table 10 Sources of Error in Solar Recording, adapted from (Muneer, 2004)	85
Table 11 Slope Irradiation Model Results	121
Table 12 Cell Temperature Model Comparison	122
Table 13 Data Logger Output	125
Table 14 Table of Results Extract	126
Table 15 Extract of Manual Inverter Power Readings (4th June) (Accuracy of displayed value)	133
Table 16 Daily Inverter Totals (condensed).....	138
Table 17 Model Correlations with Measured Irradiation	145
Table 18 Comparison of Temperature Correlations	148
Table 19 Cell Efficiency Correlation Results	151
Table 20 Shading Data Sample, Points 1 & 2.....	153
Table 21 - Energy output scenario one	196
Table 22 - Energy output scenario two.....	198
Table 23 Energy output comparison.....	200
Table 24 - List of angles and orientations to be studied.....	204
Table 25 - Technical specifications of PV module.....	204
Table 26 - Cell temperature - PV module facing south at 40°	205
Table 27 - Main characteristics of Design 1	206
Table 28 - Main characteristics of Design 2	207
Table 29 - Main characteristics of Design 3	209
Table 30 - Data collated from all designs—first design phase	210
Table 31 - Relevant data for the Design 4A	212
Table 32 - Relevant data for the Design 4B	212
Table 33 - Relevant data for the Design 4C	213
Table 34 - Relevant data for the Design 5	214
Table 35 - Relevant data for Design 6A.....	216
Table 36 - Summarized data table of all possible designs.....	218
Table 37 - Temperature conditions	221
Table 38 - Charging times for Renault Zoe.....	225
Table 39 - Data Renault Zoe e-car	229
Table 40 - Operating expenditures for 2017	233
Table 41 - Detailed cost distribution	235
Table 42 - Operating expenditures—2020.....	237
Table 43 - Detailed cost distribution	238
Table 44 - Financial results for the solar charging station.....	239
Table 45 - Detailed breakdown of individual material phase for a single module	242
Table 46 - Individual life-phase CO2 footprint details	243
Table 47 - Summary embodied energy and CO2 released by the facility	244
Table 48 - Financial analysis, scenario 2.....	246

List of Equations

Equation 1 - Yallop Solar Equations, Source: ((Muneer, 2004))	82
Equation 2 - Solar Altitude, Source: ((Muneer, 2004))	82
Equation 3 - Solar Azimuth, Source: (Muneer, 2004)	82
Equation 4 - Apparent Solar time	82
Equation 5 - Angle of Inclination, Source: (Muneer, 2004)	83
Equation 6 - Sin Rule	103
Equation 7 - Height Determination	103
Equation 8 - Clarke Seasonal (Summer) Calculation, Source (Clarke et.al. 2007).....	116
Equation 9 - Clarke June Calculation, Source: (Clarke et al., 2007)	116
Equation 10 - Muneer Calculation, Source: Software Program Calc4-08 in (Muneer et.al, 2000)	116
Equation 11 - Beam Component of Slope Irradiation, Source: Software Program Calc4-08 in (Muneer, Tariq; N, Abodahab; G, Weir; J, 2000).....	117
Equation 12 - NOCT Cell Temperature Calculation	117
Equation 13 - HOMER Cell Temperature, Source: (HOMER Energy, 2013)	118
Equation 14 - Convective Loss.....	118
Equation 15 - Radiative Loss	118
Equation 16 - Effective Sky Temperature, Source: (Aldali, Y; Celik, A.N; Muneer, 2013)	119
Equation 17 - Air Heat Transfer Coefficient, Source: (Aldali, Y; Celik, A.N; Muneer, 2013).....	119
Equation 18 - Sky Heat Transfer Coefficient, Source: (Aldali, Y; Celik, A.N; Muneer, 2013)	119
Equation 19 - Thermal Model Cell Temperature.....	119
Equation 20 - Cell Efficiency from Output	119
Equation 21 - Cell Efficiency	119
Equation 22 - Data Conversion	126
Equation 23 - Sun declination.....	177
Equation 24 - Equation of time	177
Equation 25 - Sun altitude	178
Equation 26 - Sun azimuth	178
Equation 27 - Sun inclination	178
Equation 28 - Extra-terrestrial spectrum (Muneer, 2004)	179
Equation 29 - Clearness index.....	180
Equation 30 - Hourly horizontal diffuse irradiation.....	180
Equation 31 - Hourly global slope irradiance.....	180
Equation 32 - Hourly slope beam irradiance (Muneer, 2004).....	180
Equation 33 - diffuse irradiation on a sloped surface	181
Equation 34 - Ground reflection.....	182
Equation 35 - Horn shading analyse equation	183
Equation 36 - Profile angle equation.....	184
Equation 37 - Slope beam & diffused irradiation (Muneer 2004)	185
Equation 38 - Sky view	186
Equation 39 - Total Blocked Irradiance	186
Equation 40 - Global irradiation on a sloped surface	186
Equation 41 - Global irradiation on a sloped surface in shade.....	187
Equation 42- Approach 1 for energy delivery calculation	187
Equation 43 - Approach 2 for energy delivery calculation	188
Equation 44 - Approach 3 for energy delivery calculation	188
Equation 45 - Hourly temperature equation.....	188
Equation 46 - Cell temperature equation on the basis of global radiation	189
Equation 47 - Cell efficiency.....	190
Equation 48.....	204
Equation 49.....	221

Equation 50.....	221
Equation 51.....	222
Equation 52.....	222
Equation 53.....	222
Equation 54.....	223
Equation 55.....	223
Equation 56.....	224
Equation 57.....	224
Equation 58.....	229
Equation 59.....	230
Equation 60.....	230
Equation 61.....	239
Equation 62.....	239
Equation 63.....	239
Equation 64.....	239
Equation 65.....	244
Equation 66.....	244
Equation 67.....	245

Chapter 1 Introduction

1.1 Chapter Summary

This chapter will introduce the research, the background to the solar meadow at Edinburgh College, introduce the research site and provide an overview of the current position of further education within the education sector. It will provide justification for this research, and where it sits alongside other research being carried out by the college to support the green initiatives and ambitions of the organisation. It will provide data on the campus consumption in terms of electricity and the carbon emissions of the campus where the Solar Meadow is based.

1.1.2 Research Question

This research will establish the viability of Photovoltaic solar generation at a latitude of 56° and its impact on energy saving for a medium sized further education (FE) campus based in Midlothian, Edinburgh. This is a unique piece of research for Scotland and marries aspects of modern technology with key environmental concerns.

This research will aim to discover if a 675kWp solar array can generate enough energy output to support a carbon neutral Further Education College campus and whether the energy delivery meets the forecast outputs claimed by the installer.

As this study is the first of its kind, on this scale, at a latitude of 56° north, it offers an important look at the impact of shading on solar power generation for Scotland. This will inform further development of such arrays as part of Scotland's renewable energy solution. The study will also look to validate the pedagogical impact on the college and any potential for wider research within the solar farm to form a qualitative approach to biodiversity and environmental impact.

1.1.2 Aims and objectives

This research aims to cover a number of different elements, which lead towards the achievement of the research question and the following research objectives:

- The identification of a site and array to study the impact of shading
- To obtain real and original solar and meteorological data specific to the site being studied, in contrast to using published data for the general area, or yearly-averaged data from public databases. This will form a strong basis for the calculations and model implementation.

- To perform a survey of the site using correct surveying tools and methods in order to produce a better understanding of any shading issues. This information will assist in energy forecasting for the site, which has real financial implications in terms of energy use and investment payback.
- Monitoring of solar radiation, current production and efficiencies of all the component parts of the system. Module orientation and tilt will be considered, although the installation parameters have already been optimised at the time of installation.
- The data collected on site will allow for an assessment of the applicability and accuracy of a range of commonly-used mathematical models of solar resource and photovoltaic module performance. Direct comparisons will be made between the measured values and those calculated from site-specific input data, showing how well these models perform under the given circumstances at this latitude.
- Analyse and inspect large data sets produced with the development of software tools.
- Compare and validate findings against actual energy output, available energy, modelled energy output and energy output with respect to shading.

1.1.3 Research Site and Further Education Context

Jewel & Esk College merged, in 2012, with Edinburgh's Telford College and Stevenson College Edinburgh in order to create the biggest college in Scotland. This was the first merger of Further Education (FE) Colleges within the Scottish Governments regionalisation agenda (see section 1.6 for more detail). This has created opportunities to update and upgrade the curriculum offer, and vocational delivery opportunities at the college. A key area for enhancement during this merger has been the drive to better the STEM activity undertaken by the college and enhance opportunities for all communities in the region, this is clearly referenced through the College STEM Manifesto. Sustainability and Clean Technology has been top of the agenda and through industry engagement there have been many positive developments to both curriculum content and up-to-date industrial technologies being utilised in the vocational areas. These take the form of an Electric Vehicle project, Biodiesel production, sustainable building technologies, enhanced energy curriculum, micro and macro renewable energy including the Solar Meadow based at the Midlothian Campus of Edinburgh College in Dalkeith.

Renewable energy production has become a key element for Further Education to address through improvements in curriculum offer and in terms of energy consumption across a large

and aging estate nationally (Edinburgh College, 2016). A key development for Edinburgh College, post-merger, was the installation of a Solar Array at the Midlothian Campus. As well as the energy benefits for the College, the site (which was designated for industrial use) has become an outdoor classroom for engineering, science, environmental and technology students to gather data and understand the technology and biodiversity. The ground surrounding the Solar array has been planted with wild flowers and grasses, allowing students to analyse the interaction between biodiversity and the panels, as well as monitor and assess the operation and performance of the solar panels.

The Solar Meadow at Edinburgh College's Midlothian Campus is a 5 acre development which provides 627.5kW of energy in the midst of a bio-diversity meadow. This is a unique installation for Scotland and marries aspects of modern technology with key environmental concerns. The energy produced is expected to go some way to reduce the carbon footprint of the Campus and the meadow is said to produce enough electricity for the Midlothian Campus to be self-sufficient and not rely on the National Grid. If surplus electricity is produced it will be sold back to the Grid, helping to off-set electricity bills at the College's Edinburgh Campus based at Milton Road in Edinburgh. This research aims to analyse actual performance to ratify these claims.

Initially planned as a small scale solar roof, to run the Engineering workshops, evolving quickly into a large scale solar PV installation. The 5 acre site has been developed into a 2560 panel installation that has been created in partnership with Scottish & Southern Energy (SSE). Their involvement has allowed the project to grow and make it a viable installation for generation of sustainable energy to the College and the National Grid. The site earthworks were completed with the bund and site levelling, the addition of an earth-ship classroom, where the monitoring equipment will be based, will complete the installation. Commissioning of the facility was due in November 2012, but was delayed until March 2013 due to complications with the groundworks, with the installation of the PV technology taking 3-4 weeks. It is assumed that the energy produced will in part be used for the charging of the college electric vehicle fleet and to offset electrical energy consumption from the grid. The system will be monitored from the outset to allow for a clear picture to be developed of the practicalities and viability of such a large scale project. Being the first of its kind in Scotland this research will play a major role in informing the energy industry to the viability of producing solar electricity at this scale in a high latitude location. Aspects covered in the monitoring will be solar radiation, current production and efficiencies of all the component parts of the system. Module orientation and

tilt will be considered, although the installation parameters will already be optimised at the time of installation, considering that the aspect and tilt must be given. The data collected will be analysed in order to accurately determine viability and the impact on the College ambition to have self-sustaining campus in relation to energy demands. The data collected will be off-set with information obtained through the Campus Buildings Management System which will monitor real-time energy consumption of the Campus. A study of the local environment impacts will be devised and incorporation of wild flora and fauna will be available for inclusion. Economic analysis will take the form of viability of the facility and its direct impact on the campus. The data collected through the monitoring of the installation will also inform efficiency and energy analysis which will provide a complete analysis of a large scale solar PV installation. A notional view of the site, from the south west, is presented in figure 1. Interestingly upon completion it was noted that areas of shade were cast upon the Solar Meadow due to obstacles surrounding the array. This is expected to impact adversely on the proposed energy generation of the site and therefore have negative impact on the assumed impacts for the college.

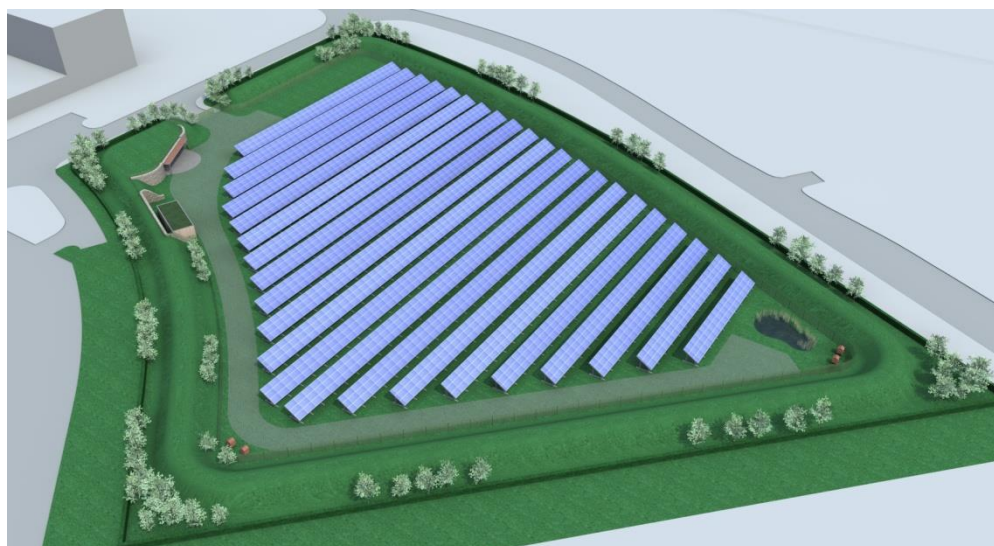


Figure 1 Proposed solar meadow at Edinburgh College

The advent of solar power as a viable method of energy generation promises great changes for the future of the energy economy across the globe. Along with other renewable technologies, it heralds a move away from the traditional system of fuel-to-energy-to-waste to a more cyclical system, where we utilise existing natural processes to support our energy needs.

1.2 Economic Arguments for Renewables & Solar

There are many arguments for a move towards renewable energy sources and at present the economic arguments are ever more pressing. The utilisation of natural phenomena, such as sunlight and wind, as an inexhaustible energy supply (as energy is derived from the sun's nuclear processes) is in stark contrast to the finite and decreasing reserves of traditional type fossil fuels. The combined factors of having zero fuel costs, in the running of a renewable power plant, coupled with the lack of production of any significant waste products requiring disposal also adds to the viability of the process. Of course, the lack of CO₂ as a waste product is an unparalleled advantage, which has a positive environmental impact and also now important economic effects under the current legislation of penalising CO₂ production (Department of Energy and Climate Change, 2013).

Renewable resources are generally available world-wide, as they are not dependent on access to traditional fossil fuels. Some countries are heavily resourced in fossil fuels whilst others are very poorly resourced. By turning to renewable resources results in an increase in energy security and decreases the need to transfer energy or fuel over large distances. Even though there is variability in renewable resource country to country, this is much reduced compared to traditional resource variability, every country having sun, wind and rain. Distributed energy supply, while bringing with it its own set of problems, theoretically allows for much more efficient energy transfer with international and local economic benefits, as sources of generation can be sited nearby to large consumer populations and can bypass a transmission system altogether. Solar is particularly well-suited in this respect, as solar panels can be installed almost anywhere there is empty ground, wall or roof-space available. Other advantages of the use of solar technology include:

- Low maintenance costs compared with traditional generation and even other renewable sources.
- A huge available resource: the theoretical limit is the whole sunlit surface of Earth. While the achievable is only a tiny fraction of this, it is still many times that of renewable sources such as hydro, tidal or geothermal (Perez et al., 2011).
- The ability to make use of brown field sites, land with little other purpose (eg desert), or land can be dual purpose (eg solar meadow).
- Little visual impact on surroundings. This is important for local acceptance and to ensure planning consent is granted. Wind power has run into many problems in the UK in this regard.
- Ease of incorporation into the existing built environment, saving costs and ensuring true distributed supply.

However there are still some important barriers to uptake of solar on a larger scale:

- It is a variable and uncontrollable energy supply.
- A relatively low energy density in terms of land use (possible kW produced per unit land area).
- The high price per unit of electricity produced due to high installation costs (Hernandez-Moro & Martinez-Duart, 2013). This is possibly the most important barrier, however prices have come down dramatically in recent years (Candelise et al., 2013).
- The production process of most renewable technology (solar modules in particular) is energy-intensive and uses rare materials.
- Many problems are created with energy transmission: grid capacity, voltage level and power factor control, and also the need to change the current centralised grid design drastically. This will require both significant R&D and economic investment.

Some of these barriers are offset by incentivised financial support for installation of emerging technologies throughout the renewables industry with room for future improvement, innovation and cost-reduction, which is less likely for fossil fuels or nuclear power.

1.3 Drivers for Uptake of Solar in the UK

The real difference in the UK in recent years has been the introduction of attractive government incentives towards developing renewable energy sources in general, and solar power in particular.

The Renewables Obligation (RO) refers to an incentivisation mechanism introduced in 2009 and effectively penalises electricity suppliers for failing to source a percentage of their energy from renewable sources (House of Commons, 2012). These percentage targets are met through the purchase of Renewable Obligation Certificates (ROCs) from certified renewable generators. At the end of an accounting year, any shortfall must be paid off into a buy-out fund, which is then divided amongst the suppliers who met their targets.

The purpose is two-fold: on one hand, suppliers are pressured to conform to government- set (and increasing) targets; on the other, generators are afforded an extra source of income. ROCs were originally issued to suppliers at the rate of 1 per MWh of electricity produced, but now this rate varies with the type of renewable technology.

The equivalent scheme for the small-scale (<50kW) and domestic market is the Feed In Tariff scheme (FITs), introduced in 2010. This is somewhat simpler than the ROCs, in that owners of installations are paid directly for each unit of electricity they generate, and are

offered a guaranteed price for any energy they would like to sell. The introduction of the FITs brought about massive uptake in solar systems in the UK, leading to greater production volumes, higher efficiencies and falling system prices (Cherrington et. al. 2013). However, FITs rates were cut dramatically at the end of 2011, leading to a slump in the domestic market which is only just starting to pick up. The effects on manufacturing, however, are still present. The Department of Energy and Climate Change (2012) produced a report on the future of the RO, taking feedback from industry stakeholders and presenting some important points:

- While previously there was an attempt to provide equivalency between ROCs and FITs, this has been abandoned due to the inherent risk in the market-linked ROCs.
- FITs contracts are more attractive to investors, as the return on investment is guaranteed for the 20-year period, allowing for accurate profit forecasts to be made.
- Ground and roof mounted systems will be considered separately in the ROC rates, as the performance is quite different. While roof systems are desirable as they make use of existing infrastructure, avoid using un-developed land, and are in close proximity to consumers, ground mounted systems perform better as they can be better situated and oriented (due south, optimum tilt, no shading). Thus ground-mounted rates will be made lower.
- There are significant economies of scale in larger systems, on materials and labour.

An important point to be noted in the recent changes in solar funding, is that government incentives are becoming less critical. A drop in incentives, coupled with dramatic decreases in module and system prices, make the savings on electricity an increasingly important factor. Martin (2012) gives the case of a 5MW plant in Cornwall, which was built despite a reduction in incentives, simply because capital costs had fallen to the point that it was worth it even on the reduced incomes.

This view must be balanced however, in that the near future for solar in the UK is not so easily predictable. Worldwide total installed capacity of solar photovoltaic has indeed increased from 1.4GW in 2000, to over 67GW in 2011 (Candelise, et al., 2013), partly due to the reasons discussed above. Uptake has also been boosted by the emergence of China as a major, cheap, producer of solar PV. However the decreases in costs, and increases in capacity, have not been at all linear (Candelise, et al., 2013). Plateaus and sharp drops have increased and the continued uncertainty over the future of Chinese involvement leave developments over the next 10 years in doubt.

1.4 Existing Medium-Large Scale Solar Installations in UK

Whilst domestic and small-scale solar projects are common across the UK, the site that serves as a subject for this investigation is the first >500kW ground-mounted solar facility to be installed in Scotland. This is due to the generally lower solar availability at these latitudes, and the increased annual cloud cover, reducing the economic viability of the site. A rough evaluation of the available solar resource in the UK is shown below (Figure 2):

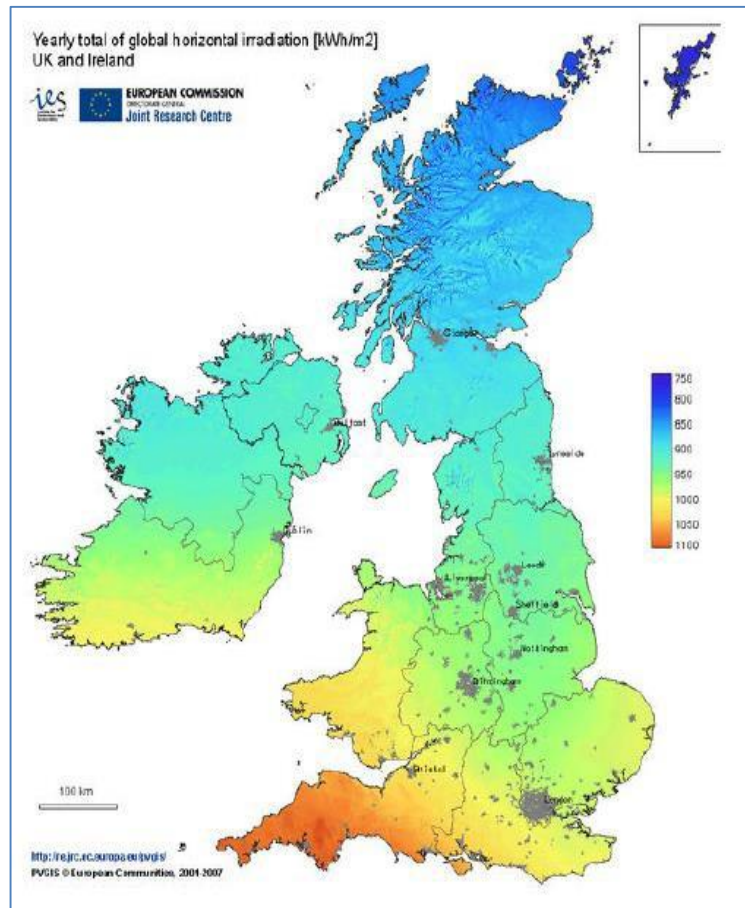


Figure 2 UK Solar Resource, Source: PVGIS in (Rugg, 2012)

It should be noted, however, that the colour scheme chosen for the plot exaggerates the difference between north and south, in fact the irradiation in central England is only 10% lower than that of Cornwall, and Scotland only 15% lower than that. Allowing for local differences in climate, a range of sites across Scotland may well be viable for solar exploitation.

Other comparable sites in the UK, to that assessed in this project, include:

Kernow, Hendra Holiday Park, Trenouth, and Wheal Jane solar parks in Cornwall.

Shipton Bellinger, Hatchlands Farm and a set of West Midlands solar plants in England.

As yet, large scale solar has yet to see significant development in Scotland. However, this is due to change as investment is starting to be put into large rooftop systems such as IKEA

(Colville, 2013) and farm-based schemes. An article in the Scotsman (Horton, 2012) highlights plans of 'TGC Renewables' to install 5MW schemes on Scottish farmland.

1.5 Existing Large-Scale Solar Installations in the UK

1.5.1 Cornwall Solar Parks



Figure 3 5MW Trenouth Solar PV Farm, Source: (Rugg, 2012)

Cornwall is one of the most attractive locations for large-scale photovoltaic (PV) projects in the UK, due to its high yearly insolation. A report produced by Cornwall Council (Rugg, 2012) includes a few of the notable solar farms, such as the site pictured (Figure 3) at Trenouth, a 1.4MW facility at Hendra Holiday Park, Newquay and a 1.4MW solar farm at Wheal Jane, Truro.

According to Rugg (2012), the Wheal Jane site consists of 5,760 solar panels installed over an area of 3.88ha. A report from Solar Century (2012) estimated the plant output at 1,427MWh per year, enough energy to power 432 homes, saving 737 tonnes of carbon. The plant is built on a disused tin mine, re-using waste land rather than greenfield (un-developed land). A number of issues, common to most solar installations were overcome in the development of the plant, consideration of the visual impact – work was carried out on landscaping the site to reduce any potential impact, ecological impact – surveys carried out to ensure the ecological impact was limited and the effect on land use was also considered with reference given to the value held in the site to the mining industry – it was determined that the site posed no risk regarding future mineral extraction efforts.

The considerations mentioned above also bore resemblance to the planning requirements for the development of the site in Dalkeith.

1.5.2 Other UK Installations

Some other large-scale plants currently being developed/commissioned across the UK include (OrtaSolar, 2012):

- Shipton Bellinger Solar Park: 5.4MWp, 21,500 panels built on farmland. Issues included proximity to archaeological sites and bird nesting sites.
- Hatchlands Farm Solar Park: 5.1MWp, 20,500 panels built on farmland. Issues included shooting rights over the land in question, which had to be resolved.
- Westmill Solar Park, 5MWp, 22,500 panels. Here, the plant had to be planned around archaeological sites, and also existing wind turbine infrastructure.

A report from Stepnell (2011), a construction company, gives a closer insight into the performance of a set of four 5MW solar parks built around the West Midlands. The energy generation figure is quoted at 4,500MWh per year per park, enough energy to power 1,350 homes. Construction times were extremely short at only 10 weeks (this timescale is mirrored by the short time to produce the Edinburgh College site, once the initial groundworks were completed). The whole project required high initial investment, £48M, paid for by the construction company, however £26M of this was 're-financed' by RBS. This indicates the strong financial viability of the project, shown in the willingness of both parties to invest substantial sums of money based on economic and production forecasts. The report makes a comparison with domestic systems, which it claims would cost 30% more to produce the same amount of energy per year, highlighting the advantage of large-scale over small-scale PV. The parks are estimated to have a 30-year operational lifespan (as a minimum), very low operation costs, and to offset 225,000 tonnes of CO₂ over this period (Stepnell, 2011).

1.5.3 Errol Estate Solar Farm

Construction was completed on Scotland's largest solar farm on the Errol Estate in Tayside in 2016. The 13MW scheme has been developed on 70 acres of land on the estate. The solar farm was completed and operational in March 2017 and provides power for over 3,500 homes. Errol estate was one of the first locations in Scotland, alongside Edinburgh College site, to be identified as a potential solar farm site, with this land being promoted for development by Savills Smiths Gore in 2011. The college site was developed in-house by the College. The site is shown in figure 4 over.



Figure 4 Errol Estate Solar Farm (Source: ROAVR 2016)

1.6 Further Education Colleges Overview

This Section will provide an overview of the Further Education Sector in Scotland. It will provide relevant information and background to the reasoning and requirement for Colleges to begin to make progress against the Scottish governments expectations set out in their Climate Change Act 2009. It will also provide information on the learner demographic and their role in providing a skilled workforce within a country of aging population (Canning, 1999). It will also outline the key policy drivers the sector currently engages with. Finally it will point towards particular initiatives one College has undertaken that the Sector could participate in more widely.

1.6.1 Scottish FE college regionalisation

Between 2012 and 2014, the Scottish Funding Council (SFC) and the Government approved ten mergers involving 26 colleges and one Higher Education Institution (HEI); one of the college mergers involved a two phase merger (New College Lanarkshire). The programme of mergers was prompted by Government policy which outlined the benefits of a regional structure for the college sector. Mergers were chosen by the colleges in most regions with more than one college to be the most effective and financially efficient way to achieve the desired outcomes of improving the delivery of education through coherent provision within the region, with benefits for all stakeholders.

The creation of larger colleges of scale, operating mainly on a regional basis, has led to a reduction in the number of publicly-funded colleges from 43 in August 2010 to 25 now. Outside the Highlands and Islands region there are now only 15 general colleges (and Newbattle Abbey College).

At the outset, the Scottish Government indicated that they expected the reform programme to deliver a number of high-level benefits, including reduced duplication, better outcomes for students and high quality learning, enhanced engagement with employers and financial savings for the sector. In addition, it was anticipated that there would be improved planning, co-ordination and delivery of skills provision in a region to meet the needs of employers at a local level but also for Scotland's economy. SFC later confirmed that they anticipated recurring savings of about £50 million each year from 2015-16 (Scottish Funding Council, 2016).

Colleges are located throughout Scotland and within 13 regions outlined in figure 1. The reasoning outlined above give a clear rationale for the merger process to take place.

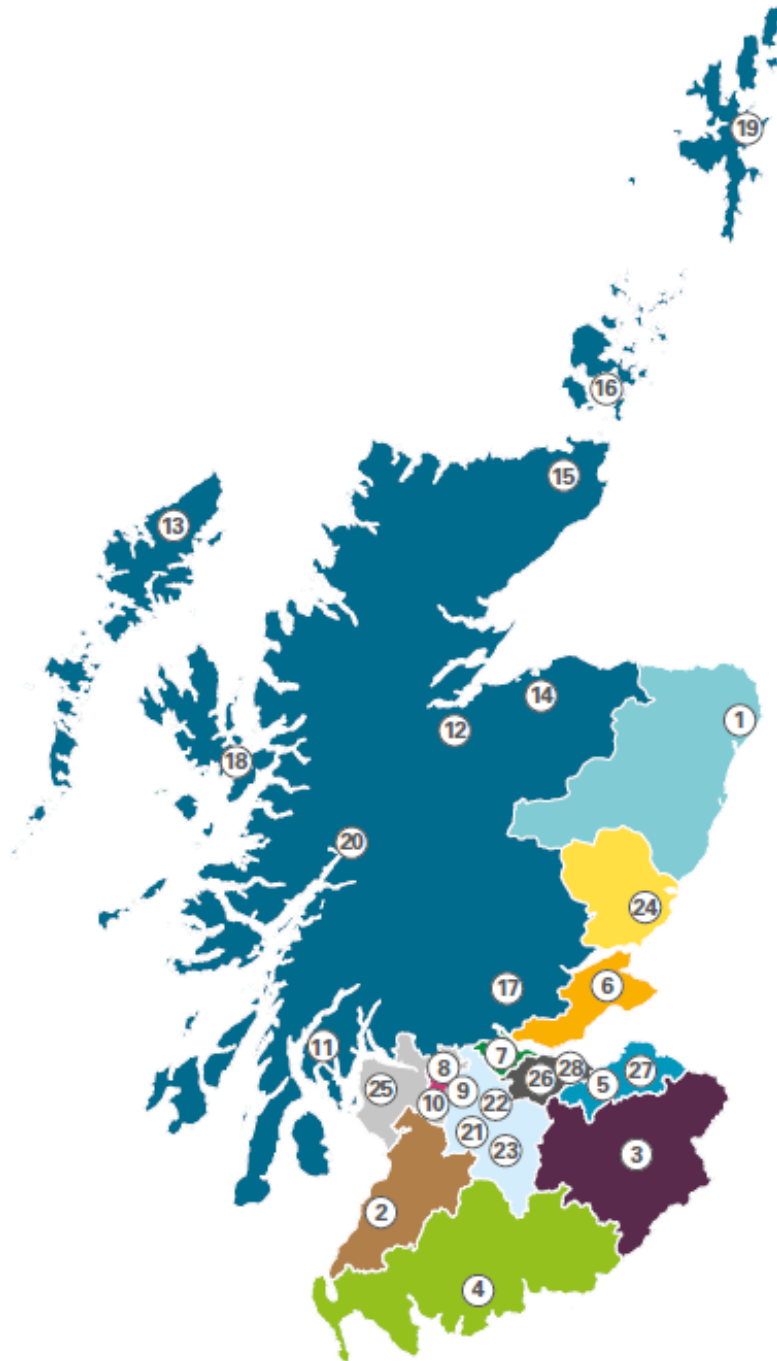


Figure 5 Map of Scotland (SFC, 2013)

1.6.2 Expectations of FE colleges and the Scottish Governments STEM agenda

Scotland's college sector creates value in a number of ways. The Colleges play a key role in helping learners increase their employability and achieve their individual potential. With a vast range of courses and apprenticeships, the colleges' provision enables learners to acquire qualifications and develop the skills they need in order to have the skills necessary to succeed in employment.

However, the contribution of the sector consists of more than solely influencing the lives of learners. The expenditures of Scotland's colleges, along with the spending of their staff and learners, further support the local economy through the output and employment generated at local level. (EMSI, 2015)

Colleges cater for all people, regardless of background, age or gender. The learner demographic is outlined in section 1.6.3. Colleges also play a crucial role in widening access into education for learners with additional needs and those from deprived communities. By providing opportunities in the community, colleges help reduce poverty and promote social inclusion (Scottish Funding Council, 2016).

Colleges are a key driver for the Developing the Young Workforce (DYW) agenda through their partnership working with local schools, universities and businesses across within their region and across Scotland. Through these partnerships, colleges are able to provide the right courses to students that match the demands of local economies around the country. With the assistance of Skills Development Scotland's (SDS) Regional Skills Investment Plans (RSIPs) local industry needs are met, and planned, for the future to ensure the relevant skills are delivered through the FE sector across Scotland. This is monitored by the SFC through the Regional Outcome Agreement (ROA) which monitors the agreed targets for individual colleges (Scottish Funding Council, 2016).

To deliver the best learning experience possible, colleges are constantly investing in upgrading campuses to provide modern, fit for purpose facilities for students. In the last ten years £900m has been spent on modernising college campuses across Scotland (Scottish Funding Council, 2016).

1.6.3 Learner Demographics

Scotland's colleges provided education to 267,226 learners, with an average learner representing roughly 50% of a full-time equivalent (FTE) in session 16/17. Included within these learners are 2,322 learners for whom Scotland's colleges contracted with other institutions to carry out provisions. The average age of learners attending Scotland's colleges was 17 years old. The breakdown of these learners by gender was 48% male and 52% female, and the breakdown by ethnicity was 85% white and 15% minority. Data on ethnicity and gender becomes important in the calculation of marginal earnings change since earnings by gender and ethnicities differ, sometimes widely, depending on the area under analysis (EMSI, 2015). This is important when the nature of regional skills requirement is taken into account. The

likelihood of skilled labour requirements being met by the FE sector in terms of vocational training should not be overlooked. This will provide the sector training requirements in growing industries across their regions, with a key growth industry being renewables and energy, across Scotland, it is important the opportunity to deliver relevant training is captured through the ROA and RSIPs to create real job opportunities for learners.

1.6.4 DYW

Scotland's colleges play an important role in helping young people of all backgrounds and abilities develop skills that are vitally important to our economy while exposing them to the more independent and self-reliant environment of college education. They cover a wide spectrum from their distinctive and significant contribution to higher education through the development of higher level applied technical skills to engagement with those young people furthest from the labour market. The option of full-time college education plus the range of options offered by colleges for those in work are critical elements of Scotland's education system.

The regionalisation of Scotland's colleges provides a significant opportunity for the sector to continue to enhance the perception of college education. Larger colleges will be well placed to play a key role in the planning and delivery of education within their regions, in the development of highly valued vocational education pathways starting with school pupils leading onto higher education, apprenticeships and employment, and in the development of advanced.

1.6.5 FE in the Future

Scotland's colleges must continue to build and grow on the success of the sector to date. The SFC's Regional Outcome Agreement process is a powerful lever in ensuring that colleges deliver in return for public investment, and reporting on those measures is now reinforced by Education Scotland's new quality framework, "How good is our college?" (Scottish Funding Council, 2016). There are also a number of other specific ways in which improvement is being sought in Scotland's colleges including: College Improvement Programme boosting retention and attainment rates among FE students, and in particular for those students currently most at risk of withdrawing without achieving a qualification or moving to a positive destination. A national college improvement programme has been introduced to look in detail at individual college level solutions to raise attainment and improve retention. On behalf of the college sector, five colleges will form an improvement team and undertake testing, gather information about what works to share across the sector, contributing to an increase in attainment and

retention within and between the five colleges. Their success will also be used to drive improvement across the sector as a whole.

1.6.6 College Innovation

There is also a desire for colleges to be more involved in innovation - our economy needs a highly skilled, adaptable and confident workforce, and colleges have excellent links with SMEs. An action plan has been put in place by the SFC's College Innovation Working Group to ignite collaboration between colleges and businesses. This includes bringing colleges further into the community of Scotland's eight Innovation Centres, while the Scottish Government announced a College Innovation Fund (£500,000 in 2017/18) to support Scotland's colleges to work with businesses on innovation activity (Scottish Funding Council, 2018).

1.7 Further Education Estate targets

The college estate across Scotland is reasonably old on the whole, with a number of colleges being refurbished or new builds in the last decade. This process of renewal is long overdue with some buildings being no longer fit-for-purpose for teaching vocational training. Maintaining facilities and also moving with technological change within organisations that are now fully in the public sector and governed through ONS makes it more difficult to invest. That being said, a sizable amount of investment has been made to manage current estate but very little has been invested in sustainable technologies to enable colleges to do their part in meeting carbon reduction targets and participating in the move to a low carbon economy. Whether green technologies are planned within refurbishment and/or new builds it would appear, on the surface, that these are the first things to go when feasibility studies are undertaken (Scottish Funding Council, 2017).

1.7.1 Overview of Scotland College Estate

Over the past ten years nearly £900 million has been invested in the college sector estate. Table 1 shows the capital value of the most significant new builds and major refurbishments completed in the last ten years:

Table 1 College Building expenditure (SFC, 2017).

College	Project	Total Cost £M
Ayrshire College	New campus NPD - Kilmarnock	48.5
Ayrshire College (formerly Ayr College)	Aeronautical Engineering Centre	4.0
Borders College/Heriot Watt University	New campus- <u>Netherdale</u> , Galashiels	28.2
City of Glasgow College	New campus NPD - Riverside & City	193.0
Dumfries & Galloway College	New campus	38.5
Dundee & Angus College (formerly Dundee College)	Major refurbishment of <u>Gardyne</u> campus	48.9
Edinburgh College (formerly Jewel & <u>Esk</u> College)	Milton Road campus development	57.0
Fife College	<u>Levenmouth</u> campus development	6.0
<u>Forth Valley</u>	- <u>Alloa</u> New campus	18.8
<u>Forth Valley</u>	Stirling New Campus	27.5
Glasgow Clyde College (formerly Anniesland College)	Redevelopment of main campus, Anniesland Hatfield Road	50.2
Glasgow Clyde College (formerly <u>Cardonald</u> College)	Major refurbishment of campus	23.4
Glasgow Clyde College (formerly <u>Langside</u> College)	New campus	36.2
Glasgow Kelvin College (formerly North Glasgow College)	New build, Springburn	42.0
Inverness College UHI	New campus NPD - <u>Beechwood & Balloch</u>	45.0
New College Lanarkshire (formerly Coatbridge College)	Major refurbishment of campus	22.6
New College Lanarkshire (formerly Motherwell College)	New build, <u>Ravensraig</u>	69.8
North East Scotland College (formerly Banff & Buchan College)	Major refurbishment of main <u>Fraserburgh</u> Campus	23.4
North East Scotland College (formerly Aberdeen College)	New – <u>Altens</u> construction Facility	15.3
North Highland College UHI	Engineering Skills Centre & Centre for Energy/Environment	15.3
South Lanarkshire College	East Kilbride Campus Development	34.5
West College Scotland (formerly Clydebank College)	New Build – Queens Quay	34.7

This first independent review of the college estate in Scotland for 10 years was undertaken when Gardiner and Theobald were appointed by SFC in January 2017 to undertake an estates condition survey across Scotland's colleges. For colleges with a campus capital project completed in the last 3 years, those campuses were excluded from the exercise. For colleges that held condition survey information less than 5 years old, that college information was used to inform the exercise. Where information was available but it was 5 years old or more and where there was little or no information, those colleges were surveyed. The purpose of an estate condition survey like this is to assess the general fabric and services of a building and estimate the cost to bring that building up to a generally sound (wind and watertight) condition, defined by the Royal Institute of Chartered Surveyors (RICS) as 'condition B'. It is important to emphasise that these surveys take no account of any costs required to improve fitness-for-purpose or redevelopment and enhancement, such as curriculum changes, improved flexibility or space efficiency, digital/ICT infrastructure or carbon reduction measures.

If tackled over a five-year period, the total backlog maintenance figure is around £360M. This does not take into account work that would not be undertaken where the relevant estate is being completely replaced or significantly refurbished. In addition to an assessment of backlog maintenance, the survey also provides a comprehensive information base to feed into high-level considerations of complete replacement or significant refurbishment of campuses (Scottish Funding Council, 2017).

1.7.2 Funding options

This analysis will feed into the Scottish Government's Learning Estate Investment Plan (Scottish Funding Council, 2017) which will include examination of opportunities to collaborate across education and the wider public sector to support joined-up services and efficient use of assets. This will include how colleges should develop their estates strategies in conjunction with local partners and taking full account of the Scottish Government's Learner Journey review and new developments in curriculum delivery. It should be noted that currently much of this funding is made up through European Structural Funds (ESF), which is potentially limiting due to the impacts of BREXIT being unknown. Further campus improvements will be hindered in the short term.

1.7.3 College Surveys

The task of surveying a College comprised a combination of site surveys. The survey and update follows on from the previous high-level desktop backlog maintenance assessment in November 2016. Resulting from this survey process, the estimated nett total backlog maintenance and renewals cost is £163,308,518 excluding contingencies, any related operational and management costs of the colleges, professionals Fees, VAT, Optimism Bias, and inflation allowance. It is also prudent to apply a level of the Optimum Bias to the estimated numbers. Based on the nett figure of £163,308,518 the additional costs when taken into account are as follows:

- Professional Fees, Contingencies, Other Costs and VAT £81,654,259
- Optimism Bias £73,488,833
- Inflation Allowance £44,869,418

This results in a total gross estimated backlog maintenance and removals cost, taking all of the above cost headings into account, is £363,321,028. Whilst noting that a notional allowance of client contingency costs has been made, it is important to note that the operational costs associated with facilitating any remedial works or renewals especially in and around occupied buildings, will vary on a building by building basis, its surroundings and function, and will depend entirely upon the colleges own preferred programming and packaging of works which may need to align with their specific wider estate strategy and other considerations. It should therefore be understood that variable packages of major works which may or may not also desirably include potential redevelopment and campus improvement strategies would have to be considered for further budgetary enhancement on a case by case basis at the time of presentation and further substantiation. An assessment was made of the cashflow uplift to the figures based on a 10 year programme of works. The complication with this is that the buildings that have identified issues and are not actioned, deteriorate further and what would be previously have been dealt with as a remedial / refurbishment exercise could actually result in a complete replacement. The added cost of these elements cannot be allowed for until a sequence of works required is agreed and an appropriate expenditure profile developed.

For the avoidance of doubt, the surveys and resulting costs also do not consider works and the costs associated with fitness-for-purpose or (re)-development and enhancement of colleges' campus or facilities or other initiatives, such as changes in curriculum delivery, carbon footprint reduction or similar upgrading works as may be determined by separate agenda or other focused individual college or sector wide strategies.

1.7.4 Scotland's Energy Efficiency Programme (SEEP)

Energy efficiency is fundamental to Scotland meeting its ambitious climate change targets. Heating and cooling Scotland's homes and businesses costs £2.6 billion a year and accounts for just under half of the country's greenhouse gas emissions (Scottish Government, 2017b). Scottish Ministers announced, in June 2015, that they would take long-term action to reduce the energy demand of our residential, services and industrial sectors through designating energy efficiency as a national infrastructure priority, as subsequently confirmed in the Scottish Government's Infrastructure Investment Plan 2015. Ministers announced that the cornerstone of this will be Scotland's Energy Efficiency Programme (SEEP) which is under development and will be rolled out from 2018. It will be a co-ordinated programme to improve the energy efficiency of homes and buildings in the commercial, public and industrial sectors (Scottish Government, 2017a).

1.7.5 Aims of SEEP

In making a long-term commitment to SEEP, the Scottish Government recognises the multiple benefits that can, and must, accrue from a programme of this magnitude and duration. These benefits not only include substantive contributions to meeting our climate change targets through the decarbonisation of heat and reduced energy demand, but also offer significant wider economic, social, health and regeneration benefits: measures to make homes warmer and places of work more comfortable, promoting more affordable energy for consumers, helping to tackle fuel poverty and improve the competitiveness of the Scottish economy; the opportunity to create a substantial Scottish market and supply chain for energy efficiency services and technologies, with an estimated 4,000 jobs per annum across Scotland, including in remote areas, based on an initial estimated minimum investment of around £10 billion; measurable health and early years improvements through people living in warmer homes; regeneration of communities through upgraded building stock; and substantially reduced greenhouse gas emissions contributing to meeting the ambitious climate change targets (Scottish Government, 2017b).

1.7.6 Pathfinder Fund

As the first step in preparing for the launch of SEEP in 2018, the Government offered funding for a range of SEEP pilot projects last year. Eleven local authorities are receiving over £9million of funding to carry out SEEP pilots in 2016-17. This investment started the process of demonstrating ways of delivering an integrated programme before the wider roll out from 2018, of which Edinburgh College is one. The Government is now inviting local authorities and/or

their partners to submit new proposals for SEEP pilot projects for delivery by February 2019. This second phase of pilot projects will further help the development of SEEP, contribute to the design of future programmes aimed at tackling fuel poverty and reducing greenhouse gas emissions and inform how future SEEP funding is best deployed to achieve Ministerial objectives. Alongside the ongoing consultation on the draft Energy Strategy (and the related consultations on the broad design and objectives of SEEP1, and on Local Heat & Energy Efficiency Strategies (LHEES) and District Heating Regulation²), this call will help us to further test and demonstrate some of the issues in delivering a Programme of this scale (Scottish Government, 2017a).

1.7.6 College sector activity

The College Sector in Scotland must embrace emergent technologies and more sustainable sources of energy if it is to reach a sustainable position moving forward. Guidance should be produced to direct college estate funding in the direction of affordable, sustainable and future focussed buildings in order to get best value for money from the public purse. This should include a requirement for more ongoing improvements being made to refurbishment or new build activities in the sector and a drive towards utilising available funding streams such as SEEP funding. Colleges are also committed to moving towards Environmental management systems (EMS) with growing public pressure on organisations to adopt production systems that do not unduly impinge upon the natural environment is reflected in the adoption of of EMSs in business activities. An EMS can change an organisation's structure, responsibilities, practices, procedures, processes and resources for environmental management, so that it is able to reduce negative environmental impact while improving management control (Renwick et al., 2008; Bansal and Hunter, 2003). In addition, a certified EMS such as ISO 14001, a globally recognised standard for environmental management, provides a strong signal to external stakeholders of its environmental management commitment (Linnenluecke and Griffiths, 2010; Jiang and Bansal, 2003).

Therefore, it is expected that EMS implementation, in colleges, brings about organisational benefits with an increase in the demand of environmentally conscious customers, achievement of environmental objectives and cost reductions through improved productivity. According to Segersen and Miceli (1998) and Welch et al. (2002), it is widely believed that organisations adopt such environmental standards because they recognise that the accrued benefits, not just production and economic benefits (Jabbour et al., 2008) of doing nothing. Although the effect of EMS implementation through an increase in demand is a direct effect, and an improvement in productivity is regarded as an indirect effect, because an EMS only provides

a management framework for environmental objectives, it is expected that several environmental management activities for the objectives actually improve productivity and provide an economic benefit (Hertin at al., 2008).

1.7.6.1 Edinburgh College (A Case study for good practice)

Edinburgh College is committed to becoming a leading low-carbon organisation. The carbon management plan, it has created, is the key mechanism for delivering the college's vision and sets out the formalised approach to reducing carbon emissions from college activities over the next six years. The introduction of EMS will contribute to a more thoughtful organisation with the aim to reduce carbon emissions by a minimum of 18% by 2020 from the 2013-14 baseline. This will be tackled by undertaking a variety of carbon-reduction projects across energy, water, waste and transport including encouraging positive behaviours by our students, staff and visitors (Edinburgh College, 2016)

In 2012/13 Edinburgh College spent approximately £1.6million on utilities and transport. With rising utility prices and the additional costs of water and waste management, it's clear how important it is that the College actively engages in reducing this cost. A Carbon Management Plan (Edinburgh College, 2016) is a proven mechanism for reducing carbon emissions from an organisation's activities. Since 2009, Napier University has seen a 25% decrease in carbon as a result of its plan (Edinburgh College, 2016). There are many drivers to reduce carbon emissions, including:

Climate change, although contested, there is near universal agreement that it is driven to a large degree by human activity and will have significant impacts on our future (Metz, 2013). The Scottish Government introduced the world-leading Climate Change (Scotland) Act 2009, which places a public duty on public sector organisations to reduce carbon emissions by 42% by 2020 and 80% by 2050. The college has signed up the Universities and Colleges Climate Commitment for Scotland, which requires them to take steps to reduce the impact on climate change.

Edinburgh College, as a case study for good practice, is committed to being a sustainable and socially responsible institution. In order to achieve this, the college aims to integrate and encourage sustainable practices across the organisation, from how it runs the estate through to what curriculum is taught. A dedicated sustainability team are an integral part of ensuring

action is taken and promoted through the sustainability strategy (Edinburgh College, 2017).

The main areas of focus for the Sustainability strategy are:

- **Carbon Management** - The College's carbon footprint in 2014-15 from electricity and gas alone was around 7500 t/CO₂. – something the college will need to reduce, not only because the College is identified as a 'Major Player' in the Climate Change (Scotland) Act 2009, but because it will also save money. Currently the College's utilities spend is over £1million.
- **Carbon Management Plan** – The College's Carbon Management Plan is the main mechanism for addressing this. A commitment to reducing carbon emissions by a minimum of 18% by 2020 from a 2014-15 baseline. In order to achieve this the College will implement a number of projects. Some, such as the recently installed voltage optimisation at 3 campuses, are already making savings. Other projects are relatively low cost and involve raising awareness amongst staff and students to encourage positive behaviours – sometimes as simple as switching the lights off. The facilities of the College include photovoltaic panels on the roof of our Granton campus which provide energy for the campus and offset around 18t/CO₂ per year. One of their Hair and Beauty Salon is eco-friendly and has the latest technology installed including a fuel cell, LED lighting and heat recovery system. Whilst this is just the start and there will be major challenges ahead if the college is to meet the targets, there will also be many opportunities – particularly linking the curriculum, where it can effect positive change.
- **Waste** - In 2014-15 the college produced around 900 tonnes of waste and had an on-site recycling rate of only 27% - something the College is committed to changing. The College has developed a waste strategy aimed at improving the recycling rate and are working with Zero Waste Scotland to deliver improvements. We have started our 'sort it' campaign in 2015-16 and will be looking to make significant inroads in the first year.
- **Sustainable Travel** - The College has a major impact on the transport infrastructure around Edinburgh and have developed a 'Green Travel plan' with the aim of reducing our impact from all aspects of travel and we want to encourage a shift towards more sustainable travel. For us that means, investing in facilities, such as our new secure cycle parking at Sighthill or the eCycles for staff use. On top of that the College is providing information and advice on using public transport through 'real time information screens' at all the main campuses. Edinburgh College has an entirely-electric pool car fleet, which has resulted in enormous benefits for the college, staff, community and planet. Aside from the reductions in tailpipe emissions and lower carbon, the electric vehicles are fully integrated into the curriculum, offering hands on experience to students on Engineering, Automotive and Electrical courses. This experience

increases their understanding of environmentally friendly transport technologies and the associated infrastructure, and provides them with the skills to work with electric vehicles as their use becomes more widespread. To date College Staff have travelled over 90,000 miles in them and seen a £40,000 saving compared to business mileage expenses. The electric car project has been selected as a finalist in the 2015 Green Gown award.

1.7.7 College Energy Efficiency Partnership (CEEP)

The college also received an offer of funding for the CEEP project which amounted to £2,147,434. This was accepted and the college has to provide reports on future carbon emissions as part of their outcome agreement, with government, from 2018 until 2020.

A number of Energy Saving Measures (ESMs) were considered and developed, taking cognisance of the available energy saving and carbon reduction measures. The measures included:

- LED lighting and controls
- Main Boiler Replacement for Milton Road Campus
- Combined Heat and Power plant for Granton Campus
- Replacement of electric heating with gas heating for motor vehicle workshops at Sighthill Campus
- Variable Speed Drive (VSD) installation and optimisation of air handling units
- Building Management optimisation of operating schedules
- Heat Exchanger installation to improve hot water supply temperature in the Club Building
- Various time controls on vending, hot water and refrigeration equipment

As with all energy and carbon reduction measures this project brings several benefits for the college and will provide a platform to further improve the estate in years to come. Immediate benefits include a measured and verified savings guarantee of £200K per annum. A summary of the main benefits of these ECMs are:

- 12% reduction in annual energy costs
- Extended life of and optimisation of existing equipment
- Improved comfort levels for students, staff and visitors
- Introduction of new technologies such as LED lighting and CHP
- Maximisation of energy efficiency measures available

- Verification of savings by independent consultant for a period of one year

1.8 Edinburgh College Electricity Consumption

Table 2 shows the electricity consumption of Edinburgh Colleges Midlothian Campus. One of the aims of the installation was to support the college's ambition of creating an offgrid campus and provide a means to reducing the carbon footprint of the campus. This research will provide an evidence base to prove or disprove the assumptions made prior to installation. It is important to point out that the information below notes a 12% decrease on the previous financial year (kWh consumption for previous financial years available in appendix I). This pushes the previous year's consumption above 700kWh thus making it unlikely that array will generate enough electricity to meet the expectations of the college, when the notable shading is factored in, and the likelihood of supporting an offgrid FE campus unlikely.

Table 2 Electricity consumption (kWh) of the Midlothian Campus

2017-18 Financial year – Electricity Consumption kWh (1st April - 31st March)		
Midlothian Campus	kWh	% Change
April 2017	48,287.2	-18%
May 2017	60,668.8	6%
June 2017	53,550.2	-2%
July 2017	41,246.6	-8%
Aug 2017	44,305.9	-14%
Sept 2017	51,211.6	-16%
Oct 2017	51,177.0	-17%
Nov 2017	57,314.3	-20%
Dec 2017	53,361.7	-15%
Jan 2018	57,433.0	-12%
Feb 2018	55,483.3	-13%
Mar 2018	61,595.7	-8%
Total (by site)	635,635.2	-12%

1.9 Edinburgh College Travel Costs

1.9.1 Scottish Government decarbonisation of the road transport sector

The Scottish government has committed to almost complete decarbonisation of the road transport sector by 2050. As such a major element of this transformation will be a shift towards the electrification of road transport. A sustainable fleet of electric vehicles aligns with Scottish investment in a renewable energy sector. Furthermore, there is a 100% funding for the installation of home charging points.

1.9.2 Edinburgh College green fleet – research project

The e-car project is monitoring 15 plus vehicles data with respect to location, acceleration, start/stop, speed and plug-in charge time. The research includes drivers' usage across all partners. The partners involved in this project are: SQA, Edinburgh College, Siemens, Midlothian Council and SESTran. There are also interested parties that are looking to become partners; East Lothian Council and Lothian and Borders Police.

The aim is to give vehicle life cost as a low/zero carbon alternatives to conventional transportation. All journeys will be full monitored through GPS and the vehicles planned route will be determined as the optimum. The route efficiency can be determined for a journey.

The electric vehicle has to be taken as a serious alternative to the conventional engine vehicle and there are many questions surrounding their practical use. From purchase costs, running costs to their practicality and what changes have to occur to the users' lifestyle, journey route and time. This is a real-time project that will have the research requirement as well as solving a commercial transportation requirement.

1.10 Edinburgh College eCar research

1.10.1 Edinburgh College BEV - early adopters

The College has twelve electric vehicles, two located at each campus with the exception of the Midlothian Campus, where there are three vehicles. There is also an electric mini-bus available for staff use. There are a total of twelve charging points, three located at each campus. The electric vehicles are for staff use only and for College business. Figure 5 indicates the user plots captured over a five year period. The College has leased the electric vehicles since 2011 with the first year operating as a trial period, following full roll out of vehicles to the four main campuses. Trials are still frequently undertaken to understand the efficiency of the vehicles in

servicing the operational needs of the staff at the College to maximise the integration to the changing business requirements.

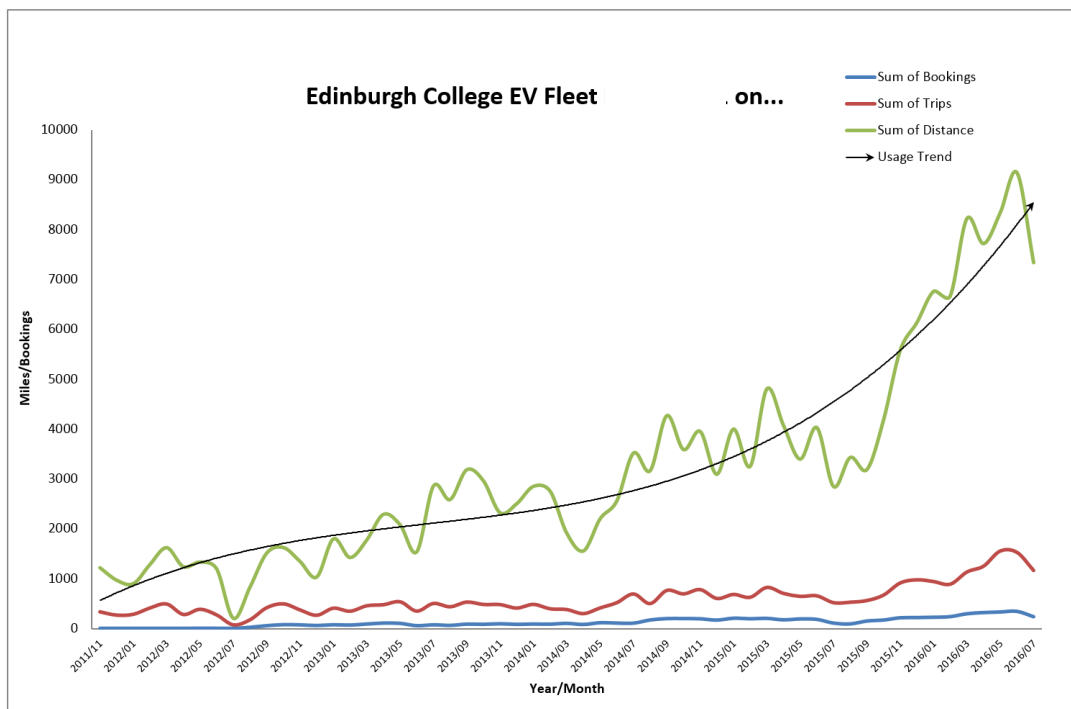


Figure 6 Battery electric vehicle usage 2011-2016 (Edinburgh College, 2016)

As an alternative option to purchasing Edinburgh College opted to design and manufacture our own model of electric vehicle (EV) charging post designed with on-charge/off-charge illumination for the user. These will be strategically positioned on routes and at businesses that will have the maximum impact to the BEV user without the attached high cost from a proprietary version.

1.10.2 Edinburgh College travel

A research study at Edinburgh College conducted analysis to determine the most suitable method of vehicle procurement. It was decided that due to the nature of the business the lease option was most applicable.

The advantages of leasing a fleet vehicle may include:

- reduced capital costs
- operation of a more fuel efficient fleet
- reduced fuel costs in the longer term
- removing maintenance and servicing issues
- flexibility to choose the vehicle that meets the College's requirements
- ability to select low carbon vehicles with the latest technology
- easy disposal of used vehicles

The disadvantages of leasing a fleet vehicle may include:

- restrictions within the terms and conditions of the lease
- vehicle is not owned
- repayments may be higher than financing the purchase
- vehicle cannot be modified
- high penalty costs can be incurred at end of lease period
- potential limitations to vehicle use and mileage restrictions

1.10.3 College commuting requirements

Post-merger and consolidation of the three Edinburgh Colleges a decision was taken to develop an innovative idea to the inter-campus travel initiative using electric vehicles. Introducing the battery electric vehicle into Edinburgh College brings important societal benefits as it improves energy efficiency, air quality and reduces urban noise, and CO₂ emissions when conducting the inter-campus commute. As part of the corporate travel plan all mobility activity should be subject to the required analysis as reported by Baddeley (2008), initially determining whether the journey is absolutely necessary.

1.10.4 Edinburgh College and staff mobility

Due to the nature of the College transport requirements over 85% of journeys are under 10 miles long due to the travel distance between campuses and the local journeys that the vehicles are mainly used for. Similar figures have been reported by Weiss *et al.* (2014) in a previous study. Figure 7 confirms the frequency of travel over 19000 recorded trips for BEV short range mobility.

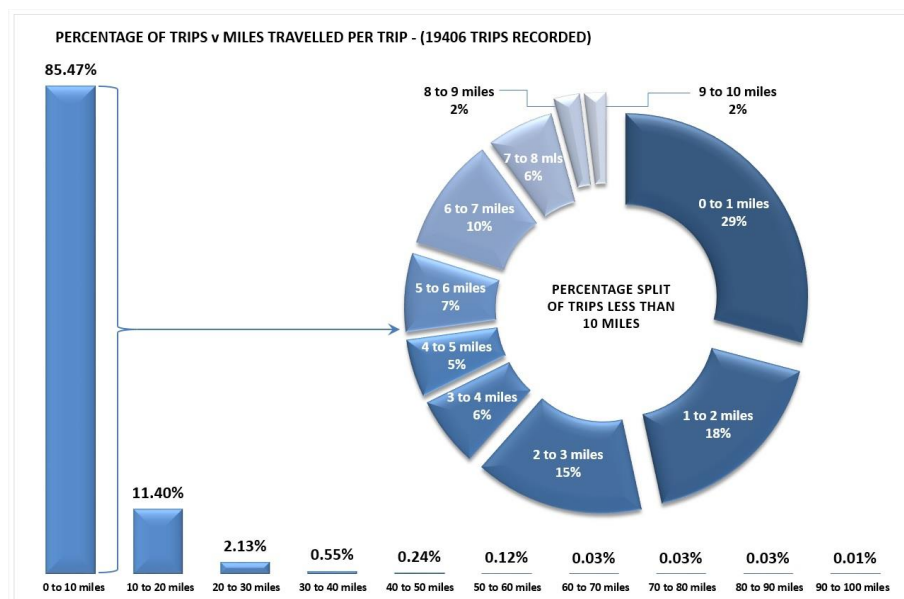


Figure 7 Percentages of travel distance (Edinburgh College, 2016)

The field data used in this study was collected as part of a nationwide BEV project in Midlothian, Scotland, UK. Nissan LEAF's, eNV200's and Mitsubishi i-MiEV's were trialled for a six-month period. The participants were selected from different genders and geographical areas in order to achieve a representative sample of the drivers in the area.

The data loggers installed in the vehicles were configured to read information from vehicle sensors available on the vehicle's CAN (Control Area Network) bus and to store these data in the logger's internal memory along with the vehicle's GPS position. GPS data and CAN bus messages were logged every five seconds and every one second respectively when the vehicle ignition was on. Specifically, the vehicle's velocity was logged every second from the CAN bus (Milligan, 2016).

1.11 Future developments

The total energy required to charge the College's eFleet has been estimated at 18,027.75 kWh, what is the feasibility of charging the college's eFleet through the use of solar charging stations situated on site supporting the college aspirations of creating a carbon neutral campus? In theory about 2.5% of the Solar Meadow's generated electricity would be required to fulfil the full charging of the eFleet at a cost of £1,261.94. This will be reviewed in chapter 6.

This chapter has outlined the research to be carried out, the main areas of interest for the researcher, provided an overview of the research site, facility and provided a contextual overview of the FE sector in Scotland along with a sector wide estate summary that highlights the current condition of College buildings. The consumptions of Edinburgh College's Midlothian campus has been presented in order to justify the need for research to provide an evidence based review of the viability of such an installation, of scale, in Scotland.

Chapter 2 – Literature Review, review of worldwide trends in solar photovoltaic technologies

2.0 Chapter Summary

The following chapter will look at the implementation and policy drivers in the world in more detail, particular attention will be paid to Scotland and Scottish government targets due to the location of the array in question. This section will also show the influence the international solar PV market is having across the leading countries and how individual country uptake can support growth in other countries.

2.0.1 Existing Literature and previous works

There is a vast amount of information available within the field of Solar Energy, most of which has been carried out in countries centred on, or in close proximity to the equator.

Almost all of the research agrees on the fact that Solar PV is a promising source of energy production, electricity generation and CO₂ reduction. Sherwani and Usmani (2010) report that further development in the efficiency of solar cells, the amount of material used in their composition and the amount of recycled material used will greatly benefit the overall sustainability of this for technology. Muneer *et al.* (2006) have shown that in order to maximise the output and efficiency of a photovoltaic facility, it is paramount to optimise the orientation and tilt of the solar panels. Myrans (2009) found that solar PV results show that it is the best choice of technology for meeting the criteria of carbon displacement. *et. al.* (2011) carried out research in Libya and have concluded that in Libya a solar PV system can have the capacity factor and Solar capacity factor of 26% and 63% respectively. This determines that the payback period of a 50MW system will be only 2.7 years, therefore, what will the conclusions for such systems in Scotland be, such as the facility at Edinburgh College? Although the current research agrees that Solar PV is a real competitor in the renewables market, efficiency and cost reduction are very important aspects of their installation. Further research and development is required to realise the true potential of Solar PV.

This analysis of a Scottish solar array will assess a number of aspects associated with the development of solar PV and any potential impacts throughout the products life. This research will serve to further the current research in terms of utilisation at high latitudes.

2.0.2 Previous works relevant to this research

Slope Irradiation, Cell Temperature and Cell Efficiency Model

In their paper, Aldali et.al.(2013) report on a similar investigation to that in this research on a small experimental PV setup in a city in southern Turkey. The experimental setup measured the current and voltage output of the PV modules, the cell temperature, ambient temperature and solar irradiance (horizontal, and in the plane of the modules). This work formed a strong basis for the research carried out on the Dalkeith solar array.

Data from each of the sensors was logged automatically every 30s; the only variable not recorded was the wind speed, where climactic average speeds for the location were used. Slope irradiation was calculated using solar geometrical equations and the diffuse irradiation model proposed by Muneer (2004) and cell temperature from a thermal model based on the work of (Mattei, 2006). Cell efficiency was calculated directly from the current and voltage output (not compared with cell temperature-based calculations, as in this project).

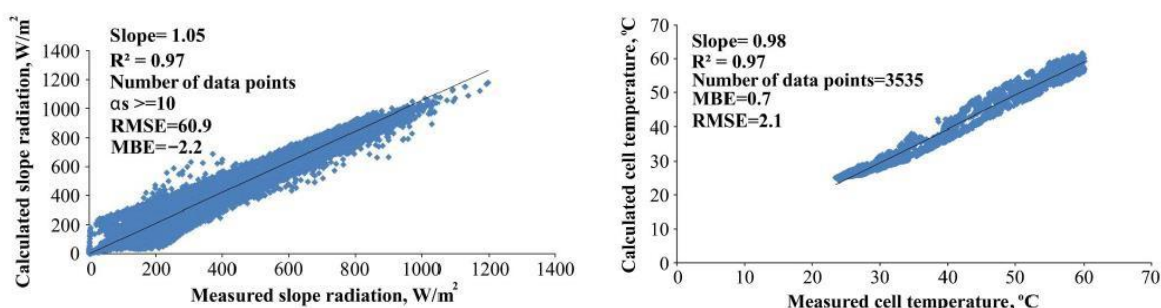


Figure 8 Correlations between measured and calculated Slope Irradiation and Cell Temperature, Source: Aldali et al.(2013)

The results (Figure 8) show very good model performance for the slope irradiation and cell temperature, with R^2 values of 0.97 for both. This indicates that good results should be achievable in this research.

2.1 Worldwide countries leading PV development and installation

By the end of 2014 the total global PV cumulative installation reached 415GW (*International Energy Agency, 2018*) this means 1.7% of world electricity generation comes directly from PV. By the end of the same year there were 20 countries worldwide which have passed the gross recorded output of 1GW from the combined solar installations in that country (*International Energy Agency, 2015*).

2017 was the fourth year in a row that Asia has led the world for PV capacity with around 60% of the total global PV installations. China, one of the largest PV contributors in Asia in the last decade, has installed 131.1 GW by 2017. The USA installed 51GW in the same year

consisting mostly of large scale installation and new business models dominating the market. Europe, on the other hand, has significantly declined from an annual installation total of 22GW down to around 7GW in 2014. Nevertheless, 2017 saw PV contributing 3.5% of electricity demand in Europe and 7% of the total peak demand (*International Energy Agency, 2017*). Germany sits top of the European countries list for PV installation with 42.4GW of PV projects in 2017, with U.K and France at 12.7GW and 8GW respectively.

The International Energy Agency (IEA) 2017, reports that the top countries for PV installation in 2014 were China, Japan, USA, Germany and the UK. The Renewable Energy Country Attractive Index (RECAI) is a report published by multinational the consultancy firm Ernst & Young (EY), which ranks the countries on the basis of their potential in terms of renewable energy investment and opportunities for growth. The RECAI and European Photovoltaic Industry Association (EPIA) reported that the highest ranking countries for PV installation in 2016 were China, Japan, USA, Germany and the UK (*International Energy Agency, 2018*). These five countries combined PV installation accounted for 65% in the year 2012, around three quarters in 2013 and almost 80% of the world's total PV installation in 2014 and in 2016 supply more than 1GW. Figure 9 represents the leading countries by PV installation in 2017. That being said it should be noted that China and Japan installed five times the amount than that of Germany and therefore four times the amount of the UK and the USA have just over half the number of Chinese installations. Figure 10 shows the combined total installations from the leading countries for 2017.

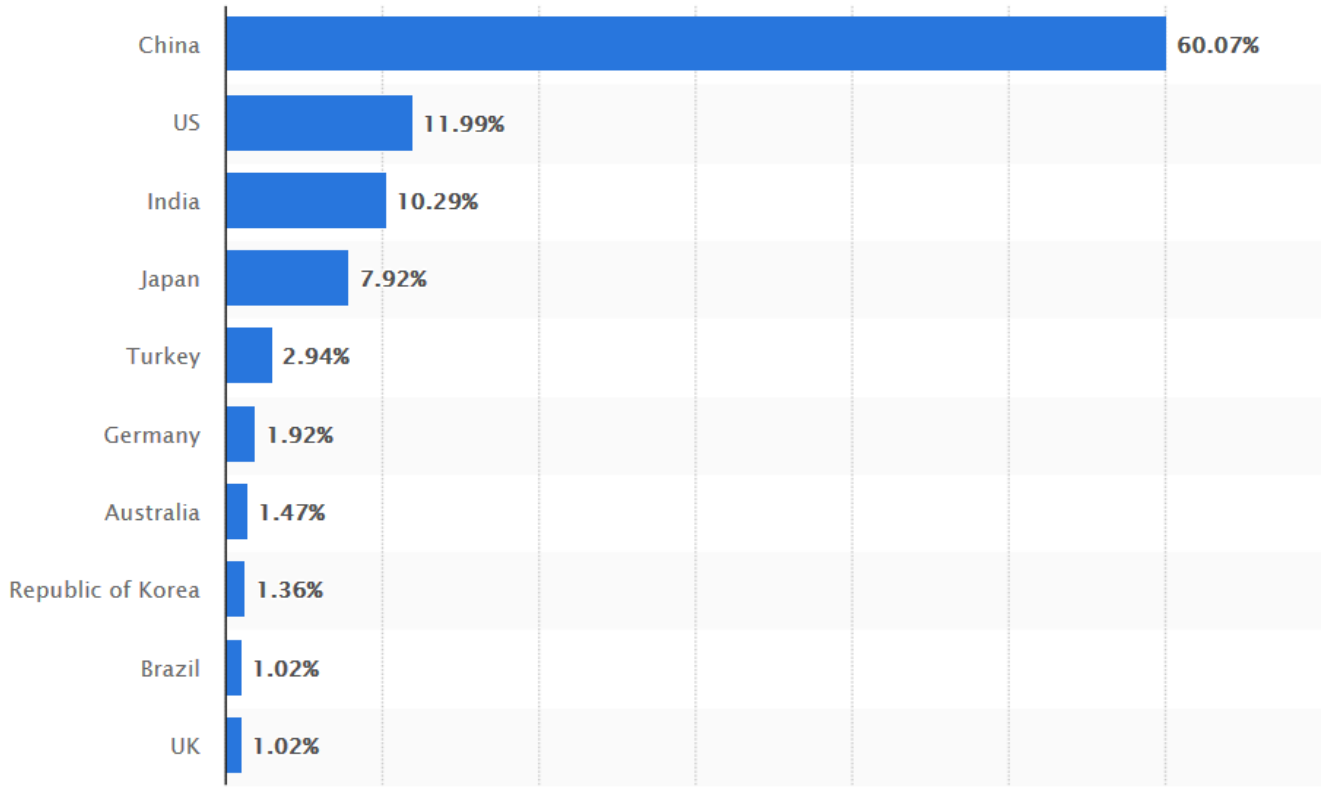


Figure 9 PV installation in the year 2017 for leading countries (Statista.com)

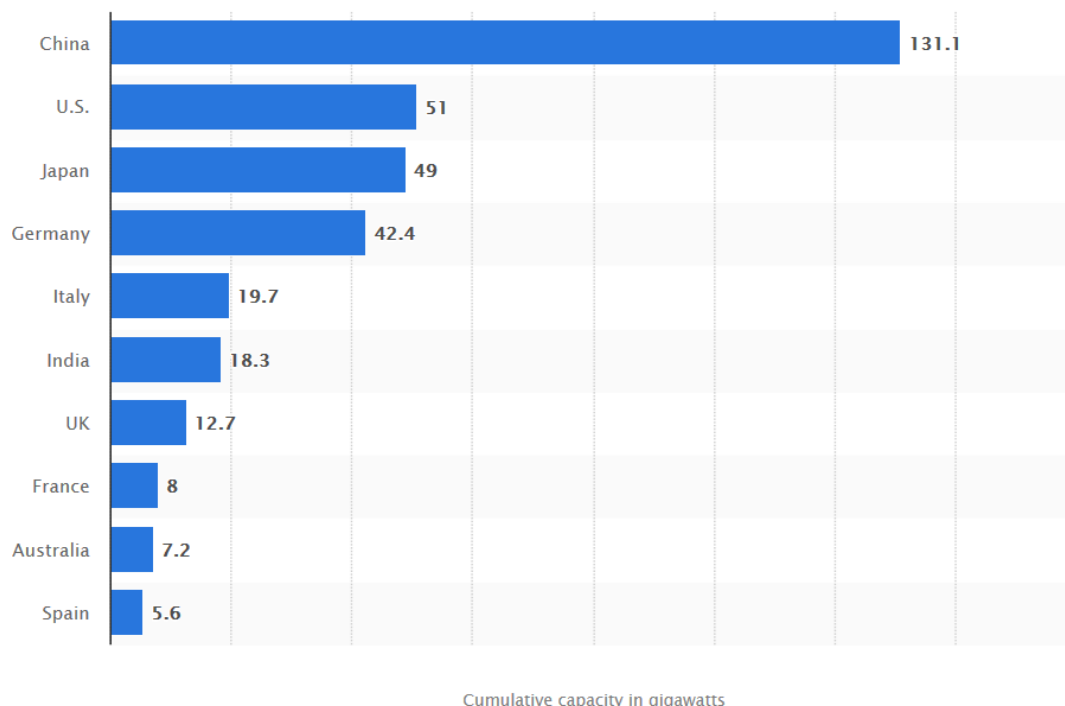


Figure 10 Cumulative installation capacity of the leading countries for 2017 (Statista.com)

2.2 China

2.2.1 Key policy drivers

The solar industry of China is growing faster than any other country in the world, mainly due to the extremely rich solar energy resources found there (Liu et. al. 2010). The Chinese government has created policy and incentivised the solar industry which has allowed such rapid growth in the use of solar technologies.

The Renewable Energy Law (China) was planned in 2005 by the National People Congress (NPC) (Calde´s et.al. 2009) and implemented in 2006. It is based on five key structures: (a) national targets for the development of renewable energy (it focuses the investment towards all sources of renewable energies) (b) a mandatory connection and purchase policy created between grid companies and renewable energy electricity generating schemes, grid companies need to sign an agreement stating that they will purchase renewable electricity from all renewable electricity generating schemes and provide the grid connection services (c) Feed in Tariff (FiT) system and price, FiT prices are fixed and will be paid to the renewable electricity generating schemes owners for each kWh of electricity generated (d) a cost sharing mechanism, the cost of the grid connection and the renewable energy generation will be divided between utility companies and the end users (consumers) by implementing a surcharge on sold electricity and (e) the renewable energy development special funds, funds

will be provided and apportioned to activities such as research and development of renewable energy technologies and schemes, setting up pilot projects or renewable resources assessments (Solangi et.al 2013).

Additionally, following this law, several different policies were implemented in China by the government to support growth, such as the Tentative Management Method for Renewable Energy Development Special Fund (2006), Provisional Administrative Measure on Pricing and Cost Sharing for Renewable Energy Power Generation (2006), the Medium and Long term Renewable Energy Development Plan (2007) and the 11th Five year Plan of Renewable Energy Development (2008).

The Brightness and Township Electrification Programme is a group of programmes which is one of the main driving forces behind the expansion of the solar PV market in China. The brightness programme was implemented in 1996 with an aim to use PV modules and provide electricity for the day-to-day requirements of the population of china, which are without any grid connections (Zhang et.al. 2013). Thereafter, in 2002, the National Development and Reform Commission (NDRC) put forward a Township Electrification Program for more remote areas and the western regions of China. Under this programme, 20MW of solar PV stations was installed in 688 towns and resulted in the first large scale attempt, by Chinese government, to solve the problem of electricity supply requirements for un-electrified areas within China. Based on the success of this attempt, the government is now supporting the programme with funding and development and therefore the manufacture PV modules and associated industry is rapidly rising (*Actions taken by the Chinese Government, 2015*).

The Rooftop Subsidy Programme and Golden Sun Demonstration Programme implemented by the Ministry of Finance (MOF), Ministry of Housing and Urban Rural development of China (MOHURD) were initiated in 2009 (Finance, 2009a). This programme allows eligible consumers, access to a subsidy for £1.54/W (RMB 15/W) for a rooftop system. The Ministry of Science and Technology (MOST) and the National Energy Administration (NEA) initiated the golden sun demonstration programme, which provides 70% of the total cost of an off-grid system and 50% for an on-grid system (Finance, 2009b), there is an attached condition to this subsidy in that the size of the plant should be more than 300kW et.al. 2011). By 2012 both programmes had approved more than 500MW of solar PV projects clearly showing the government incentivisation of solar PV projects in country (PJM, 2011).

In July 2011 the NDRC introduced the first **national FiT Scheme**, named as Notice on perfection of policy regarding FiT of power generated by solar PV. The first phase, under this scheme, was for the projects approved prior to July 2011, and for those due to have completed construction and commercial operation prior to 31st December 2011. All projects meeting

these requirements are entitled to a tariff of £0.12/kWh (RMB 1.15/kWh). The second phase of the scheme is allocated to those projects which were approved post July 2011 or approved prior to that date but cannot be completed by the end of 2011, these projects are entitled to a tariff of £0.10/kWh (RMB1/kWh) (Wigmore, 2012).

Another important policy is the **Free grid-connection services** policy, provided by the State Grid Corporation of China (SGCC). It declared that, as of November 2012, it would provide free connection services for distributed solar PV electricity producers that are located in close proximity to customers and meet the requirements of having installed capacities of less than 6MW for each installation (*The Golden Sun of China*, 2015).

2.2.2 Photo Voltaic Research & Development activities and associated funding

Numerous R&D activities have been reported on technologies such as crystalline silicon solar cells, thin-films, Concentrated Photovoltaic (CPV), Balance of System (BOS) components and testing technologies. China has been conducting all PV R&D under the National High tech R&D Programme since 1986 (Thornley et.al. 2011). All basic research in relation to PV technology is carried out under the National Basic Research Programme of China (2015) and further research into storage, transmission and demonstrations of PV generated electricity is held by MOST. Under China's 12th Five Year Plan (2011–2015) for R&D, targets are set to increase the conversion efficiency of crystalline silicon solar cells and amorphous thin films solar cells with a view to commercialise the use of CIGS and CdTe thin-films. In 2005, NDRC funded £3.51 million (€5.02 million) for development and demonstration projects for PV manufacturers and R&D institutions. Similarly, from 2006 to 2010, £15.38 million (€22 million) was spent on basic research programmes as well as high-tech programmes for R&D on PV (Grau, 2011).

In addition, MOST created a programme to support small firms specialising in high-tech PV manufacturing plants. This programme provided about £2.06 million (¥ 20 million) to support high-tech PV projects in 2009. Chinese state banks (government) provide a variety of support packages for investment for PV manufacturers including refund of loan interest, refund of electricity consumption fees, refund of land transfer fee, refund of corporate income tax, refund of value added tax payment, loan guarantees and credit facilities are all available (Grau, 2011).

The Chinese government has set ambitious targets, based on the policies mentioned previously, of installing 100GWp of PV projects by 2050 (Dincer, 2011). In fact, China's cumulative solar PV (photovoltaic) capacity reached 131.1 gigawatts at the end of 2017 (Statista.com).

2.3 Japan

2.3.1 Key Policy Drivers

The Japanese government has set policies which greatly favour the use of PV technology. The government has consistently applied these policies and are targeting the investment in R&D on PV technology or on the issue of climate change. After the 1973 oil crisis, Japan introduced the Sunshine Project in 1974 in response. This was the countries first solar PV industry support programme. This scheme was introduced by Ministry of Economy, Trade and Industry (METI) (Lewis, 2009). The main aim of this scheme was to carry out research and development in clean energy technologies. At the outset of the scheme the majority of the focus, and budget, was on solar thermal technology (Kurokawa and Osamu, 2001). 1993 (Chowdhury et.al. 2014) saw the introduction of a new scheme, the New Sunshine Project, with a particular focus on the PV technologies and its residential PV system monitoring programme. This scheme also saw rise to providing subsidies to consumers for offsetting the initial cost of residential PV systems. A 3kW PV system was installed in Japan in 1994 and was 50% subsidised by this programme. The total cost of this installation was £0.03 million (¥5 million). Due to the success of this type of incentivisation and subsidy, a new programme was introduced to support the development of large scale PV installations in 1997. The **Residential PV System Dissemination Programme** provided a means for consumers to sell their excess electricity back to the government through the grid. This was monitored by the introduction of a net monitoring system. To support this a significant amount of funding was provided to national R&D labs for more research on PV technology (Osamu, 2003).

Japan started reducing the available subsidies to an average low from £319.12 (¥60000) to £372.31 (¥70000) per household in 2005. Unfortunately 2006, the Japanese government removed subsidies at national level which resulted in a significant fall in solar PV technology related installations.

The government's estimated PV target of 2020 and 2030 is, however, 10 to 40 times greater than the current level. METI recognised, in 2008, that to achieve these targets, it was important for the government to reintroduce the residential PV system subsidies (Takase and Suzuki, 2011), which would consequently rank Japan as the largest installer of solar PV worldwide (Negishi and Lawson, 2008). In the same year, METI, the Ministry of Education, Culture, Sport, Science and Technology, Ministry of the Environment, The Ministry of Land, Infrastructure, Transport and Tourism mutually implemented an **Action Plan for Promoting the Introduction of Solar Power Generation**. Through this programme a 50% subsidy will be provided for the cost of installing solar power generation systems in public facilities including airports, highway service areas and within railway infrastructure (METI, 2008b). Local

government will also support the subsidizing of local PV projects by providing budget to support a range of other subsidies.

The Japanese prime minister introduced the country's Cool Earth Initiative (Cool Earth 50) (METI, 2008a) in 2007. The main aim is to see a reduction of greenhouse gases by 50% by 2050. This initiative includes the development of 21 of the latest technologies which includes solar cell technology. One of the key policies under this initiative is the development of low cost solar cells with a conversion efficiency of up to 40% and generate power at £0.04/kW (¥7/kW) compared to the current rate of £0.21/kW (¥40/kW) (METI, 2008b). In 2008 Japan introduced an **Action Plan for Achieving a Low Carbon Society**, to support the cool earth initiative, with the ultimate goal to make Japan a world leader in solar electricity generation, cutting the current price of solar electricity by 50% within 3 to 5 years and creating a significant amount of reduction in the countries carbon emission

2012 saw the introduction of a FiT scheme (Muhammad-Sukki et.al. 2014), which resulted more than 20.9GW of PV installation projects, all of which were approved by the end of May 2013 (GreenPeace International, 2011).

The Japanese government has set an ambitious goal of installing 53GW of PV projects by 2030 (Kumar and Sahu, 2015) as a result of the policies, R&D activities and funding as outlined in the next section.

2.3.2 Photo Voltaic Research & Development activities and associated funding

Japan has a number of on-going R&D programmes including the New Energy and Industrial Technology Development Organization (NEDO) funding programmes such as **Innovative Solar Cells** and **High Performance PV Generation Systems for the Future**. Also, Development of Organic Photovoltaics supporting a move toward a Low-Carbon Society and low carbon economy. The Innovative Solar Cells and High Performance PV Generation Systems for the Future programmes have a key focus on crystalline silicon, thin-film silicon, thin-film CIGS, and organic thin-film solar cells. Within the Innovative Solar Cells programme there are 5 research projects to be completed by the end of 2015 (*Japan International Corporation Agency*, 2011). The University of Tokyo is running a programme focusing specifically on organic PV technology, under the Development of Organic Photovoltaics towards a Low-Carbon Society.

Other Japanese projects include the **Photoenergy Conversion Systems and Materials for the Next Generation Solar Cells (2009)** and **Creative Research for Clean Energy Generation Using Solar Energy (2011)**, both are funded by the Ministry of Education, Culture, Sports, Science and Technology and Japan Science and Technology Agency (JST).

In 2013 NEDO initiated a project of demonstration in the diversification of PV application programmes in order to extend installation areas for PV systems i.e. agricultural lands, tilted slopes and water surfaces. METI introduced a practice demonstration project on the development of power output forecasting technology for PV power generation programmes, in order to enhance the country's power system infrastructure and to promote and increase the use of PV power generation. In October 2013 the National Institute of Advanced Industrial Science and Technology (AIST) founded a new research facility, Fukushima Renewable Energy Institute (2014), for research & development in photovoltaic technologies (Fukushima Renewable Energy Institute, 2014).

2.4 USA

2.4.1 Key Policy Drivers

The USA differs from most other countries in that the regulation of investment and growth in renewable energy happens at state and/or regional level and not at national level. This makes it more difficult to analyse the impact of specific state policy affecting the growth of solar PV. There are a few major policy drivers that are worth noting in terms of impact.

The **Renewable Portfolio Standards (RPS)** is one of the most common policies in place to actively encourage the utilisation renewable energies (Wiser, 2010). Washington D.C adopted this policy, with another 29 states, at the end of 2011 to help stimulate the renewable energy sector in the USA. It covers the whole spectrum of renewable energy technology (including PV), however its uptake and implementation varies state by state.

Renewable Energy Certificates (REC) are made available across all states in the USA and it is mandatory for utilities companies to hold a renewable energy certificate, which is the equivalent of 1MWh of energy created via renewables. The REC can be compared to a European policy such as a **Tradable Green Certificate**, which can be produced or purchased by energy providers by paying an **Alternative Compliance Payment (ACP)** however the price of each ACP varies region by region. There is a provision within the RPS, known as Set Aside or Carve Out, where utility companies have the opportunity to take into account a certain percentage of PV electricity generation, depending on their sales. For example, Ohio's RPS has a 2025 target of 12.5% renewable energy production out of which 0.5% is from solar, as per its solar set-aside terms (US Energy Information Administration, 2015).

Solar Renewable Energy Credit (SREC) has been implemented in nine out of the fifty states in North America. An SREC can be generated for every MWh of solar energy produced in a given energy year. There is no consideration given to the usage of the solar PV electricity,

either it is consumed by residential/owner themselves or sold back to the government through the grid. It is good practice for utilities companies to build on current solar production or they can purchase SRECs from private solar PV energy producers or pay the Solar Alternative Compliance Payments (SACP). To generate SREC, installed PV systems must be approved by the state authorities on the basis of safety and technical requirements (DSIRE, 2015). SREC registration is a simple, straightforward process that takes around 2 months (PJM, 2011), roughly ten times shorter compared to other Green Credit Market processes in the USA (Dusonchet and Telaretti, 2010). The tracking of SRECs generated is also fairly straightforward; the solar PV system owner must set up an approved tracking system, which monitors the generated kWh and creates an SREC for each MWh produced (Burns and Kang, 2012).

Tax Credit policy is a policy allotted by the federal government meaning it applies to all 50 states in the USA and is known as the Residential Renewable Energy Tax Credit and is a non-refundable personal tax credit. However, it can only be to residential renewable energy systems. It was established in 2006 and was set to expire in 2011 but due to an extension in its use it was extended to the end of 2016 (Verbruggen, 2004). Under this policy, a taxpayer can claim a credit of up to 30% of qualified expenditures for a PV system that serves a dwelling unit that is owned, and used as a residence, by the taxpayer (*Tax Credits, Rebates & Savings*, 2015).

Net Metering is one of the most widespread mechanisms for supporting PV systems in the USA (Darghouth, 2011). This policy specifies that every person generating electricity through a PV system should have a specified meter which records the amount of electricity generated by the owner of the PV plant and the electricity consumed from the government grid. In addition, if there is an excess amount of electricity generated by the PV plant, termed as Net Excess Generation (NEX), then this can be returned to government grid. This net total and included adjustment of inflow and outflow of electricity is monitored by these meters. The payment of the NEX will be settled at the end of each year, however due to the way the states within the USA are run each state has different price/rate of electricity, so it is quite difficult to glean a generalised summary (DSIRE, 2015; SEIA, 2015). 99% of all USA PV installations were net metered in 2012 (Brown, 2013).

Cash Rebates is a form of financial incentive, where the scheme helps during the initial installation a PV system. Under this policy every installer of PV plant will be rewarded with a dollar per watt installed. According to Wisser et al., (2010) and Barbose et al., (2011), this is a useful scheme, as it reduces the installation cost and outlay of PV projects.

2.4.2 Photo Voltaic Research & Development activities and associated funding

In the US Department of Energy (DOE) is accelerating its PV research under a programme known as the Solar Energy Technologies Programme (SETP). SETP funded research includes sub-programmes on: applying scientific research in solar PV to improve its efficiency, progress on new concepts of innovating new materials and manufacturing processes, R&D on BOS, demonstrate the increase in the installation of rooftop PV technology to name a few. In 2011, the SunShot initiative was introduced and supported by the DOE, with an aim to lower the cost of solar technologies. Their goal is to reduce the cost of solar electricity by up to £0.04/kWh (\$0.06/kWh). In order to achieve this reduction the DOE is receiving help and support from all sectors such as: education, private industry and national laboratories, which in turn will lead to increase the share of electricity, generated by solar PV, up to 18% by 2030. According to a 2014 SunShot Initiative Portfolio Book (Sunshot Initiative, 2014), the projects in the portfolio currently represent nearly £131.34 million (\$200 million) of investment, in which 66% is invested by National Laboratories, 30% by participating academic institutions and 4% by private industries.

There are other funding sources and programmes which provide loans and mortgages for solar PV such as: Energy Efficient Mortgage (2015), FHA PowerSaver (2015), High Energy Cost Grants (2015), Multi-Family Housing Loans and Grants (2015), Rural Energy for America Programme (2015). All of these funding sources and programmes are supported by Department of Housing & Urban Development and the Department of Agriculture (2015).

2.5 Germany

2.5.1 Policy Drivers

Germany hosts more than 80% of all solar PV installations in the whole of EU (comprising of 27 countries). The **Electricity Feed-in Act** (Stromeinspeisegesetz 1991-1999/2000) was the first policy to provide incentives for PV electricity generation. The first PV-specific policy scheme to provide low interest loans for PV installation was the "1000 Solar Roofs Initiative", which was implemented between 1991 and 1995 and was followed up by the "100,000 Solar Roofs Initiative" and funded by the German development bank Kreditanstalt fuer Wiederaufbau Bank (KfW). A FiT scheme for solar installations was established in 2000 (Renewable Energy Sources Act, Erneuerbare-Energien-Gesetz (EEG)) and has been amended several times since.

EEG have played a major role in the expansion of renewable energy in the electricity network of Germany. Since 2012 the FiT is has been adjusted on monthly basis and from July 2013 the residential tariff was set to £0.11/kWh (€0.151/kWh). Furthermore, from November 2013

under FiT scheme, PV installations over 1 MW receive £0.07/kWh (€0.0974/kWh) and systems under 10kW receive £0.10/kWh (€0.1407/kWh). Due to favourable policies for solar in Germany there are 3500 PV companies, of which 50 are manufacturing PV cells, modules and other components, utilised within solar PV technologies (Jager-Waldau, 2014b).

Other projects such as Waschen mit der sonne (doing laundry with the sun), is helping to increase people participation and reduce peak demand during morning and evening hours (Lichner 2010). Under this scheme, customers will receive a phone call between 10am to 1pm, stating that their PV systems are generating a substantial amount and whoever responds to the call will be rewarded with £0.35/reply.

2.5.2 Photo Voltaic Research & Development activities and associated funding

The German Federal Government, the Federal Ministry for the Environment, Nature Conservation, and Nuclear Safety (BMU) hold the responsibility of developing and encouraging the utilisation and use of renewable energy (including solar PV). R&D in different aspects of PV is supported by the BMU as well as the Federal Ministry of Education and Research (BMBF). In 2008, BMBF granted 8 PV projects for R&D totalling £13.63 million (€19.5 million). This budget was increased to as total of £37.90 million (€39.9 million) in 2009 and was shared between 130 projects (Grau, 2011). Alongside these R&D projects, the public PV R&D budgets, industrial R&D investments totalled £113.96 million (€163 million Euro) in 2008. In 2010, BMU and BMBF started a joint programme to promote Innovative Alliance PV for the reduction in PV production costs. Together they have supported this programme with £69.91 million (€100 million) of investment. Due to its success, to date, a new programme FuE for Photovoltaic was created in 2013, with £34.96 million (€50 million) funding (*Innovationsallianz Photovoltaik*, 2015). This incetivisation has had a positive impact in reaching the 80% share of all solar PV installations in Europe.

In 2011, a new programme, the countries 6th, was introduced. The Research for an environmentally friendly, reliable and economically feasible energy supply, under which the current R&D is carried out. This programme covers almost all sectors, from the basics of PV through to its application and is carried out with support from BMU and BMBF departments (*Research for an environmentally sound, reliable and affordable energy supply.*, 2011). That being said, both departments are working on separate concepts of PV, BMU has prioritised the use of silicon technology, thin-film technologies, systems engineering, alternative solar cell concepts and new research approaches (such as concentrator PV), as well as general issues such as building-integrated photovoltaics and recycling while BMBF focuses its R&D on organic solar cells and thin-film solar cells (including nanotechnology) (*Research for an environmentally sound, reliable and affordable energy supply.*, 2011).

In 2013 BMU funded 242 projects costing £34.05 million (€48.7 million) (Energieforschung, 2013). According to EuPD the research PV industry was supported by £245 million (€300million Euro) for R&D during 2010. Furthermore, the German patent and Trademark office registered 290 German patents in PV technology during the same year (Grigoleit and Lenkeit, 2011).

Germany offers funding options, alongside this R&D, as investment incentives to manufacturing plants. These incentives and support can be categorised into three major groups. The first group, grant/cash incentives (including the Joint Task program and the Investment Allowance program). These incentives reimburse direct investment costs during the initial investment phase of projects (before operations have started). The second group is known as reduced interest loans (at national and state level). These loans are provided by publically owned banks, to investors in Germany. Most often these loans have a lower interest rate compared to the actual market interest rate and provide an attractive grace period. The third group is known as public guarantees (at state and combined state/federal level). In order to facilitate the financing of investment projects in young and innovative businesses, through the capital market, companies lacking security guarantees may apply for public guarantees (Naam, 2011).

As a result of these policies, R&D activities and funding, Germany has set a target of reaching 51GW PV generation by 2020. Overall, Germany's long term policies and funding have had significant impact on reducing the setup costs that are associated with solar installation, such as permitting, inspection, interconnection, financing (Naam, 2011).

2.6 U.K

2.6.1 Policy Drivers

It should be noted that the UK government has been trying, for a long time, to make valuable changes in policy and increase the awareness of PV in order to attract more public interest in solar technology. The first programme, SCOLAR, was introduced in 1998, as a coherent programme by British commercial companies and academicians to spread awareness and understanding of PV nationwide, with an integral research extended to the applications of PV. This programme was valued as £2.5 million which included £1 million from the Government's Foresight initiative and the remainder from participating schools and colleges (Wolfe and Conibeer, 1998). Under this programme 100 small PV projects were initiated and installed for schools and colleges each sizing between 2-3kW. These projects were possible due to the main policies in place in the UK at the time. In 2002, the Renewable Obligation (RO) came

into effect in England, Wales and Scotland, followed by Northern Ireland in 2005. Its main aim is to place an obligation on the UK electricity suppliers to source an increasing proportion of the electricity, which they supply, is from renewable energy sources. ROCs is a green certificate issued to operators of accredited renewable generating stations for the eligible renewable electricity which they generate. Operators can trade ROCs with other parties, ROCs are ultimately used by suppliers to demonstrate that they have met their obligation. Where suppliers do not present a sufficient number of ROCs to meet their obligation, they must pay an equivalent amount into a buy-out fund. However, an amendment (referred to as the RO Closure Order 2015) closes the RO and the Renewable Obligation (Scotland) (ROS) schemes for large-scale solar PV systems on the 1st April 2015. The report by Office of Gas and Electricity Markets (Ofgem) (Chowdhury et.al. 2014) explains the details of this closure scheme.

In October 2012 UK government launched a new policy called the "Green Deal" which was operational at the start of 2013. The purpose of the Green Deal is to allow householders to apply for loans for energy efficiency and renewable energy technologies (including solar PV) supporting them with the upfront costs. This money is paid back through instalments via their energy bills. The repayments are arranged in such a way that, the money householders are due to pay is about equal to the savings they are making as a result of the installation (Nicholson J, 2015). This scheme can be merged with FiT to increase the net savings. For example, a typical 3.5kW domestic solar PV system installation under FiTs (over the whole 20 year duration) will generate a net saving of £5835 to the homeowner (DECC., 2015). The Green Deal was thought to 'revolutionize the energy efficiency of British properties' (DECC, 2015), but was pulled in July 2015 due to low uptake (Fawcett and Killip, 2014). Currently the deployment of renewables schemes in the UK (under the FiT scheme) has exceeded all expectations, to the point where spending has breached the limits of the government's Levy Control Framework, which itself sets limits on the amount of money that can be added to consumer bills to support low carbon electricity generation. The DECC proposed (at the end of August 2015) a range of reductions, including an 87% cut to the FiT provided for electricity generated by solar rooftop panels from 12.4p to 1.6p from January 2016 (Energy Institute, 2015).

The current PV market, in the UK, is driven by two policies: FiT's and Renewable Obligation Certificates (ROCs). The FiT scheme was introduced in 2010 (Sweetnam et.al. 2013), which led to installation of 1.8GW of solar PV capability by the end of 2012. This significant rise in installation was also due to the fast track review of large-scale solar projects by Department of Energy and Climate Change (DECC) (Smit et.al. 2011; *Feed-in Tariff*, 2015) which expects

that UK will install up to 20GW worth of installations by 2020 (Department of Energy and Climate Change, 2011). In order to be eligible for the FiT scheme, PV installations must undertake an accreditation process to determine with Fit scheme each installation is eligible under. PV installations below 50kW are eligible under (Microgeneration Certification Scheme) MCS-FiT accreditation process (2015) and PV installations greater than 50kW are eligible under the ROO-FiT process (2015). OFGEM website publishes the rates that PV system owners receive under the FiT scheme (2015).

2.6.2 PV Research & Development activities and associated funding

Between the years 2000 to 2006, the PV Field Trials Programme was introduced with associated funding of £9.4million and as a result 1.5MW of PV plants were installed under this programme. During the same time period, the Major Photovoltaic's Demonstration Programme was also introduced with £31 million supporting 8MW projects. From 2006 through 2010, the Low Carbon Building Programme was introduced with £13.4 million support for 4428 PV projects.

Currently, R&D funding is provided by the Engineering and Physical Sciences Research Council (EPSRC). The UK Energy Research Centre (*UKERC*, 2015) Research Atlas provides details of publicly funded, past and ongoing research activities within in the solar sector. Research is, in the main, carried out at academic institutions and by a few companies (increasingly with those who have a collaborative approach with academic institutions). Overall in 2008, EPSRC provided £8.6 million of funding for 82 PV and PV related research programmes. Of this total funding, £6.3 million was invested in new PV materials for the 21st Century (PV-21) programme, which, was in collaboration with eight universities and nine industrial partners aiming to make solar energy more economically reasonable. Prior to this activity, Woking Borough Council invested in PV projects and had installed 10% of the UK's solar PV by 2004 (Allen SR, 2008) and had also proved that a typical solar PV system can provide 51% of electricity demand (DTI, 2006).

In 2012, the Research Council UK (RCUK) research portfolio was around £40 million for solar PV which encourages and supports the UK PV manufacturing industry through the innovation of both existing products and new products. In 2013, the UK National Solar Centre (NSC) was launched in collaboration with Building Research Establishment (BRE) jointly aiming to grow the PV industry in the UK. During Intersolar (2013) the U.K government announced that it will provide £7.6 billion per year by 2020 of targeted subsidy to support the deployment of renewable energy technologies (including PV) in Britain (Department of Energy and Climate Change, 2013).

2.7 PV electricity production in leading countries

PV technology has seen rapid installation growth and its contribution to electricity demand is significantly rising. Around 415GW of PV is installed by 2017 across the world, which is at least 10 times higher than in 2008. It has been calculated that, globally, at least 443TWh of PV electricity was generated in the 2017 (Statista.com).

It is relatively easy to measure the electricity production of an individual PV plant, but much more complicated to accurately estimate it for an entire country. Unfortunately, it is also difficult to compare the installed PV systems to date with the production of electricity. For example, for a PV system installed in December it will only contribute a small fraction of its regular annual generation, it should also be noted variations in the weather conditions will have an impact the reliability of a long term average. There are several other issues that need to be accounted for, such as, the optimum orientation or partial shading for Building Integrated PV Systems (BIPV) which can also impact the output of PV systems. For these reasons, the PV electricity production calculation is theoretical and is based on cumulative PV capacity for specific countries. Figure 11 (Statista, 2017) shows the largest solar photovoltaic power plants, based on optimum siting, panel orientation and average weather conditions (statista 2017). India has installed the largest PV system called Kurnool Mega Solar Park producing 1000MW, as shown in figure 11.

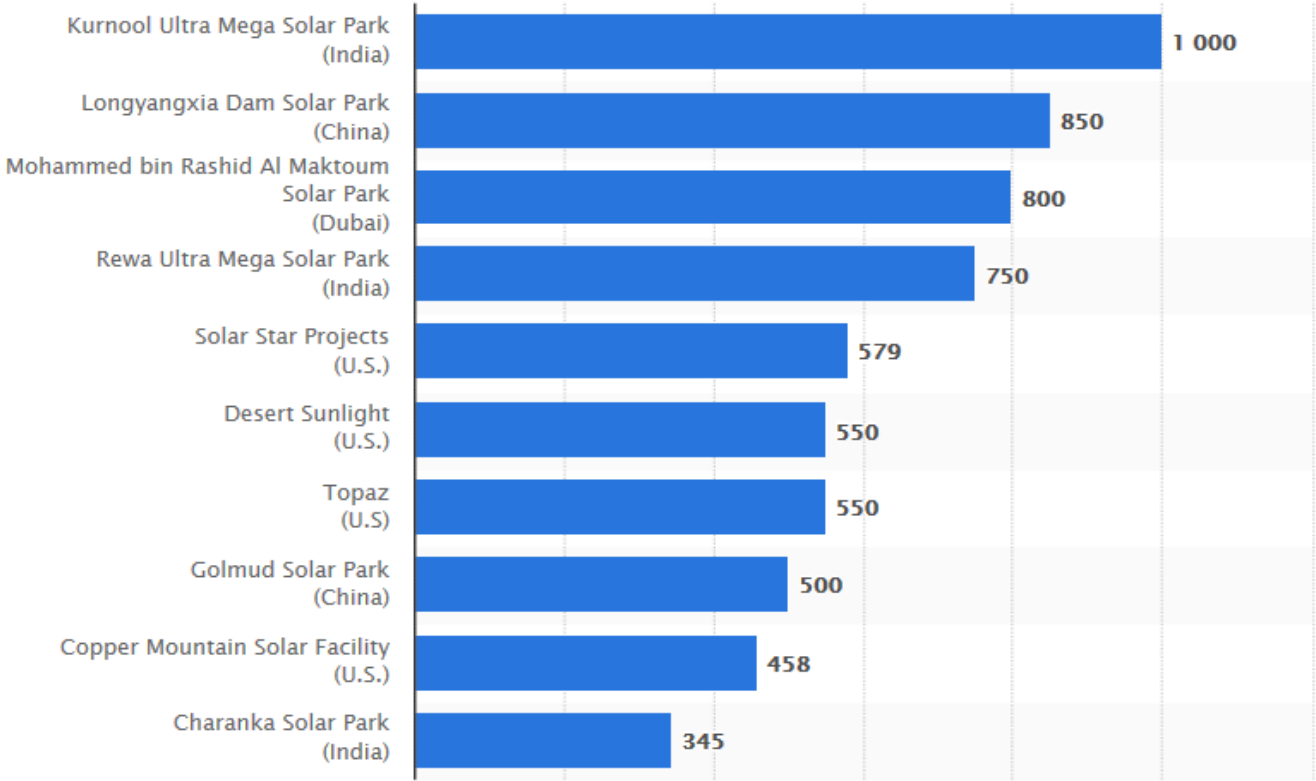


Figure 11 Largest solar photovoltaic power plants worldwide by capacity (MW) (Statista.com)

There are nineteen other countries, alongside the 5 leading countries, around the world whose PV electricity contribution to total electricity demand has surpassed 1% (International Energy Agency, 2015). It should be noted that 5% of European electricity demand is fulfilled through PV generation and Italy is contributing 7.92% in 2015. This is more than any of the major leading countries mentioned previously. That being said China and USA are still leading the market in terms of yearly installations as well as cumulative installed capacity but they are behind in terms of generation of PV electricity compared to the countries actual demand.

2.8 PV cost analysis

For several decades the price of production of solar modules has been decreasing. This decrease in price has largely been due to the following factors (a) innovations in material technology and design (b) an increase in the overall amount of production (c) improvements in the efficiency by innovative design (d) increasing lifespan of PV systems (e) favourable policies for solar technology (GreenPeace International, 2011). From figure 12 (GreenPeace International, 2011; Naam, 2011; *Cost of solar panels-10 charts tell you everything*, 2013, *German Solar Industry Association*, 2015, *Growth of Photovoltaics*, 2015; Department of Energy and Climate Change, 2013; Feldman et.al. 2014; SolarBuzz, 2015), it can be observed that the price of PV cells has drastically reduced from £15.18/W (\$23/W) in 1980 to £0.79/W (\$1.2/W) in 2014, and in June 2015 it has reached a new low of £0.20/W (\$0.30/W), which is a decrease of more than 75 times, over a period of thirty five years.

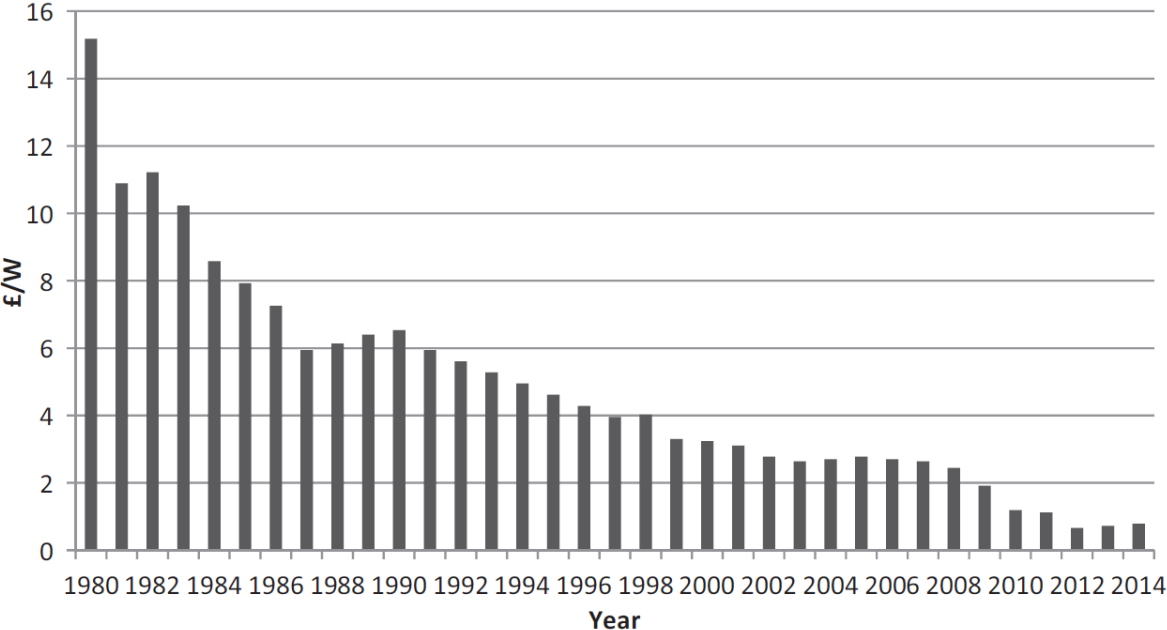


Figure 12 - Solar PV cells price trend (Cost of Solar, 2013; Feldman et al., 2014; German Solar Industry Association, 2015; Growth of photovoltaics, 2015; GreenPeace International, 2011; Naam, 2011; SolarBuzz, 2015; UK Solar Photovoltaic Roadmap, 2013)

A complete PV system combines PV modules with a set of additional application dependent system components like the mounting frame structure, inverters, charge controllers, electrical components, to name a few, which are known as Balance of System (BOS) to form a complete PV system. Similarly, like PV modules, BOS components are also decreasing and this trend can be seen from an example within the US market. There are several reasons to use the USA as an example including, government investment, market diversity, climate diversity and high labour costs. Figure 13 shows the BOS system cost from 2010 to 2013 for 10MW fixed tilt blended c-Si projects. It shows that BOS costs have reduced by almost 20 times since 1980 and reduced to approximately £0.18/W (\$0.29/W) between 2010 and 2013.

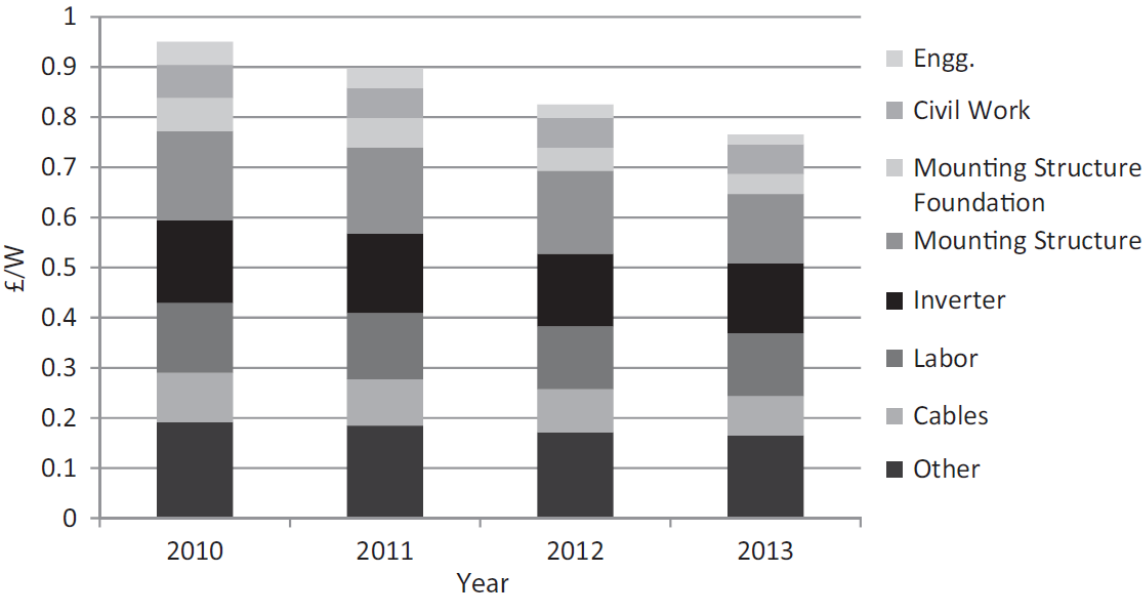


Figure 13 - BOS price trend for 10MW fixed-tilt blended c-Si projects in USA (Aboudi, 2011; Media, 2013).

According to a GreenTech Media (GTM) Research report Solar PV BOS Market: Technologies, Cost and leading companies, 2013 - 2016, in 2011, the ratio of cost of BOS to module was 68:32 and by 2012, the ratio had reached 50:50 (Greentech Solar, 2012), which clearly shows that not only the price of modules is decreasing but BOS costs are also decreasing in line with modules. This significant fall in both, module price and BOS price has gained the attention of investors and as a result, there are several new projects being built all over the world.

To get the broad overview of installed project costs worldwide, Table 3 lists 98 installed PV projects and describes the total building cost and cost per watt (£/W) of all PV projects. The table shows China is the cheapest country in terms of total installation costs of PV project, while South Africa is the most expensive country for total installation costs of a PV project. More importantly it shows there is a significant difference of £3.97/W between the minimum and maximum cost of projects. In considering the overall size of a project, the table shows that for a 5MW installed PV plant in Panama is the costliest when compared to the likes of Bulgaria, China and India. Similarly, for 10, 20 and 30 MW plants, South Africa is the most expensive when compared to China, the Dominican Republic, India and Thailand. However, for 50MW projects Chile is the most expensive when compared to the likes of the Dominican Republic, Ecuador, India, Indonesia and even (the notably more costly) South Africa. This differential can be attributed to many factors such as the cost of modules, BOS and labour costs which vary from country to country. Please note that this table is based on the availability of data and not specifically on any one country.

Table 3 Size and cost of PV projects (D. C, 2011; I, 2011; S. C, 2011; T, 2011; Tech, 2014; Lieberose Photovoltaic Park, 2015; Lopburi Solar Farm, 2015; Bank, 2015; Energy, 2015; Ranch, 2015; Station, 2015) (over)

Project Name	Location	Size, MW	Total Cost, Million £	£/W
Helios Sredetz Solar Plant	Bulgaria	1.8	4.69	2.6
Helios Zelena Svetlina Solar Plant	Bulgaria	2	5.15	2.57
Helios Montana Solar Plant	Bulgaria	3	7.72	2.57
CEZ Oreshets Solar Plant	Bulgaria	5	8.58	1.72
Helios Yerusolimovo Solar Plant	Bulgaria	5	12.87	2.57
LS/CHINT Yambol Solar Plant	Bulgaria	14.5	24.68	1.7
Devnya Solar Plant Phase 1	Bulgaria	15	43.89	2.93
Moncada Solar Plant	Bulgaria	16	24.75	1.55
Apriltsi-Sbor Solar Plant	Bulgaria	60	156.82	2.61
MEMC Karadzhalovo Solar Plant	Bulgaria	60.4	155.63	2.58
Sky Solar PV	Chile	18	49.5	2.75
Acciona Solar PV	Chile	25	54.12	2.16
Element Power Altos de Pica Solar Plant	Chile	30	63.36	2.11
Element Power de Huasco Solar Plant	Chile	30	63.36	2.11
Element Power Lagunas Solar Plant	Chile	30	63.36	2.11
Element Power Pica Solar Plant	Chile	30	63.36	2.11
Atacama Solar Plant Phase 1	Chile	50	102.04	2.04
Mainstream - El Aguila Solar PV	Chile	70	118.8	1.7
Igenostrum - Laberinto Oeste PV	Chile	70	128.7	1.84
Igenostrum - Laberinto Este PV	Chile	77	141.9	1.84
Domeyko Este PV - Ingenostrum	Chile	112	205.92	1.84
Ingenostrum - Domeyko Solar PV	Chile	160	297	1.86
Mainstream - Diego de Almagro PV	Chile	162	277.2	1.71
Fotones de Chile - Encuentro Solar	Chile	180	264	1.47
Fotones de Chile Crucero Solar PV	Chile	180	290.4	1.61
AES Loa Andes Solar PV	Chile	220	343.2	1.56
Zhenjiang	China	3.5	7.26	2.07
Siyang	China	4	9.57	2.39
Gansu Jinchang Technology PV Plant	China	5	11.09	2.22
Dongying	China	7	16.5	2.36
Shizuishan, Ningxia Hui	China	20	29.7	1.49
Yangjiang Hanergy Roof PV Plant	China	27	8.55	0.32
Yili Zhenfa PV Plant Phase 1	China	30	41.84	1.39
Jiangsu nantong LDK-Haidong PV Plant	China	30	49.42	1.65
Yichun City Hongxing Solar Power Project Phase II	China	250	660	2.64
Electronica JRC Solar PV	Dominican Republic	30	79.2	2.64
Isofoton solar PV	Dominican Republic	50	99	1.98
Isofoton - Calderon Solar PV	Ecuador	50	66	1.32
Lieberose Photovoltaic Park	Germany	70.8	157.08	2.22
Nzema Solar PV	Ghana	155	341.22	2.2
Azure Rooftop Solar Project	India	2.5	3.3	1.32
Sun Edison Rooftop Solar Project	India	2.5	3.3	1.32
Sunborne Energy Rajasthan Solar Private Limited	India	5	6.53	1.31
Moser Baer (Porbandar) Solar Project	India	15	22.97	1.53
Essel MP Energy Limited	India	20	25.81	1.29
SEI Solar Power Joghpur Solar Project	India	20	33.4	1.67

GMR Charanka Solar Plant	India	25	37.03	1.48
SLREPL Banskantha Solar Project	India	25	47.98	1.92
Tata Mithapur Solar Plant	India	25	51.61	2.06
Gunthawada	India	30	62.7	2.09
Welspun Energy Jodhpur Solar Project	India	50	59.4	1.19
SGL - Mitabu Solar Plant Phase 1	Indonesia	50	68.64	1.37
Puerto Rico Convention Centre	Isla Grande, Panama	5	13.2	2.64
Berjaya Berhad Solar Plant	Malaysia	100	217.8	2.18
Sonora Solar PV	Mexico	39	52.8	1.35
Wah Sanjwal Solar Plant	Pakistan	1	2.51	2.51
Conduit Panamericana/Tacna Solar Plant	Peru	40	138.6	3.47
EDPR Hehendinti, Olt & Dolj Solar Plants	Romania	39	100.32	2.57
Samsung Giurgiu Solar Plant	Romania	45	104.87	2.33
Gascom Kursumlija Solar Plant	Serbia	2	4.29	2.15
Inspired RustMo Solar Plant	South Africa	7	16.5	2.36
Biothem - Aries Solar PV	South Africa	10	22.4	2.24
Konkoonsies Solar PV	South Africa	10	22.4	2.24
Mulilo De Aar Solar plant	South Africa	10	23.1	2.31
Old Mutual - Greefspan Solar PV	South Africa	10	31.68	3.17
Mulilo Prieska Solar Plant	South Africa	20	46.2	2.31
Old Mutual - Herbert Solar PV	South Africa	20	63.36	3.17
MEMC Soutpan Solar Plant	South Africa	28	118.8	4.24
MEMC Wiktop Solar Plant	South Africa	30	128.7	4.29
Mainstream Droogfontein Solar Plant	South Africa	50	99	1.98
Mainstream De Aar Solar Plant	South Africa	50	99	1.98
Sctec Kalkbult Solar Plant	South Africa	72.5	170.94	2.36
Solar Capital De Aar Solar Plant	South Africa	75	170.94	2.28
SolarReserve Letsatsi Solar Plant	South Africa	75	18438	2.46
SolarReserve Lesedi Solar Plant	South Africa	75	194.04	2.59
Kathu Solar Plant	South Africa	81	260.04	3.21
Kaohsiung	Taiwan	5.92	13.79	2.33
EGCO SPP5 Solar Plant	Thailand	8	18.35	2.29
IFEC Bo Phloy Solar Plants	Thailand	10	21.12	2.11
Solarta Nakhon Pathom Solar Plant	Thailand	12.4	12.28	0.99
SPCG Nakhon Tratchasima & Loaei Solar Plants	Thailand	18	36.43	2.02
GPS Nakhon Sawan & Chai Nat Solar Plants	Thailand	19.5	36.04	1.85
SPCG Khon Kaen	Thailand	24	17.23	0.72
Sumikin Rojana Solar Plant	Thailand	24	60.75	2.53
Korat Solar Plants	Thailand	36	25.87	0.72
EGCO SunWat Solar Plants	Thailand	36	34.78	0.97
Yanhee Nakorn Pathom & Suphanburi Solar Plants	Thailand	57	151.34	2.66
Lopburi Soar Farm	Thailand	84	178.86	2.13
Renegy Porogi Solar Plant	Ukraine	4.5	4.95	1.1
Acytiv Mityaev Solar Plant	Ukraine	31.6	81.18	2.57
Active Starokozache Solar Plant	Ukraine	43	110.55	2.57
Activ Dunayskaya Solar Plant	Ukraine	43.1	110.88	2.57
Perovo Solar Power Station	Ukraine	10.5	255.42	2.42
Active Crimea Solar Plant	Ukraine	300	1193.81	3.98
Conergy's	United States	1.8	0.99	0.55
Gloucester Marine Terminal Rooftop Solar Array	United States	9	27.72	3.08
Copper Mountain Solar Facility	United States	150	93.06	0.62
California Valley Solar Ranch	United States	250	1056	4.22

2.9 Discussion and recommendations

It is important to review current materials in light of reducing costs as solar PV technology has enormous potential and benefits for society. Currently, several new materials are emerging on the PV market. Notwithstanding these new materials, efficiency improvement is still one of the key factors for the establishment of all PV technology in the market. Due to the availability of silicon, as a raw material, and its relatively simple manufacturing process, multi crystalline efficiency has reached 20.4%, at a maximum, and as a result it holds 80% et.al. 2011) of the PV market. However, to achieve PV as a major player in the power sector, efficiency of other types of materials need to increase with no compromise in the cost (Powalla and Bonnet, 2007). It is believed that under all scenarios, solar PV will continue to increase its share of the energy mix in Europe and around the world.

Table 4 (Fthenakis et.al. 1999; Razykov et.al. 2009; Razykov et.al. 2011) provides a brief comparison and comments between all type of material utilised along with their advantages, disadvantages, industrial manufacturing aspects and R&D areas. Table 7 shows that crystalline materials have the highest percentage of module efficiency (circa 20.4%) when compared to all other available POV materials. However, CIS/CIGS (categorised as thin film materials) and Hybrid cell materials (categorised as emergent technologies) have a commercially available module efficiency of 15% and 17.8% respectively. Then general advantages and disadvantages of each material are noted in the fourth and fifth column of the table. The R&D activity based around these materials, all five leading countries have their own individual programmes as noted in the Leading PV countries section. The sixth and seventh columns summarise the main areas of R&D of each material that researchers, from all countries, are working towards. In general, the overall aim of all of these programmes is to innovate with new PV materials, minimise production costs and increase the PV market share within electricity generation. This project aims to add to this by developing a clearer understanding of PV installation at high latitudes and what the unique factors are that impact on solar PV generation at 56° north, the detail of this is discussed in chapter 3.

Table 4 Comparison and comments on all PV materials and their development (Fthenakis et.al. 1999; Razykov et.al. 2009; Razykov et.al. 2011)

Material Type	Material sub type	Company Ref No. Income and max. commercial module efficiency (%)	Advantages	Disadvantages	Industry Manufacturing aspects	Research & development areas
Crystalline	Monocrystalline	US17	1. made from the purest form of silicon results in maximum efficiency	1. Most Expensive	Si consumption < 5 grams/Watt (g/W)	1. Productivity and cost optimisation in production
		20.4	2. Consumes less space	2. any Kind of shade, dust or moisture on the module would break the circuit unless supported by micro inverter		2. New silicon materials and processing
			3. Longest lifetime and performs better including in low light conditions			
			4. More heat tolerant and therefore performs better in higher ambient temperatures			
	Multi-crystalline	T10	1. Easy to Install and Maintain	1. made of impure silicon - less efficient		
		16.9	2. Wastes smaller amount of silicon and therefore more cost effective	2. Occupies a larger area		
Thin Film	Amorphous Silicon	US13	1. Lower Manufacturing costs	1. Lower efficiency than mono-crystalline solar cells/poly-crystalline solar cells	1. High rate deposition	1. improved deposition techniques
		13.8	2. Produce in variety of shapes and sizes	2. manufacturing processes are more complex	2. simplified production process	2. improved substrates and transparent conductive oxides
			3. Easy to create modules in varying voltages	3. expected lifetime is shorter than crystalline	3. management of toxic materials	3. improved cell structures
			4. Much less susceptible to breakage during transport and installation		4. recycling of modules	4. advanced materials and concepts
			5. Experience higher results at increased temperatures			
	CdTe/CdS	First solar	1. Ease of manufacturing a simple mix. Of molecules cadmium sulphide and cadmium telluride with different compositions	1. Lower efficiency levels: lower than the typical efficiencies of silicon solar cells		
		13.9	2. good match with sunlight: captures energy at shorter wavelengths than is possible with silicon materials	2. Tellurium is an extremely rare element		
			3. cadmium is abundant	3. Harmful to the environment: Cadmium is toxic		
	CIS/CIGS	US7	1. Consumes less energy while manufacturing than crystalline silicon technology	1. they are not as efficient as crystalline silicon solar cells. However, it is the most efficient of the thin film technologies		
		15	2. Much lower level of cadmium is used. Hence, less harmful to the environment than CdTe	2. Cost of manufacture is higher than crystalline silicon and CdTe		
			3. Better resistance to heat than silicon based solar modules			
	GaAs	N/A	1. High resistivity to heat and radiation	Expensive		
Emerging Technologies	Hybrid Cell	J2	1. Better resistant to low light and high temperature	1. Complex to Manufacture	1. Reducing cost of manufacture	1. Finding new compounds
		17.8			2. Making cost competitive 3. manufacturing complete modules rather than cells	2. Improving cell stability
	CNT	N/A	1. Can convert 75% of light to electricity	1. CNT is difficult to produce		
	DSSC	N/A Lab efficiency is 11%	1. Works in simple pn junction	1. TiO2 is expensive		
	Tandem/Multi-junction Cell	N/A Lab efficiency is 44.4%	1. High efficiency	1. Stacking of several compounds may increase price		

After analysing the policies of the five leading countries in ‘Leading PV countries Worldwide’ section (Dusonchet and Telaretti, 2015), it should be noted that the PV market still remains as a policy-driven market and the right decisions of creating smart and sustainable support schemes for PV, along with a valuable amount of funding for R&D activities, can influence the overall market. So far, FiTs are the most utilised and widespread support mechanism adopted all over the world, with a market share equal to approximately 60% in 2012 (IEA - PVPS, 2015). Direct subsidies and tax rebates are in second place, with a share of 20%, followed by self-

consumption (12%) (Dusonchet and Telaretti, 2015), RPS (4%) and net-metering (2%). However, the following section recommends a few changes that could be made in policies for deployment of PV systems. These recommendations could be applied globally, including in the five leading countries.

2.9.1 Policy recommendations – Change is required

To achieve high deployment of PV systems, a complete PV analysis from raw material, module technologies and BOS components, to product development, demonstration and deployment, need to make a number of changes. This section presents a set of key actions required to create an effective policy framework, which will directly or indirectly support solar PV to be successful in the market (International Energy Agency, 2015).

2.9.2 Incentive and framework

A. Financial incentive scheme and regulatory framework

To gain more interest, from investors, for high capital investment for PV installations and the PV module manufacturing industry, it is essential to have clear, long term, effective and predictive financial incentive schemes like FiT, portfolio standards and investment subsidies with a framework like access to grids. Governments should implement long term schemes and energy policies for PV deployment. Additionally a framework should continue to be developed for the actual market, where net metering systems are involved with an economic incentive scheme for PV electricity generators and users.

Providing only economic support is not enough, it would help if proper regulations for non-economic hurdles, which can hinder the effectiveness of policies and supportive schemes, were put in place. There are additional administrative problems such as planning delays, lack of coordination between authorities, long lead times for approval and connectivity with grids. There should be some timescales set out for each legal step and a procedure developed to allow for good coordination between all departments, authorities and government bodies.

The majority of PV incentive schemes are provided for grid connected systems with standalone systems hardly ever being supported, despite the fact that they can offer an efficient and effective solution (replacing diesel generators with PV systems) within many settings.

B. Regulatory framework for PV grid integration

The two main issues with a PV system is its connection to the grid and load management. This will require better ways of generating and distributing electricity which is simple, safe and reliable. One way of mitigating this issue is by improving transmission and management technologies, which include smart grids, metering and improved energy storage systems.

Therefore, for better grid integration, governments should initiate long term planning for system flexibility and grid management. For example, a region with a high irradiation can be connected with a greater number of grid connected PV installations with a better distribution management system and time dependent electricity tariffs.

2.9.3 Market transformation

A. Globally accepted standards and codes

With the aim to continue to introduce large scale PV deployment IEA has identified that, there should be internationally accepted set of standards, codes and certificates for PV products (International Energy Agency, 2015). This will support safety and quality but will also avoid the bureaucratic barriers. The set of standards, codes and certificates will need to include energy and performance of PV modules, quality assurance, reuse and recycling and for grid connections. Overall, an accepted standard agreed on a worldwide level will enhance the deployment of a wider variety of PV technologies.

B. Promote new investment and business models

There is a high initial outlay for PV system installation but results in a low operating cost. At present, most of the incentive schemes are for large scale grid connected projects. However, the high capital investment requirements are a major hurdle for residential and small commercial customers with an offgrid application. One option to resolve this issue is to support/partner with Energy Service Companies (ESCOs), which will own the system and provide the energy to end user for a periodic fee (like the partnership set up to support the Solar Meadow and Edinburgh College). The user will never be the owner of the system and are not responsible for any maintenance.

According to the IEA, PVPS (Photovoltaic Power System Programme), in 2008 there should be some sort of financing mechanism options like direct cash sales, credit sales or lease purchase arrangements(IEA - PVPS, 2015).

C. Skilled PV workforce

From research, to installation and on to maintenance, the PV market requires a highly skilled workforce. Highly skilled and suitably trained people are required for technology development, customer's confidence in quality of installation, reliability and cost reduction. To ensure this workforce is in place and available, there should a programme of delivery adopted by educational institutes and training providers to target specific professional groups such as government planners, architectures and home builders (US Department of Energy's Programme, 2015). Training of new and upskilling of current workers will be a big part of meeting the growing demand for PV installation and maintenance in the years to come. This

will require curriculum development in vocational areas to ensure the training is fit-for-purpose and at the level required to meet the demand. Development of apprenticeships and embedding within STEM curriculum and agenda's would go some way to supporting this, however, vocational curriculum at a skills level requires further development.

2.9.4 Development of technology and Research & Development

A. Assured long term R&D funding

The PV sector utilises several different materials and technologies, which required ongoing improvements. Appropriate long term high level funding assurance is required to develop and improve system technology and to introduce innovative concepts to the market as outlined in table 5. It should be noted that R&D Funding for PV has increased in recent years, however, it still needs to be increased further over the next few years to achieve the targets like BLUE MAP and to reduce carbon emissions by 50% by 2050 (IEA, 2010).

B. Develop smart grids and energy storage technologies

As described in section 2.9.2 B, the requirement for improved smart grid technology will significantly increase as the numbers of installed PV systems increases. Smart Grids provide a wide range functions for both the generator and the end user in the monitoring of bidirectional flow of electricity. This technology can keep a controlled monitor of conventional generation with variable PV electricity generation and storage. It can maintain the proper flow of electricity in times of peak demand, from the storage to the end user with an accurate calculation of generated electricity from both conventional sources and PV. It can also process real time meteorological data and an evaluation to predict the PV electricity generation. An advanced metering system, which is an integrated part of smart grids, can be deployed alongside the PV systems because it will provide a better operational characteristic consumption of grid electricity and generated PV electricity i.e. if the user has installed its own PV plant and learn from the usage of the end user making a more adaptive system that can meet individual user requirement and maximise delivery back to the grid and/or storage.

The IEA vision for PV electricity to hold 5% of global share of electricity after the year 2030. At that stage, there will be need to see major improvements made with storage technologies, which will provide flexibility to the system and minimise the impact of variable PV generation. Various R&D activities are ongoing on redox flow batteries, Compressed Air Energy Storage (CAES), electric double layer capacitors, flywheel systems, Li-ion batteries, and Superconducting Magnetic Energy Storage (SMES). We are yet to see a long term solution to PV energy storage but progress is being made. This is an area of study which requires more detailed analysis to provide robust commentary on R&D activities. Hopefully this research can add to the argument for further research to assist in the storage of generated energy.

2.9.5 International expansion and collaborations

A. Expansion of Research & Development internationally

It is necessary to have R&D activities, taking place in individual countries & across the globe and therefore, it is important that both short term and long term issues are addressed by each country and existing infrastructure facilities will be provided for the improvements made of PV materials and BOS components. One of the examples of such international collaborations is PVPS by IEA between 21 expert countries, of the 66 sunbelt countries, in the EPIA.

B. International aid

Since 1993, the World Bank (WB) and Global Environmental Facility (GEF) have been providing funds and support for renewable energy technologies to developing countries. From 1997 through to 2007, the WB and GEF supported China with \$40 million in the form of grants and loans (The World Bank, 2015). Due to that support, within the time period stated, China became one of the top manufacturers globally, for solar PV modules and BOS components. Another Similar example is of the German state owned bank KfW (see 'Driving Policies section'), who financed £160.80 million (€230 million) for renewable energy products in 2008. Growth is clearly linked to sustainable funding and therefore, this sort of funding facility for the PV sector should be increased.

2.10 Scotland's Key policy drivers

2.10.1 Kyoto Protocol

Over 10 years' worth of climate policy negotiations have produced the Kyoto Protocol, the first legally binding international agreement on climate protection with a focus on reducing greenhouse gas emissions, based on the consensus within the scientific community that climate change is indeed a real effect impacting heavily on the planet and that it is becoming an agreed position that human activity and man-made CO₂ emissions have contributed to the effect of global warming and indeed speeded the process up. This protocol came into force in 2005 and includes 192 parties from across the globe (United Nations, 1998).

2.10.2 Paris UN Climate Conference

At the Paris summit in December 2015, 196 countries met to sign a new climate change agreement. The Paris agreement seems set to achieve where the Kyoto agreement has fallen short, in that the USA did not ratify the Kyoto protocol and have since left the agreement with the introduction of a new president. Ambitious Global outcomes have been set that will have

a real impact on tackling climate change, by keeping the rise in global temperature below 2 degrees Celsius and by tackling global greenhouse gas emissions (United Nations, 2015).

Originally countries like the US and China were working to ensure an outcome is likely in 2015; and the years since the 2009 Copenhagen negotiations have seen some significant breakthroughs, however this has become more challenging since the USA left the agreement.

The 2009 negotiations were fraught and chaotic, with a last minute agreement emerging after frantic scenes on the conference floor. Yet international negotiations remain vital for countries to build on national approaches, providing reassurance that they are not acting alone, and making it easier for nations to work together towards a low carbon future (United Nations, 2015).

This is why the 2015 Paris summit was so important. To ensure meaningful action on climate change, the deal must contain the following elements:

- ambitious action before and after 2020
- a strong legal framework and clear rules
- a central role for equity
- a long term approach
- public finance for adaptation and the low carbon transition
- a framework for action on deforestation and land use
- clear links to the 2015 Sustainable Development Goals

The strong deal will make a significant difference to the ability of how individual countries plan to tackle climate change. It will provide a clear signal to business, to guide investment toward low carbon outcomes. It will reduce the competitiveness impacts of national policies, and create a simpler, more predictable framework for companies operating in different countries. For instance the French government's plan to ban petrol and diesel vehicles by 2040 (United Nations, 2015).

However, on June 1st 2017, the President of the USA withdrew the US from the Paris accord under the premise that it will undermine the US economy and put the USA at a permanent disadvantage compared with the other countries who have signed up (United Nations, 2015). A four year period, as set out in article 28 of the Paris Agreement, means the earliest withdrawal for the USA will be November 2020.

2.10.3 Climate Change (Scotland) act 2009

The Scottish Government's ambition to achieve carbon reduction and climate change targets are bound within its plan for an inclusive, improving sustainable low carbon economy. In

tackling the climate change issue it is assumed that general wellbeing, air quality and employment opportunities will all be improved. Therefore the Climate Change (Scotland) Act passed by the Scottish Parliament in 2009 has helped to elevate Scotland to a world leader in terms of its climate change agenda and ambitious target setting. In the years since, Scotland has made significant progress against the targets set out in the act. GHG emissions are reported annually by the government in order to monitor the achievement of targets being met.

The Scottish Government is playing a vital role in the Paris agreement by limiting global temperature rises and in turn allowing for opportunities and access to \$23 trillion worth of climate smart incentives and investments by 2030 (International Finance corporation – climate investment opportunities) (Scottish Government, 2017a). Within the Climate Change (Scotland) Act 2009 there are specific requirements for reporting and planning to be published by the Scottish Government in order to maintain the required scrutiny of progress being made. The final climate change plan, expected in February 2018, is a directive on how the Government plans to cut emissions by a further 66% by 2032. In order to maintain the positive momentum garnered by the government there is a proposed Climate Change Bill, set out by the government in Scotland that will introduce even more ambitious targets to ensure Scotland meets its obligations within the Paris Agreement around GHG emissions and set out the bold commitments required to decarbonise the Scottish economy with a progressive move towards a low carbon economy (Scottish Government, 2017a).

2.10.4 Low Carbon Scotland

Even though climate change is contested, it is seen as one of the greatest threats faced around the globe, real action must be taken to reduce its impact regardless. Moving towards a low carbon economy and in turn creating a low carbon society is regarded as a key investment strategy for the Scottish government as the country strives to minimise the impact of global climate change for future generations. It is also a real contribution being made to the global economy but also sets a standard for other countries looking to follow Scotland's lead. With world leading target on emissions reduction of 42% by 2020, Scotland's Climate Change (Scotland) Act is deemed one of the most ambitious climate change legislations in the world. With the rest of the UK set to reduce its emissions by 34% (Committee on Climate Change, 2017). in the same time period it is clear that the framework adopted by the Scottish Government and the annual reporting strategies set their legislation apart from other parts of the UK and indeed the wider world.

Despite positive progress being made by Scotland against its own targets for GHG emissions baseline revisions, stalling talks at both EU and international levels have led Scotland missing

its original targets set out in the Climate Change (Scotland) Act 2009 in both 2010 and 2011 (Scottish Government, 2017b). It is useful to reiterate that these negative results are based against a backdrop of poorly performing EU-15 members and fall in emissions of 25.7% in 2011 compared with a planned 23.9%. A planned over achievement of targets would help recover the position lost in 2010 and 2011 but with ambitious targets already set in years up to 2020, this will be a very challenging realisation especially with potential impacts after BREXIT.

Five themes have been identified by the Scottish Government that apply to all six of the sectors requiring improvements in a low carbon economy. The key themes are;

- Understanding external factors driving the pace of change
- Transition to the low carbon economy
- Funding and Financing opportunities
- Understanding and influencing behaviours
- Planning frameworks

These five themes outline potential moves in the future that highlight the need to be agile, adaptive and flexible, providing a sound economic decision making process to progress towards the planned targets and utilising natural resources in renewable energy sources whilst upskilling and reskilling the workforce, capitalising on funding methodologies and opportunities such as Green Deal, influencing the ten main household behaviours 'installing a more energy efficient energy system; keeping the heat in; better heating management; saving electricity; walking, cycling, using public transport and or car sharing; avoiding food waste; eating a healthy diet in season where we live; and reducing and reusing, in addition to the efforts we already make on recycling (Audit Scotland, 2011). And finally utilising the National Planning Frameworks down to local improvement plans at locality level. Only by making progress in all themes will the Scottish Government manage to realise the targets set out in the plan.

2.10.5 Scottish Government Climate Change Plan (2018)

In 2009, the Scottish Parliament passed the most ambitious climate change legislation anywhere in the world. In 2017 the government developed its third Report on the Policies and Proposals, the Climate Change Plan (CCP), which will take Scotland's climate agenda to 2032. Between 2009 and the present time much has changed and we are in a fundamentally different political, economic, social and technological landscape to that of 2009. The Climate Change (Scotland) Act 2009 outlines a set of criteria that can be used to monitor progress and ensures that the government reports effectively on progress made against targets. To date there have

been three such reports published which includes the draft CCP outlining the proposed emission reduction targets set for 2017-2032 (Scottish Government, 2018).

Internationally the UN Paris Agreement, as discussed earlier, is the first global legally binding agreement to limit greenhouse gas emissions. With the agreement coming into full force in 2016 it surprised the international community by coming significantly earlier than anticipated. The world is now seeing much more momentum towards environmental management in a low carbon future which, although it will not be a straightforward or smooth journey, appears to be a real force for change.

While the UN climate change processes provided much-needed confidence at the global level, many people have expressed fears about the potential impact of the UK's damaging Brexit vote on the climate change agenda. One major concern is a potential hampering of climate ambition.

There were a number of emission reduction pathways suggested, with the government selecting what they have deemed, the most beneficial to the people of Scotland.

Consideration has been given to emergent technologies, issues of delivery, costs and disruption (as discussed earlier in this chapter). Further efforts have been made to ensure future growth in the Scottish economy by taking steps to prevent industries moving away from Scotland due to the carbon reduction constraints, set by the government, are perceived to be too tight and challenging to meet in comparison to other economies, especially that of the rest of the UK, leading to the potential for 'carbon leakage'. Innovation within best business practice will also be heralded and the emerging economic opportunities being demonstrated will drive change within the low carbon economy (Scottish Government, 2018).

Alongside the Scottish Government's CCP a further strategy has been developed, the Scottish Government's first Energy Strategy. Designed to sit alongside and complement the CCP, the Energy Strategy sets out a number of key questions which lead to successful decarbonisation the supply of affordable, clean safe and reliable energy. The ambitions held within the Economic Strategy for Scotland have been used to set the Energy strategy and CCP, with an aim to boost productivity and secure competitive advantage, protect and preserve the environment and deliver a low carbon economy within Scotland (Scottish Government, 2018).

The CCP sets out outcomes in transport, heat, electricity generation, and energy efficiency along with increased natural carbon sinks and more efficient and profitable agricultural

practices. By the start of the 2030 it is expected the low carbon economy will have positively impacted on Scotland by drastically reducing the emissions from buildings, residential and industrial settings, by dramatically improving progress made against the decarbonisation of heat and improvements made in energy efficiency measures across the country. Electricity generation in Scotland is expected to be carbon neutral by 2025 through increasing the mix of energy generation technologies and their uptake, through the large scale introduction of carbon capture and storage gas utilisation from plant materials and biomass waste. The heating of the countries homes is set to move towards the use of electricity and the countries daily travel requirements are also expected to move towards electrically powered vehicles. Current EU and UK legislation determines the reduction required in industrial emissions and the Scottish Government's planning is in line with the expected fall in industrial emissions of 19% by 2032 through the use of emissions trading, fuel diversification and energy mix and savings related to energy efficiency and heat recovery. The Scottish Government's plans for reducing transport emissions by a third by 2023 also fit with their low carbon economy plans but actively promoting the wide-scale uptake of low carbon vehicles, improvements made to the efficiency of freight and improvements made to zoning for low carbon emission areas (Scottish Government, 2018). Recently Scottish & Southern Energy (SSE) announced that they will be the first green energy provider in 2018 by generating solely through wind.

There is ongoing good work in the reduction of the GHG emissions from waste, with the phase out process planned for landfilling of biodegradable waste ahead of the statutory ban coming into force from 2021 (Scottish Government, 2018). The UN's Sustainable Development Goals, set to facilitate the reduction of food waste by 50% by 2030 have been adopted by the Scottish Government who plan to employ a circular economy approach to deliver on the emission reduction targets set by 2050.

The planned move away from fossil fuel based technologies for energy generation, heating and transportation and progress made towards the circular economy will provide the Scottish business and research community with real opportunities for innovative practice along with the knowledge transfer of this leading practice. The co-development of policy with business leaders will allow for this transformation to take place in the face of difficult choices in terms of maximising commercial potential, export and employment opportunities on a cohesive scale. The Scottish Energy Efficiency Programme will support supply chain and market activity by supporting thousands (Scottish Government, 2017) of jobs within Scotland within the energy sector, providing a skilled workforce that can operate in country and indeed in the international arena for renewable heat services and related technologies. With the likelihood of millions

saved in fuel bills, having a positive impact on fuel poverty and recycling money back into local economies, this will drive community development and planning through the 31 community planning partnerships across Scotland. The CCP is a plan that, if it is to be realised in its entirety, must sit at the heart of the Scottish people. Climate conversations must be developed through local economy impact plans and community planning partnerships will need to play a role in supporting the development of inclusive local plans. If done right, improvements towards a low carbon economy based on the way travel, freight logistics, heating and energy utilisation within domestic and industrial settings, agricultural developments and the newly created jobs will sit at the heart of community and the people of Scotland. The Climate Challenge Fund is an example of how CPP's and their localities can raise awareness and become more involved in the climate debate. Change will inevitably only achieve the ambitions of the government should the public react and get behind the many initiatives discussed here. In this section I have shown the importance of this research if the ambitions of the Scottish Government, and the world, are to be met.

2.10.6 Political Background

In this section I will provide an overview of the current Scottish position against UK policy. This will set out the direction of travel for Scotland, as a country, in combatting the effects of global climate change and highlight the importance of understanding local impacts on renewable installation decisions.

Scottish Position on UK policy

Scottish Renewables is the representative body for the renewable energy industry in Scotland, providing a voice for more than 320 member organisations working across the full range of technologies delivering a low-carbon energy system integrating renewable electricity, heat and transport. Scottish Renewables has been created to ensure Scotland harnesses the full economic, social and environmental potential of all forms of renewable energy in order to provide the country with secure, low-carbon supplies of energy at the lowest possible cost.

District Heating Projects

More than half the energy consumption in Scotland is in the form of heat, therefore the decarbonisation of this sector will have a big impact on the reduction plans in Scotland. There is recognised support for the Scottish Government's ambition for district heating, in order to achieve the wider renewable heat targets by 2020; however, there is a significant proportion of these schemes that will need to include renewable heat. The Scottish Government's draft Heat Generation Policy Statement had indicated that, to achieve the required emission reductions, a much higher proportion of heat will need to come from renewable sources such

as geothermal, solar thermal, biomethane or biomass as well as low-carbon sources like excess unused industrial heat (Scottish Government, 2017). There is however no clear indication of the reduction targets recommended, the inclusion of the 11% renewable heat target needs to be clearly defined here to ensure the challenging target is realised.

Community Scale Energy Storage

The importance of energy storage in shaping our future energy systems, is becoming more prevalent as the move towards introducing more renewable generation gains momentum. A systems approach should be taken to ensure a joined-up approach to electricity, heat and transport in particular. There are real benefits to the range of energy storage schemes but more should be made to the variety of ancillary services provided to the grid by energy storage, such as frequency response.

Cost is often the key barrier to the roll out of energy storage. There is a growing expectation that the capital costs of storage technologies will fall while a number of projects taken forward under the Low Carbon Networks Fund have shown that it is possible to significantly improve commercial viability by realising the additional value that such technologies can add to the system (Energy Savings Trust, 2015).

Post EU referendum

Scotland is recognised as a leader in climate change and setting even more ambitious targets through the new climate change bill cements the need for change as an over-arching priority for the government. Membership of the EU has ensured progress on a range of important issues due to protocols such as the Paris Agreement and thus has enabled the application of high standards in vital environmental protections to the benefit of natural assets found in the country. There is widespread acceptance that the EU has been a catalyst for driving up environmental standards since the UK joined in 1973. Scotland provides the major part of the UK's contribution to Natura 2000, with over 15% of land area designated for a wealth of habitats and species (Scottish Government, 2018). With BREXIT looming there is the realisation that by no longer being part of the EU negotiating block on climate change will make the ambitious targets set out by the Scottish Government harder to achieve, however it is impingent on the nation to ensure the drive to strive to achieve the targets are maintained. The loss of access to financial support programmes and the loss of influence on the big decisions will likely impact on Scotland's ability to negotiate in terms of international recognition but alignment to policy making can still be achieved. Climate change targets are challenging, and the best way of achieving them is to continue with collective effort, which is vital for delivering on Paris Agreement commitments. With colleges expected to become more

sustainable, in terms of aging estate (as discussed earlier), BREXIT impacts and potential loss of EU funding will make this particularly challenging.

2.11 Solar PV Technologies

This section will look at the specifics of current PV module materials, outline the efficiencies of the materials and modules and the companies producing the modules. I will then introduce new technologies on the market and summarise their position within the market. Finally I will present the economics of the installation at Edinburgh College, site layout and design and the plant specifications.

2.12 Solar PV Materials

In a technological age seeing great changes and developments in electricity systems and low carbon economies across the globe, demand for, and a growing dependence on, electricity is increasing. The environmental impact of electricity generation is being thrown into the spotlight, due to the effect of global warming, resulting in a worldwide focus on reducing carbon footprints and greenhouse gas emissions (World, 2015). This has led to the promotion of a more diverse mixture of developing technologies in renewable generation, namely solar photovoltaic (PV) and wind generation. This is leading to a decarbonised, low carbon economy in many countries. In developing clean, affordable, scalable, and importantly, reliable electricity generation solar PV has a great role to play (Tyag et.al. 2013). In realising the ambitions of governments the world over, incentivisation schemes have been introduced to promote and facilitate the installation of solar PV. On the world stage hundreds of manufacturers are providing a range of PV technology and producing modules with varying efficiencies and weaknesses. Cost of installation also fluctuates depending on type of module, location in the world and they type of system being installed in specific projects. This chapter will look at recently published information from a range of projects and focus on materials, efficiency, policy drivers, research & development (R&D), funding sources and the global status of solar PV including its potential for electricity generation.

The most common PV materials and associated efficiencies will be reviewed under the following headings, crystalline silicon, thin film technology and newer emerging technologies. The efficiencies of 143 manufacturing firms and their modules are highlighted with the aim to review the most current improvements in material testing and efficiencies (lab based) and compare & contrast them against the common PV modules available on the market. This chapter will provide a list of the 143 manufacturers and outline the 29 countries of origin of the manufacturers. When looking at the installation of an array such as the one at Edinburgh

College this type of information is important to offer an overview of the growing market with a large amount of variables.

As this thesis is focussed on a solar array in Edinburgh, Scotland, this section will focus on manufacturers from the United Kingdom and its leading competitors, namely United States of America, China, Germany and Japan. For detailed analysis of the cost implications for the Edinburgh Array see chapter 3 (3.4).

2.13 Photovoltaic module material and associated efficiencies

The 20 largest solar PV manufacturers worldwide were identified in a 2014 report by JRC (2014) which also states that some 350 companies are involved in the manufacture of PV cells worldwide (Jager-Waldau, 2014b). However an internet search has heralded the manufactures listed in table 6. This 143 manufacturers in this table falls short of the above reported figure but illustrates well the countries of manufacture and supports the above decision to focus on the UK and its 4 main competitors. It is clear from this list that China boasts the highest number of companies at 43, with Germany at around half that of China, 21, the USA at 19 and Taiwan at 15. These countries are manufacturing and developing more compared with the UK, Spain, Italy, Japan and India, all around the 7 mark, with the remaining 20 countries supporting 1 or 2 manufacturers. The table 5 lists the countries and manufacturers with the country initials and numerical position of the company in the list, for example the first country listed in Australia (AU) with the first manufacturer being E-solar giving the reference AU1. These identifiers will aid in the company identification later in this chapter. This list does not account for popularity or success but is yielded from internet research. As these factors are of no merit to this study, they have been left out to remain focussed and within context.

Table 5 List of companies based on relevant countries and their reference numbers (Frankl and Tanaka, 2014)

S.No.	Country	Company Name	Ref.No.
1	Australia	E-Solar	AU1
2	Austria	PVT	A1
3	Belgium	GH Solar	B1
4	Brazil	SunLab Power	BR1
5	Canada	Eclipsall Energy Corp	C1
6	China	Astronergy co.,Ltd.	CH1
7		Canadian Solar Inc	CH2
8		Chengdu Xushuang Solar Technology	CH3
9		CN Solar Technology Co., Ltd.	CH4
10		CNPV	CH5
11		CSUN	CH6
12		Eging PV	CH7
13		ET Solar Group	CH8
14		FF Solar	CH9
15		General Solar Power Co., Ltd.	CH10
16		Golden Sun Solar Technology Ltd	CH11
17		Gongchuang PV	CH12
18		Hangzhou Amplesun Solar Technology	CH13
19		Hanwha SolarOne	CH14
20		Harbin Gerui Solar Energy Corporation	CH15
21		JA Energy Co., Ltd.	CH16
22		JA Solar Holding	CH17
23		Jiawei Solarchina	CH18
24		Jiangyin Hareon Power Co., Ltd.	CH19
25		Jinko Solar Holding	CH20
26		LDK Solar Co., Ltd.	CH21
27		Polar Photovoltaics Co., Ltd	CH22
28		Pvled Technology Co., Ltd.	CH23
29		QS Solar	CH24
30		ReneSola Co., Ltd.	CH25
31		Shanghai ST Solar Co., Ltd.	CH26
32		Shanghai SunhiSolar	CH27
33		Shenzen Global Solar Energy Technology	CH28
34		Shenzhen Suoyang New Energy	CH29
35		Sunflower Solar Tech Co., Ltd.	CH30
36		Suntech Power Co. Ltd	CH31
37		Sunvim Solar	CH32
38		Topray Solar	CH33
39		Trina Solar Ltd.	CH34
40		Trony Solar	CH35
41		UpSolar	CH36
42		Weihai China Glass Solar Co., Ltd.	CH37
43		Wiosun China Co., Ltd.	CH38
44		Yingli Green Energy Holding	CH39
45		Yunnan Tianda photovoltaics	CH40
46		Zhejiang Energy Technology	CH41
47		Znshine PV-Tech	CH42
48		ZONEPV Co., Ltd.	CH43
49	Croatia	Idea Solar	CR1

50	Cyprus	GESolar Cyprus Ltd	CY1
51	Finland	Naps System	F1
52	France	Auvergne Solaire	FR1
53		Imex Cgi	FR2
54	Germany	Aleo Solar AG	G1
55		Alfasolar GmbH	G2
56		Avancis	G3
57		Axitec GmbH	G4
58		Bosch Solar	G5
59		Conenergy AG	G6
60		DCH Colar GmbH	G7
61		GSS Gebaude - Solarsysteme GmbH	G8
62		G-Tec	G9
63		Hanwha Q Cell	G10
64		Heckert Colar AG	G11
65		Inventux Solar Technologies	G12
66		Jurawatt Vertrieb GmbH	G13
67		LCS Solarstrom AG	G14
68		Schott Solar AG	G15
69		Schuco	G16
70		SI Module GmbH	G17
71		Solarion	G18
72		Solland Solar Cells	G19
73		Solteure GmbH	G20
74		SPS Solar	G21
75	Hong Kong	Sungen International	HK1
76	India	Emmvee Photovoltaic Power Private Ltd.	I1
77		Novergy Energy Solutions Pvt. Ltd.	I2
78		Vikram Solar Pvt. Ltd.	I3
79		Vorks Energy	I4
80	Italy	Albasolar Srl	IT1
81		General Membrane	IT2
82		Istar s.r.l	IT3
83		Silfab S.p.A	IT4
84	Japan	Honda Soltec Co., Ltd.	J1
85		Sanyo Electric	J2
86		Sharp Corporation	J3
87		Solar Frontier K.K	J4
88	Korea	Shinsung Solar Energy Co., Ltd	K1
89	Malaysia	Advanced Solar Voltaic Sdn Bhd	M1
90	Netherlands	Scheuten	N1
91	Portugal	Martifer Solar	P1
92	Russia	Hevel Solar	R1
93	Slovenia	Bisol Group	S1
94	South Africa	Chi Components	SA1
95		Setsolar	SA2
96	Spain	Atersa	SP1
97		Eastech Solar S.A.U	SP2
98		EPS Solar	SP3
99		Gadir Solar S.A	SP4

100		Siliken	SP5
101		YohKon Energia	SP6
102		Zytech	SP7
103	Sweden	Latitude Solar AB	SW1
104	Switzerland	Astom AG	SL1
105		Solar Swiss SD GmbH	SL2
106	Taiwan	A2peak	T1
107		ANJI Technology Co., Ltd.	T2
108		Axuntek Solar Energy	T3
109		Gintech Energu Corporation	T4
110		Green Energy Technology Incorporation	T5
111		Jenn Feng New Energy Co., Ltd.	T6
112		Kenmos Photovoltaic Co., Ltd.	T7
113		Ligitek Photovoltaic Co., Ltd.	T8
114		Motech Industries Inc.	T9
115		Neo Solar Power Corporation	T10
116		NexPower Technology Corporation	T11
117		Ritek	T12
118		Sinonar Solar Corporation	T13
119		Sunshine PV Corporation	T14
120		TSMC Solar	T15
121	Thailand	Bangkok Solar Co., Ltd.	TH1
122	United Kingdom	Antaris Solar	UK1
123		Romag Ltd.	UK2
124		Viridian Solar	UK3
125	United States of America	AEE, Inc	US1
126		Ascent Solar Technologies Inc.	US2
127		Crown Renewable Energy	US3
128		Global Solar Energy Inc	US4
129		HelioVolt Corporation	US5
130		ISET	US6
131		Mia Sole	US7
132		NanoPV Corporation	US8
133		Nanosolar Inc.	US9
134		REC Solar	US10
135		Solar World NC	US11
136		SoloPower	US12
137		Stion Corporation	US13
138		Sungreen Systems US	US14
139		Suniva Inc.	US15
140		SunPerfect Solar, Inc.	US16
141		SunPower Corporation	US17
142		Sunside Solar, Inc.	US18
143		Xunlight Corporation	US19

The following section will discuss and review a number of different materials and their associated efficiencies utilised in the manufacture of PV modules. These are the raw materials utilised to create the desired efficiencies based on supply chain and company business model.

2.14 Crystalline Silicon (c-Si)

Bruton (2002) states that silicon is the most prevalent semiconductor utilised in PV technology. The original designs of PV modules used a crystalline structure of silicon. Due to the development of the bipolar transistor in 1948, a new age of research and development of silicon semiconductors was ushered in and due to this development the efficiencies of silicon based solar cells were increased to 15%. The next leap forward happened in 1970 where the efficiency was pushed to 17% based in the development of micro-electronics. Since then ongoing R&D has led us to circa 25% efficiency being reached by the 2000's et.al. 2001). Efficiency levels of 24.7% and 24.5% have been reached through research by the University of New South Wales by means of Passivated Emitter, Rear Locally (PERL) on Flat Zone (FZ) silicon substrate and Passivated Emitter, Rear Totally (PERT) diffused silicon solar cells fabricated on Magnetically Confined Czochralski (MCZ) substrates respectively (Zhao, 2011). Goetzberger et al. (2000) have reviewed the background history of photovoltaic materials and suggested possible future scenarios for silicon based technologies.

In the broadest sense of classification, mono crystalline and multi crystalline are two basic forms of crystalline technology. As compared to all other types of solar PV technology, crystalline silicon technology has the highest commercial efficiency and therefore the most developed. This has led to a market dominance worldwide of some 80% market share today and has proven efficiencies based on standard test conditions (Key and Peterson, 2009).

2.14.1 Mono crystalline

Mono crystalline structures are widely used due to a high level of efficiency compared to multi crystalline structures. Zhao et al. (1998) reported that with a honeycomb textured, mono crystalline solar cell can achieve an efficiency of 24.4%. It must be noted that overall module efficiency will be lower than this tested 24.4% efficiency. SunPower Corporation (2015) (US17) measured 20.4% overall module efficiency at the National Renewable Energy Laboratory (NREL), 2015. The next table (6) presents 60 companies and their associated module efficiencies which utilise monocrystalline silicon technology. From this table it is seen that a range of 16-16.9% module efficiency is achieved by 36 of the 60 companies (the majority being Chinese and German manufacturers) with the global leader being SunPower (US17) with its 20.4% module efficiency.

Table 6 Efficiency of mono crystalline PV modules ((NREL), 2015)

S.No.	Monocrystalline efficiency Range (%)	Companies
1	20.0-20.9	US17
2	19.0-19.9	J2
3	18.0-18.9	CH19, US3
4	17.0-17.9	CH40, CR1, CH8, CH18, T4, T10
5	16.0-16.9	A1, SP7, CH35, CH21, G15, SP2, CH1, CH20, CH32, US15, K1, C1, CH9, G2, G17, IT4, T8, UK3, CH2, CH15, CH31, CH37, CH41, CH43, G9, G14, US1, B1, CH6, CH26, G6, G8, G13, IT3, SL2, US14
6	15.0-15.9	CH22, F1, FR1, G10, G16, CY,1, G5, I1, G4, SP1, UK1
7	14.0-14.9	US11, J3
8	13.0-13.9	UK2

2.14.2 Multi crystalline or Poly crystalline

As previously mentioned Zhao et al. (1998) also reported on the honeycomb textured solar cells, with an efficiency of 19.8% for multi crystalline based silicon structured technology. Being cheaper to manufacture, multi crystalline are the preferred silicon structures for modules across the market. However, they are less efficient than their mono crystalline counterparts as shown in section 2.15.1. In table 7 a list of multi crystalline modules and associated efficiency is given and shows, again, that half of the 38 companies are from either China or Germany. It is also clear that the majority of the manufactures are sitting with module efficiency of 15-16.9%, some 4-5% lower than their mono crystalline counterparts. In fact the highest module efficiency of the multi crystalline modules listed is 16.9% from Neo Solar Power Corporation in Taiwan. In comparison, the highest efficiency in mono crystalline modules is 20.9%. R&D is currently underway to improve the efficiency found in multi crystalline technology to reach comparable efficiencies found in mono crystalline technology et.al. 2011).

Table 7 Efficiency of multi crystalline PV modules ((NREL), 2015)

S.No.	Multi-Crystalline efficiency range (%)	Companies
1	16.0-16.9	CH20, CH26, CH32, CH35, G19, CH1, CH40, US17, T4, CH18, CH15, CH21, T10
2	15.0-15.9	G10, S1, T12, G11, N1, P1, T8, T9, US10, CH7, CH43, G1, J4, G15, SW1, CH6, CH39, T1, I3, SP5, CH22, CH2, CH8
3	14.0-14.9	US11, UK2

2.15 Thin film technology

Thin film is an alternative to the silicon based technologies, this alternative used less or no silicon in the manufacturing process. There have been extensive reviews undertaken in the field of amorphous and crystalline thin film silicon solar cells, one such review has been carried out by Roedern (2003) and reports that in the initial phases of this technology development of thin film solar cells, the achievement of 10.7% efficiency has been demonstrated by Yamamoto et al. (2004).

2.15.1 Amorphous Silicon (a-Si)

The most developed form of non-crystalline allotropic silicon is amorphous silicon. Even though it is prone to degradation, it is still the most commonly used form of thin film technology. Some examples of a-Si are amorphous silicon-nitrite (a-siN), amorphous silicon germanium (a-SiGe), amorphous silicon carbide (a-SiC) and microcrystalline silicon (μ -Si) (Parida et.al. 2011). A-Si has a high band gap of 1.7eV due to the random nature of its structure (Boutchich et.al. 2012) and when compared to mono crystalline silicon. It has a much higher rate of light absorptivity, 40 times higher (Mah, 1998). It is also the most common thin film material found in the commercial market today. In 1976 the first amorphous thin film solar cell has produced an efficiency of 2.4%, from a cell of $\sim 1 \mu\text{m}$ thickness, achieved by Carlson and Wronski (1976). Furthermore, improvements in the potential of thin film solar cell is detailed by Rech and Wagner (1999).

A list of 49 manufacturers utilising a-Si in their commercial modules is shown in table 8. Stion Corporation, based in the USA, is currently manufacturing a-Si modules with an efficiency of 13.8%, the highest in the market. However, as we have seen with the previous technologies described, China and Germany still have the majority of manufacturers with more than half situated within the 2 countries. We also see that there is a higher disparity between highest and lowest available efficiency with a 10% difference shown. Efficiency of the modules from the majority of manufacturers listed is in the range of 5-9.9%. When comparing tables 9,10 & 11 it is clear that a-Si has some development required in order make it a viable market alternative to both mono and multi silicon varieties. It can be seen that the maximum efficiency of current a-Si modules is a mere 13.8%, when compared to the other 2 module types. This sits around the lowest efficiency found. In reviewing the maximum module efficiency found, in a-Si modules, this technology lags behind mono crystalline by 6.6% and multi crystalline by 3.1%.

Table 8 Efficiency of a-Si PV modules ((NREL), 2015)

S.No	a-si efficiency range (%)	Companies
1	13.0-13.9	US13
2	11.0-11.9	SP3
3	10.0-10.9	CH43, T11
4	9.0-9.9	I2, CH17, G12, J4, CH13
5	8.0-8.9	CH3, CH4, G13, G15, T13, G21, T5, i\$, R1, CH42
6	7.0-7.9	CH12, CH16, FR2, IT2, CH34, CH23, CH27
7	6.0-6.9	CH28, T7, US8, CH14, US16, SL1, US19, CH38, SP4, CH10, CH11, CH25, SA2, HK1, BR1
8	5.0-5.9	CH29, CH5, CH30, IT1, TH1
9	4.0-4.9	M1, AU1
10	3.0-3.9	CH36

2.15.2 Cadmium Telluride (CdTe) / Cadmium Sulphide (CdS)

Cadmium Telluride solar cells are created by combining from cadmium and tellurium to form a thin film material. Due to the ideal band gap found in this particular material, 1.45 eV, and better long term stability (Boer, 2011)(in comparison with a-Si) it is a very promising technology for use in thin film solar modules. It should be noted that there are several remarkable results reported by Compaan (2004), Schock and Pfisterer (2011), Razykov et al. (2004) and an efficiency of 10.6% and 11.2% obtained on thin film 0.55- μm - and 1- μm -thick CdTe by Nowshad et.al. (2001). Upadhyaya et al (2007) have reported an efficiency of 11.4% on CdTe on plastic foil. In general 15 to 16% cell efficiency has been obtained by Britt and Ferekides (1993), Aramoto et al. (1997)and Wu et al. (2001). In July 2011, First solar (2011) company set the world record for cell efficiency at 17.3%, confirmed by NREL.

2.15.3 Copper Indium Gallium Selenide (CIGS) / Copper Indium (Di) Selenide (CIS)

There has been a multitude of advanced research carried out into Copper Indium Gallium Selenide. This material is created by adding Gallium to Copper Indium (Di) Selenide (Schock, A; Shah, 1997)to form the semiconductor structure. In 2006 the best cell efficiency of CIGS was recorded at 20% (Repins et.al. 2008) which is circa 13% module efficiency (Powalla, 2006). However, in 2013, Siva Power reported the highest cell efficiency of 18.8% confirmed by NREL (Osborne, 2014).

In table 9 a list of top CIGS/CIS manufacturers is provided. This shows that of the 26 listed manufacturers half reside in the USA and Germany. This is unlike mono, multi and amorphous silicon technologies described previously, in that China is not a leading manufacturer of this technology. It is also clear from table 12 that the majority of the manufacturers deal within a module efficiency range between 9 and 12.9% with the maximum efficiency of a commercial module, utilising this form of material, of 15%. The most efficient modules here are manufactured by Mia Solé in USA (US7). However, this material is still lagging behind both mono and multi crystalline silicon materials by 5.4 and 1.9% respectively. It is important to note that CIGS/CIS based modules are an improvement on a-Si modules by a higher efficiency of 1.2% in comparison. As with a-Si modules research and technology advancement is required to ensure CIGS/CIS technology is a viable alternative to mono or multi crystalline modules.

Table 9 Efficiency of CIS/CIGS PV modules ((NREL), 2015)

S.No	CIS/CIGS efficiency range (%)	Companies
1	15.0-15.9	US7
2	14.0-14.9	IT3, T15
3	13.0-13.9	US9, US12
4	12.0-12.9	US5, IT2, SP6, J1, US4, G10, G3,
5	11.0-11.9	G20
6	10.0-10.9	T12, US6, T3, US2, CH33, G18
7	9.0-9.9	T2, CH24, T6, US18, T14
8	8.0-8.9	G7, SA1

2.15.4 Gallium Arsenide (GaAs)

Gallium Arsenide is a compound semiconductor formed of Gallium (Ga) and Arsenide (As). It has a similar structure to silicon cells with high efficiency and less thickness. In addition, it is lighter as compared to mono crystalline and multi crystalline silicon cells (Iles, 2001). Its energy band gap is 1.43eV (Streetman, S; Banerjee, 2005; Saas, 2009) which can be improved by alloying it with Aluminium (Al), Antimony (Sb), Lead (Pb), which in turn will form a multi junction device (Satyen, 1998).

The Dutch Radboud University Nijmegen made a single junction GaAs cell that reached up to 28.8% efficiency (Yablonovitch et.al. 2012) while Sharp Company has reached up to 36.9%

(Sharp, 2011) and Spire Corporation, has manufactured the most efficient triple-junction, GaAs cell, with an efficiency of 42.3%, which was verified by NREL (Osborne, 2010). However, this technology is still under research and hence, there are negligible commercial modules available in market.

2.16 New emerging technologies

2.16.1 Hybrid cell

Hybrid cell technology is comprised of crystalline silicon with non-crystalline silicon (Itoh et al. 2001), which makes the manufacturing process of combining them complex. It has been found that a high ratio of performance to cost is evident in hybrid cell Wu et al. (2005). As a result of this, Sanyo has manufactured a hybrid cell with module efficiency of 17.8% (Zipp, 2011). Panasonic manufactured a hybrid cell, in 2014, that is a combination of a thin crystalline silicon wafer coated with amorphous silicon which gives better performance in low light situations and at high temperature with the highest conversion efficiency of 25.6%. This was confirmed by the National Institute of Advanced Industrial Science and Technology (AIST) (Panasonic, 2014; Evoenergy, 2015).

2.16.2 Carbon Nanotube (CNT) cells

Carbon nanotube cell is a cutting edge technology where a transparent conductor material made of CNT provides excellent current flow. CNT is manufactured by forming a hexagonal lattice carbon (Manna and Mahajan, 2007). It is believed that this type of cell technology can convert as much as 75% of light to electricity, (Meiller, 2013). In 2012, a Titanium Dioxide (TiO_2) coated CNT silicon solar cell with efficiency up to 15% was delivered et al. 2012).

2.16.3 Dye Sensitized Solar Cells (DSSC)

Due to the issues encountered with the manufacture of solar cells, namely their lack of efficiency, relatively high production costs and environmental issues with some of the materials utilised researchers have produced a new technology and material called Dye sensitized solar cells (Twidell and Weir, 1986). Research into the sensitization of wide band gap semiconductor materials, such as Zinc Oxide (ZnO), by way of organic dyes for photoelectrochemical (PEC) process was undertaken (Gerischer and Tributsch, 1968; Hauffe et al. 1970). The first use of TiO_2 in PEC process was reported by Deb et al. (1978), although these cells are still considered under early stage development. École Polytechnique Fédérale De Lausanne (EPFL) scientists recorded 15% exceeding the power conversion efficiencies of conventional, amorphous silicon-based solar cells and they believe that this will create a new market place for DSSC solar cells (Ayre, 2013; Papageorgiou, 2013). It is also surmised that this technology will be a

leading competitor over existing materials available in market for solar cells (Gratzel, 2003), however this is yet to be realised.

2.16.4 Tandem cells / Multi Junction solar cell

Another emerging technology is Tandem cells. In this technology several cells of differing band gaps are stacked together so that the gap energy decreases from the top of the stack so that each cell converts the solar spectrum at its maximum efficiency. Overall this means that there will be an increase in the efficiency of a completely stacked cell. In this stacked, Tandem arrangement different thin film materials are used according to their individual band gaps (Goetzberger and Hoffman, 2005). A review of the efficiency and status of multi junction solar cells was carried out by Yamaguchi et al. (2005; 2008). In theory the efficiency of a single junction cell is around 31% (Shockley and Queisser, 1961), the stabilised efficiency is 9.3% for a single junction cell, 12.4% for double junction cells and 13% for a triple junction cell (Guha, 2004). Fuji Electric & Co and Phototronics (Japanese and German respectively) created a double junction cell of intrinsic layers of Hydrogenated amorphous silicon (a-Si:H) which had a stabilised cell efficiency (lab based) of circa 8.5% and 5.5% efficiency for the commercially available modules on the market (Diefenbach, 2005). An efficiency of 14.7% has been recorded by Yamamkoto et al. (2004) for intermediate Transparent Conducting Oxides (TCO) reflector layer for light trapping based on the stacked concept. Sharp, in 2013, heralded the highest recorded efficiency for a triple junction solar cell of 44.4% which was verified by the Fraunhofer Institute (Wesoff, 2013).

This section has outlined the various types of solar PV module technology available on the market, it has covered new and emerging technologies along with the more traditional forms of the technology. This has served to provide an overview in order to highlight the options available to installers.

2.17 Conclusion

Every year, global energy consumption is increasing (an expected rate of 28% between 2015 and 2040 (*International Energy Agency, 2017*)) and several different technologies are used to meet this increasing energy demand. One of the emerging technologies, solar PV is reviewed in this research. In the last decade it is clear that solar PV technology is rapidly growing and becoming a mainstream player within the power industry. Several countries are installing significant amounts of solar PV plants every year, which proves its importance. This progressive growth of PV was put in perspective with the development of renewable power sources in several countries in 2014.

The concepts which are explored in this chapter are, (a) leading countries - this section looked into the policies drivers for the lead countries, R&D activities and funding for the five leading countries China, USA, Japan, Germany and U.K. Based on this review it can be said that, PV is still a policy driven market and rest of the world should take into account the policies of the leading countries in order to participate in PV deployment. (b) PV electricity production - it has been shown that it is difficult to analyse the precise amount of PV electricity generated for an individual country. However, analysis has shown that 1% of global electricity demand will be fulfilled, by PV electricity, by the end of 2015. (c) PV cost analysis – for more than a decade, the PV materials price and BOS components system prices are decreasing. Consequently, the overall costs of a PV project has decreased to £0.32/W (\$0.48/W).

In conclusion, a look at all the major aspects covered in this chapter, it is difficult to define an exact global pattern. Though, it can be said that PV hasn't reached widespread development and deployment across the globe but is still driven by a few leading countries. PV technology has gained a significant amount of attention by policymakers in numerous countries and hence, plans for PV development have increased all over the world. However, this hasn't contributed drastically to an increase of the PV market with deployment up to 2014 was in less than 40 countries. Hence, all the concepts explored and covered in this chapter would be useful for the solar PV system installers, academicians and researchers. This study can contribute knowledge transfer to inform decisions around installation of solar PV arrays at high latitudes. The assumption that the bad weather in Scotland deems PV irrelevant will be challenged through the findings in this thesis.

2.18 Thesis Outline

This thesis will follow the structure outlined below, the structure also represents the order in which various studies, experiments and theoretical research which has taken place throughout the process of carrying out this research.

Chapter 2 covers the extensive literature review undertaken within this study which forms the basis of understanding current worldwide solar PV trends, module materials and types and how these can be implemented in modern solar PV farms at high latitudes.

Chapter 3 explains, in detail, the cost of Scotland's first solar meadow and attributed payback periods. This chapter will present how the accuracy and applicability of existing methods of solar resource modelling and solar photovoltaic (PV) module performance are investigated in the case of a ground array installation at Edinburgh College, Midlothian Campus, the principal derived quantities consisting of slope irradiation, cell temperature, and cell efficiency. Experimental data were obtained on site through both automated and manual measurements for comparison with the calculated quantities.

Chapter 4 will investigate the importance of solar panel positioning in maximising energy delivery, especially at higher latitudes. As solar altitude decreases obstacles and blockages become more of a hindrance and careful planning is required to ensure the amount of shading on the panel surface is kept to a minimum. This chapter looks at the impacts of shading on the Edinburgh College Solar Meadow from obstacles along the Southern and Eastern edges.

Chapter 5 describes how this research has provided scope for further research in an array linked, but not directly, is around the pedagogical impact of having a resource, such as the solar farm studied, on the site of a college campus. This study has provided a good example of a research approach that breaks away from the more traditional University based research work. One of the real advantages of this particular work is the partnership between FE and HE institutions (Edinburgh College and Edinburgh Napier University in the case, and Industry (SSE).

Chapter 6 provides conclusions to the study, contribution to knowledge and recommendations for further study within the solar farm at Edinburgh College. It also outlines lessons learned which should be taken into account within further study.

Chapter 3 – Evaluation of Solar Modelling Techniques Edinburgh College – Midlothian campus, Scotland

3.1 Chapter Summary

This chapter shows, in detail, the cost of Scotland's first solar meadow and attributed payback periods. This information is pertinent to other PV projects, particularly those local to the college and further afield in Scotland. It also lends relevant information to other Colleges looking to consolidate sustainability issues and further their environmental management in a low carbon economy. As we will see the investment required and opportunities vary as much as panel efficiency itself and are heavily influenced by the country in which the project is based.

This chapter will present how the accuracy and applicability of existing methods of solar resource modelling and solar photovoltaic (PV) module performance are investigated in the case of a ground array installation at Edinburgh College, Midlothian Campus, the principal derived quantities consisting of slope irradiation, cell temperature, and cell efficiency. Experimental data were obtained on site through both automated and manual measurements for comparison with the calculated quantities. Results indicate that the horizontal-to-slope conversion models used are extremely accurate, with a greater than 99% degree of confidence in the calculated results. Likewise, correlations between measured and calculated cell temperature were very high at up to 94%. Estimations of the cell efficiency and hence module output were less reliable however, with only one of the models used, for one of the days studied, giving reasonable results. Efficiency values were, however, in the correct range of 15-20%.

3.2 Introduction

Solar energy has not traditionally been a focus of investment in Scotland, where the weather is generally considered to be unfavourable and the amount of solar irradiation low. However, a thriving domestic solar market and developing commercial market (examples given below) both indicate that this intuitive judgement may not match the reality. In fact, the average solar resource available in the south of Scotland is only 10% lower than that of middle-England (Rugg, 2012). When factoring in regional variation, some sites in Scotland are likely to be very favourable to solar development indeed.

A critical factor in the swift uptake of solar generation in Scotland and the whole of the UK has certainly been governmental incentivisation, largely through the Renewables Obligation.

The Renewables Obligation (RO) refers to an incentivisation mechanism which was introduced in 2009 and effectively penalises electricity suppliers for failing to source a percentage of their

energy from renewable sources (House of Commons, 2012). These percentage targets are met through the purchase of Renewable Obligation Certificates (ROCs) from certified renewable generators. At the end of an accounting year, any shortfall must be paid off into a buy-out fund, which is then divided amongst suppliers who met their targets.

The purpose here is two-fold: suppliers are pressured to conform to government-set (and increasing) targets; and generators are afforded an extra source of income.

The equivalent scheme for the small-scale (<50kW) and domestic market is the Feed In Tariff scheme (FIT), introduced in 2010. This is somewhat simpler than the ROCs, in that generators are paid directly for each unit of electricity they generate, and are offered a guaranteed price for any energy they would like to sell. The introduction of the FITs brought about massive uptake in solar systems in the UK, leading to greater production volumes, higher efficiencies and falling system prices (Cherrington, et al., 2013). FIT rates were cut dramatically at the end of 2011, leading to a severe slump in the domestic market which is only just starting to recover.

An important point to be noted in the recent changes in solar funding is that government incentives are becoming less critical. Drops in incentives, coupled with dramatic decreases in module and system prices, are making the savings on electricity an increasingly important factor. Martin (2012) gives the case of a 5MW plant in Cornwall, which was built despite a massive reduction in incentives, simply because capital costs had fallen to the point that it was worth it even on the reduced incomes.

A specific example of a successful implementation of medium-scale solar is the 15kWp façade-mounted array at Edinburgh Napier University. This system, installed in 2005, produces approximately 8MWh of electrical energy each year, avoiding the use of 1.4 metric tons of carbon (Muneer, et al., 2006). All this with next to zero maintenance or upkeep requirements. Other systems successfully using the power of solar in Scotland include:

A 150kWp, 792-module array installed on the Malcolm Allen House builders warehouse in Kintore, predicted to generate 114MWh per year (Solar Power Portal, 2012).

A solar installation of 150kW of solar panels on the roof of the byre to reduce the company's dependence on fossil fuels even further. All the solar energy produced is used on site to power the byre and the milking robots, replacing the dependency on power from the National grid produced by fossil fuels at Westerton Farm, Aberdeenshire

3.3 Summary of Analysis Process

The research methodology is covered throughout the chapters within this thesis, however in summary the following steps were employed to collect data, understand and analyse:

1. Experimental data was recorded on site over a set period. Data collected includes horizontal and slope irradiation, air and cell temperature, rate of heat loss from the module and module power output.
2. The expected slope irradiation will be calculated from the recorded horizontal irradiation, and the results compared with those measured.
3. The expected cell temperature will be calculated from the recorded solar irradiation and air temperature, and the results compared with those measured.
4. The expected cell efficiency will be calculated from the recorded cell temperature, and the results compared with those derived from the module power output.

By completion of the above steps, it is expected that the reliability of the chosen models can be verified in a real-world situation.

3.3.1 Methodology

This research will utilise quantitative data in order to analyse the feasibility of the facility. Aliaga and Gunderson (2002) describe quantitative data collection in research studies as 'Explaining phenomena by collecting numerical data that is analysed using mathematically based methods (in particular statistics)'. This is a good explanation of this type of collection method and explains the purpose and methods of analysing quantitative data and this is the data collection technique that will predominantly be used. There will be data collected from other sources, not just the meadow. Met office data will be utilised to cross-reference the findings along with data collected from SSE used in their modelling process. Other forms of data and data collection methods are to be neglected as they will have little use in this particular piece of research, however, future study into the impact of the array on the biodiversity of the solar farm will require other forms of data (such as qualitative) to analyse a full life cycle analysis.. Given the nature of this research quantitative data will give in-depth detail that could be used in future research and provide its presentation with real relevance to the field of solar energy. The following section provides an overview of the methods, calculations and experimental data recording utilised in this study to provide practicable data and analysis to support the findings of this research.

3.3.2 Solar Geometry Calculations to be utilised in this research

An analysis of the solar resource requires detailed knowledge of the movement of the sun across the sky, as the minute-by-minute position of the sun in the sky affects both the irradiation received on a plane, and the effect of any possible sources of shading. The sun's position in the sky relative to an observer can be described by the use of two co-ordinates, the solar altitude (y_s , or SOLALT) and azimuth (a_s , or SOLAZM). This position can then be related to the plane of a solar module as shown below (Figure 29).

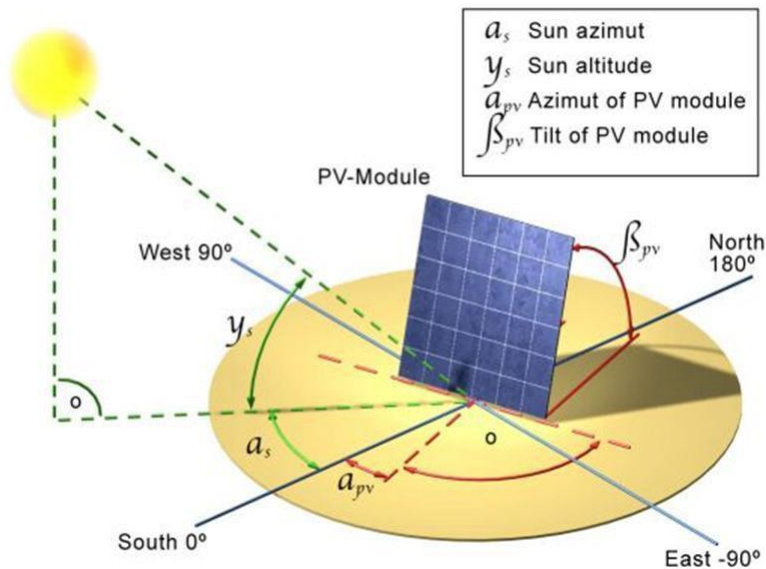


Figure 14 Solar Position Relative to a Plane, Source: Thomas Markvart in(Grassie, 2012)

The data derived here is the angle between horizontal (0°) and the plane of the PV module and a vector drawn to the centre of the sun (INC). A smaller angle will give higher irradiation on the PV module's surface and hence a higher electrical output. In addition, the reflectivity of a solar module's glass cover increases significantly with a large angle of incidence (Muneer, et.al. 2000). The sun's absolute position is also important, as the higher in the sky the more solar irradiation hits the earth's surface (on low cloud days).

The solar altitude and azimuth can be calculated from the latitude (LAT) and longitude (LONG) of the chosen position, and the exact time (ie year (y), month (m), day (D), hour (h), minute (min), Second (s)). This time indicates the current equation of time (EOT), which relates clock time to solar time, and the solar declination (DEC), which indicates the 'tilt' of the earth (ie the angle between the earth-sun vector and the equatorial plane).

These quantities are calculated using the following process. First, the time must be encoded in an appropriate way and the DEC and EOT derived. A quantity called the Greenwich Hour Angle (GHA) is also used. This is calculated by Yallop in the following way Equation 1.

Equation 1 - Yallop Solar Equations, Source: ((Muneer, 2004))

$$t = \frac{\frac{UT}{24} + D + [30.6m + 0.5 + [365.25 (y - 1976)] - 8707.5]}{365.25}$$

Where $UT = h + \frac{min}{60} + \frac{s}{3600}$, other letters as in above paragraph

$$\begin{aligned} G &= 357.528 + 3599.05t \\ C &= 1.915 \sin G + 0.020 \sin 2G \\ L &= 280460 + 36000.770t + C \\ \alpha &= L - 2.466 \sin 2L + 0.053 \sin 4L \\ GHA &= 15UT - 180 - C + L - \alpha \\ \varepsilon &= 23.4393 - 0.013t \\ DEC &= \tan^{-1} (\tan \varepsilon \sin \alpha) \end{aligned}$$

$$EOT = \frac{L - C - \alpha}{15}$$

Finally, SOLALT and SOLAZM may be calculated (equations Equation 2 and Equation 3):

Equation 2 - Solar Altitude, Source: ((Muneer, 2004))

$$\sin SOLALT = \sin LAT \sin DEC - \cos LAT \cos DEC \cos GHA$$

Equation 3 - Solar Azimuth, Source: (Muneer, 2004)

$$\cos SOLAZM = \frac{\cos DEC (\cos LAT \tan DEC + \sin LAT \cos GHA)}{\cos SOLALT}$$

Also, the apparent solar time (AST) (where the sun is at zenith at exactly 12 noon) can be calculated from these parameters and the position of the local standard meridian (LSM) shown in equation 4:

Equation 4 - Apparent Solar time

$$AST = \text{stand time (LCT)} + EOT \pm \frac{LSM - LONG}{15}$$

As well as direct calculations, these equations can be used to produce a sun chart or sun diagram for the location in question, showing the path that the sun takes across the sky for different days in the year. The following sun chart was downloaded from the University of Oregon's extremely helpful sun chart program (Figure 30):

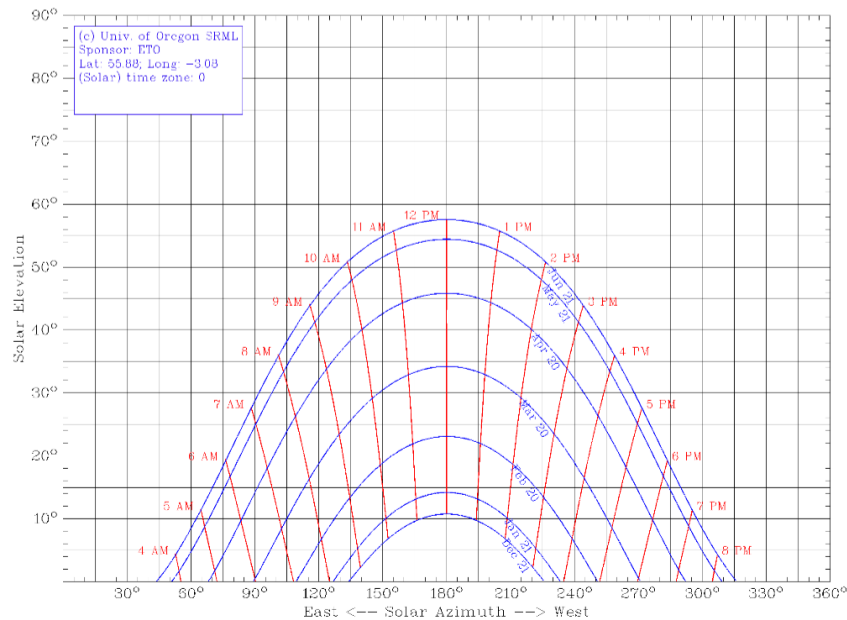


Figure 15 Solstice Sun Chart for Dalkeith, Source: (UO Solar Radiation Monitoring Laboratory, 2007)

This contains much of the information required for a solar analysis, for example it can be seen that the sun rises at an (azimuth) angle of 40° from north (ie NE) on the summer solstice and that the day is only a little over 6 hours long on the winter solstice, with a maximum angle of elevation from horizontal of around 9.5°. The angle of incidence (INC) for a solar panel can then be derived from (Equation 5):

Equation 5 - Angle of Inclination, Source: (Muneer, 2004)

$$INC = \cos^{-1} [\cos SOLALT \cos(SOLAZM - WAZ) \sin TLT + \cos TLT \sin SOLALT]$$

Where WAZ indicates the angle of orientation of the panel and TLT indicates the angle of inclination from horizontal.

3.3.3 Solar Data Recording

Solar data measurements are often taken using pyranometers, global and diffuse values being recorded separately. 'Global irradiation' indicates the total solar energy density received by a collector, while 'diffuse irradiation' only consist of the light coming from the sky, not directly from the sun. From QUARSC (2012), "...this device essentially measures the difference in temperature between a perfect absorber and perfect reflector, the difference in temperature is proportional to the solar radiation." Recording diffuse irradiation is accomplished with the same device as for global, but with a 'shade ring' attached. This covers the arc that the sun will take across the sky, so preventing beam irradiation arriving at the

receiver (a mobile sun-tracking disc may be used instead). The ring requires weekly recalibration. Pyranometer examples are shown in figure 31 below (Note: diffuse measurements were not taken as part of this research.)

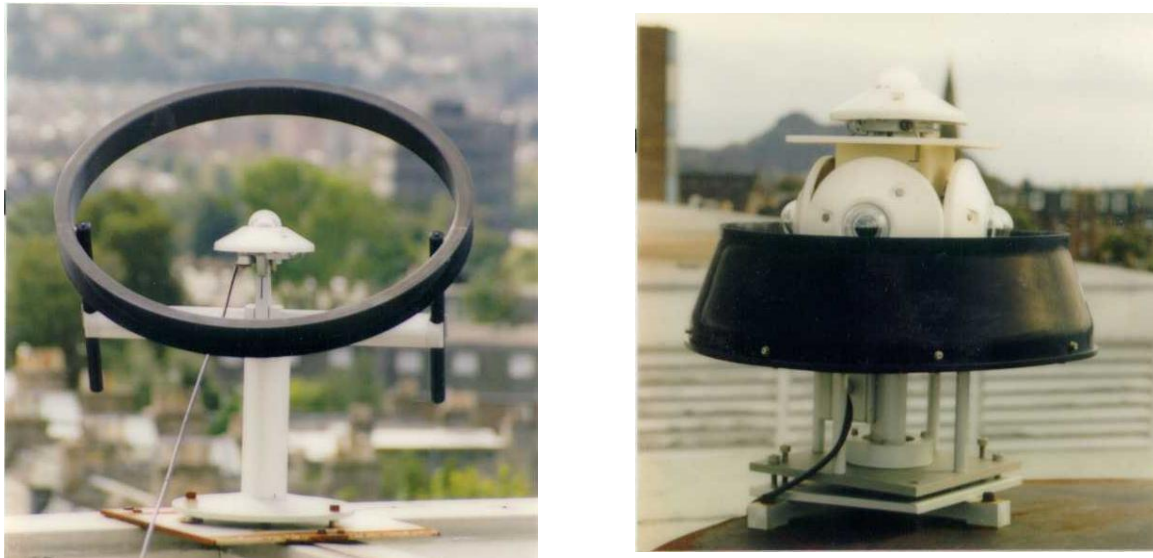


Figure 16 Diffuse, and Global (with N,S,E,W detectors) Pyranometers, Source: (Muneer, 2012)

There are many possible sources of error associated with solar data recording. Problems with correct sensor setup, the position of the shade ring as mentioned, and defects in the equipment (such as a non-uniform glass dome) can all cause errors. The most likely cause for this is the offset caused by the sensor re-radiating to the sky (as the sky is cold and the sensor, being an operating piece of electronic equipment, is relatively warm).

According to UO Solar Radiation Monitoring Laboratory (2007), this error occurs due to the sensor using variations in temperature to record irradiation. Radiating to the sky introduces an error here of up to 20W/m^2 , and should be corrected for. Inadequate or inexact correction could well produce negative values of irradiation. They experimented with a Schenk pyranometer, which removes this particular error source.

Muneer (2004) includes an exhaustive list of sources of error (Table 10 over):

Table 10 Sources of Error in Solar Recording, adapted from (Muneer, 2004)

Equipment Error	Operational Errors
cosine response	complete or partial shade-ring misalignment
azimuth response	dust, snow, dew etc
temperature response	incorrect sensor levelling
spectral selectivity	shading from buildings
stability	electric fields in vicinity of cables
non-linearity	mechanical loading on cables
thermal stability	improper screening from ground-reflected
zero offset due to nocturnal	station shutdown
radiative cooling	improper diffuse correction factor application
	inaccurate programming of calibration constants

3.3.4 Effects of Shading on String Output

The primary effect of any shading on a PV module or string of PV modules is apparent: a proportion of the available solar energy will be blocked from the PV module by the obstruction causing shade, and so will not be translated into electrical output. However, there is a secondary, and perhaps more problematic, effect caused by shading which is the increase in resistance of the shaded cells.

Since all cells in a series string carry the same current, the shaded cells still have a high current flowing through them despite only generating a small photon current themselves. According to Ramabadran & Mathur (2009), this causes reverse-biasing in the affected cells, turning them into loads rather than sources of power. They performed a software analysis, showing that a high degree of power will be dissipated in module cells when only a few of the module total are shaded (Figure 32). As well as power loss, this can cause damage to the cells.

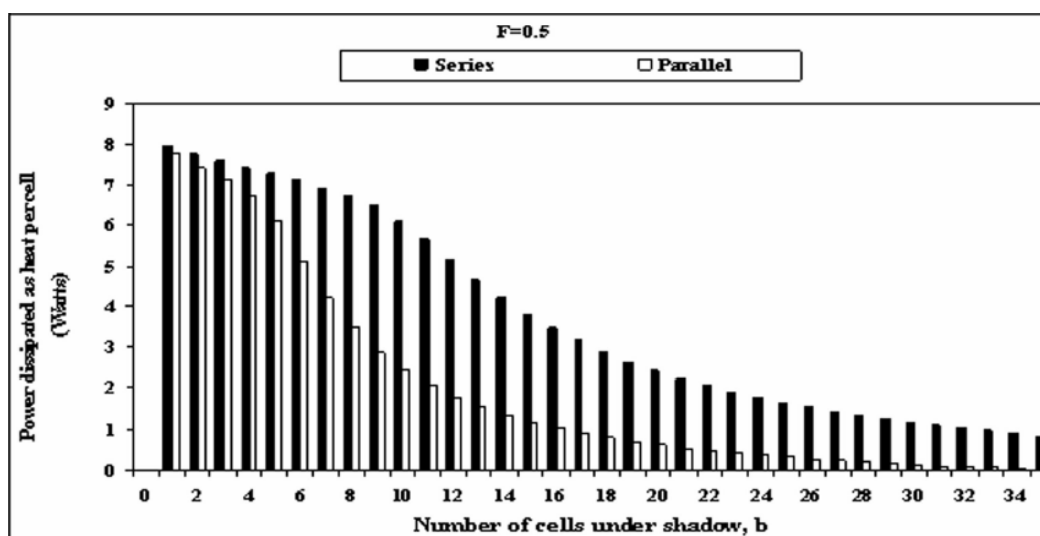


Figure 17 Power Dissipation as a function of shaded cells, Source: (Ramabadran, R; Mathur, 2009)

Deline, et al. (2012) compare two cases, that of a regular string inverter and the use of 'micro- inverters' (effectively, having an inverter per module, avoiding any serial connection shading issues). They show that for 'light shading', performance is increased by 4% when using micro-inverters; 8% for 'moderate shading' and 12-13% for 'heavy shading'. This increase indicates the approximate additional losses associated with using a string inverter, and should correspond roughly to a case such as Dalkeith. An additional complication is highlighted, in that each individual module is often supplied with bypass diodes which 'turn off' a portion of their cells to avoid shading losses and damage (for example, if there is severe shading on one cell, of a 60-cell module, with bypass diodes the result would indicated 20 cells may be bypassed, reducing the output by a third).

3.3.5 Data Presentation

The data will be presented through tables, charts and calculations. The information from the quantitative research will be coded to allow for charts to be produced which will give a pictorial representation of the findings. This highlights any themes or differences more clearly, and is visual proof to any interpretations made. The data will be presented in a simple form to allow for deductions to be made and clearly shown. The charts back up the findings from the tables in a simpler, graphical manner to allow for triangulation and consistency in the resulting findings. Tools, such as NVIVO, will be used to determine correlations and trends through analysis. This research will mainly utilise quantitative collection techniques due to the nature of the data, some quantitative data will be harnessed, however the research offers a solid foundation of data collected from the source which will be used comparatively against other projects currently underway in the UK. Data will be collected on shading analysis techniques, irradiance calculations, cell temperature, cell efficiency, modelling and will be presented against comparative analysis of current solar ventures around the UK. This is covered at length in chapters 3 and 4.

3.3.6 Horizontal to Slope Irradiation Conversion

Clarke *et al.* (2008) proposed a more accurate set of relationships to complete an important step in determining the slope irradiation. As directly measuring the diffuse irradiation is difficult, requiring calibrated shading rings, it is advantageous to be able to work from the global horizontal irradiation value only. In fact, only 9 out of 93 UK Met Office stations record diffuse irradiation (Clarke *et al.*, 2008). The diffuse value must be calculated, and this is achieved by utilising a polynomial regression relationship between the 'beam clearness index' and the

'diffuse ratio'. (Clarke *et al.*, 2008) produced a set of equations, to use for the Edinburgh area, in particular: one yearly, 4 seasonal and 12 monthly average.

From a number of attempts, they determine that a cubic equation with limits is the best to use, and that while the monthly regressions give better accuracy for some months, the advantage over the use of seasonal regressions is marginal. The increase in accuracy over previous methods shown indicates that these equations would be a reliable basis to work from in the current project.

3.3.7 Thermal Model for Cell Temperature

Mattei, et. al. (2006) investigate the use of a thermal model of a solar cell to determine the cell temperature, as opposed to using a simple equation with only solar irradiation as an input. In an experimentally-verified process, they show that by modelling the mechanisms of heat gain and loss from a cell, more accurate predictions of the cell temperature can be made. Some important points made are:

- There are a large range of coefficients in the model, such as that for convective heat transfer, which need to be selected and, if possible, optimised.
- Wind speed has a strong effect on model output. High-resolution wind data is required to get the best results from this type of thermal model.
- Radiative heat transfer is neglected (this is included in the model used by Aldali, et.al, 2011), Aldali et al. 2013)

3.3.8 Alternative Thermal Model

Lobera & Valkealahti (2013) have produced a much more complex thermal model for predicting cell temperature, which is a little beyond the scope of this investigation. An important feature of their work is that they take into account the thermal mass of the PV cell, and incorporate the rate of change of cell temperature with respect to time into the energy balance equation. In addition, they incorporate the radiative heat transfer, providing an alternative model for how to do this. This more complex model produces good quality predictions of the cell temperature, but requires a larger range of input variables than the Mattei, et.al. (2006) model, some difficult to ascertain, such as the module heat capacity. Again, Lobera & Valkealahti (2013) highlight high-resolution irradiation and wind data as important in implementing the model.

This section has summarised the main renewable technologies available and given some context around the Solar Meadow installation at Edinburgh College. It has covered the main research question, aims and objectives, briefly summarised the analysis process and

methodologies utilised within the research, presented expected outcomes and how the data will be presented. It also covers existing literature in brief and presents previous works of note within this research.

3.4 Edinburgh College Solar Meadow Technology

3.4.1 Purpose and Investors

The solar plant at Dalkeith, which is the focus of this research, is a joint project between Edinburgh College and Scottish & Southern Energy, who installed and maintain the site. The plant was commissioned and built for a number of different purposes, not only to take advantage of the aforementioned Renewables Obligation Certificate programme. In addition, the site constitutes an important source of carbon-free energy. For the college, there is also the opportunity to use it as a research and learning environment, where students can get hands-on experience with modern renewable technology. The site will also be made dual-purpose by planting wild meadow-grasses and encouraging the growth of local wildlife. An area of wetland, and a bank of beehives on the site will further exploit the potential ecological benefit to the area.

3.5 The Solar Meadow Farm

The solar plant at Edinburgh College, Midlothian Campus, South East Scotland, (Figure 14) is a £1.2M, equal-partnership project between Edinburgh College and Scottish & Southern Electricity (SSE) Energy Solutions, who installed and maintain the site. Located in Dalkeith, to the south-east of Edinburgh, the plant was commissioned and built for a number of different purposes: to produce carbon-free, renewable energy, to generate an extra revenue stream for the college and to make good use of previously waste land. For the college, there is also the opportunity to use it as a research and learning environment, where students can get hands-on experience with modern renewable technology. The site has now been made dual-purpose by planting wild meadow-grasses and encouraging the growth of local wildlife, making this plant Scotland's first solar meadow. An area of wetland, and a bank of beehives on the site will further expand the potential ecological benefit to the area.



Figure 18 Midlothian Solar Meadow Farm

The 627.5kWp installation, as shown in Figure 15, comprises 2,560 solar panels each rated at 245W, 32 P Aurora power one trio-20.0-TL inverters 20kW inverters and attendant cabling, framing and housing. In fact, over 11km of cable was laid out to connect the AC and DC sides of the system, while almost 1,000 ground screws were planted to support the module mountings. In one year, the site is predicted to produce 568MWh of electrical energy, enough energy to power 170 homes. Feeding directly into the National Grid, this energy will offset conventional electricity production to save approximately 293,000 kg of CO₂ per year.

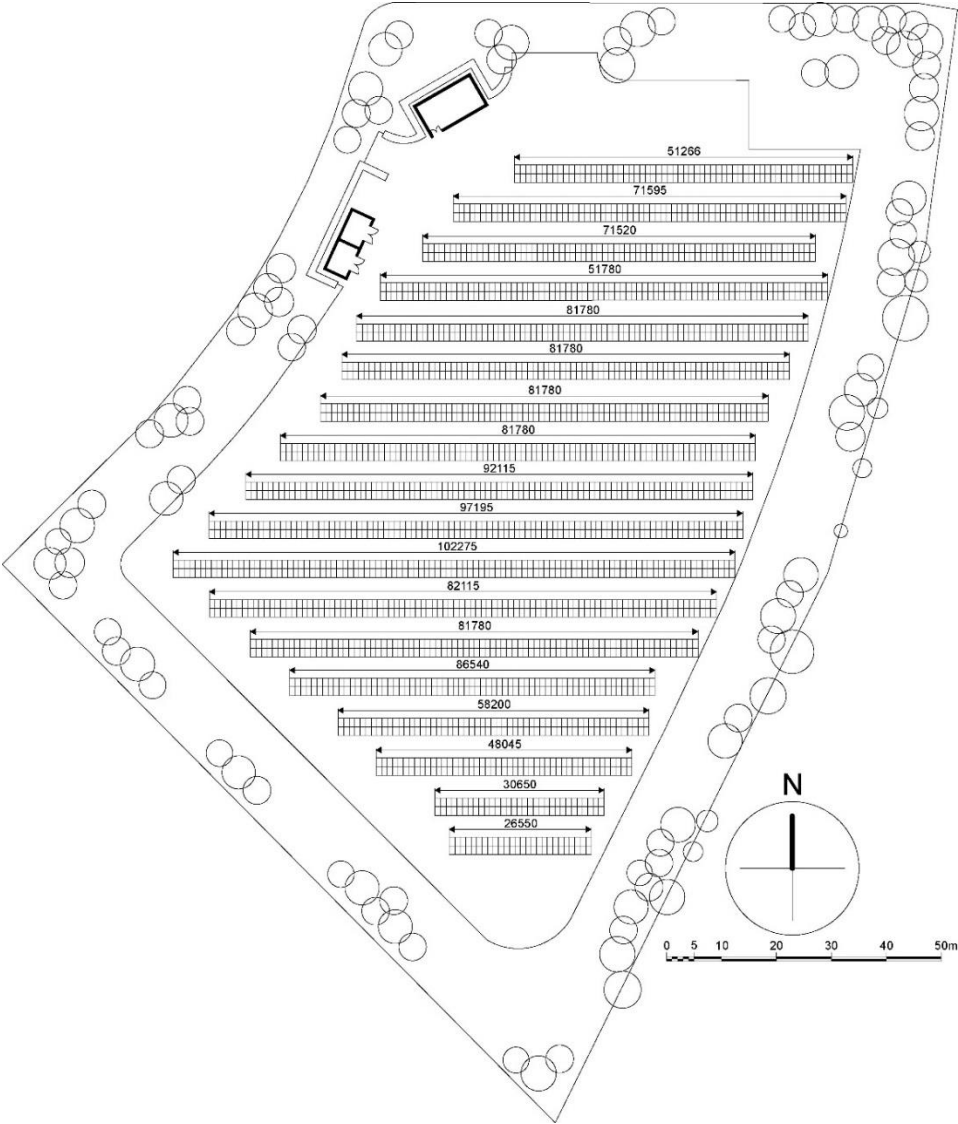


Figure 19 Site Plan of the Meadow

The photovoltaic modules used for the plant are CSUN245-60P series modules. The polycrystalline modules have a nominal power output of 245W, with an overall module efficiency of 16.78%. Modules are connected in series strings of 20 modules each, with 4 parallel strings per inverter. Power-One Aurora Trio inverters are used, with a maximum power input of 20kW each a nominal efficiency of 98%. The modules are mounted on framing orientated due south, with an inclination of 30° degrees.

While the site has now been completed, and in fact started producing on the 28/03/2013, contractual details have only recently been finalised. This proved problematic for the completion of this project, and for the College in general, as the site and data access were not always available.

There were a number of issues to overcome in the first year of operation. Initially 6 out of the 32 inverters were not available for the parallel connection, thus preventing maximum yields for the first 2 months of operation. This limiting effect culminated in the inverters only being able to operate at 12kW instead of the 20kW expected, i.e. these inverters were only operating at 60% of their maximum input power. A problem with transformer balancing and variable phasing problems caused the substation to trip out on the Solar Meadow side. This has meant that a total of 4-5 weeks generation have been lost. Both of these factors have contributed to the shortfall in production during year 1 of operation. By May 2014, 440MWh of power had been generated against a projected SAP projection of 431MWh which included reduction due to shading. Subsequently further works have been carried out to install fans and heatsinks to all the inverters to increase heat dissipation. In addition the transformer taps have been changed on the national grid side to lower the operating level to a point where phase shifts and grid fluctuations will have less impact at peak times.

3.6 Specifics of Location and Site

The plant was constructed adjacent to Edinburgh College Midlothian Campus, just south of the village of Eskbank in the Dalkeith area. The map over (Figure 16) shows the undeveloped site as a satellite image from Google Maps. The solar site roughly corresponds to the green area bounded by a road to the right, while the college is just out of frame to the north.



Figure 20 Google Maps Satellite Image of Site

The area to the left of the image has been developed into parking for the new Eskbank railway station, and so site access between the two projects had to be coordinated carefully.



Figure 21 Initial Site Layout and Design, Source: (Archial, 2013)

Figure 17 shows the initial site design and photovoltaic (PV) module layout, modules aligned to south, following the shape of the field, with spaces in between the rows of modules to allow for access and to avoid any self-shading between rows. As part of the planning requirement a raised embankment was stipulated in order to isolate the site from the surrounding area. Apart from the modules themselves, and the plant room to house the transformers and electrical board, the site is due to contain:

- A classroom (top-left), allowing students access to live data from the site.
- A demonstration/experimentation area (at the north end) where students can set up their own modules and framing, and experiment with factors such as orientation and inclination of the panels.
- A pond/wetlands area at the south of the site, to collect water from drainage and to encourage wildlife.

- A set of beehives, likewise set up at the south end of the site.
- A range of meadow grasses and wild plants, to be seeded over the whole site.
- Some trees, to be planted around the site. These will be planted on the far side of the embankment, and are assumed not to cause any shading issues.

A computer-generated image, based on the above design, is shown below in Figure 18.

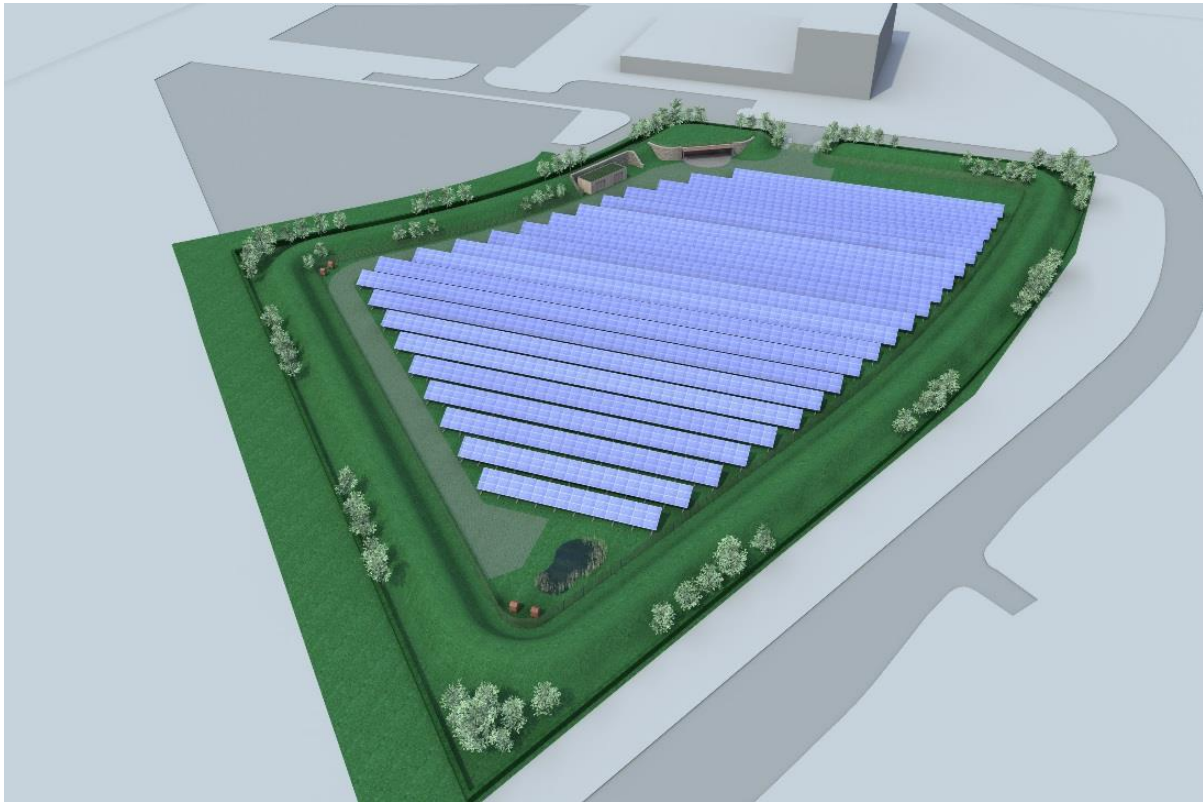


Figure 22 Computer-Generated Image of Completed Site, Source: (SSE, 2013)

A number of photos of the site were taken during an initial inspection for the purposes of this project:



Figure 23 View from SW of Site towards College

This photo (Figure 19) shows a view across the site towards the college in the background. The plant room can just be seen to the left of the picture. Also visible is the module configuration: aligned in portrait, two modules one above the other. The framing raises the modules roughly a meter above the ground at the lowest end, at an angle of 30°. The ground is still bare, sandy earth at this point, but will be seeded as mentioned above.



Figure 24 View from W of site (front of panels)

Another view across the site Figure 20 Here the earth wall on the east side (which is considered in the shading analysis) is shown more clearly, also the east-side side stand of trees can be seen along the horizon.



Figure 25 View from W of Site (back of panels)

Figure 21, showing the rear side of the modules and framing, the locations of inverters mounted on the framing of the rows of modules can be seen.



Figure 26 -View from NE, showing Classroom and Plant Room

In Figure 22, the site entrance is from the right while the plant room (completed) and space for the classroom are centre-frame. The walls of the classroom area are constructed from tire bales, cutting costs and environmental impact.



Figure 27 View from NE across Site

Figure 23 shows the whole site, looking towards the south-west line of trees. These are significant as they will have a shading effect on the solar modules, particularly on those at the south end of the site.



Figure 28 Inverter and AC Distribution Box Setup

Figure 24 shows a closer view of two inverters and one of the distribution boxes, which collects the inverter outputs before transmission to the plant room. The wiring along the back of the modules is also visible.



Figure 29 Front View of Inverter and Detail of Display Screen

The inverters used are Power One Aurora Trio inverters (Figure 25). The display screen shows (among other data) the power output, at this time registering 12.1kW for this inverter.



Figure 30 View along Central Trench

The inverters are located along a central trench dug for the power cables (Figure 26). There are 32 inverters on the site, which are fed into the distribution boxes and then to the plant room for input into the college or the grid.

3.7 Plant Specifications

The 2,560 photovoltaic modules used for the plant are all CSUN 245-60P modules produced by China Sunergy. Polycrystalline, they have a nominal power output of 245W each at a cell

efficiency of 16.78%, and consist of 60 photovoltaic cells per module. The module datasheet is included in Appendix B: Datasheets, containing all the relevant technical specifications. As mentioned, the inverters are Power One Aurora Trio inverters, with a maximum power input of 20kW each and nominal efficiency of 98% (datasheets reproduced in Appendix B). These each have 2 maximum power point tracking inputs, which ensure that the power conversion efficiency of the system is as high as possible regardless of the amount of solar irradiation.

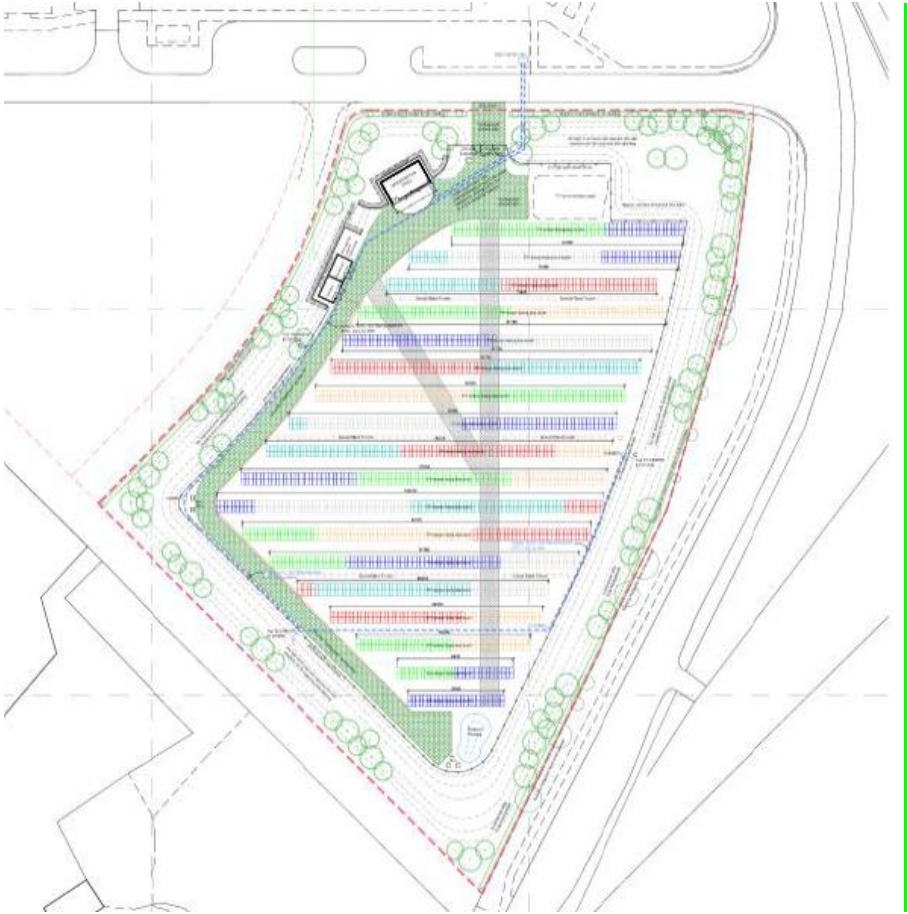


Figure 31 Site String Plan, Source: (Archial, 2013)

In the above plan (Figure 27), the string configuration is shown, with the modules that are connected to each inverter highlighted in different colours. This is important as it allows expected inverter outputs to be determined, and also the approximate power output per module if the inverter output is known. It can be confirmed from this plan that each of the 32 inverters is fed by an equal number of modules (80). These each consist of 4 strings of 20 modules each, pairs connected in parallel into each MPP input of the inverter (this was confirmed through inspection of the site). Another factor to note is that module groups are often split across rows, requiring extra cable runs (and hence greater wiring losses). The 'y'-shaped shaded area indicates the main trenches for cabling, connecting the inverters and distribution boxes through to the plant room.

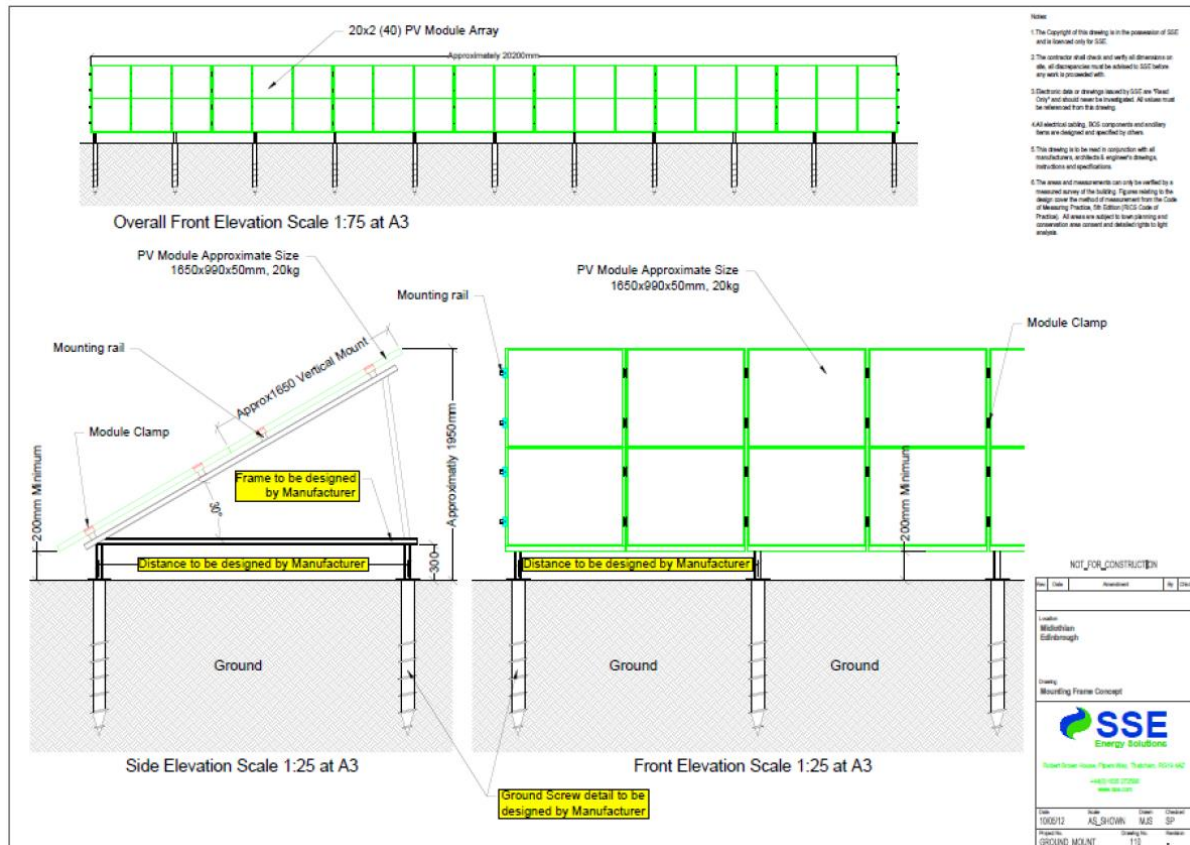


Figure 32 Solar Module Mounting Initial Design, Source: (SSE, 2013).

Figure 28 shows the initial plans for the module framing. This was not the design ultimately used, as it was decided to raise the modules a height of 1m off the ground, however is included as many of the important features remain the same. As shown clearly in Figure 18, the modules are mounted in portrait (ie. with the short side horizontal) with two modules per vertical section. Two points of connection run along the back of each panel, where they are bolted to the framing. At an angle of inclination of 30° from horizontal, the top of the rear panel is approximately 1.75m higher than the bottom of the front panel.

The system cost for the entire project was quoted by SSE at **£879,356**, while the annual generation figure given was **568,611kWh** (see Appendix D: SSE System Documents). The payback period for this installation is expected to be 9.3 years with a life expectancy of 25 years of operation. The average income is anticipated to be circa £90,000 with an overall income and saving of £1,730,434 across a 25 year period. This equates to a profit of nearly £1 million over the lifetime of the installation (Appendix J has full cost recovery).

This chapter has discussed the ongoing and emerging PV materials and efficiency – where it was found that mono crystalline modules have the highest efficiency of 22.5% and other emerging materials like CNT are still under lab R&D and will take some time to become commercially viable. Overall, the common concepts of R&D for all materials is to increase efficiency, develop new methods of manufacturing and cost optimisation.

This chapter has outlined the number of different modules materials currently on the market, the main manufacturers and countries of origin. It has covered the associated efficiencies dependant on material selection and has given plant specifications for the Solar Meadow on which this research is based. It has also given the expected costs and savings anticipated across the lifetime of the array. These forecasts will be tested in the following chapters to ascertain whether the expectations will be met.

3.8 Shading Analysis

The two main sources of shading on site are stands of trees along the south-west and east sides of the site (see Figure 22). The east trees are further away, across the road, and so have a lesser effect but the south-west trees could significantly affect the output of modules at the south end of the site, particularly in the winter when the sun is much lower in the sky. There is also a 3m high earth wall or 'bund' surrounding the site, as mentioned previously as part of the planning consent.

5 points were considered as part of the shading analysis, toward the south and east limits of the site (see Figure 33). The goal of the shading assessment was to obtain an accurate shading sun chart for each which would allow the severity of shading to be determined. It should be noted that SSE, in their site survey and generation forecast, assumed zero shading on the site (see SSE shading analysis, Appendix D: SSE System Documents). Any significant shading will impact significantly on this forecast.

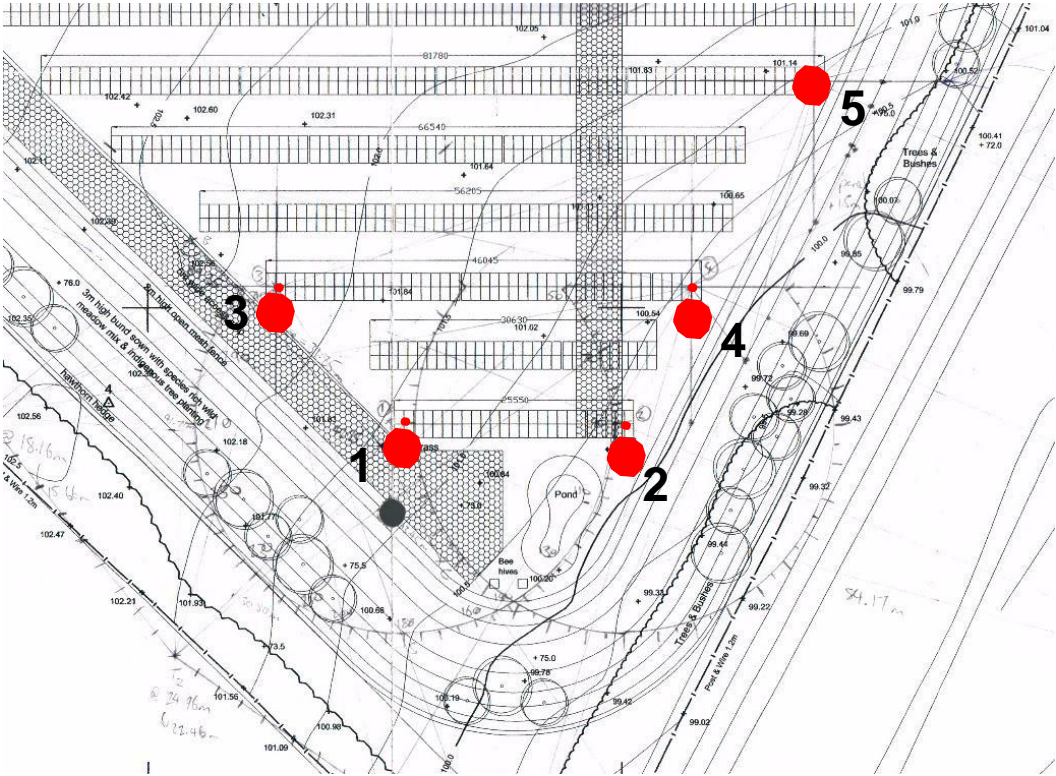


Figure 33 Shading Reference Points, Adapted from (SSE, 2013)

These 5 points of interest were selected due to their proximity to the main identified obstacles, the trees and/or surrounding 3m bund.

3.8.1 Site Survey and Triangulation

A visit was made to the site with the surveying technician from Edinburgh Napier University in order to survey the site accurately.. The pictured surveying instrument (a theodolite) was used to make the necessary measurements (Figure 34).



Figure 34 Theodolite

First, a baseline was set up for each line of trees (as Figure 35). The theodolite required to be positioned accurately at a known point (A or B) and levelled accurately. 0° was set when sighting along the baseline, then the angle between this and a known point on the treeline (T1 or T2) could be measured (the instrument also gave the vertical angle from horizontal).

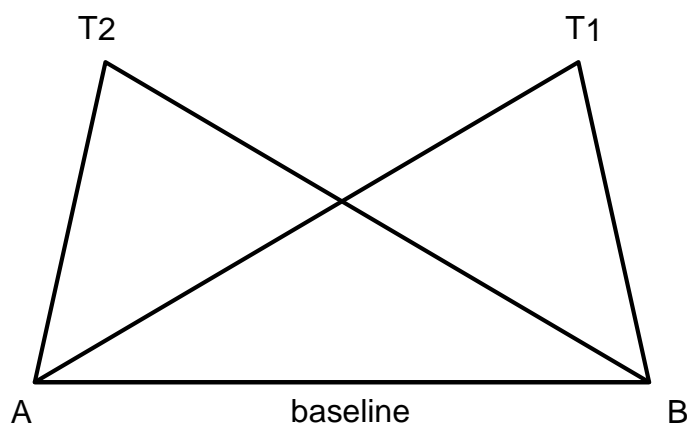


Figure 35 Determination of Tree Distance and Height (Angles/Lengths not to Scale)

Points A and B are the two ends of the original baseline, 1.6m above which the surveying instrument was placed to take the measurements. T1 and T2 indicate the tops of two trees

on the SW treeline, which were chosen to be distinct, allowing them to be found from different locations.

The distances to, and heights of, the trees chosen were then determined through triangulation for each point separately (explanation follows).

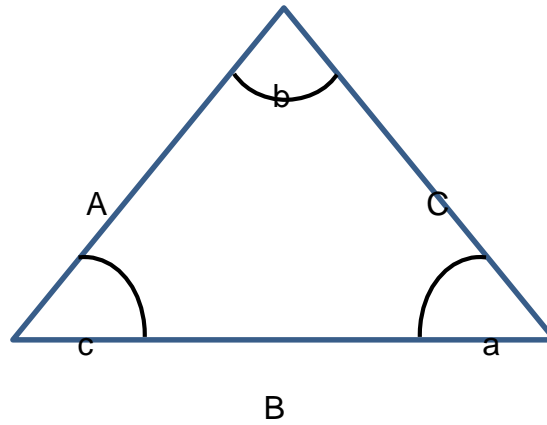


Figure 36 Triangulation

Figure 36 shows three arbitrary points, in an x-y (horizontal) plane.

Equation 6 - Sin Rule

$$\frac{A}{\sin a} = \frac{B}{\sin b} = \frac{C}{\sin c}$$

By rearranging Equation 6 once two angles and one side of a triangle (Figure 36) have been measured, all the other properties of the triangle may be calculated. Furthermore, if one point of the triangle (for example that at the top) were raised vertically (ie, in the z-direction), this would then form a right-angled triangle with the ground, allowing the height to be found from (Equation7):

Equation 7 - Height Determination

$$\text{vertical height} = \text{horizontal distance} \times \tan(\text{vertical angle})$$

Where the 'horizontal distance' is that seen on the original triangle, figure 36.

This process was performed using the solar plant site plan as shown below (Figure 37) (baseline at top-right) with the angles measured on site, and repeated for the east-side line of trees:

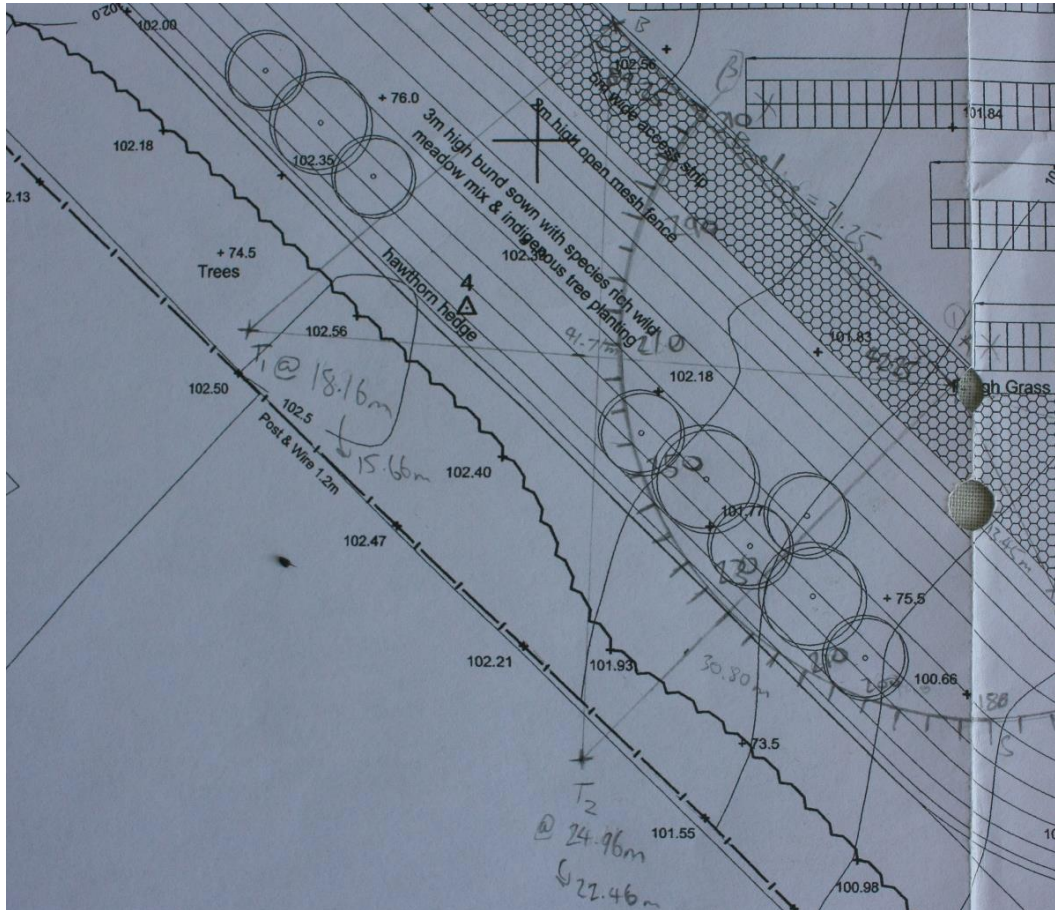


Figure 37 Tree Line Triangulation, detail from (SSE, 2013)

3.8.2 Shading Charts

From each of the 5 shading reference points indicated (Figure 33), measurements were taken at a range of angles of orientation (0-360°), and the distances to and heights of any obstacles (trees or surrounding bund) were recorded, in order to work out the horizon line elevation angle. The results are shown in section 3.13, Experimental Results.

3.9 Experimental Setup

3.9.1 Position on Site



Figure 38 Location of Experimental Setup, Adapted from (Archial, 2013)

In Figure 38 above, the location of the experimental setup is indicated by the red circle. The module on which sensors were placed is part of the group of modules shown in blue, and was connected to 'Inverter 15'. Pyranometers were installed adjacent to this module, in a gap between modules (see figure 39).

3.9.2 Sensor Specifications

The experimental setup consisted of the following:

- 4 Hukseflux HPF01 heat flux sensors mounted on the back panel of one of the PV modules. These were used to determine the rate of heat transfer between the module and its surroundings. Calibration was performed by the manufacturer, certification is shown in appendix B
- 4 K-type thermocouples. Two of these were mounted similarly to the heat flux sensors to determine cell temperature, while two were twisted together and attached to the module framing to record air temperature.
- 3 Kipp & Kozen CM11 solar pyranometers. These were mounted on tripods, one above the modules, facing directly upwards to record the horizontal solar

irradiation, and two in the plane of the modules to record the slope irradiation (Specification available in appendix B).

- 2 Grant 2020 series 'Squirrel' data-loggers, which the sensors were wired into and which recorded periodic averaged values of the sensor outputs. Specifications for these data-loggers is shown in appendix B.

Setup and calibration of the thermocouples and data-loggers, and equipment setup on site was performed by the author with technician support from Edinburgh Napier University.

Calibration certificates for the heat flux sensors and pyranometers can be seen in Appendix B: Datasheets as the calibration was carried out by the manufacturer.

3.9.3 Pyranometer Setup

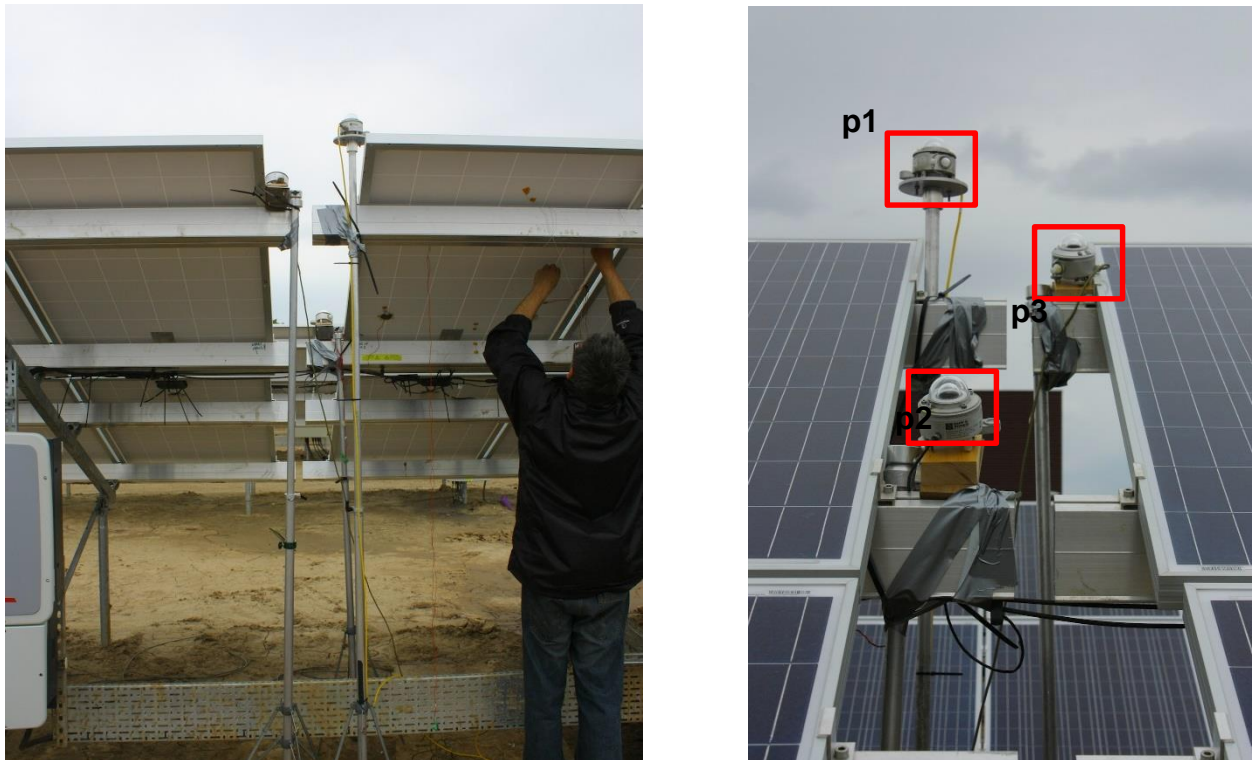


Figure 39 Pyranometer Setup (Front and Back)

Here (Figure 39) can be seen the 3 pyranometers set up for the experiment. The meter for measuring horizontal irradiation, designated 'p1', can be clearly seen at the top of the right-hand photograph. The two meters for measuring the slope irradiation, designated 'p2' and 'p3', are situated lower, in the plane of the solar modules. When these photos were taken, the covers (like that visible in Figure 43) had not yet been applied.

Figure 40 & Figure 41 below show the positioning of the sensors in greater detail. The close proximity of p1 and p2 will be returned to in section 3.13, Experimental Results.



Figure 40 Detail of Horizontal and Upper Slope Pyranometers (p1 & p2)



Figure 41 Detail of Lower Slope Pyranometer (p3)

The following two figures (Figure 42 & Figure 43) show the alignment of the slope pyranometers in the plane of the solar module. While not perfect, the angle of inclination is considered to be as good as reasonably achievable with purely visual inspection.



Figure 42 Alignment of Upper Slope Pyranometer (without cover)

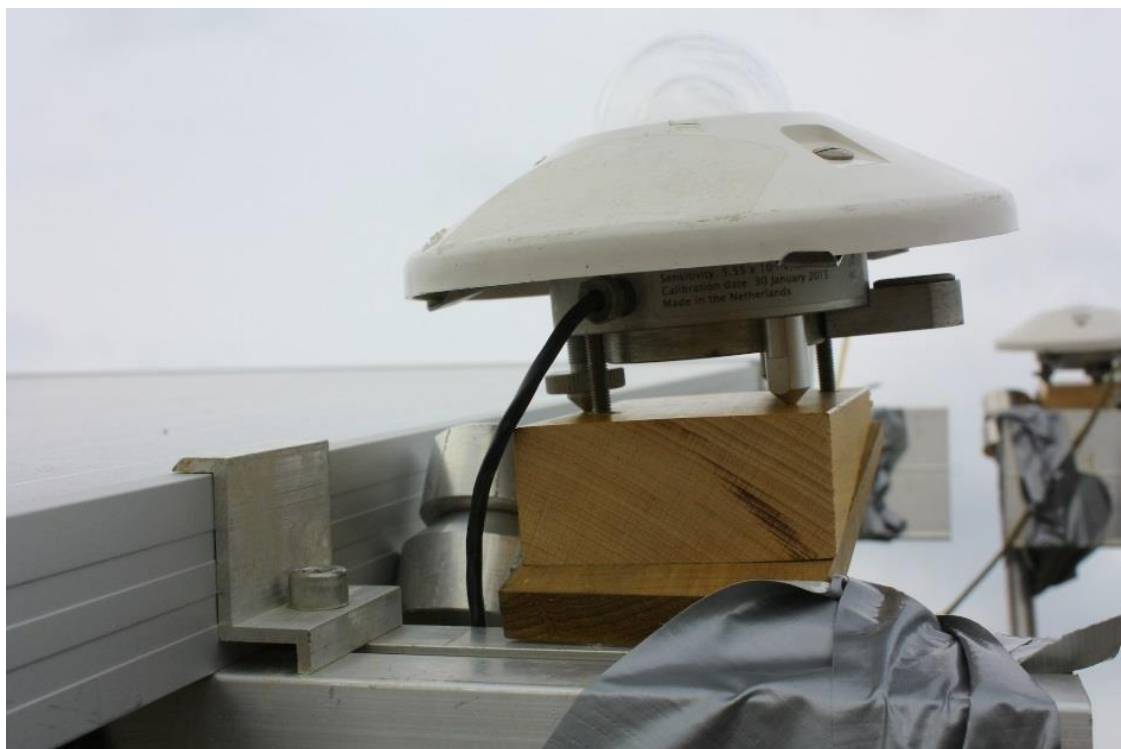


Figure 43 Alignment of Lower Slope Pyranometer (with cover)

3.9.4 Flux Sensor and Thermocouple Setup

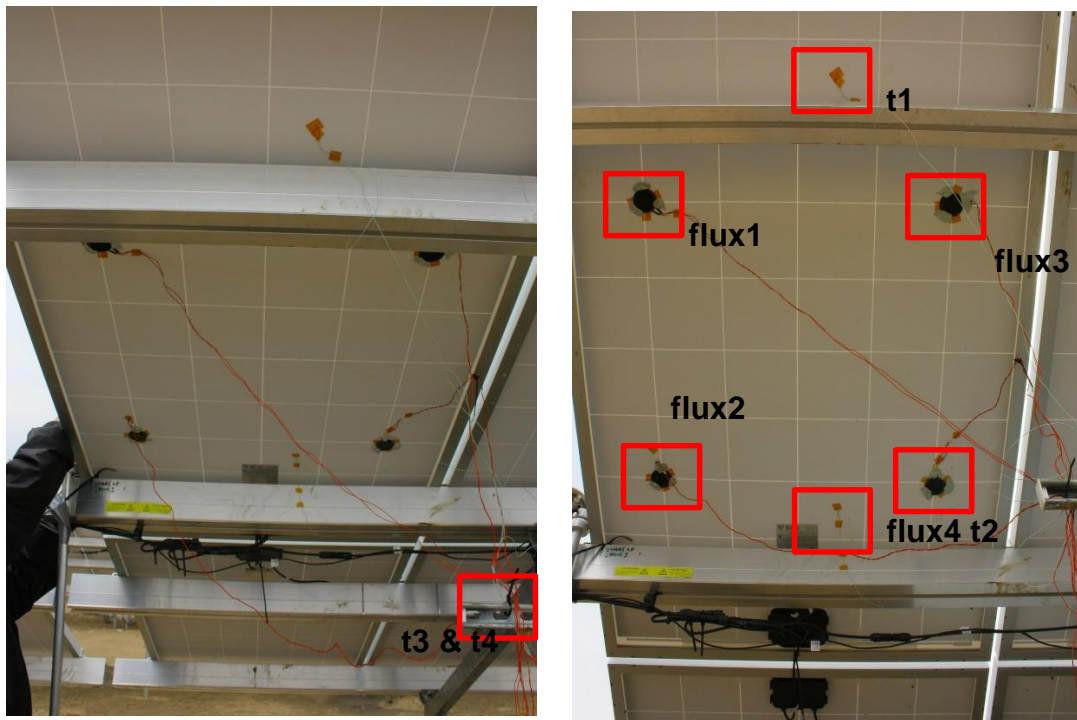


Figure 44 Placement of Flux & Temperature Sensors

The photos in Figure 44 show the overall placement of the flux sensors and thermocouples on the back of the solar module. (The solarimeters are located just to the left of shot.) The four flux sensors were affixed at symmetrical locations, two cells out from the centre of the module, while the two thermocouples were located near the top and bottom centre. Flux sensors are designated 'flux1' to 'flux4', thermocouples 't1' to 't4'.

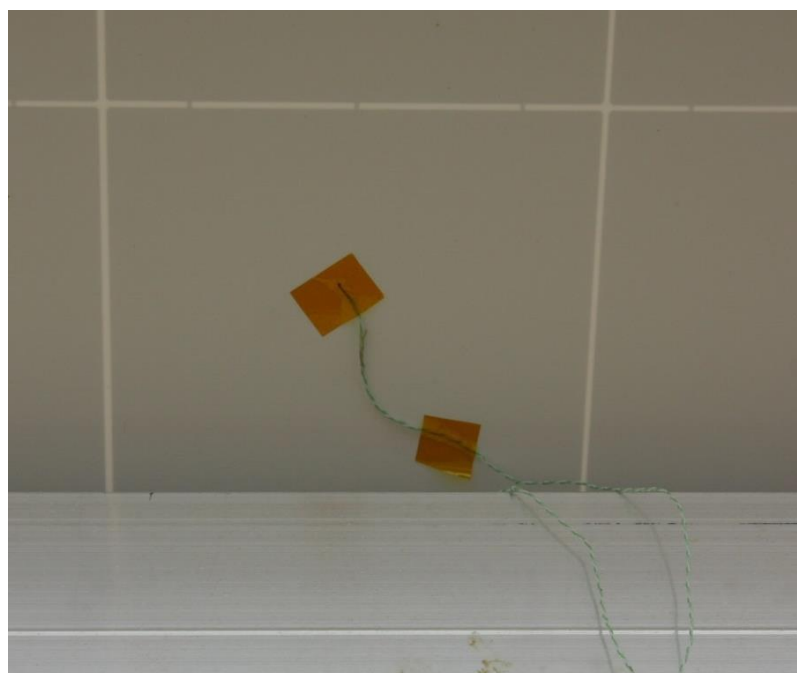


Figure 45 Detail of Thermocouple

The thermocouples were simply affixed with electrical tape (Figure 45), one piece to cover the end pair completely, and one to support the wire.

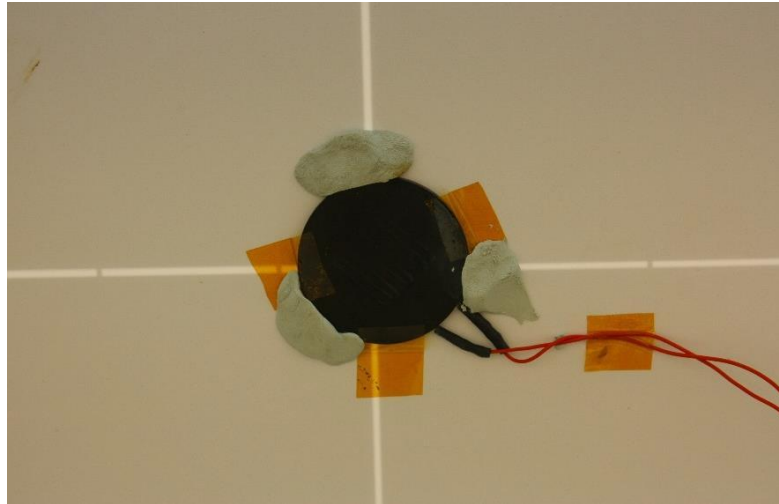


Figure 46 Detail of Flux Sensor

The flux sensors were more difficult to affix, as they required a good contact with the module back cover across the whole of their top surface, and at the same time no obstruction or covering of the bottom surface to allow efficient heat transfer. A thermally-conducting glue would have been the perfect solution, however damage to the module itself had to be avoided and ease of removal ensured. The sensors fixed firmly in place as shown in Figure 46. A small amount of oil was applied to the top surface prior to this to increase the heat transmission between panel and sensor. In future study heatsink compound will be utilised to improve heat transfer as opposed to oil. This will provide better clarity in data collection and more reliable data analysis.

3.9.5 Data-Loggers



Figure 47 Data-Logger Housing

The data-loggers were kept in this metal storage box (Figure 46), bound to the solar panel framing using only cable ties to avoid any damage. A hole was drilled in the bottom of the box to allow the sensor wires to enter. The holes through the back of the container were sealed to ensure no water could enter.

Grant 2020 series 'Squirrel' data-loggers were used, and are pictured over (Figure 48). Technical information is supplied in Appendix B: Datasheets.



Figure 48 Data-Loggers, Source: (Grant Instruments, 2011)

As one logger was insufficient for the number of sensors used, two of this same type were used in tandem, one for the flux sensors and the other for the thermocouples and pyranometers. Data was extracted periodically from the loggers by a college based technician assisting on the project. This was carried out using the ‘SquirrelView’ software supplied with the loggers (Grant Instruments, 2013) and collected manually, due to WiFi signal strength issues, on a weekly basis.

3.10 Experimental Measurements at Solar Meadow Farm

Experimental data was collected at the site to fulfil two goals. Firstly to obtain detailed, specific data on the day-to-day operation of the plant, and secondly to assess the accuracy of solar models used to predict such values as in-plane (or slope) irradiation, PV module cell temperature, and cell efficiency.

The experimental setup consisted of the following:

- heat flux sensors mounted directly on the back panel of one of the PV modules. These were used to determine the rate of heat transfer between the module and its surrounding air.

- K-type thermocouples. Two of these were mounted in a similar way to the heat flux sensors to determine cell temperature, while another two were used to record air temperature under shade.
- solar pyranometers. These were mounted on tripods: one above the modules facing directly upwards to record the horizontal solar irradiation, and two in the plane of the modules (with equal inclination and orientation) to record the slope irradiation.
- Two data-loggers, which the sensors were wired into and which recorded 5-minute periodic averaged values of the sensor outputs.

The sensors were positioned around the solar modules as shown in Figures 49 & 50.

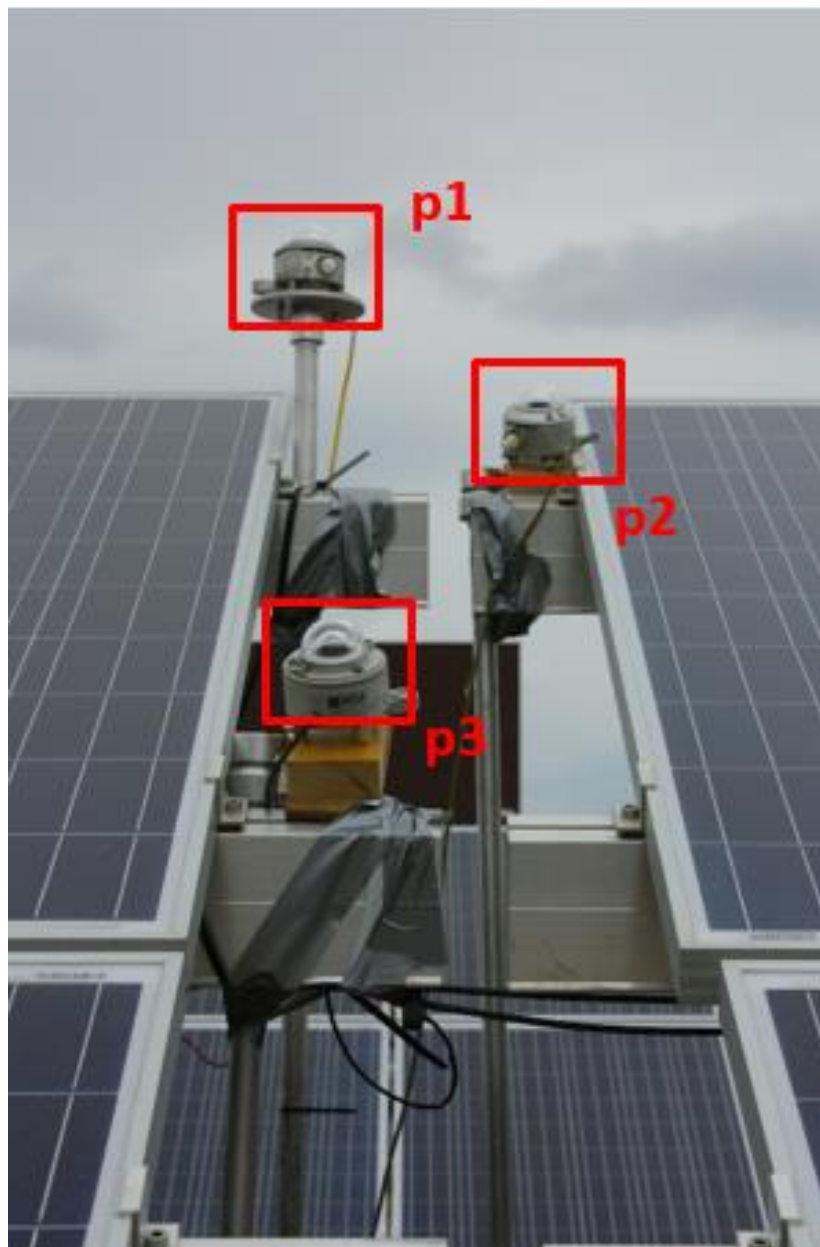


Figure 49 Position of Pyranometers

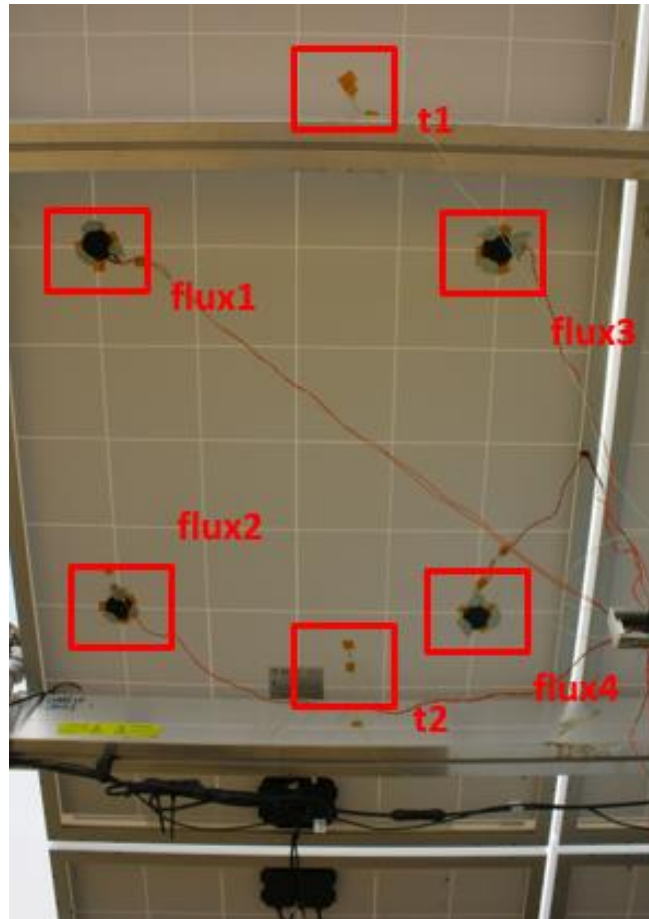


Figure 50 Position of Flux Sensors

Data from each of the temperature, flux and irradiation sensors was logged using two Grant 2020 series 'Squirrel' data-loggers, taking measurements every 5 minutes throughout the day. These data points constituted the average value (temperature, irradiation or heat flux) registered over the 5-minute period, forming the basis for the calculation process.

The final data values required were the power output of the solar module being measured. Unfortunately, no method of automated logging of module output was available, and a compromise had to be made. Manual readings from the string inverter corresponding to the chosen PV module were taken, 9am, 12 noon and 4pm, over the course of three days. The module output was simply estimated as a fraction (1/80) of the input power to the inverter; as per technical specifications. In future study it is suggested that time lapse cameras are setup up as required to better capture accurate data sets.

3.11 Calculation Process

The comparison of measured and calculated variables was completed according to Figure 51.

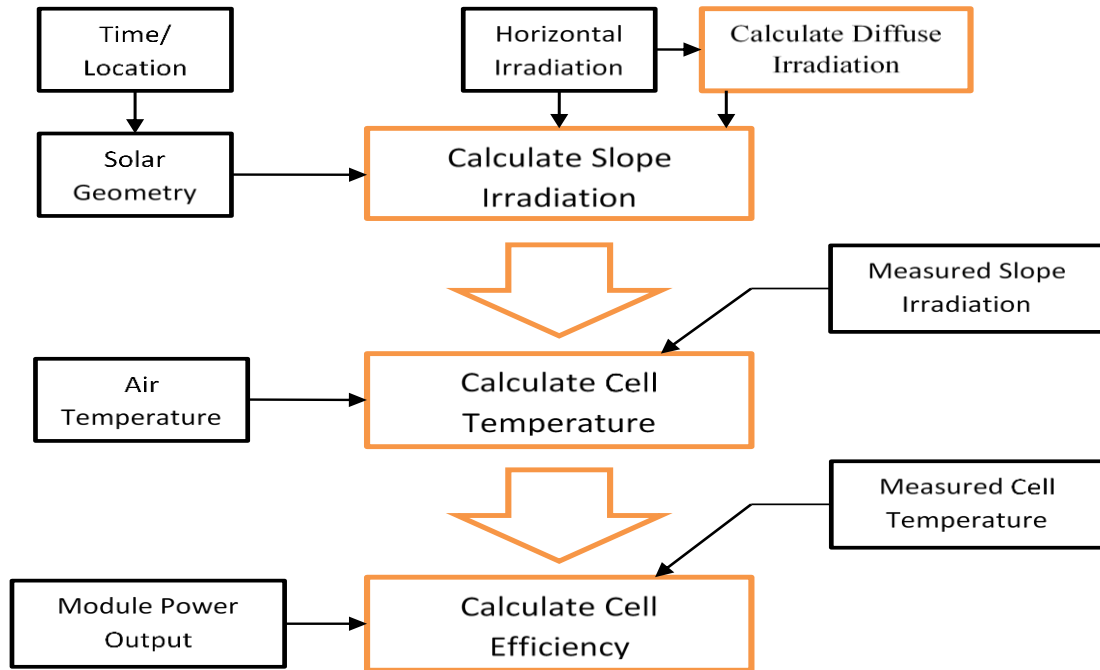


Figure 51 Calculation Flow Chart

This being a linear calculation process, each stage relying on the previous, any errors or inaccuracies picked up would be propagated through the calculations, making an accurate, independent assessment of each stage difficult. For this reason, calculations were based on measured data along with previous-stage calculated values.

3.11.1 Slope Irradiation

As indicated in Figure 51, the principal input variables to determine the slope irradiation (once the position of the slope has been decided) are the horizontal irradiation and the time of day (and date), which allow the position of the sun in the sky to be calculated. As data readings were taken over 5 minute time intervals, not at an exact time, it was decided to follow the approach used by (Clarke, 2007) and take the mid-point of the time period as the data point, i.e. 2.5 minutes before the logged time.

As used by Muneer (2004) Figure 52 demonstrates how time/date and irradiation data was used with solar geometry equations to calculate slope irradiation.

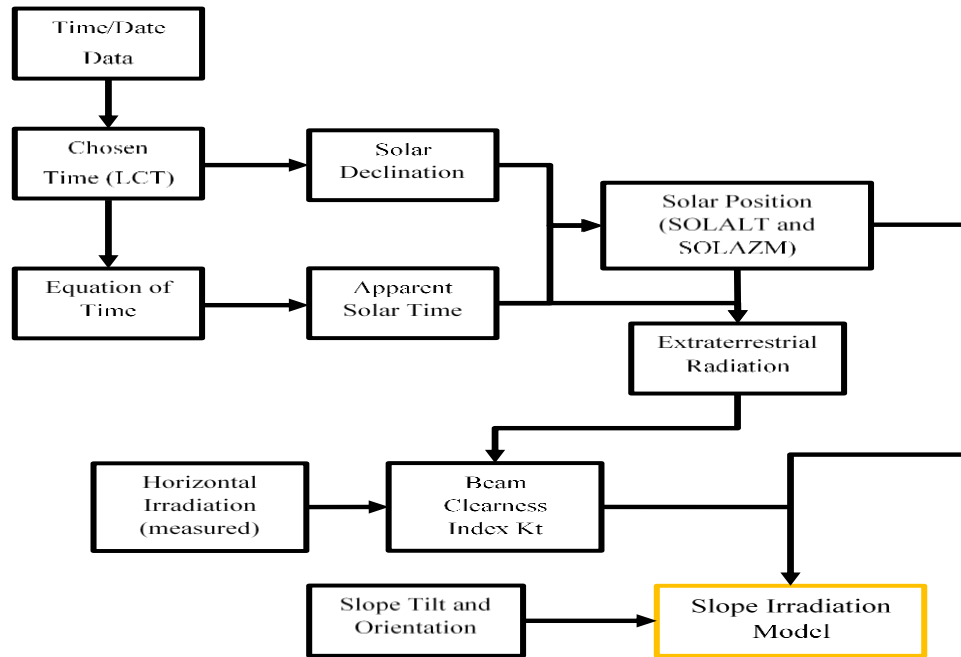


Figure 52 Solar Geometry and Slope Irradiation

The final important factor to be determined was the diffuse irradiation component, i.e the solar energy emitted across the whole hemisphere of the sky rather than directly from the sun. This was achieved through use of separate models for relating the relationship between the global clearness index $k_t = I_G/I_E$, and the horizontal diffuse to global ratio $k = I_D/I_G$. (Where I_G is the global irradiation, I_E is the extra-terrestrial irradiation and I_D the diffuse).

This relationship allows us to calculate the diffuse irradiation, rather than directly measure it, which is a critical step towards determining the slope irradiation.

Three different equations (8, 9, and 10) were selected to generate a range of results, one from Muneer et al. (2000), the others from Clarke et al.(Clarke, 2007). They are shown below with coefficients selected for Edinburgh:

Equation 8 - Clarke Seasonal (Summer) Calculation, Source (Clarke et.al. 2007)

$$k = 0.8721 + 1.7619k_t - 6.2135k_t^2 + 3.9467k_t^3, 0.25 \leq k_t \leq 0.8 \text{ for } k_t > 0.8$$

Equation 9 - Clarke June Calculation, Source: (Clarke et al., 2007)

$$k = 0.8798 + 1.7195k_t - 6.1193k_t^2 + 3.8769k_t^3, 0.2 \leq k_t \leq 0.85$$

Equation 10 - Muneer Calculation, Source: Software Program Calc4-08 in (Muneer et al, 2000)

$$k = 1.006 - 0.317k_t + 3.1241k_t^2 - 12.7616k_t^3 + 9.7166k_t^4$$

Once both the diffuse and global (total) horizontal irradiation are known, it becomes possible, for a given collector inclination and orientation, to calculate the global slope irradiation

(generally referred to as the slope irradiation). This method is adapted directly from the Windows in Buildings (Muneer et. al. 2000) software. Three quantities are calculated separately for the plane of the collector:

- beam irradiation
- diffuse irradiation
- ground-reflected irradiation

Beam irradiation depends on the global and diffuse horizontal irradiation, the Sun's angle of incidence on the centre of a solar panel (SOLINC) and the Sun's Altitude as seen in the sky above a solar panel (SOLALT). It is set to zero if either SOLALT is less than 7°, or SOLINC is greater than 90°. In other words, if the sun is not in 'view' of the collector. Otherwise, the beam component is given by (equation 11):

Equation 11 - Beam Component of Slope Irradiation, Source: Software Program Calc4-08 in (Muneer, Tariq; N, Abodahab; G, Weir; J, 2000)

$$Beam_{slope} = Beam_{horizontal} \frac{\cos SOLINC}{\sin SOLALT}$$

Diffuse slope irradiation is more complex to determine, as in the model proposed by Muneer(2004), the sky is not considered isotropic. This method has been shown to give better results for diffuse irradiation (Muneer, 2004). Complete algorithmic details for the calculation of the above mentioned slope irradiation and computations are provided in the latter reference. The final value used for the slope irradiation during the given time period is simply the sum of the beam, diffuse and ground-reflected components.

3.11.2 Cell Temperature

The cell temperature, similarly to the slope irradiation, was estimated through the use of three different models. The Nominal Operating Cell Temperature (NOCT) model is based on the behaviour of a solar module under certain test conditions, and utilises a simple calculation relating the solar irradiation to the temperature (equation 12):

Equation 12 - NOCT Cell Temperature Calculation

$$T_c = T_a + \frac{G_{slope}}{G_{noct}} (T_{c,noct} - T_{a,noct}) \left(1 - \frac{\eta_{stc}}{\tau\alpha}\right)$$

Where: T_c is the cell temperature, T_a is the air temperature, G_{slope} is the global slope irradiation, G_{noct} equals 800W/m², $T_{c,noct}$ and $T_{a,noct}$ are the cell and air temperatures at NOCT, η_{stc} indicates the cell efficiency at STC (standard test conditions) and $\tau\alpha$ is related to the transmissivity-absorptivity of the module to solar irradiation.

The HOMER software model alters equation 12 to include a linearly variable, rather than static cell efficiency (equation 13).

Equation 13 - HOMER Cell Temperature, Source: (HOMER Energy, 2013)

$$T_c = \frac{T_a + (T_{c,noct} - T_{a,noct}) \frac{G_{slope}}{G_{noct}} \left[1 - \frac{n_{stc}(1-\alpha_p T_{c,stc})}{\tau\alpha} \right]}{1 + (T_{c,noct} - T_{a,noct}) \frac{G_{slope}}{G_{noct}} \frac{\alpha_p n_{stc}}{\tau\alpha}}$$

In the third case, a thermal model was implemented based on the method proposed in (Aldali et.al. 2013). This avoids the assumption of the previous methods: that the module's thermal parameters will not change under different circumstances such as air temperature or irradiation.

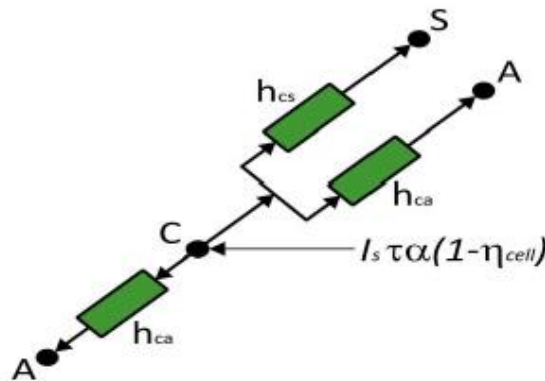


Figure 53 Heat Transmission from a Solar Module, Source: (Aldali et.al. 2013)

In Figure 53, it can be seen that there are three main mechanisms for thermal energy transfer from the cell (or module) to its surroundings. These correspond to convective losses to the air on both sides of the cell, and radiative losses to the sky (radiative losses to the ground are much smaller, and are neglected).

The convective losses are a function of the temperature difference between cell and air (equation 14):

Equation 14 - Convective Loss

$$\text{Convective Loss} = 2h_{ca}(T_c - T_a)$$

The radiative losses likewise, but to the sky (equation 15):

Equation 15 - Radiative Loss

$$\text{Radiative Loss} = h_{cs}(T_c - T_{sky})$$

In which T_{sky} , the effective sky temperature, and h_{ca} and h_{cs} can be determined from equations 16, 17 and 18:

Equation 16 - Effective Sky Temperature, Source: (Aldali, Y; Celik, A.N; Muneer, 2013)

$$T_{sky} = 0.0552T_a^{1.5}$$

Equation 17 - Air Heat Transfer Coefficient, Source: (Aldali, Y; Celik, A.N; Muneer, 2013)

$$h_{ca} = 5.67 + 3.8v$$

Equation 18 - Sky Heat Transfer Coefficient, Source: (Aldali, Y; Celik, A.N; Muneer, 2013)

$$h_{cs} = \frac{\sigma \epsilon_c (T_c^4 - T_{sky}^4)}{T_c - T_{sky}}$$

The cell temperature value is found by combining the energy losses with the heating effect from the sun (equation 19):

Equation 19 - Thermal Model Cell Temperature

$$T_c = \frac{I_{slope} \tau \alpha (1 - \eta_{cell}) + h_{cs} T_{sky} + 2h_{ca} T_a}{h_{cs} + 2h_{ca}}$$

Where: I_{slope} is the incident irradiation. The value for T_c is derived iteratively as T_c affects the heat transfer coefficients h_{cs} and h_{ca} .

3.11.3 Cell Efficiency

While the other variables could be measured fairly directly, the cell efficiency had to be estimated from the measured data (using equation 20).

Equation 20 - Cell Efficiency from Output

$$Cell\ Efficiency = \frac{P_{out}}{P_{in}} = \frac{P_{module} / No.\ of\ Cells}{Solar\ Irradiation \times Cell\ Area}$$

P_{module} was derived from the manually-recorded inverter power readings at each time interval. This was done in two ways to get the best possible result: first of all as an average of a set of instant power readings taken around the sample time, and secondly from the change in total inverter energy reading over the time period, divided by the sample time. Each reading had its own advantages. In general, the instant readings were highly variable, whereas the averaged readings were adversely affected by the low resolution of the energy counter (nearest 0.1 kWh).

Equation 21 - Cell Efficiency

$$\eta_{cell} = \eta_{stc} [1 + \alpha_p (T_c - T_{c,stc})]$$

3.12 Results & Discussion

3.12.1 Slope Irradiation

The measurement of slope irradiation was relatively simple and reliable, as the use of a manufacturer calibrated pyranometer (see appendix B for calibration certificate) aligned to match the slope and orientation of the solar module in question gave accurate readings with which to check the calculated values against. More complex was the method used for calculating the slope irradiation from only the horizontal global irradiation, requiring a number of different steps and intermediate quantities; regardless it was expected that the calculation accuracy would be relatively high, as has been demonstrated in the papers presenting the methods used (Aldali et. al. 2013) (Clarke, 2007) .

The three models for determining the clearness index and hence the slope irradiation gave similar results, the best of which is shown in Figure 54, derived from the Clarke Summer model (Clarke at.al. 2007)

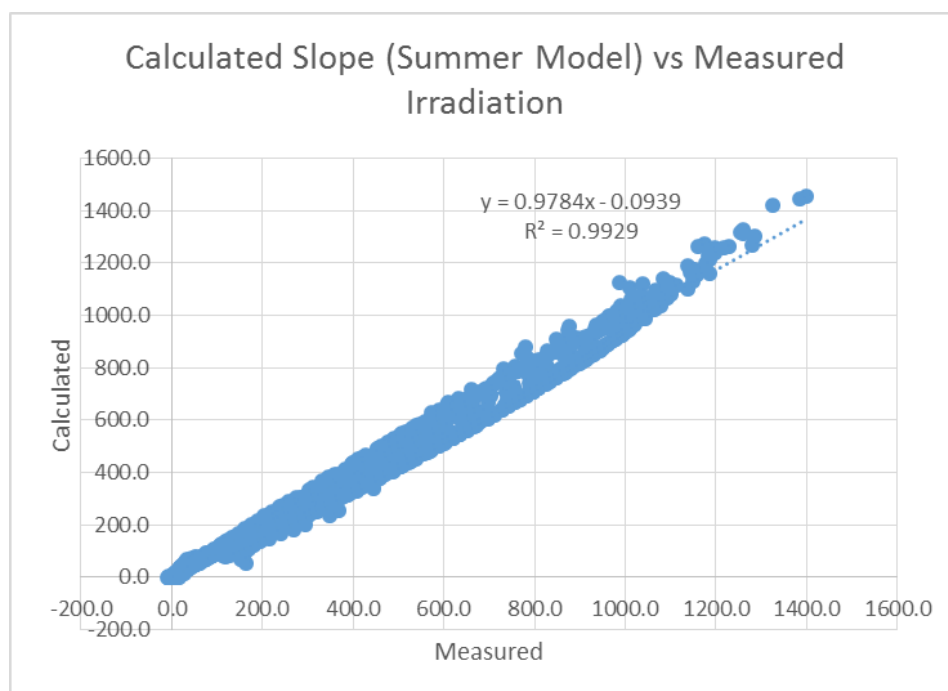


Figure 54 Slope Irradiation Results

It can be seen that Figure 54 shows an excellent, almost entirely linear, correlation for the site studied.

While all three methods show a high degree of accuracy, as expected the calculations optimised for the given location give slightly better results. Table 11 makes a direct comparison

in terms of the same quantities highlighted in Figure 54: gradient, y-axis intercept and regression coefficient, R^2 , between the computed and measured quantities.

Table 11 Slope Irradiation Model Results

Slope Irradiation Comparison			
Model	Gradient	Offset	R^2
Summer	0.9784	0.0939	0.9929
June	0.9761	0.3164	0.9929
Muneer	0.9738	0.405	0.9897

The difference between using the seasonal and monthly models follows the assessment in Clarke et al.(Clarke, 2007), namely that the increased complexity of using monthly coefficients (as in the June model) in a project gives a low return in increased accuracy (in this case, little to none).

3.12.2 Cell Temperature

As detailed in Section 3.13.2, the cell temperature was modelled in three ways; the simple but widely-used NOCT or nominal operating cell temperature model, the slightly more complex one used in the HOMER software, and finally the full thermal model. It was expected that each would give successively better results when compared with the cell temperature directly measured from the back of the PV module, with the thermal model being significantly more accurate than the other two due to its consideration of a greater number of factors. Figure 55 shows the output of the thermal model only across the full time range of the experiment, while Table 12 compares the outputs of the three models.

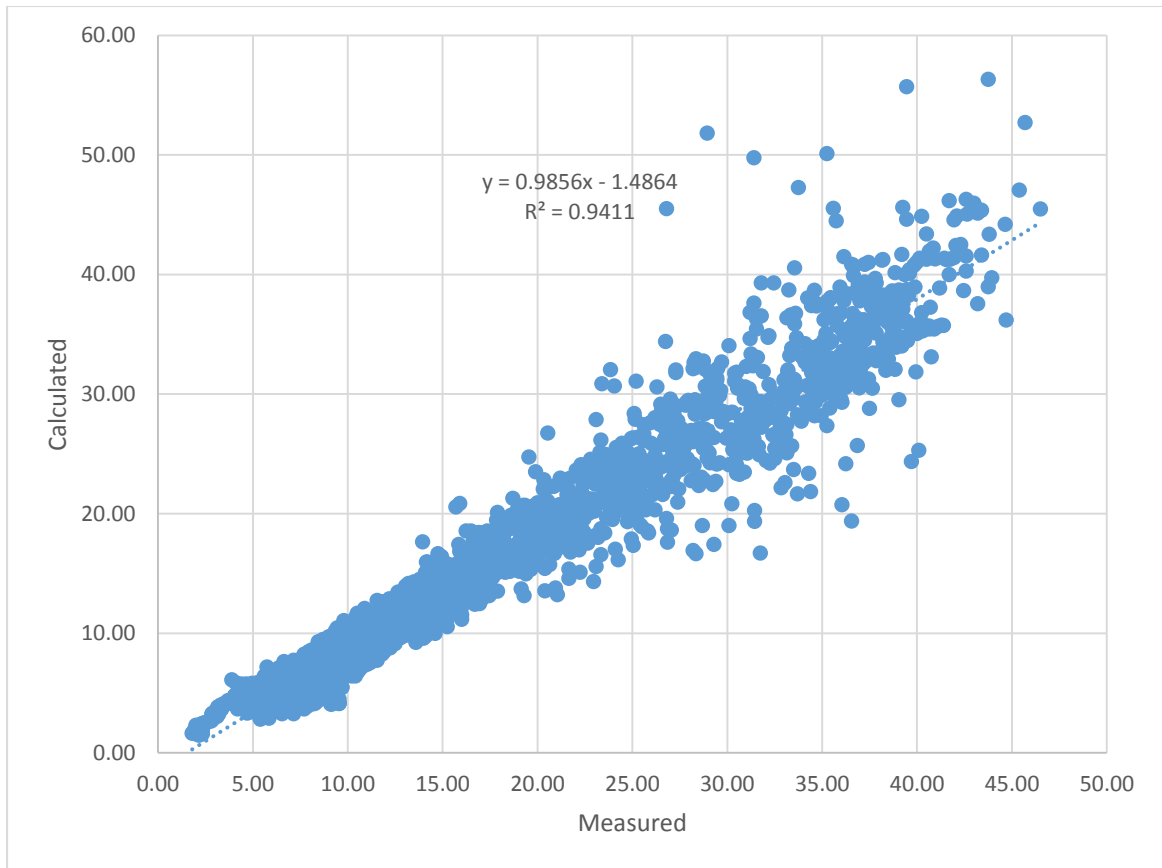


Figure 55 Cell Temperature Results

Table 12 Cell Temperature Model Comparison

Cell Temperature Comparison			
Model	Gradient	Offset	R ²
NOCT	1.0662	0.7332	0.9401
Homer	0.8876	2.303	0.9452
Thermal	0.9856	1.4864	0.9411

These results clearly show the relatively high reliability of the simple NOCT method. Comparing the three methods, we can see the reliability (or R² value) of every method is around 94%. A larger difference can be seen in the gradient, which indicates the average percentage error if we utilise the given method of calculation. Here, the thermal model gives

the best results, corresponding to only a 1.5% degree of error compared to 6.6% for the NOCT model and 11.3% for the HOMER model.

It is proposed that with the inclusion of reliable and high-resolution wind data, the thermal model could be optimised to give even better results than it has done, particularly at higher temperatures when the measured value starts to vary further from that calculated. This requires further study and with the college undertaking wind measurements on site through a meteorological test station being set up, a prime opportunity to further this work.

3.12.3 Cell Efficiency

The cell efficiency differed from the other two quantities since it is not a directly-measured quantity. Efficiency is derived from the power in to and useful power out from a system, in this case solar irradiation and electrical power. Since automatic logging of electrical power was not possible as part of the experiment and manual measurements had to suffice, two problems arose: which method of determining the average power value for the time period to use (as described in Section 3.13.2) and assuring accuracy in the timing of measurements. Thus only a very limited set of data, recorded manually, could be used for evaluating the efficiency model and results for equation 21 are presented in figure 56.

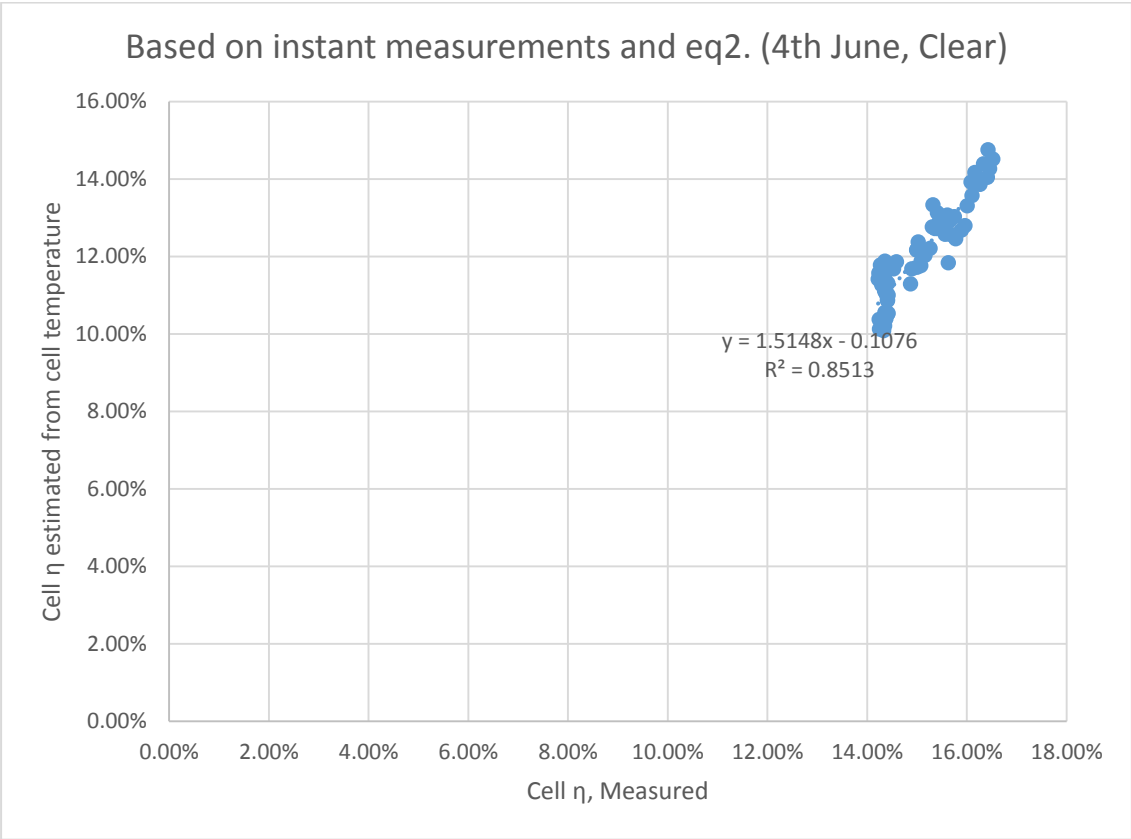


Figure 56 - Clear-Day Efficiency and Cloudy day efficiency

As can be seen in Figure 56, a good correlation is seen over the course of a clear day.

The range over which the measured cell efficiency varied was within the correct range, and had a close concordance to the computed values, as shown in Figure 57. An average efficiency value of close to 16% is observed.

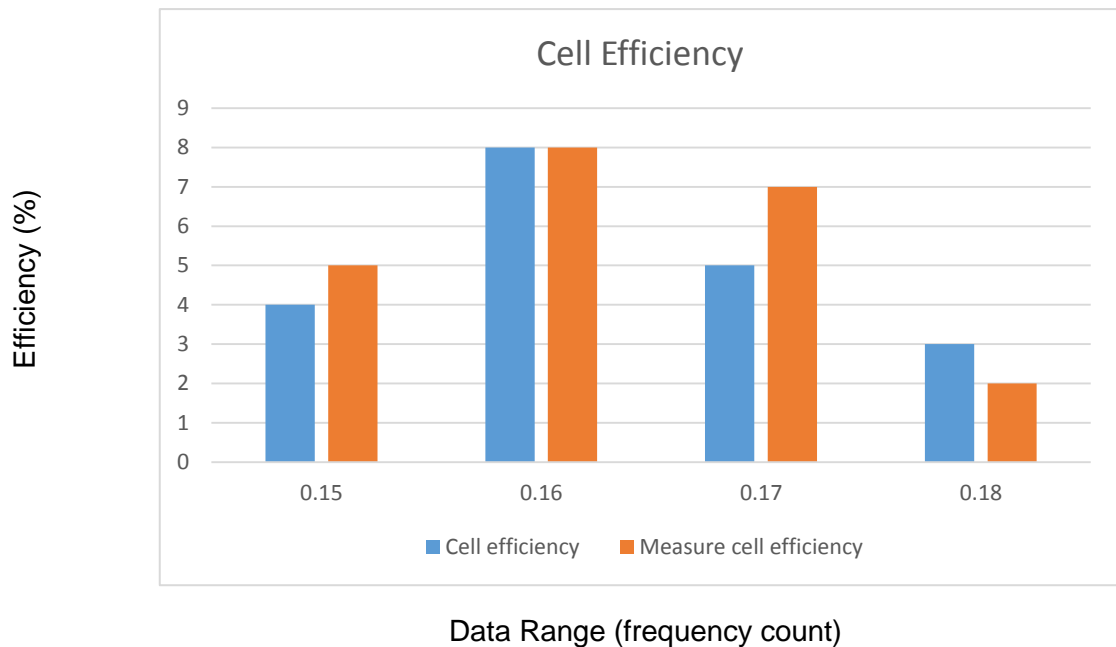


Figure 57 - Cell Efficiency: measured and computed values (note y-axis is the frequency count)

3.13 Experimental Results

3.13.1 Overview

This section presents the numerical data obtained from the experiment. Solar irradiation and flux readings were recorded via the data-logger as voltage levels, and so needed to be converted into meaningful units by use of the sensor sensitivities given in the calibration documents (Appendix B: Datasheets). The thermocouples used for recording air and cell temperature were already calibrated with the data-logger, and so did not require any further conversion. All times displayed are local civil time (LCT), not GMT or solar time, and as mentioned previously (section 3.13.2) each datum represents an average of the value over the previous time period. This was initially set at 10 minutes for the 28th through to the 30th, however was changed to 5 minutes for the remainder of the experiment to allow for greater detail in the data.

Graphs are largely produced by the software developed in excel (see section 3.17) and, due to limitations discussed, formatting is incomplete. Units are given in the figure captions, other information in the accompanying text. Any blank areas in the graphs correspond to missing data, most often due to the downtime caused by data from the data-loggers being downloaded mid- experiment. More detailed research should be undertaken here to acquire more accurate data, with the sign off of contract between SSE and Edinburgh College taking place in July 2018 accurate data analysis can now be undertaken through the data sharing protocol now in place.

3.13.2 Sensor Readings

Shown below and over (tables Table 13 and Table 14), are examples of the output direct from the data- loggers. (These can be seen in greater detail in Appendix A: Data Tables.) The two data-loggers' clocks were off by about 30s; for simplicity's sake the time from the second logger (which recorded both irradiation and temperature) was used. This inconsistency is small in comparison to the 5 or 10 minute period over which the data has been averaged. Clock 2 was checked against atomic clock on first activation (accurate), Inaccuracy is 19% of the sample time this introduced a small error, however quantities are generally slow-changing, Change in alignment is 1.5% of the sample time this was deemed small for this initial study.

Table 13 Data Logger Output

Arm Time	30/05/2013 15:11					Arm Time	30/05/2013 15:12							
Disarm Time	03/06/2013 13:39					Disarm Time	03/06/2013 13:40							
Duration	3 days 22:27:37					Duration	3 days 22:27:41							
Job Description	Job Description					Job Description	Job Description							
Channel Info						Channel Info								
Description	flux1 (V)	flux2 (V)	flux3 (V)	flux4 (V)		Description	p1 (V)	p2 (V)	p3 (V)	t1 (°C)	t2 (°C)	t3 (°C)	t4 (°C)	
Sample Interval	00:05:00	00:05:00	00:05:00	00:05:00		Sample Interval	00:05:00	00:05:00	00:05:00	00:05:00	00:05:00	00:05:00	00:05:00	00:05:00
Logging Interval	00:05:00	00:05:00	00:05:00	00:05:00		Logging Interval	00:05:00	00:05:00	00:05:00	00:05:00	00:05:00	00:05:00	00:05:00	00:05:00
Date/Time	Type	flux1 (V)	flux2 (V)	flux3 (V)	flux4 (V)	Date/Time	Type	p1 (V)	p2 (V)	p3 (V)	t1 (°C)	t2 (°C)	t3 (°C)	t4 (°C)
30/05/2013 15:11	Interval	-0.013375	-0.000388	-0.009126	0.000206	30/05/2013 15:12	Interval	0.003594	0.004878	0.00527	35.3	35.5	16.1	16.2
30/05/2013 15:16	Interval	-0.011042	-0.006603	-0.009986	-0.004846	30/05/2013 15:17	Interval	0.003514	0.004755	0.00514	37.4	37.3	18.3	18.4
30/05/2013 15:21	Interval	-0.010655	-0.00761	-0.008407	-0.0058	30/05/2013 15:22	Interval	0.003512	0.00473	0.005123	36.9	37.1	18.1	18.2
30/05/2013 15:26	Interval	-0.012973	-0.007684	-0.009841	-0.005575	30/05/2013 15:27	Interval	0.003429	0.004811	0.005006	37.4	37.1	15.8	15.8
30/05/2013 15:31	Interval	-0.014497	-0.007748	-0.01248	-0.005912	30/05/2013 15:32	Interval	0.003468	0.004842	0.005061	36.9	36.5	17.1	17.3
30/05/2013 15:36	Interval	-0.012744	-0.007937	-0.009707	-0.005939	30/05/2013 15:37	Interval	0.003591	0.004756	0.005218	37.7	36.8	17.9	18
30/05/2013 15:41	Interval	-0.010958	-0.008311	-0.011474	-0.006961	30/05/2013 15:42	Interval	0.000929	0.001096	0.001255	36.4	35.7	18.3	18.2
30/05/2013 15:46	Interval	-0.009704	-0.008063	-0.007147	-0.006962	30/05/2013 15:47	Interval	0.001177	0.001404	0.001579	28.7	28.7	15.4	15.2
30/05/2013 15:51	Interval	-0.007991	-0.007794	-0.007458	-0.006017	30/05/2013 15:52	Interval	0.000962	0.00117	0.001334	26.8	26.9	16.2	15.8
30/05/2013 15:56	Interval	-0.006499	-0.00764	-0.006363	-0.006463	30/05/2013 15:57	Interval	0.003288	0.004397	0.00482	28.6	28.1	18.1	15.9
30/05/2013 16:01	Interval	-0.00714	-0.00728	-0.00574	-0.005148	30/05/2013 16:02	Interval	0.00347	0.004518	0.005	34.9	33.9	17.9	18
30/05/2013 16:06	Interval	-0.010734	-0.00732	-0.008481	-0.005212	30/05/2013 16:07	Interval	0.001545	0.001992	0.002219	33.2	32.7	16.9	16.8
30/05/2013 16:11	Interval	-0.00794	-0.008234	-0.007294	-0.006471	30/05/2013 16:12	Interval	0.003369	0.004425	0.004873	35.1	34.2	18.5	18.6
30/05/2013 16:16	Interval	-0.010292	-0.007898	-0.008433	-0.005919	30/05/2013 16:17	Interval	0.003746	0.004786	0.005277	37.3	36.4	18.1	18.2

Table 14 Table of Results Extract

Sensor Sensitivities		V/W/m2	0.0000564	0.0000595	0.0000577	0.0000545	0.00000467	0.00000528						
Heat Loss		Irradiance				Temperature								
Date/Time (GMT+1)	Type	flux1 (W/m2)	flux2 (W/m2)	flux3 (W/m2)	flux4 (W/m2)	p1 (W/m2)	p2 (W/m2)	p3 (W/m2)	t1 (°C)	t2 (°C)	t3 (°C)	t3 (°C)		
30/05/2013 15:12	Interval	237.15	6.52	158.16	-3.78	769.6	923.5	949.5	35.3	35.5	16.1	16.2		
30/05/2013 15:17	Interval	195.78	110.97	172.72		88.92	752.5	900.6	926.1	37.4	37.3	18.3	18.4	
30/05/2013 15:22	Interval	188.92	127.90	145.70	106.42		752.0	895.8	923.1	36.9	37.1	18.1	18.2	
30/05/2013 15:27	Interval	230.02	129.14	170.55	102.29		734.3	873.3	902.0	37.4	37.1	15.8	15.8	
30/05/2013 15:32	Interval	257.04	130.22	216.29	108.48		742.6	879.2	911.9	36.9	36.5	17.1	17.3	
30/05/2013 15:37	Interval	225.96	133.39	168.23	108.97		769.0	900.8	940.2	37.7	36.8	17.9	18	
30/05/2013 15:42	Interval	194.26	139.68	198.86	125.89		198.9	207.6	226.1	36.4	35.7	18.3	18.2	
30/05/2013 15:47	Interval	172.06	135.51	123.86	128.11		252.0	265.9	284.5	28.7	28.7	15.4	15.2	
30/05/2013 15:52	Interval	141.68	130.99	129.25	110.40		206.0	221.6	240.4	26.8	26.9	16.2	15.8	
30/05/2013 15:57	Interval	168.42	133.45	110.28	118.59		704.1	832.8	868.5	28.6	28.1	16	15.9	
30/05/2013 16:02	Interval	126.60	122.35	99.48		94.46	743.0	855.7	900.9	34.9	33.9	17.9	18	
30/05/2013 16:07	Interval	190.32	123.03	146.98		95.63	330.8	377.3	399.8		33	32.7	16.9	16.8
30/05/2013 16:12	Interval	140.78	138.39	126.41	118.73		721.4	838.1	878.0	35.1	34.2	18.5	18.6	
30/05/2013 16:17	Interval	182.48	132.24	163.48	108.61		802.1	906.4	950.8	37.3	36.4	18.1	18.2	
30/05/2013 16:22	Interval	134.01	130.34	121.75	108.15		321.6	328.0	351.7	33.8	33.6	17.2	17.3	

Table 14 shows an example of the tabulated results used to produce the graphs in this section, and is derived directly from Table 13. The time (here at 5-min intervals) can be seen on the left, while the data values for each time period can be seen in the table itself. The decoded values, in W/m^2 , were obtained from the following formula:

Equation 22 - Data Conversion

$$Data Value [W/m^2] = \frac{\pm Data Value [V]}{Sensitivity [V/W /m^2]}$$

Equation 22 is used to represent heat leaving the solar module as an absolute value.

3.13.2.1 Solar Irradiation Data Readings

Here, reference will be made to the three solarimeters (or pyranometers) as 'p1', 'p2' and 'p3'. These were the designations used in the data-logger and excel workbook so will be kept for consistency. 'p1' refers to the horizontal irradiation sensor, while 'p2' and 'p3' refer to the sensors in the plane of the solar module. In the plots below, these are represented by green, blue and red- orange lines.

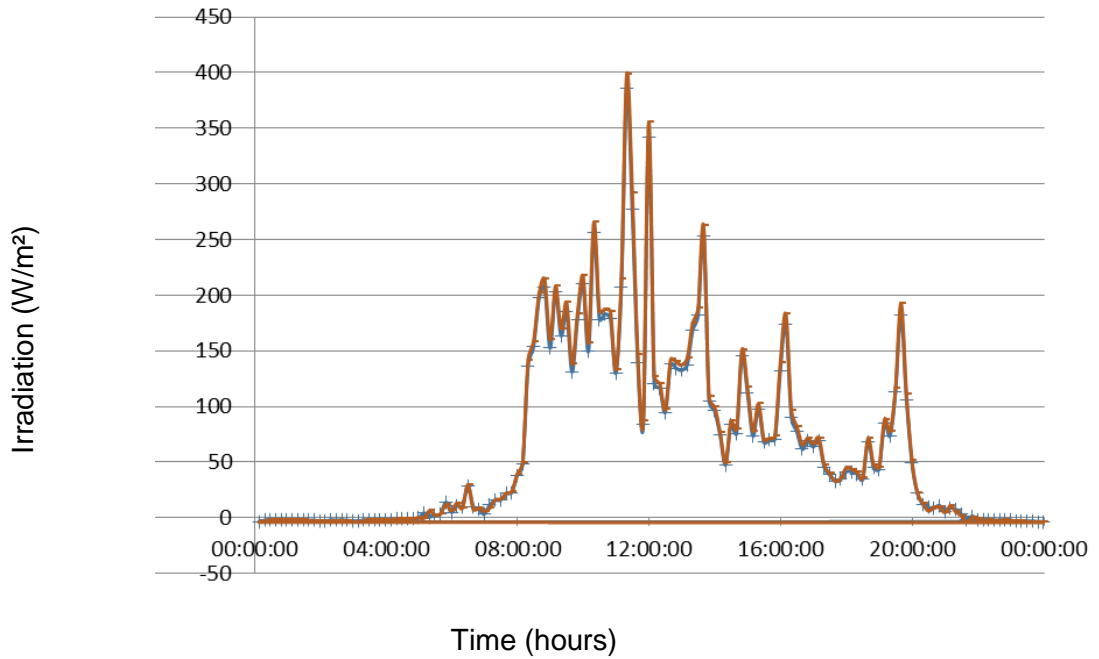


Figure 58 - Example Slope Irradiation Measurements (29th May) (W/m²)

Figure 58 shows an example of a typical, mixed-cloud day. Only p2 and p3, the slope irradiancies, are shown. It can be seen that the sensor values correspond extremely closely; this largely holds true across the days when both sensors were active. Once it was ascertained the slope irradiation readings were accurate, the experiment was completed using one slope solarometer only.

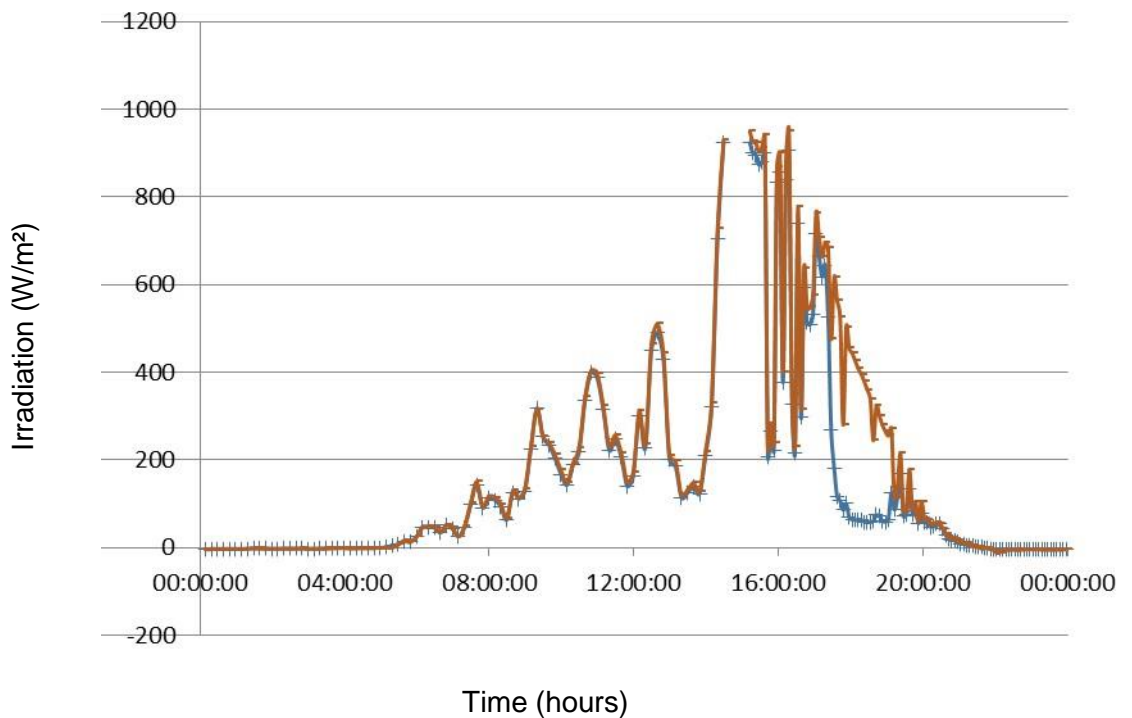


Figure 59 - Slope Irradiation Shading (30th May) (W/m²)

A problem was identified in the setup of p2 and figure 59 (colours as previous), shows the issue by noting the high irradiation due to a sunny afternoon, it can be seen that the output of sensor p2 drops significantly at around 6pm. This is due to the poor relative positioning of sensors p1 and p2 (see Figure 46 in section 3.9.4) where not enough distance was allowed to avoid shading. The effect is not visible on cloudy days, only clear high-irradiation days, but as p3 did not have any similar shading issues the experimental results are not adversely affected by this error. The blank section around 2pm corresponds to the data-loggers being read and reset, as mentioned previously.

Once data had been recorded for a clear, sunny day, it became apparent that the remaining slope irradiation sensor had been poorly oriented towards south (see Figure 60).

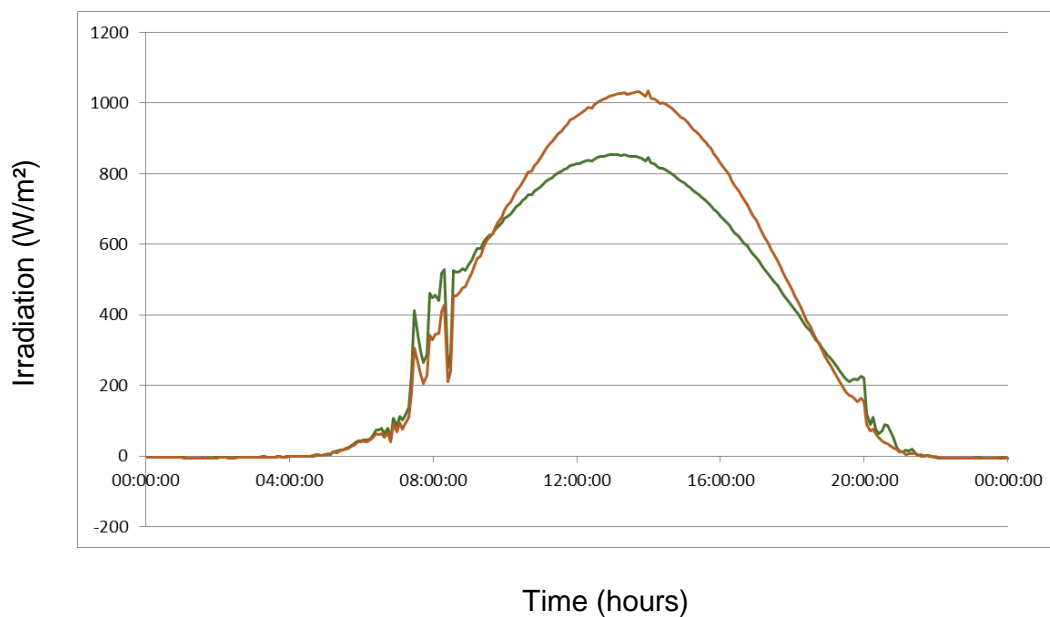


Figure 60 - p3 Misalignment (4th June) (W/m²)

Unfortunately, when setting up the sensors care was taken to ensure the correct inclination, that the sensor was closely aligned with the plane of the solar module, however a mistake was made with the sensor orientation. While variations in intensity between the horizontal and slope sensors align well, indicating there was no error in data handling, the peaks of each graph occur at different times: horizontal at 13:15 and slope at 13:35. This 20 minute inconsistency is caused by the slope sensor facing a few degrees towards the west (a simple calculation of $360/72$ returns 5°).

While the error is immediately apparent from viewing this graph, the same thing cannot be said of the other days recorded, with mixed or heavy cloud. The error will be present throughout the recorded data, but is not likely to be significant as there were few clear-sky periods within the test period. However, in further study more care needs to be taken to ensure that test equipment is set up with better correlation to remove the potential for error. This assumption is borne out by the high correlations between calculated and recorded slope

irradiation (seen in section 3.11), and also the good match between sensor p2 and p3 outputs as reported previously. However, further tests should be undertaken to verify this assumption.

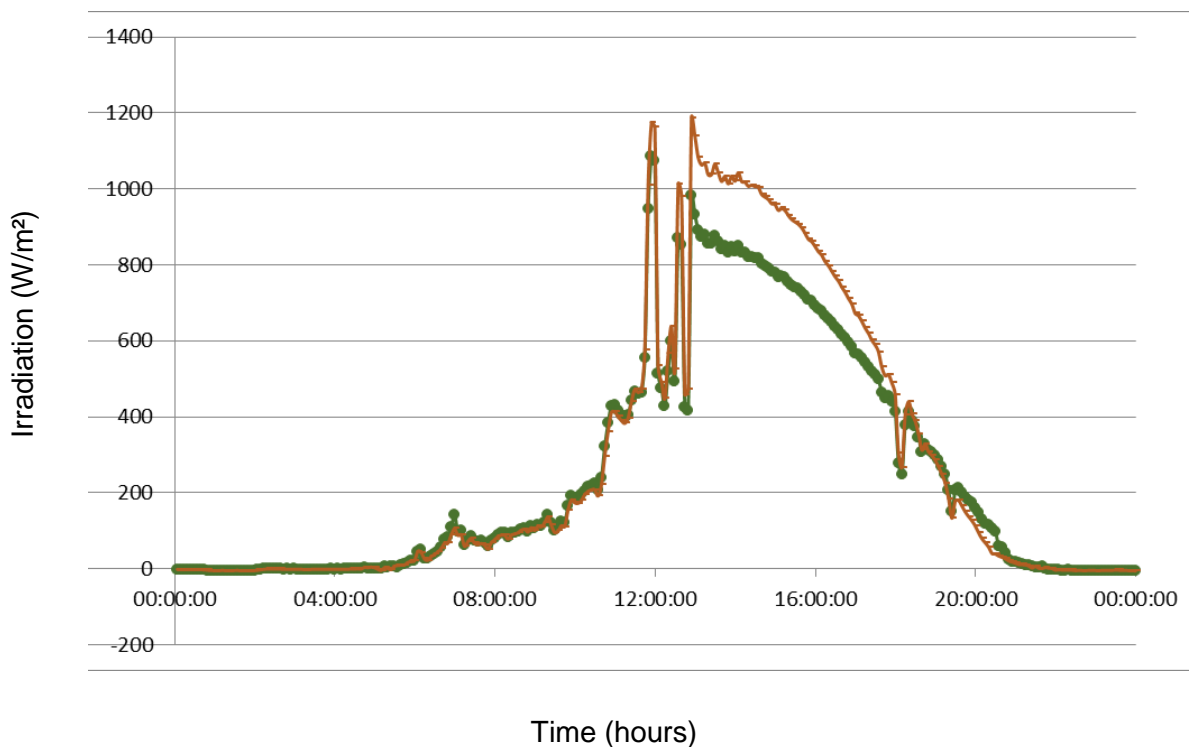


Figure 60 Slope and Horizontal Measurements (6th June) (W/m^2)

Figure 60 shows both p1 (horizontal), green, and p3 (slope), orange, readings for a single day. A number of characteristics may be observed and meet expectations. With heavy cloud, horizontal and slope readings are very similar, with horizontal even a little higher. This is due to the low levels of beam irradiation rendering the angle of incidence between the sun vector and a normal to the collector plane less important, while p1 picks up slightly more diffuse irradiation, being exposed to the whole hemisphere of the sky.

During sunny periods, p2 gives significantly higher readings for much of the day, as it is facing more directly into the sun. This is, in fact, the main reason for positioning solar modules on a tilt. In the evening, this advantage decreases until p1 is actually picking up slightly more beam irradiation in the hour or so before sunset (when the sun is slightly to the north).

There were no possible sources of shading on the horizontal detector and no inconsistencies observed in the recorded data. It is inferred that the horizontal irradiation readings are accurate.

3.13.2.2 Air and Cell Temperature Readings

The temperature readings were made using thermocouple sensors calibrated in the lab (see section 3.12).

The thermocouples were then denoted as 't1', 't2', 't3' and 't4', the first two sensors indicate those measuring the cell temperature from the back panel of the solar module, the second two giving air temperature. The graph shown, in figure 61, corresponds to the same day as previously shown for irradiation readings (Figure 61).

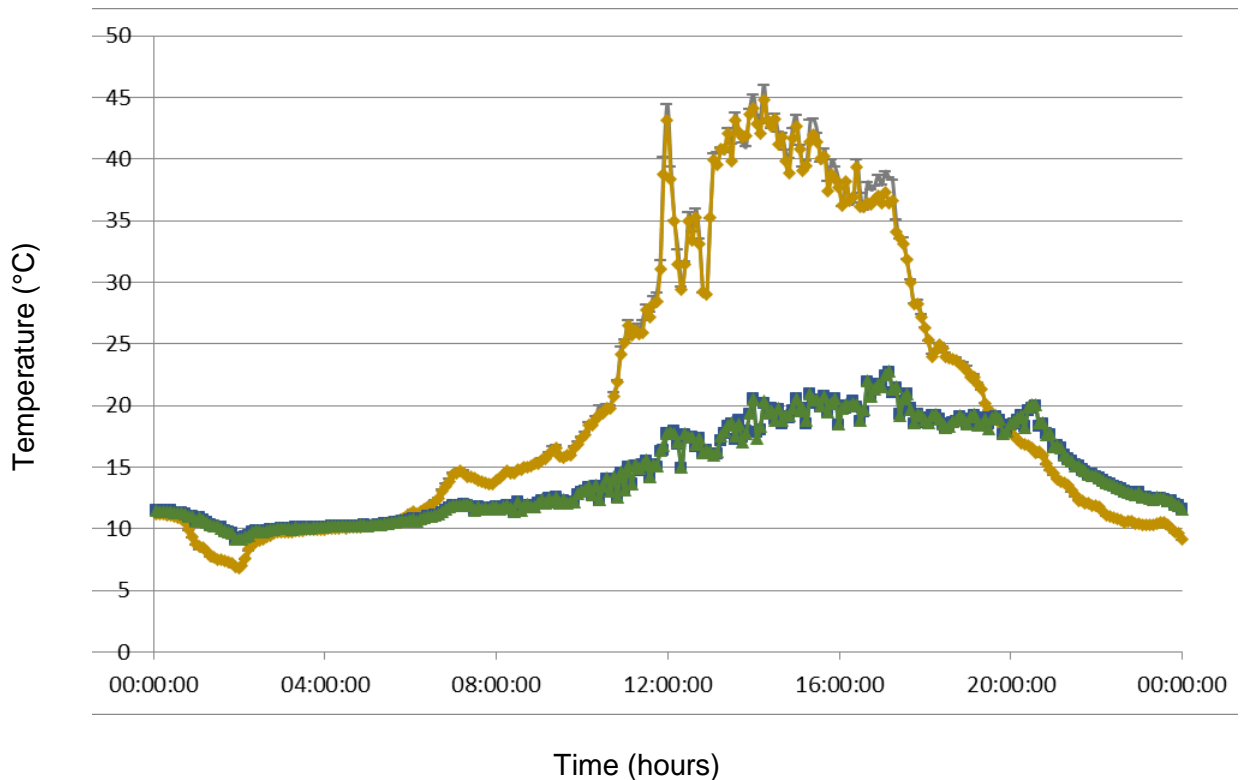


Figure 61 - Thermocouple Temperature Readings (6th June) (°C)

Here, t1 is shown in purple (with dashes), t2 is shown in orange, t3 is shown in blue and t4 in green. Comparing figures 60 and 561 shows a close correlation between the cell temperature and level of solar irradiation measured. The air temperature, meanwhile, shows a much smoother curve, increasing in temperature throughout the day and peaking in the late afternoon. This corresponds to expectations. There is a slight variability between t1 and t2, as these are placed at different locations on the panel; t3 and t4 were intertwined and rarely differ by even as much as 0.2°C.

A few erroneous readings were recorded during the following day (see figure 62), most likely down to poor connection of the termocouples themselves.

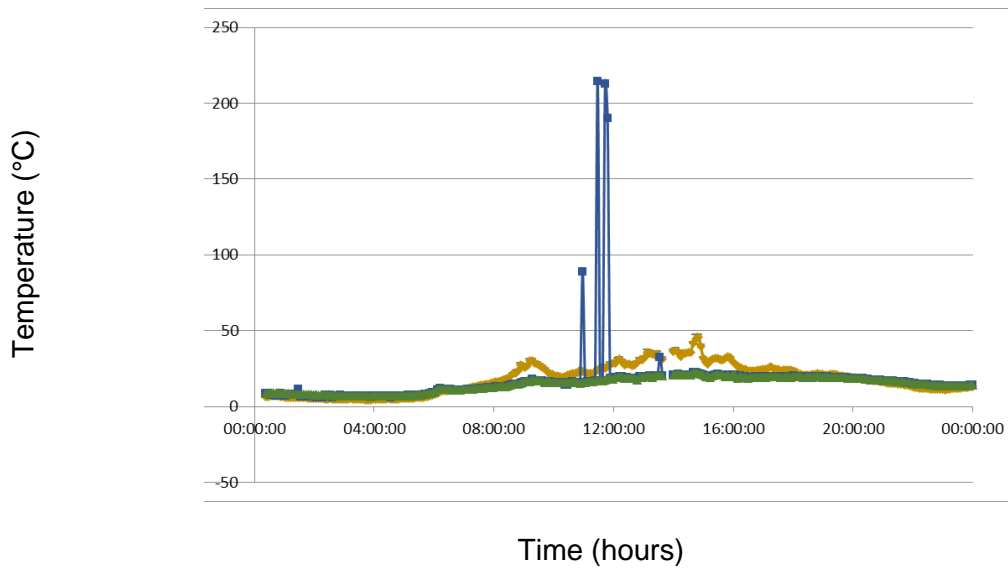


Figure 62 – Erroneous readings in t3 (3rd June) (°C)

Curiously, sensor t3 gave some single readings of over 200°C for this day. It is not known why these values were recorded, however an electrical connection or software issue is likely to be the fault as no physical change in the sensor could cause such a fast temperature change. This magnitude of error was observed on this day only, and on no other. Discounting these few error readings, the remainder of the data from sensor t3 is judged to be reliable.

3.13.2.3 Heat Flux Readings

The heat flux sensors were denoted 'flux1', 'flux2', 'flux3' and 'flux4' and are represented by dark orange, grey, orange and blue respectively.

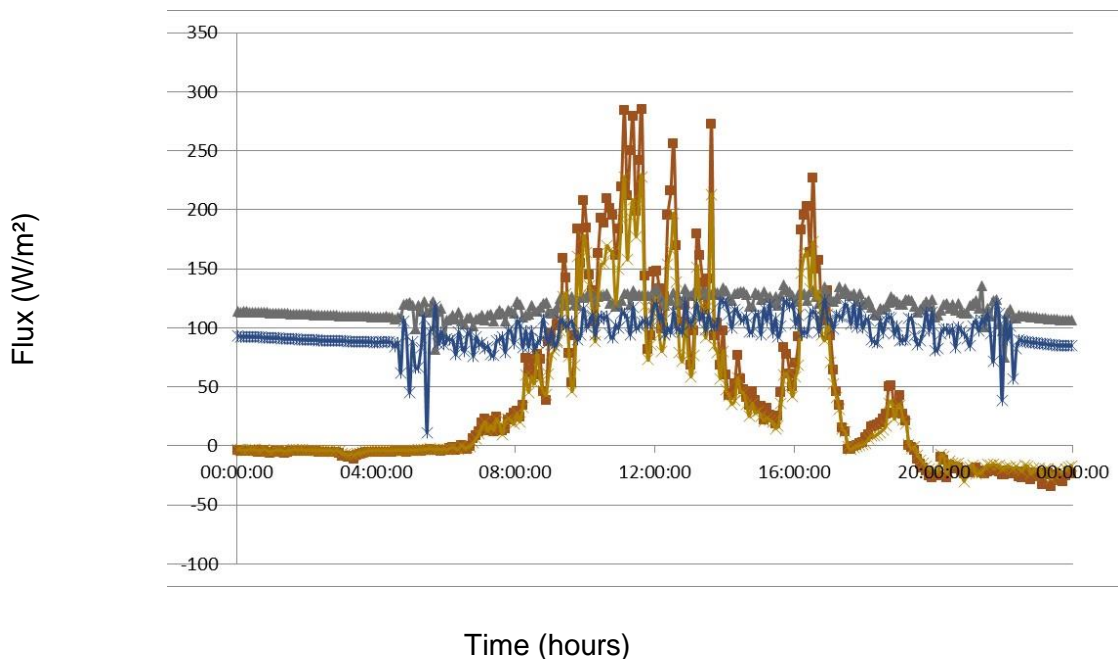


Figure 63 - Example Heat Flux Readings (1st June) (W/m²)

The example day shown in Figure 63 displays most of the characteristics observed across the range of recorded days. Clearly, only two of the sensors are responding correctly. Flux2 and flux4 centre around a value of 100W/m², even into the night, whereas flux1 and flux3 follow the expected trend of high heat loss during the day (relating well to cell temperature) and even slightly negative heat loss at night, where the panel becomes cooler than the surrounding air. No reason to explain the roughly consistent, yet incorrect, operation of flux2 and flux4 has been found, and so these results are excluded from further analysis. A problem likely existed with the sensors themselves, or with the connection to or operation of the data-logger.

Sensor 'flux4' was replaced part-way through the experiment it was judged the instantaneous readings were unreliable. No significant change was seen in the final results, however, which reinforces the hypothesis that there was a problem with the data-logger. The graph below (Figure 64) shows the 30th May, when the change was made:

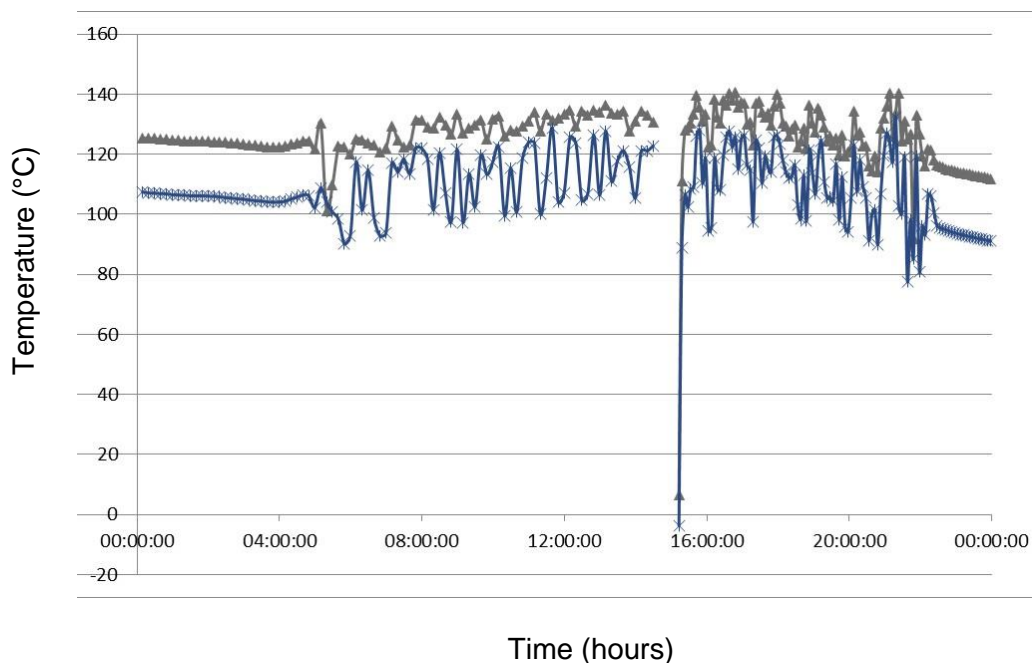


Figure 64 - Change of Sensor Flux4 (30th May) (W/m²)

3.14 Manual Readings

3.14.1 Inverter Power Output

Unfortunately, it was not possible to arrange access to automatically logged power output data from either the inverter in question, or the system as a whole. This was a major setback in the implementation of the project, and not only required alternative solutions to be found, but limited the applicability and accuracy of the results of the experiment. Only three days of manual readings were taken, and the whole-system power output could only be inferred. The

College and SEE have now agreed on contract specifics and access to inverter data is now available. This will allow for analysis of 6 years' worth of inverter data, further study is required in this area.

As the power output of the module being measured was a critical data value, it was decided to go on-site and take the appropriate readings directly from the display screen of the inverter that the module was connected to. This was done for three consecutive days, the 3rd, 4th and 5th of June. Readings were taken every 5 minutes to correspond with the data-logger period, however there was no way to ascertain the exact sampling time, so there is a small inconsistency between the manual reading times and the data-logger times. This will introduce a source of error in later results using output power.

Table 15 Extract of Manual Inverter Power Readings (4th June) (Accuracy of displayed value)

Date:	04/06/2013							
	Inverter 15						Inverter 16	
Time:	P1/kW	P2/kW	P3/kW	E-day/kWh	V/V	I/A	P/kW	E-day/kWh
09:30	11.66	11.65	11.65	18.1	577	20.6	11.75	18.3
09:35	11.94	11.92	11.93	19.4	572	21	12.03	19.5
09:40	12.18	12.16	12.14	20.2	572	21.6	12.03	19.5
09:45	12.36	12.36	12.38	21.1	570	22	12.42	21.4
09:50	12.68	12.69	12.69	22.5	570	22.6	12.67	22.7
09:55	12.84	12.86	12.87	23.3			12.87	23.5
10:00	13.12	13.13	13.15	24.4			13.16	24.6
10:05		13.3	13.31	13.31	25.6		13.34	25.8
10:10	13.53	13.54	13.53	26.6			13.6	26.8
10:15	13.76	13.76	13.76	27.8			13.81	28
10:20	13.98	13.98	13.98	28.9			14	29.1
10:25	14.17	14.17	14.17	30.1			14.21	30.3
10:30	14.31	14.32	14.32	31.3			14.38	31.5
10:35	14.53		14.5	14.52	32.6		14.56	32.8
10:40		14.7	14.7	14.7	34		14.78	34.2
10:45	14.73	14.75	14.76	35			14.82	35.2

In Table 15, clock time (LCT) is shown on the left; this was checked and synchronised each day to the atomic clock website. Three instantaneous power readings were taken from the inverter fed by the module being measured (inverter 15), one 10s before the time shown, one during and one 10s after. Following this, the remaining values were taken consecutively, as

quickly as possible. These correspond to the total energy produced by the inverter so far that day, the voltage and current levels, and lastly the power and energy levels from an adjacent inverter (inverter 16), for comparison. Voltage and current values were only recorded for the whole of the first day, and were not used in later calculation.

There is a degree of inaccuracy in the reading time shown. For a subset of the data, 6.8%, the actual reading time was up to 90 seconds after the time shown. This was due to mistakes made during the manual readings, predominantly lapses in concentration, and introduces a further (although not severe) source of error into the results. Better use of technology, such as a time lapse cameras, is proposed for use in further study to avoid inaccuracies and the potential for cumulative errors occurring.

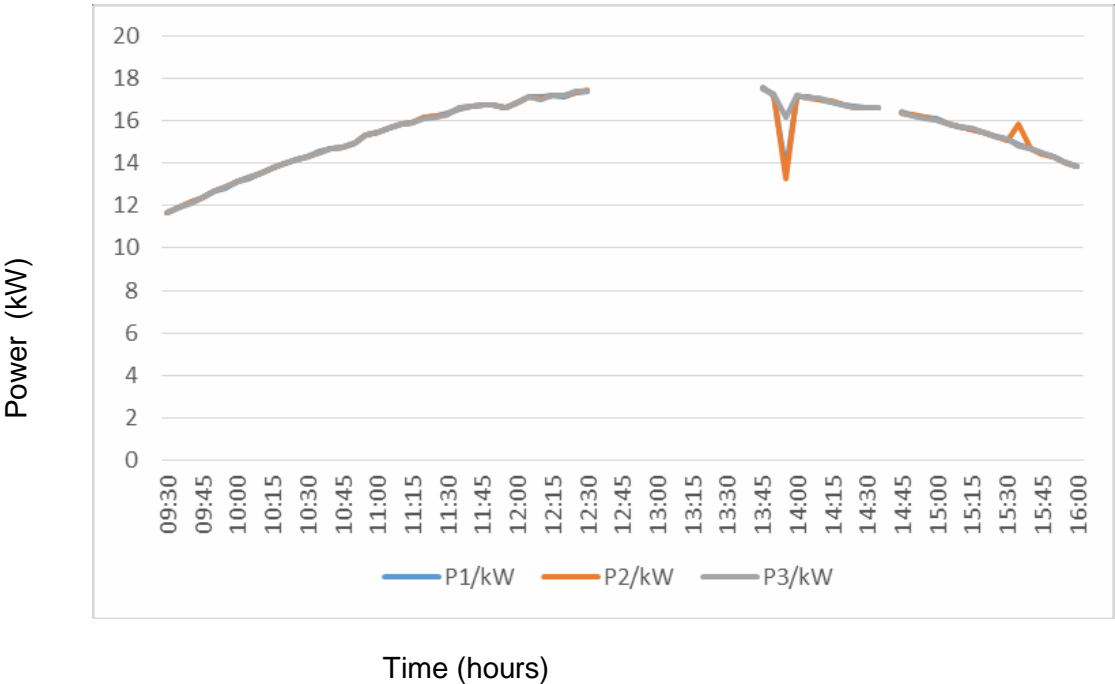


Figure 65 - Inverter 16 Power Readings (4th June)

Figure 65 plots the three power values recorded for inverter 15 for the same day as the tabulated data. They correspond extremely well due to the slow change in inverter output, and are so likely very close to the correct value of power output.

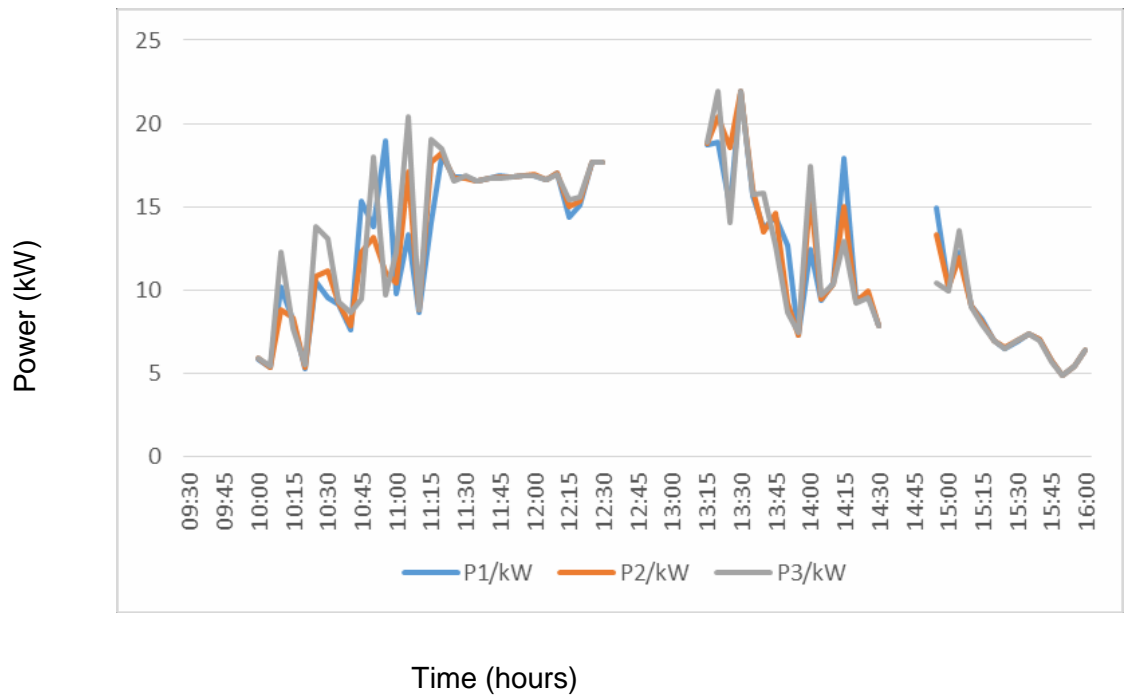


Figure 66 - Inverter 16 Power Readings (5th June)

Figure 66, on the other hand, shows results from the 5th, a much cloudier day. Here, due to the high variability in power output, the power readings differ significantly even over the 20 second reading period.

The power value to be carried on from this data was determined in two ways: as the average of the three power readings, and as the difference in total energy from the previous sample over the time period of 5 minutes (see section 3.17.1).

3.14.2 Inverter kWh output

Further data collection was undertaken to review kWh production per inverter. Due to the lack of available data direct from inverter, manual collection was undertaken. On a daily basis, readings were collected from the 32 inverters each morning and evening. This gave or daily energy production per inverter per day. This data was collected over a period of 3 months, November through January. Figures 67 and 68 have been produced for November and January due to more data collected (an outage in December meant limited data was secured).

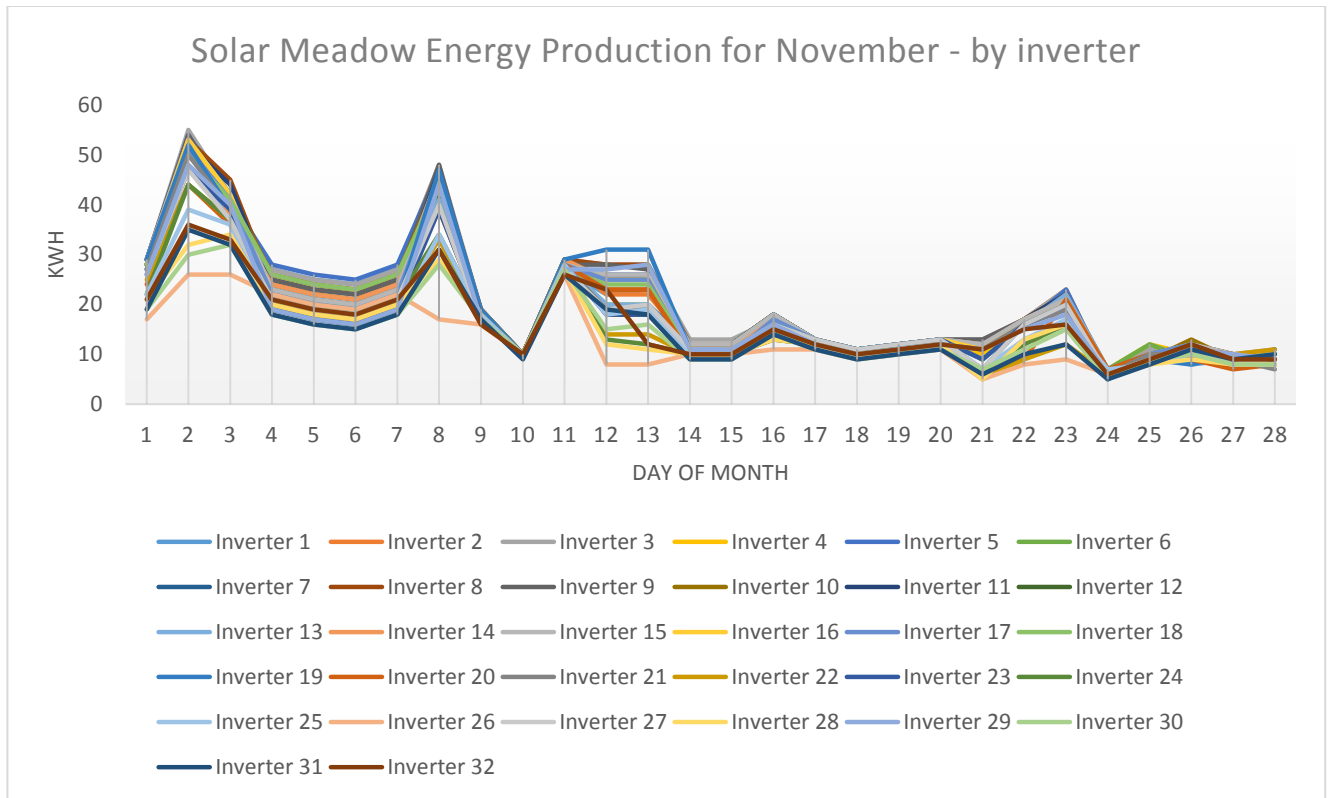


Figure 67 daily energy production chart for the month of November

As can be seen from figure x, a variation in production across the inverters can be viewed. On better days, the best and worst producing inverters can be out by a factor of 2. This is a sizeable variation, which supports the argument of their being significant shading affecting the meadow.

On days where the energy production values are lower (such as day 18), the range across inverters is much lower. The difference between best and worst inverters was 2 kWh, a difference from the 25 kWh seen in the better days at the start of the November.

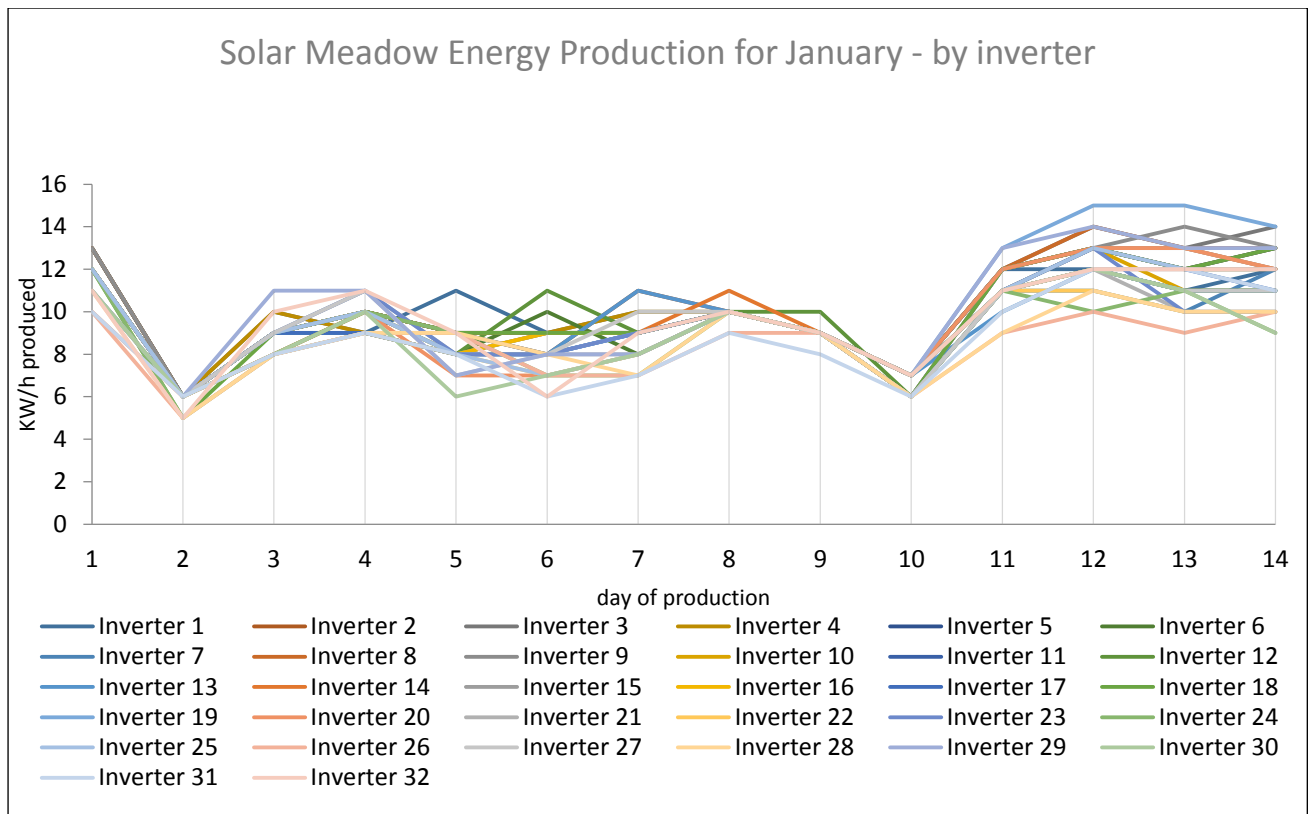


Figure 68 daily energy production chart for the month of January

January provided lower production figures over the course of the month than November, though this is much as expected, due to occurring just after the shortest day of the year, and the sun being lower in the sky for longer periods of the day.

Similarly to November, the variation over the course of the day across January is a small range between inverters.

Through the data collected from both months, we can see there is a difference between the inverters at the front of the meadow (numbers 1-6) and those at the rear side of the meadow (28-32). This supportive finding of the assumptions made by SSE, that the sight will have little impact from shading, led to further study as outlined in chapter 4.

3.14.2 Overall System Output

In addition to individual inverter readings, at the start and end of each day the total energy produced by each inverter was recorded, in order to get a better picture of the whole system performance. Recording the data took around 5 minutes from start to finish (sometimes longer) as the site is relatively large and so the timing was manually recorded as data was collected. Table 16 shows the kWh readings from each inverter across the entire site (1-32).

Table 16 Daily Inverter Totals (condensed)

Date:	03/06/2013	04/06/2013	04/06/2013	05/06/2013	05/06/2013
Order:	32->1	1->32	32->1	1->32	32->1
Time:	16:19	09:20	16:05	09:57	16:04
Inverter	kWh	<u>kWh</u>	<u>kWh</u>	<u>kWh</u>	<u>kWh</u>
32	59.1	16.8	97.7	13.7	75.5
31	58.5	16.75	97.7	13.5	75.1
30	59	16.5	97.6	13.5	75.3
29	59.4	16.6	97.3	13.7	75.6
28	59.9	16.4	97.7	13.5	75.6
27	59.3	16.2	96.8	13.7	75.8
26	61.2	16.2	122.6	13.6	90.9
25	60.5	16.3	123.4	13.4	90.6
3	63.5	15.2	124.6	13.2	93.1
2	63.5	14.8	123.9	13.1	93
1	63.5	15.1	124.7	13.1	93.2
Time:	16:31	09:16	16:10	09:51	16:11

The second line of Table 16 shows the order in which readings were taken, starting from inverter 1, or from inverter 32. While there is some variation to be seen, the data is mostly consistent across the site (taking the time difference into account). It is judged that by extrapolating the data of inverter 15 to the whole site will give a reasonable approximation to its performance.

However, significant differences can be seen in the afternoon outputs of inverters 27-32 only. These are situated at the south end of the site, and so it was initially hypothesised that there could be some shading issues with these strings. This was quickly abandoned as shading should be a factor in the morning, not in the afternoon when the sun is high, and would be unlikely to cause such a large drop in system output across the day unless it was severe.

The second cause considered was that these inverters were fed by smaller numbers of panels, contrary to the site string plan. Consistent morning values would have to be explained away by assuming these strings over-performed during this period for some reason, rendering this explanation unsatisfactory.

Alternatively, 1 out of the 4 strings connected to each of these inverters could have been faulty (outputs can be seen to have dropped by roughly a quarter). The fact that only afternoon levels showed a differentiation and that this was almost non-existent on the first (cloudy) day pointed to a problem which only manifested at high outputs/temperatures. A wiring problem, perhaps cable overloading at high power outputs, was considered as a cause.

Finally, in a meeting with Scottish and Southern Energy on the 2nd of July, it was found that this problem had been identified by them and they were working to fix it. The inverters in question had been supplied with the wrong type of cable ends, limiting their power output to 12.5kW, rather than the full 20kW of the remaining inverters. This explains the inconsistencies observed in the data.

3.15 Derived Quantities

A large number of quantities were derived in a range of ways from the sensor and manual data, coupled with solar calculations based on the date, year and time of day. In deriving certain quantities an element of potential inaccuracy is introduced in to the results. Had explicit data been available directly from the source, the accuracy of the data have been improved. This will warrant future data collection once agreement and contracts have been signed between the College and SSE. The data sharing protocol and contract were agreed in late 2018 and further data analysis should now be undertaken in through further study. Some of the principal results are related here.

3.15.1 Module Power Output

Two methods were used to determine the module power output, a value required to determine the cell efficiency. Module output was assumed to be equal to 1/80 of the inverter output. This approximation neglects losses between the modules and the inverter, and the inverter efficiency.

A comparison between inverter power determined from instantaneous readings (highly variable on cloudy days) and energy readings (low decimal accuracy) follows (Figure 69). The derivation of these values is explained in section 3.14, and in more detail in section 3.15. Instantaneous readings are shown in dark orange, averaged readings in light.

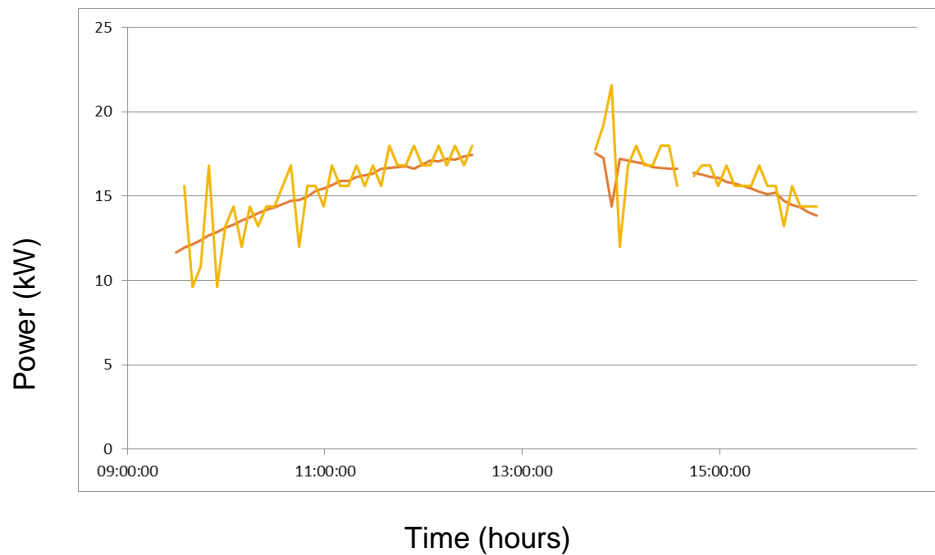


Figure 69 Inverter 15 Output, Instant vs. Averaged (4th June) (kW)

From the smoothness of the graph, and a visual correlation with the irradiation levels (shown in Figure 60), it can be inferred that the instantaneous power readings are relatively good. This is to be expected, as the main problem with this method is that power output can change dramatically from second to second, does not apply on clear-sky days.

The averaged readings, on the other hand, show significant fluctuation around the ‘correct’ value. This fluctuation is caused by two factors: the low resolution of the energy data (0.1kWh) and the inaccuracy in time of measurement.

Figure 70 shows the same data, but with instantaneous power plotted against averaged power. Again, the low resolution of the averaged-power value can be clearly seen with the fluctuation apparent in figure 70, this is a result of the energy data resolution and the inaccuracy in the time measurement. The correlation between results is poor.

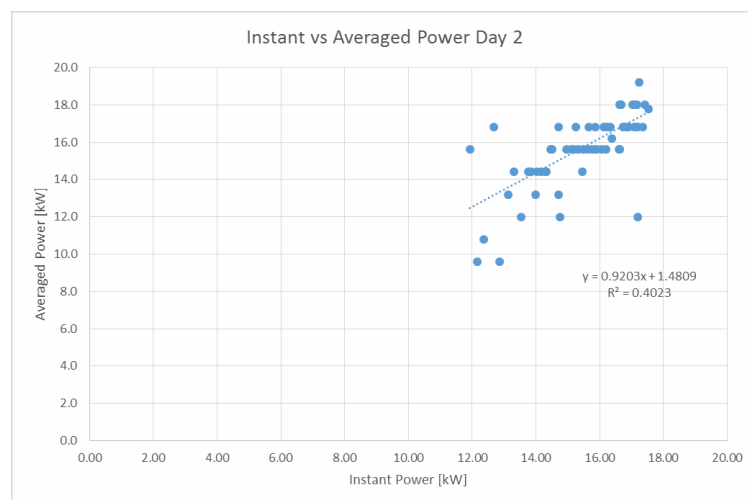


Figure 70 Instant vs Averaged Inverter Power Output (4th June)

This situation is not exactly reversed, but is quite different on the other days measured, when there was significant cloud cover and highly variable irradiation levels.

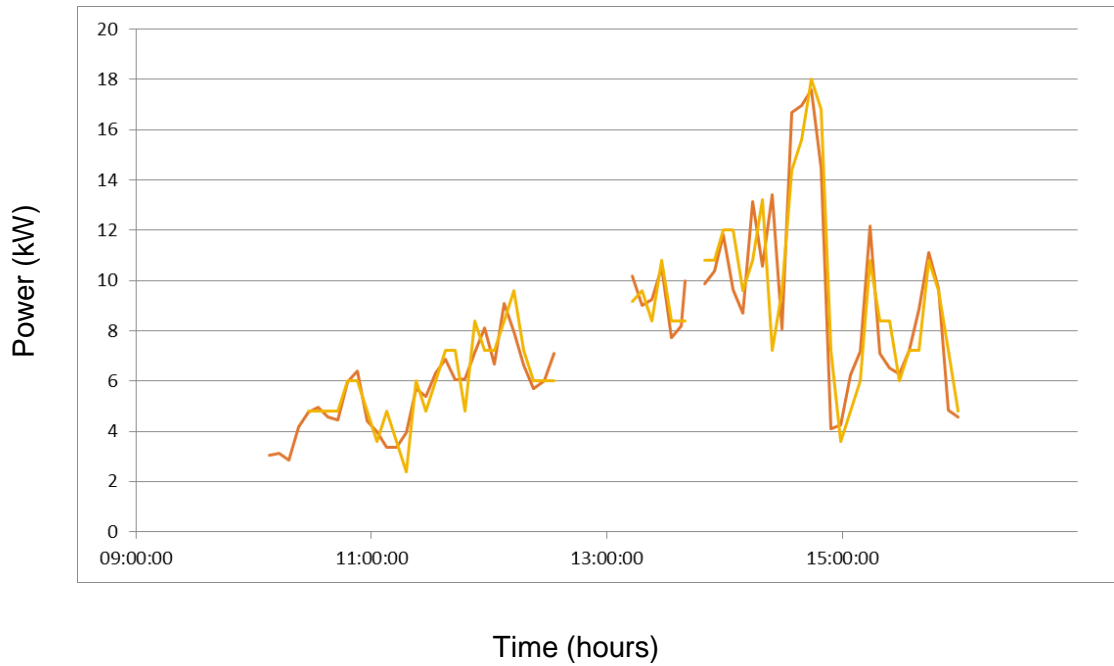


Figure 71 - Inverter 15 Output, Instant vs. Averaged (3rd June) (kW)

It can be said that on a cloudy day, both methods are comparable (Figure 71). The actual average value of power output over the time period in question is unlikely to correspond well with the instantaneous power reading due to the high variability. However, the averaged value still exhibits the low quantisation and fluctuation problems highlighted earlier. This creates a problem for quantifying an accurate cell efficiency for use later in the project. The instant vs average chart, similar to that shown previously, for the 3rd of June is shown below (Figure 72).

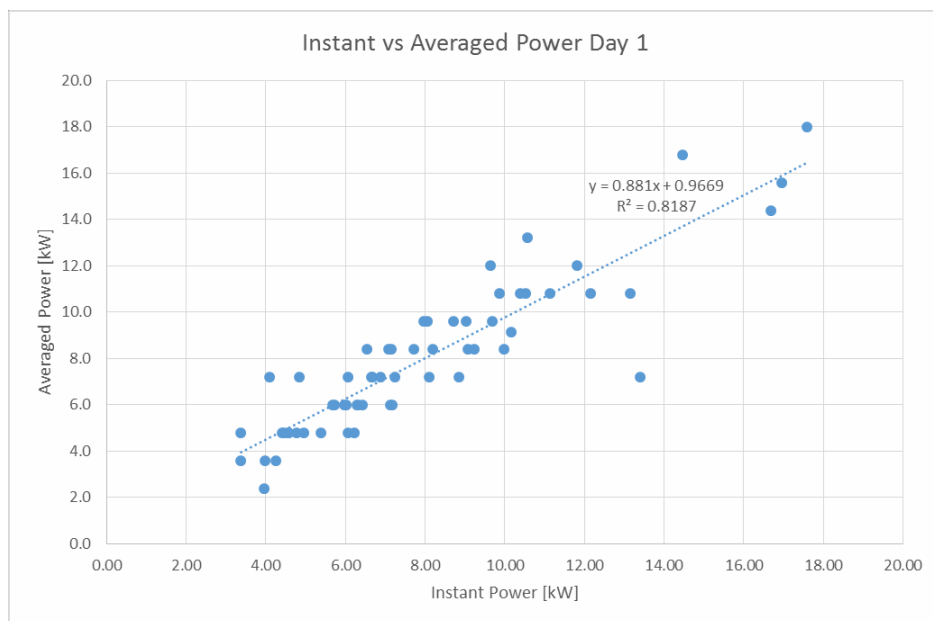


Figure 72 - Instant vs Averaged Inverter Power Output (3rd June)

3.15.2 Energy Balance

As covered earlier, the energy balance of the solar module could be used to determine the expected cell output, and cell efficiency. However, the problems encountered with the heat flux sensors and their resultant data streams (see section 3.13.2) made it unlikely that this approach would give good quality results.

This assumption is borne out in the following comparison of results (Figures 73, 74 & 75). The cell efficiency calculated from the heat flux readings is plotted in grey.

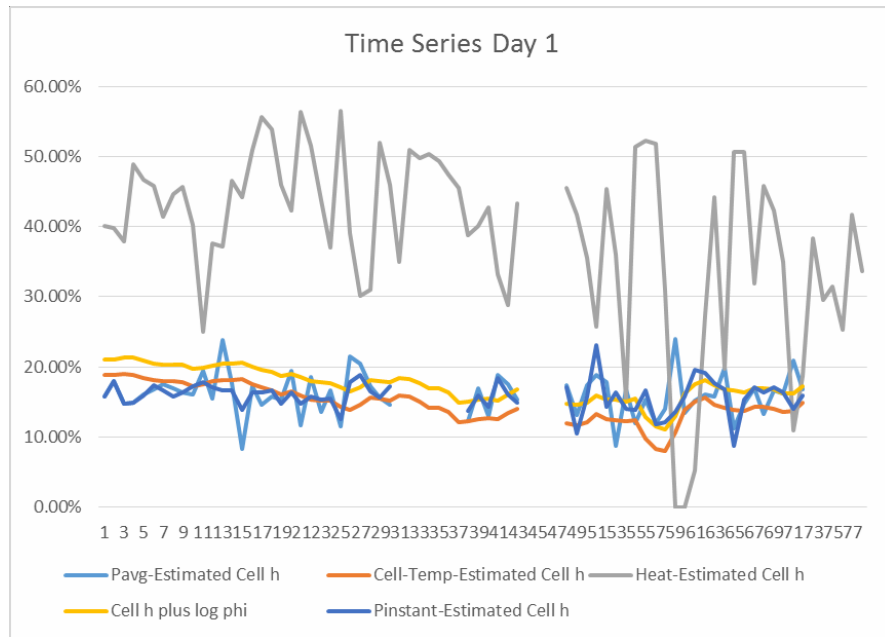


Figure 73 -Time Series of 5 Different Measures of Cell Efficiency (3rd June)

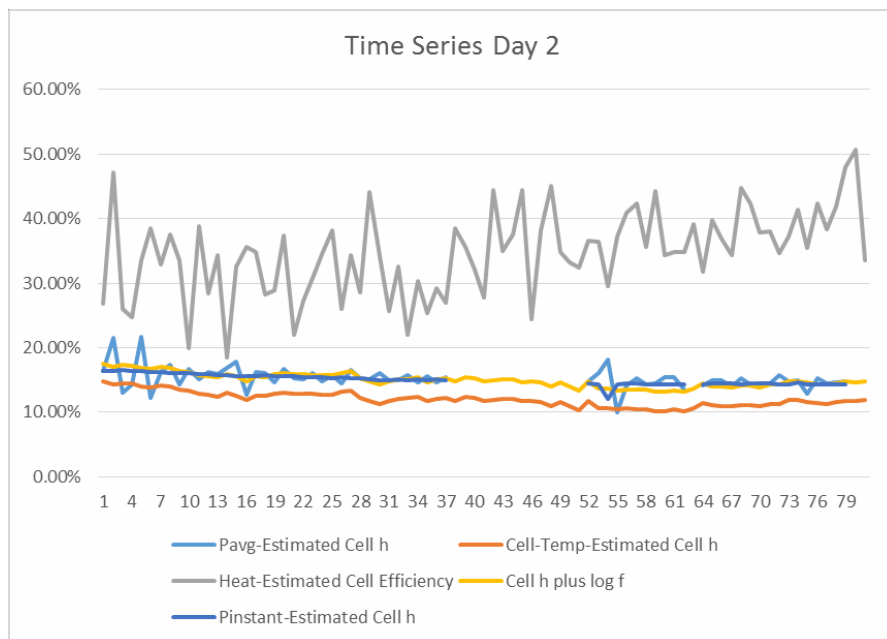


Figure 74 - Time Series of 5 Different Measures of Cell Efficiency (4th June)

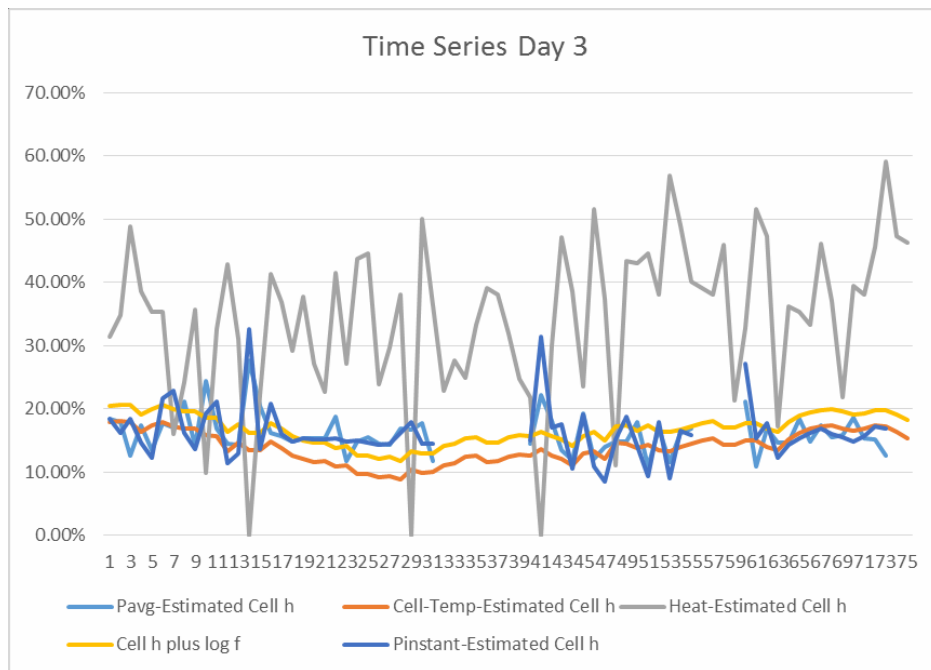


Figure 75 - Time Series of 5 Different Measures of Cell Efficiency (5th June)

It can be concluded that the flux measurements taken, or the method used for interpreting them, are insufficient to produce a reasonable estimate of either the energy output of a cell, or the relative cell efficiency. The calculation method was re-checked to ensure the error did not lie within this method, the same results were identified. Improvement is required to the way the heat flux readings have been collected to improve the dataset in future.

3.15.3 Measuring Correlation

To determine the accuracy of any type of calculation against measured data, a consistent and reliable method of quantifying this correlation is required. As used by Aldali et al. (2013), Clarke et al. (2007) and Mattei, et al. (2006), a linear equation and measure of R² (the coefficient of determination) was obtained, the line in this case being produced by Excel's built-in graph-plotting software. While the line equation indicates the difference in absolute terms between the measured and calculated values (a gradient of 1 and zero offset shows a perfect match), the R² value indicates how dependent one value is on the other (a value of 1 indicating maximum dependence, or correlation).

3.15.4 The Slope Irradiation

The measurement of slope irradiation was relatively simple and reliable, as the use of a professionally calibrated pyranometer aligned to match the slope and orientation of the solar module in question should have given an accurate reading with which to check the calculated values against. However, as explained in section 3.11.1, the method of calculating the slope irradiation from only the horizontal global irradiation is not so simple, and requires a number of different steps and intermediate quantities. Regardless, it was

expected that the calculation accuracy would be relatively high, as has been demonstrated in the papers presenting the methods used (Aldali, et al., 2013) (Clarke, et al., 2007).

3.15.5 Results

The correlation of the best calculated value (using a seasonal equation) against the measured is shown below (Figure 76).

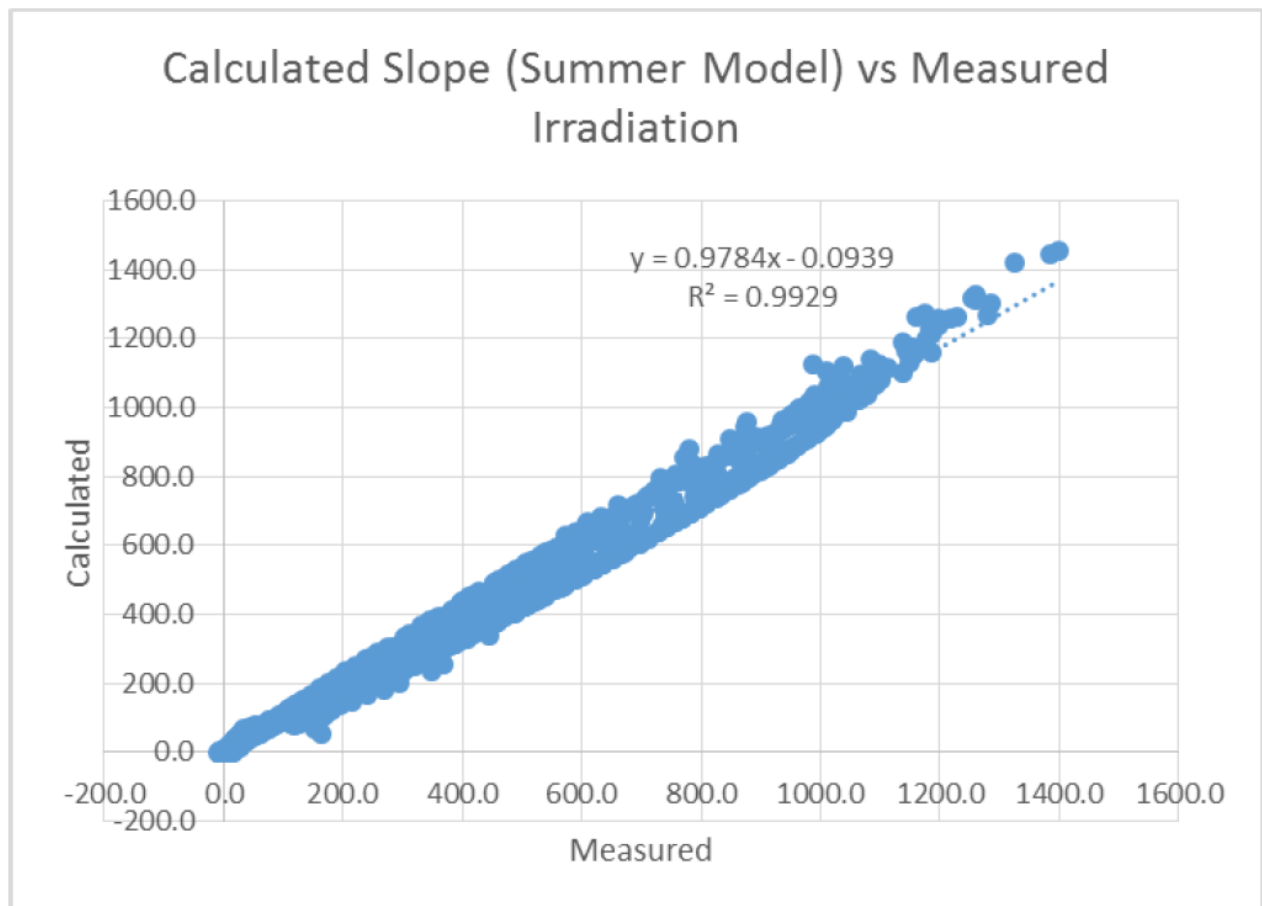


Figure 76 Summer Model vs. Measured Irradiation (W/m²)

It can be seen that figure 76 shows an excellent, almost entirely linear, correlation for the site studied, beyond even the high accuracy expected. This is even more surprising when considering the small sources of error in slope irradiation data collection as discussed previously (section 3.13.2). The small impact on accuracy due to the misalignment is attributed to the fact already proposed, the short duration of entirely clear weather during the period of the experiment. While this is purely speculative, the misalignment error could be the cause of the slight hysteresis visible on the plot.

3.15.6 Model Comparison

Three alternative methods, two proposed by Clarke et al. (2007) and one by Muneer et al. (2000) as discussed previously, were also used to obtain similar results. A comparison of the four model outputs is shown below (Table 17).

Table 17 Model Correlations with Measured Irradiation

Period 1 Averaged			
Model	Gradient	Offset	R ²
Summer	0.9926	1.3145	0.9948
June	0.9927	1.363	0.9948
Muneer	1.0063	0.7338	0.9946

Period 2 Averaged			
Model	Gradient	Offset	R ²
Summer	0.9784	0.0939	0.9929
June	0.9761	0.3164	0.9929
Muneer	0.9738	0.405	0.9897

While all four methods show a high degree of accuracy, as expected the calculations optimised for the given location give slightly better results. The difference between using the seasonal and monthly models follows the assessment in Clarke et al. (2007), namely that the increased complexity of using monthly coefficients (as in the June model) in a project gives a low return in increased accuracy (in this case, little to none).

3.15.7 The Cell Temperature

The cell temperature was again calculated using a range of methods (as detailed in section 3.11.2), the simple but widely-used NOCT or nominal operating cell temperature model, the slightly more complex one used in the HOMER software, and finally the full thermal model. It was expected that each would give successively better results, with the thermal model being significantly more accurate than the other two due to the consideration of a greater number of factors. Graphs and tabulated results are shown below (figures 77 to 80), and Table 18). As before, 'Period 1' refers to the first two days, while 'Period 2' refers to the remainder of the data recording period. Only one example of period 1 data is given, the larger sample size of period 2 should give clearer results.

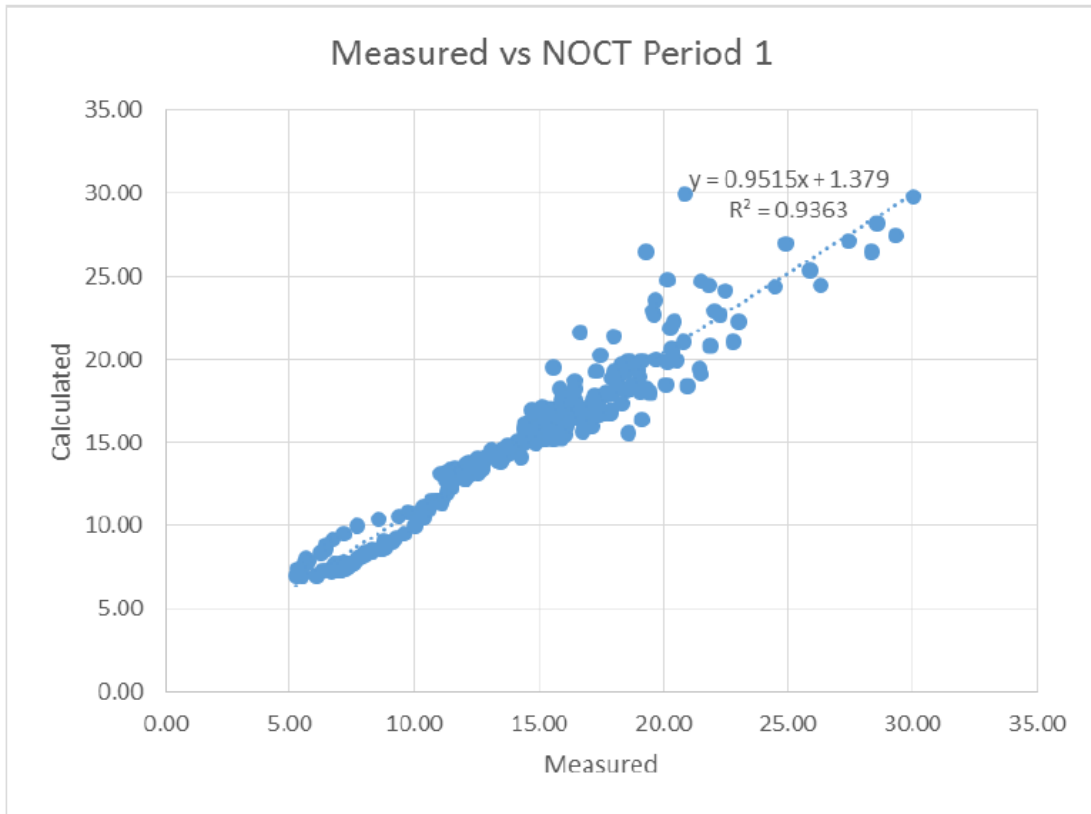


Figure 77 Measured vs. NOCT-Calculated Cell Temperature during Period 1 (°C)

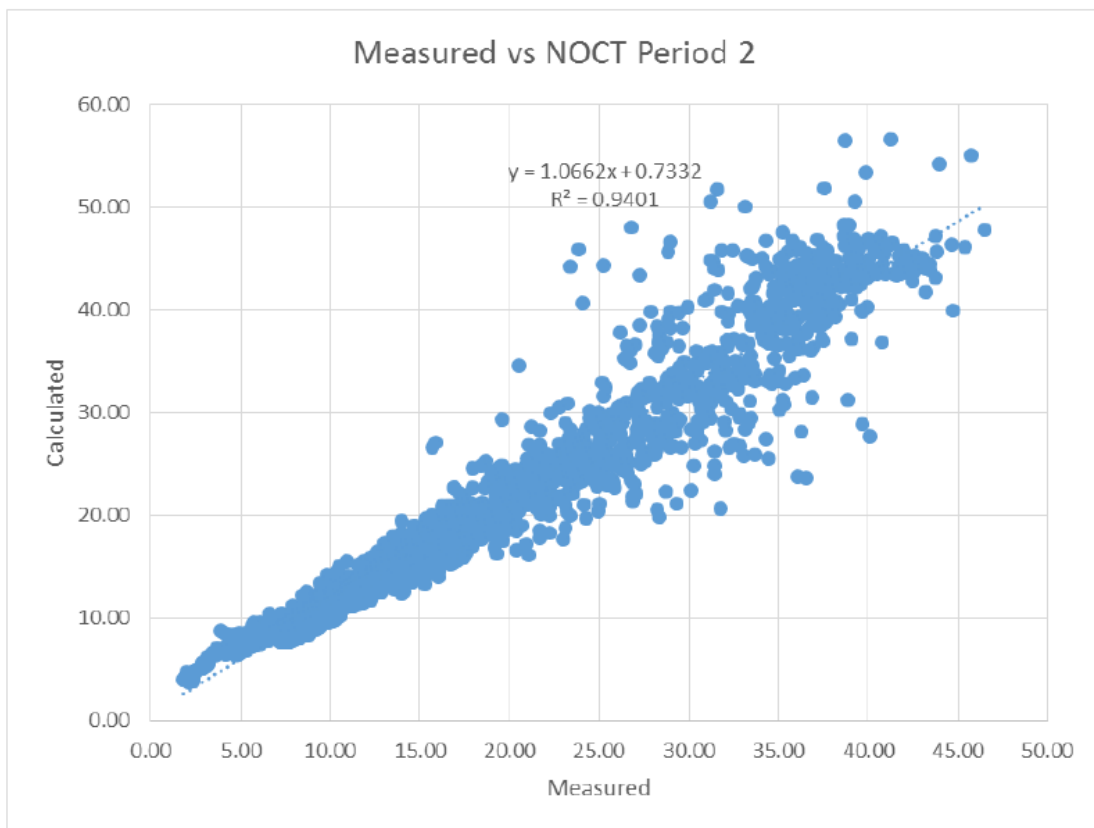


Figure 78 Measured vs. NOCT-Calculated Cell Temperature during Period 2 (°C)

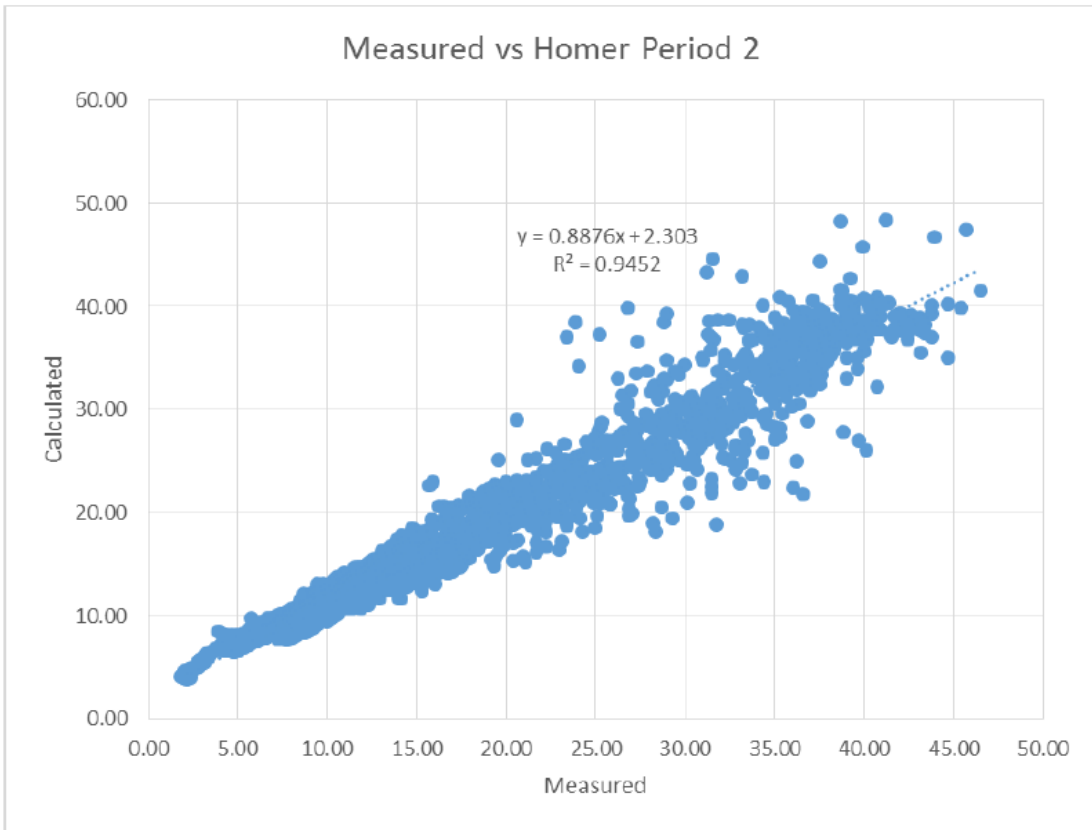


Figure 79 Measured vs. Homer-Calculated Cell Temperature during Period 2 (°C)

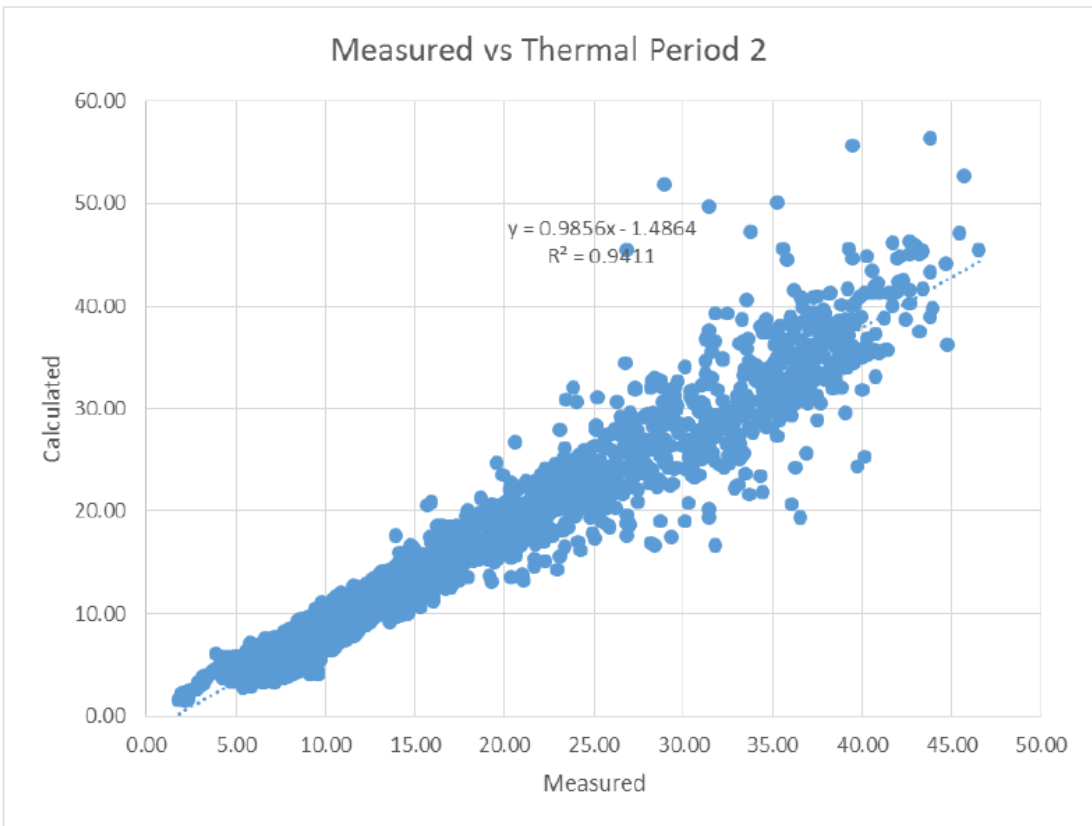


Figure 80 Measured vs. Thermal-Model-Calculated Cell Temperature during Period 2 (°C)

Table 18 Comparison of Temperature Correlations

Period 1			
Model	Gradient	Offset	R ²
NOCT	0.9515	1.379	0.9363
Homer	0.8179	2.6428	0.9347
Thermal	0.8998	-0.8016	0.9255

Period 2			
Model	Gradient	Offset	R ²
NOCT	1.0662	0.7332	0.9401
Homer	0.8876	2.303	0.9452
Thermal	0.9856	-1.4864	0.9411

These results clearly show the reliability of the simple NOCT method. Focusing on the period 2 results, as these are based on a much larger set of data points, we can see the reliability (or R2 value) of every method is around 94%, with the HOMER software calculation performing very slightly better than the others. A larger difference can be seen in the gradient, which indicates the average percentage error if we utilise the given method of calculation. Here, the thermal model gives the best results, corresponding to only a 1.5% degree of error compared to 6.6% for the NOCT model and 11.3% for the HOMER model. It is proposed that with the inclusion of reliable and high-resolution wind data, the thermal model could be optimised to give even better results than it has done, particularly at higher temperatures when the measured value starts to vary considerably from that calculated.

3.15.8 The Cell Efficiency

A problem encountered with correctly assessing the accuracy of methods of cell efficiency estimation was determining a reliable 'measured' value to test the models against. As opposed to the slope irradiation and cell temperature, which could be measured directly by sensors and so a fairly high degree of confidence could be held in the results, a value for the cell efficiency had to be derived from other variables, reducing confidence in the results. In this section, 'estimated' efficiencies refer to those derived from power readings, while 'calculated' efficiencies refer to those derived from temperature readings.

3.15.9 Daily Variability

Section 3.15 showed the time series data for the cell efficiency. First it should be noted that, despite a degree of error, the cell efficiency across each data series is approximately consistent, generally lying in the range 12-18%. Below (Figure 81), the same data is represented as a correlation between the value calculated from the measured cell temperature, and that from either the averaged power, or instantaneous power (see section 3.15).

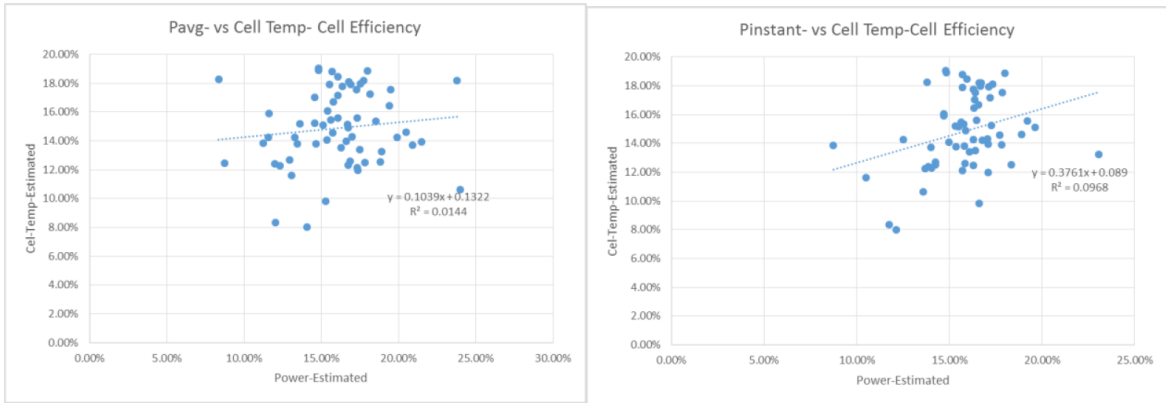


Figure 81 Correlations between Pavg (left) and Pinstant (right) Cell Efficiency against Cell Temperature Cell Efficiencies for 3rd June

This indicates a very low degree of certainty in the calculated value. While a trend line can be drawn, the results merely show a cluster of points within the range 8-20%, with little indication of any linear relationship. It is proposed that this very low degree of certainty is due in part to the low range of values represented in the data, coupled with the high degree of variability over time and correspondent uncertainty. These results would be clearer if the behaviour of the module could be tested over a much wider temperature and efficiency range.

The results are similar for the 5th of June, however the 4th shows quite different results (Figure 82).

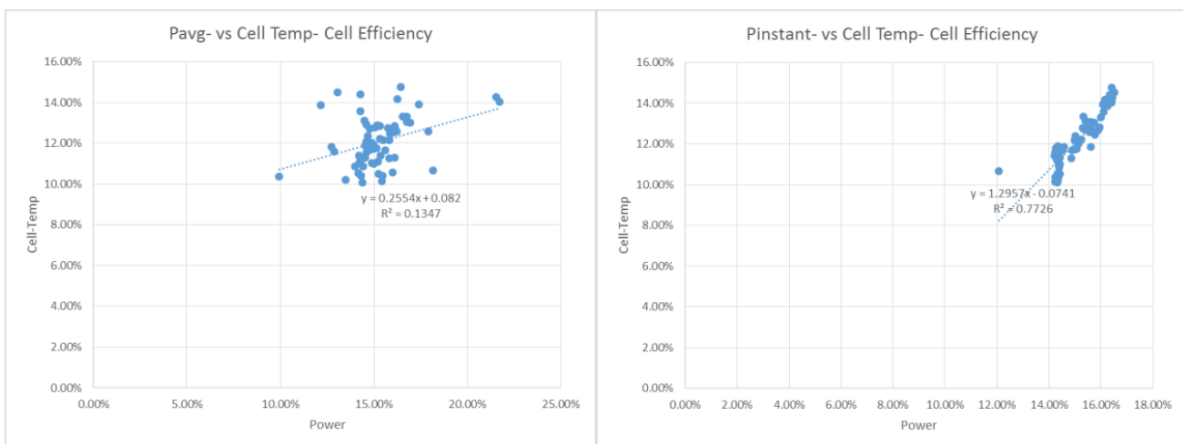


Figure 82 Correlations between Pavg (left) and Pinstant (right) Cell Efficiency against Cell Temperature Cell Efficiencies for 4th June

As discussed previously (section 3.15), the values of $P_{instant}$ for the 4th of June can be assumed to be more accurate than any of the other power readings, and much less sensitive to the exact time. Under these conditions only, a good and reliable result is produced. This is important as it indicates the viability of prediction of cell efficiency from cell temperature under the right circumstances. The R^2 value of 0.77 is relatively high, however the trend line still indicates an error of approximately 30% in the scaling which is far from perfect. The inclusion of the log of solar irradiation in the cell efficiency formula did not produce any significant changes in the correlations between estimated and calculated values, however for the 4th (only), the absolute calculated value is pushed significantly closer to the estimated with an average offset of 3% as opposed to the 7.4% shown.

3.15.10 Averaged Values

In an attempt to reduce the impact of minute-to-minute errors in readings and reading times, the calculated cell efficiencies were averaged both over each hour of the day, and over morning/afternoon of each day.

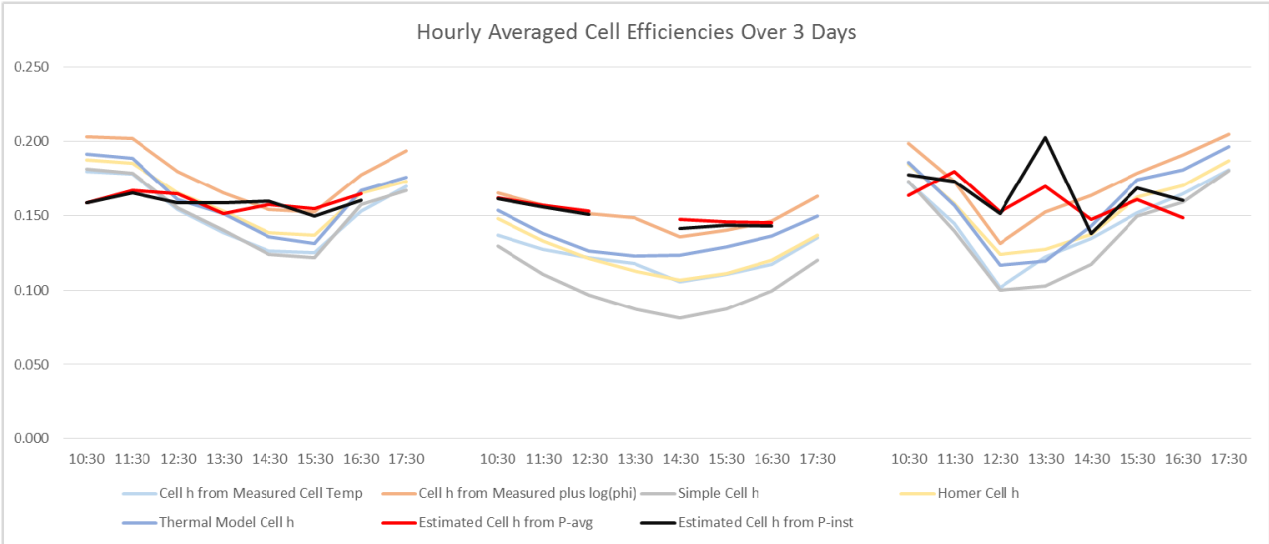


Figure 83 Hourly-Averaged Efficiencies (3rd, 4th and 5th June)

In Figure 83, all 5 calculated series follow a similar curve for each given day (which is to be expected, as the principal input is the cell efficiency). This curve only seems to bear a passing relation to the estimated values, which in general indicate a fairly linear, but shallow, decrease in efficiency across the day.

An example of the correlation is shown below (Figure 84). The other data series' graphs are all very similar, with no R^2 values of greater than 0.3 but are shown in table 19 for completeness.

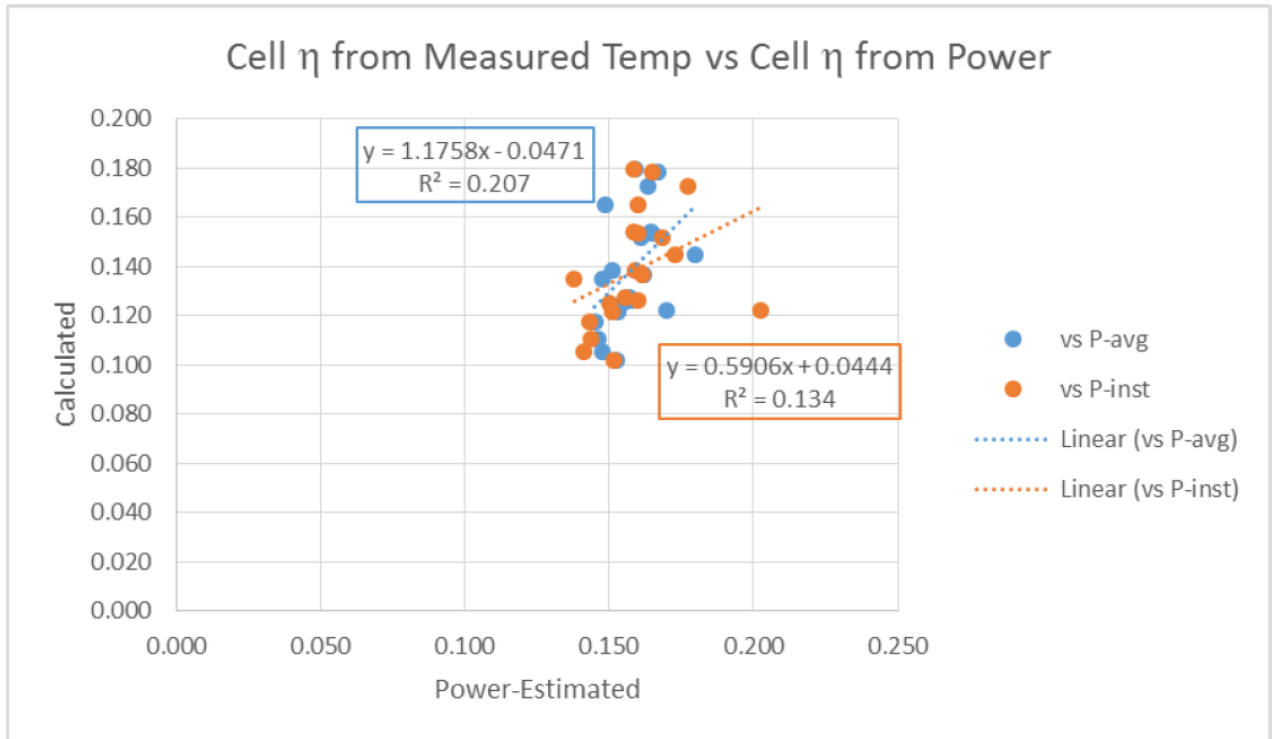


Figure 84 3-Day Hourly Results for Pavg and Pinstant against Cell Temperature-Cell Efficiency

Table 19 Cell Efficiency Correlation Results

Against P-avg			
Model	Gradient	Offset	R ²
Cell Temp	1.1758	-0.0471	0.207
C.T + log(phi)	1.0961	-0.0068	0.2128
Simple/NOCT	1.6617	-0.1316	0.2378
Homer	1.4222	-0.0773	0.2693
Thermal	0.9579	-0.0004	0.1288

Against P-inst			
Model	Gradient	Offset	R ²
Cell Temp	0.5906	0.04444	0.134
C.T + log(phi)	0.5629	0.0765	0.144
Simple/NOCT	0.7813	0.0062	0.1349
Homer	0.6939	0.366	0.1646
Thermal	0.4295	0.0824	0.0664

Finally, even the half-daily results (Figure 85) still show a high degree of variability between the estimated and calculated values. The models used seem to predict a much greater

variability in efficiency than that observed. It is hypothesised that they are too sensitive to input variables: perhaps the published value of α_p , the coefficient of power, is too large in order to err on the safe side (a high value of α_p indicates poor temperature performance).

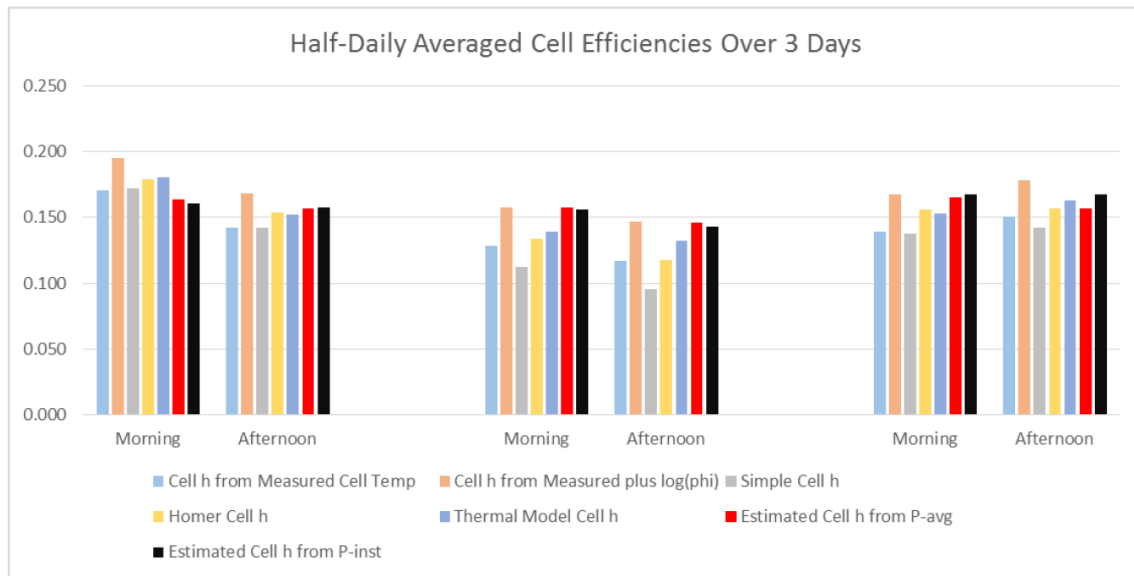


Figure 85 Morning/Afternoon-Averaged Cell Efficiencies

3.16 Shading Analysis

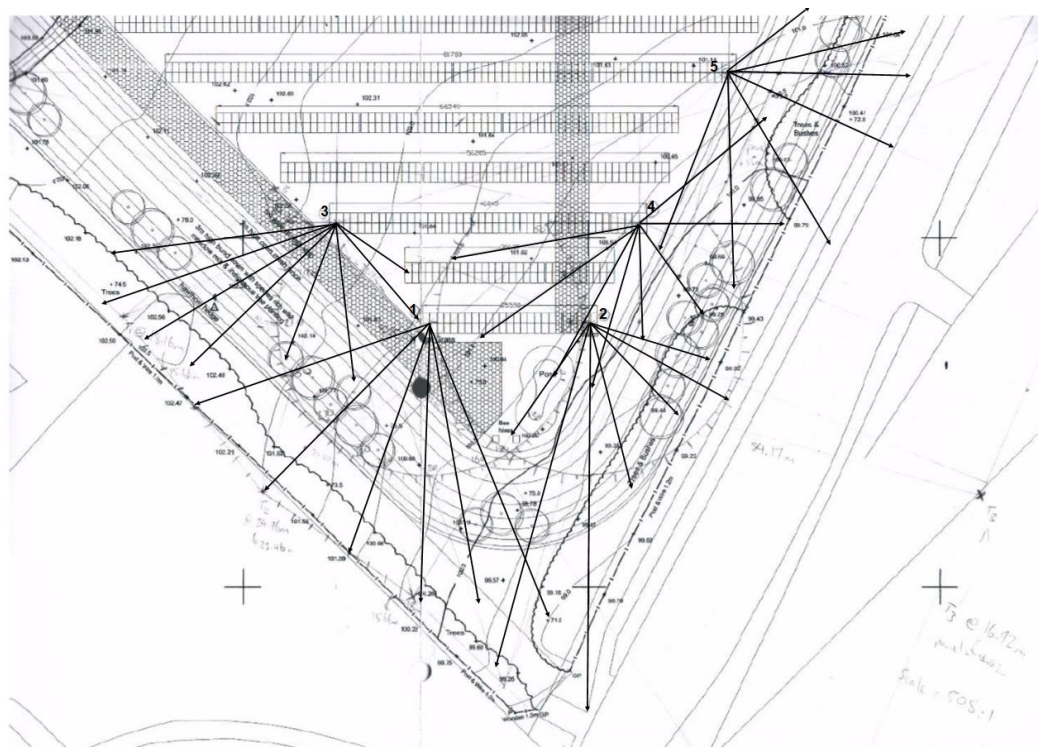


Figure 86 -Shading Acquisition, based on (SSE, 2013)

The five points chosen for the shading analysis (see section 3.8) are shown above (Figure 86), along with the lines drawn and measurements made to calculate the horizon line. An exhaustive method of calculating the horizon elevation angle for every 5° of arc was only undertaken for the two southernmost points, the remaining three were characterised by

measurements taken at important or notable angles only (where obstacles were clearly casting shade ie a tall tree line or the earth bund), the assumption being that this would still give a reasonable approximation. A sample of the numerical results are shown below (Table 20 & Table 21) (full results in Appendix A: Data Tables

Table 20 Shading Data Sample, Points 1 & 2

Point 1				Point 2				
Azimuth (0=N)	Horizon Height (m)	Distance (cm)	Distance (m)	Azimuth (0=N)	Horizon Height (m)	Distance (cm)	Distance (m)	Elevation
50	1.5	1471.12	1.208253	50	1.5	4.2	21.336	4.021489
55	1.5	1260.96	1.409553	55	1.5	3.9	19.812	4.3297
60	1.5	10.553.34	1.610818	60	14.42	20	101.6	8.077988
65	14.42	24.3 123.444	6.662759					
	1.5	9.2546.99	1.828357		1.5	2.9	14.732	5.813773
70	14.42	22.5 114.3	7.190404	65	14.42	18.75	95.25	8.608699
75	14.4220.75	105.41	7.789663	70	14.42	16.5	83.82	9.761346
80	14.42	19.297.536	8.409852	75	14.42	15.5	78.74	10.37783
85	14.42	18.593.98	8.723255	80	14.42	14.25	72.39	11.26579
90	14.42	17.689.408	9.161944	85	14.42	13.75	69.85	11.66441
95	14.42	17.86.36	9.479535	90	14.42	13	66.04	12.31735
100	14.42	16.684.328	9.703664	95	14.42	12.5	63.5	12.79413
105	14.42	16.483.312	9.819712	100	14.42	12.25	62.23	13.04638
110	14.42	16.282.296	9.93854	105	14.42	12.1	61.468	13.20248
115	14.42	16.282.296	9.93854	110	14.42	12	60.96	13.3086
120	14.4216.25	82.55	9.908567	115	14.42	12	60.96	13.3086
125	14.42	16.583.82	9.761346		1.5	1.7	8.636	9.853487
				120	14.42	12.1	61.468	13.20248

Table 21 - Shading Data Sample, Points 3 & 4

Point 3				Point 4				
Azimuth (0=N)	Horizon Height (m)	Distance (cm)	Distance (m)	Azimuth (0=N)	Horizon Height (m)	Distance (cm)	Distance (m)	Elevation
72.5	1.512.75	64.77	1.326668	50	1.5	4.3	21.844	3.928262
	14.42	26.132.08	6.230662	65	14.42	17.75	90.17	9.085816
90	14.42	21.5109.22	7.521097		1.5	2.7	13.716	6.24114
112	14.4219.75	100.33	8.178866	90	14.42	13	66.04	12.31735
147	14.4223.25	118.11	6.960768		1.5	1.85	9.398	9.0684
160	15.66	1471.12	12.41787	113	14.42	11.8	59.944	13.52595
169	15.6610.75	54.61	16.00081		1.5	1.6	8.128	10.45613
180	17.12666667	8.945.212	20.74709	144	14.42	13.8	70.104	11.6233
	1.5	3.517.78	4.822308		1.5	1.8	9.144	9.315942
196	22.46	7.940.132	29.2337	180	1.5	2.8	14.224	6.019909
220	1.5	1.99.652	8.833571	196	15.66	13.75	69.85	12.63646
	19.196	6.533.02	30.17135	211	15.66	12.5	63.5	13.85352
246	15.66	6.533.02	25.37302	235	22.46	13.1	66.548	18.64958
270	15.66	8.945.212	19.10446	259	15.66	14.8	75.184	11.76585
289	15.66	14.774.676	11.84364	270	15.66	17.5	88.9	9.990331
				283	15.66	23	116.84	7.633827

When there was a question over whether the treeline or bund would be dominant, two readings for the same orientation angle were taken. The lower, discountable, reading in this case is shown in red. In fact, for the given assumptions, the earth bund never has a larger shading effect than the treeline (neglecting relative opacity and proximity), indicating that it could possibly be neglected entirely.

5 shading charts based on the Dalkeith sun chart were produced from this data, and are reproduced here (figures 87 to 91). Monthly average charts were used, as opposed to the 20th/21st chart shown in previously. This was done to give a better representation of the sun path for each month.

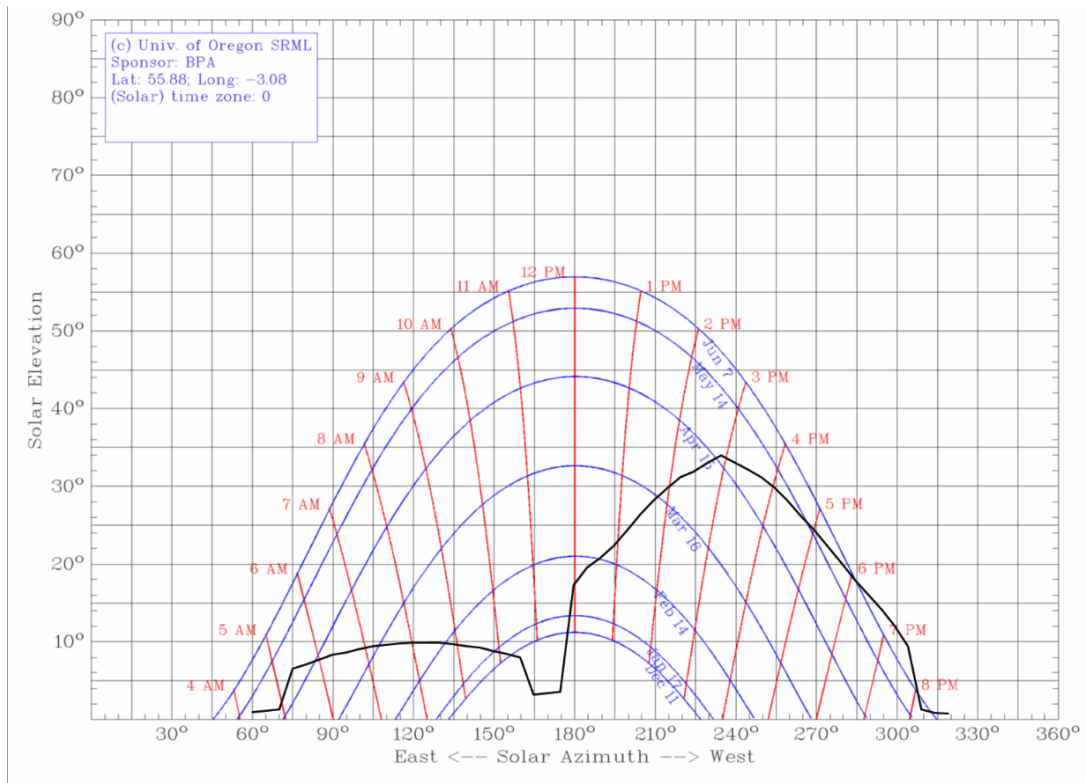


Figure 87 - Monthly Average Shading Chart, Point 1

Point 1 has possibly the most severe shading, with the South West treeline obscuring the sun through much of the afternoon in all but the summer months.

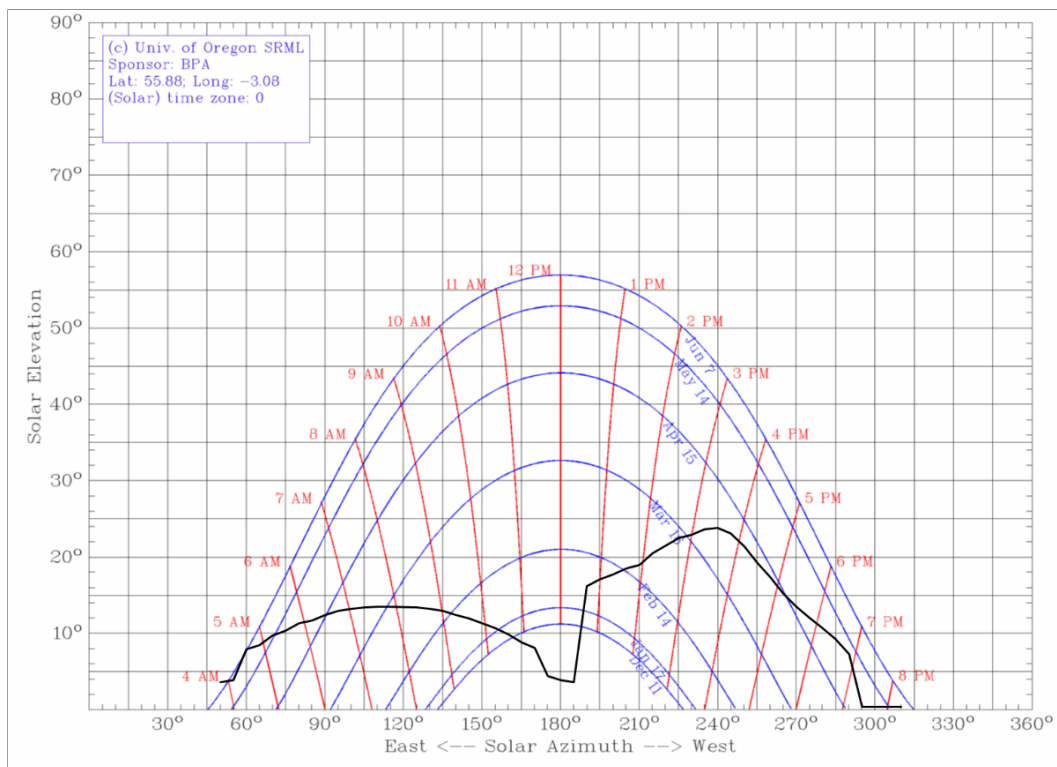


Figure 88 - Monthly Average Shading Chart, Point 2

Point 2 has less severe shading, although the effect of the East treeline can be seen to be comparable to the closer, South West treeline.

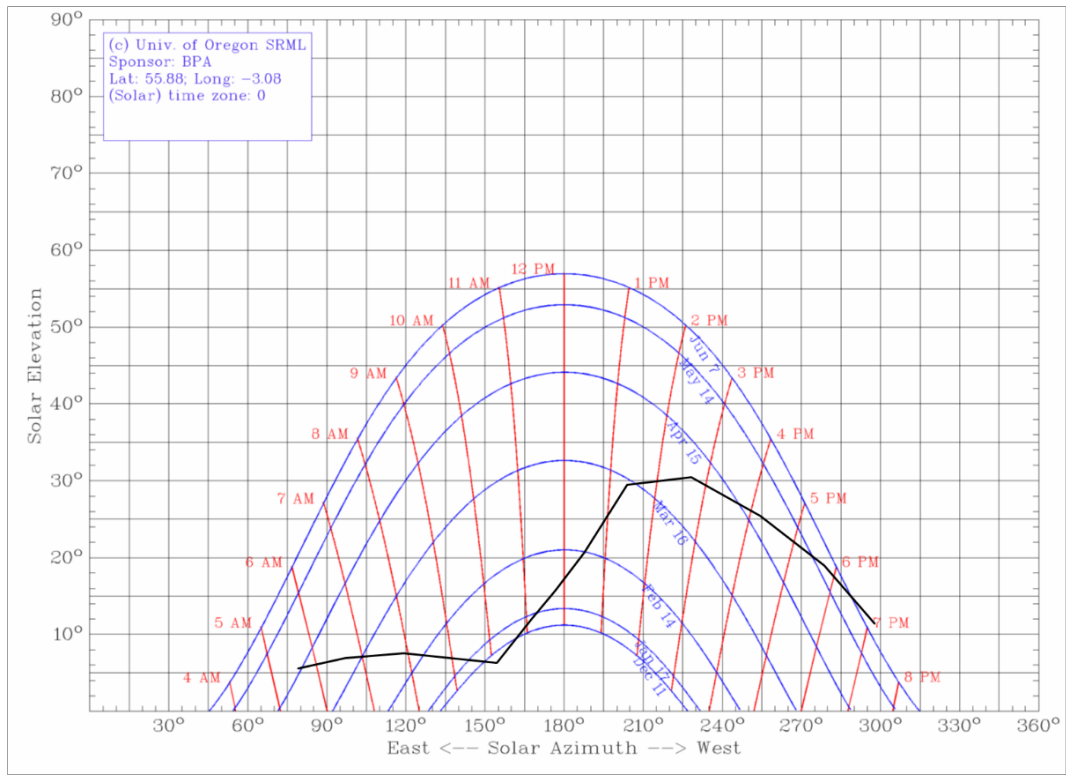


Figure 89 - Monthly Average Shading Chart, Point 3

Much fewer points were calculated for point 3, giving the rougher diagram seen. Shading is similar to point 1, although slightly less severe now the reference point is further from the site boundary.

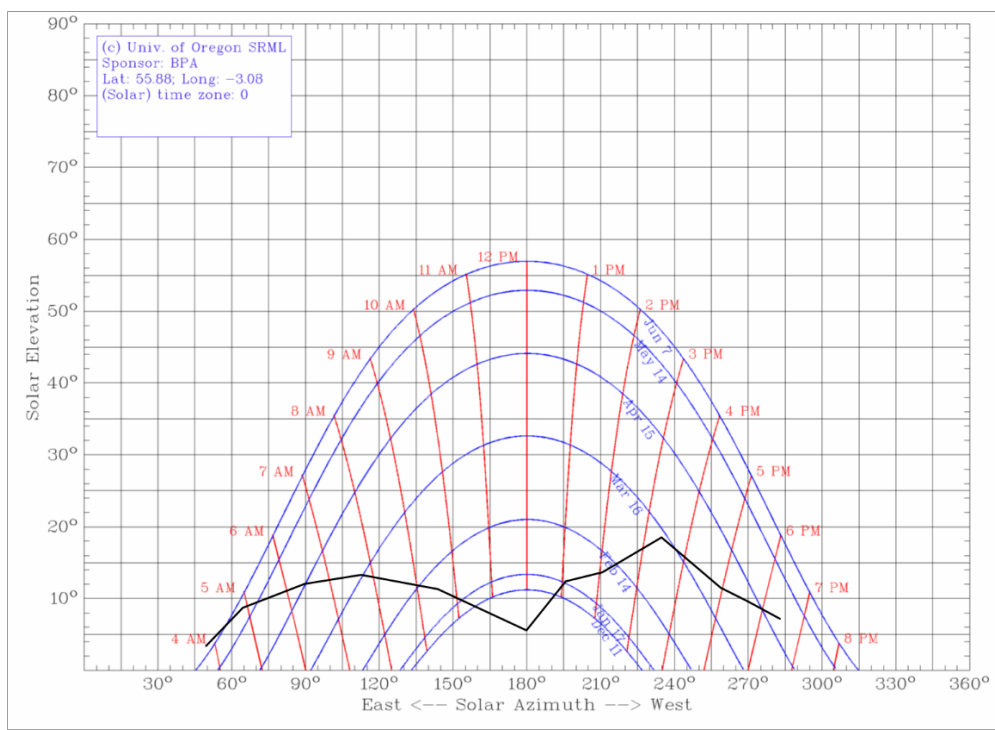


Figure 90 - Monthly Average Shading Chart, Point 4

Shading at point 4 is much less severe, although a fair amount of morning sunlight is lost. Note: shading falls almost to zero after the last point plotted.

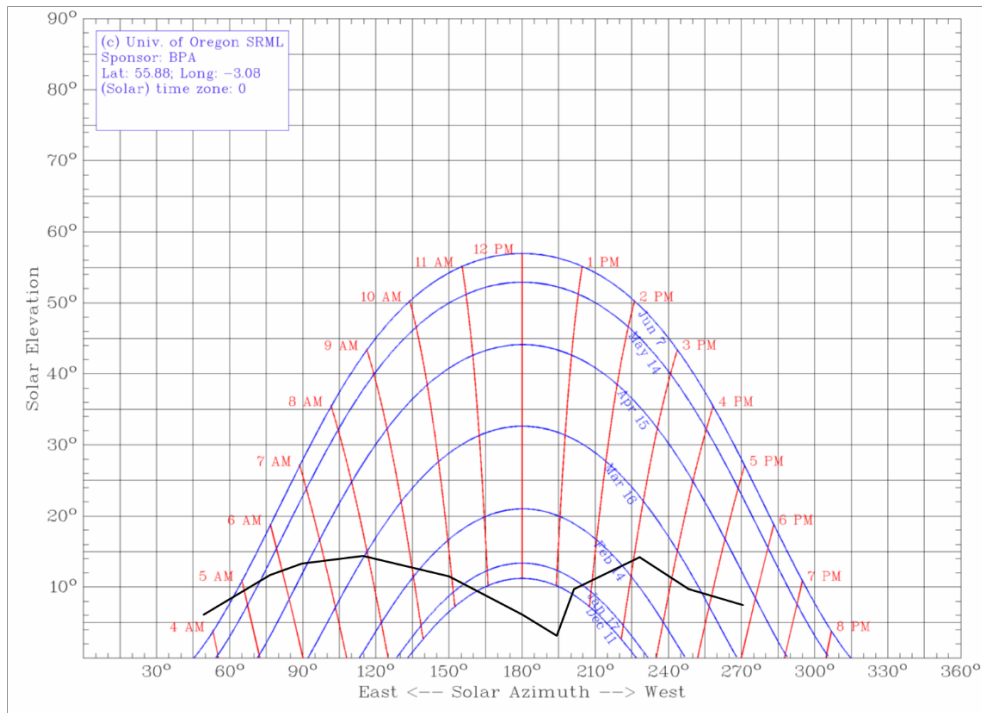


Figure 91 - Monthly Average Shading Chart, Point 5

Point 5 is similar to point 4 (Figure 90) but is affected slightly more by morning shading. There is very little shading in the afternoon.

From these results, bearing in mind that these represent some of the most affected points on the site, it can be seen that shading, while not being a huge problem, is not only present at the site, but will result in a noticeable drop in performance of some of the PV strings. Modules at the south end of the site will be affected particularly badly in the winter months, when the low sun path will keep it behind the trees for much of the day, and shading from the SW line of trees will continue to affect the west end of strings for much of the year. Further study and analysis will be required to ascertain the actual impact of shading. This will be covered in chapter 4.

3.17 Software

The methodology for this project was implemented in the Excel software environment, making use of both the embedded functionality and the extension available through VBA, Visual Basic for Applications, a programming language which interfaces closely with Excel. Full printouts of all code used are available in Appendix C: VBA Code Transcripts. Code written by the author is commented.

3.17.1 Workbook Structure

The excel workbook, titled 'Processed Test Results' consists of the following tabs or 'sheets'. Some are hidden by default to reduce clutter, but can be easily viewed by right-

clicking on any tab title (seen at the bottom left of screen) and choosing 'unhide' from the resultant menu.

- 'Logger Data' [hidden] - this sheet contains the raw logger data produced by the SquirrelView
- (Grant Instruments, 2013) software.
- 'Crichton Gogarbank Weather Data' [hidden] - wind data from the nearest available weather station operated by the Met Office.
- 'Sorted Gogarbank' [hidden] - wind data processed and sorted for use in the thermal model.
- 'Processed Data' - initial calculations done on logger data, including decoding of voltage levels.
- 'Solar Geometry, Diffuse, Slope' - solar geometry and horizontal->slope calculations.
- 'Manual Data' - data manually recorded from inverters (3 days).
- 'Daily Inverter Totals' - likewise, manual readings from inverters.
- 'Compared Processed + Manual' - calculations done only over the period when manual data was available, including comparisons of cell efficiency.
- 'Heat Transfer Model' [hidden] - subset of data used for development and checking of thermal model.
- 'Modelled Cell Efficiency' - all cell temperature and cell efficiency calculations from models.
- 'Averaged Cell Efficiencies' - averaged values of the previous sheet's results.
- 'Graphical Display Data' [hidden] - full table of all data in spreadsheet where columns can be
- 'turned on/off', used as input for 'Graphical Display'.
- 'Graphical Display Data 2' [hidden] - full table of all data in spreadsheet, no column switching,
- used as input for 'Graphical Display'.
- 'Graphical Display' - described in section 3.20, produces graphs of data (in fact, displayed near beginning of tabs in the workbook for easy access).

There is also an additional excel file, 'Shading Estimation', which was used to produce the lines on the shading sun charts shown in section 3.16.

3.17.2 Excel-Only Implementation

Excel affords a fairly wide range of computations to be performed as part of its default functionality. In fact, simple multiplications, additions, subtractions and averages make up a lot of the required calculations. A summary of the main calculations performed is presented here, arranged by section of the workbook.

3.17.2.1 'Processed Data'

- **Average Irradiance (W/m^2)** is computed as the average of p2 and p3 (to avoid errors caused by sensor shading).
- **Average Cell Temp** is the average of sensors t1 and t2, while **Average Air Temp** is the average of t3 and t4.
- **Average Heat Loss (W/m^2)** is the average of sensors flux1 and flux3 only

The following calculations are performed for both cell and module, and are done relative to the cell or module area

- **Solar Power (W)** is the multiple of average irradiance and area, calculated on solar cell area.
- **Heat Loss (W)** is the multiple of Average Heat Loss (W/m^2) and area, calculated by solar cell area.
- **Energy Balance (W)** is given by 80% of the solar power (to simulate reflection losses) minus Heat Loss. To provide a better representation of the losses incurred.
- **Estimated η** is given by Energy Balance divided by Solar Power. This is only calculated if both Energy Balance and Solar Power are positive, and the resultant value is less than 20%.

3.17.2.2 Compared Processed and Manual

There is some overlap with Processed Data, duplicate calculations are been removed.

- **Heat Loss Should be... (W/m^2)** indicates the estimated heat loss derived from 80% of 'Average Irradiance' minus 'Estimated Cell Power' divided by the area of a cell.
- All energy values are calculated for inverter and whole plant, as well as cell and module.
- **Instance Inverter Power (kW)** is the average of the three power readings P1, P2 and P3 from sheet 'Manual Data'.

- **5-min Inverter Energy (kWh)** is given by the difference between the current period's 'E-day(kWh)' and the previous period's, both from 'Manual Data'.
- **Estimated Av. Power (kW)** is given by '5-min Inverter Energy' divided by the length of the time period (5 minutes unless value is in bold).
- **Inverter-level η** is given by 'Estimated Av. Power' divided by 'Solar Power per Inverter'. A bold value indicates no 'Estimated Av. Power' value available, 'Instance Inverter Power' used instead.
- **Estimated Cell Power (W)** is given by 'Estimated Av. Power' divided by the number of cells feeding each inverter (80 modules*60 cells per module). Note the unit conversion from kW to W.
- **Pavg-Estimated Cell η** is given by 'Estimated Cell Power' divided by 'Solar Energy per Cell'
- **Pinstant-Estimated Cell η** is calculated in the same way as 'Pavg-Estimated Cell η ', except using 'Instance Inverter Power'.

3.18 Use and Adaptation of solar analysis Software

The solar analysis software, made available to me, was written in VBA and provided with the Windows in Buildings textbook (Muneer et.al. 2000) was used as a basis for the solar geometry and slope irradiation calculations (in sheet 'Solar Geometry, Diffuse, Slope'). Where code has been used from these software programs, it is clearly indicated in the attached transcripts (see Appendix C: VBA Code Transcripts), directly after the macro (or 'Sub') name. Any alterations to the original code are identified by commented asterisk (*). Note: some functions and variables have the same name (but only when a function defines a variable). This software was deemed most suitable by author due to its use at high latitudes (Muneer et.al. 2000) , within solar studies already carried by a number of researchers including Gago et.al. (2011).

List of Windows in Buildings functions used:

- EOT - Determines the equation of time using the Yallop algorithm (see section 3.3.2), from the time/date variable (GMT) and the local standard meridian (LSM).
- DEC - Uses the same processing and input variables as EOT, above, but determines the solar declination.
- SOLALT - Determines the solar altitude from the apparent solar time (AST), the latitude and DEC (see methodology).

- SOLAZM - Determines the solar azimuth from the same input data as SOLALT, above.
- DAYNUM - Determines the day number, for use in calculation of ERAD, from the time/date variable (GMT).
- ERAD - Determines the intensity of the extra-terrestrial irradiation, from the time/date variable and SOLALT. Utilises function DAYNUM.
- INC - Determines the angle of solar inclination from the solar altitude and azimuth, and the module orientation and inclination (see section 3.3.2).
- BSRAD - Determines the slope irradiation beam component from the horizontal global and diffuse irradiation, SOLALT and SOLINC (see section 3.11).
- DSRAD - Determines the slope irradiation diffuse component from the same variables as BSRAD, above, with the addition of the module angle of inclination (TLT) and the extra-terrestrial irradiation (ERAD) (see section 3.11).
- Additionally some extra functions were produced by the author for solar calculations. Some of these are simple additions or multiplications, but were rendered in function form to keep all the spreadsheet functionality in the same place:
- AST – Calculates the apparent solar time from the clock time (see methodology).
- decimalhour – converts time in hours, minutes and seconds to a decimal value in hours only
- clearness – simply calculates the ratio of global to extra-terrestrial irradiation, set to zero if either input value is zero or less
- DiffuseCalc – implements the clearness regression formulae (see section 3.11).
- GroundR – calculates the ground reflected component (see section 3.11).
- GSRAD – simply adds the ground, diffuse and beam slope irradiation components

3.18 Implementation of Thermal Model

As opposed to the preceding examples, the thermal model was implemented as a macro due to its iterative nature. In fact, a central macro runs, calling functions which execute the various equations shown in section 3.11 (thermal model methodology). Unlike a function, in excel a macro must be called in order to work. This is accomplished in the workbook through the use of a button object on the relevant sheet, labelled 'Calculate'.

3.19 Cell Efficiency Calculations

This code implements the following equations as functions (Muneer et.al. 2000):

- SimpleTemp: Equation 12: NOCT Cell Temperature Calculation
- HOMERTemp: Equation 13: HOMER Cell Temperature, Source:
- CellEfficiency: Equation 12: Cell Efficiency
- CellEfficiency2: Equation 21: Cell Efficiency

The following flowchart in figure 92 outlines the VBA model proposed by Aldali et.al (2011) of which elements were utilised to compute the above equations as functions. The program is capable of calculating dew-point, slope radiation, sky and cell temperature, module efficiency and maximum power for operation of the PV modules. Furthermore, the program calculates the current, voltage and fill factor. The program is designed to compute results for 10 h each day for a period of 1 year. Not all of these parameters were required in this study but it will be useful to have these results for planned further research in the future.

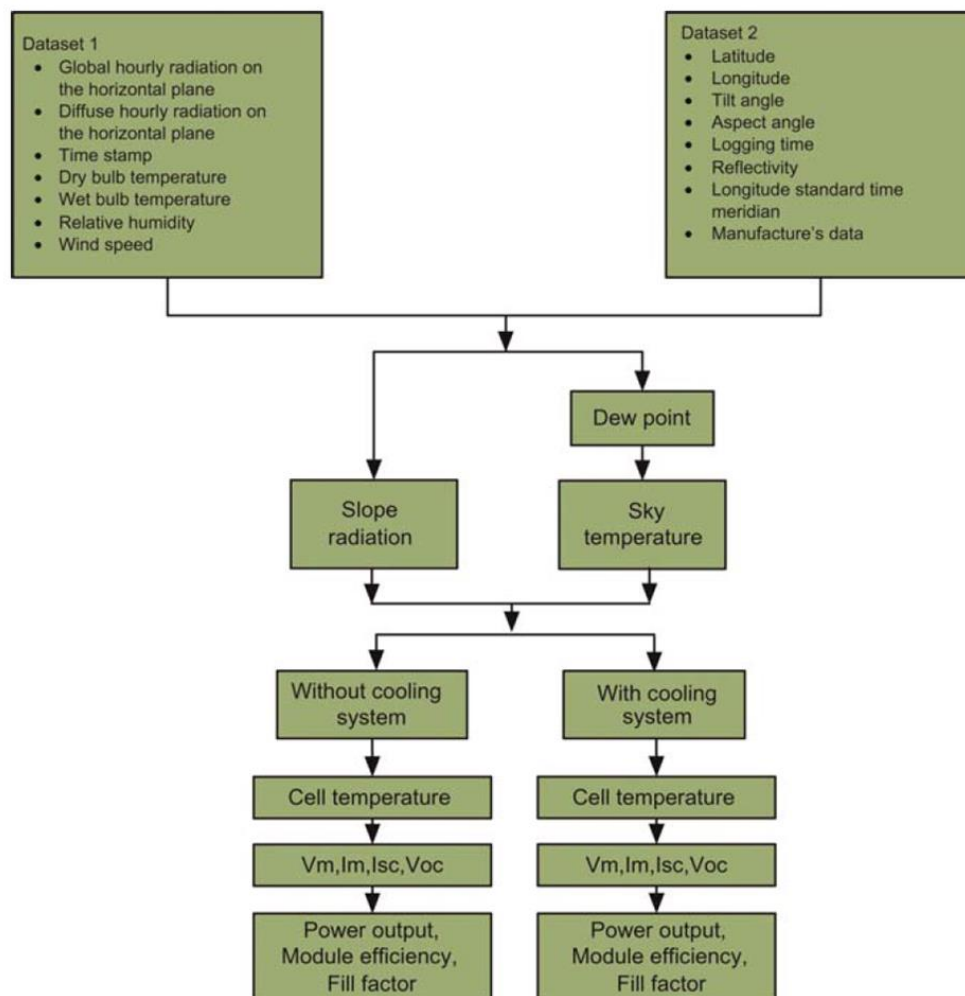


Figure 92 Flow chart for the computer model. Source:(Aldali et. al. 2011)

3.20 Graphical Display Interface

Software was used to quickly and easily display the many different data streams was developed to aid in the data analysis of the project. The below figure (Figure 93) shows the display screen for this software (input values are cut off for purposes of presentation):

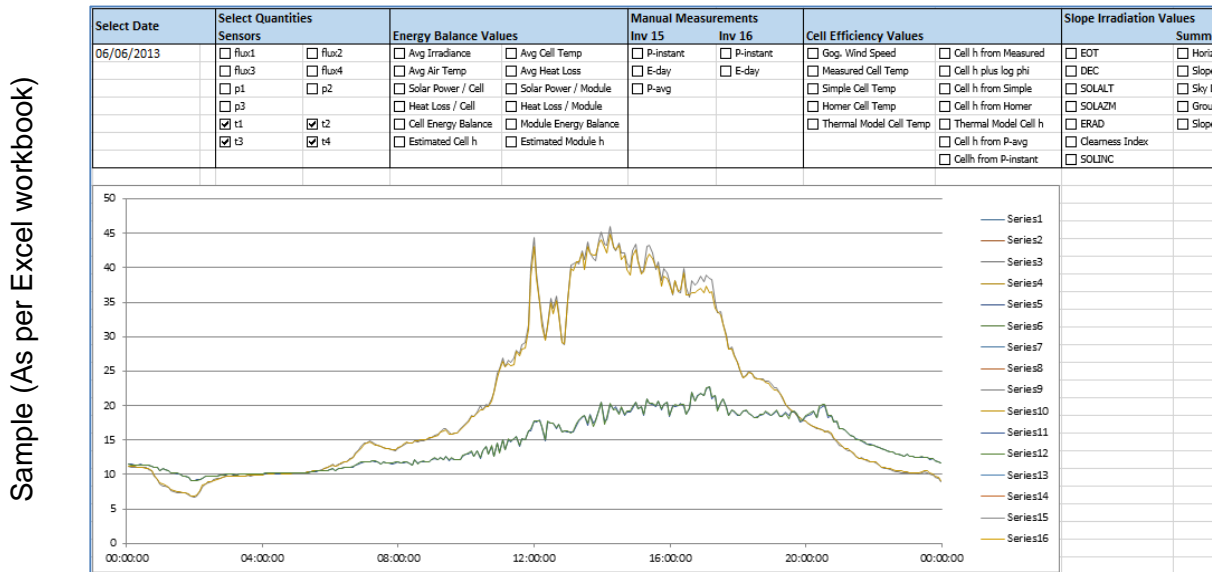


Figure 93 - Graphical Display Screen (Time Series Plot)

The software allows the user to select any combination of sensor inputs, manually-recorded data variables or calculated values to display on the graph. One day only is displayed, from midnight until midnight, which can be selected from a list contained in the top-left cell.

The software works from a reference data table, in which data columns are switched on and off dependent on the status of the corresponding check-box, above. The range of rows to be displayed (the data table containing the entire 2500 sample times) is changed by macro whenever a new date is selected. The chart is set to automatically scale to the given data.

One drawback of this method is that all data sets are selected at once, and so the 'legend' function of excel which displays which variables correspond to which colours has about 60 entries. When graphs produced by this software are used in this report, variables are identified in the text.

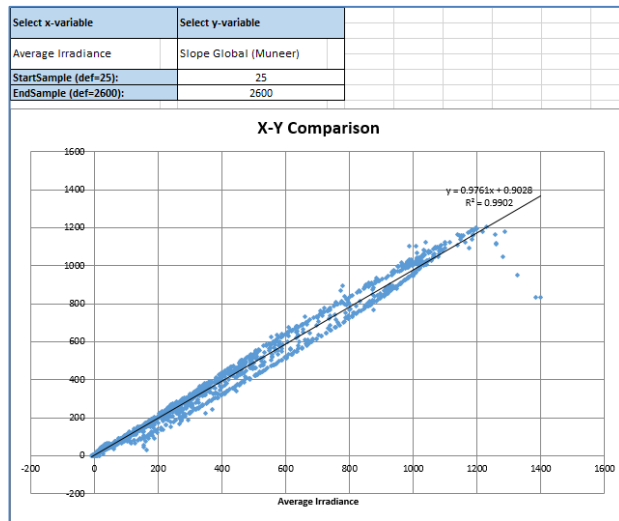


Figure 94 - Graphical Display Screen (correlation graph)

The second section of the display screen allows for the plotting of one variable against another, as opposed to showing many variables concurrently against time. The same list of data columns as available to the previous graph (Figure 93) can be selected from the two drop-down lists 'Select x- variable' and 'Select y-variable' (Figure 94). A macro, triggered by the change in cell value, then deletes the existing plot and creates a new chart with the correct cell references and formatting. By default, this plots over the whole range of the data variables, however it is possible to manually set the sample range in the table shown (the actual data table would have to be referred to in order to determine which times/dates these sample numbers refer to).

3.21 Problems Encountered

The entire selection of software developed was implemented as a single excel workbook. This was managed with consideration, but did hold the advantage of data continuity: any changes made to one section of the workbook could be immediately propagated to all other sheets and tables. The serious drawback was that of computer resource demand: with some sheets constituting thousands of calculations, some being run in code, even on a relatively fast computer a full update of the spreadsheet would take around 2 minutes. Excel automatically updates sections of an open file whenever changes are made, and updates the whole document periodically. There is also a risk that errors within complex spreadsheets, such as this, could go un-noticed. It is recommended that a revised approach is undertaken in future studies to mitigate against the potential for error.

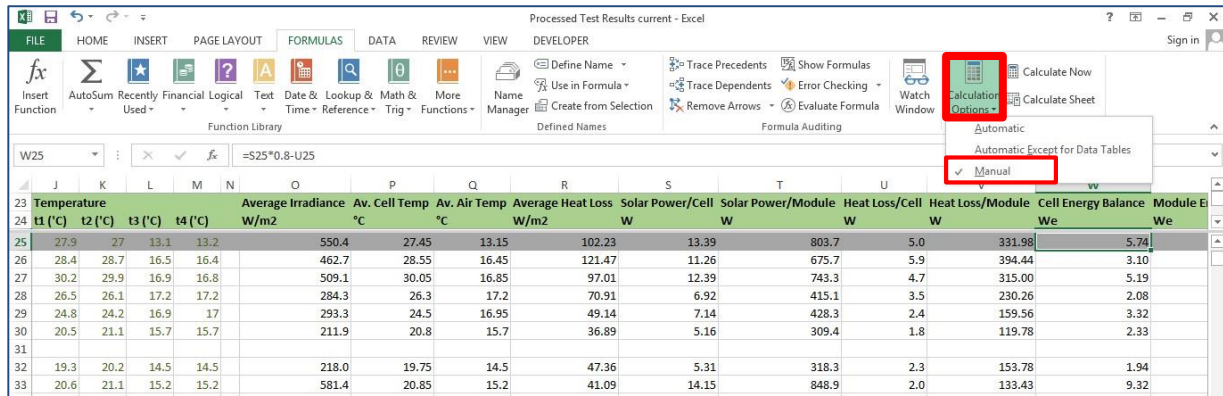


Figure 95 - Setting Manual Calculation Mode

This problem was avoided by changing excel to 'manual' calculation mode (see Figure 95). This caused its own problems, unfortunately, as it became difficult to ensure that data was correctly updated, particularly when being passed between sheets. Further code was developed to deal with this problem, basically updating certain sheets whenever changes were made and leaving only the most resource-intensive sections to be updated manually by the user. The code is reproduced in Appendix C: VBA Code Transcripts.

3.22 Conclusions

As covered previously, the estimated generation of the solar meadow farm is 568,611kWh over a full year's operation. This is a significant amount of energy, avoiding the production of 293,000kg of CO₂. The actual energy produced in year 1 was 439,276kWh.

The solar meadow at Edinburgh Midlothian campus is more than just a valuable financial investment, it is a firm indication of the viability and importance of large-scale solar in Scotland. It supports the strong likelihood of the future uptake of projects of this kind as part of a greener, more sustainable energy solution.

The performance of solar irradiation, PV cell temperature and efficiency models have been assessed through a study done on a commercial solar plant in the Edinburgh area. An experiment to measure a range of data quantities was designed and implemented, and a survey of the site to obtain an estimate of the degree of shading was performed. To overcome limitations on data available to the researcher, three days of manually-recorded measurements were made to support the experimental data.

The shading characteristic of the site was not as detailed at this stage (the next chapter covers the impact of shading on the array in greater detail), but it was clearly shown that the figure of zero shading for the site assumed by the contractors will prove to be inaccurate, particularly in the winter months. Shading was shown to be most severe at the south end of the site, and still notable along the east side. Any shading on the solar modules will adversely affect the performance of the entire string in question, having a disproportionately large effect on plant output.

The conversion of solar irradiation data from horizontal intensity to intensity received on a slope has been shown to be extremely accurate when using location-specific regression formulae. It was concluded that the seasonal model proposed by Clarke et al (2007) was the most suitable to use over the recorded time period, by a small margin. A further advantage of the given method is the slightly simpler implementation compared to the monthly model, which requires a different set of regulated coefficients to be used for every month.

The prediction of a solar photovoltaic module's cell temperature from environmental data such as air temperature and solar irradiation was shown to be accurate (within the expected tolerance shown) across three different calculation methods. The simplest, based on the 'nominal operating cell temperature' of the module, actually gave results almost as good as the much more complex thermal model, indicating that this is a reliable and useful method to use. The thermal model was assumed to be limited by the lack of good quality, high resolution wind data for the site studied. In addition, the range of assumed input variables requires better definition.

Finally, the calculation of cell efficiency over the three days of manual data recordings was performed, the average measured value being 16%. On a clear-sky day when the cell efficiency was predicted by the model presented herein and within the tolerance range of 12-18%, the efficiency being generally lower on hotter days, or in the afternoon.

The implementation of more accurate and high-resolution data collection methods on the site in the future, currently under discussion, will open up excellent opportunities for further analysing and refining the results of this investigation. High level data is now available through direct inverter data download along with this use of calibrated sensors will provide a detailed analysis for future work.

This chapter has investigated module performance through, modelling, of a ground array installation at Edinburgh College, Midlothian Campus, the derived quantities consisting of

slope irradiation, cell temperature, and cell efficiency. The experimental data was obtained on site through both automated and manual measurements for comparison with the calculated quantities. Results indicate that the horizontal-to-slope conversion models used provide a greater than 99% degree of confidence in the calculated results. Likewise, correlations between measured and calculated cell temperature were very high at up to 94%. Estimations of the cell efficiency and hence module output were less reliable however, with only one of the models used, for one of the days studied, giving reasonable results. Efficiency values were, however, in the approximately correct range of 15-20%.

Chapter 4 – Analysis of Energy Delivery of the Edinburgh College solar PV meadow: Effects of Shading

4.1 Chapter Summary

This chapter will investigate how important solar panel positioning is as a factor in maximising energy delivery, especially at higher latitudes. As solar altitude decreases obstacles and blockages become more of a hindrance and careful planning is required to ensure the amount of shading on the panel surface is kept to a minimum. Edinburgh College's Solar Meadow comprises of 2,560 solar panels over a 20,000m² site with 32 P Aurora power one trio-20.0-TL inverters 20kW inverters. The site is predicted to produce 568MWh of electrical energy and is estimated to save approximately 293,000 kg of CO₂ per year. This study looks at the impacts of shading on the Edinburgh College Solar Meadow from obstacles along the Southern and Eastern edges. The impact of shading throughout the months of 2015 have been analysed and the effect on energy delivery captured throughout the year. The Solar Meadow delivers 90 – 100% energy output for seven months of the year. Only one month of the year is the energy delivery drop to around 50% of its expected output due to the shading impact from the obstacles along the southern edge.

4.2 Introduction

In chapter 3, the research carried out by (Jeffrey *et al.*, 2015) it was recommended that further study was required into the effects of shading on the solar array in Dalkeith Scotland. The initial site survey that was undertaken to ensure accuracy of the layout and electrical connections through the available site plans. The array, figure 96, had clear areas of shade impacting on a number of panels around the site and an initial shading analysis was undertaken to ascertain its impact.

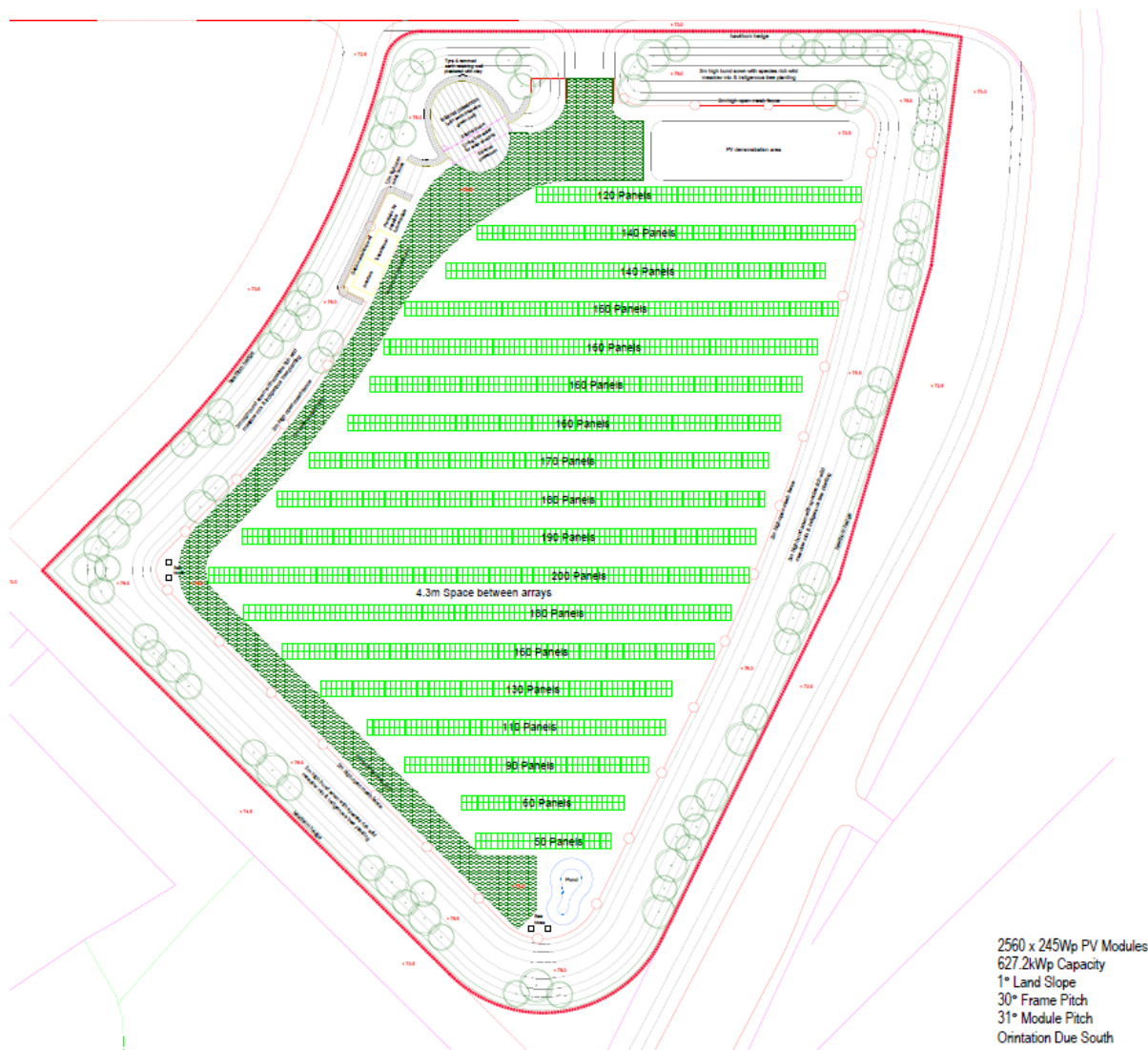


Figure 96 - Solar Meadow layout and markup (SSE, 2013)

The analysis undertaken previously (Jeffrey *et al.*, 2015) looked at five critical points towards the southern edge of the site where shading was most prevalent due to a line of high trees on both the south-east and south-west edges along with the earth bund that surrounds the site. Horizon lines were constructed for each point. An example is shown in figure 97, this initial analysis suggested a significant amount of shading will occur along the southern-most row of modules. This study was undertaken to analyse, in much greater detail, the overall shading implications on the array, how much energy will be lost due to modules being in shade and the overall cost implications of shade on the site of a planned PV array. The need, or not, for full site shading analysis will also be considered as part of the planning process for future large scale installations.

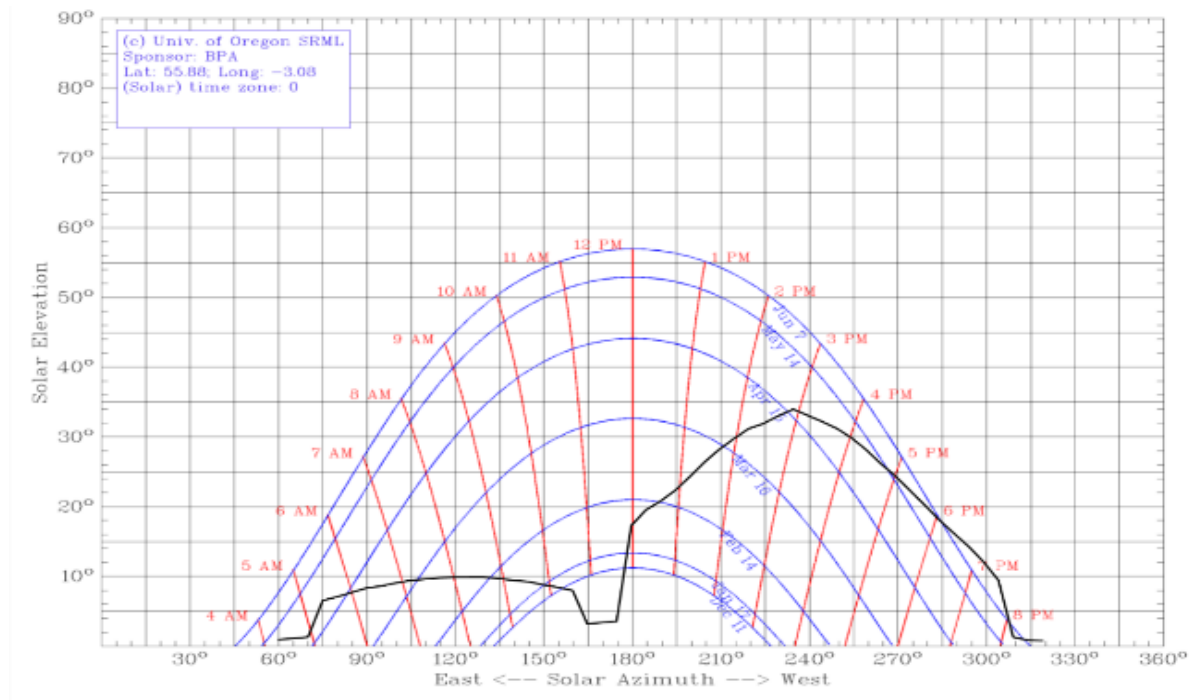


Figure 97 - Shading along the southern edge

4.3 PV modules in shade

Researchers have studied the characteristics of PV modules under partial shading conditions. Experimental work has been undertaken to characterize the I–V curve during partial shading but the scope was limited to module-level shading (Alonso-Gracia, 2006). (Sathyanarayana *et al.*, 2015) found that the impact of uniform shading on a panel resulted in a linear decrease in power output but not in the efficiency of the panel. Interestingly non-uniform shading was found to have a greater impact with a drop in current, power and efficiency as a result. It is therefore important to avoid non-uniform shading at the earliest stages of installation onwards. Ekpenyong and Anyasi (2013) confirm this finding and Pachpande and Zope (2012) verify, through findings, that the non-uniform shading will push a solar panel into operating like a ‘load’ on the string. All agree that to mitigate this occurrence a bypass and blocking diode can be connected in parallel with a particular group of panels. However, initial planning will also play an important role in minimising the effects of shading.

In large solar PV farms, PV arrays are constructed by connecting large numbers of PV modules to each other in series, or strings. To investigate the shading effect it would not be useful to do so at a modular level, but it is necessary to analyse at string level to appreciate the actual impact on output. The string of PV modules can be connected in different interconnected topologies. Series–parallel (SP), bridge link (BL), and total cross tied (TCT) are the main interconnection topologies used in industry. Figure 98 depicts the

stated configurations for a 20 x 3 PV array with different types of shading patterns labelled A-D. In series-parallel (SP) configuration, due to the effect of shading the maximum power point tracker (Mpp) is forced to move from the non-shaded modules to the modules that are in shade. However, for the BL and TCT connections, due to the additional wires in the modules connections, new current paths are created and the PV output power can be increased under the non-uniform insolation conditions. These connections can be useful under certain shading conditions.

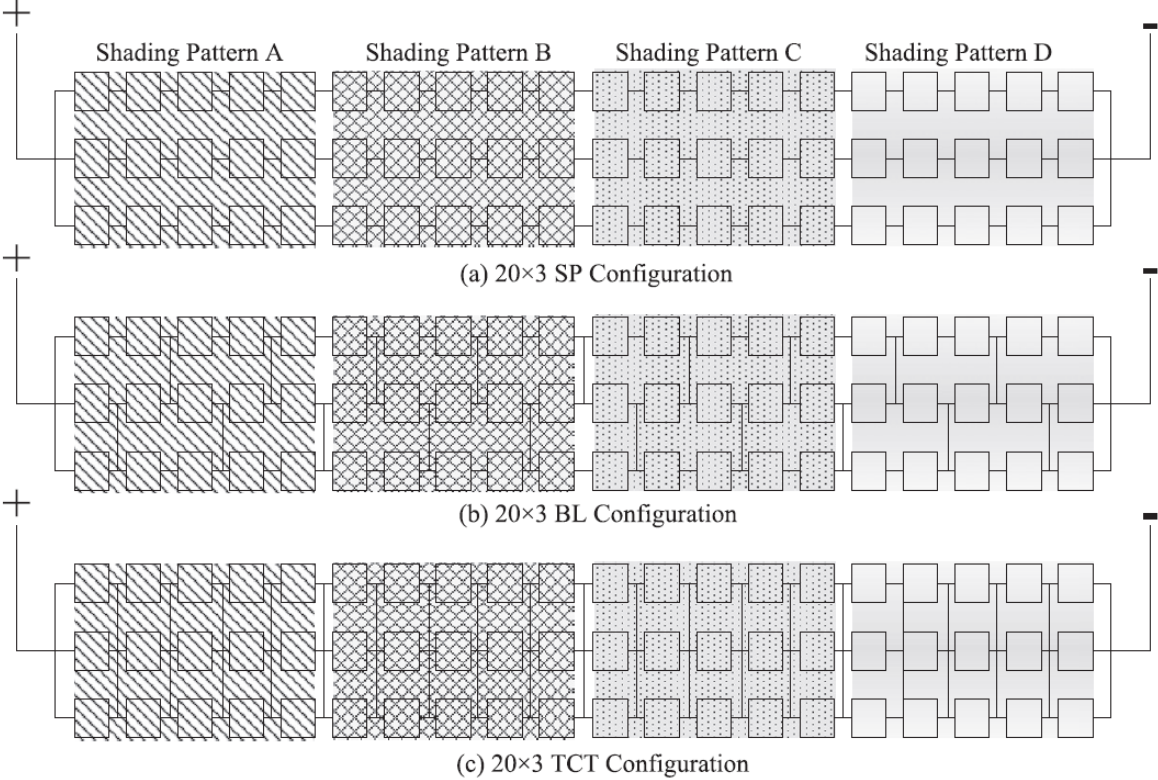


Figure 98 - SP, BL and TCT connections for 20*3 array (Ishaque, 2011)

The characteristics of a PV module in shade with a bypass diode has been described as follows; during times where no shade is apparent on the PV module, the bypass diode are reverse biased, the current will then flow through the module as presented in figure (99 a). During times when the module is in the shade, the module cells act as a load instead of a conductor and cause the problem of creating hot spots. To avoid the hot spot issue it is necessary to drive the current away from shaded cells. This has been implemented by the use of a bypass diode as shown in figure (99 b), this bypass diode is forward biased when the module is in the shade, and therefore it conducts the current produced by non-shaded modules (Ishaque, 2011)

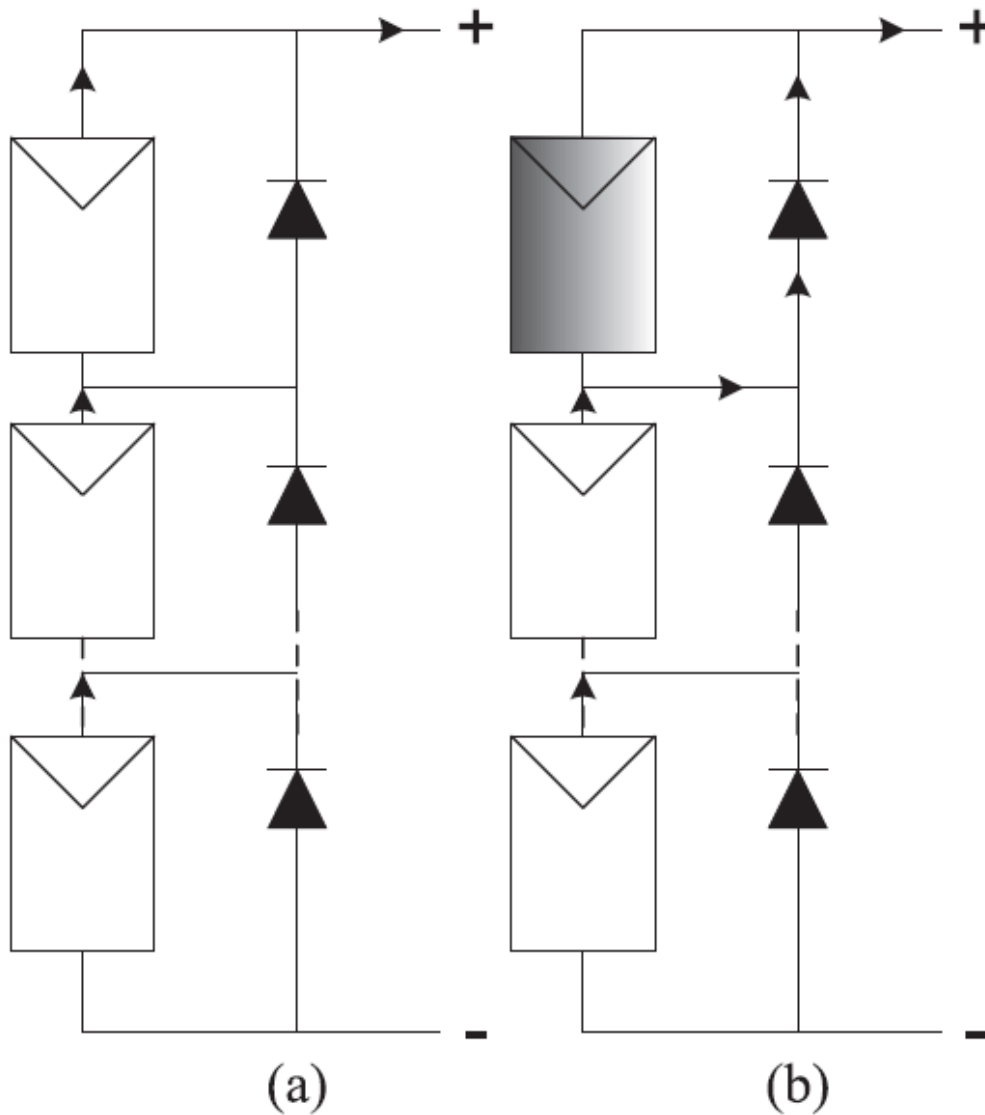


Figure 99 - (a) Module in normal condition and (b) bypass operation as the module is in shade (Ishaque, 2011)

4.4 Problems caused by shading

There are several problems caused by shading that can have a big impact on the overall performance of the panels. Partial (non-uniform) shade, can have a significant impact on the performance and result in a reduction in overall output. Even a small section of the cells being shaded will result in the entire series-linked section of cells being affected and a significant reduction in power output to due to the string current reducing to the lowest level as per the shaded cell. Partial shade reduces the overall current impacting on overall power output (Sathyanarayana *et al.* 2015).

Another problem caused by partial shading is the phenomena of hot spots caused by thermal stresses incurred on the weaker, shaded cell(s). This stress can cause overheating

which will, in turn, further reduce the power output of the panel. The cells not in shade will generate a high voltage forcing extra current through the good cells resulting in forward bias of the 'good' string (Ekpenyong and Anyasi, 2013). If the short-circuit current of the shaded cell is balanced by the overall current of the unshaded cells the forward bias will become reverse bias in the shaded cell. This results in the entire generating power of the unshaded cells dissipating through the shaded cell resulting in localised power dissipation and hot-spot phenomena. This phenomena will reduce the lifespan of the panel and in extreme circumstances can result in catastrophic malfunction through combustion of the panel. This ultimately results in the shaded cells acting like a load on the panel string array (Sun *et al.*, 2014).

4.4.1 Establishing critical points of shade within the Solar Meadow at Edinburgh College

In order to better understand the impact and the amount of shading experienced by the panels within the Solar Meadow at Edinburgh College, algorithms were used to calculate the amount of shade that a surface experiences. In analysing the impacts of shade affecting the solar array a number of these shading algorithms were considered and evaluated. Establishing a comprehensive approach to shading analysis is important to the overall level of detail required to critically analyse the impact shading can have on a surface within a given point on the site. It was also necessary to further develop the points of shade outlined in the initial piece of research (see chapter 3), and create a more accurate representation of the shading impact on the array.

The angle of the solar panels was measured using a theodolite to ensure accurate data on the solar plane of the panels. The measurements were taken at each critical point and the theodolite was mounted at a height near to the centre (the junction point of two modules) and east set as 0°. In intervals of 30° in azimuth, due east, the height of the panel angle was recorded. The measurements recorded for the front row where shading is most prolific is shown (Table 22). The setup of the theodolite can be seen in figure 100.

Table 22 - Inclination of Trees from specific plots

First Row- Left	Angle (degrees°)		Degrees	Minutes	Seconds	Degrees	Inclination
	0°(east)	76°05'20"	76	5	20	76.089	13.911
	30°	74°15'20"	74	15	20	74.256	15.744
	60°	80°03'40"	80	3	40	80.061	9.939
	90°	74°33'00"	74	33	0	74.550	15.450
	120°	67°19'40"	67	19	40	67.328	22.672
	150°	76°34'40"	76	34	40	76.578	13.422
	180°	-	-			-	-
First Row- Centre	0°(east)	80°33'00"	80	33	0	80.550	9.450
	30°	77°52'40"	77	52	40	77.878	12.122
	60°	77°36'00"	77	36	0	77.600	12.400
	90°	80°38'20"	80	38	20	80.639	9.361
	120°	69°59'00"	69	59	0	69.983	20.017
	150°	64°50'10"	64	50	10	64.836	25.164
	180°	72°49'30"	72	49	30	72.825	17.175
First Row- Right	0°(east)	85°58'10"	85	58	10	85.969	4.031
	30°	78°59'40"	78	59	40	78.994	11.006
	60°	81°19'50"	81	19	50	81.331	8.669
	90°	69°02'20"	69	2	20	69.039	20.961
	120°	61°24'20"	61	24	20	61.406	28.594
	150°	63°47'10"	63	47	10	63.786	26.214
	180°	73°16'50"	73	16	50	73.281	16.719



Figure 100 - Theodolite

From this data it was established that the main areas of shading were experienced in the east and south of the farm, where trees and the earth bund are having the highest shading effect on the modules. 12 critical points were chosen and are shown in the figure 101. The view of the southern tree line is shown in figure 102.

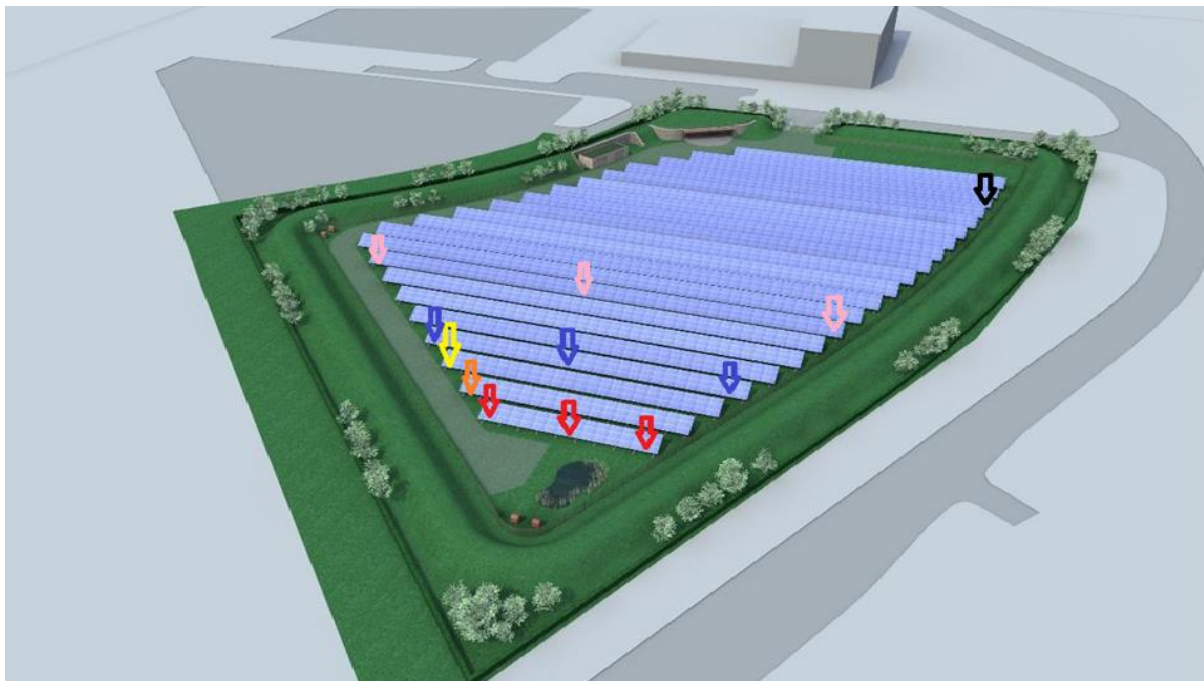


Figure 101 - Position of critical points of shading (Burns 2015)



Figure 102 - View of Solar Meadow from southern obstacles

4.5 Modelling Approaches

After the initial study (discussed in chapter 3) a number of modelling approaches were undertaken, sun-earth geometry calculations, solar radiation calculations, manual data collection, shading analysis, and energy calculations in order to answer the impact shading has on the energy delivery of the farm. It was first important to determine the interaction of solar radiation with the atmosphere and the earth's surface for the site through the following three steps: 1- Solar geometry: the available extra-terrestrial radiation on earth's surface which varies due to the earth rotation around the sun and the sun-earth position above that horizon, 2- The attributes of the PV surface: surface tilt, aspect of the surface, shade effect of the neighbouring objects around the surface and 3- Atmospheric influences on the attraction of solar energy on the earth's surface (i.e. impacts of clouds and all particles in the atmosphere). The shading analysis of the Edinburgh College PV farm focussed on the first 2 steps in order to demonstrate the impact of shading on the overall output.

4.5.1 Sun-Earth Geometry description

The geometric relationship between the sun and the earth can be described in terms of the latitude of the site, the time of the year, the angle between sun and earth and the altitude & azimuth of the sun. The main factors and variables which are necessary for the calculation of the sun's position in the sky in respect to a specific plane on earth's surface has been

investigated. The factors included in the investigation are day number (DN), sun declination (DEC), equation of time (EOT), solar altitude, solar azimuth and sun inclination.

4.5.2 Day number description

Day number is defined as the number of days passed in any given year to a specific date in that year. It is used to calculate the extra-terrestrial irradiance and through the use of VBA codes which are transferred to MATLAB to calculate all the day numbers for each data point with consideration given to leap years. All the MATLAB codes related to this have been provided in appendix (F) (Muneer, 2004).

4.5.3 Solar Declination description

Solar declination is defined as the angle between the earth–sun vector and the equatorial plane. Solar declination, as function that varies with the day of the year, is a significant parameter for the estimation of solar radiation. As presented in figure 103, the change in solar declination throughout the year ranges from 0° at the spring equinox to 23.44° at the summer solstice and it drop again to 0° at the autumn equinox and becomes -23.44° at the winter solstice. Because the earth's orbit around the sun is elliptical, the earth's velocity varies during the year and by changing the solar declination, sun light intensity changes during this time and results in the different seasons. This is the reason that the declination is not a strict sinus tidal curve (Budin, 1995).

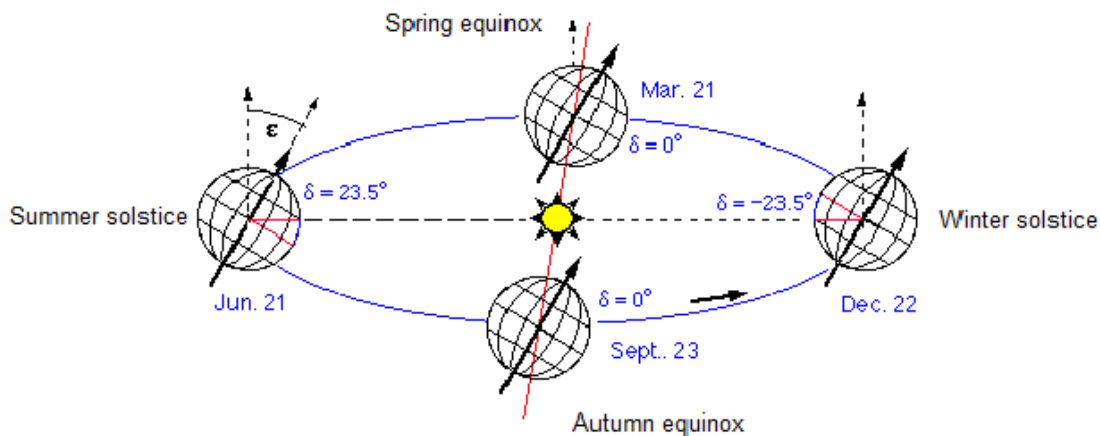


Figure 103 - Solar declination in different seasons

In this research Yallop's algorithm (1992) has been used to calculate solar declination due to it having very high precision and accuracy (1 min of arc) and is valid for the period 1980-2050 (Muneer, 2004).

For a given year (Y), month (m), day (D), hour (h), minute (m) and second the amount of solar declination will be obtained through this algorithm:

$$t = \{(UT/24) + D + [30.6m + 0.5] + [365.25(y - 1976)] - 8707.5\}/365.25$$

Where $UT = h + \left(\frac{min}{60}\right) + \left(\frac{s}{3600}\right)$ and if $m > 2$ then $y = y$ and $m = m - 3$, otherwise $y = y - 1$ and $m = m + 9$. The following terms are then determined:

$$G = 357.528 + 35999.05t$$

$$C = 1.915 \sin G + 0.020 \sin 2G$$

$$L = 280.460 + 36000.770t + C$$

$$\alpha = L - 2.466 \sin 2L + 0.053 \sin 4L$$

$$GHA = 15UT - 180 - C + L - \alpha$$

$$\varepsilon = 23.4393 - 0.013t$$

$$DEC = \tan^{-1}(\tan \varepsilon \sin \alpha)$$

4.5.4 Equation of Time description

Equation of time (EOT) is defined as the difference between standard time and solar time. Solar day is the interval of the time that the sun crosses from one local meridian to the subsequent time it crosses that same meridian. Solar day varies due to the solar declination and the earth's position in the plane of the elliptical orbit containing the sun and the earth. The orbital distance of sun-earth varies from a maximum 152 million Km to a minimum 147 million Km. There is a difference between solar day and a full rotation of the earth due to the fact that the earth rotates in a diurnal cycle and has forward movement in its orbit. Standard time is a time recorded by clocks that has constant speed (Muneer, 2004).

Equation 24 - Equation of time

$$EOT = (L - C - \alpha)/15$$

4.5.5 Solar Altitude and Azimuth description

The position of sun can be described with consideration given to two angles, SOLALT and SOLAZM. SOLALT is defined as the elevation angle of the sun from horizon and SOLAZM is described as the angle from north, and that of the perpendicular projection of the sun down onto the horizontal plane. This will proceed from sunrise to sunset in a clockwise rotation. The sun position is dependent on Greenwich Hour Angle (GHA), the latitude (LAT) and longitude (LONG) of the location and solar declination. SOLALT and SOLAZM can be calculated respectively through arc sin and arc cosine of these two equations:

$$\sin(SOLALT) = \sin(LAT) * \sin(DEC) - \cos(LAT) * \cos(DEC) * \cos(GHA)$$

$$\cos(SOLAZM) = \cos(DEC) \times (\cos(LAT) * \tan(DEC) + \sin(LAT) \times \cos(GHA)) / \cos(SOLALT)$$

4.5.6 Sun Inclination description

Sun inclination (INC) is defined as the angle of sun's beam on a sloped surface, which can be calculated from the solar altitude, azimuth and the orientation of the surface, which is known as wall azimuth angle (WAZ). Wall azimuth angle is described as the angle of a sloped surface from north, same as the azimuth clockwise, see figure 104. Arc cosine of the following equation, 27, will reveal sun inclination (INC):

$$\cos(INC) = \cos(SOLALT) * \cos(SOLAZM - WAZ) * \sin(TLT) + \cos(TLT) * \sin(SOLALT)$$

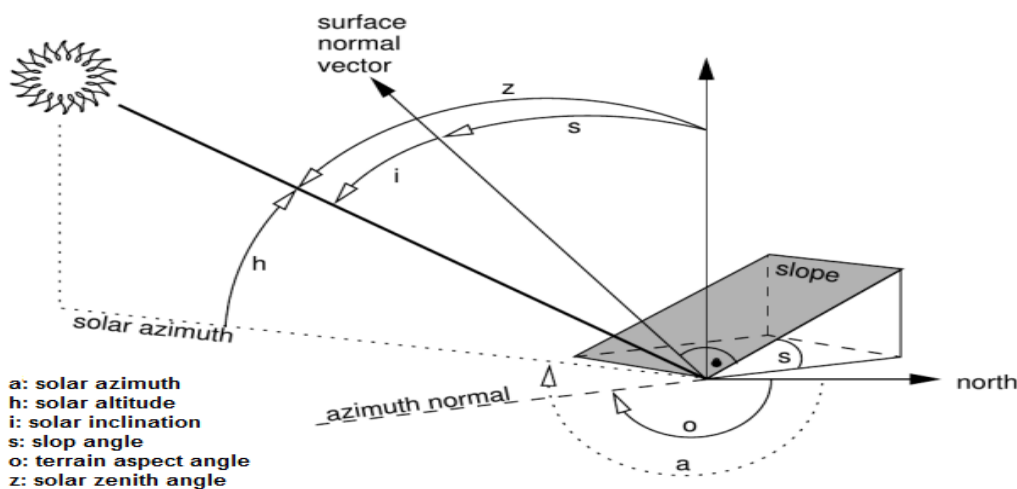


Figure 104 - Sun geometry in a tilted surface (Team, 2008)

4.5.7 Extra-terrestrial spectrum description

The spectrum of the solar radiation outside the earth's atmosphere is known as extra-terrestrial spectrum (ETS). The first step required in calculating extra-terrestrial spectrum is to consider the sun as a blackbody radiating at a temperature of approximately 5780 K, and by taking advantage of Planck's law, the corresponding spectral irradiance from that temperature can be estimated. The sun's energetic output represents a huge departure

from the smooth Planck spectral curve, especially at wavelengths below 800 nm. The recent extra-terrestrial measurements represent that ETS is variable on a day-to-day basis according to solar activity. Total solar irradiation (TSI) varies because of day-to-day change in EST. TSI has been measured between November 1978 to January 2003 and the results were respectively 1363 and 1368 W/m². The extra-terrestrial constant value can be obtained as the average value of TSI, defined as the mean between the minimum and maximum values of TSI, after a 27 day smoothing filter is applied to reduce the sun's rotation effect. The value of the solar constant is given for the average sun-earth distance, 1 Astronomical unit, because the earth's orbit around sun is not circular but elliptical. Around 3 April and 5 October sun-earth distance is 1 astronomical unit. For any other days except 3 April and 5 October, extra-terrestrial value should be multiplied to a correction factor S, to gain the daily extra-terrestrial irradiance at normal incidence (Muneer, 2004). For more accurate results Day number (DN) and SOLALT have been used in the following equation, 28, to calculate the hourly values of extra-terrestrial irradiance (I_E):

Equation 28 - Extra-terrestrial spectrum (Muneer, 2004)

$$I_E = 1367 * (1 + 0.033 * \cos(0.0172024 * DN)) * \sin(SOLALT)$$

4.5.8 Solar radiation description

When extra-terrestrial radiation enters to the atmosphere a part of the incident energy is lost due to the composition of the earth's atmosphere. The earth's atmosphere includes a mixture of gases, ozone, water vapour and aerosols which all cause the incident sun energy to be divided into two main radiations, beam radiation (which arrives at the surface of the earth directly from the sun) and the scattered radiation (which is called diffuse radiation). To calculate energy from the sun, hourly beam irradiance and hourly diffuse irradiance must be attained.

4.5.8.1 Hourly horizontal global irradiation (IG) description

Hourly horizontal global irradiation varies depending on local position (latitude and longitude) on earth and time of the year due to the variance in the sun-earth distance. In this research hourly horizontal global irradiation for Edinburgh (latitude: 55.95 N and longitude: 3.32 W) was collected from GOGARBANK site.

4.5.8.2 Hourly clearness index (K_T) description

The clearness index (K_T), equation 29, is defined as the ratio of the horizontal global irradiance to the corresponding irradiance available out of the atmosphere. The transparency of the sky is then indicated (Ndilemeni; Momoh, 2013).

Equation 29 - Clearness index

$$K_T = \frac{I_G}{I_E}$$

4.5.8.3 Hourly horizontal diffuse irradiance (I_D) description

Hourly horizontal diffuse irradiance is calculated by the usage of hourly global horizontal irradiance and hourly clearness index values with equation 30 (Muneer, 2004).

Equation 30 - Hourly horizontal diffuse irradiation

$$I_D = I_G * (1.006 - (0.317 * K_T) + (3.1241 * K_T^2) - (12.7616 * K_T^3) + (9.7166 * K_T^4))$$

4.5.9 Hourly global slope irradiance description

Solar photovoltaic panels are mounted with a specific tilt to take the most advantage of the sun. To calculate hourly global slope irradiance, it is necessary to obtain the incident slope beam and diffuse irradiance. Diffuse irradiance in a sloped surface consists of sky-diffuse and ground reflection. The irradiances that land on PV panel are beam irradiance, diffuse irradiance and ground reflection (equation 31).

Equation 31 - Hourly global slope irradiance

$$I_{G,slop} = I_B + I_{D,TLT} + I_{Ground}$$

4.5.9.1 Hourly slope beam irradiance (I_B) description

Hourly slope beam irradiance is calculated from hourly horizontal global irradiance, hourly horizontal diffuse irradiance, sun inclination, and solar altitude through equation 32.

Equation 32 - Hourly slope beam irradiance (Muneer, 2004)

$$I_B = \frac{(I_G - I_D) * \cos(inc)}{\sin(solalt)}$$

4.5.9.2 Sky diffuse irradiance models

The Sky diffuse calculation is important because it is a dominant component of energy calculations in an overcast sky or at times when beam irradiance has been blocked. The Sky diffuse model has been divided into three different generation models with respect to their evolution and precision.

4.5.9.3 First generation models

This model is the simplest and earliest model used to describe the sky diffuse as in this model it was assumed an isotropic sky. Diffuse irradiation is not isotropic in nature and is an angular function of the solar altitude and azimuth. Only in the intensity of overcast skies case it is possible to consider isotropic as an acceptable case even in the partial overcast skies it is unrealistic. Another model which belongs to the first generation is to consider the sky diffuse and beam radiation originate from the direction of the solar disc. This model unlike the isotropic model is acceptable for the clear sky conditions (Muneer, 2004).

Equation 33 - diffuse irradiation on a sloped surface

$$I_{D,TLT} = I_D * \cos^2\left(\frac{TLT}{2}\right)$$

4.5.9.4 Second generation models

The second generation models offer a better and more precise result than first generation because these models differentiate between the radiation distribution of clear and overcast skies. By putting functions that vary for different conditions from clear to overcast skies (Muneer, 2004).

4.5.9.5 Third generation models

In these models the sky diffuse component consider as anisotropic. A great majority of the models in this generation analyse non-overcast irradiance as the sum of two components, circumsolar and background sky diffuse (Muneer, 2004).

This research adopted a first generation model approach as the main objective is to analyse energy delivery.

4.5.10 Ground reflection

One of the components of the solar radiation incident on a sloped surface is ground reflected radiation. Ground reflection changes due to ground materials and their reflectivity, for example, a ground covered by snow has a high value of reflectivity and in northern latitudes due to the low elevations of sun. To estimate an accurate amount of ground reflected radiation, knowledge of foreground type and geometry, its reflectivity, degree of isotropy, the details of the surrounding skyline and the condition of the sky are required (Muneer, 2004).

The ground reflected radiation incident on a tilted surface can be calculated by assuming that the ground is an isotropic diffuse reflector and by taking advantage of equation 34 (Efim and Evseev, 2008).

$$I_{Ground} = \rho * I_G * \sin^2\left(\frac{TLT}{2}\right)$$

Where, ρ , is ground albedo which is a constant value 0.2 for temperate and humid tropical places and 0.5 for dry tropical places and it will change regarding to geographically position.

The process of carrying out detailed calculations was important in understanding the interaction of solar radiation with the Earth's surface and atmosphere was important in pin pointing the site's specific attributes for the capture of solar energy. This last section has given an overview of the required site specific attributes identified through the modelling process, which are required to accurately model the shading algorithm used to determine the shade present at the site. The next section will discuss the shading algorithm options available, in brief, and describe the chosen algorithm in more detail.

4.6 3 Shading algorithms considered:

4.6.1 Budin shading algorithm

The shading algorithm proposed by (Budin and Budin, 1982) is a detailed mathematical approach requiring coordinates on the earth's surface used to pin-point the location of a point on the surface of the planet. The sun's position with respect to the hour angle, site altitude and solar declination (DEC) are also required to accurately use this algorithm. Here, the relationship between sun's position (in a spherical coordinate system) and the local tilted surface is calculated through two transformations:

The first consists of the local tilted surface to the horizontal surface of that in the spherical coordinate system.

The second uses the spherical coordinate system of the horizontal surface to that of the equator.

The shading calculation is defined as the calculation of the shadow of a blocked point on the plane surface with an arbitrary orientation. The position of the shade in a particular site on a certain day and time can be calculated from solar altitude (SOLALT) and solar azimuth (SOLAZM) with consideration to site latitude, solar declination (DEC), surface azimuth (orientation), surface tilt and solar hour angle for that day. A lengthy process when looking at a number of potential obstacles.

4.6.2 Horn shading algorithm

(Horn, 1981) proposed an 'automatic hill shading algorithm', which, removed the mathematics and physics aspect of the Budin's shading algorithm and replaced it with Digital Terrain Models (DTMs) and the reflectance map. In order to accurately demonstrate shade through a reflectance map it is necessary that the scene brightness is captured on the surface orientation with consideration to slopes and different elevations from east to west and south to north direction. Relief shading methods were divided in these groups by Horn:

- rotationally symmetric reflectance maps-grey tone depends on slope only
- average reflectance are modulated by methods based on different thickness
- ideal diffuse reflectance and various approximations
- the group that only depends on the angle of the plane in the direction away from the assumed light source (grey tones)
- methods which are more dependent on more sophisticated models of diffuse reflectance from porous material, such as that covering the lunar surface
- models for gloss and lustrous reflection-smooth surface, extended source and rough surface, point source

4.6.3 Geographic Information system packages

The third algorithm is the model used by shading commands in Geographic Information system (GIS) packages. The brightness of a specific surface point can be determined by its orientation with respect to the observer and the sun. The amount of the radiation that can be absorbed by a surface point will depend on its inclination compared to the incident beam.

It is generally assumed that the radiation received on a surface point is also proportional to cosine of the surface elevation, however this is not the main issue here because sun radiation is likely to be reflected in different directions. Shading can be obtained through equation 35:

Equation 35 - Horn shading analyse equation

$$S = 225 \times \cos\theta_z \times \cos\beta + \sin\theta_z \times \sin\beta \times \cos(\gamma_s - \gamma)$$

Where 255 is the maximum gradient for a 16-bit colour system and θ_z is the incident angle, β surface tilt and γ_s is the sun azimuth and γ is the surface azimuth.

This method requires a simulation of the Sun's path through the sky, this can be calculated manually through the use of solar altitude (SOLALT) and solar azimuth (SOLAZM) for a specific time and location from the solar position and intensity calculator, through the GIS package. For each point of interest, on the surface, the shadow of obstacles around the

point will vary and are obtained by calculating the horizon of each point of interest. A profile line is the line between two pixels connecting them together. An angle is the dedicated to each profile line giving the profile angle. A point of interest not in shade will be the maximum of all the possible angles and therefore must be equal to the profile angle. The profile angle α_p is defined by Duffie and Beckman (2013) as the angle through which a plane, that is initially horizontal, must rotate around the axis, of the plane in question, in order to include the sun. Mathematically the profile angle is calculated through equation 36:

Equation 36 - Profile angle equation

$$\tan\alpha_p = \frac{\tan\alpha_s}{\cos(\gamma_s - \gamma)}$$

Where α_s is the surface angle, γ_s is the surface azimuth, and γ is the sun azimuth. In different sun positions, as it changes with time, the profile angle is checked to investigate whether the point of interest is in shade or not. Figure 105 represents the final flow chart of this algorithm and shows the clear process required to be undertaken in order to capture the losses due to shading (Nguyen and Pearce, 2012). Within the GIS modelling algorithm the site is reasonably easy to evaluate due to the groundworks undertaken to provide a clear, flat site for the array to be easily installed.

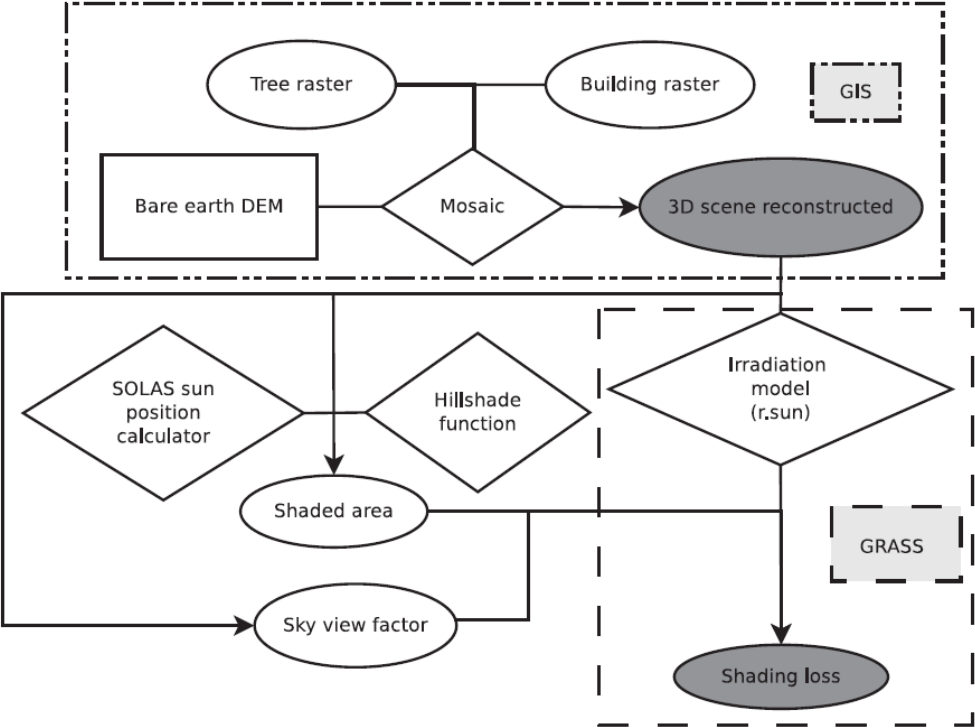


Figure 105- Final scene construction and irradiance modelling for this algorithm (Nguyen and Pearce, 2012)

4.7 Algorithm selected – Sky View Factor (SVF)

Sky View Factor (SVF) has been shown to be one of the most useful urban spatial indicators for radiation and thermal assessment (Zeng et.al. 2018). Estimating SVF is straightforward and convenient and can account for obstruction by buildings and vegetation such as trees. Undertaking shading calculations within a cluttered sky space would better suit the algorithms described previous, however, with few obstructions within the available sky space on the site of the solar farm.

4.7.1 Sky view factor

After consideration was given to the previous methods described, this study utilises Sky View Factor (SVF) to establish the shading effects encountered in the Edinburgh College Solar Meadow. SVF is the ratio of radiation received by a surface to the radiation emitted by the entire hemispheric environment (Nguyen and Pearce, 2012). It expresses the relationship between the visible area of the sky and the portion of the sky covered by surrounding buildings, and other obstacles, viewed from a specific point of observation. The SVF encompasses reduction of visibility due to the slope of an inclined plane and obstacles in the surrounding built environment. The diffuse radiation incident is thus obtained through the product of SVF (%) by available diffuse radiation on unobstructed horizontal surfaces (Carneiro, 2009). In analysing SVF one can acquire the impact of shading on the 12 critical points of shade within the array.

This section will look at the methods used to collect the data required to understand the impact of shading on the solar farm. The Critical points of interest were selected through a topographical survey of the entire site in order to analyse areas of high shading as described in section 4.4.1. The method used theodolite data and the following equations, 37, 38 and 39, to calculate the total irradiance being blocked by obstacles surrounding the array.

The first calculation, from (Muneer, 2004), is used to calculate the beam and diffused irradiation of a point at a given time. Equation 37 will provide the calculation:

Equation 37 - Slope beam & diffused irradiation (Muneer 2004)

$$Total\ Visible\ Sky, TF = \cos^2\left(\frac{\beta}{2}\right)$$

$$I, Beam\ Slope\ (G, Global - D, Diffused) \frac{\cos INC}{solALT}$$

$$I, Diffused\ slope = D, Diffused \times TF$$

When the slope beam and diffused values are calculated they need to be cross referenced with the angular values of any obstruction to the solar panels this allows the total irradiance being blocked to be calculated. This can be done using equation 38:

Equation 38 - Sky view

$$Sky\ View = 1 - \sum \frac{(d\phi, \text{deg} \times \frac{\pi}{180}) \times (d\alpha, \text{deg} \times \frac{\pi}{180})}{\cos^2\left(\frac{\beta}{2}\right)}$$

Where:

$d\phi$, deg: is the angle between two points in degrees

$d\alpha$, deg: is the angle of inclination from a 90° plane to the highest point of the obstacle

By using the results from the previous equations (37 & 38), the total solar irradiance blocked can be calculated using equation 39:

Equation 39 - Total Blocked Irradiance

$$Total\ Blocked\ Irradiance = \left((ID, Slope \times Sky\ View) + (IB, Slope \times Sky\ View) \right) \times \left[\sin^2\left(\frac{\beta}{2}\right) \right]$$

This calculation, 39, gives the cumulative value of all irradiance being blocked and therefore shows the total impact of the shading effect incurred by the PV panels. To achieve more reliable results, shading analysis was implemented every 30 minutes once a week for the whole year. For this shading analysis four main steps have been used in MATLAB to provide the calculated results.

1. Allocate measured panel's elevation for specific azimuth in each critical point.
2. Investigate whether the critical points are in shade, or not, by comparing solar altitude and panels elevation in each specific time. In this step panels have been modified and divided in two groups. If the panel altitude on that specific time is lower than solar altitude the point is not in shade and for (SVF) has been considered as zero.
3. Calculate sky view factor which varies between 1 & 0. 1 = no shade, 0 = high shade.
4. Determine global slope radiation in two different conditions. Firstly, where the point is not in shade, the following calculation using equation 40 is used:

Equation 40 - Global irradiation on a sloped surface

$$I_{G,stop} = I_B + I_{D,TLT} + I_{Ground}$$

And when the point is in the shade (no beam radiation therefore diffuse values must be multiplied to sky view factor (SVF)) the following calculation through equation 41 is used:

Equation 41 - Global irradiation on a sloped surface in shade

$$I_{G,slop} = I_{D,TLT} \times (SVF) + I_{Ground} \times (SVF)$$

All the calculated data was transferred into an excel spreadsheet for further analysis. Through this process the ability to produce graphical outputs of the calculations was achieved. Each month's data was separated and, for each day, available energy has been evaluated and then available energy in each critical point (with consideration to shading effect) has been estimated. Three different approaches have been applied to investigate each month's energy delivery and are described in the next section.

4.8 Calculation Process

4.8.1 Energy delivery from the solar meadow – the three approaches utilised

In the first approach, equation 42, each day's energy delivery ratio has been evaluated as the average of the 12 critical points. The available energy, at these points, was divided by that day's available energy without shading effect, and in the end average of those 4 days represents the percentage of energy delivered for that month.

In the second approach, equation 43, the whole the month's available energy without shading has been obtained and the available energy for each critical point during the month has been estimated, the ratio of critical point available energy to the whole month available energy without shading presents the point's delivery percentage and average of the 12 points represents the percentage of energy delivered in that month.

In Third approach, equation 44, all 18 rows of solar panels, in the solar meadow, have been included. Each row has been divided into three different parts (left, centre and right). All 54 of these points were included in the shade investigation. This research assumed that the 2nd and 3rd row have the same shading analysis as the 4th row and all other rows, except row 1 and row 17 which have the same shading effect as eighth row. The entire month's energy delivery has been obtained on the basis of these 54 points.

Equation 42- Approach 1 for energy delivery calculation

$$approach\ 1 = \frac{\sum \left(\frac{\text{points daily energy after shading analysis}}{12} \right)}{\text{available energy without shading}} \div \text{number of days in that specific month}$$

Equation 43 - Approach 2 for energy delivery calculation

$$\text{approach 2} = \frac{\sum \frac{\text{one month point energy after shading analysis}}{\text{one month available energy without shading}}}{12}$$

Equation 44 - Approach 3 for energy delivery calculation

approach 3

$$= \frac{(frled + frced + frred + srred + trred + (forled * 3) + (forced * 3) + forred + (erled * 14) + (erced * 14) + (erred * 13) + srled)}{54}$$

4.8.2 Calculating Energy Output with relation to shading

To calculate the overall energy output of the farm, 6 steps have been implemented and explained. Global slope radiation is the major contributor; therefore all the data must be highly accurate. Muneer's (2004) VBA programs (calculation 4.8 and calculation 10) have been used to calculate the hourly global slope irradiation.

Step 1: To calculate the hourly horizontal diffuse irradiation from measured hourly horizontal global irradiation in GOGARBANK, program calculation 4.8 has been used. By putting the measured data in the program, hourly horizontal diffuse irradiation has been obtained.

Step 2: Hourly slope irradiation has been calculated by using inputting the data into program calculation 4.10.

Step 3: Hourly temperature of Edinburgh has been calculated through equation 45 as proposed by ASHRAE (figure 106).

Equation 45 - Hourly temperature equation

$$T_a = z(T_{max} - T_{min}) + T_{min}$$

Where z values are for the diurnal temperature swing in 24 hours proposed by ASHRAE which has been presented in figure 94 and maximum and minimum temperature values of day 16 of each month has been collect from TUTIEMPO website (10/2015). The performance of the ASHRAE model evaluated with comparing measured hourly temperature and computed one in different places and it represented reasonably good similarity (Gago *et al.*, 2010).

Hour	Z	Hour	Z
1	0.12	13	0.95
2	0.08	14	1.00
3	0.05	15	1.00
4	0.02	16	0.94
5	0.00	17	0.86
6	0.02	18	0.76
7	0.09	19	0.61
8	0.26	20	0.50
9	0.45	21	0.41
10	0.62	22	0.32
11	0.77	23	0.25
12	0.87	24	0.18

Figure 106 - ASHARAE for diurnal temperature changing (Gago et al. 2010)

Step 4: To calculate cell temperature using Normal operating cell temperature (NOCT). It is defined as the cell temperature of a solar module operating in a specific condition as zero current, 800 W/m² irradiation, 20^oc air temperature and wind speed of 1 m/s. Here cell temperature has been calculated (equation 46) relating to solar irradiation:

Equation 46 - Cell temperature equation on the basis of global radiation

$$T_C = T_a + \frac{G_{slope}}{G_{noct}} (T_{c,noct} - T_{a,noct}) \left(1 - \frac{\eta_{stc}}{\tau\alpha}\right)$$

Where: T_C is the cell temperature, T_a is air temperature, G_{slope} is the global slop irradiation, G_{noct} is equal to 800 w/m², $T_{c,noct}$ is the cell temperature at NOCT, $T_{a,noct}$ is the air temperature at NOCT, η_{stc} is the cell efficiency in standard test conditions (STC), and $\tau\alpha$ is the module light absorptivity.

Step 5: There are 3 different methods to calculate cell efficiency: 1- from power output and available solar irradiation, 2- using the heat flux energy balance, and 3- by using the cell temperature. In this instance method 3 was used, in calculating cell efficiency from cell temperature a coefficient factor, heat coefficient for power output, is required. This coefficient is a value accounting for a drop in power output with an increase in temperature. This coefficient is gathered from the manufacturer's datasheet. The equation (47) for efficiency calculation is:

$$\eta_{cell} = \eta_{stc}(1 + \alpha_p(T_c - T_{c,stc}))$$

Where: η_{cell} is the cell efficiency η_{stc} is the cell efficiency in standard test condition, α_p the heat coefficient of the cells.

Step 6: The energy output of the farm in each month, energy output for one square meter has been calculated. The area of each cell has been worked out as 0.0243 m² and each module in the Edinburgh College solar PV farm contains 60 cells, therefore each module has a useful area of 1.485 m² with each module area being 1.62 m² including margin. There are 2560 PV modules in the array giving a net, useful, area of circa 3732.48 m². By using this detail, the energy output for one square metre can be calculated and the overall energy output in a specific month has been calculated.

4.9 Results

4.9.1 The three approaches in results

The shading results will be presented in 2 ways, linear plots and radar plots. This will achieve a clear understanding of the impact of shading on the solar farm. Table 23 and figure 107 show the energy delivery percentage in each month with consideration to different approaches is presented with respect to impact of shading on modelled output. Table 23 provides a monthly breakdown of energy production of the overall site.

Table 23 - Shading analysis of three approaches

Month	Approach 1	Approach 2	Approach 3
January	70%	70%	70%
February	72%	70%	80%
March	86%	84%	91%
April	99%	99%	99%
May	100%	100%	100%
June	100%	100%	100%
July	100%	100%	100%
August	99%	99%	99%
September	93%	93%	95%
October	74%	80%	88%
November	73%	54%	69%
December	59%	52%	54%

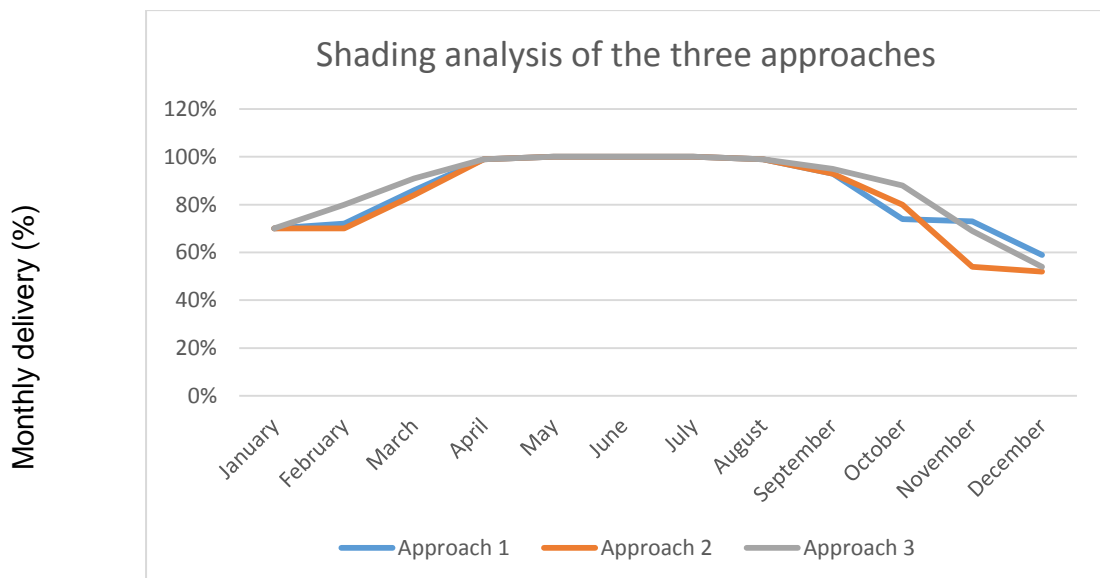


Figure 107 - Shading analysis of the three approaches

As presented in table 22 and figure 107 December has the lowest percentage of energy conversion power production in the year, with near to half of the energy being lost due to shading. May, June and July are generating at 100% with a further 4 months operating at 90% or above. This gives an average of around 90% for the full year. From this it is clear that shading on this site has a significant impact on energy production for one month of the year and a further three months where energy delivery is only 70%-80% of maximum potential.

4.9.2 Linear plots

Linear plots have been used here to illustrate the sun’s altitude at two of the 12 critical points in the Solar Meadow. The First row-right’s blockage altitude and the eighth row-centre’s blockage altitude, on four different days, in each month throughout the year are represented by these linear plots and clearly justify the findings of the three approach shading analysis undertaken.

For three months of the year it is clear that Solar altitude is at its highest point at nearly 60° which is twice the height of the maximum altitude of the blockages along the southern and eastern edges of the meadow. Figure 108 is an example of one such month, July, and clearly shows the differences in altitude in a linear fashion.

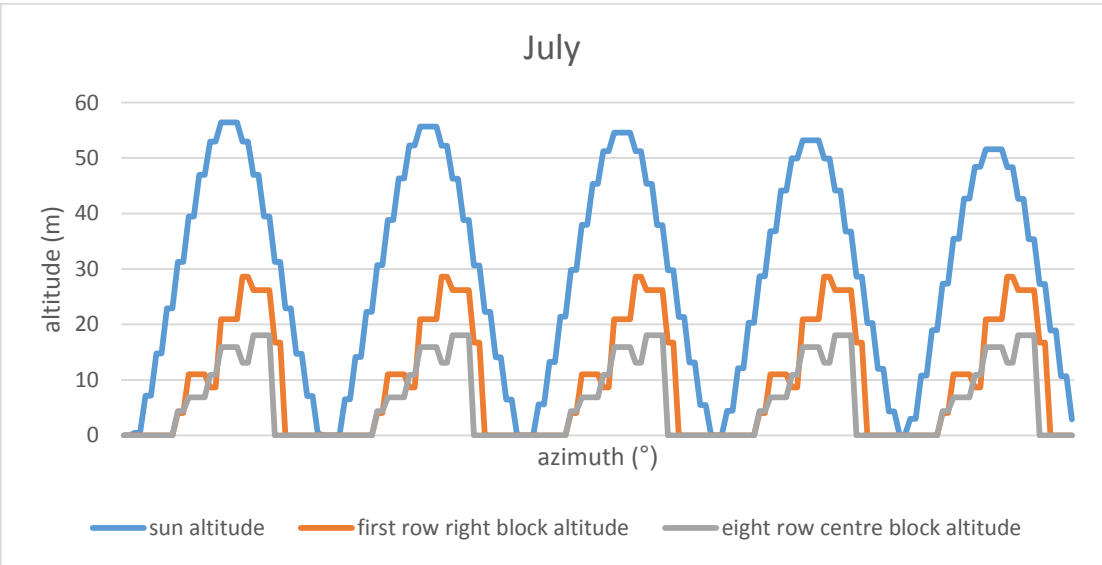


Figure 108 - July shading analysis

December is the worst month in terms of energy delivery, as figure 109 shows, the sun’s altitude is at its lowest point above the horizon in the year. This is as expected but the main issue with the 2 points in question is that they are both in shade at all times throughout the entire month of December. This clearly illustrates the poor positioning of the solar panels

with respect to the southern and eastern blockages and the impact shading can have on the amount of energy produced.

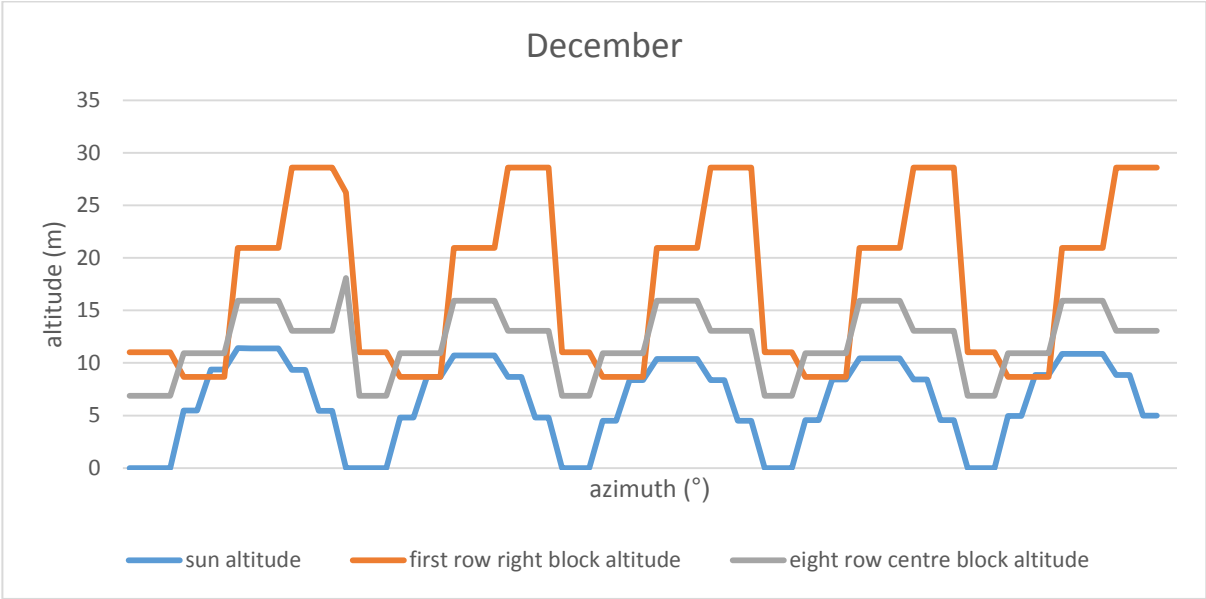


Figure 109 - December shading analysis

Appendix G shows the remaining month’s linear plots and highlights shading impacts throughout the year. It can be seen that in most of the hours in January both of the points are in shade as the solar altitude is lower than the blockages altitude. In this month the solar PV modules also have a shading effect on each other, along with the blockages around the site, as the energy delivery at the critical point in the eighth row-centre is only 62%.

During February the sun’s altitude is increasing and in the last two weeks of the month, during the morning, the two points are not in shade as the sun’s altitude is higher than blockages altitude. The energy delivery, as a percentage, at the point eighth row-centre reaches to 91%, but the first row-right is still low at only 53%. This is a result of the large trees that dominate the southern edge having an impact on the first row of solar panels.

From the second week in March the solar altitude passes 30° and is higher than the maximum block altitude which is near to 29°. This means there is an expected increase in energy production from March onwards. In March the energy delivery at the point, first row-right, reaches 70%.

In April energy delivery of the two points arrives at 99%, as shown in appendix G. During the times plotted the solar altitude is higher than blockages altitude. As, all the data has been collected every seven days, so in this month five days have been investigated.

In May 100% of energy is delivered and the plot shows in all the times of the month solar altitude is higher than blockages altitude. In June and July the solar altitude remains at its highest point above the horizon, near to 60°. However, during July we do see a slight decrease in the energy delivery.

From the final two weeks of August it appears that the blockages, again, start to impact on the energy delivery of farm. In September energy delivery of farm has dropped to 95% as the sun's altitude in the sky begins to decrease along with the earth's tilt away from the sun. From the second week of September the first row of solar panels is experiencing shading for half of the day, as can be seen in the September plot, and its energy delivery has decreased to 88%.

During October the energy delivery of farm remained at 88%, until the last week of the month when the Sun's altitude reaches roughly 20° as shown in the October plot. Finally the November plot shows that point, first row-right, is in shade during most of the times throughout November. Only during the first week of November is the solar altitude higher than the blockages altitude at point eighth row-centre and the energy delivery at this point has dropped to 66%.

4.9.3 Radar plots

A different representation of the sun's altitude verses the blockages altitude can be shown through the use of radar plots. These plots have also been included for a better visual presentation of findings. As shown, in figure 110, the altitude varies as the circle's radius changes and azimuth changes clockwise. Each day is represented by one quarter of the radar plot and by three values of solar altitude, the two points, first row-right blockage altitude and eighth row-centre, can be evaluated by consideration given to their distance from centre. Figure 110 and 111 represent the best and worst months in terms of shading impact. Appendix H shows all remaining months of the year for comparison with the linear plots provided. In essence giving a clear pictorial representation of the impacts of shading and the sun's altitude on the energy delivery of the solar meadow during each month.

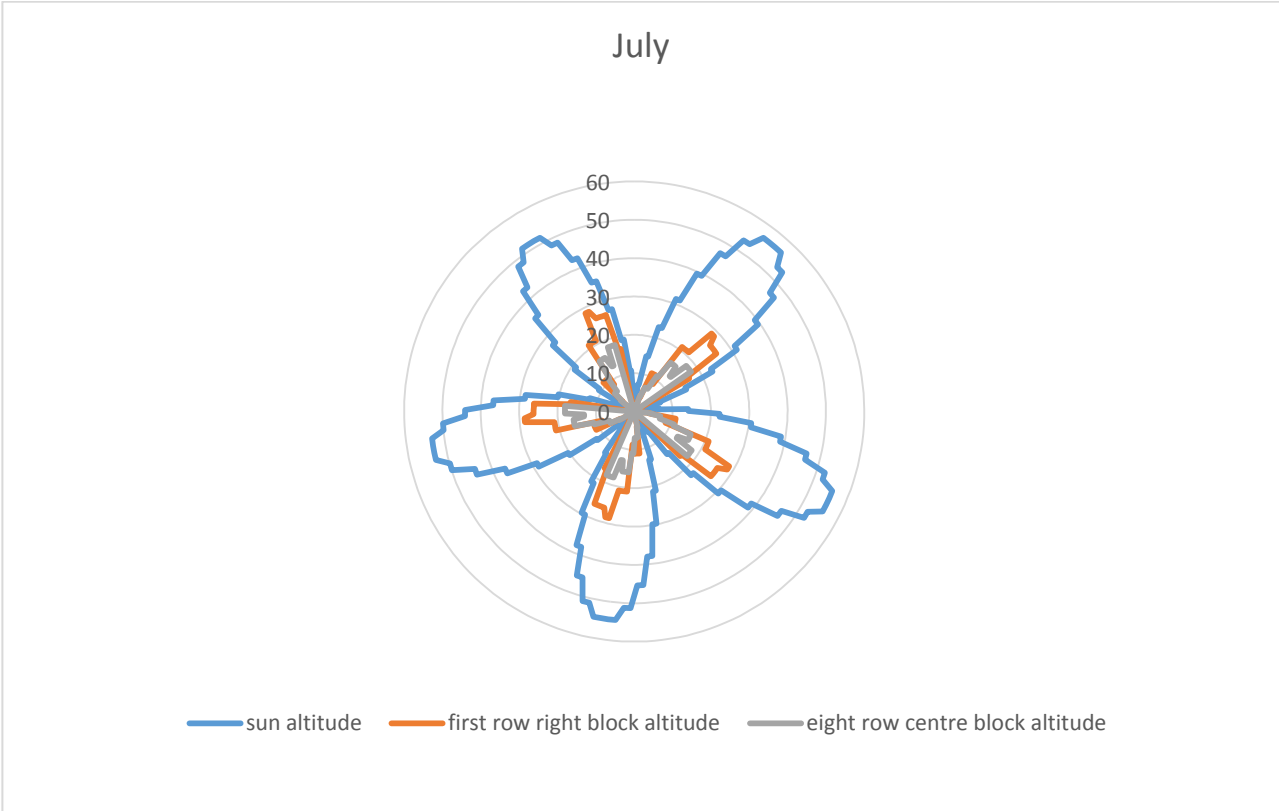


Figure 110 - July Radar Plot

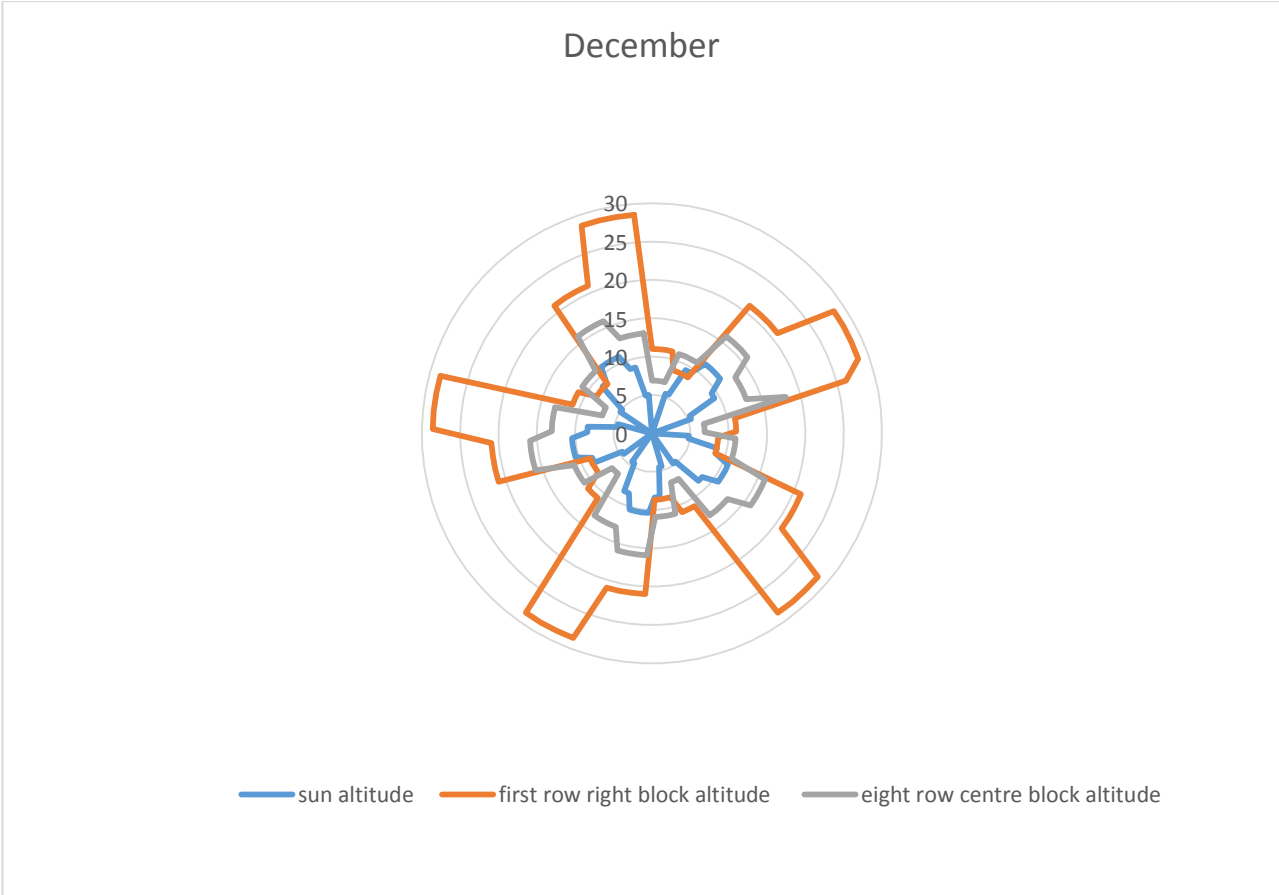


Figure 111 - December Radar Plot

4.10 Energy output of the Solar Farm

4.10.1 Scenario one

To calculate energy output, two scenarios have been considered and evaluated. In the first scenario energy output is on the basis of hourly global irradiation on the 16th day of each month and then extended to the monthly value by multiplying that number by the number of days on that specific month. Results have been provided in table 24. The total annual energy available in the farm is 717,111 kWh and this value after the shading effect is implemented will change to 675,943 kWh. This is 94% of the energy available being delivered. 41,167 kWh of energy will be lost due to the impact of shading and it is equivalent to a £2,700 monetary loss in annually. Figure 112 shows these findings in graphical form across the year and shows the expected outcome from the energy output with relation to the impact of shading outlined in the previous section.

Table 21 - Energy output scenario one

Month	Monthly Energy (KWh/m ²)	Farm Monthly Energy (KWh)	Shade Delivery Percentage %	Output Energy with Shading (KWh)
January	5.27	19659	70.00	13762
February	13.93	52013	80.00	41610
March	12.10	45152	91.00	41088
April	17.24	64364	99.00	63720
May	27.71	103440	100.00	103439
June	36.47	136113	100.00	136113
July	25.45	95003	100.00	95003
August	21.90	81749	99.00	80931
September	10.05	37515	96.00	3614
October	13.42	50092	88.00	44081
November	5.17	19299	69.00	13316
December	3.41	12713	54.00	6865

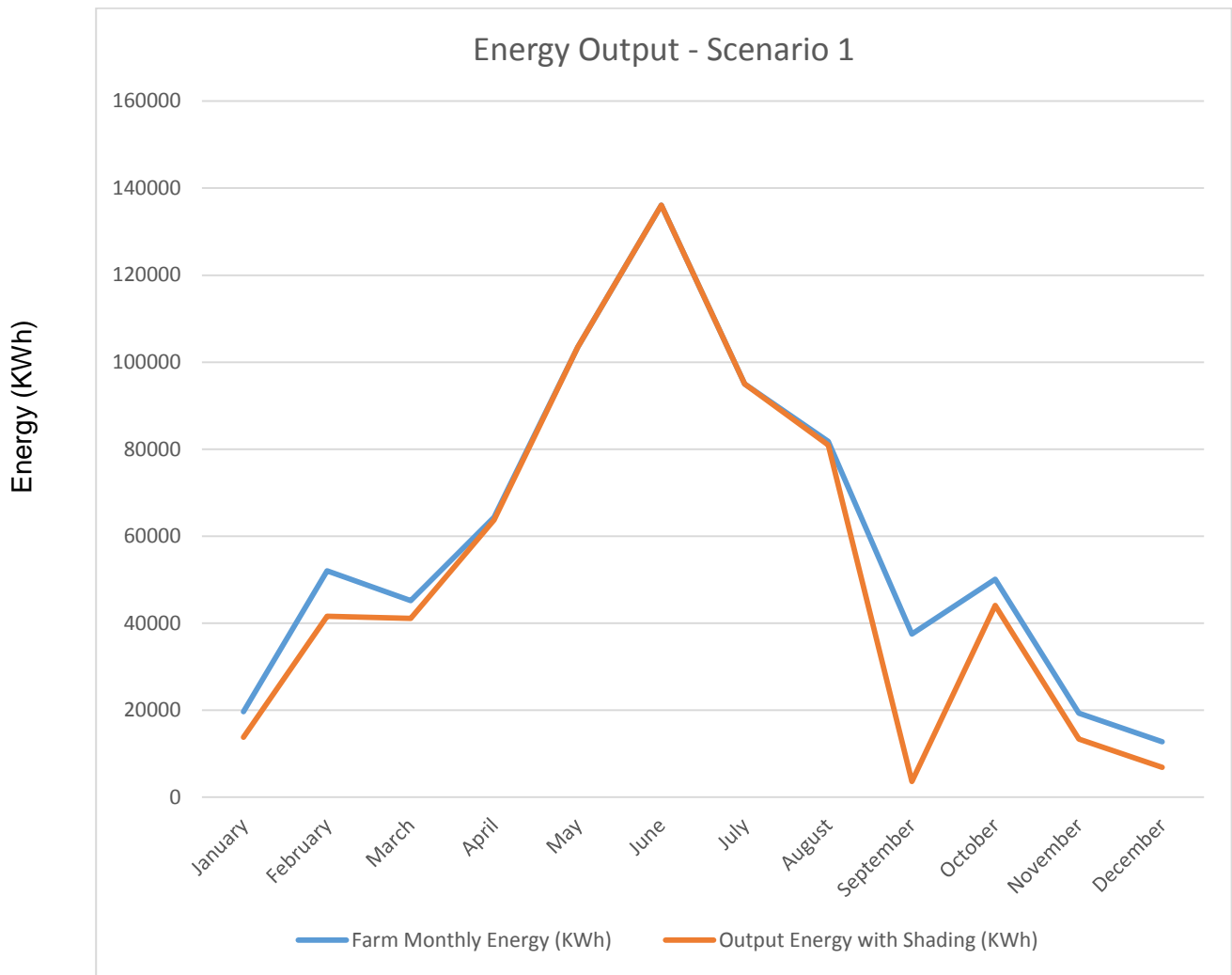


Figure 112 - Energy Output - Scenario 1

4.10.2 Scenario 2

In the second scenario, the mean value of hourly horizontal global irradiation for each month has been calculated using MATLAB software. Instead of using single day values, the mean value of each specific hour, in one day, for whole the month has been calculated. The hourly global slope irradiation has been calculated for each month on the basis of the mean values. Table 24 and figure 113, show the results related to second scenario. The total annual energy available has been estimated as 525,674 kWh, decreasing to 498,776 kWh after the impact of shading is applied. 26,898 kWh of energy has been lost due to shading, equivalent to £1800 with consideration to FIT scheme of the site.

Table 22 - Energy output scenario two

Month	Monthly Energy (KWh/m ²)	Farm Monthly Energy (KWh)	Percentage %	Output Energy with Shading (KWh)
January	2.16	8053	70	5637
February	8.24	30758	80	24606
March	14.23	53119	91	48339
April	15.2	56745	99	56177
May	17.52	65411	100	65411
June	20.01	74707	100	74707
July	23.43	87473	100	87473
August	15.08	56301	99	55738
September	11.45	42772	96	41061
October	8.37	31246	88	27497
November	3.25	12144	69	8379
December	1.86	6946	54	3751

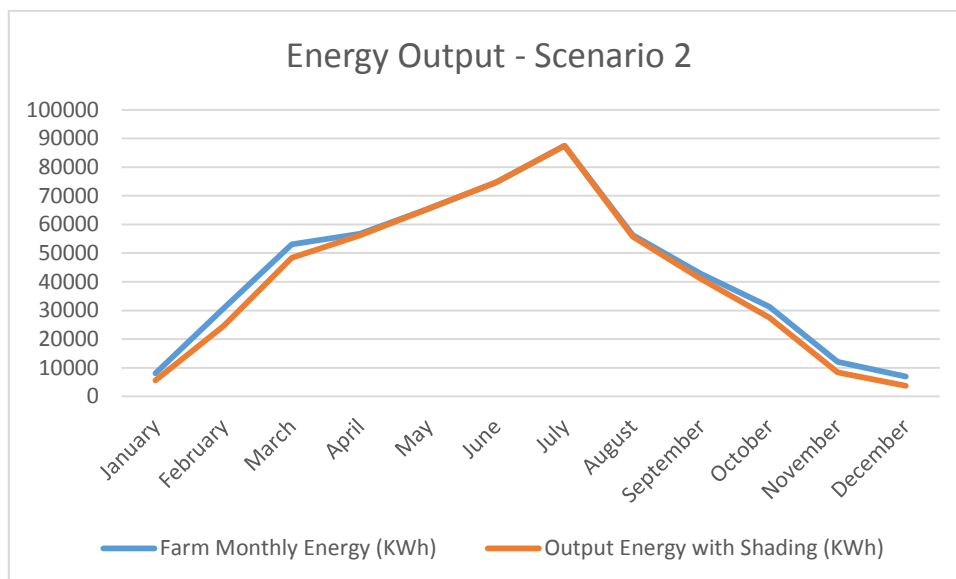


Figure 113 - Energy output - scenario two

4.11 Conclusions

This Chapter set out to research the impact shading, from obstacles around the solar array, has, if any, on the solar array at Edinburgh College's Midlothian campus. The energy delivery has been assessed with consideration to the shading effect. Energy production, especially in the renewable sector, requires reliable and precise calculations in terms of the available source of energy and the net energy production. It is important for installers to make the most of available solar sources and to ensure the highest possible energy conversion is realised. The installers of the array attributed little to no shading effect on the farm during the entire year.

After an initial inspection of the site, 12 critical points were selected from south, east and the centre of the array. All data related to the obstacles around the farm at each critical point was collected by the theodolite and for every 30° due east, the height (altitude) of the obstacle was recorded for each point. Sun position in the sky (solar altitude and azimuth) has been calculated. For each specific azimuth due east, solar altitude (SOLALT) and the obstacles height was compared. The duration of shading experienced at each point was analysed by taking advantage of sky view factor (SVF) shading model and the relationship between the visible area of the sky and the proportion of the sky covered by surrounding obstacles was assessed.

Energy delivery for each month has been calculated on the basis of the energy delivered at these points. December has the lowest energy delivery with only 54% with November and January second and third lowest with 69 and 70% energy delivery respectively. The energy delivery increases gradually until it reaches 100% in May, June and July. The solar PV farm at Edinburgh College delivers more than 94% annually when accounting for the impact of shade.

The solar farm's energy has been calculated by use of the measured 2014 global radiation and farm's PV modules specifications. The available energy in the Edinburgh college solar PV farm has been estimated at 525,674 kWh, which, due to the shading effect decreases to 498,776 kWh. For this specific installation 95% of the energy is produced in the months where energy delivery is higher than 80% and only 5% of energy is produced in the months from November through February. The main shading factors have been recognised as the trees in the south and south east of the farm.

This chapter has investigated the importance of solar panel positioning in maximising energy delivery, especially at higher latitudes. The chapter has shown that as solar altitude

decreases obstacles and blockages become more of a hindrance and careful planning is required to ensure the amount of shading on the panel surface is kept to a minimum. This chapter has presented the impacts of shading on the Edinburgh College Solar Meadow from obstacles along the Southern and Eastern edges. The Solar Meadow delivers 90 – 100% energy output for seven months of the year. There is only a single month in the year when the energy delivery of the farm drops to around 50% of the expected output. This chapter has shown that shading can have a significant impact on solar PV installations at high latitudes, extra care should be afforded in the planning process to ensure maximum potential is met through the orientation and positioning of panels. A comparison of Actual, Available, modelled and energy output with respect to shading is shown below. This table (23) shows the site suffers from shading as shown in section 4.9. PV*SOL modelling or a GIS package should be utilised to fully appreciate the shading impact across the entire site, not just the 12 critical points studied in this theses. This will build a strong picture of the site and shading across the array.

Table 23 Energy output comparison

Actual Energy	538,388 kWh
Available Energy	525,674 kWh
Modelled	560,000 kWh
Energy output with respect to shading	498,776 kWh

Chapter 5 Future plans: Implementation of a solar charging station for e-cars at Edinburgh College

5.0 Chapter Summary

One aspect of this study that has provided scope for further research in an array linked, but not directly, is around the pedagogical impact of having a resource, such as the solar farm studied, on the site of a college campus. This study has provided a good example of a research approach that breaks away from the more traditional University based research work. One of the real advantages of this particular work is the partnership between FE and HE institutions (Edinburgh College and Edinburgh Napier University in the case, and Industry (SSE).

This is not an original concept but is one that is not necessarily the norm in the UK. A real benefit of this specific site is access to the land, equipment, data and research facility for the students, at all times. The number of partners involved and opportunities this brings to study and curriculum, stakeholder involvement and student exposure to industry standard technology. The training opportunities now embedded in the curriculum and the bolt on training options now available to students, let alone potential for knowledge transfer and upskilling with industry. The sum of the parts is the main output along with the college becoming a research active organisation.

The requirement for the development of higher-level vocational skills within industry, and the needs of regional market demands increasingly prioritised by both devolved and national governments, has highlighted the need for FE colleges to devise different partnerships with HEIs in order to deliver advanced skills training. Removing the focus on transition through FE to HE and providing advanced skills training utilising the benefits of practices already associated with FE, could offer opportunities to meet regional and economic requirements whilst recontextualising the nature and provision of the higher education offered in FE. There are several challenges presented in the pursuit of developing HE in FE and the maintenance of partnerships and successful current practices. The intention is not to suggest a replacement for HE and HEIs but to add an additional complementary route into valid and quality-driven higher education. Ensuring that a distinction is drawn between the respective focus and purpose of the alternative routes will provide clarity for employers, students and educational providers (Husband and Jeffrey, 2016).

The requirement for universities to continue in the production of high-quality research that fuels innovation and knowledge transfer is vital in the development of industry. However, of

equal importance is the recognition of the requirement to focus on higher-level vocational routes that allow for skilled implementation of the research outputs. Focusing on advanced vocationally based HE delivered in FE, enables the bespoke development of courses and apprenticeships that are industry led and directly address the identified skills gaps within the current workforce (Scottish Government 2014).

This chapter will present the theoretical next steps the College could undertake to marry two active research projects together and present the case for the construction of solar charging booths for the Colleges green fleet. It is important to note at this stage that if the college is to succeed in their ambitions of having an offgrid campus it will need to incorporate a number of additional measures due to the fact that the installed solar array does not meet consumption requirements at the present time. This issue can be managed in a number of different ways however, this chapter introduces an option that could be considered. Both of these projects are curriculum based, active learning research projects where students are exposed to real life industry issues. The impact on student learning is clear, anecdotally, but certainly warrants further research and study. This is an area of suggested work for the college going forward and would provide research not currently underway in the sector.

Given the outlined possibilities by Husband and Jeffrey (2016) for increased access to employment opportunities and skills development within the Scottish workforce, perhaps there is scope for greater value to be placed on the skills and methods prevalent in FE to deliver a vocationally focused HE provision that values the practices of both sectors? The impact on pedagogy in this research warrants further study with potential outcomes open of implementation across the curriculum within the college.

The college has seen growth in the use of electric vehicles; yet little has been done to support a 'greener' way to charge them. This chapter aims to determine the optimal orientation and inclination of the solar panels according to different designs providing a technical and financial analysis as well as an environmental impact assessment of Edinburgh College's Midlothian campus in order to establish the feasibility of such a project.

5.1 Calculation process: Slope irradiation, cell temperature and cell efficiency

The process to calculate the slope irradiation, cell temperature, and cell efficiency was the same carry out in the calculations done for the solar meadow farm; see Section 3.11.

5.1.1 Slope irradiation

The methodology followed in this section was the same as that used in Section 3.11. The different steps to reach the slope irradiation were carried out using a software programme adapted directly from Windows in Buildings (Muneer et al., 2000). Some modifications to the software programme relating to the process of calculating the diffuse irradiation, were carried out and the slope irradiation was calculated according to different tilt angles in order to find the optimal orientation and inclination for solar panels at the Midlothian Campus.

To calculate the diffuse irradiation, a new diffuse ratio (k) was used according to the article 'Monthly averaged-hourly solar diffuse radiation model for the UK' (Muneer et. al 2014). Figure 114 shows the relation between the diffuse ratio (k) and the clearness index (k_t), showing a single regression curve for United Kingdom.

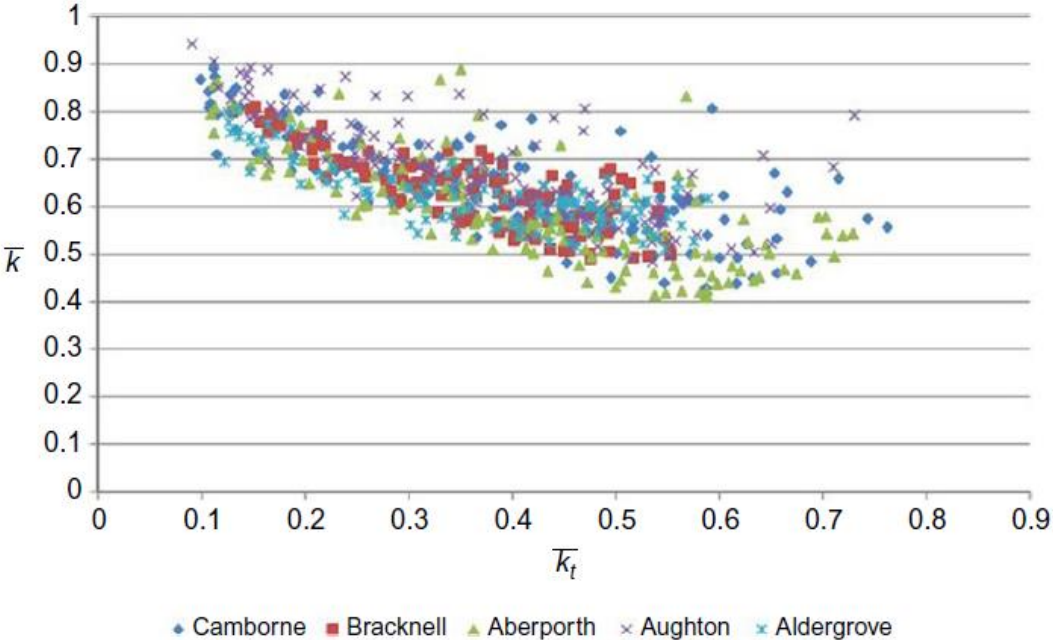


Figure 114 - Monthly-average hourly k - k_t plot for UK (locations arranged in an increasing order of latitude). (Muneer et.al. 2014)

To analyse the optimum inclination, the annual slope irradiation for tilt angles between 0° and 55° facing south and east-west was evaluated. Table 24 shows the angles and orientations considered for the theoretical study.

Table 24 - List of angles and orientations to be studied

Orientation	Angles								
	0°	10°	20°	30°	35°	40°	45°	50°	55°
South	0°	10°	20°	30°	35°	40°	45°	50°	55°
East-west	0°	10°	20°	30°	35°	40°	45°	50°	55°

Equation 48 was used to establish the resulting regression model (Gago et al.,2010):

Equation 48

$$k = 0.89k_t^2 - 1.185k_t + 0.95$$

5.1.2 Cell temperature

Cell temperature was calculated according to equation 13 and the PV module selected to carry out the calculations was an ASP-400GSM monocrystalline, which is a good option given the technical specifications shown in Table 25.

Table 25 - Technical specifications of PV module

Parameter	Value
Model	ASP-400GSM
Rated power (Pmax)	400 W
Maximum power voltage (Vmp)	49.25 V
Maximum power current (Imp)	7.92 A
Open-circuit voltage (Ioc)	59.62 V
Short-circuit current (Voc)	8.42 A
Dimensions	(1977 × 1315 × 34 mm)
Module efficiency	15.2%

The cell temperature was calculated according to different scenarios (different tilt and azimuth angles) in order to ascertain if the variation of temperature from one tilt and azimuth position to another would be significant or not.

The angles utilised to obtain the cell temperature for every month and every hour were as follows:

South orientation, $\alpha = 30^\circ$, $\alpha = 40^\circ$, and $\alpha = 50^\circ$

West-east orientation, $\alpha = 0^\circ$, $\alpha = 30^\circ$, $\alpha = 40^\circ$, and $\alpha = 50^\circ$

Table 26 shows the cell temperature for the PV module facing south at 40°. The cell temperature will be different from the hourly temperature only during the hours when radiation is emitted (coloured cells in the tables).

Table 26 - Cell temperature - PV module facing south at 40°

Hourly cell temperature, 40 degrees												
Month/ time	Jan	Feb	Mar	Apr	May	Jun	Jul	Aug	Sep	Oct	Nov	Dec
1	1.87	1.94	2.98	4.14	6.18	9.08	10.52	11.09	8.48	6.63	5.33	4.93
2	1.65	1.70	2.68	3.72	5.86	8.72	10.18	10.73	8.08	6.29	5.09	4.69
3	1.48	1.51	2.47	3.42	5.61	8.45	9.93	10.46	7.79	6.03	4.91	4.51
4	1.31	1.32	2.25	3.11	5.36	8.18	9.67	10.18	7.50	5.77	4.72	4.32
5	1.20	1.20	2.10	2.90	5.20	8.00	9.50	10.00	7.30	5.60	4.60	4.20
6	1.31	1.32	2.25	3.52	6.70	9.96	11.23	11.00	7.50	5.77	4.72	4.32
7	1.70	1.76	2.98	6.01	9.55	12.75	13.90	13.55	9.33	6.37	5.15	4.75
8	2.66	3.00	7.03	10.42	13.89	16.79	17.83	17.64	13.32	8.41	6.46	5.79
9	4.70	8.34	11.29	15.22	18.51	21.02	21.91	22.05	17.78	13.38	10.11	7.03
10	5.68	12.02	15.35	19.65	22.70	24.79	25.60	26.06	22.01	17.19	14.92	8.69
11	9.78	15.16	18.71	23.27	26.03	27.81	28.57	29.31	25.51	20.40	18.48	14.39
12	10.31	17.04	20.67	25.42	28.00	29.61	30.32	31.26	27.58	22.32	20.46	15.85
13	10.73	17.53	21.25	26.24	28.65	30.33	31.00	31.99	28.37	23.01	20.95	16.36
14	11.04	16.59	20.36	25.64	27.92	29.88	30.52	31.43	27.76	22.40	19.86	15.79
15	7.81	14.34	18.12	23.56	25.81	28.21	28.85	29.52	25.74	20.46	17.21	11.01
16	7.45	11.35	14.87	20.26	22.53	25.43	26.07	26.51	22.61	17.59	13.07	10.02
17	6.02	6.72	11.39	16.57	18.81	22.19	22.93	23.10	19.23	13.57	10.09	9.45
18	5.46	5.91	7.87	12.92	15.04	18.78	19.60	19.65	15.90	12.14	9.24	8.84
19	4.62	4.98	6.55	9.59	11.54	15.27	16.24	16.37	13.28	10.85	8.32	7.92
20	4.00	4.30	5.75	8.05	9.30	12.50	13.75	14.55	12.20	9.90	7.65	7.25
21	3.50	3.74	5.09	7.12	8.56	11.69	12.99	13.73	11.32	9.13	7.10	6.70
22	2.99	3.18	4.44	6.20	7.82	10.88	12.22	12.91	10.44	8.35	6.55	6.15
23	2.60	2.75	3.93	5.48	7.25	10.25	11.63	12.28	9.75	7.75	6.13	5.73
24	2.21	2.32	3.41	4.75	6.68	9.62	11.03	11.64	9.06	7.15	5.70	5.30

5.1.3 Cell efficiency

The equation used to calculate the cell efficiency is equation 11. Finally, the average cell efficiency according to different tilt and azimuth angles had a value of 16.2%

5.1.4 Design of the solar charging station: First phase

In the first phase of the design, three different designs with different shapes were analysed (see Figures 103 – 105) to establish, for each case, the total energy output generated, the number of panels and the geometry required. This information will be essential in determining which design would be the most suitable for a solar charging station in terms of annual solar energy available and feasibility. To start with an area of 400 m², 20 x 20 m was considered for building the solar charging station.

5.1.5 Design 1: South orientation

The tilt angles studied for this design were 30°, 40°, and 50°. All dimensions, the number of PV modules that may be installed on the roof, the annual energy generated, and the slope irradiation of this facility (Figure 115) for different tilt angles are presented in Table 27.

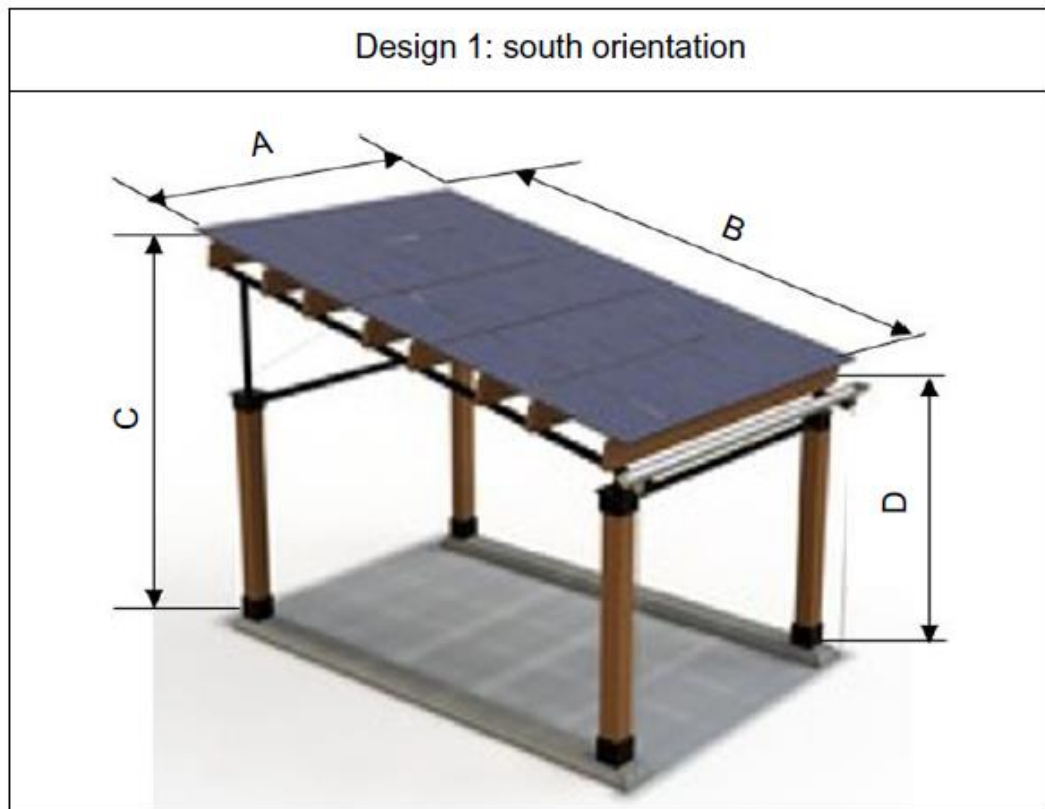


Figure 115 - South facing design. Based on Formfont, 2016.

Table 27 - Main characteristics of Design 1

Design	Tilt angle	Roof length	Roof width	Height, max	Height, min	N° PV module	Output	Slope irradiation
Unit	α	A (m)	B (m)	C (m)	D (m)	–	(MWh)	(kWh/m ²)
1A	30°	20	23.1	14	2.5	180	78.6	1037
1B	40°	20	26.1	19.3	2.5	195	85.7	1044
1C	50°	20	31.1	26.3	2.5	240	103.7	1026

5.1.6 Design 2: East-west orientation

In the second design, figure 116, half of the panels will be facing west, and the other half will be facing east. The tilt angles studied for this design were 0°(facing any orientation), 30°, 40°, and 50°. All the relevant data for this designs is shown in Table 28.

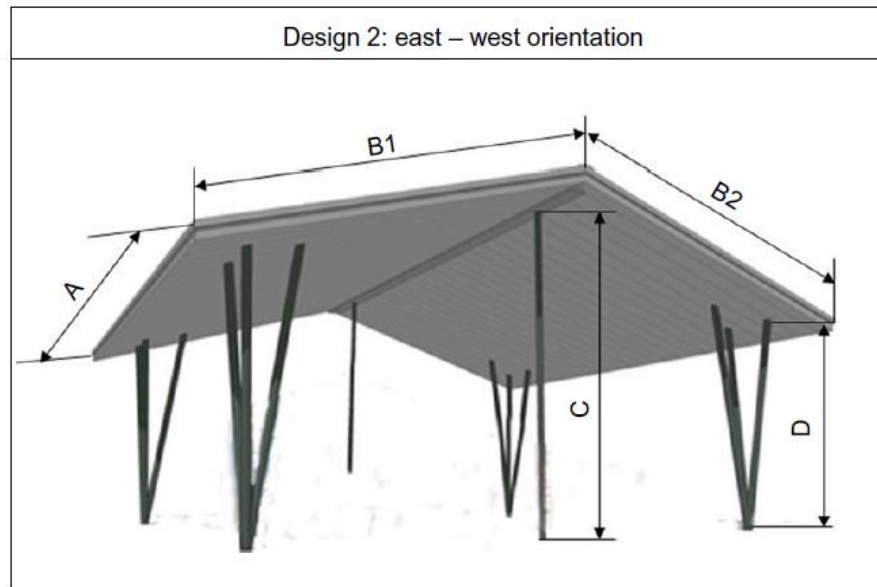


Figure 116 – East - West facing design. Based on Formfonts, 2016.

Table 28 - Main characteristics of Design 2

Design	Tilt angle	Roof length	Roof width	Height, max	Height, min	N° PV module	Output	Slope irradiation
Unit	α	A (m)	B1 + B2 (m)	C (m)	D (m)	–	(MWh)	(kWh/m ²)
2A	0°	20	20	— ^a	2.5	150	56.5	893.8
2B	30°	20	23.1	8.3	2.5	180	64.1	846.5
2C	40°	20	26.1	10.9	2.5	200	68.8	817.2
2D	50°	20	31.1	14.4	2.5	240	78.6	778.3

Design 2A yields the maximum slope irradiation for this orientation (east - west) but with the drawback that the number of panels to be installed is the lowest. As a general observation, it could be said that this V-shape design is less efficient than that of the south-facing designs but it allows for half the height with the same number of panels thus improving the ease of installation and reducing the overall costs.

The worst design presented, 2D, in comparison with design 1C, the energy generated is 24% lower in this design. In design 1C, the total energy obtained was 103.7 MWh/yr compared with 78.6 MWh in design 2D. However, if 2D is compared with the previous designs in terms of height, 2D with the same height as design 1A, generates the same amount of energy, but the uses more PV modules (240 instead of 180). Therefore, making it more expensive.

5.1.7 Design 3: East-West orientation

For the third design, Figure 117, shows a curved design and heights of 10 and 5 m were reviewed. As the roof is curved, each string of PV modules will be placed at different angles; in order to determine the orientation of each string of PV modules and calculate the number of strings, some designs were created in AutoCAD (see Figures 118 and 119). Table 29 presents the main characteristics of the two heights noted above.

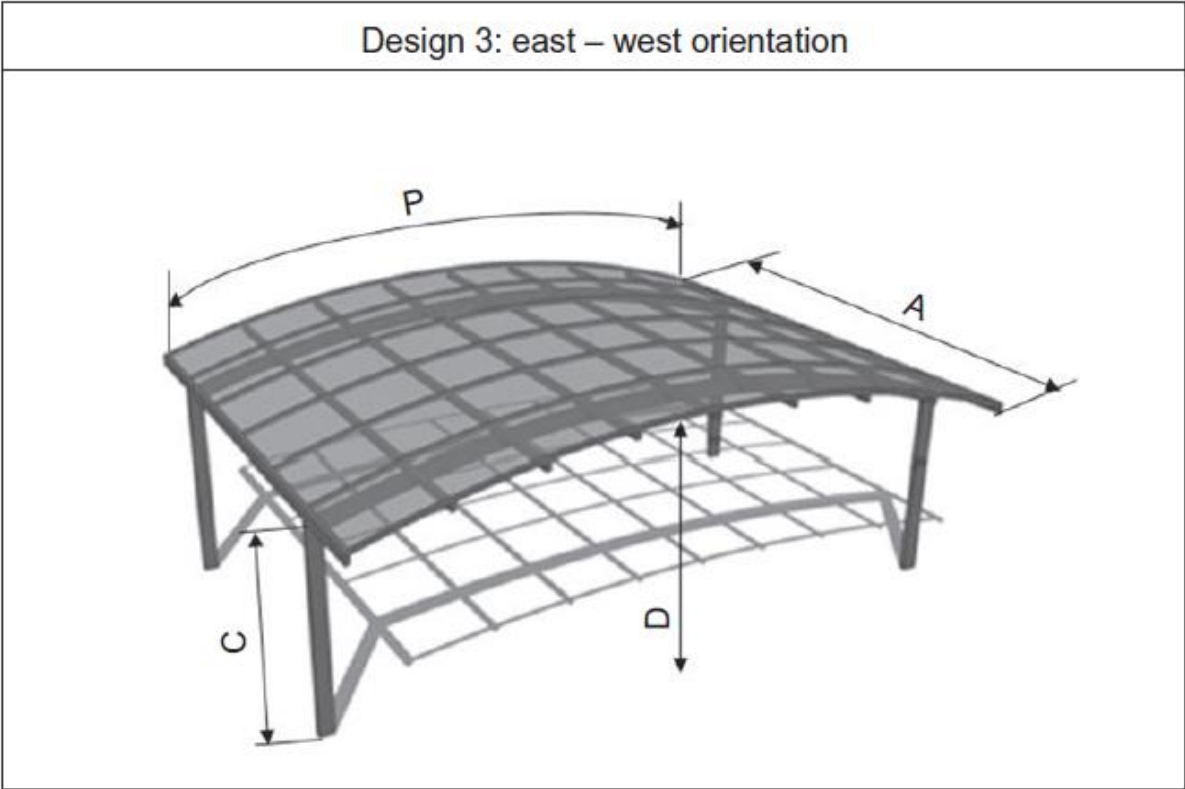


Figure 117 – East - West facing curved design. Based on Formfonts, 2016.

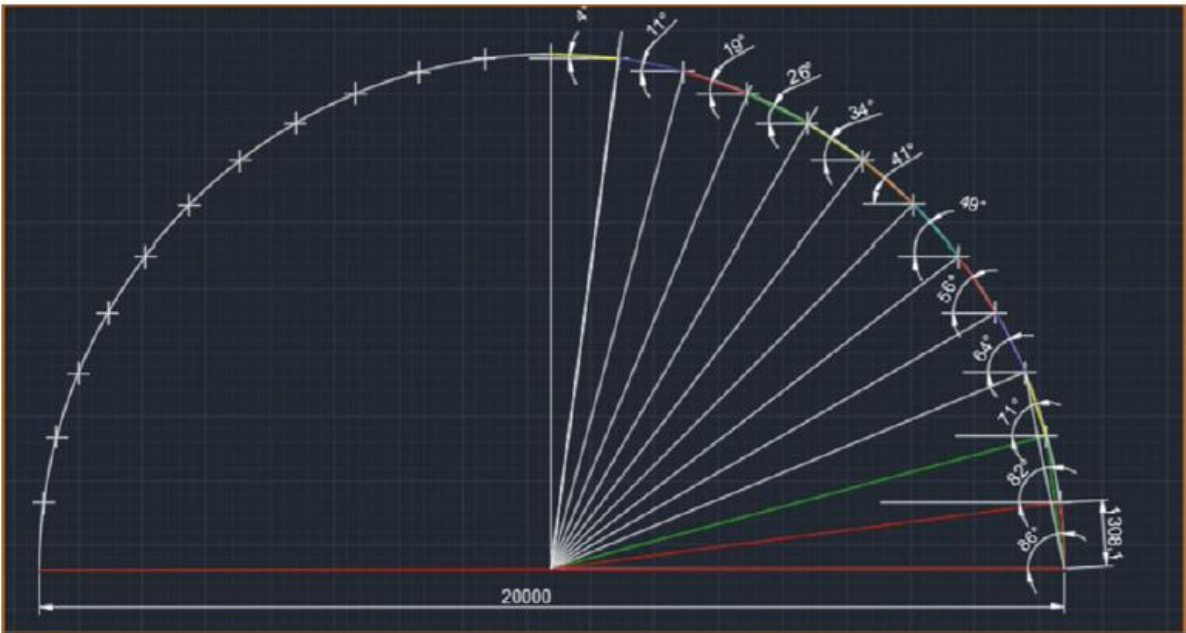


Figure 118 - Design 3A—Orientation of PV modules on the roof.

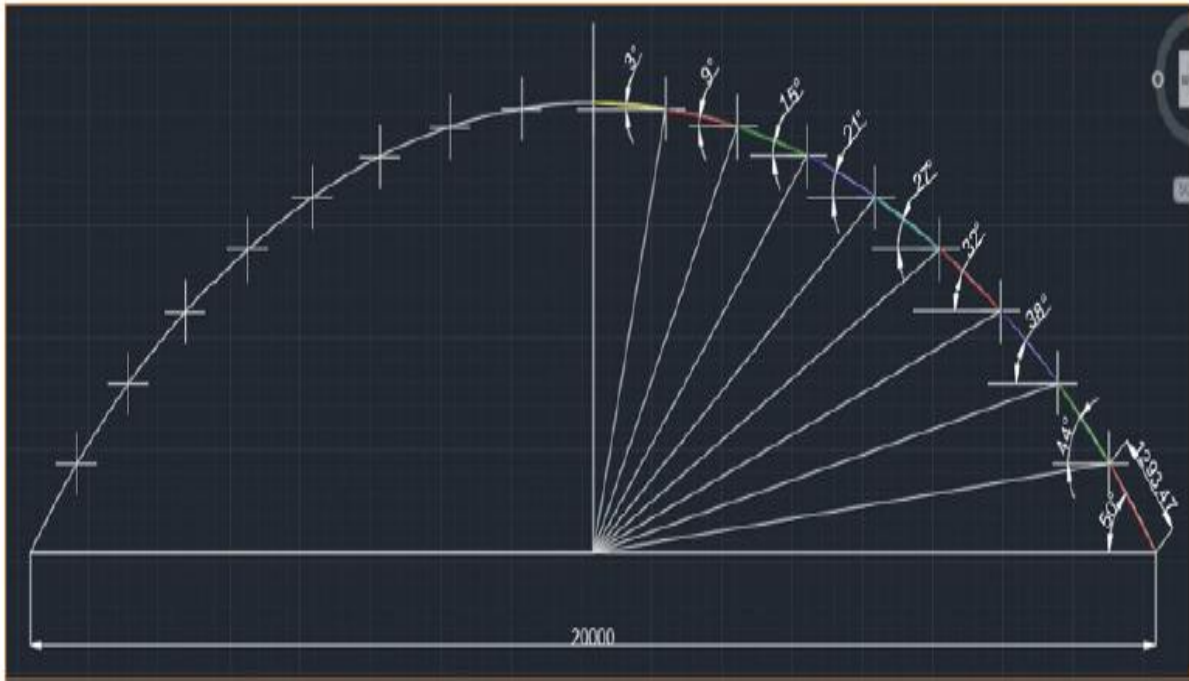


Figure 119 - Design 3B—Orientation of PV modules on the roof.

Table 29 - Main characteristics of Design 3




Design	Tilt angle	Roof length (m)	Roof perimeter (m)	High max (m)	High min (m)	N° PV module	Output (MWh)	Slope irradiation (kWh/m ²)
Unit	α	A (m)	P (m)	C (m)	D (m)	–	(MWh)	(kWh/m ²)
3A	Various	20	31.4	12.5	2.5	240	77.8	769.5
3B	Various	20	23.2	7.5	2.5	180	64.4	849.3

ªThe height of the solar roof could be any with an area of 400 m².

5.1.8 Design summary

The results are summarised in table 30 which is arranged according to the shape of the design, tilt angle, number of panels used, slope irradiation, generated energy per year, and height of the solar canopy. To carry out the second phase of the design, some specifications were defined according to the results shown in Table 30; for example, the maximum height for the facility is 8.5 m (keeping it below the height of the campus workshop area, which is the lowest roof height in the campus); therefore, designs 1A, 1B, 1C, 2C, 2D, and 3A were rejected from the first round of design options. This leaves design 2B & 3B the only available options with canopy heights of 8.3m and 7.5m respectively.

Table 30 - Data collated from all designs—first design phase

	Design	Shape	Tilt angle	PV No.	Slope irradiation (kWh/m ²)	Output (MWh)	Height, max (m)
First design South	1A		$\alpha = 30^\circ$	180	1037	78.6	14
	1B		$\alpha = 40^\circ$	195	1043	85.6	19.3
	1C		$\alpha = 50^\circ$	240	1026	103.7	26.3
Second design W-E	2A		$\alpha = 0^\circ$	150	893.82	56.47	–
	2B		$\alpha = 30^\circ$	180	846.48	64.14	8.3
	2C		$\alpha = 40^\circ$	200	817.23	68.8	10.9
Third design W-E	2D		$\alpha = 50^\circ$	240	778.28	78.6	14.4
	3A		$\alpha = \ddagger$	240	769.48	77.78	12.5
	3B		$\alpha = \ddagger$	180	849.31	64.39	7.5

This next section covers the next phase of design, where both the designs chosen will be studied further and adaptations suggested to optimise the carport.

5.1.9 Design of the solar carport: Second phase

In the second phase of design, it was important to review Edinburgh College's Midlothian campus, located in the Dalkeith and suggest how new carports could be designed according to the available space. Figure 120 shows the area available where the facility could be installed. The carpark to the left of the building is an area in which infrastructure is already in place with carpark spaces and electric vehicle chargers already installed. This has the benefit of keeping potential costs low as site preparation will not need to be undertaken.



Figure 120 - Edinburgh college—Midlothian Campus. From Google maps.

Two aspects have been taken into account: the area of the car park and its accessibility. Generally speaking, the dimensions of a standard parking space are 2.4 m width and 4.8 m depth (Jackson, 2016).

5.1.10 Design 4: South orientation

In the initial design phase, all of the south-facing designs were rejected due to their heights exceeding the maximum height permitted; therefore, the aim of this secondary phase of the design is to reduce this height with new models by:

- Decreasing the inclination of the roof
- Modifying the width and length of the area, maintaining a consistent area of 400 m²



Figure 121 - Area selected for designs 4A & 4B, from Google maps.

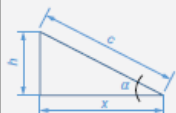
For a southern orientation, three variations of designs were created. The first with an area of 80 × 5 m, the second one with an area of 40 × 10 m and the third one with the dimensions established in the first phase, 20 × 20 m, solving the previous problem by decreasing the height of the solar carport. Based on this, the geometrical dimensions of the solar roof and

energy output (MWh/yr), slope irradiation (kWh/m²), and number of PV modules will be calculated (figure 121).

Design 4A

This design consists of a string of parking spaces with an area of 80 × 5 m. The tilt angles studied were 30°, 40°, and 50°. The geometry of this design and further calculations for the following angles are shown in Table 31 and can be seen in figure 122.

Table 31 - Relevant data for the Design 4A

Shape	Name	Tilt angle	Width	Length	Height ^d	Inclined surface	No. PV mod.	Output	Slope I
	4AA	30°	5	80	2.88	5.77	180	78.62	1037
	4AB	40°	5	80	4.2	6.52	200	87.96	1044
	4AC	50°	5	80	5.96	7.78	240	103.72	1026

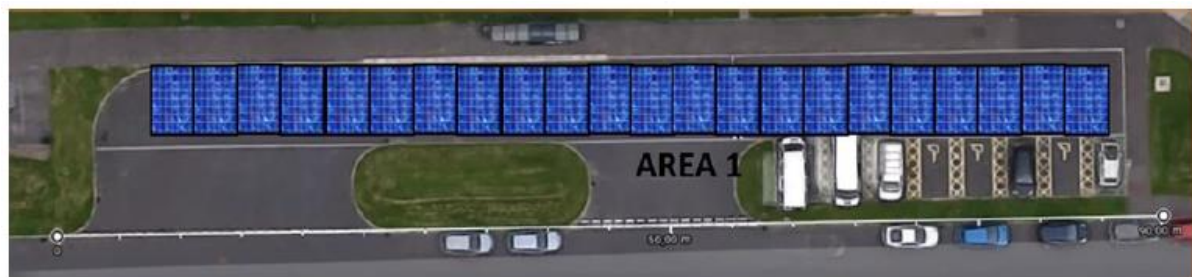


Figure 122 - Area to place the designs 4A. Modified from Google maps.

Design 4B

This design will consist on a double string of parking spaces with an area of 40 × 10m; see Figure 123. For this area, an canopy inclination of >30° will not be possible due to the height exceeding the maximum height permitted, therefore, the angles analysed were 20° and 30° Table 32.

Table 32 - Relevant data for the Design 4B

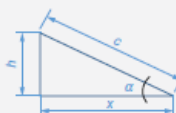
Shape	Name	Tilt angle	Width	Length	Height	Inclined surface	No. PV mod.	Output	Slope I
	4BA	20°	10	40	3.64	10.64	160	68.04	1010
	4BC	30°	10	40	5.67	10.64	180	78.62	1037



Figure 123 - Area to place the design number 4B. Modified from Google maps.

Design 4C

The area chosen to install this solar carport design is shown in Figure 124 located in the main carpark at the campus. As shown in Table 33, tilt angles >15° will not be permissible due to the roof height being >6 m.

Table 33 - Relevant data for the Design 4C

Shape	Name	Tilt angle	Width	Length	Height	Inclined surface	No. PV mod.	Output	Slope I.
	4CA	α	x (m)	l (m)	h (m)	c (m)		(MWh)	(kWh/m ²)
	4CB	10°	20	20	3.52	20.3	156	63.17	961.4
		15°	20	20	5.35	20.7	159	66.17	988.0



Figure 124 - Area to place the design number 4C, Modified from Google maps.

5.1.11 Design 5: East-west orientation

In this solar carport design, the panel orientation will be facing east-west and for this reason a new design was created. The height of the carport was minimised whilst the energy production was maximised. For this design the most suitable tilt angle was 0° , and the design would look like the diagram shown in figure 125.

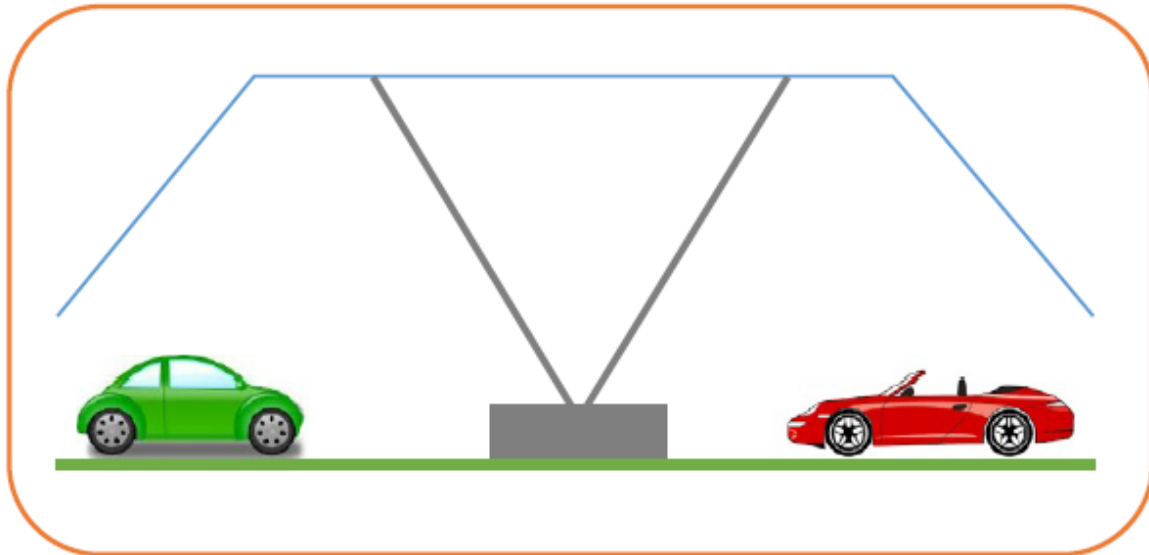


Figure 125 – Diagram of design 5

The area chosen to locate this design is shown in Figure 126 and was developed with potential canopy panel angles of 30° , 40° , and 50° . Table 34 summarises the most relevant data including the dimensions of the facility, total number of PV modules, and total output by all PV modules.

Table 34 - Relevant data for the Design 5

Shape	Name	Tilt angle	a = c	b	Length	Height	Inclined surface	No. PV mod.	Output	Slope I.
	5A	$30^\circ/0^\circ$	(m)	(m)	l (m)	h (m)	r (m)		(MWh)	(kWh/m ²)
	5B	$40^\circ/0^\circ$	5	10	20	2.9	5.77	160	58.6	870.15
	5C	$50^\circ/0^\circ$	5	10	20	4.2	6.53	180	64.5	851.26
			5	10	20	5.96	7.78	200	69.5	824.5



Figure 126 - Area to place the design 5 Modified from Google maps.

6.1.12 Design 6: East-west orientation

Figure 127 details the different areas chosen within the main carpark of the campus to support design 6. Area A has dimensions of 40 × 10 m and area B's dimensions being 67 × 6 m. Heights of 5m and 3m were chosen for these designs.




Figure 127 - Area to place the designs 6. Modified from Google maps.

Design 6A

In this design 2 canopy heights were reviewed, table 35 details the most relevant data for the two heights, 6AA and 6AB.

Table 35 - Relevant data for Design 6A

Shape	Name	Tilt angle	Width	Length	Height	Roof perimeter	No. PV mod.	Output	Slope I
	6AA	α Various	x (m) 10	l (m) 40	h (m) 5	p (m) 15.7	240	(MWh) 78.18	(kWh/m ²) 773.37
	6AB	Various	10	40	3	12.25	180	63.34	835.45

For a height of 5m, the tilt angle of each string of PV modules was calculated with AutoCAD as shown in Figure 128.

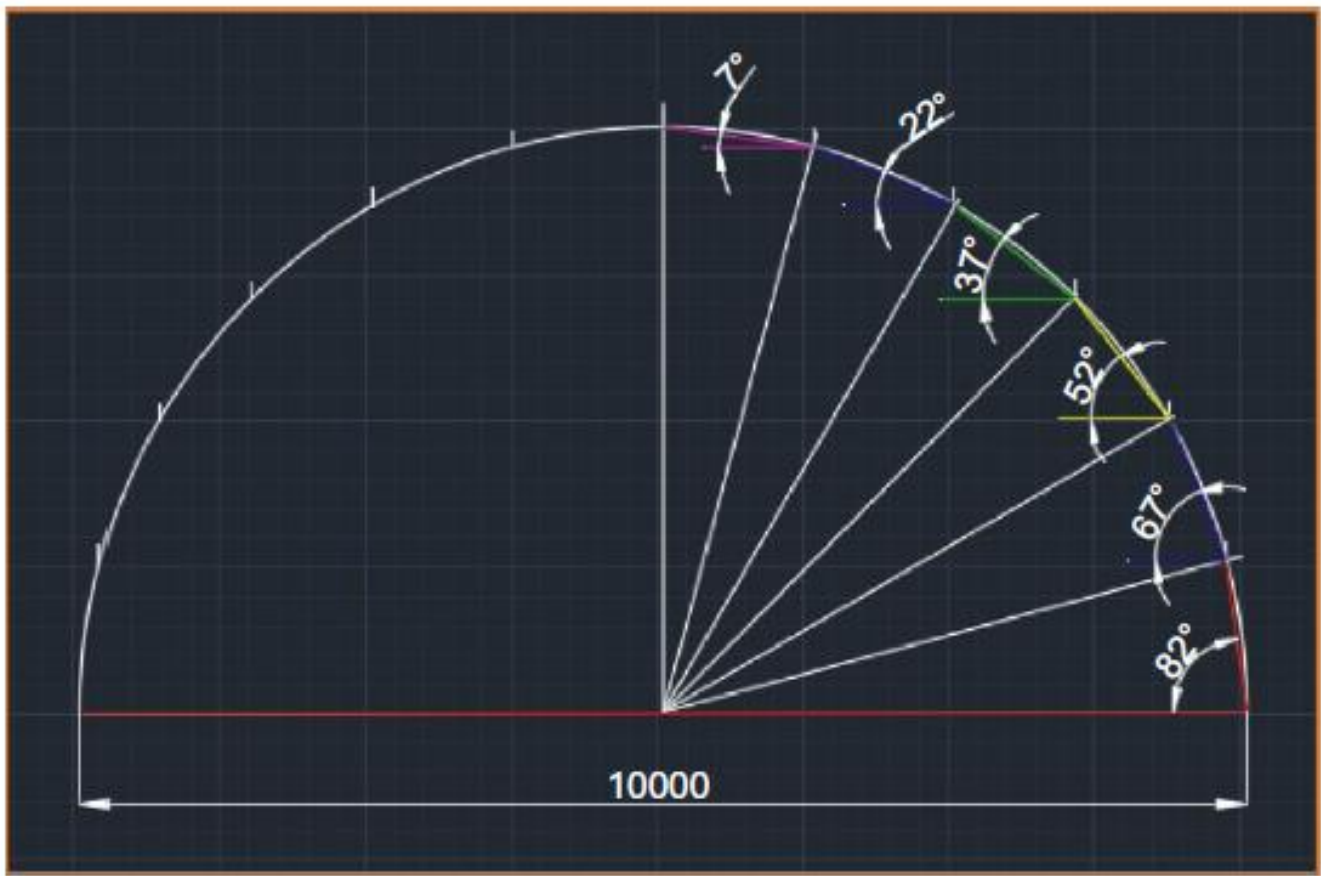


Figure 128 - Design 6AA—Orientation of PV modules on the roof

Figure 129 shows a representation of a life-size solar carport based on design 6A with a canopy height of 5m. In this case, the roof can accommodate 12 strings of PV modules and 20 PV modules along its 40 m of length, totalling 240 PV modules.

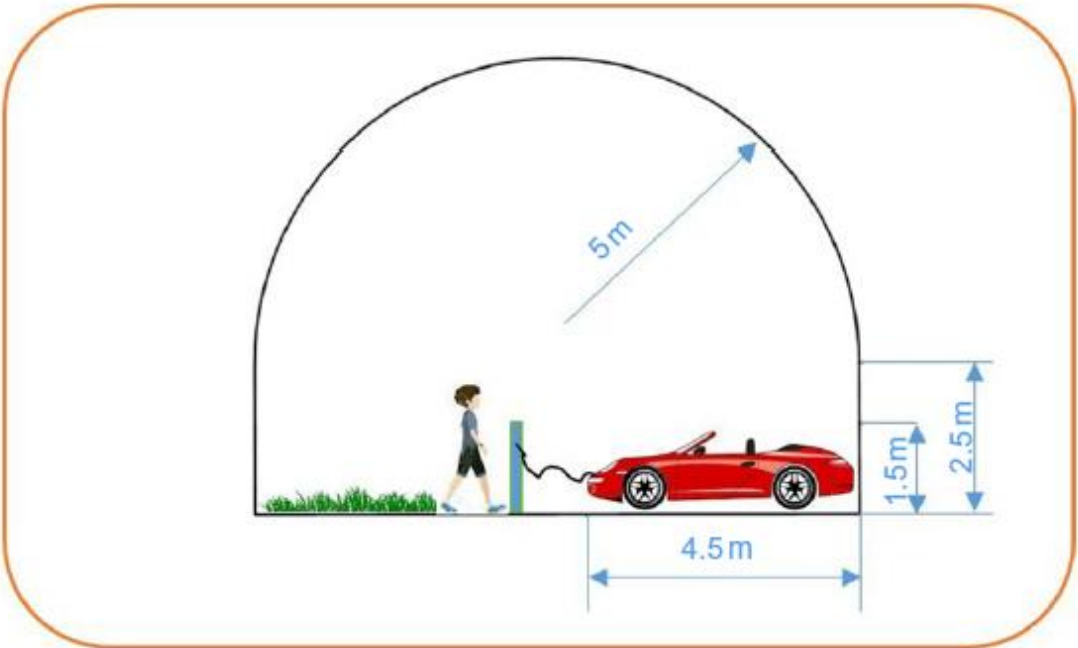


Figure 129 – representation of design 6A

For a height of 3 m, the canopy can only be divided into nine parts; the inclination angles for the PV modules are shown in Figure 130.



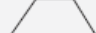
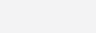


Figure 130 - Design 6AB—Orientation of PV modules on the roof.

5.2 Summary of results by design shape for the first and second phase

Table 36 summarises all the designs developed in the first and second phase of the design, disregarding the designs height over 8.5 m. This table shows all the relevant data in order to choose the best design for the project.

Table 36 - Summarized data table of all possible designs

Orientation	Design	Shape	Tilt angle	No. PV Modules	Slope I (kWh/m ²)	Output (MWh/yr)	Height, max ^a (m)
W-E	2B		$\alpha = 30^\circ$	180	846.48	64.14	8.3
	3B		$\alpha = \neq^b$	180	849.31	64.34	7.5
W-E	6AA		$\alpha = \neq$	240	773.37	78.18	7.5
	6AB		$\alpha = \neq$	180	835.45	63.34	5.5
	6BB		$\alpha = \neq$	238	794.76	79.67	5.5
	5A		$\alpha = 30^\circ$	160	870.15	58.6	5.4
W-E	5B		$\alpha = 40^\circ$	180	851.26	64.5	6.7
	5C		$\alpha = 50^\circ$	200	824.5	69.5	8.46
	4AA		$\alpha = 30^\circ$	180	1037	78.62	5.38
	4AB		$\alpha = 40^\circ$	200	1044	87.96	6.7
South	4AC		$\alpha = 50^\circ$	240	1026	103.72	8.46
	4BA		$\alpha = 20^\circ$	160	1009.6	68.04	6.14
	4C2		$\alpha = 30^\circ$	180	1037	78.62	8.17
	4CA		$\alpha = 10^\circ$	156	961.4	63.17	6.02
	4C2		$\alpha = 15^\circ$	159	988.0	66.17	7.85

aThis height includes the minimum height of 2.5 m.

bStrings of PV modules oriented at different tilt angles.

5.2.1 Design Review

Among all the designs proposed in the table above, the most effective designs were those facing south, in particular designs 4AB and 4 AC. These designs feature the best total energy output and consisted of only a single row of cars, which allows for an increase in the tilt angle of the canopy in order to obtain better slope irradiation. From these two designs, design 4AB has better features in terms of height, around 1.8 m lower than design 4AC, and because this southern orientation, at 40°, being the most efficient. This results in benefits including the amount of energy produced. Therefore, the optimal design is proposed to be the design 4AB facing south at 40°. It is also worth mentioning that southern orientation may not always be the most optimal for solar carports; account must be taken of the existing solar carport layouts or the shadows cast by blockages in the surroundings such buildings or foliage as is evident from the research carried out in chapters 3 and 4 of this thesis. For example, according to Table 38, for an east-west orientation, the best design for the solar carport would be design 5B, which would generate 64.5 MWh/yr.

5.2.2 Characteristics of the chosen design

The optimal orientation for the modules in the chosen design, 4AB, is horizontally as shown in Figure 131. This allows for more PV modules to be installed, maximising the space and

therefore generating more output. The dimensions of the carport are 403m² and the roof area of 526.5 m².

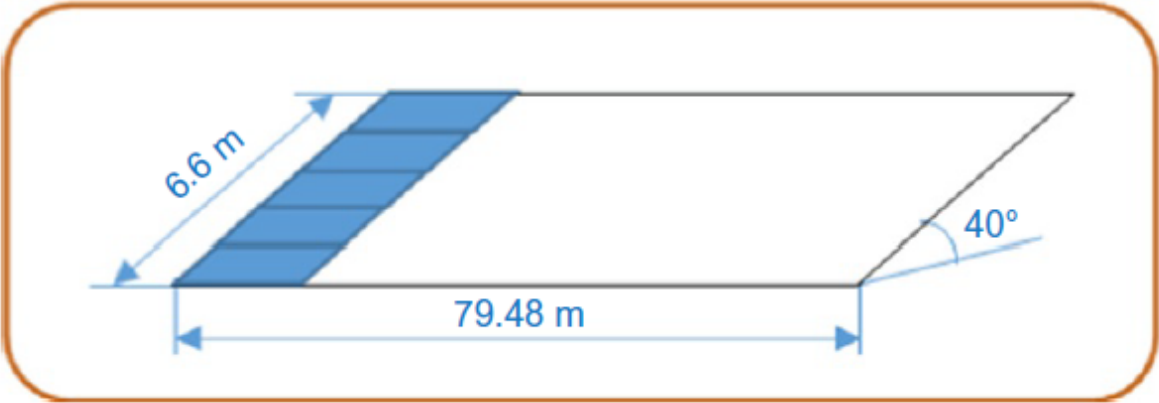


Figure 131 - Horizontal positions of the PV modules

Design 4AB with southern orientation at 40° consists of 200 PV modules rated at 400Wp placed horizontally in a roof area of 526.5 m². This design can generate 87.96 MWh/yr as it receives a slope irradiation of 1044 kWh/ m². The installed capacity is 80 kWp in theory. Taking into account that the standard car parking area for a single car is 4.8 × 2.4 m, as the proposed facility has a ground area of 79.5 × 5.07 m, this solar charging station will be able to provide space for 33 vehicles. The solar carport has a minimum height of 2.5 m and a maximum height of 6.7 m. Figure 132, 133 and 134 present how the facility would look with real dimensions.

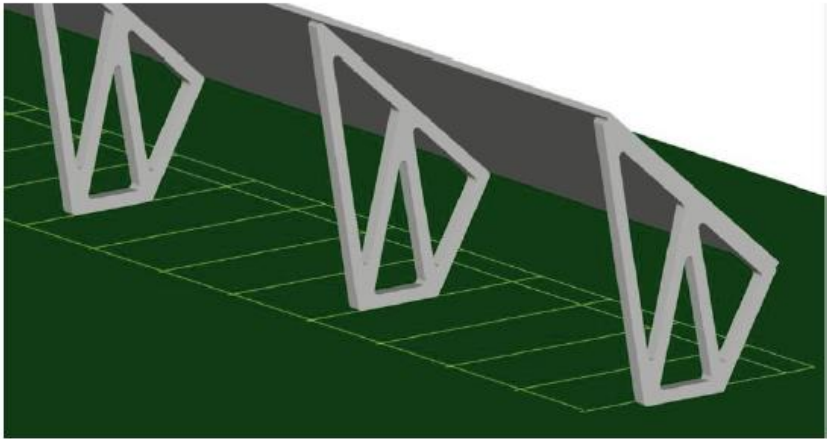


Figure 132 - Solar carport, rear view



Figure 133 - Solar carport, front view.

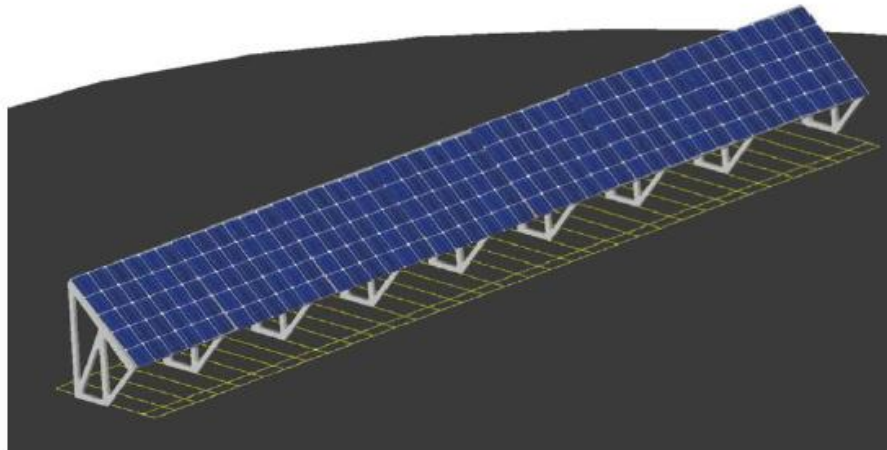


Figure 134 - Full view of the solar carport.

5.2.3 Design of the PV system

This section deals with the hardware required for the proposed design 4AB including the type and number of inverters, PV modules, charger stations, and its connection to the grid.

5.2.4 Selection of the inverter

The chosen inverter was a TRIO-20.0-T, as used within the Solar Meadow at the College, with a maximum power input of 20 kW and a peak efficiency rating of 98.3% (Power-One, 2016) see appendix B. In order to calculate the number of inverters needed by the facility, an example provided by SMA called 'Example Design of a PV Array' (SMA, 2016) was used.

Table 37 - Temperature conditions

Temperature data	Edinburgh
Tmax	19.1°C
Tmin	1.2°C
Tmax cell	32°C
Tmin cell	1.2°C
Tstc	25°C

PV modules per string and maximum number of strings required along with the temperature data for Edinburgh, see table 37, are required to perform the following calculations. Equation 49 was used to calculate the maximum open-circuit voltage of the PV module, which had a value of 65.3 V, the open-circuit voltage of the PV module being 59.62 V, the voltage temperature coefficient being $-0.4\%/^{\circ}\text{C}$, and the temperature at STC and minimum ambient temperature being -23.8°C :

Equation 49

$$V_{DCmaxMOD} = V_{OC} \left(1 + \frac{T_{DCUocMOD} \times \Delta T_{LOW}}{100\%} \right)$$

where

- $V_{DCmaxMOD}$: maximum PV module voltage
- V_{OC} : open-circuit voltage of the PV module
- $T_{DCUocMOD}$: voltage temperature coefficient
- ΔT_{LOW} : temperature at STC and minimum ambient temperature ($T_{cellmin} - T_{stc}$)

The open-circuit voltage decreases as temperatures rises. The minimum PV module open-circuit voltage is calculated with Equation 50, where the value of the voltage of the PV module at maximum power is 49.25 V and the temperature at STC and maximum cell temperature is 7°C , the result of the minimum PV open circuit voltage being 47.87 V:

Equation 50

$$V_{DCminMOD} = V_{mpp} \left(1 + \frac{T_{DCUocMOD} \times \Delta T_{max}}{100\%} \right)$$

where

- $V_{DCminMOD}$: minimum PV module voltage
- V_{mpp} : voltage of the PV module at maximum power
- ΔT_{max} : temperature at STC and maximum cell temperature ($T_{maxMOD} - T_{stc}$)

The PV modules within a string will have the same current as the string because they are placed in series. Equation 51 was used to calculate the maximum PV module current, which

had a value of 8.39 A, the short-circuit current of the PV module being 8.42 A, and the current temperature coefficient being 0.05%/°C:

Equation 51

$$I_{DCmaxSTR} = I_{SC} \left(1 + \frac{T_{DCIocMOD} \times \Delta T_{max}}{100\%} \right)$$

where

$I_{DCmaxSTR}$: maximum string current

I_{SC} : short-circuit current of the PV module

$T_{DCIocMOD}$: current temperature coefficient

The maximum string voltage must not exceed the maximum permitted system voltage of the photovoltaic modules. The maximum number of modules per string is 15 as per equation 52, with the maximum input voltage of the inverter being 1000 V:

Equation 52

$$n_{maxMODSTR} \leq \frac{V_{DCmaxINV}}{V_{DCmaxMOD}}$$

where

$n_{maxMODSTR}$: maximum number of PV modules per string

$V_{DCmaxINV}$: maximum input voltage of the inverter

Equation 53 shows the calculation to obtain the minimum number of PV modules per string that should be installed would be 9 with the minimum MPP voltage of the inverter being 450 V.

Equation 53

$$n_{minMODSTR} \leq \frac{V_{DCmppinINV}}{V_{DCminMOD}}$$

where

$n_{minMODSTR}$: minimum number of PV modules per string

$V_{DCmppinINV}$: minimum MPP voltage of inverter

The optimum number of strings per array must not be less than the minimum number of strings and must not exceed the maximum number. In order to avoid system damage, such as current surge, it is important not to choose the maximum number of strings. Therefore, the number of PV modules per string is calculated as follows:

$$n_{minMODSTR} \leq n_{MODSTR} \leq n_{maxMODSTR}$$

where n_{MODSTR} is the number of PV modules per string.

Therefore;

$$9 \leq 15 \leq 15$$

In knowing the value of the power of the inverter, 20,000 W, and the maximum power of the PV modules, 400 W, the minimum and maximum number of strings needed to achieve the total power can be calculated. The minimum and maximum number of strings required, according to Equations 54 and 55 was the same in each equation:

Equation 54

$$n_{minSTR} = \frac{P_{DCGEN}}{P_{maxMOD} \times n_{MODSTR}}$$

Equation 55

$$n_{maxSTR} = \frac{I_{DCmaxINV}}{I_{DCmaxSTR}}$$

where

P_{DCGEN} : power of the inverter

P_{maxMOD} : maximum power of the PV modules

The optimum number of strings per array must not be less than the minimum number of strings and must not exceed the maximum number:

$$n_{minSTR} \leq n_{STRCHOOSE} \leq n_{maxSTR}$$

Therefore;

$$3 \leq 3 \leq 3$$

The number of PV modules connected to a single inverter and the total number of inverters required can be calculated using equations 56 and 57 and ensuring that the maximum voltage and current values of the string do not exceed the maximum voltage and current values of the inverter.

$$V_{Array} = V_{DCmaxSTR} = n_{MODSTR} \times V_{DCmaxMOD}$$

$$I_{DCmaxSTRarray} = n_{STR} \times I_{DCmppMOD}$$

Once this has been calculated, the total number of PV modules connected to a single inverter can be obtained.

From these calculations, the maximum number of strings is 13 and that each string consists of 3 modules, the total number of PV modules connected to a single inverter will be 39. Design 4AB chosen had 200 PV modules, so if an inverter can be connected to 39 PV modules, the total number of inverters that the facility would need would be:

$$n_{TOTALINV} = \frac{200}{39} = 5.1 \sim 5 \text{ invertors}$$

5.2.4 Selection of the PV module

See Section 5.1.2

5.2.5 Selection of the charging station

There are three main types of EV chargers (Jackson, 2016):

1. Slow charging (up to 3 kW), suitable for charging during 6–8 h overnight.
2. Fast charging (7–22 kW) that can fully recharge some models in 3–4 h.
3. Rapid charging (43–50 kW), able to provide an 80% charge over 30 min. They can be used in AC or DC connected configurations.

The charging station chosen for the facility was a twin rapid charger CHAdeMO, an AC rapid charger. This type of charger is currently installed at Napier University, figure 135, and features a charge time of around 1 hour which results in enough charge to allow for an 80 mile range from 1 hour of charging. Table 38 shows the charging times for a Renault Zoe. For the proposed facility, three twin rapid charger stations were installed.

Table 38 - Charging times for Renault Zoe

Charging times					
Charger type	Phases	Current (A)	Voltage (V)	Power (kW)	Charge time
Very slow	1	10	230	2.3	9.5 h
Slow	1	16	230	3.7	6.0 h
Fast	1	32	230	7.4	3.0 h
AC-Rapid	3	32	230	22	1.0 h
DC-Rapid	3	63	230	43	0.5 h
Battery Swap	–	–	–	–	90 s



Figure 135 - Rapid charger CHAdeMO at Napier University. (Plugshare 2016)

5.2.6 Layout

The PV carports will be connected to the grid; as shown in figure 136 below. This diagram outlines how the connection of the PV system to the grid. Battery storage is not considered in this grid connection as the purpose is to store the generated electricity in the electric vehicles battery. This creates an advantage of reducing the costs of not requiring battery storage in the connection to the grid.

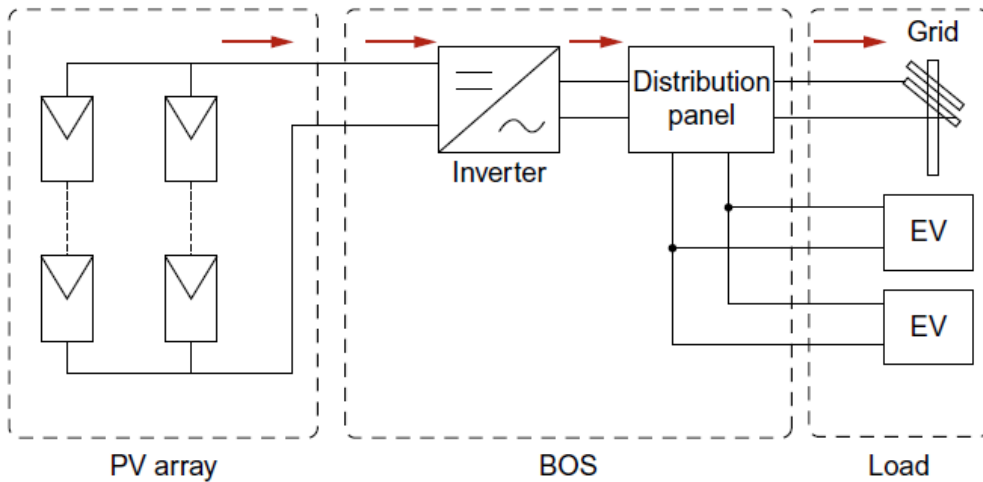


Figure 136 - Typical grid-connected PV system without battery storage From Narayan, N. (2013). Solar charging station for light electric vehicles. A design and feasibility study. Master of Science Thesis. Delft University of Technology.

Figure 137 shows the circuit diagram of the proposed 80 kW solar carport facility. It has been divided into five arrays, each made up of 39 PV modules rated at 400 Wp connected to the inverter that converts DC power from the PV modules into AC power. The facility will be connected to the national grid through a transformer.

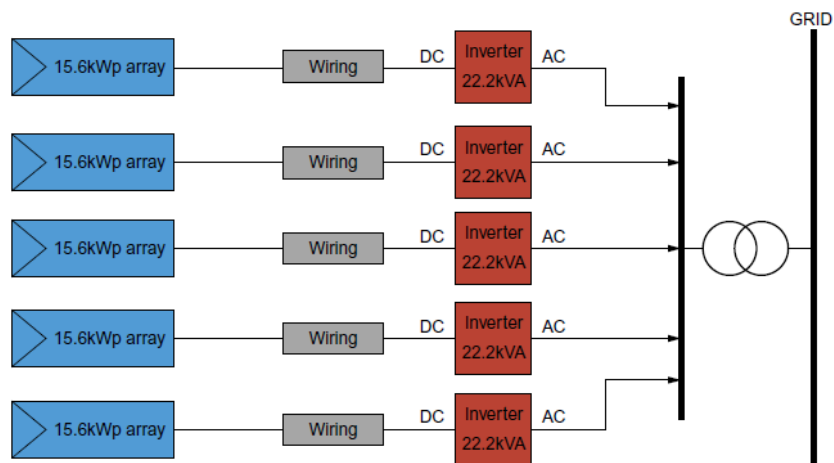


Figure 137 - Schematic circuit diagram of the 80kWp facility.

5.2.7 Driving behaviour

This next section will aim to calculate the average driving distance by a single vehicle in a day and the average energy consumption of the vehicle per day. To achieve this, a report called 'Energetic, environmental and economic performance of electric vehicles: Experimental evaluation' (Muneer et al., 2015) is used to gain the required information.

5.2.7.1 Review of average driving distance and trips undertaken

According to the Department for Transport, in 2014, individual people, in England, travelled around 6500 mi annually (covering all means of transport), where cars accounted for 78%, i.e. the number of miles travelled by car was around 5067 (8107 km) per year (Department for Transport, 2015). Therefore, the average trip length per car and per person would be of around 22 km, while in Scotland, the average car journey per person, also in 2014, was 20.8 km (Transport Scotland, 2015).

Trips in progress by time and day in the UK

Figure 138 below shows the number of journeys with a vehicle along the day during weekdays and weekends. As shown, peak journeys take place around 8 a.m. and 4 p.m.

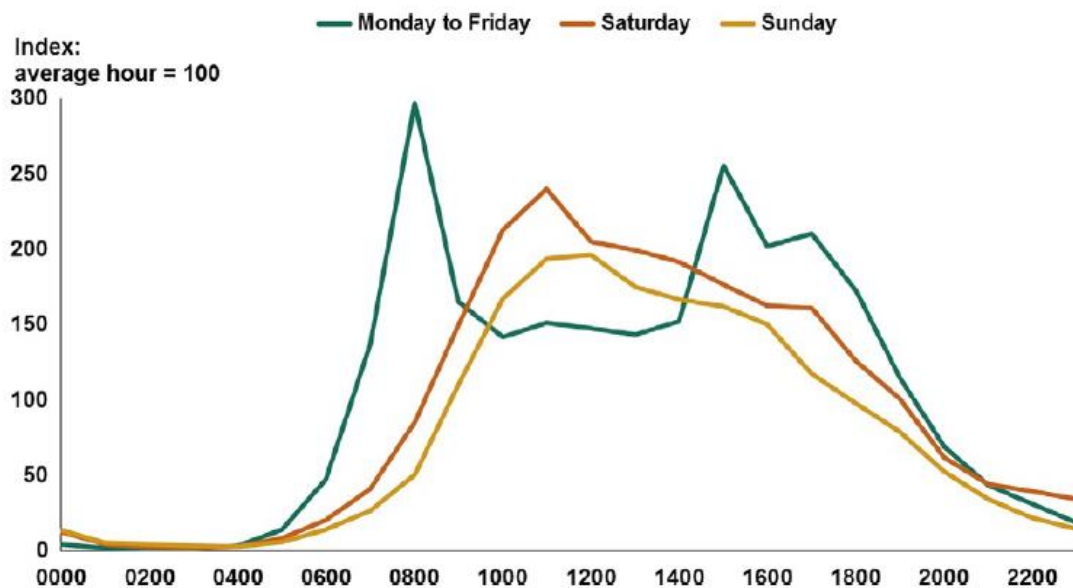


Figure 138 - Trips by time of day and day of week. From Department for Transport (2015). (National travel survey 2014)

According to the National Travel Survey, education and work have a big impact on travel patterns, because it is the time when people go to work and school and come back home; Figure 139 shows an alternative view of trips made by vehicle and categorises the events into trips such as leisure, most of that at weekends; shopping, most shopping trips are made

between 9 a.m. and 3 p.m. and one-fifth on Saturdays or commuting; and business where 68% of the trips start between 6 a.m. to 9 a.m. and 4 p.m. to 7 p.m.

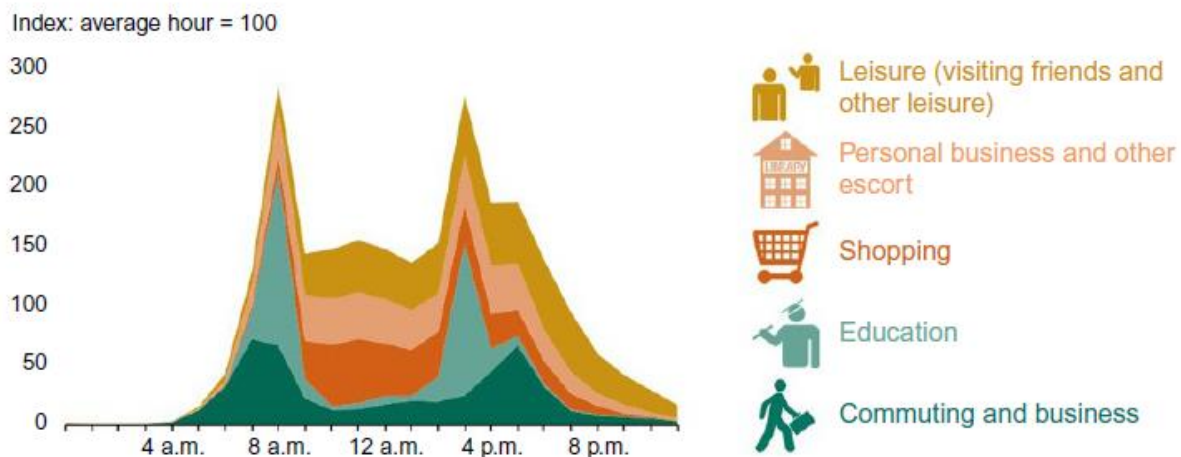


Figure 139 - Trips in progress by start time and purpose, Monday to Friday.(National travel survey 2014)

5.2.7.2 Estimation of energy consumption by electric vehicles

Obtaining information relating to energy consumption by electric vehicles can be carried out simply, by analysing and calculating the number of best-selling electric cars in the United Kingdom and, based on the manufacturer's datasheets, calculate the average energy consumption of the cars. However, the energy consumption specified by the manufacturer rarely matches the reality of actual road conditions, therefore, based Muneer et al.(2015), it was decided to take the data from this report instead of any manufacturer's data to improve the accuracy of this theoretical research.

Car model: Renault Zoe e-car

The French manufacturer Renault introduced their e-car Zoe in the year 2013. Edinburgh Napier University obtained the very first model that was made available. In this study, the Renault Zoe e-car was used for an experimental evaluation, where the speed and energy were recorded in a journey from Morningside to Leith. To calculate the consumption per kilometre (kWh/km) of this car, information about time, speed, and altitude of this journey was required, which was being logged at specific times during the test drives.

With this data collected, the next step was to calculate the driven distance in metres, the gradient in radians (angle of inclination), and the acceleration in metre per second squared of the car. Once these unknown quantities are known and some data from the Renault Zoe car, table 39, and equation 58 is utilised to calculate the energy consumption by a single car:

Table 39 - Data Renault Zoe e-car

A, m ²	g, m/s ²	μ	ρ	m, kg	Cd
2.75	9.81	0.030	1.23	1693	0.28

Equation 58 (Walsh et. al. 2011)

$$E = \left[\mu mg \cos\theta + mg \sin\theta + \frac{1}{4} CdAp(v_f^2 + v_i^2) \right] \Delta d + \frac{1}{2} m(v_f^2 + v_i^2)$$

This equation takes the following into account:

- Tyre friction: $[\mu mg \cos\theta] \Delta d$
- Hill climbing: $[mg \sin\theta] \Delta d$
- Wind drag: $\left[\frac{1}{4} CdAp(v_f^2 + v_i^2) \right] \Delta d$
- Change in kinetic energy: $\frac{1}{2} m(v_f^2 + v_i^2)$

The most relevant features of the Renault Zoe for all calculations are shown below where

A: front area of the car

g: gravity

μ: friction coefficient

ρ: air density

m: weight

Cd: aerodynamics coefficient

By applying the time, speed, and altitude data and the manufacturer's data, Table 41, the amount of energy consumed during the different types of driving such as acceleration, cruise, and deceleration can be calculated.

The breakdown of events during a driving episode is illustrated in Figure 140 and shows that 47% of the driving episode is spent decelerating; in this drive mode energy is generated instead of consumed due to regenerative braking and engine braking, where 27% of that deceleration is due to a descending gradient which results in a greater potential for energy recovery (Walsh et.al. 2011).

According to the study conducted by Muneer et al. (2015), the Renault Zoe was reported to have a power usage 12% higher than the manufacturer’s values. The analyses shows that the average energy consumption by a single car, the Renault Zoe, was 0.164 kWh/km compared with 0.146 kWh/km (Muneer et al., 2015). The purpose of studying the driving behaviour has been to estimate how much energy an electric car could use in a day. As the carport is going to be placed in Edinburgh, the average number of kilometres travelled by car per day is 20.8 km, as noted through Transport Scotland’s data (2015).

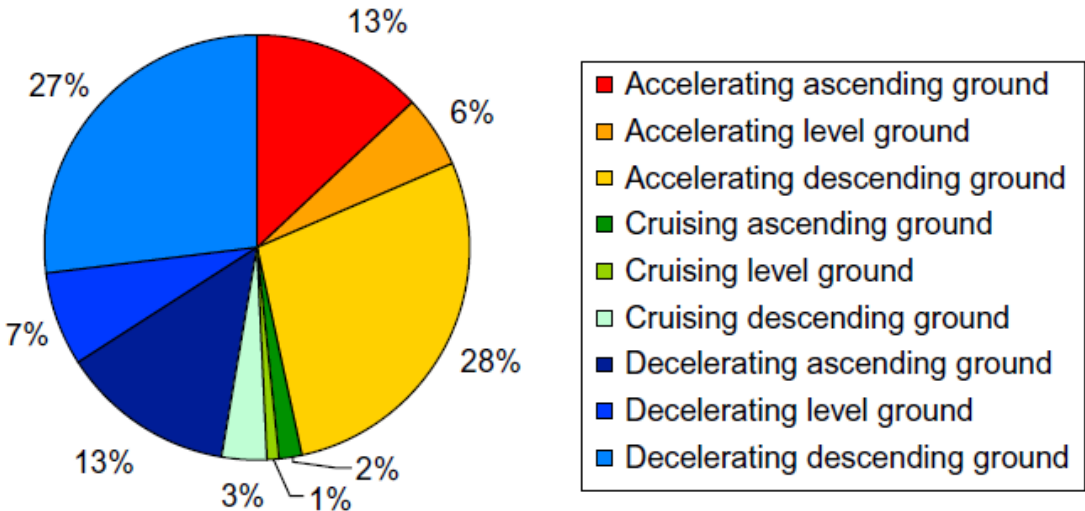


Figure 140 - Driving episodes in Edinburgh City (Walsh, J., Muneer, T., & Celik, 2011)

With this data equation 59 can be used to to calculate the energy consumption per day for this specific car.

Equation 59

$$E = \text{km travelled by car per day} \times \text{Energy consumption} = \mathbf{3:41kWh/day}$$

5.2.8 Number of vehicles to be charged during a day by the solar carport

The average daily slope irradiation per year in Edinburgh is circa 2.85 kWh/m², the 200 PV modules of the carport could generate a potential daily output of 240.08 kWh/daily as shown through the use of equation 60 (Muneer, 2017).

Equation 60

$$E_{daily} = A_m \eta_{sys} I_{tilt} No_{.PV} = 240.08 kWh/daily$$

According to Section 5.2.7, the consumption of a car was estimated to be 0.164 kWh/ km; therefore, with 1 kWh, a car could drive 6.1 km or 3.8 mi. Thus, with an amount of energy of 240.08 kWh generated by the facility daily, 912.3 mi could be driven in a day. If the average

trip per passenger by car was 20.8 km or 13 mi in a day (Muneer T, et.al. 2017), a total of 70 cars could be charged. Therefore, the energy consumption for these 70 cars per day would be 238.7 kWh, the energy that a car consumes per day being 3.41 kWh.

5.3 Energy production and energy consumption by the carport

The monthly energy production and energy consumption for the carport is estimated in figure 131 for an entire year.

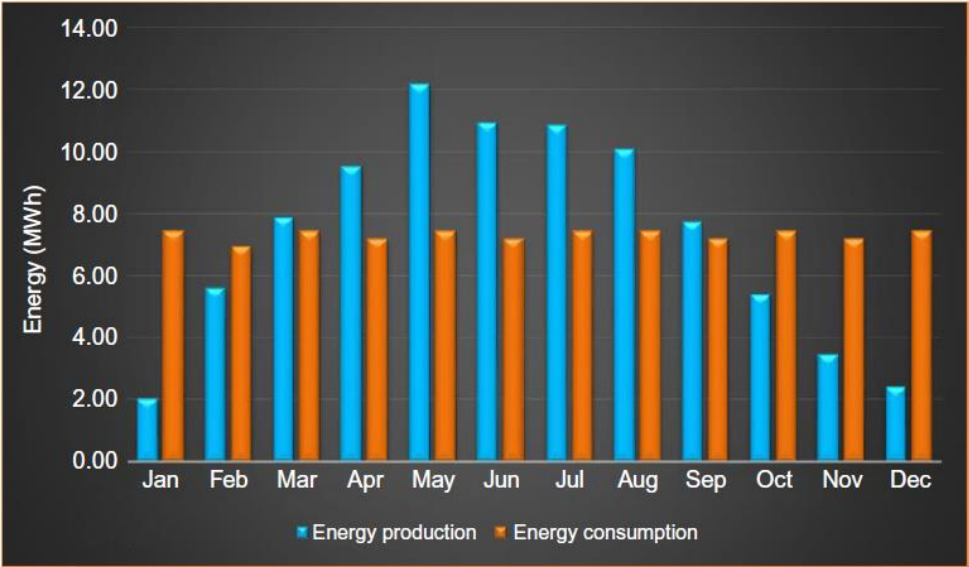


Figure 141 - Energy production vs. Energy consumption.

Figure 141 shows that during the months of January and December, the energy produced by the solar carport does not meet the expected demand. This correlates to findings from the earlier research studies highlighting lowest generation within the solar meadow in the same months. This problem could be mitigated due to the national grid connection. So, during the months where the carport does not generate enough energy the grid can feed the charging of electric vehicles and when the carport generates energy in excess; this energy can be sold back to the national grid.

5.4 Load profile

In order to model the monthly energy consumption used by electric cars, it is necessary to create a load profile that simulates the load behaviour. The number of electric vehicles that could be charged was defined in the previous section. This load behaviour can be simulated based on trips made during a day according to the journey and peak times, as mentioned in Section 5.2.7. However, as this solar charging station is located at the college, it is difficult to estimate how the load would change over the months and throughout the year, because

staff & students usually do not come and go at the same times, such as during holiday periods.

It was therefore decided to define the range of hours when the vehicles could be charged, estimating that this energy supply would be constant in that period, therefore simplifying the load profile. The hours range chosen for charging the vehicles was between 07:00 to 22:00, these are the opening hours of the college so will capture the most traffic. Figure 142 and 143 show the energy consumption of the 70 cars and the energy generated by the carport during the months of March and May.

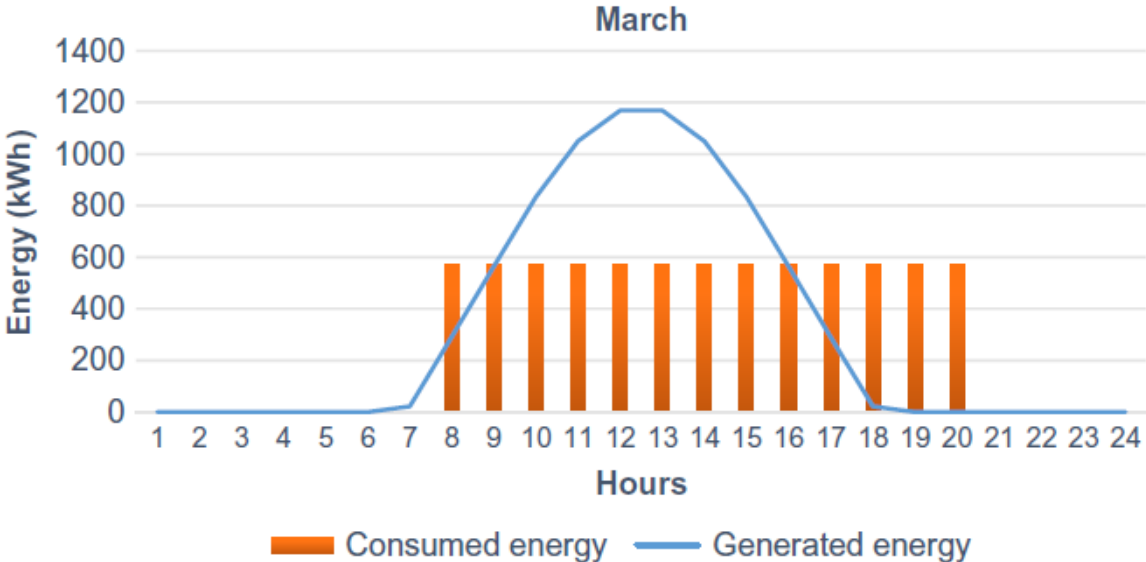


Figure 142 - Consumed and generated energy in March.

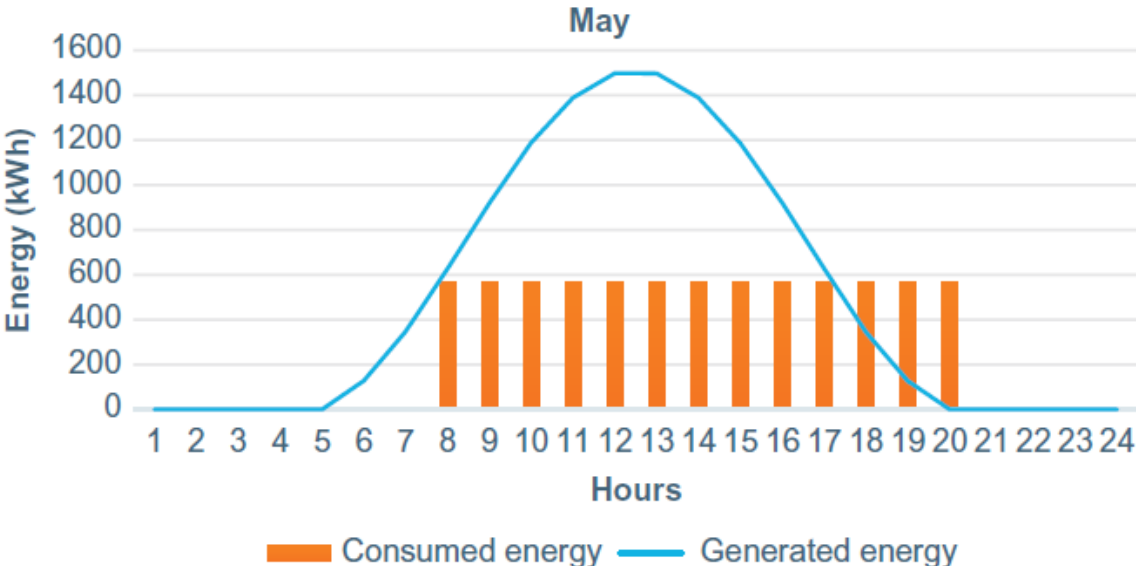


Figure 143 - Consumed and generated energy in May.

Figures 132 and 133 show the potential energy generated will vary month to month and meet the demand for charging for longer periods throughout the day during the months the solar azimuth is higher as shown in the findings in chapter 4.

5.5 Financial analysis

The economic viability of the solar carport facility needs to be ascertained prior to making a recommendation. In order to do so a study of the market situation was undertaken, a financial plan was developed for three different scenarios: the first scenario for the present year 2017; the second scenario for 2020, the year Edinburgh College could implement the project, and the third scenario based on unsubsidised generation. Various methods are reviewed such as payback period time, net present value (NPV), internal rate of return (IRR), and the debt-service coverage ratio (DSCR) were studied to determine the feasibility of the project, made even more pertinent in terms of the funding changes and challenges outlined in chapter 2.

5.6 Scenario 1

This scenario will be developed with reference to 2017.

Expenses: Operating Expenditure (OPEX) and investment costs

In OPEX the main components of a carport are PV systems, canopies, frames, and foundations. The budget needed for the investment (80kWp of installed capacity) is presented below, with a breakdown of all components of the PV facility. All the data used for this analysis were taken from a study published by Fraunhofer Institute for Solar Energy Systems entitled 'Current and Future Cost of Photovoltaics' (ISE, 2015). The total operating expenditures were found to be 15.4 £/kWp. These costs were categorised and are shown in Table 40. From this table the operational expenses for this 80kWp solar carport facility will be £1232 per year.

Table 40 - Operating expenditures for 2017

OPEX			Total costs
Maintenance and operating cost	25%	3.85 £/kWp	£308
Replacing and cleaning cost	35%	5.40 £/kWp	£432
Insurance and taxes	40%	6.15 £/kWp	£492
Total	100%	15.4 £/kWp	£1232

The investment costs of the carport represent the measurable technical factors in the money involved in the production. For the proposed facility, it will be necessary to take into account the costs for the following:

- PV modules
- Inverters
- Balance of system
- Charging station

Frames and foundations

The balance of system cost includes the cost of the installation, mounting system, infrastructure, transformers, grid connection, wiring, planning and documentation (ISE, 2015), mounting structure, and grid connection accounting for the most expensive cost. The cost breakdown as a percentage for the proposed carport and the breakdown of the balance of costs are shown in Figures 144 and 145.

PV modules, inverters, and balance of system costs are based on a ground-mounted PV plant; therefore, charging stations, frames, and foundations costs are not included in this document. Presently, the charging stations are manufactured by the staff of Edinburgh College at an approximate cost of £600. Three chargers and the frame and foundation costs were estimated to be around £200/kWp (Jackson, 2016).

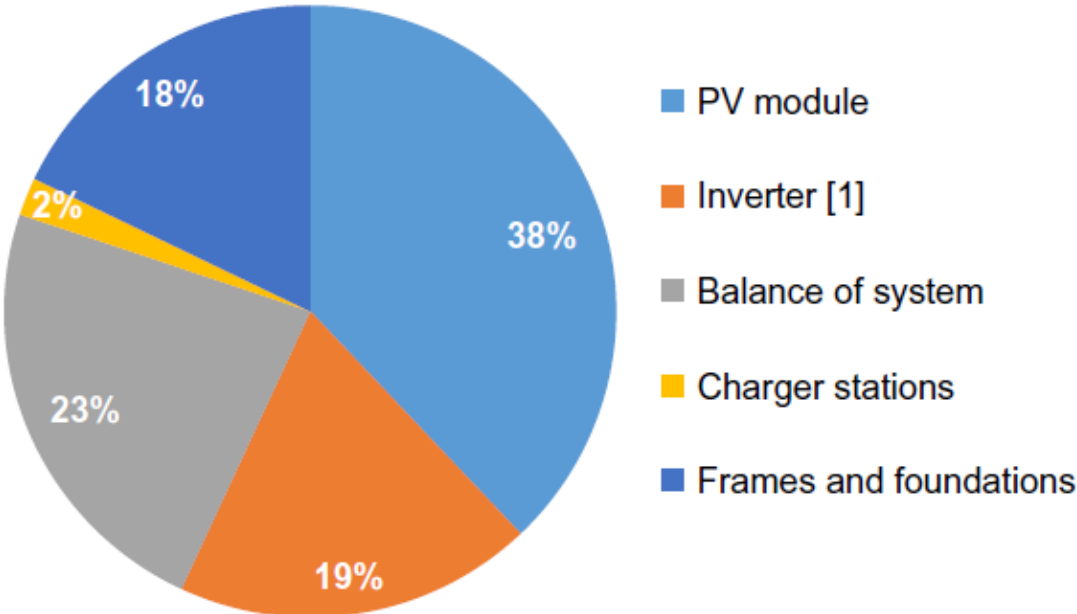


Figure 144 - Main costs distribution

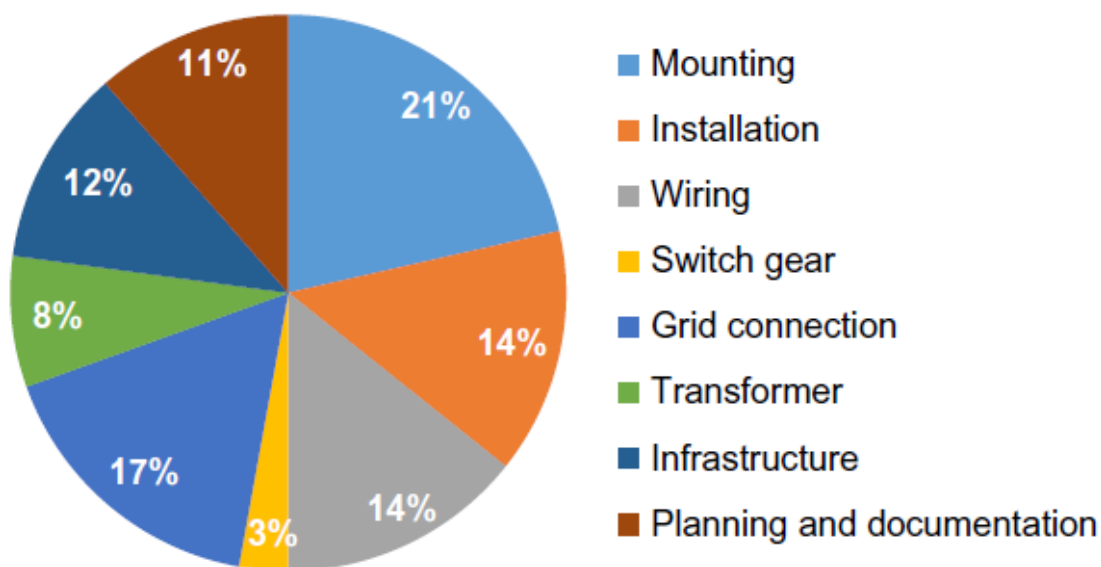


Figure 145 - Balance of System costs distribution.

Table 41 details the breakdown of the distributed costs and the total expenses of the carport is £90,832, £1232 from operational expenses annually and £89,600 from the initial investment.

Table 41 - Detailed cost distribution

Investment cost			Total costs
PV module	55%	425 £ ^a /kWp	£34,000
Inverter ^b	11%	85 £/kWp	£17,000
Balance of system	34%	260 £/kWp	£20,800
Mounting	8%	61 £/kWp	£4500
Installation	5%	38 £/kWp	£3000
Wiring	5%	38 £/kWp	£3000
Switch gear	1%	2.5 £/kWp	£600
Grid connection	6%	15.5 £/kWp	£3500
Transformer	2%	5 £/kWp	£1600
Infrastructure	4%	10.5 £/kWp	£2400
Planning and documentation	4%	10.5 £/kWp	£2400
Total ^c	100%		£71,800
Charging stations	—	600 £/unit	£1800
Frames and foundations		200 £/kWp	£16,000
Total			£89,600

Indicative revenues for the proposed installation

Revenue can be obtained through a variety of methods, as outlined in chapter 2, and for simplicity the following have been selected for this proposed installation:

Feed-in tariffs

Selling the electricity generated to the electric car fleet

Feed-in tariff (FIT) earnings The feed-in tariff applicable to the proposed facility was 2.70 p/kWh, and the export tariff was 4.85 p/kWh (Ofgem.gov.uk, 2016). It is important to note that if the facility capacity of the project is below 50 kW, the payments from FIT will be much better, 4.59 p/kWh instead of 2.70 p/kWh (Ofgem.gov.uk, 2016). According to Ofgem, the FIT payments will last for 20 years for PV system (Recc.org.uk, 2016). The total energy generated for the facility in the first year is suggested to be 87.96 MWh; thereafter, the PV modules will suffer a degradation of 0.4% per year (Stu, 2014), and the generating potential of the carport will reduce annually.

Selling the electricity generated to the electric vehicles fleet In order to sell the electricity to the electric vehicles, consideration was given to the possibility of setting two different pricing options, peak and off-peak.

The estimated hours during which the vehicles are going to be charged is between 8:00–21:00. During this period, from 8:00 to 9:00 and from 18:00 to 21:00, the cost of electricity is suggested to be 18 p/kWh, during this period most of energy should be bought from the grid due to low generation capacity, and therefore creating an additional cost. For the remaining hours, the price of the electricity would remain at its present value, 12 p/kWh, which means that 70% of the total time the price of electricity would be lower, benefitting the consumers.

5.7 Scenario 2

This scenario has been developed for 2020, where the feed-in tariff will likely be a lower rate but the PV system costs is also expected to decrease and should offset one another.

Expenses: Operating Expenditure (OPEX) and investment costs

According to the study published by Fraunhofer Institute for Solar Energy Systems, by 2050, the OPEX will have been reduced to 7.7 £/kWp (ISE, 2015). The estimation for 2020 is 14.1 £/kWp as per table 42. The operating expenditure for this scenario is estimated to be £1,128 in 2020.

Table 42 - Operating expenditures—2020

OPEX			Total costs
Maintenance and operating cost	25%	3.53 £/kWp	£282
Replacing and cleaning cost	35%	4.94 £/kWp	£395
Insurance and taxes	40%	5.64 £/kWp	£451
Total	100%	14.1 £/kWp	£1128

Figure 146 shows an approach to estimating investment costs by including the assumptions for 2050 where the costs of the PV system will decrease between 610 £/kWp in the worst-case scenario and 280 £/kWp in the best-case scenario. It is estimated that by 2020, these costs will be 935 £/kWp in the worst-case scenario and 880 £/kWp for the best-case scenario. For the purposes of this project, the average of these two costs was used. The estimated distributed costs for 2020 in pounds are shown in Table 43, where the charging station costs were also reduced. The total expenses will decrease by 8.8% by 2020 compared with 2016.

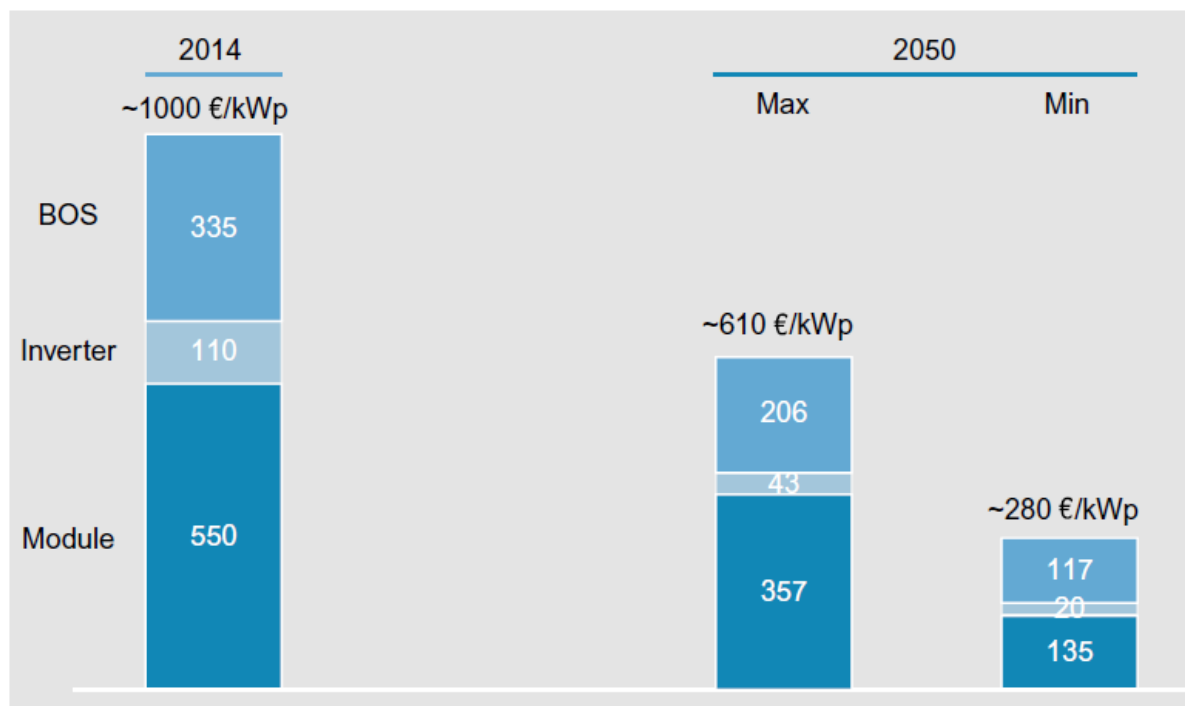


Figure 146 - PV system costs in 2015 combining minimum and maximum assumptions. (Kleiner, 2015)

Table 43 - Detailed cost distribution

Investment cost			Total costs
PV module	55%	384 £/kWp	£30,720
Inverter ^a	11%	75 £/kWp	£15,000
Balance of system	34%	235 £/kWp	£18,800
Charging stations	–	400 £/unit	£1200
Frames and foundations	–	200 £/kWp	£16,000
Total	100%		£81,720

aTaking into account the replacement of the inverter every 10 years.

Revenues

Feed-in tariff (FIT) earnings According to Ofgem, feed-in tariffs for 2019 will have a rate of 1.76 p/kWh, and export tariffs will have a rate of 4.85 p/kWh (Ofgem.gov.uk, 2016).

5.8 Scenario 3

Feed-in tariffs are decreasing as each year passes; also the costs for PV technology is falling quickly; and subsidies are no longer guaranteed in the future. In this scenario, the same assumptions as in Scenario 2 have been taken into account, where FIT was disregarded.

5.9 Financial assumptions

Firstly, it was assumed that the bank would support a loan for 100% of the investment costs over a term of 15 years at a fixed rate of 3%. The project life is 25 years, and the duration of feed-in tariff is 20 years. The inflation rate (RPI) for FIT payments over 20 years was considered to be 2% and the electricity price inflation over the 25 years' lifetime of the project 3%. The lifetime for the PV modules, the mounting system, and the wiring was estimated to be of 25 years (Narayan, 2013), whereas the lifetime of the inverter was estimated as 10 years a rolling replacement scheme will need to be employed to ensure timeous replacement and ensure downtime is minimised.

Payback period, NPV, IRR and DSCR

Equations 61 – 64 (over) are applied in the financial analysis in order to determine the feasibility of the carport. The payback period time, the net present value (NPV), the internal rate of return (IRR), and the debt-service coverage ratio (DSCR) were calculated for the different scenarios (Prentice, 2015):

$$\text{Payback} = \frac{\text{Investment costs}}{\text{Net annual cash in flow}}$$

$$NPV = -C_o \sum_{t=0}^n \frac{C_t}{(1+r)^t}$$

where t is the number of years, n the project time, r the discount rate in %, C_t the cash flow in year t, and C_o the initial investment:

$$NPV = -C_o \sum_{t=0}^n \frac{C_t}{(1+r)^t} = 0$$

$$DSCR = \frac{\text{Net operating income}}{\text{Debt service}}$$

Financials the three different scenarios

Table 44 details the financial results for the carport and shows them to be profitable. The payback period between the scenarios ranged from 8.8 to 9.3 years; the NPV that determined the profitability of the project was found to be higher in Scenario 1, with a benefit of £170,676, and the percentage of IRR showed the financially robust project. According to the results, even in Scenario 3, the worst-case scenario (assuming that the facility will not benefit from subsidies) the economic benefits are still positive. This project has broadly proved the feasibility of the solar charging stations at Edinburgh College's Midlothian Campus and can provide a more sustainable way of charging their green fleet and other electric vehicles on site, further research should be undertaken with a mock investigation bay being established to verify findings.

Table 44 - Financial results for the solar charging station

	Scenario 1	Scenario 2	Scenario 3
Payback	8.8 years	8.4 years	9.3 years
NPV (25 years)	£175,033	£170,676	£144,374
IRR (25 years)	15%	15%	13%
DSCR (15 years)	1.9	1.96	1.71

5.10 Environmental analysis

To conclude the feasibility study, a life-cycle assessment (LCA) was carried out in order to determine the environmental impact of this proposal. As solar charging stations are a relatively novel proposal the life-cycle assessment was carried out for the main components: PV modules, balance of system, inverters, and mounting system to the limited information available. The amount of CO₂ saved when using solar energy, as a source to generate electricity, instead of the electricity from the grid will also be reviewed.

5.11 Life cycle assessment (LCA) of the project

A LCA is important to determine the life of products, materials, system, process, and impact on the environment (Asif and Muneer, 2006).

Eco-audit of the PV module selected

As the PV module is the most important element in the facility, the LCA was carried out using software, CES EduPack, along with the eco-audit tool to evaluate the environmental impact of the selected PV module by focusing on two known environmental stressors, CO₂ footprint and energy usage identifying which of the main life phases (material, manufacture, transport, use, and end of life) is the most demanding of all, Figure 147 gives an example of a products life-cycle.

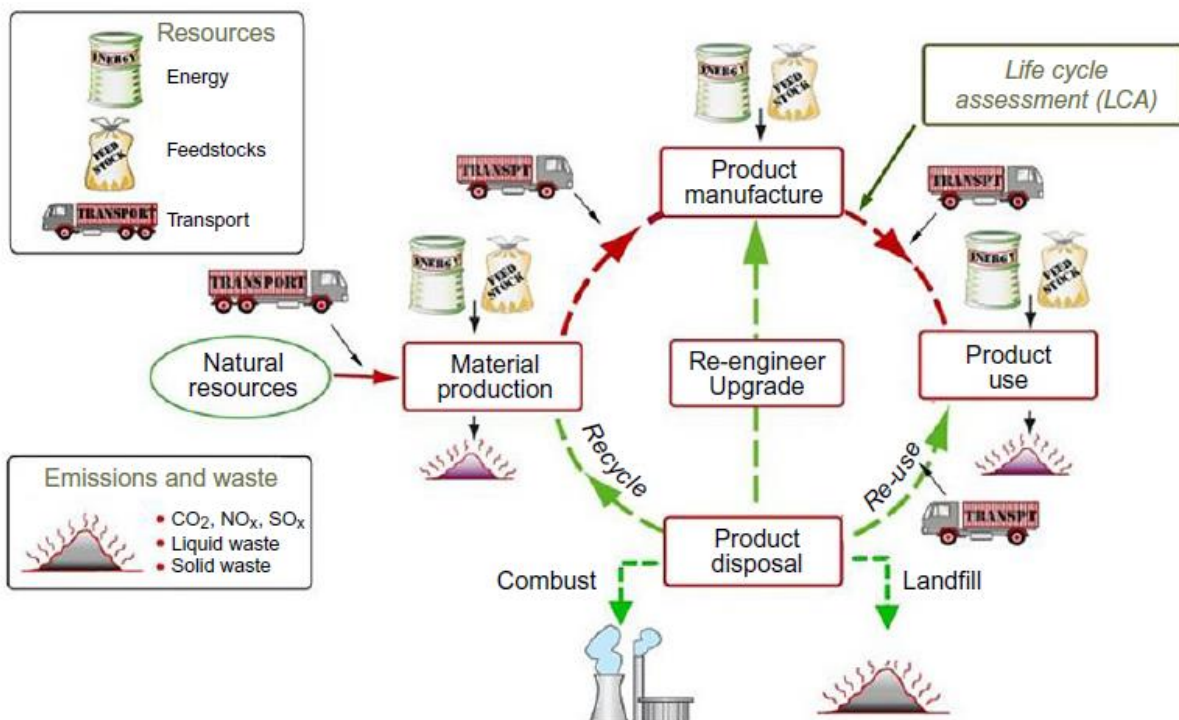


Figure 147 - The product life-cycle (Granta, 2016)

Materials

A typical structure of a monocrystalline silicon PV (see chapter 2) module can be seen in figure 148 (Bagher, 2015). All the relevant data is entered into the software programme including manufacturing materials required for the PV module, the type of process used to manufacture them and their masses, based on a study carried out by Phylipsen and Alsema (1995). This data was adapted with respect to the characteristics of the PV module used for this project.

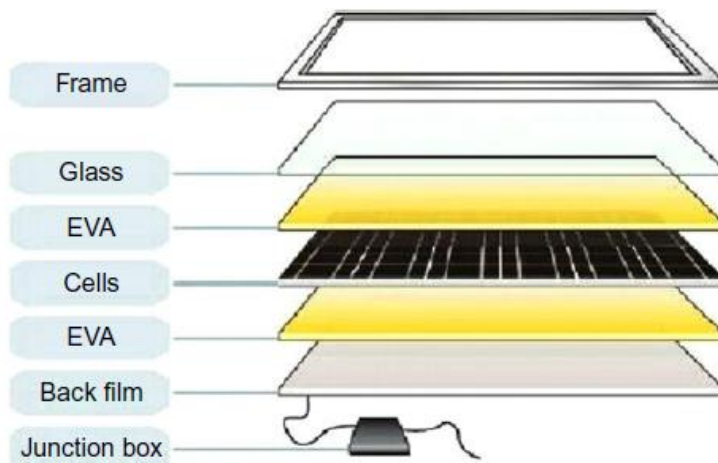


Figure 148 - Monocrystalline solar cell structure *Mohammad Bagher (2015)*.

Transport assumptions

The PV modules used, ASP-400GSM, are produced in the United States. The energy and CO₂ released during transport must be taken into account to carry out the LCA. The distance from the United States to Edinburgh is approximately 6500 km. The likely distance travelled is likely more than this as the route will not be door-to-door, however an accurate representation of the distance travelled for the PV panels will not be available.

Use

Finally, the LCA is used to define the use of the PV module during its lifespan, which was 25 years. As its mode of operation is static, the power rating, duty cycle, and the product efficiency were defined. With all the data collected, the programme could provide detailed information about the breakdown of energy usage and CO₂ footprint of a single PV module or for the 200 PV modules used for the facility. Figure 149 shows that the largest energy demand and the largest release of CO₂ occur during the production phase of the materials where the most polluting material was the silicon, with a percentage of 78% as detailed in table 45.

The results extracted from the CES EduPack report for the 200 PV modules used is detailed in Table 46; the table shows all the energy consumption and CO2 footprint of each individual phase. A total of 70,300 kg of CO2 would be emitted during all the life phases of the product, and 998,000 MJ would be required during the lifespan of the PV module after the end of its life.

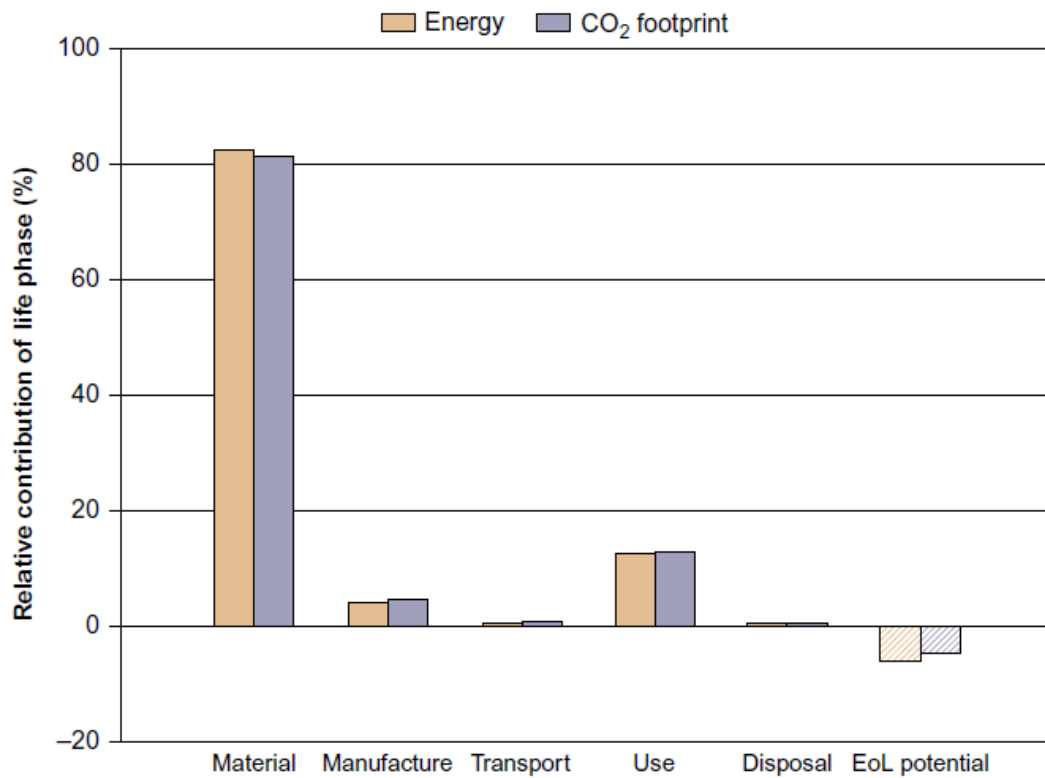


Figure 149 - Energy and CO2 footprint details of a single module. Data from CES Edupack, 2016.

Table 45 - Detailed breakdown of individual material phase for a single module

Component	Material	Recycled content (%)	Part mass (kg)	Qty.	Total mass (kg)	Energy (MJ)	%
	Single crystalline silicon, photovoltaics	Virgin (0%)	2,2	1	2,2	3,7e+03	78,0
	Alkaline-earth lead glass	Virgin (0%)	28	1	28	7e+02	14,7
	EVA (Shore A95/D50, 12% vinyl acetate)	Virgin (0%)	1,9	2	3,8	3e+02	6,3
	PVC (flexible, Shore A60)	Virgin (0%)	0,7	1	0,7	42	0,9
Total				5	35	4,7e+03	100

Data from CES EduPack (2016).

Table 46 - Individual life-phase CO2 footprint details

Phase	Energy (MJ)	Energy (%)	CO ₂ footprint (kg)	CO ₂ footprint (%)
Material	9,39e+05	94,0	6,56e+04	93,4
Manufacture	4,69e+04	4,7	3,75e+03	5,3
Transport	7,11e+03	0,7	505	0,7
Use	720	0,1	51,1	0,1
Disposal	4,7e+03	0,5	329	0,5
Total (for first life)	9.98e+05	100	7.03e+04	100
End-of-life potential	-6.5e+04		-3.66e+03	

Data from ES EduPack (2016).

5.12 Life cycle assessment of the balance of system (BOS) and system mounting

In order to gain an accurate hypothesis, this LCA was based in a study entitled 'Life cycle assessment of a medium-sized photovoltaic facility at a high latitude location', at the Napier University's Merchiston Campus (Muneer et al., 2006).

Balance of system

The components to be taken into account in BOS, as previously mentioned, are the inverters, cables, fuses, and transformers. Due to the lack of data, this theory only considers the inverter and cables. According to Peyser (2010), the contribution of greenhouse gases from BOS is relatively small compared with other components of PV systems. The inverter used for the installation at Napier University was a Fronius (IG60) with a nominal power of 4.6 kW, the amount of CO₂ released per inverter being 850 kg, and the embodied energy 1 MWh (Muneer et al., 2006). Based on this information, the CO₂ released by the inverter selected for the solar carport, an Aurora Trio of 20 kW of nominal power, would be 3700 kg of CO₂ per inverter and 4.35 MWh of embodied energy. As the facility has five inverters, the total amount of CO₂ released would be 18,500 kg and the energy used would be 22 MWh. For the carport, the use of around 450 kg of copper for cabling was estimated; the amount of CO₂ released was estimated being 2280 kg and 8.4 MWh of embodied energy for the facility of 400 m². Again a mock investigation bay being installed will further these findings.

System mounting

The mounting system for the 520m² photovoltaic canopy installation, where the 200 PV modules are going to be placed, the use of around 9750 kg including spigots, vertical rails,

tie brace, and schuco rails was estimated (Muneer et al., 2006). The amount of CO₂ released was estimated to be 21,000 kg and 159 MWh of embodied energy.

5.12.1 Energy payback time (EPBT) and global warming potential (GWP) summary

Based on the LCA, it is estimated that the solar carport (PV modules, BOS, and system mounting) would release a total of 130 tonnes of CO₂ and it would have 488 MWh of embodied energy. Table 47 provides a summary of the most relevant data.

Table 47 - Summary embodied energy and CO₂ released by the facility

Element	Number	Material	Mass (Kg)	Embodied energy (MWh)	Embodied energy (MJ)	CO ₂ released (kg)
PV module (400 Wp)	200	Mixed	6940	277	998,000	70,300
BOS						
Inverter (20 kW)	10 ^a	Mixed	355 × 2	22 × 2	79,200 × 2	18,500 × 2
Cables	–	Copper	450	8.4	30,240	2280
Mounting	–	Steel	9750	159	572,400	21,000
Total				488.4	1,759,040	130,580

^a Assuming the inverters are replaced every 10 years.

Once the total energy used to manufacture the PV system components has been calculated, it is necessary to determine if the PV facility is a net positive producer of energy in its 25 years of lifetime. The energy payback time estimates the energy reimbursement of a product; for the proposed facility, the energy payback time calculated was 5.55 years Equation 65 (McEvoy et.al. 2012).

Equation 65

$$EPBT = \frac{\text{Total energy input during the system life cycle}}{\text{Yearly energy generation by the system}}$$

The global warming potential (GWP) is a measurement to quantify the impact on global warming, the facility will release 130,580 kg of CO₂ and that the lifetime of the installation is 25 years, the ratio of the lifetime emissions of CO₂ for the solar carport was found to be 0.059 kg CO₂/kWh Equation 66 (Muneer et al., 2006) is used.

Equation 66

$$GWP = \frac{\text{Total CO}_2 \text{ released during the system life cycle}}{\text{Energy generation along the lifetime of the system}}$$

5.12.2 CO₂ emissions saved

In order to determine the amount of CO₂ saved by this carport, it was important to take account of the carbon content of the UK grid. Measurements were taken during a 10 day period at specific times (10 a.m., 17 p.m., and 22 p.m.) in August through a website that provides live data on how much electricity is being made nationally and the percentage from fossil fuels, nuclear, or renewable energy, giving information about the grams of CO₂ emitted for every unit of electricity generated in the United Kingdom.

As the average carbon content of the UK grid was 274 g CO₂/kWh during these 10 days of measurements and, according to (Muneer and Kolhe 2017) the carbon footprint that solar energy has is 50g CO₂/kWh, the amount of CO₂ saved by this facility yearly generating an output of 87.96 MWh is calculated using equation 67.

Equation 67

$$CO_2 \text{ saved} = (0.274 - 0.05) \times 87,960 = 19.7 \text{ tonnes of } CO_2$$

5.13 Conclusions

Solar charging station at Edinburgh College

The proposed design of the solar carport has met expectations, proving to be a cost-effective and environmentally friendly design and technically and financially viable. The main findings of this study are: The average solar energy available in Edinburgh is 2.47 Kwh/m² daily, and due to the low temperatures in the city, it was determined that the cell efficiency of the PV module chosen increased from 15.2 to 16.2%. It was found that the best tilt and azimuth angle to install the PV modules was a southern orientation at 40°, this allows the carport to generate 87.96 MWh of energy per year. The car park area identified for the location of the solar charging station is approximately 400 m², providing parking spaces for 33 vehicles. The canopy area will have enough space to accommodate 200 monocrystalline PV modules rated at 400Wp; five Aurora Trio inverters rated at 20 kW, and three twin AC rapid charger CHAdeMO charging stations are required. This facility will be connected to the national grid.

According to the average car journey per person in the Scotland, 20.8 km, and the average energy consumption by an electric car, 0.164 kWh/km, the total energy demand for a single electric car in a day is 3.41 kWh. According to these results, the carport could theoretically charge 70 electric vehicles during the day.

A financial analysis was carried out for three different scenarios. The result of the financial analysis for Scenario 2 during a lifetime of 25 years is shown in Table 48 (over).

Table 48 - Financial analysis, scenario 2

Expenditures		Revenues	
Operating expenditures (annually)	£1128	Feed-in tariff and export tariff	£53,532
PV modules	£30,720	Sale of electricity	£430,006
Inverters	£15,000		
Balance of system costs	£18,800		
Charging stations	£1200		
Frames and foundations	£16,000		
Buying electricity from the grid (25 years)	£81,063		
Interest to pay 3%	£20,960		
Total in 25 years	£211,943	Total in 25 years	£483,538

The payback, i.e. the recovery of the investment for Scenario 2 starts in year 8; the net present value (NPV) analysis shows the best-case NPV of £176,676 and an internal rate of return (IRR) of 15%.

In the environmental analysis, the energy payback time (EPBT) was found to be recovered within 5 years and 5 months, and the global warming potential was 0.059 kg CO₂/kWh. The CO₂ saved by installing this facility, compared with the electricity produced by the UK grid, was 19.7 t of CO₂.

This chapter has presented an option that Edinburgh College could consider in its attempts to create an offgrid and carbon neutral campus. The options presented in this chapter point to the use of current space available to the college within its current estate. Three scenarios have been investigated and presented finding that the financial benefit of undertaking the second option would create significant benefits of the college. With this solution, adding to the campus' solar farm, a real opportunity presents itself for the organisation to meet its aspirations. As a result of this initial study a mock carport is planned for summer 2019 to further scrutinise the findings and assumptions made in this chapter. This chapter also provides an evidence base warranting future study within the area of pedagogical impact of applied research within an FE institution. The undertaking would not have been possible for individual partners, but the combination of partners and stakeholders has given the opportunity for students to gain access to a research facility which is not, in the traditional sense, normally available to students studying within the FE sector. The Education Working for All report (Scottish Government 2014) outlines several areas of interest that add to the debate regarding the nature and validity of HE delivered in FE. The report focussed on the requirement to develop and promote higher-level technical vocational training to support the

increased requirement for associate professional skills. This training is to be developed and delivered in partnership with employers, colleges and universities with a focus on the applied, technical and practical skills available within the vocational FE sector (Husband and Jeffrey, 2016).

Chapter 6 – Conclusion

6.1 Introduction

Through this research the energy delivery of the Edinburgh College solar PV farm has been assessed with consideration to the shading effect. Energy production especially in the renewable sector, which is intermittent, requires a reliable and precise calculation in terms of available sources of energy and net produced energy. It is important for the installers to have the highest efficiency and to take the most of available sources. As in the Edinburgh college solar PV farm project, the installers of the farm claimed that there would be little to no shading effect on the farm across the year. This project was implemented to review the comparison of actual energy produced/available energy/modelled energy output/output with respect to shading. To fully understand this comparison, the secondary study was implemented to review the shading impact in greater detail, with the farm being investigated, in terms of shading for every 30 minutes across seven day intervals for the entire year. This secondary study has relied heavily on the use of MATLAB in order to better analyse the vast amount of data. This thesis shows the importance of the impact shading has on solar installations in northern latitudes.

6.2 Site identification

Site identification was straightforward with the introduction of the Solar farm at Edinburgh College's Midlothian Campus is a 5 acre development which provides 627.5kW of energy in the midst of a bio-diversity meadow. This is a unique installation for Scotland and marries aspects of modern technology with key environmental concerns. The energy produced is expected to go some way to reduce the carbon footprint of the Campus and the meadow is said to produce enough electricity for the Midlothian Campus to be self-sufficient and not rely on the National Grid. If surplus electricity is produced it will be sold back to the Grid, helping to off-set electricity bills at the College's Edinburgh Campus based at Milton Road in Edinburgh. The site was commissioned in March of 2013 however, complications within the contracting process, which were resolved in 2018, has meant access to valuable data directly from the site infrastructure has been limited up to this point. Manual methods of data collection at the site were adopted to ensure data was available for analysis.

6.3 Site specific data

Chapter 3 sees the performance of a range of solar module parameters studied in this research and includes experiments used to measure a range of data quantities designed

and implemented. An initial survey of the site, was carried out to obtain an estimate of the degree of shading incurred. To overcome the limitations of the data available to the researcher, a period of manually-recorded measurements was carried out to support the experimental data. Through the collection the site's power and energy data, as well as providing a useful picture of site operation, a problem with a subset of the inverters on site was identified. Upon discussion with the Engineer overseeing the site, it was found to correspond with the data collected by SSE, the contractors, who resolved the issues as a result of the research taking place.

6.4 Site survey

The shading characteristic of the site was assessed in chapter 4 which describes this process in detail, but it was clearly shown that the assumption of zero shading for the site assumed by the contractors (see Appendix B: SSE System Documents) was shown to be inaccurate, particularly in the winter months. Shading was shown to be most severe at the south end of the site, and still notable along the eastern edge of the site. Any shading on the solar modules will adversely affect the performance of the entire string in question, having a disproportionately large effect on overall output. This certainly requires a revision of the initial SAP calculations to be carried out.

Within this survey of the site an inspection of the farm was carried out and 12 critical points of shade have been established within the farm, situated along the south, east and centre. All the data related to the obstacles around the farm at each critical point and was collected via a theodolite. Increments every 30° due east, the height (altitude) of each identified shade creating blockage was recorded for each of the identified critical points. The Sun's position in the sky (solar altitude and azimuth) was also calculated for each specific azimuth due east, solar altitude (SOLALT) and blockage height were compared. The periods of shade impacting on the critical points was assessed by taking advantage of sky view factor (SVF) shade model the relationship between the visible area of the sky and the portion of the sky covered by surrounding solar blockage was assessed.

6.5 Site monitoring

The conversion of solar irradiation data, from horizontal intensity to intensity received on a slope, has been shown to be accurate when using location-specific regression formulae. It was concluded that the seasonal model proposed by Clarke et al (2007) proved the most accurate of those considered over the recorded time period, by a small margin. A further

advantage of the given method is the slightly simpler implementation compared to the monthly model, which requires a different formula to be used for every month.

The prediction of a solar photovoltaic module's cell temperature from environmental data such as air temperature and solar irradiation was shown to be within close alignment across three different calculation methods. The simplest, based on the 'nominal operating cell temperature' of the module gave results within tolerance, as the much more complex thermal model, indicating that this is a useful method to use. The thermal model was limited by the lack of good quality, high resolution wind data for the site studied. In addition, the range of input variables require better definition. Future study should incorporate a thorough investigation of the thermal model.

Finally, the calculation of cell efficiency over the three days of manual data recordings was performed, giving the results described in chapter 3. The results obtained here require further ratification to extract a reliable data set and it is suggested that this work is carried out as a matter of interest in further study. The difficulty encountered was whether to ascribe the poor quality of results to the models used, or the data collected. The one exception, on a clear-sky day when the related uncertainties were small, indicated that with reliable, automatically logged power data the models used could yield much more favourable results between 16 – 18%. The cell efficiency was predicted, in as far as lying between 14 – 16% and being lower on hotter days, or in the afternoon at 12- 16%. The implementation high-resolution data collection through longer term study on the site in the future opens up excellent opportunities for further analysing the results of this project.

6.6 Site Modelling

Software models were produced or adapted from a range of source material to implement the required calculations which formed the investigative assessment, and associated data organisation and display tools were developed through the use of Excel (Aldali et. al. 2011).

Software implementation of the data analysis and processing models was successfully implemented with the data collected, constituting a valuable learning experience. However, time could have been saved and errors avoided with a more organised approach to design and testing of the software before full implementation in the project spreadsheet. With the site now operational for 6 years, initial technical issues (as outlined in this thesis) have been resolved allowing for further analysis of actual energy output versus modelled output. MATLAB software was used to carry the calculations and as the day number and sunrise &

sunset values vary daily. Excel has been used for data evaluation and to clearly present findings in chapter 4. This has allowed an evaluation of the impact of shading has on the solar farm in a visual format.

6.7 Data Analysis

The experimental setup produced results that could be analysed, but introduced some unnecessary sources of error (such as shading/misalignment of the slope irradiation sensors, and slight inconsistency in data-logger times) and didn't incorporate enough redundancy in the data recording.

Errors were encountered due to the implementation equipment used. Human error is to blame and the researcher should validate these results through further study. The data-logger evidently recorded some spurious data values, and the heat-flux readings were either incorrect or were incorrectly interpreted. A much more timely analysis, in particular graphical analysis, of the data obtained may have allowed some of these problems to be fixed. (Inspection of the numerical results was made as the experiment progressed, but this proved to be insufficient.) This also applies to the sensor problems mentioned above. All the data related to the solar blockages has been collected in 30° intervals due east improved precision could have been achieved by undertaking 10° intervals. For calculating monthly energy output the mean value of monthly, hourly horizontal global irradiation has been used but for more clear results it should be carried out every 5 or 10 days to reflect the ever changing air temperature and clearness index. Energy delivery for each month, within a year, was calculated on the basis of energy delivery at the critical points. December has the lowest energy delivery with only 54% of the total available being delivered and November & January are the second and third lowest with 69% and 70% delivered respectively. The energy delivery increases gradually until it arrives at 100% in May, June and July. The energy delivery of the Edinburgh College solar PV farm is more than 94% for the entire year with the impact of shading taken into account.

6.8 Comparison of solar output

The farm energy has been calculated on the basis of measured 2014 global radiation and farm's PV module specifications. Available energy in the Edinburgh college solar PV farm has been estimated at 525,674 KWh and by accounting for shading decreases to 498,776 KWh. 95% of the energy is produced during the months where energy delivery is higher than 80% and only 5% of energy is produced in the months from November to February. Shading occurs in two main areas along the southern edge, due to the tree foliage, and the

eastern edge due to the earth bund which encloses the site. The modelled output for the site was estimated to be 560,000kWh the actual energy based on location and meteorological data has been shown to be 538,388kWh with the available energy of the site being 526,674kWh. With the shading apparent on the site taken into account the value of energy delivered drops to 498,776kWh. The solar farm does not currently provide enough energy to cover the campus requirements with the campus energy consumption of 635,635 kWh for academic year 2017/18. This represents a shortfall of 136,859 kWh.

6.9 Pedagogical impact on the College

Chapter 5 presented an option that Edinburgh College could consider in its attempts to create an offgrid and carbon neutral campus. The options presented in this chapter point to the use of current space available to the college within its current estate. Three scenarios have been investigated and presented finding that the financial benefit of undertaking the second option would create significant benefits of the college. With this solution, adding to the campus' solar farm, a real opportunity presents itself for the organisation to meet its aspirations. As a result of this initial study a mock carport is planned for summer 2019 to further scrutinise the findings and assumptions made in this chapter. This chapter also provides an evidence base warranting future study within the area of pedagogical impact of applied research within an FE institution. The undertaking would not have been possible for individual partners, but the combination of partners and stakeholders has given the opportunity for students to gain access to a research facility which is not, in the traditional sense, normally available to students studying within the FE sector. The Education Working for All report (Scottish Government 2014) outlines several areas of interest that add to the debate regarding the nature and validity of HE delivered in FE. The report focussed on the requirement to develop and promote higher-level technical vocational training to support the increased requirement for associate professional skills. This training is to be developed and delivered in partnership with employers, colleges and universities with a focus on the applied, technical and practical skills available within the vocational FE sector (Husband and Jeffrey, 2016).

6.10 Lessons learned

Time management of the project could have been improved. Work was commenced early and quickly, however the latter stages of the project, in particular the report write-up, suffered from an inconsistent work-rate and poorly-defined work goals. A more organised

approach throughout the 15 weeks would have allowed for more to have been accomplished, and a more polished report to have been produced. The generation of research data and application of (thus far) purely theoretical knowledge in a practical environment has provided an extremely positive experience for the author. In addition to hopefully making a useful contribution in the field of solar research, the work undergone will prove useful to Edinburgh College in their operation of, and knowledge of, the solar plant at Midlothian Campus. The gap in this research is the lack of GIS modelling or PV*SOL modelling as part of the review of the site.

6.11 Recommendations for future study

There are some clear gaps within this study, such as the use of PV*SOL to accurately depict a 3D representation of an array and provided detailed information on the shadow cast, throughout the year, to provide likely reductions in overall yield. This should be utilised in further study to ratify the results obtained through this research. Furthermore, now that contracts between the college and SSE have been agreed access to high resolution data will inform further research into the actual output versus modelled output.

The following recommendations for future work, on areas relating to this study were proposed or considered as part of the research, but were abandoned due to time constraints, or lack of access to data or equipment.

- To calculate the farm energy delivery with consideration to cell temperature.
- To calculate the farm energy delivery with consideration to different module configuration.

Further study in these areas will provide a more robust assessment of the site and present excellent opportunities for college students to carry out applied research on a live, fully operational system within their coursework.

The comparison of power/energy readings from a single inverter, or indeed all 32 inverters across the site, with the overall metered power output being exported to the grid would allow for detailed analysis of overall system efficiency, allowing for losses such as through dc and ac wiring, module mismatch and inverter efficiency would provide an analysis of other losses within the site.

The application of the existing findings to a different seasons, or even across the whole year, would allow for the solar models to be more accurately assessed, and would give a much more detailed representation of system performance. This applies particularly to any detailed shading analysis, but also to the cell temperature, slope irradiation and low-power performance of the system (inverters, for example, perform less well at low power outputs).

The use of yearly-average climactic data for the given location, in conjunction with the solar models used and detailed shading data, would allow for accurate forecasts of plant output to be produced with real economic gain for the college and SSE. Knowing what revenues the site will generate in years to come (from generation and subsidies) would be a real gain.

The recording and inclusion of detailed wind data into the thermal model used should provide more accurate estimates of the cell temperature, and would allow for further optimisation and testing of the model. The aforementioned possibility of implementing automated data logging of all inverters on site (including power, current and voltage) would greatly improve the potential for future study.

The use of modelling packages such as GIS based approached or PV*SOL modelling should be undertaken across the site to build a comprehensive analysis of shading across the site. Both studies within this research have highlighted that the site suffers from shading, which impacts on the overall energy generated. An in depth review of the overall site could lead to suggested improvements for this site or other proposed fixed frame urban arrays.

References

- (IEA), I. E. A. (2014) *Snapshot of Global PV 1992–2013*.
- (NREL), N. R. E. L. (2015) *National Renewable Energy Laboratory (NREL)*. Available at: <http://www.nrel.gov> (Accessed: 18 March 2016).
- Aboudi, M. (2011) *Solar PV balance of system (BOS):Technologies and markets blog, GTM Research*.
- Actions taken by the Chinese Government* (2015). Available at: <http://cdm.ccchina.gov.cn/english/> (Accessed: 19 December 2015).
- Aldali, Y., Henderson, D. and Muneer, T. (2011) 'AldaliCelikPV.pdf', *International Journal of Low-Carbon Technologies*, pp. 277–293. doi: 10.1093/ijlct/ctr015.
- Aldali, Y; Celik, A.N; Muneer, T. (2013) 'Modelling and Experimental Verification of Solar Radiation on a sloped surface, Photovoltaic Cell Temperature and Photovoltaic efficiency', *Journal of Energy Engineering*, 1(139), pp. 8–11.
- Aliaga, M; Gunderson, B. (2002) *Interactive statistics*. New Jersey: Prentice Hall.
- Allen SR, H. G. and M. M. (2008) 'Prospects for and barriers to domestic micro generation: A United Kingdom perspective.', *Applied Energy*, 85, pp. 528–554.
- Alonso-Gracia, M. C. (2006) 'Experimental study of mismatch and shading effects in the I–V characteristic of a photovoltaic module', *solar cells*, pp. 329–340.
- Aramoto T, Kumaza S, Higuchi H, et al. (1997) '16.0% efficient thin-film CdS/CdTe solar cells', *Journal of Applied Physics*, 36(Part 1: Regular Papers and Short Notes and Review Papers), pp. 6304–6305.
- Audit Scotland (2011) 'Reducing Scottish greenhouse gas emissions', *Environment*, (December).
- Ayre, J. (2013) *Clean technica: Dye-sensitized solar cells achieve record efficiency of 15%*. Available at: <http://cleantechnica.com/2013/07/15/dye-sensitized-solar-cells-achieve-record-efficiency-of-15/> (Accessed: 19 December 2015).
- B, R. (2003) 'Status of amorphous and crystalline thin film silicon solar cell activities', in *NCPV and Solar Program Review Meeting 5*, pp. 552–555.
- Baddeley, S. (2008) 'Reducing our dependence on the car', (April 2012), pp. 37–41.
- Becker C, Sontheimer T, Steffens S, et al. (2011) 'Polycrystalline silicon thin films by high-rate electronbeam evaporation for photovoltaic applications – Influence of substrate texture and temperature', *Energy Procedia*, 10, pp. 61–65.
- Boer, K. W. (2011) 'Cadmium sulfide enhances solar cell efficiency', *Energy Conversion and Management*, (52), pp. 426–430.
- Boutchich M, Alvarez J, Diouf D, et al. (2012) 'Amorphous silicon diamond based hetero

junctions with high rectification ratio.’, *Journal of Non-Crystalline Solids*, (358), pp. 2110–2113.

Brown, N. (2013) *Clean Technica*. 99% Of 2012 US solar PV installations were net metered. Available at: <http://cleantechnica.com/2013/04/19/99-of-2012-us-solar-pv-installations-were-net-metered/> (Accessed: 18 December 2015).

Budin, R. and Budin, L. (1982) ‘A Mathematical Model for Shading Calculations’, 29(4), pp. 339–349.

Burns, J; Kang, J. (2012) ‘Comparative economic analysis of supporting policies for residential solar PV in the United States: Solar Renewable Energy Credit (SREC) potential.’, *Energy Policy*, (44), pp. 217–225.

C, B. J. and F. (1993) ‘Thin film CdS/CdTe solar cell with 15.8% efficiency.’, *Applied Physics Letter*, (62), pp. 2851–2852.

Calde´s N, Varela M, Santamari´a M, et al. (2009) ‘Economic impact of solar thermal electricity deployment in Spain.’, *Energy Policy*, (37), pp. 1628–1636.

Canning, R. (1999) ‘Post-16 education in scotland: credentialism and inequality’, *Journal of Vocational Education & Training*, 51(2), pp. 185–198.

Carneiro, C. (2009) ‘Assessment of solar irradiance on the urban fabric for the production of renewable energy using LIDAR data and image processing techniques’, *Advances in GIScience*, p. 30.

Cherrington, R; Goodship, V; Longfield, A; Kirwan, K. (2013) ‘The feed-in tariff in the UK: A case study focus on domestic photovoltaic systems’, *Renewable Energy*, 50, pp. 421–426.

Chowdhury S, Sumita U, Islam A, et al. (2014) ‘Importance of policy for energy system transformation: Diffusion of PV technology in Japan and Germany.’, *Energy Policy*, (68), pp. 285–293.

Clarke, P. et al. (2008) ‘Models for the estimation of building integrated photovoltaic systems in urban environments’, *Proceedings of the Institution of Mechanical Engineers, Part A: Journal of Power and Energy*, 222(1), pp. 61–67. doi: 10.1243/09576509JPE474.

Clarke, P. et al. (2007) ‘Technical note: An investigation of possible improvements in accuracy of regressions between diffuse and global solar irradiation.’, *Building Services Engineering Research and Technology*, 28(2), pp. 189–197.

Committee on Climate Change (2017) ‘Advice on the new Scottish Climate Change Bill.’

Compaan, A. D. (2004) ‘The status of and challenges in CdTe thin-film solar-cell technology.’, *MRS Symposium Proceedings*, (808), pp. 545–555.

Cost of solar panels-10 charts tell you everything (2013) *Cost of Solar*.

CR, C. D. and W. (1976) ‘Amorphous silicon solar cell’, *Applied Physics Letters*, (28), pp. 671–673.

Darghouth NR, B. G. and W. R. (2011) 'The impact of rate design and net-metering on the bill savings from distributed PV for residential customers in California.', *Energy Policy*, 9(39), pp. 5243–5253.

Deb SK, C. S. and W. H. (1978) 'No Title.' USA.

DECC. (2015) *Green Deal: Energy Saving for Your Home*. Available at: <https://www.gov.uk/govern> (Accessed: 26 February 2016).

Deline, C; Meydbray, J; Donovan, M; Forrest, J. (2012) *Photovoltaic Shading Testbed for Module-Level Power Electronics*. Colorado.

Department of Energy and Climate Change (2011) *UK Renewable Energy Roadmap*. Available at: https://www.gov.uk/government/uploads/system/uploads/attachment_data/file/48128/2167-ukrenewable- (Accessed: 18 June 2016).

Department of Energy and Climate Change (2013) *UK Solar Photovoltaic Roadmap, Doing solar business in the UK*.

Diefenbach, K. (2005) 'Wiped away.', *Photon International*, (February), pp. 48–67.

Dincer, F. (2011) 'The analysis on photovoltaic electricity generation status, potential and policies of the leading countries in solar energy', *Renewable and Sustainable Energy Reviews*, (15), pp. 713–720.

DSIRE (2015) *US National database of state incentives for renewable energy, Interstate Renewable Energy Council*. Available at: <http://www.dsireusa.org/> (Accessed: 3 February 2016).

DTI (2006) *Domestic Photovoltaic Field Trials-Final Technical Report*. London.

Dusonchet, E ; Telaretti, L. (2015) 'Comparative economic analysis of support policies for solar PV in the most representative EU countries.', *Renewable and Sustainable Energy Reviews*, (42), pp. 986–998.

Dusonchet, E; Telaretti, L. (2010) 'Economic analysis of different supporting policies for the production of electrical energy by solar photovoltaics in eastern European Union countries.', *Energy Policy*, (38), pp. 4011–4020.

Edinburgh College (2016) *Carbon Management Plan*. Available at: edinburghcollege.ac.uk (Accessed: 1 October 2017).

Edinburgh College (2017) *Sustainability Strategy*. Available at: www.edinburghcollege.ac.uk (Accessed: 1 October 2017).

Efim, G; Evseev, A. (2008) 'the assessment of different models to predict the global solar radiation on a surface tilted to the south', *Solar Energy*, 86, p. 16.

Ekpenyong, E. Anyasi, F. (2013) 'Effect of Shading on Photovoltaic Cell', 8(2), pp. 1–6.

EMSI (2015) 'Demonstrating the economic value of Scotland's Colleges', (September).

Energieforschung, B. (2013) *Innovation durch Forschung – Jahresbericht zur Forschungsfortschreibung im Bereich der erneuerbaren Energien*. Available at: <https://www.ptj.de/> (Accessed: 17 December 2015).

Energy Institute (2015) *Energy World, Linking Electric System-Power System Heading Towards Low Carbon Future*. London.

Evoenergy (2015) *Evoenergy*. Available at: <http://www.evoenergy.co.uk> (Accessed: 14 March 2016).

Fawcett, G; Killip, T. (2014) 'Anatomy of low carbon retrofits: Evidence from owner-occupied Super Homes.', *Building Research Information*, 4(42), pp. 434–445.

Feed-in Tariff (2015). Available at: <https://www.ofgem.gov.uk/sites/default/files/docs/2015/02/fitfact> (Accessed: 18 January 2016).

Feldman D, Barbose G, Margolis R, et al. (2014) *Photovoltaic system pricing trends, NREL*. Available at: <http://www.nrel.gov/docs/fy14osti/62558.pdf> (Accessed: 18 January 2016).

Finance, M. of (2009a) *Interim management method for financial assistance fund supporting golden sun demonstration programs*. Beijing, China.

Finance, M. of (2009b) *Interim management method for financial subsidy fund for building integrated PV systems*. Beijing, China.

First Solar (2011). Available at: <http://investor.firstsolar.com/releasedetail.cfm?ReleaseID=593994> (Accessed: 18 January 2016).

Fthenakis V, Morris S, Moskowitz P, et al. (1999) 'Toxicity of cadmium telluride, copper indium diselenide, and copper gallium diselenide', *Progress in Photovoltaics*, (7), pp. 489–497.

Fukushima Renewable Energy Institute (2014) *Fukushima Renewable Energy Institute*. Available at: <https://www.aist.go.jp/fukushima/en/> (Accessed: 18 January 2016).

Gago, E. J. et al. (2010) 'Inter-relationship between mean-daily irradiation and temperature, and decomposition models for hourly irradiation and temperature', pp. 1–16. doi: 10.1093/ijlct/ctq039.

Gago, E. J. et al. (2011) 'Inter-relationship between mean-daily irradiation and temperature, and decomposition models for hourly irradiation and temperature', *International Journal of Low-Carbon Technologies*, 6(1), pp. 22–37. doi: 10.1093/ijlct/ctq039.

Gardiner M, White H, Munzinger M, et al. (2011) *Low carbon building programme. Final Report 2006–2011*. Available at:

https://www.gov.uk/government/uploads/system/uploads/attachment_data/file/48484 (Accessed: 18 January 2016).

Gerischer, H; Tributsch, H. (1968) 'Electrochemische Untersuchungen zur spectraleu sensibilisierung von ZnO-Einkristalien.', *Berichte der Bunsengesellschaft fu"r Physikalische Chemie*, (72), pp. 437–445.

German Solar Industry Association (2015). Available at: <http://www.solarwirtschaft.de/> (Accessed: 18 January 2016).

Goetzberger A and Hebling (2000) 'Photovoltaic materials, past, present, future.', *Solar Energy Materials and Solar Cells*, (62), pp. 1–19.

Goetzberger and Hoffman (2005) 'Photovoltaic solar energy generation', *Springer Series in Optical Sciences*, p. 112.

Grant Instruments (2013) *Squirrel View (Online)*. Available at:

<http://www.grantinstruments.com/squirrelview/> (Accessed: 2 April 2014).

Granta (2016) *Granta's eco audit methodology*.

Gratzel, M. (2003) 'Dye-sensitized solar cells', *ournal of Photochemistry and Photobiology C: Photochemistry Reviews*, (4), pp. 145–153.

Grau T, H. M. and N. K. (2011) *Survey of Photovoltaic Industry and Policy in Germany and China., CPI Report*. Available at: <http://climatepolicyinitiative.org/wp-content/uploads/2011/12/> (Accessed: 21 January 2016).

Green MA, Zhao J, Wang A, et al. (2001) 'Progress and outlook for high-efficiency crystalline silicon solar cells.', *Solar Energy Materials and Solar Cells*, (65), pp. 9–16.

GreenPeace International (2011) *Solar generation 6 solar photovoltaic electricity empowering the world, EPIA*. Available at:

<http://www.greenpeace.org/international/Global/international/publica> (Accessed: 26 February 2016).

Greentech Solar (2012) *Solar balance-of-system costs account for 68% of PV system pricing, New GTM report blog*. Available at:

<http://www.greentechmedia.com/articles/read/Solar-Balance-of-> (Accessed: 14 April 2016).

Grigoleit, D; Lenkeit, T. (2011) *The renewable energy industry in Germany. A glance at industry promotion policies in selected energy sectors*. Available at:

<https://www.gtai.de/GTAI/Content/EN/> (Accessed: 20 December 2015).

Growth of Photovoltaics (2015). Available at:

https://en.wikipedia.org/wiki/Growth_of_photovoltaics (Accessed: 2 February 2016).

Guha, G. (2004) 'Thin film silicon solar cells grown near the edge of amorphous to microcrystalline transition.', *Solar Energy*, (77), pp. 887–892.

H, R. B. and W. (1999) 'Potential of amorphous silicon for solar cells.', *Applied Physics A*

Materials Science & Processing, (65), pp. 155–167.

Hauffe K, Danzmann HJ, Pusch H, et al. (1970) 'New experiments on the sensitization of zinc oxide by means of the electrochemical cell technique', *Journal of the Electrochemical Society*, (117), pp. 993–999.

Horn, B. K. P. (1981) 'Hill Shading and the Reflectance Map', *Proceedings of the IEEE*, 69(1), pp. 13 – 47.

House of Commons (2012) *The Renewables Obligation*. Available at: www.parliament.uk/briefing-papers/sn05870.pdf (Accessed: 19 August 2014).

Husband, G. and Jeffrey, M. (2016) 'Advanced and higher vocational education in Scotland: recontextualising the provision of HE in FE', *Research in Post-Compulsory Education*, 21(1-2), pp. 66–72. doi: 10.1080/13596748.2015.1125670.

IEA (2010) *Global Gaps in Clean Energy RD&D*. Available at: <https://www.iea.org/publications/> (Accessed: 28 February 2016).

IEA - PVPS (2015) *Rural electrification with PV hybrid systems. Report, IEA-PVPS T9-13:2013*. Available at: http://www.iea-pvps.org/fileadmin/dam/public/report/national/Rural_Electrification_with_PV (Accessed: 17 February 2016).

Iles, P. (2001) 'Evolution of space solar cells.', *Solar Energy Materials and Solar Cells*, (68), pp. 1–13.

Innovationsallianz Photovoltaik (2015). Available at: <http://www.innovationsallianz-photovoltaik.de/> (Accessed: 18 February 2016).

International Energy Agency (2015). Available at: <http://www.iea-pvps.org/> (Accessed: 18 February 2016).

International energy Agency (2015) *Technology Roadmap: Solar Photovoltaic Technology*. Available at: http://www.iea.org/publications/freepublications/publication/pv_roadmap.pdf (Accessed: 19 March 2016).

Itoh M, Takahashi H, Fujii T, et al. (2001) 'Evaluation of electric energy performance by democratic module PV system field test.', *Solar Energy Materials and Solar Cells*, (67), pp. 435–440.

Jager-Waldau (2014a) *JRC scientific and policy report*. Luxembourg.

Jager-Waldau (2014b) 'Technology Roadmap Solar photovoltaic energy', *International Energy Agency*, pp. 1–42. doi: 10.1787/9789264088047-en.

Japan International Corporation Agency (2011). Available at: <http://www.jica.go.jp/usa/english/office/> (Accessed: 21 March 2016).

Jeffrey, M. et al. (2015) 'Evaluation of solar modelling techniques through experiment on a 627 kWp photo- voltaic solar power plant at Edinburgh College — Midlothian Campus ,

Scotland Evaluation of solar modelling techniques through experiment on a 627 kWp photo-voltaic solar power', 033128. doi: 10.1063/1.4922450.

Kashif Ishaque (2011) 'Modeling and simulation of photovoltaic (PV) system during partial shade', *Elsevier*, (19), p. 14.

Key and Peterson (2009) 'Solar Photovoltaics: Status, Costs, and Trends. Palo Alto, CA', *EPRI*, p. 1015804.

Kleiner, M. M. (2015) *Current and future cost of photovoltaics.*, *ISE*.

Kumar, K; Sahu, B. (2015) 'A study on global solar PV energy developments and policies with special focus on the top ten solar PV power producing countries.', *Renewable and Sustainable Energy Reviews*, (43), pp. 621–634.

Kurokawa, i and Osamu, K. (2001) 'The Japanese experiences with national PV system programme', *Solar Energy*, (70), pp. 457–466.

L, S. Z. and X. (2012) 'Large scale wind power integration in China: Analysis from a policy perspective', *Renewable and Sustainable Reviews*, (16), pp. 1110–1115.

Lewis J, S. A. and T. T. (2009) *International Motivations for Solar Photovoltaic Market Support: Findings from the United States, Japan, Germany and Spain*. San Francisco.

Lichner C (2010) *Washing the Sun.*, *Photovoltaik*. Available at: <http://www.photovoltaik.eu/Archiv/> (Accessed: 18 February 2016).

Liu LQ, Wang ZX, Zhang HQ, et al. (2010) 'Solar energy development in China – A review.', *Renewable and Sustainable Energy Reviews*, 1(14), pp. 301–311.

Mah, O. (1998) *Fundamentals of photovoltaic materials*, *National Solar Power Research Institute, Inc*. Available at: <http://userwww.sfsu.edu/ciotola/solar/pv.pdf> (Accessed: 17 March 2016).

Manna, SM ;Mahajan, T. (2007) 'Nanotechnology in the development of photovoltaic cells', *In: IEEE conference on clean electrical power Capri, 21–23 May*, pp. 79–86.

Mattei, M. et. al. (2006) 'Calculation of Polychrystalline PV module temperature using a simple method of energy balance', *Renewable Energy*, 31, pp. 553 – 567.

Media, G. (2013) *How are solar PV BOS costs trending in the US?*, *blog. regenerate Power*. Available at: <http://www.regeneratepowerllc.com/news/14-opportunity-in-solar-as-balance-of-syst> (Accessed: 18 February 2016).

Meiller, R. (2013) *Future looks bright for carbon nanotube solar cells*, *University of Wisconsin-Madison News*. Available at: <http://www.news.wisc.edu/21890> (Accessed: 17 March 2016).

METI (2008a) *Cool Earth Initiative*. Available at: <http://www.meti.go.jp/english/newtopics/data/pdf/> (Accessed: 6 May 2016).

METI (2008b) *METI*. Available at: <http://www.meti.go.jp/english/index.html> (Accessed: 2

February 2016).

Metz, B. e. al (2013) *Mitigation of climate change, International panel on climate change.*

Muhammad-Sukki F, Abu-Bakar SH, Munir AB, et al. (2014) 'Feed-in tariff for solar photovoltaic: The rise of Japan', *Renewable Energy*, (68), pp. 636–643.

Muneer, T. (2004) *Solar radiation and daylight models*. Second.

Muneer, T. et al. (2006) 'Life cycle assessment of a medium-sized photovoltaic facility at a high latitude location', *Proceedings of the Institution of Mechanical Engineers, Part A: Journal of Power and Energy*, 220(6), pp. 517–524. doi: 10.1243/09576509JPE253.

Muneer, Tariq; N, Abodahab; G, Weir; J, K. (2000) *Windows in Buildings: Thermal, Acoustic, Visual and Solar Performance*. First Edit. Oxford: Butterworth - Heinemann.

Muneer, T., Etxebarria, S., & Gago, E. (2014) 'Monthly averaged-hourly solar diffuse radiation model for the UK', *Building Services Engineering Research and Technology*, 35(6), pp. 573–584.

Myrans, K. (2009) *Comparative Energy and Carbon Assessment of Three Green Technologies for a Toronto Roof*. University of Toronto.

Naam, R. (2011) *Smaller, cheaper, faster: Does Moore's law apply to solar cells?*, blog. *Scientific America*. Available at: <http://blogs.scientificamerican.com/guest-blog/2011/03/16/smaller-cheaper-faster-> (Accessed: 18 March 2016).

National travel survey (no date) *National travel survey*.

Ndilemeni; Momoh (2013) 'Evaluation of clearness index of sokoto using estimated global solar radiation', *Iosrjournals*, 5(3), p. 4.

Negishi, H; Lawson, M. (2008) *Reuters. Japan aims to restart solar subsidies next year*. Available at: <http://www.reuters.com/article/environmentNews/idUST20760420080624> (Accessed: 18 March 2016).

Nguyen, H. T. and Pearce, J. M. (2012) 'Incorporating shading losses in solar photovoltaic potentiation assessment at the municipal scale', *Solar Energy*, 86(5), pp. 1245–1260.

Nicholson J (2015) *FIT and the green deal for solar PV installations*.

Nowshad A, Takayunki I, Akira Y, et al. (2015) 'High efficient 1 mm thick CdTe solar cells with textured TCOs', *Solar Energy Materials and Solar Cells*, (67), pp. 195–201.

Osamu, I. (2003) 'Present status and future prospects of PV activities in Japan', *Solar Energy Materials and Solar Cells*, (75), pp. 729–737.

Osborne, M. (2010) *GaAs solar cell from Spire sets 42.3% conversion efficiency record.*, *PV Tech*. Available at: http://www.pv-tech.org/news/gaas_solar_cell_from_spire_sets_42.3_conversion_effici (Accessed: 18 March 2016).

Osborne, M. (2014) *Siva Power claims 18.8% lab CIGS efficiency, PVTECH*.

Pachpande, smita G. and Prof. Zope, P. (2012) 'Studying The Effect of Shading on Solar Panel using MATLAB', *International Journal of Science and Applied Information Technology*, 1(2278), pp. 46–51.

Panasonic (2014) *solar cell achieves world's highest energy conversion efficiency*1 of 25.6%*2 at research level, Panasonic HIT_*. Available at: <http://panasonic.co.jp/corp/news/official.data/data.dir/> (Accessed: 18 March 2016).

Papageorgiou, N. (2013) *E´ cole Polytechnique Fe ´de ´rale De Lausanne News*.

PJM (2011) *About GATS*. Available at: <http://www.pjm-eis.com/gettingstarted/about-GATS.aspx> (Accessed: 18 March 2016).

Plugshare (no date) *PlugShare*.

Powalla, M. (2006) 'The R&D potential of CIS thin-film solar modules.', in *Proceedings of the 21st European photovoltaic solar energy conference*. Dresden, pp. 1789–1795.

Powalla, D; Bonnet, M. (2007) 'Thin film solar cells based on the polycrystalline compound semiconductors CIS and CdTe', *Advances in Optoelectronic*, pp. 1–6.

Rajka Budin (1995) 'investigation of solar declination', *Pergamon*, 7(3), p. 7.

Ramabadran, R; Mathur, B. (2009) 'Effect of Shading on series and parallel connected solar PV modules', *Modern Applied Science*, 3(10), pp. 32–41.

Razykov TM, R. B. and T. A. (2004) 'Special issue on thin Film PV.', *Solar Energy*, (77), pp. 665–666.

Razykov TM, Contreras-Puente G, Chornokur GC, et al. (2009) 'Structural, photoluminescent and electrical properties of CdTe films with different compositions fabricated by CMBD', *Solar Energy*, (83), pp. 90–93.

Razykov TM, Ferekides CS, Morel D, et al. (2011) 'olar photovoltaic electricity: Current status and future prospects.', *Solar Energy*, (85), pp. 1580–1608.

Repins I, Conteras M, Egaas B, et al. (2008) '19.9%-efficient ZnO/CdS/CuInGaSe₂ solar cell with 81.2% fill actor.', *Progress in Photovoltaics: Research and Application*, (16), pp. 235–239.

Research for an environmentally sound, reliable and affordable energy supply. (2011) *6th energy research programme of the federal government*. Available at: <http://www.bmwi.de/DE/Mediathek/pub> (Accessed: 18 March 2016).

Rugg, P. (2012) *Renewable Energy Planning guidance Note 2: The development of large scale (>50kW) solar PV arrays*. Available at: [http://www.solar-trade.org.uk/media/2 Large Scale Solar PV August 2012.pdf](http://www.solar-trade.org.uk/media/2_Large_Scale_Solar_PV_August_2012.pdf) (Accessed: 19 August 2014).

Saas, F. (2009) *A bright spot in a dark economy*. Available at: <http://www.pddnet.com/articles/2009/10/> (Accessed: 19 March 2016).

Sathyanarayana, P. et al. (2015) 'Effect of Shading on the Performance of Solar PV

Panel', 5, pp. 1–4. doi: 10.5923/c.ep.201501.01.

Satyen, K. (1998) 'Recent developments in high efficiency photovoltaic cells', *Renewable Energy*, (15), pp. 467–472.

Schock, F. P. H. W. (2011) 'Thin-film solar cells: past, present and future', *Renewable Energy World*, (4), pp. 75–87.

Schock, A; Shah, H. (1997) 'Proceedings of the 14th European PV solar energy conference', in. Barcelona, Spain.

Scottish Funding Council (2016) *impact and success of the programme of college mergers in Scotland*. Available at: www.sfc.ac.uk (Accessed: 1 November 2016).

Scottish Funding Council (2017) *College sector estates condition survey*.

Scottish Funding Council (2018) *College Innovation fund*. Available at: www.sfc.ac.uk (Accessed: 5 July 2018).

Scottish Government (2017a) 'The draft third report on policies and proposals 2017-2032', (January).

Scottish Government (2017b) 'The Scottish Greenhouse Gas Emissions Annual Target Report for 2015', (October).

Scottish Government (2018) 'Climate Change Plan 2018-2032', pp. 1–52.

SEIA (2015) *Net Metering*. Available at: <http://www.seia.org/policy/distributed-solar/net-metering> (Accessed: 18 March 2016).

Sharp (2011) *Sharp develops solar cell with world's highest conversion efficiency of 36.9%*. Available at: <http://sharp-world.com/corporate/news/111104.html> (Accessed: 19 March 2016).

Sherwani, a. F. and Usmani, J. a. (2010) 'Life cycle assessment of solar PV based electricity generation systems: A review', *Renewable and Sustainable Energy Reviews*, 14(1), pp. 540–544. doi: 10.1016/j.rser.2009.08.003.

Shi E, Zhang L, Li Z, et al. (2012) *TiO₂-coated carbon nanotube-silicon solar cells with efficiency of 15%.*, *PMC Scientific Report*. China.

Shockley, T ; Queisser, W. (1961) 'Detailed balance limit of efficiency of p–n junction solar cells', *Journal of Applied Physics*, 3(32), pp. 510–519.

Smit A (2005) 'The alternative technology movement: An analysis of its framing and negotiation of technology development.', *Research in Human Ecology Review*, (12), pp. 106–119.

Solangi KH, Islam MR, Saidur R, et al. (2011) 'A review on global solar energy policy', *Renewable and Sustainable Energy Reviews*, (15), pp. 2149–2163.

SolarBuzz (2015) *Module pricing*. Available at: <http://www.solarbuzz.com/facts-and-figures/retailprice-> (Accessed: 19 March 2016).

SSE (2013) *No Title*. Available at: <http://www.sse.co.uk/> (Accessed: 19 August 2014).

Streetman, S; Banerjee, B. (2005) *Solid State Electronic Devices*. 6th ed. Upper Saddle River, NJ: Prentice Hall.

Sun, Y. *et al.* (2014) 'Investigating the Impact of Shading Effect on the Characteristics of a Large-Scale Grid-Connected PV Power Plant in Northwest China', 2014.

SunPower Corporation (2015). Available at: <http://www.sunpowercorp.co.uk> (Accessed: 19 March 2016).

Sunshot Initiative (2014) *Tackling challenges in solar: 2014 portfolio*. Available at: <http://energy.gov/sites/> (Accessed: 19 March 2016).

Sweetnam T, Spataru C, Cliften B, *et al.* (2013) 'PV system performance and the potential impact of the green deal policy on market growth in London, UK', *Energy Procedia*, (42), pp. 347–356.

Takase, T; Suzuki, K. (2011) 'The Japanese energy sector: Current situation, and future paths', *Energy Policy*, (39), pp. 6731–6744.

Tax Credits, Rebates & Savings (2015). Available at: <http://energy.gov/savings/residential-renewableenergy-> (Accessed: 19 March 2016).

Team, G. (2008) *No Title*.

The Golden Sun of China (2015). Available at: http://www.pvgroup.org/events/ctr_031358 (Accessed: 20 March 2016).

The World Bank (2015) *Private participation in renewable energy database*.

Thornley B, Wood D, Grace K, *et al.* (2011) *Case study 13: National High-Tech R&D (863) Program*.

TM, B. (2002) 'General trends about photovoltaics based on crystalline silicon', *Solar Energy Materials and Solar Cells*, (72), pp. 3–10.

Twidell, T; Weir, J. (1986) *Renewable energy resources*. 2nd edn. London: Taylor & Francis.

Tyag VV, Rahim Nurul AA, Rahim NA, *et al.* (2013) 'Progress in solar PV technology: Research and achievement', *Renewable and Sustainable Energy Reviews*, (20), pp. 443–461.

UKERC (2015). Available at: <http://ukerc.rl.ac.uk> (Accessed: 20 March 2016).

United Nations (1998) 'KYOTO PROTOCOL TO THE UNITED NATIONS FRAMEWORK KYOTO PROTOCOL TO THE UNITED NATIONS FRAMEWORK.'

United Nations (2015) 'Paris agreement.'

Upadhayaya HM, Razykov TM, Tiwari A, *et al.* (2007) 'Photovoltaics fundamentals, technology and application.', in *Goswami DY and Kreith F (eds) Handbook of Energy Efficiency and Renewable Energy*. New York: CRC Press, pp. 23–1–23–63.

US Department of Energy's Programme (2015) *Solar Powering America Home*.

US Energy Information Administration (2015) *Electric power annual—U.S. electric industry residential average retail price of electricity by state*. Available at: <http://www.eia.gov/cneaf/electricity/epa/> (Accessed: 20 March 2016).

Verbruggen, A. (2004) 'Tradable green certificates in Flanders (Belgium).', *Energy Policy*, (32), pp. 165–176.

Walsh, J., Muneer, T., & Celik, A. (2011) 'Design and analysis of kinetic energy recovery system for automobiles: Case study for commuters in Edinburgh.', *Journal of Renewable and Sustainable Energy*, 3(1).

Weiss, C. et al. (2014) 'Capturing the Usage of the German Car Fleet for a One Year Period to Evaluate the Suitability of Battery Electric Vehicles - A Model based Approach', *Transportation Research Procedia*. Elsevier B.V., 1(1), pp. 133–141. doi: 10.1016/j.trpro.2014.07.014.

Wesoff, E. (2013) *Sharp hits record 44.4% efficiency for triple-junction solar cell*, *GreentechSolar*. Available at: <http://www.greentechmedia.com/articles/read/Sharp-Hits-Record-44.4-Efficiency-> (Accessed: 20 March 2016).

Wigmore GS, L. S. and R. J. (2012) *China: China policy: Shedding light on the recently enacted solar feed-in-tariff*. Available at: <http://www.mondaq.com/x/159390/Renewables/ChinaPolicy> (Accessed: 20 March 2016).

Wiser R, B. G. and H. E. (2010) *Supporting solar power in renewables portfolio standards: Experience from the United States. Prepared for the: US Department of Energy Office of Energy Efficiency and Renewable Energy Office of Electricity Delivery and Energy Reliability and the National*. Available at: <http://eetd.lbl.gov/ea/ems/> (Accessed: 20 March 2016).

Wolfe, G; Conibeer, J. (1998) 'The scholar programme for photovoltaics in the U.K.', *Renewable Energy*, (15), pp. 598–601.

World, E. (2015) *Renewable Energy: What Does 2015 Holds for Bioenergy in the UK?* London.

Wu L, T. W. and J. X. (2005) 'Silicon based solar cell system with a hybrid PV module', *Solar Energy Materials and Solar Cells*, (87), pp. 637–645.

Wu X, Keane JC, DeHart C, et al. (2001) '16.5% efficient CdS/CdTe polycrystalline thin film solar cell.', in *Proceedings of the 17th European photovoltaic solar energy conference, Munich, 14–17 October 2001*. Munich, pp. 995–999.

Xu H, Charlie D, Wang S, et al. (2011) *Co-Operation programme on photovoltaic power system., National survey report on China*. IEA. Available at: <http://www.iea-pvps.org/> (Accessed: 20 March 2016).

- Y, Z. S. and H. (2013) 'Analysis on the development and policy of solar PV power in China. Analysis on the development and policy of solar PV power in China.', *Renewable and Sustainable Energy Reviews*, (21), pp. 393–401.
- Yablonovitch E, M. O. and K. S. (2012) 'The opto-electronic physics that broke the efficiency limit in solar cells.', in *38th IEEE photovoltaic specialists conference (PVSC), IEEE, Austin, TX, 3–8 June 2012*, pp. 001556–001559.
- Yamaguchi M, Nishimura K, Sasaki T, et al. (2008) 'Novel materials for high-efficiency III–V multijunction solar cells.', *Solar Energy*, (82), pp. 173–180.
- Yamaguchi M, Takamoto T, Arak K, et al. (2005) 'Multi-junction III–V solar cells: current status and future potential.', *Solar Energy*, (79), pp. 78–85.
- Yamamoto K, Nakajima A, Yoshimi M, et al. (2004) 'A high efficiency thin film silicon solar cell and module.', *Solar Energy*, (77), pp. 939–949.
- Yamamoto K, Yoshimi M, Tawada Y, et al. (2001) 'Cost effective and high performance thin film Si solar cells towards the 21 century.', *Solar Energy Materials and Solar Cells*, (66), pp. 117–125.
- Zeng, Liyue; Lu, Jung; Li, Wuyan; Li, Y. (2018) 'A fast approach for large-scale Sky View Factor estimation using street view images', *Buildings and Environment*, 135, pp. 74–84.
- Zhang S, Zhao X, Andrew-Speed P, et al. (2013) 'The development trajectories of wind power and solar PV power in China: A comparison and policy recommendations.', *Renewable and Sustainable Energy Reviews*, (26), pp. 322–331.
- Zhao J, W. A. and G. M. (2011) 'High-efficiency PERL and PERT silicon solar cells on FZ and MCZ substrates', *Solar Energy Materials and Solar Cells*, (65), pp. 429–435.
- Zhao J, Wang A, Green MA, et al. (1998) '19.8% efficient "honeycomb" textured multicrystalline and 24.4% monocrystalline silicon solar cells.', *Applied Physics Letters*, (73), pp. 1991–1993.
- Zipp, K. (2011) *Solar power world. Hybrid solar panel generates more power.*

Appendices

Appendix A: Data Tables

Logger Details:					Logger Details:									
Logger Type	1F8				Logger Type	1F8								
Serial Number	KS0718014				Serial Number	KS0805005								
Controller Firmware	4.3				Controller Firmware	4.3								
Acquisition Firmware	4.3				Acquisition Firmware	4.3								
Logger ID	Logger ID				Logger ID	Logger ID								
Job Details					Job Details									
Number of Analogue Channel	4				Number of Analogue Channel	8								
Number of Digital Channels	0				Number of Digital Channels	0								
Total Number of Channels Us	4				Total Number of Channels Us	8								
Arm Time	28/05/2013 14:33				Arm Time	28/05/2013 14:34								
Disarm Time	28/05/2013 15:31				Disarm Time	28/05/2013 15:32								
Duration	00:58:01				Duration	00:57:51								
Job Description	Job Description				Job Description	Job Description								
Channel Info					Channel Info									
Description	flux1 (V)	flux2 (V)	flux3 (V)	flux4 (V)	Description	p1 (V)	p2 (V)	p3 (V)	t1 (°C)	t2 (°C)	t3 (°C)	t4 (°C)		
Sample Interval	00:10:00	00:10:00	00:10:00	00:10:00	Sample Interval	00:10:00	00:10:00	00:10:00	00:10:00	00:10:00	00:10:00	00:10:00		
Logging Interval	00:10:00	00:10:00	00:10:00	00:10:00	Logging Interval	00:10:00	00:10:00	00:10:00	00:10:00	00:10:00	00:10:00	00:10:00		
Date/Time	Type	flux1 (V)	flux2 (V)	flux3 (V)	flux4 (V)	Date/Time	Type	p1 (V)	p2 (V)	p3 (V)	t1 (°C)	t2 (°C)	t3 (°C)	t4 (°C)
28/05/2013 14:33	Interval	-0.006243	-0.00165	-0.005411	-0.00084	28/05/2013 14:34	Interval	0.002462	0.002866	0.003097	27.9	27.9	27.9	13.2
28/05/2013 14:43	Interval	-0.007673	-0.006999	-0.006168	-0.005346	28/05/2013 14:44	Interval	0.002152	0.002411	0.002602	28.4	28.7	28.4	16.4
28/05/2013 14:53	Interval	-0.006314	-0.007831	-0.004735	-0.006584	28/05/2013 14:54	Interval	0.002312	0.002651	0.002864	30.2	29.9	29.9	16.9
28/05/2013 15:03	Interval	-0.00429	-0.007902	-0.003794	-0.006589	28/05/2013 15:04	Interval	0.001404	0.001478	0.001602	26.5	26.1	17.2	17.2
28/05/2013 15:13	Interval	-0.00297	-0.007902	-0.002632	-0.006587	28/05/2013 15:14	Interval	0.001398	0.001525	0.001653	24.8	24.2	16.9	17
28/05/2013 15:23	Interval	-0.002285	-0.008076	-0.001919	-0.00759	28/05/2013 15:24	Interval	0.001043	0.001103	0.001193	20.5	21.1	15.7	15.7
Arm Time	28/05/2013 15:38				Arm Time	28/05/2013 15:39								
Disarm Time	30/05/2013 14:35				Disarm Time	30/05/2013 14:36								
Duration	1 day 22:57:02				Duration	1 day 22:57:04								
Job Description	Job Description				Job Description	Job Description								
Channel Info					Channel Info									
Description	flux1 (V)	flux2 (V)	flux3 (V)	flux4 (V)	Description	p1 (V)	p2 (V)	p3 (V)	t1 (°C)	t2 (°C)	t3 (°C)	t4 (°C)		
Sample Interval	00:10:00	00:10:00	00:10:00	00:10:00	Sample Interval	00:10:00	00:10:00	00:10:00	00:10:00	00:10:00	00:10:00	00:10:00		
Logging Interval	00:10:00	00:10:00	00:10:00	00:10:00	Logging Interval	00:10:00	00:10:00	00:10:00	00:10:00	00:10:00	00:10:00	00:10:00		
Date/Time	Type	flux1 (V)	flux2 (V)	flux3 (V)	flux4 (V)	Date/Time	Type	p1 (V)	p2 (V)	p3 (V)	t1 (°C)	t2 (°C)	t3 (°C)	t4 (°C)
28/05/2013 15:38	Interval	-0.002865	-0.007589	-0.002534	-0.006987	28/05/2013 15:39	Interval	0.001065	0.001114	0.001249	19.3	20.2	14.5	14.5
28/05/2013 15:48	Interval	-0.002602	-0.008097	-0.00208	-0.006951	28/05/2013 15:49	Interval	0.002545	0.002995	0.003305	20.6	21.1	15.2	15.2
28/05/2013 15:58	Interval	-0.002584	-0.008041	-0.002291	-0.005886	28/05/2013 15:59	Interval	0.001049	0.001177	0.001288	19.5	19.9	14.2	14.3
28/05/2013 16:08	Interval	-0.002874	-0.007848	-0.002121	-0.006126	28/05/2013 16:09	Interval	0.001742	0.002091	0.00235	20.3	20.3	14.4	14.4
28/05/2013 16:18	Interval	-0.005811	-0.007478	-0.004632	-0.005319	28/05/2013 16:19	Interval	0.001471	0.001604	0.00182	22.2	22.5	14.7	14.6
28/05/2013 16:28	Interval	-0.002895	-0.007567	-0.002313	-0.005556	28/05/2013 16:29	Interval	0.001441	0.001425	0.001618	19.9	20.6	14.7	14.7
28/05/2013 16:38	Interval	-0.001279	-0.007666	-0.001262	-0.005395	28/05/2013 16:39	Interval	0.000781	0.000761	0.000827	17.1	17.3	13.9	13.9
28/05/2013 16:48	Interval	-0.001857	-0.00793	-0.00128	-0.006724	28/05/2013 16:49	Interval	0.001074	0.001065	0.001173	17.2	17.4	14	14
28/05/2013 16:58	Interval	-0.00302	-0.008001	-0.002161	-0.006842	28/05/2013 16:59	Interval	0.001404	0.001493	0.001675	17.9	18.1	14	14
28/05/2013 17:08	Interval	-0.003447	-0.007937	-0.002806	-0.005705	28/05/2013 17:09	Interval	0.002322	0.002639	0.003017	19.1	19.5	13.2	13.2
28/05/2013 17:18	Interval	-0.002615	-0.007402	-0.002193	-0.005677	28/05/2013 17:19	Interval	0.001699	0.001949	0.002144	19.6	19.8	14	14
28/05/2013 17:28	Interval	-0.002965	-0.007406	-0.00274	-0.005513	28/05/2013 17:29	Interval	0.001029	0.001217	0.001301	18.7	19.2	13.5	13.4
28/05/2013 17:38	Interval	-0.005356	-0.007734	-0.003839	-0.006712	28/05/2013 17:39	Interval	0.001239	0.001075	0.001475	21.3	21.7	13.2	13.3
28/05/2013 17:48	Interval	-0.003197	-0.007854	-0.002403	-0.006941	28/05/2013 17:49	Interval	0.001632	0.001116	0.002105	21.5	21.5	15.1	15
28/05/2013 17:58	Interval	-0.003817	-0.007805	-0.003327	-0.006746	28/05/2013 17:59	Interval	0.001405	0.00136	0.001699	22.2	21.9	15.8	15.8
28/05/2013 18:08	Interval	-0.00226	-0.007707	-0.002149	-0.005688	28/05/2013 18:09	Interval	0.000799	0.000852	0.000935	20.3	20.5	15.7	15.7
28/05/2013 18:18	Interval	-0.001821	-0.007589	-0.00147	-0.005726	28/05/2013 18:19	Interval	0.000533	0.00054	0.000593	18.5	18.5	15.5	15.5
28/05/2013 18:28	Interval	-0.000752	-0.007383	-0.000604	-0.005716	28/05/2013 18:29	Interval	0.000213	0.00023	0.000219	16.1	16.1	15.1	15.1
28/05/2013 18:38	Interval	-0.000407	-0.007929	-0.000391	-0.005953	28/05/2013 18:39	Interval	0.000294	0.000328	0.000346	15.5	15.4	14.8	14.8
28/05/2013 18:48	Interval	-0.000762	-0.007857	-0.000655	-0.006539	28/05/2013 18:49	Interval	0.000482	0.000546	0.000584	16.1	16.1	14.8	14.8
28/05/2013 18:58	Interval	-0.00112	-0.007755	-0.00087	-0.005859	28/05/2013 18:59	Interval	0.00049	0.000535	0.000571	16.3	16.3	14.7	14.6
28/05/2013 19:08	Interval	-0.000883	-0.007825	-0.000768	-0.00688	28/05/2013 19:09	Interval	0.000431	0.000484	0.000523	16.1	16.1	14.5	14.5
28/05/2013 19:18	Interval	-0.000655	-0.007739	-0.000603	-0.005739	28/05/2013 19:19	Interval	0.00042	0.000483	0.000519	15.8	15.8	14.4	14.4
28/05/2013 19:28	Interval	-0.00077	-0.007846	-0.000654	-0.005797	28/05/2013 19:29	Interval	0.000399	0.000427	0.000459	15.3	15.3	14.2	14.2
28/05/2013 19:38	Interval	-0.000494	-0.007308	-0.000438	-0.006591	28/05/2013 19:39	Interval	0.000431	0.000449	0.000491	14.9	14.8	14.1	14.1
28/05/2013 19:48	Interval	-0.000279	-0.007767	-0.000249	-0.005616	28/05/2013 19:49	Interval	0.000484	0.000432	0.000521	14.6	14.6	14.1	14.1
28/05/2013 19:58	Interval	-0.000174	-0.007628	-0.00014	-0.005722	28/05/2013 19:59	Interval	0.000468	0.000401	0.00049	14.4	14.4	13.7	13.8
28/05/2013 20:08	Interval	-0.000309	-0.007604	-0.000213	-0.006697	28/05/2013 20:09	Interval	0.000342	0.000313	0.000374	14.1	14.1	13.5	13.5
28/05/2013 20:18	Interval	-0.000077	-0.007486	-0.000067	-0.005463	28/05/2013 20:19	Interval	0.000234	0.000214	0.000233	13.3	13.3	12.9	12.9
28/05/2013 20:28	Interval	0.000193	-0.007788	0.00013	-0.00657	28/05/2013 20:29	Interval	0.000197	0.000182	0.000201	12.3	12.4	12.8	12.8
28/05/2013 20:38	Interval	-0.000228	-0.007973	-0.000229	-0.006847	28/05/2013 20:39	Interval	0.000126	0.000134	0.000141	11.1	11.1	10.7	10.7
28/05/2013 20:48	Interval	-0.000005	-0.007688	-0.000027	-0.006561	28/05/2013 20:49	Interval	0.000104	0.000109	0.000116	10.6	10.5	10.4	10.4
28/05/2013 20:58	Interval	0.000481	-0.005462	0.00036	-0.003096	28/05/2013 20:59	Interval	0.000126	0.000046	0.000042	10.9	10.9	10.5	10.5
28/05/2013 21:08	Interval	0.000568	-0.007832	0.000443	-0.005702	28/05/2013 21:09	Interval	0.000063	0.000061	0.000047	9.8	9.7	10.5	10.5
28/05/2013 21:18	Interval	0.000767	-0.007044	0.000568	-0.006157	28/05/2013 21:19	Interval	0.000044	0.000018	0.000012	9.4	9.3	10.5	10.4
28/05/2013 21:28	Interval	0.000903	-0.008322	0.000798	-0.006562	28/05/2013 21:29	Interval	0.000019	0.000031	-0.000009	8.6	8.5	10.3	10.3
28/05/2013 21:38	Interval	0.001137	-0.007604	0.001154	-0.005826	28/05/2013 21:39	Interval	0.000009	-0.000004	-0.000002	7.7	7.7	10	10
28/05/2013 21:48	Interval	0.001249	-0.007644	0.001066	-0.006762	28/05/2013 21:49	Interval	-0.000002	-0.000019	-0.00001	7.2	7.1	9.6	9.5
28/05/2013 21:58	Interval	0.001333	-0.007459	0.000981	-0.006421	28/05/2013 21:59	Interval	-0.000006	-0.000019	-0.00002	6.8	6.7	9.3	9.3
28/05/2013 22:08	Interval	0.001158	-0.007063	0.000938	-0.00619	28/05/2013 22:09	Interval	-0.000024	-0.000022	-0.000027	6.5	6.4	9	9
28/05/2013 22:18	Interval	0.001319	-0.006998	0.001079	-0.005147	28/05/2013 22:19	Interval	-0.000021	-0.000021	-0.000025	6.5	6.4	8.7	8.7
28/05/2013 22:28	Interval	0.001456	-0.007											

Heat Loss		Irradiance		Temperature		Average Heat Loss		Solar Power/Cell		Solar Power/Module									
Date/Time	Type	flux1 (W/m2)	flux2 (W/m2)	flux3 (W/m2)	flux4 (W/m2)	p1 (W/m2)	p2 (W/m2)	p3 (W/m2)	t1 (°C)	t2 (°C)	t3 (°C)	t4 (°C)	Average Irradiance W/m2	Average Heat Loss W/m2	Air Temp °C	Cell Temp °C	Average Heat Loss W/m2	Solar Power/Cell W	Solar Power/Module W
28/05/2013 14:34	Interval	136.05	117.63	106.90	95.64680.8	456.6	468.8	28.4	28.7	16.5	16.4	16.5	16.5	16.45	121.47	462.728.55	102.23	13.39	883.7
28/05/2013 14:44	Interval	111.95	131.61	82.06	117.78	495.1	502.1	30.2	29.9	16.9	16.8	16.8	16.85	16.85	97.01	469.130.05	97.01	11.26	675.7
28/05/2013 14:54	Interval	76.06	132.81	65.75	117.87	300.6	279.9	288.6	26.5	26.1	17.2	17.2	17.2	17.2	70.91	284.3	70.91	12.39	743.3
28/05/2013 15:04	Interval	52.66	132.81	45.62	117.84	299.4	288.8	297.8	24.8	24.2	16.9	17	17	17.2	49.14	293.3	49.14	6.92	415.1
28/05/2013 15:14	Interval	40.51	135.73	33.26	135.73	223.3	208.9	215.0	20.5	21.1	15.7	15.7	15.7	15.7	36.89	211.9	36.89	7.14	428.3
28/05/2013 15:24	Interval													15.7	36.89		15.7	5.16	309.4
28/05/2013 15:39	Interval	50.80	127.55	43.92	124.99	228.1	211.0	225.0	19.3	20.2	14.5	14.5	14.5	14.5	47.36	218.019.75	47.36	5.31	318.3
28/05/2013 15:49	Interval	46.13	136.08	36.05	124.95	545.0	567.2	595.5	20.6	21.1	15.2	15.2	15.2	15.2	41.09	581.420.85	41.09	14.15	848.5
28/05/2013 15:59	Interval	45.82	135.14	39.71	105.30	224.6	222.0	232.1	19.5	19.9	14.2	14.3	14.3	14.3	42.76	207.5	42.76	5.54	332.2
28/05/2013 16:09	Interval	50.96	131.90	36.76	109.59	373.0	396.0	423.4	20.2	20.3	14.4	14.4	14.4	14.4	43.86	409.720.15	43.86	9.97	598.3
28/05/2013 16:19	Interval	103.03	125.68	80.28	95.15315.0	303.8	327.9	327.9	22.2	21.9	14.6	14.6	14.6	14.65	91.65	315.922.25	91.65	7.66	461.2
28/05/2013 16:29	Interval	51.33	127.18	40.09	95.35308.6	269.9	291.5	291.5	19.9	20.6	14.7	14.7	14.7	14.7	45.71	280.720.25	45.71	6.83	409.6
28/05/2013 16:39	Interval	22.68	128.84	21.87	96.5167.2	144.1	149.0	149.0	17.7	17.3	13.9	13.9	13.9	13.9	22.27	146.617.15	22.27	3.57	214.0
28/05/2013 16:49	Interval	32.99	133.28	22.18	120.29	300.0	201.7	211.4	17.2	17.4	14	14	14	14	27.55	206.5	27.55	5.03	301.6
28/05/2013 16:59	Interval	53.55	134.47	37.45	122.40	300.6	282.8	301.8	17.9	18.1	14	14	14	14	45.50	292.3	45.50	7.11	426.8
28/05/2013 17:09	Interval	61.12	138.39	48.63	102.06	497.2	499.8	543.6	19.1	19.5	13.2	13.2	13.2	13.2	54.87	521.7	54.87	12.70	761.8
28/05/2013 17:19	Interval	46.37	124.40	38.01	101.56	368.8	369.1	386.3	19.6	19.8	14	14	14	14	42.19	377.7	42.19	9.19	551.5
28/05/2013 17:29	Interval	52.57	124.47	47.49	98.62220.3	230.5	234.4	234.4	18.7	19.2	13.5	13.4	13.4	13.4	50.03	232.518.95	50.03	5.66	339.4
28/05/2013 17:39	Interval	94.96	129.98	66.53	120.07	265.3	265.8	265.8	21.3	21.7	13.2	13.3	13.3	13.3	80.75	230.5	80.75	5.61	336.6
28/05/2013 17:49	Interval	56.68	132.00	41.65	124.17	349.5	211.4	379.3	21.5	21.5	15.1	15.1	15	15	49.17	379.3	49.17	9.23	553.8
28/05/2013 17:59	Interval	67.68	131.18	57.66	120.68	300.9	257.6	306.1	22.2	21.9	15.8	15.8	15.8	15.8	62.67	281.922.05	62.67	6.86	411.5
28/05/2013 18:09	Interval	40.07	129.53	37.24	101.75	171.1	161.4	168.5	20.3	20.3	15.7	15.7	15.7	15.7	38.66	164.920.15	38.66	4.01	240.6
28/05/2013 18:19	Interval	32.29	127.55	25.48	102.43	102.3	102.3	106.8	18.5	18.5	15.5	15.5	15.5	15.5	28.88	104.6	28.88	2.54	152.7
28/05/2013 18:29	Interval	13.33	124.08	10.47	102.25	45.6	38.4	39.5	16.1	16.1	15.14	15.14	15.14	15.14	11.90	16.114.95	11.90	0.95	56.5
28/05/2013 18:39	Interval	7.22133.26			6.78106.49	63.0	62.1	62.3	15.5	15.4	14.8	14.8	14.8	14.8	7.00	62.215.45	7.00	1.51	90.5
28/05/2013 18:49	Interval	13.51	132.05	11.35	116.98	103.2	103.4	105.2	16.3	16.3	14.8	14.8	14.8	14.8	12.43	104.315.95	12.43	2.54	152.3
28/05/2013 18:59	Interval	19.86	130.34	15.08	104.81	104.9	101.3	102.9	16.3	16.3	14.7	14.6	14.6	14.6	17.47	102.1	17.47	2.48	149.1
28/05/2013 19:09	Interval	15.66	131.51	13.31	123.08	92.3	91.7	94.2	16.1	16.1	14.5	14.5	14.5	14.5	2.26	93.0	2.26	2.48	135.7
28/05/2013 19:19	Interval	11.61	130.07	10.45	102.67	89.9	91.5	93.5	15.8	15.8	14.4	14.4	14.4	14.4	11.03	92.5	11.03	2.25	135.1
28/05/2013 19:29	Interval	13.65	131.87	11.33	103.70	85.4	80.9	82.7	15.3	15.3	14.2	14.2	14.2	14.2	12.49	81.8	12.49	1.99	119.4
28/05/2013 19:39	Interval	8.76122.82			7.59117.91	92.3	85.0	88.5	14.9	14.8	14.1	14.1	14.1	14.1	8.17	86.814.85	8.17	2.11	126.7
28/05/2013 19:49	Interval	4.95130.54			4.32100.47	103.6	81.8	93.9	14.6	14.6	14.13	14.13	14.13	14.13	4.63	87.8	4.63	2.14	128.3
28/05/2013 19:59	Interval	3.05128.20			2.43102.36	100.2	75.9	88.3	14.4	14.4	13.7	13.8	13.8	13.8	2.76	82.1	2.76	2.00	119.5
28/05/2013 20:09	Interval	5.48127.80			3.69119.80	73.2	59.3	67.4	14.1	14.1	13.5	13.5	13.5	13.5	4.59	63.3	4.59	1.54	92.5
28/05/2013 20:19	Interval	1.37125.82			1.16	97.7550.1	40.5	42.0	13.3	13.3	12.9	12.9	12.9	12.9	1.26	41.3	1.26	1.00	60.2
28/05/2013 20:29	Interval	-3.42	130.89	-2.25	117.53	42.2	34.5	36.2	12.3	12.4	12.8	12.8	12.8	12.8	-2.84	35.312.95	-2.84	0.86	51.6
28/05/2013 20:39	Interval	0.05129.21			3.57122.49	27.0	25.4	25.4	11.1	11.1	10.7	10.7	10.7	10.7	0.62	25.4	0.62	10.7	37.1
28/05/2013 20:49	Interval	-8.53	91.80	-6.24	0.47117.37	22.3	20.6	20.9	10.6	10.5	10.4	10.4	10.4	10.4	0.28	20.810.55	0.28	0.51	30.3
28/05/2013 20:59	Interval	-10.07	131.63	-7.68	102.00	13.5	11.6	11.6	7.6	7.6	10.9	10.5	10.5	10.5	-7.38	8.1	-7.38	0.20	11.8
28/05/2013 21:09	Interval	-13.60	118.39	-9.84	110.14	9.4	3.4	3.4	2.29	9.3	10.5	10.4	10.4	10.4	-8.87	10.0	-8.87	0.24	14.6
28/05/2013 21:19	Interval	-16.01	139.87	-13.83	117.39	4.1	5.9	-1.68	8.5	10.3	10.3	10.3	10.3	10.3	-11.72	2.8	-11.72	0.07	4.1
28/05/2013 21:29	Interval	-20.16	127.80	-20.00	104.22	1.9	-0.8	-3.67	7.7	7.7	7.7	7.7	7.7	7.7	-20.08	-2.2	-20.08	-0.05	3.1
28/05/2013 21:39	Interval	-22.15	128.47	-18.47	120.97	-4.3	-3.6	-1.87	7.1	9.6	9.5	9.5	9.5	9.5	-20.31	-1.8	-20.31	-0.04	-2.6
28/05/2013 21:49	Interval	-23.63	125.36	-17.00	114.87	-1.3	-3.6	-3.66	6.7	9.3	9.3	9.3	9.3	9.3	-20.32	-3.6	-20.32	-0.09	-5.3
28/05/2013 21:59	Interval	-20.53	118.71	-16.26	110.73	-5.1	-4.2	-4.56	6.4	9	9	9	9	9	-18.99	-4.9	-18.99	-0.12	-7.1
28/05/2013 22:09	Interval	-23.39	117.61	-18.70	92.08	-4.5	-4.0	-4.56	6.4	8.7	8.7	8.7	8.7	8.7	-21.04	-4.5	-21.04	-0.11	-6.6
28/05/2013 22:19	Interval	-25.82	119.43	-22.55	100.59	-4.7	-4.4	-5.26	6.2	8.5	8.5	8.5	8.5	8.5	-24.18	-5.2	-24.18	-0.13	-7.6
28/05/2013 22:29	Interval	-20.52	118.86	-17.37	100.00	-5.1	-4.5	-5.85	5.6	8.2	8.1	8.1	8.1	8.1	-19.14	-5.8	-19.14	-0.14	-8.4
28/05/2013 22:39	Interval	-20.57	118.49	-16.83	99.36	-5.1	-4.2	-4.56	5.7	8.1	8.1	8.1	8.1	8.1	-18.70	-5.4	-18.70	-0.13	-7.5
28/05/2013 22:49	Interval	-22.48	117.85	-18.41	98.71	-5.1	-4.2	-4.56	5.6	7.9	7.9	7.9	7.9	7.9	-20.44	-5.4	-20.44	-0.13	-7.5
28/05/2013 22:59	Interval	-23.35	117.36	-15.98	98.16	-4.3	-4.0	-4.55	5.6	7.9	7.8	7.8	7.8	7.8	-19.67	-4.9	-19.67	-0.12	-7.1
28/05/2013 23:09	Interval	-24.15	116.79	-18.25	97.58	-4.9	-4.2	-5.65	5.3	7.5	7.5	7.5	7.5	7.5	-21.20	-5.6	-21.20	-0.14	-8.2
28/05/2013 23:19	Interval	-23.72	116.37	-19.08	97.10	-4.3	-3.8	-4.55	5.3	7.5	7.5	7.5	7.5	7.5	-21.40	-4.7	-21.40	-0.14	-8.2
28/05/2013 23:29	Interval	-18.72	116.10	-15.18	96.69	-4.1	-4.0	-4.75	5.4	7.2	7.1	7.1	7.1	7.1	-16.95	-4.7	-16.95	-0.11	-6.8

Date/Time (GMT)	Centre of time period (GMT)	LCT hrs	EoI hrs	DEC deg	AST hrs	ASTI deg	SOLAIT deg	SOIAZM deg	ERAD W/m2	Global Horizontal Irr. Kt W/m2	Summer Diffuse June Diffuse		Muneer Diffuse		
											W/m2	W/m2	W/m2	W/m2	
28/05/2013 14:34:35	28/05/2013 13:29:35	13.493	0.0449	21.54	13.33	13:19:58	52.59	211.56	1056.1	527.20.499	366.0366.7	338.5			
28/05/2013 14:44:35	28/05/2013 13:39:35	13.660	0.0449	21.54	13.50	13:29:57	51.82	215.14	1045.2	460.80.441	359.1359.7	344.2			
28/05/2013 14:54:35	28/05/2013 13:49:35	13.826	0.0448	21.54	13.67	13:39:57	50.98	218.61	1033.0	495.10.479	358.3359.0	336.4			
28/05/2013 15:04:35	28/05/2013 13:59:35	13.993	0.0448	21.54	13.83	13:49:57	50.07	221.98	1019.6	300.60.295	286.4286.9	275.7			
28/05/2013 15:14:35	28/05/2013 14:09:35	14.160	0.0448	21.54	14.00	13:59:57	49.10	225.24	1005.1	299.40.298	284.4284.8	277.8			
28/05/2013 15:24:35	28/05/2013 14:19:35	14.326	0.0448	21.55	14.17	14:09:57	48.08	228.40	989.4	223.30.226	223.3223.5	217.1			
28/05/2013 15:39:23	28/05/2013 14:34:23	14.573	0.0448	21.55	14.41	14:24:45	46.48	232.89	964.2	228.10.237	228.1227.0	220.6			
28/05/2013 15:49:23	28/05/2013 14:44:23	14.740	0.0448	21.55	14.58	14:34:45	45.34	235.81	945.8	545.00.576	315.7316.4	267.2			
28/05/2013 15:59:23	28/05/2013 14:54:23	14.906	0.0447	21.55	14.75	14:44:45	44.16	238.63	926.4	224.60.242	224.6222.9	216.6			
28/05/2013 16:09:23	28/05/2013 15:04:23	15.073	0.0447	21.55	14.91	14:54:45	42.95	241.37	906.0	373.00.412	305.8306.3	296.0			
28/05/2013 16:19:23	28/05/2013 15:14:23	15.240	0.0447	21.55	15.08	15:04:45	41.70	244.02	884.6	315.00.356	280.3280.7	273.8			
28/05/2013 16:29:23	28/05/2013 15:24:23	15.406	0.0447	21.55	15.25	15:14:45	40.43	246.60	862.3	308.60.358	273.9274.4	267.6			
28/05/2013 16:39:23	28/05/2013 15:34:23	15.573	0.0447	21.55	15.41	15:24:45	39.13	249.11	839.2	167.20.199	167.2163.9	164.1			
28/05/2013 16:49:23	28/05/2013 15:44:23	15.740	0.0447	21.56	15.58	15:34:45	37.81	251.56	815.2	230.00.282	221.5221.9	216.2			
28/05/2013 16:59:23	28/05/2013 15:54:23	15.906	0.0447	21.56	15.75	15:44:45	36.48	253.94	790.5	300.60.380	258.7259.1	252.1			
28/05/2013 17:09:23	28/05/2013 16:04:23	16.073	0.0446	21.56	15.91	15:54:45	35.12	256.27	765.0	497.20.650	236.7237.1	173.9			
28/05/2013 17:19:23	28/05/2013 16:14:23	16.240	0.0446	21.56	16.08	16:04:45	33.75	258.55	738.8	363.80.492	256.2256.7	238.3			
28/05/2013 17:29:23	28/05/2013 16:24:23	16.406	0.0446	21.56	16.25	16:14:45	32.38	260.79	712.0	220.30.309	207.0207.3	202.3			
28/05/2013 17:39:23	28/05/2013 16:34:23	16.573	0.0446	21.56	16.41	16:24:44	29.60	265.14	656.7	265.30.388	225.9226.3	219.9			
28/05/2013 17:49:23	28/05/2013 16:44:23	16.740	0.0446	21.56	16.58	16:34:44	28.20	267.26	628.3	349.50.532	225.4225.8	202.0			
28/05/2013 17:59:23	28/05/2013 16:54:23	16.906	0.0446	21.56	16.75	16:44:44	26.80	269.35	599.4	300.90.479	217.9218.3	204.6			
28/05/2013 18:09:23	28/05/2013 17:04:23	17.073	0.0445	21.57	17.08	16:54:44	25.40	271.42	570.2	171.10.285	164.3164.6	160.4			
28/05/2013 18:19:23	28/05/2013 17:14:23	17.240	0.0445	21.57	17.25	17:04:44	24.00	273.46	540.7	114.10.200	114.1115.3	112.0			
28/05/2013 18:29:23	28/05/2013 17:24:23	17.406	0.0445	21.57	17.41	17:14:44	22.60	275.48	510.9	45.60.084	45.6	44.7	45.4		
28/05/2013 18:39:23	28/05/2013 17:34:23	17.573	0.0445	21.57	17.58	17:24:44	21.21	277.49	481.0	63.00.123	63.0	61.7	62.5		
28/05/2013 18:49:23	28/05/2013 17:44:23	17.740	0.0445	21.57	17.75	17:34:44	19.82	279.48	450.8	103.20.215	103.2103.8	100.8			
28/05/2013 18:59:23	28/05/2013 17:54:23	17.906	0.0445	21.57	17.91	17:44:44	18.44	281.46	420.6	104.90.233	104.9104.7	101.7			
28/05/2013 19:09:23	28/05/2013 18:04:23	18.073	0.0444	21.57	18.08	17:54:44	17.07	283.44	390.4	92.30.219	92.3	92.6	89.9		
28/05/2013 19:19:23	28/05/2013 18:14:23	18.240	0.0444	21.57	18.25	18:04:44	15.72	285.40	360.2	89.90.230	89.9	89.8	87.2		
28/05/2013 19:29:23	28/05/2013 18:24:23	18.406	0.0444	21.57	18.41	18:14:44	14.37	287.37	330.1	85.40.237	85.4	85.0	82.6		
28/05/2013 19:39:23	28/05/2013 18:34:23	18.573	0.0444	21.57	18.58	18:24:44	13.04	289.33	300.1	82.30.280	82.3	82.2	82.6		
28/05/2013 19:49:23	28/05/2013 18:44:23	18.740	0.0444	21.58	18.75	18:34:44	11.73	291.29	270.3	92.30.280	92.3	89.2	86.9		
28/05/2013 19:59:23	28/05/2013 18:54:23	18.906	0.0444	21.58	18.91	18:44:44	10.43	293.26	240.8	103.60.345	93.5	93.6	91.4		
28/05/2013 20:09:23	28/05/2013 19:04:23	19.073	0.0444	21.58	18.91	18:54:44	9.14	295.23	211.5	100.20.371	87.4	87.6	85.3		
28/05/2013 20:19:23	28/05/2013 19:14:23	19.240	0.0444	21.58	19.08	19:04:44	7.84	297.21	182.0	73.20.304	69.1	69.3	67.6		
28/05/2013 20:29:23	28/05/2013 19:24:23	19.406	0.0443	21.58	19.25	19:14:44	6.54	299.21	152.5	50.10.237	50.1	49.9	48.5		
28/05/2013 20:39:23	28/05/2013 19:34:23	19.573	0.0443	21.58	19.41	19:24:44	5.24	301.19	123.3	42.20.231	42.2	42.1	40.9		
28/05/2013 20:49:23	28/05/2013 19:44:23	19.740	0.0443	21.58	19.58	19:34:44	3.94	303.19	93.9	27.00.175	27.0	26.4	26.6		
28/05/2013 20:59:23	28/05/2013 19:54:23	19.906	0.0443	21.58	19.75	19:44:43	2.64	305.20	64.4	22.30.176	22.3	21.8	22.0		
28/05/2013 21:09:23	28/05/2013 20:04:23	20.073	0.0443	21.58	19.91	19:54:43	1.34	311.305.21	35.9	22.00.273	22.0	26.2	26.2	25.5	
28/05/2013 21:19:23	28/05/2013 20:14:23	20.240	0.0443	21.58	20.08	20:04:43	0.04	313.05.21	7.1	13.50.187	13.5	13.2	13.3		
28/05/2013 21:29:23	28/05/2013 20:24:23	20.406	0.0442	21.59	20.25	20:14:43	-0.19	315.07.25	45.9	9.40.205	9.4	9.5	9.2		
28/05/2013 21:39:23	28/05/2013 20:34:23	20.573	0.0442	21.59	20.41	20:24:43	-1.22	316.30.30	20.4	4.10.200	4.1	4.0	4.0		
28/05/2013 21:49:23	28/05/2013 20:44:23	20.740	0.0442	21.59	20.58	20:34:43	-2.22	317.44.44	0.0	1.90.000	1.9	1.9	1.9		
28/05/2013 21:59:23	28/05/2013 20:54:23	20.906	0.0442	21.59	20.75	20:44:43	-3.19	318.54.54	0.0	-4.30.000	-4.3	-4.2	-4.3		
28/05/2013 22:09:23	28/05/2013 21:04:23	21.073	0.0442	21.59	20.91	20:54:43	-4.11	319.66.66	0.0	-1.30.000	-1.3	-1.3	-1.3		
28/05/2013 22:19:23	28/05/2013 21:14:23	21.240	0.0442	21.59	21.08	21:04:43	-5.11	319.80.80	0.0	-5.10.000	-5.1	-5.0	-5.2		
										-4.50.000	-4.5	-4.4	-4.4		

Sample of Solar Geometry Spreadsheet (1)

SOLINC deg	Calculated (Summer)				Calculated (June)				Calculated (Muneer)				Measured	
	Slope Beam	Sky Diffuse	Ground Reflected	Slope Global	Slope Beam	Sky Diffuse	Ground Refl	Slope Global	Slope Beam	Sky Diffuse	Ground Refl	Slope Global	Average Slope	Only p3
	W/m2	W/m2	W/m2	W/m2	W/m2	W/m2	W/m2	W/m2	W/m2	W/m2	W/m2	W/m2	W/m2	W/m2
18.65	192.3	354.4	9.415561	191.5	355.1	9.415559	225.0	330.2	9.415646	225.0	330.2	9.415646	550.4558.0	
20.91	120.9	342.4	8.234714	120.1	342.9	8.234712	138.6	329.4	8.23476.2	138.6	329.4	8.23476.2	462.7468.8	
23.17	161.8	344.6	8.84515.3	161.0	345.2	8.84515.1	187.8	325.4	8.84522.0	187.8	325.4	8.84522.0	509.1516.0	
25.44	16.8	266.8	5.37288.9	16.2267.2	17.0285.3	5.37288.8	24.6261.0	24.6261.0	5.37291.0	24.6261.0	24.6261.0	5.37291.0	284.3288.6	
27.71	17.5	264.9	5.34287.8	17.0285.3	25.2259.3	5.34287.7	25.2259.3	25.2259.3	5.34289.8	25.2259.3	25.2259.3	5.34289.8	293.3297.8	
29.97	0.0	200.9	3.99204.9	-0.2201.0	3.99204.8	3.99204.8	7.3201.8	7.3201.8	3.99213.0	7.3201.8	7.3201.8	3.99213.0	211.9215.0	
33.33	0.0	205.1	4.07209.2	1.2204.2	4.07209.5	4.07209.5	8.6205.1	8.6205.1	4.07217.8	8.6205.1	8.6205.1	4.07217.8	218.0225.0	
35.59	262.0	309.5	9.73581.3	261.3	310.1	9.73581.1	317.6	264.8	9.73592.1	317.6	264.8	9.73592.1	581.4595.5	
37.86	0.0	202.1	4.01206.1	2.0200.5	4.01206.5	4.01206.5	9.0201.4	9.0201.4	4.01214.5	9.0201.4	9.0201.4	4.01214.5	227.5232.1	
40.12	75.5	288.1	6.66370.3	74.5288.6	6.66370.2	6.66370.2	86.4279.6	86.4279.6	6.66372.7	86.4279.6	86.4279.6	6.66372.7	409.7423.4	
42.38	38.5	262.1	5.62306.3	38.0262.5	5.62306.2	5.62306.2	45.7256.4	45.7256.4	5.62307.8	45.7256.4	45.7256.4	5.62307.8	315.9527.9	
44.64	38.0	256.1	5.51299.6	37.5256.5	5.51299.5	5.51299.5	45.0250.5	45.0250.5	5.51300.9	45.0250.5	45.0250.5	5.51300.9	280.7291.5	
46.89	0.0	150.4	2.99153.4	3.6147.4	2.99154.0	2.99154.0	3.4147.6	3.4147.6	2.99154.0	3.4147.6	3.4147.6	2.99154.0	146.6149.0	
49.14	9.0	205.9	4.11219.0	8.6206.2	4.11219.0	4.11219.0	14.7201.2	14.7201.2	4.11219.9	14.7201.2	14.7201.2	4.11219.9	206.5211.4	
51.38	44.0	241.8	5.37291.1	43.6242.1	5.37291.1	5.37291.1	333.3	168.9	8.88511.1	333.3	168.9	8.88511.1	521.7543.6	
53.62	268.6	227.9	8.88505.4	268.2	228.3	8.88505.4	126.8	224.4	6.50357.7	126.8	224.4	6.50357.7	377.7386.3	
55.86	108.7	240.8	6.50356.0	108.2	241.3	6.50356.0	17.8188.0	17.8188.0	6.50357.7	17.8188.0	17.8188.0	6.50357.7	232.5234.4	
58.09	13.2	192.3	3.93209.4	12.5192.6	3.93209.4	3.93209.4	43.7204.5	43.7204.5	4.74252.7	43.7204.5	43.7204.5	4.74252.7	230.5265.8	
60.31	37.9	210.1	4.74252.7	37.6210.4	4.74252.7	4.74252.7	137.7	187.7	6.24331.7	137.7	187.7	6.24331.7	379.3379.3	
62.53	115.9	209.4	6.24331.6	115.5	209.8	6.24331.6	86.9189.1	86.9189.1	5.37281.8	86.9189.1	86.9189.1	5.37281.8	281.9306.1	
64.74	74.9	201.5	5.37281.8	74.5201.9	5.37281.8	5.37281.8	9.2148.7	9.2148.7	3.05161.0	9.2148.7	9.2148.7	3.05161.0	164.9168.5	
66.94	5.9	152.4	3.05161.3	5.6152.7	3.05161.3	3.05161.3	1.8100.7	1.8100.7	2.04104.6	1.8100.7	1.8100.7	2.04104.6	104.6106.8	
69.14	0.0	102.7	2.04104.7	-0.5103.7	2.04104.8	2.04104.8	0.2	40.8	0.81	0.2	40.8	0.81	39.039.5	
71.33	0.0	41.0	0.81	0.7	40.2	0.81	41.7	41.7	0.12	0.2	40.8	0.81	62.262.3	
73.50	0.0	56.6	1.12	0.9	55.5	1.12	57.6	57.6	1.12	0.3	56.2	1.12	104.3105.2	
75.67	0.0	92.8	1.84	-0.4	93.3	1.84	94.8	94.8	1.84	1.7	90.6	1.84	102.1102.9	
77.83	0.0	94.4	1.87	0.2	94.1	1.87	96.2	96.2	1.87	2.0	91.5	1.87	93.094.2	
79.98	0.0	83.0	1.65	-0.2	83.3	1.65	84.8	84.8	1.65	1.3	80.9	1.65	92.593.5	
82.11	0.0	80.9	1.61	0.1	80.8	1.61	82.4	82.4	1.61	1.3	78.5	1.61	81.882.7	
84.23	0.0	76.9	1.53	0.2	76.5	1.53	78.2	78.2	1.53	1.0	74.3	1.53	86.888.5	
86.34	0.8	80.1	1.65	0.8	80.3	1.65	82.7	82.7	1.65	1.4	78.2	1.65	87.893.9	
88.43	1.2	84.2	1.85	1.2	84.4	1.85	87.4	87.4	1.85	1.5	81.8	1.85	82.188.3	
90.51	0.0	77.4	1.79	0.0	77.5	1.79	79.3	79.3	1.79	0.0	75.5	1.79	77.3	
92.57	0.0	62.2	1.31	0.0	62.3	1.31	63.6	63.6	1.31	0.0	60.8	1.31	62.1	
94.61	0.0	45.1	0.89	0.0	44.9	0.89	45.8	45.8	0.89	0.0	43.6	0.89	41.342.0	
96.63	0.0	37.9	0.75	0.0	37.9	0.75	38.6	38.6	0.75	0.0	36.8	0.75	35.336.2	
98.63	0.0	25.1	0.48	0.0	24.6	0.48	25.0	25.0	0.48	0.0	24.7	0.48	25.425.4	
100.61	0.0	20.7	0.40	0.0	20.3	0.40	20.7	20.7	0.40	0.0	20.4	0.40	20.8	
102.56	0.0	24.3	0.48	0.0	24.4	0.48	24.9	24.9	0.48	0.0	23.7	0.48	24.2	
104.48	0.0	12.5	0.24	0.0	12.3	0.24	12.5	12.5	0.24	0.0	12.3	0.24	12.6	
106.38	0.0	8.7	0.17	0.0	8.8	0.17	9.0	9.0	0.17	0.0	8.6	0.17	8.7	
108.24	0.0	3.8	0.07	0.0	3.7	0.07	3.8	3.8	0.07	0.0	3.7	0.07	3.8	
110.07	0.0	0.0	0.03	0.0	0.0	0.03	0.0	0.0	0.03	0.0	0.0	0.03	0.0	
111.86	0.0	0.0	-0.08	0.0	0.0	-0.08	-0.1	-0.1	0.0	0.0	0.0	-0.08	-0.1	
113.62	0.0	0.0	-0.02	0.0	0.0	-0.02	0.0	0.0	0.0	0.0	0.0	-0.02	0.0	
115.32	0.0	0.0	-0.09	0.0	0.0	-0.09	-0.1	-0.1	0.0	0.0	0.0	-0.09	-0.1	
116.99	0.0	0.0	-0.08	0.0	0.0	-0.08	-0.1	-0.1	0.0	0.0	0.0	-0.08	-0.1	

Sample of Solar Geometry Spreadsheet (2)

Input				Temperature				Calculate				Efficiency				Module/Model Parameters		(from manufacturer's specifications)
Date/Time (GMT+1)	Air Temp °C	Slope W/m2	Wind Speed m/s	Measured Cell Temp °C	Simple Cell Temp °C	Homier Cell Temp °C	Thermal Model Cell Temp °C	Cell η from Measured plus log(phi)	Cell η from Measured	Simple Cell η	Homier Cell η	Thermal Model Cell η	Estimated Cell η from P-ave	Estimated Cell η from P-Instant	Parameters			
28/05/2013 14:34:35	13.15	550.4	9.2	27.42	27.14	23.95	23.95	21.42	0.158	0.1850.159	0.174	0.174	0.182	0.151	0.182	0.151		
28/05/2013 14:44:35	16.45	482.7	9.4	28.51	28.21	25.21	25.21	23.17	0.151	0.1800.155	0.157	0.157	0.182	0.151	0.182	0.151		
28/05/2013 14:54:35	16.85	509.1	9.2	30.02	29.79	26.51	26.51	24.44	0.147	0.1740.148	0.162	0.162	0.175	0.147	0.175	0.147		
28/05/2013 15:04:35	17.20	284.3	5.1	26.31	26.31	22.57	22.57	21.51	0.182	0.1870.170	0.178	0.178	0.182	0.182	0.182	0.182		
28/05/2013 15:14:35	16.95	295.3	5.8	24.51	24.41	22.45	22.45	21.47	0.170	0.1950.170	0.178	0.178	0.170	0.170	0.170	0.170		
28/05/2013 15:24:35	16.70	211.9	5.1	20.81	21.08	19.65	19.65	18.24	0.185	0.2050.184	0.189	0.189	0.185	0.185	0.185	0.185		
28/05/2013 15:39:23	14.50	218.0	5.1	19.71	20.04	18.95	18.95	17.16	0.186	0.2110.188	0.194	0.194	0.186	0.186	0.186	0.186		
28/05/2013 15:49:23	14.20	281.4	5.1	20.81	20.98	18.21	18.21	16.57	0.185	0.2110.187	0.193	0.193	0.185	0.185	0.185	0.185		
28/05/2013 15:59:23	14.25	227.5	5.1	19.71	20.03	18.51	18.51	17.11	0.186	0.2110.188	0.194	0.194	0.186	0.186	0.186	0.186		
28/05/2013 16:09:23	14.40	409.7	11.4	20.15	24.82	22.11	22.11	19.07	0.188	0.2140.169	0.180	0.180	0.188	0.188	0.188	0.188		
28/05/2013 16:19:23	14.85	315.9	11.4	22.21	22.68	20.60	20.60	17.85	0.178	0.2040.177	0.186	0.186	0.178	0.178	0.178	0.178		
28/05/2013 16:29:23	14.70	280.7	11.4	20.21	21.84	19.84	19.84	17.36	0.187	0.2110.181	0.187	0.187	0.187	0.187	0.187	0.187		
28/05/2013 16:39:23	13.90	146.6	11.4	17.15	17.63	16.63	16.63	14.48	0.200	0.2210.198	0.202	0.202	0.200	0.200	0.200	0.200		
28/05/2013 16:49:23	14.00	206.5	11.4	17.31	19.23	17.85	17.85	15.51	0.198	0.2210.191	0.197	0.197	0.198	0.198	0.198	0.198		
28/05/2013 16:59:23	14.20	292.3	11.4	18.00	21.43	19.50	19.50	16.81	0.181	0.2210.182	0.190	0.190	0.181	0.181	0.181	0.181		
28/05/2013 17:09:23	13.20	377.7	11.4	18.70	25.60	21.31	21.31	18.44	0.185	0.2150.162	0.176	0.176	0.185	0.185	0.185	0.185		
28/05/2013 17:19:23	13.45	292.5	11.4	18.94	19.38	17.81	17.81	15.51	0.182	0.2110.151	0.197	0.197	0.182	0.182	0.182	0.182		
28/05/2013 17:29:23	13.25	290.5	11.4	21.31	19.11	17.51	17.51	15.21	0.182	0.2050.162	0.198	0.198	0.182	0.182	0.182	0.182		
28/05/2013 17:39:23	15.05	379.3	11.4	21.31	24.89	22.21	22.21	19.31	0.182	0.2050.176	0.184	0.184	0.182	0.182	0.182	0.182		
28/05/2013 17:49:23	15.70	384.9	10.2	22.01	19.89	18.80	18.80	16.71	0.188	0.2110.189	0.195	0.195	0.188	0.188	0.188	0.188		
28/05/2013 17:59:23	15.90	304.6	10.2	20.11	19.38	17.48	17.48	15.41	0.194	0.2110.196	0.199	0.199	0.194	0.194	0.194	0.194		
28/05/2013 18:09:23	14.89	248.9	10.2	18.11	19.94	18.05	18.05	15.71	0.194	0.2110.205	0.205	0.205	0.194	0.194	0.194	0.194		
28/05/2013 18:19:23	14.68	104.3	10.2	15.41	15.38	15.98	15.98	13.91	0.207	0.2250.205	0.205	0.205	0.207	0.207	0.207	0.207		
28/05/2013 18:29:23	14.68	104.3	10.2	15.97	17.65	16.15	16.15	14.11	0.205	0.2110.189	0.201	0.201	0.205	0.205	0.205	0.205		
28/05/2013 18:39:23	14.50	102.1	8.1	16.51	16.56	15.24	15.24	14.15	0.204	0.2120.201	0.204	0.204	0.204	0.204	0.204	0.204		
28/05/2013 18:49:23	14.40	81.4	8.1	18.61	16.79	15.11	15.11	14.00	0.205	0.2110.201	0.204	0.204	0.205	0.205	0.205	0.205		
28/05/2013 18:59:23	14.20	81.4	8.1	18.31	16.28	15.71	15.71	13.66	0.207	0.2170.209	0.206	0.206	0.207	0.207	0.207	0.207		
28/05/2013 19:09:23	14.40	86.1	8.1	18.61	16.31	15.71	15.71	13.66	0.205	0.2150.209	0.206	0.206	0.205	0.205	0.205	0.205		
28/05/2013 19:19:23	13.95	87.4	8.1	14.61	16.18	15.65	15.65	13.11	0.210	0.2160.204	0.208	0.208	0.210	0.210	0.210	0.210		
28/05/2013 19:29:23	13.75	82.1	8.1	14.41	15.11	14.66	14.66	13.21	0.211	0.2160.208	0.207	0.207	0.211	0.211	0.211	0.211		
28/05/2013 19:39:23	12.90	63.1	10.2	13.91	13.98	13.67	13.67	11.66	0.216	0.2160.213	0.214	0.214	0.216	0.216	0.216	0.216		
28/05/2013 19:49:23	12.80	41.1	10.2	12.91	13.70	13.66	13.66	11.47	0.215	0.2150.214	0.215	0.215	0.215	0.215	0.215	0.215		
28/05/2013 19:59:23	10.70	35.4	10.2	11.51	11.39	11.17	11.17	9.16	0.229	0.2350.224	0.224	0.224	0.229	0.229	0.229	0.229		
28/05/2013 20:09:23	10.40	20.4	10.2	10.51	10.93	10.76	10.76	8.71	0.227	0.2400.226	0.226	0.226	0.227	0.227	0.227	0.227		
28/05/2013 20:19:23	10.50	10.4	10.2	9.71	10.71	10.65	10.65	8.65	0.228	0.2380.226	0.226	0.226	0.228	0.228	0.228	0.228		
28/05/2013 21:09:23	10.50	10.4	10.2	9.71	10.71	10.65	10.65	8.65	0.228	0.2380.226	0.226	0.226	0.228	0.228	0.228	0.228		
28/05/2013 21:19:23	10.45	9.51	10.2	10.51	10.52	10.50	10.50	8.50	0.232	0.2380.227	0.227	0.227	0.232	0.232	0.232	0.232		
28/05/2013 21:29:23	10.30	2.1	10.2	8.51	10.39	10.34	10.34	8.34	0.235	0.2380.228	0.228	0.228	0.235	0.235	0.235	0.235		
28/05/2013 21:39:23	10.00	-2.1	10.2	7.71	9.64	9.61	9.61	7.61	0.238	0.0000.000	0.000	0.000	0.238	0.238	0.238	0.238		
28/05/2013 21:49:23	9.55	-4.1	10.2	7.11	9.50	9.51	9.51	7.51	0.240	0.0000.000	0.000	0.000	0.240	0.240	0.240	0.240		
28/05/2013 21:59:23	9.30	-3.1	10.2	6.71	9.21	9.21	9.21	7.21	0.240	0.0000.000	0.000	0.000	0.240	0.240	0.240	0.240		
28/05/2013 22:09:23	9.00	-4.1	10.2	6.41	8.88	8.91	8.91	6.88	0.240	0.0000.000	0.000	0.000	0.240	0.240	0.240	0.240		
28/05/2013 22:19:23	8.70	-4.1	10.2	6.41	8.58	8.62	8.62	6.58	0.240	0.0000.000	0.000	0.000	0.240	0.240	0.240	0.240		
28/05/2013 22:29:23	8.50	-5.1	10.2	6.21	8.37	8.40	8.40	6.36	0.240	0.0000.000	0.000	0.000	0.240	0.240	0.240	0.240		
28/05/2013 22:39:23	8.15	-5.1	10.2	5.61	8.00	8.04	8.04	6.01	0.240	0.0000.000	0.000	0.000	0.240	0.240	0.240	0.240		
28/05/2013 22:49:23	8.05	-5.4	10.2	5.71	7.94	7.94	7.94	5.92	0.240	0.0000.000	0.000	0.000	0.240	0.240	0.240	0.240		
28/05/2013 22:59:23	7.90	-5.4	10.2	5.61	7.90	7.80	7.80	5.71	0.240	0.0000.000	0.000	0.000	0.240	0.240	0.240	0.240		
28/05/2013 23:09:23	7.85	-4.1	10.2	5.71	7.79	7.76	7.76	5.16	0.240	0.0000.000	0.000	0.000	0.240	0.240	0.240	0.240		
28/05/2013 23:19:23	7.50	-5.1	10.2	5.31	7.38	7.40	7.40	4.82	0.240	0.0000.000	0.000	0.000	0.240	0.240	0.240	0.240		
28/05/2013 23:29:23	7.50	-4.1	10.2	5.41	7.38	7.41	7.41	4.84	0.240	0.0000.000	0.000	0.000	0.240	0.240	0.240	0.240		
28/05/2013 23:39:23	7.15	-4.1	10.2	5.51	7.03	7.04	7.04	4.44	0.240	0.0000.000	0.000	0.000	0.240	0.240	0.240	0.240		
28/05/2013 23:49:23	7.10	-4.1	10.2	5.31	6.98	7.01	7.01	4.42	0.240	0.0000.000	0.000	0.000	0.240	0.240	0.240	0.240		
28/05/2013 23:59:23	7.20	-4.1	10.2	5.51	7.09	7.11	7.11	4.54	0.240	0.0000.000	0.000	0.000	0.240	0.240	0.240	0.240		
29/05/2013 00:09:23	7.10	-4.1	10.2	5.51	7.00	7.01	7.01	4.21	0.240	0.0000.000	0.000	0.000	0.240	0.240	0.240	0.240		
29/05/2013 00:19:23	7.05	-4.1	10.2	6.11	6.98	7.00	7.00	4.18	0.240	0.0000.000	0.000	0.000	0.240	0.240	0.240	0.240		
29/05/2013 00:29:23	7.30	-4.1	10.2	6.71	7.28	7.27	7.27	4.47	0.240	0.0000.000	0.000	0.000	0.240	0.240	0.240	0.240		
29/05/2013 00:39:23	7.35	-4.1	10.2	6.81	7.30	7.32	7.32	4.51	0.240	0.0000.000	0.000	0.000	0.240	0.240	0.240	0.240		
29/05/2013 00:49:23	7.35	-4.1	10.2	7.05	7.30	7.32	7.32	4.51	0.240	0.0000.000	0.000	0.000	0.240	0.240	0.240	0.240		
29/05/2013 00:59:23	7.45	-2.1	10.2	7.10	7.40	7.41	7.41	4.61	0.240	0.0000.000	0.000	0.000	0.240	0.240	0.240	0.240		
29/05/2013 01:09:23	7.55	-2.1	10.2	7.21	7.50	7.51	7.51	4.71	0.240	0.0000.000	0.000	0.000	0.240	0.240	0.240	0.240		

Sample of Modelled Cell Efficiency Spreadsheet

Point 1				
Azimuth (0=N)	Horizon Height (m)	Distance (cm)	Distance (m)	Elevation
50	1.5	1471.12	1.208253	
55	1.5	1260.96	1.409553	
60	1.5	10.553.34	1.610818	
65	14.42	24.3123.444	6.662759	
	1.5	9.2546.99	1.828357	
70	14.42	22.5114.3	7.190404	
75	14.4220.75	105.41	7.789663	
80	14.42	19.297.536	8.409852	
85	14.42	18.593.98	8.723255	
90	14.42	17.689.408	9.161944	
95	14.42	1786.36	9.479535	
100	14.42	16.684.328	9.703664	
105	14.42	16.483.312	9.819712	
110	14.42	16.282.296	9.93854	
115	14.42	16.282.296	9.93854	
120	14.4216.25	82.55	9.908567	
125	14.42	16.583.82	9.761346	
130	14.42	1786.36	9.479535	
135	14.42	17.488.392	9.265437	
140	14.42	18.292.456	8.864779	
145	1.5	5.427.432	3.129854	
	14.42	1996.52	8.497091	
150	14.42	20101.6	8.077988	
155	1.5	4.924.892	3.448492	
160	1.5	4.7524.13	3.557117	
165	1.5	4.522.86	3.754184	
170	15.66	10	50.817.13284	
175	15.66	8.844.704	19.30557	
180	15.66	8.241.656	20.60306	
185	15.66	7.638.608	22.07823	
190	16.51	7.337.084	23.99889	
195	17.36	735.56	26.02112	
200	18.21	6.834.544	27.79613	
205	19.06	6.734.036	29.24862	
210	19.91	6.633.528	30.7032	
215	20.76	6.734.036	31.38079	
220	21.61	6.734.036	32.41212	
225	22.46	6.734.036	33.4204	
230	21.70444444	6.734.036	32.52528	
235	20.94888889	6.734.036	31.61197	
240	20.19333333	6.734.036	30.68038	
245	19.43777778	6.834.544	29.36629	
250	18.68222222	735.56	27.71617	
255	17.92666667	7.337.084	25.79945	
260	17.17111111	7.638.608	23.97736	
265	16.41555556	840.64	21.99507	
270	15.66	8.543.18	19.93408	
275	15.66	9.648.768	17.80246	
280	15.6610.75	54.61	16.00081	
285	15.6612.25	62.23	14.12503	
290	15.66	14.573.66	12.00229	
295	15.66	18.593.98	9.460345	
300	1.5	10.553.34	1.610818	
305	1.5	15	76.21.127724	
310	1.5	16.583.82	1.025227	

Point 2				
Azimuth (0=N)	Horizon Height (m)	Distance (cm)	Distance (m)	Elevation
50	1.5	4.221.336	4.021489	
55	1.5	3.919.812	4.3297	
60	14.42	20101.6	8.077988	
	1.5	2.914.732	5.813773	
65	14.4218.75	95.25	8.608699	
70	14.42	16.583.82	9.761346	
75	14.42	15.578.74	10.37783	
80	14.4214.25	72.39	11.26579	
85	14.4213.75	69.85	11.66441	
90	14.42	1366.04	12.31735	
95	14.42	12.5	63.512.79413	
100	14.4212.25	62.23	13.04638	
105	14.42	12.161.468	13.20248	
110	14.42	1260.96	13.3086	
115	14.42	1260.96	13.3086	
	1.5	1.78.636	9.853487	
120	14.42	12.161.468	13.20248	
125	14.42	12.161.468	13.20248	
130	14.4212.25	62.23	13.04638	
135	14.42	12.5	63.512.79413	
140	14.42	1366.04	12.31735	
145	14.42	13.568.58	11.87434	
150	14.4214.25	72.39	11.26579	
155	1.5	2.211.176	7.644337	
	14.42	15	76.210.71587	
160	1.5	2.311.684	7.315656	
	14.4216.25	82.55	9.908567	
165	1.5	2.613.208	6.47918	
	14.42	1891.44	8.961686	
170	1.5	2.914.732	5.813773	
	14.42	19.599.06	8.282278	
175	1.5	3.517.78	4.822308	
180	1.5	3.919.812	4.3297	
185	1.5	4.221.336	4.021489	
190	15.66	10.955.372	15.79167	
195	15.66	10.352.324	16.66187	
200	15.66	9.950.292	17.29562	
205	15.66	9.548.26	17.97785	
210	15.66	9.2546.99	18.43129	
215	16.70615385	9.146.228	19.86915	
220	17.75230769	9.246.736	20.79889	
225	18.79846154	9.347.244	21.69769	
230	19.84461538	9.648.768	22.14233	
235	20.89076923	9.849.784	22.76429	
240	21.93692308	10.251.816	22.94595	
245	21.84181818	10.553.34	22.26826	
250	20.60545455	10.75	20.6725	
255	19.36909091	11.25	18.72238	
260	18.13272727	11.75	16.89782	
265	16.89636364	12.5	63.514.90027	
270	15.66	1366.04	13.3401	
275	15.66	14.573.66	12.00229	
280	15.6616.25	82.55	10.74155	
285	15.6618.75	95.25	9.336443	
290	15.66	23.5119.38	7.473261	
295	0	0	0	0
300	0	0	0	0
305	0	0	0	0
310	0	0	0	0

: Shading Estimation Points 1 & 2

Point 3				
Azimuth (0=N)	Horizon Height (m)	Distance (cm)	Distance (m)	Elevation
72.5	1.5	12.75	64.77	1.326668
	14.42		26132.08	6.230662
90	14.42	21.5	109.22	7.521097
112	14.42	19.75	100.33	8.178866
147	14.42	23.25	118.11	6.960768
160	15.66		1471.12	12.41787
169	15.66	10.75	54.61	16.00081
180	17.12666667		8.945.212	20.74709
	1.5		3.517.78	4.822308
196	22.46		7.940.132	29.2337
220	1.5		1.99.652	8.833571
	19.196		6.533.02	30.17135
246	15.66		6.533.02	25.37302
270	15.66		8.945.212	19.10446
289	15.66		14.774.676	11.84364

Point 4				
Azimuth (0=N)	Horizon Height (m)	Distance (cm)	Distance (m)	Elevation
50	1.5		4.321.844	3.928262
65	14.42	17.75	90.17	9.085816
	1.5		2.713.716	6.24114
90	14.42		1366.04	12.31735
	1.5		1.859.398	9.0684
113	14.42		11.859.944	13.52595
	1.5		1.68.128	10.45613
144	14.42		13.870.104	11.6233
	1.5		1.89.144	9.315942
180	1.5		2.814.224	6.019909
196	15.66	13.75	69.85	12.63646
211	15.66	12.5	63.5	13.85352
235	22.46		13.166.548	18.64958
259	15.66		14.875.184	11.76585
270	15.66		17.5	88.99.990331
283	15.66		23116.84	7.633827

: Shading Estimation Points 3 & 4


Point 5				
Azimuth (0=N)	Horizon Height (m)	Distance (cm)	Distance (m)	Elevation
50	1.5		2.914.732	5.813773
77	14.42		1471.12	11.46168
	1.5		1.68.128	10.45613
90	14.42		12.261.976	13.09801
	1.5		1.47.112	11.90977
115	14.42	11.25	57.15	14.1612
	1.5		1.25	6.3513.2908
150	14.42		14.272.136	11.30443
	1.5		1.68.128	10.45613
180	1.5		2.914.732	5.813773
194	1.5		5.929.972	2.865075
201	15.66		18.593.98	9.460345
228	22.46	17.75	90.17	13.98689
248	15.66		18.593.98	9.460345
270	15.66	24.25	123.19	7.244623

Shading Estimation Point 5

Appendix B: Datasheets

Solar Module

Poly Mono



**Powerguard insurance
global coverage**


Within the first year, the output power shall not be less than 97.5% of the minimum output power in CSUN's product datasheet, thereafter the loss of output power shall not exceed 0.7% per year, ending with 80.7% in the 25th year.

■ CSUN ■ Standard warranty

CSUN's **NEW** linear performance warranty



Additional value from CSUN's linear warranty



All rights reserved by CSUN



CSUN255-60P

Standard Solar Product

- CSUN255-60P
- CSUN250-60P
- CSUN245-60P
- CSUN240-60P
- CSUN235-60P



15.71%
Module efficiency

255 W
Highest power output

10 years
Material & workmanship warranty

25 years
Linear power output warranty

-  Industry leading conversion efficiency
-  Positive tolerance offer
-  Passed salt mist corrosion testing and ammonia corrosion testing
-  Certified to withstand wind (2400 Pa) and snow load (7200 Pa)
-  Excellent performance under weak light condition
-  Good temperature coefficient performance enables better output in the tropical zone

- China Sunergy (Nanjing) Co., Ltd. (NASDAQ: CSUN), established in 2004, is a hi-tech corporation with its core business in R&D, manufacturing, and sale of high efficiency silicon based solar cells and modules.
- As one of the leading PV enterprises in the world, CSUN has delivered more than 1GW solar products, to residential, commercial, utility and off-grid projects all around the world.
- Through strict selection of raw materials, stringent quality control and rigorous test in state of the art facilities in Nanjing and Shanghai, CSUN has always committed to higher efficiency, more stable and better cost performance products.

* Note: All specifications, warranties, certifications about module of „CSUN“ series also apply to that of „SST“.

All information and data are subject to change without notice.



www.csun-solar.com

Electrical characteristics at Standard Test Conditions (STC)

Module type	CSUN 255-60P	CSUN 250-60P	CSUN 245-60P	CSUN 240-60P	CSUN 235-60P
Maximum Power - P _{mpp} (W)	255	250	245	240	235
Positive power tolerance	0~3%				
Open Circuit Voltage - Voc (V)	37.5	37.3	37.1	36.9	36.8
Short Circuit Current - I _{sc} (A)	8.88	8.81	8.74	8.67	8.59
Maximum Power Voltage - V _{mpp} (V)	30.1	29.9	29.7	29.6	29.5
Maximum Power Current - I _{mpp} (A)	8.47	8.36	8.25	8.11	7.97
Practical module efficiency	17.46%	17.12%	16.78%	16.44%	16.10%
Module efficiency	15.71%	15.40%	15.09%	14.78%	14.47%

Electrical data relates to standard test conditions (STC): irradiance 1000W/m²; AM 1.5; cell temperature 25°C measuring uncertainty of power is within ±3%. Certified in accordance with IEC61215, IEC61730-1/2 and UL 1703

Electrical Characteristics at Normal Operating Cell Temperature (NOCT)

Module type	CSUN 255-60P	CSUN 250-60P	CSUN 245-60P	CSUN 240-60P	CSUN 235-60P
Maximum Power - P _{mpp} (W)	188	185	181	178	175
Maximum Power Voltage - V _{mpp} (V)	28.0	27.9	27.5	27.2	27.0
Maximum Power Current - I _{mpp} (A)	6.72	6.64	6.58	6.54	6.48
Open Circuit Voltage - Voc (V)	34.6	34.5	34.2	34.0	33.8
Short Circuit Current - I _{sc} (A)	7.16	7.1	7.02	6.95	6.9

Electrical data relates to normal operating cell temperature (NOCT): irradiance 800W/m²; wind speed 1 m/s; cell temperature 45°C; ambient temperature 20°C measuring uncertainty of power is within ±3%.

Temperature Characteristics

Voltage Temperature Coefficient	-0.292%/K
Current Temperature Coefficient	+0.045%/K
Power Temperature Coefficient	-0.408%/K

Maximum Ratings

Maximum system voltage(V)	1000
Series fuse rating(A)	20

Mechanical Characteristics

Dimensions	1640 × 990 × 40 mm (L×W×H)
Weight	19.1 kg
Frame	anodized aluminum profile
Front glass	white toughened safety glass, 3.2 mm
Cell Encapsulation	EVA (Ethylene-Vinyl-Acetate)
Back Sheet	composite film
Cells	6 × 10 pieces polycrystalline solar cells series strings (156 mm × 156 mm)
Junction Box	with 6 bypass diodes
Cable	length 900 mm, 1 × 4 mm ²

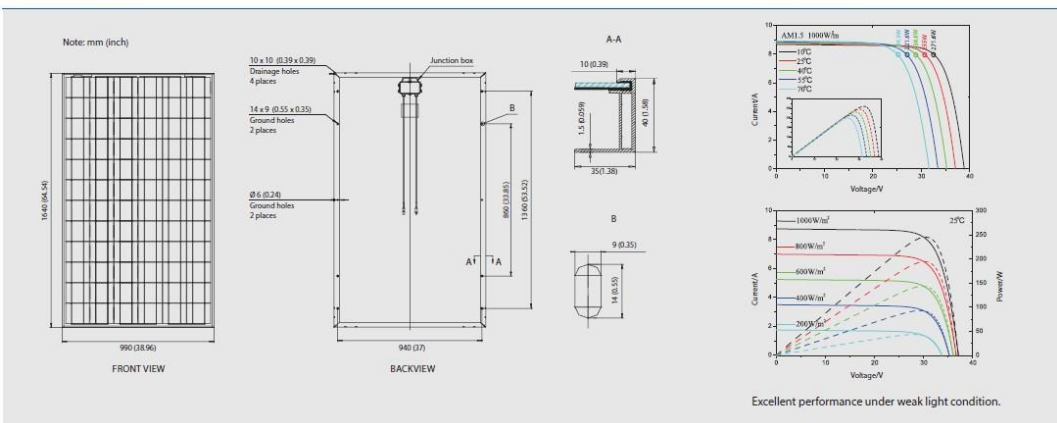
Packaging

Dimensions (L × W × H)	1690 × 1120 × 112 mm
Container 20'	300
Container 20'HC	324
Container 40'	700
Container 40'HC	756

System Design

Temperature range	-40°C to +85°C
Hail	maximum diameter of 25 mm with impact speed of 23 m/s (51.2 mph)
Maximum surface load capacity	7200 Pa

Dimensions



TRIO-20.0-TL
TRIO-27.6-TL

GENERAL SPECIFICATIONS
OUTDOOR MODELS

AURORA UNO
TRIO

The latest in Power-One's Aurora Trio range, this new-look three-phase inverter fills a specific niche in the commercial solar market. This new three-phase inverter benefits from the three-phase inverter technology perfected in the PVI-10.0 and 12.5, probably the world's most commonly used three-phase inverter which has led the way in best-in-class efficiency.

Controlling more PV panels than its smaller predecessor, the Trio-27.6 and Trio-20.0 will offer more flexibility and control to installers who have large installations with varying aspects or orientations. This device has two independent MPPTs and efficiency ratings of up to 98.2%. The very wide input voltage range makes the inverter suitable to installations with reduced string size.

The new look inverter has new features including a special built-in heat sink compartment and front panel display system. The unit is free of electrolytic capacitors, leading to a longer product lifetime.



Features

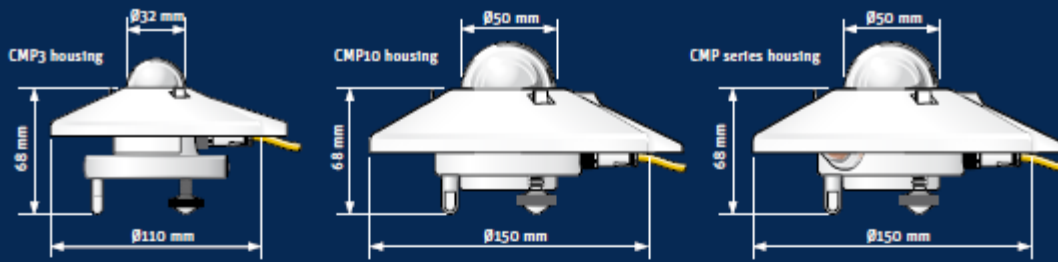
- 'Electrolyte-free' power converter to further increase the life expectancy and long term reliability
- Quiet Rail
- True three-phase bridge topology for DC/AC output converter
- Each inverter is set on specific grid codes which can be selected in the field
- Dual input sections with independent MPP tracking, allows optimal energy harvesting from two sub-arrays oriented in different directions
- Wide input range
- Detachable wiring box to allow an easy installation
- Integrated string combiner with different options of configuration which include DC and AC disconnect switch in compliance with international Standards (-S2, -S2F and -S2X versions)
- High speed and precise MPPT algorithm for real time power tracking and improved energy harvesting
- Flat efficiency curves ensure high efficiency at all output levels ensuring consistent and stable performance across the entire input voltage and output power range
- Outdoor enclosure for unrestricted use under any environmental conditions
- Capability to select via display the Active Power reduction and the Reactive Power regulation (fixed cos(phi), standard cos(phi)=f(P) curve, Fixed Q (Q/Pn))
- Capability to connect external sensors for monitoring environmental conditions
- Availability of auxiliary DC output voltage (24V, 300mA)

PARAMETER	TRIO-20.0-TL-OUTD	TRIO-27.6-TL-OUTD
Input Side		
Absolute Maximum DC Input Voltage ($V_{max,dc}$)	1000 V	1000 V
Start-up DC Input Voltage (V_{start})	360 V (adj. 250...500 V)	360 V (adj. 250...500 V)
Operating DC Input Voltage Range ($V_{dcrtr} \dots V_{dcrmax}$)	0.7 x $V_{max,dc}$...950 V	0.7 x $V_{max,dc}$...950 V
Rated DC Input Power (P_{dc})	20750 W	28600 W
Number of Independent MPPT	2	2
Maximum DC Input Power for each MPPT ($P_{dc,MPPT,max}$)	12000 W	16000 W
DC Input Voltage Range with Parallel Configuration of MPPT at P_{dc}	440...800 V	500...800 V
DC Power Limitation with Parallel Configuration of MPPT	Linear Derating From MAX to Null [800V ≤ V_{MPPT} ≤ 950V]	Linear Derating From MAX to Null [800V ≤ V_{MPPT} ≤ 950V]
DC Power Limitation for each MPPT with Independent Configuration of MPPT at P_{dc} , max unbalance example	12000 W [480V ≤ V_{MPPT} ≤ 800V] the other channel: P_{dc} 12000W [350V ≤ V_{MPPT} ≤ 800V]	16000 W [500V ≤ V_{MPPT} ≤ 800V] the other channel: P_{dc} 16000W [400V ≤ V_{MPPT} ≤ 800V]
Maximum DC Input Current ($I_{max,dc}$) / for each MPPT ($I_{MPPT,max}$)	500 A / 25.0 A	64.0 A / 32.0 A
Maximum Input Short Circuit Current for each MPPT	30.0 A	40.0 A
Number of DC Inputs Pairs for each MPPT	1 (4 in -52X and -52F Versions)	1 (5 in -52X and -52F Versions)
DC Connection Type	Tool Free PV Connector WM / MC4 (Screw Terminal Block on Standard and -52 versions)	Tool Free PV Connector WM / MC4 (Screw Terminal Block on Standard and -52 versions)
Input Protection		
Reverse Polarity protection	Yes, from limited current source	Yes, from limited current source
Input Over Voltage Protection for each MPPT - Varistor	2	2
Input Over Voltage Protection for each MPPT - Plug In Modular Surge Arrester (-52X Version)	3 (Class II)	3 (Class II)
Photovoltaic Array Isolation Control	According to local standard	According to local standard
DC Switch Rating for each MPPT (Version with DC switch)	40 A / 1000 V	40 A / 1000 V
Fuse Rating (Versions with fuses)	12 A / 1000V	12 A / 1000V
Output Side		
AC Grid Connection Type	Three phase 3W or 4W+PE	Three phase 3W or 4W+PE
Rated AC Power (P_{ac})	20000 W	27600 W
Maximum AC Output Power ($P_{ac,max}$)	22000 W ¹⁾	30000 W ¹⁾
Rated AC Grid Voltage ($V_{ac,r}$)	400 V	400 V
AC Voltage Range	320...480 V ¹⁾	320...480 V ¹⁾
Maximum AC Output Current ($I_{ac,max}$)	33.0 A	45.0 A
Rated Output Frequency (f_r)	50 Hz	50 Hz
Output Frequency Range ($f_{min} \dots f_{max}$)	47...53 Hz ²⁾	47...53 Hz ²⁾
Nominal Power Factor ($\cos\phi_{NAC}$)	> 0.995 (adj. ±0.9, or fixed by display down to ±0.8 with max 22 kVA)	> 0.995 (adj. ±0.9, or fixed by display down to ±0.8 with max 30 kVA)
Total Current Harmonic Distortion	< 3%	< 3%
AC Connection Type	Screw terminal block	Screw terminal block
Output Protection		
Anti-Islanding Protection	According to local standard	According to local standard
Maximum AC Overcurrent Protection	34.0 A	46.0 A
Output Overvoltage Protection - Varistor	4	4
Output Over Voltage Protection - Plug In Modular Surge Arrester (-52X Version)	4 (Class II)	4 (Class II)
Operating Performance		
Maximum Efficiency (η_{max})	98.2%	98.2%
Weighted Efficiency (EURO/CEC)	98.0% / 98.0%	98.0% / 98.0%
Feed In Power Threshold	40 W	40 W
Stand-by Consumption	< 8W	< 8W
Communication		
Wired Local Monitoring	PVI-USB-RS232 485 (opt.), PVI-DESKTOP (opt.)	PVI-USB-RS232 485 (opt.), PVI-DESKTOP (opt.)
Remote Monitoring	PVI-AEC-EVO (opt.), AURORA-UNIVERSAL (opt.)	PVI-AEC-EVO (opt.), AURORA-UNIVERSAL (opt.)
Wireless Local Monitoring	PVI-DESKTOP (opt.) with PVI-RADIOMODULE (opt.)	PVI-DESKTOP (opt.) with PVI-RADIOMODULE (opt.)
User Interface	Graphic display	Graphic display
Environmental		
Ambient Temperature Range	-25...+60°C / -13...140°F with derating above 45°C/113°F	-25...+60°C / -13...140°F with derating above 45°C/113°F
Relative Humidity	0...100% condensing	0...100% condensing
Noise Emission	< 50 dB(A) @ 1 m	< 50 dB(A) @ 1 m
Maximum Operating Altitude without Derating	2000 m / 6560 ft	2000 m / 6560 ft
Physical		
Environmental Protection Rating	IP 65	IP 65
Coding	Natural	Natural
Dimension (H x W x D)	1061 mm x 702 mm x 292 mm / 41.7" x 27.6" x 11.5"	1061 mm x 702 mm x 292 mm / 41.7" x 27.6" x 11.5"
Weight	< 70.0 kg / 154.3 lb (Standard Version)	< 75.0 kg / 165.4 lb (Standard Version)
Mounting System	Wall bracket	Wall bracket
Safety		
Isolation Level	Transformerless	Transformerless
Marking	CE	CE
Safety and EMC Standard	EN 50178, AS/NZS 3100, AS/NZS 60950, EN61000-6-1, EN61000-6-3, EN61000-3-11, EN61000-3-12	EN 50178, AS/NZS 3100, AS/NZS 60950, EN61000-6-1, EN61000-6-3, EN61000-3-11, EN61000-3-12
Grid Standard	Enel Guideline (CEI 0-21 + Attachment A70 Terna, CEI 0-16 ³⁾ , VDE 0126-1-1, VDE-AR-N 4105, GS 9/2, EN 50438, RD1663, AS 4777, BDEW	Enel Guideline (CEI 0-21 + Attachment A70 Terna, CEI 0-16 ³⁾ , VDE 0126-1-1, VDE-AR-N 4105, GS 9/2, EN 50438, RD1663, AS 4777, BDEW
Available Products Variants		
Standard	TRIO-20.0-TL-OUTD-400	TRIO-27.6-TL-OUTD-400
With DC+AC Switch	TRIO-20.0-TL-OUTD-S2-400	TRIO-27.6-TL-OUTD-S2-400
With DC+AC Switch and Fuse	TRIO-20.0-TL-OUTD-S2F-400	TRIO-27.6-TL-OUTD-S2F-400
With DC+AC Switch, Fuse and Surge Arrester	TRIO-20.0-TL-OUTD-S2X-400	TRIO-27.6-TL-OUTD-S2X-400

- The AC voltage range may vary depending on specific country grid standard
- The Frequency range may vary depending on specific country grid standard
- Limited to 20000 W for Germany
- Limited to 27600 W for Germany
- Since their applicability dates

Remark: Features not specified by listed in the present data sheet are not included in the product

Pyranometer specifications



Specifications	CMP 3	CMP 6	CMP10 & CMP 11	CMP 21	CMP 22
Classification to ISO 9060-1990	Second Class	First Class	Secondary Standard	Secondary Standard	Secondary Standard
Spectral range (50% points)	300 to 2800nm	285 to 2800nm	285 to 2800nm	285 to 2800nm	200 to 3600 nm
Sensitivity	5 to 20 $\mu\text{V}/\text{W}/\text{m}^2$	5 to 20 $\mu\text{V}/\text{W}/\text{m}^2$	7 to 14 $\mu\text{V}/\text{W}/\text{m}^2$	7 to 14 $\mu\text{V}/\text{W}/\text{m}^2$	7 to 14 $\mu\text{V}/\text{W}/\text{m}^2$
Impedance	20 to 200 Ω	20 to 200 Ω	10 to 100 Ω	10 to 100 Ω	10 to 100 Ω
Expected output range (0 to 1500 W/m^2)	0 to 30 mV	0 to 30 mV	0 to 20 mV	0 to 20 mV	0 to 20 mV
Maximum operational irradiance	2000 W/m^2	2000 W/m^2	4000 W/m^2	4000 W/m^2	4000 W/m^2
Response time (63%)	< 6s	< 6s	< 1.7s	< 1.7s	< 1.7s
Response time (95%)	< 18s	< 18s	< 5s	< 5s	< 5s
Zero offsets (a) thermal radiation (at 200 W/m^2) (b) temperature change (5 K/h)	< 15 W/m^2 < 5 W/m^2	< 12 W/m^2 < 4 W/m^2	< 7 W/m^2 < 2 W/m^2	< 7 W/m^2 < 2 W/m^2	< 3 W/m^2 < 1 W/m^2
Non-stability (change/year)	< 1%	< 1%	< 0.5%	< 0.5%	< 0.5%
Non-linearity (100 to 1000 W/m^2)	< 1.5%	< 1%	< 0.2%	< 0.2%	< 0.2%
Directional response (up to 80° with 1000 W/m^2 beam)	< 20 W/m^2	< 20 W/m^2	< 10 W/m^2	< 10 W/m^2	< 5 W/m^2
Spectral selectivity (350 to 1500 nm)	< 3%	< 3%	< 3%	< 3%	< 3%
Temperature response	< 5% (-10°C to +40°C)	< 4% (-10°C to +40°C)	< 1% (-10°C to +40°C)	< 1% (-20°C to +50°C)	< 0.5% (-20°C to +50°C)
Tilt response (0° to 90° at 1000 W/m^2)	< 1%	< 1%	< 0.2%	< 0.2%	< 0.2%
Field of view	180°	180°	180°	180°	180°
Accuracy of bubble level	< 0.2°	< 0.1°	< 0.1°	< 0.1°	< 0.1°
Temperature sensor output				10K Thermistor (optional Pt-100)	10K Thermistor (optional Pt-100)
Detector type	Thermopile	Thermopile	Thermopile	Thermopile	Thermopile
Operational temperature range	-40°C to +80°C	-40°C to +80°C	-40°C to +80°C	-40°C to +80°C	-40°C to +80°C
Storage temperature range	-40°C to +80°C	-40°C to +80°C	-40°C to +80°C	-40°C to +80°C	-40°C to +80°C
Humidity range	0 to 100% non-condensing	0 to 100% non-condensing	0 to 100% non-condensing	0 to 100% non-condensing	0 to 100% non-condensing
Ingress Protection (IP) rating	67	67	67	67	67
Recommended applications	Economical solution for routine measurements in weather stations, field testing	Good quality measurements for hydrology networks, greenhouse climate control	Meteorological networks, PV panel and thermal collector testing, materials testing	Meteorological networks, reference measurements in extreme climates, polar or arid	Scientific research requiring the highest level of measurement accuracy and reliability

Note: The performance specifications quoted are worst-case and/or maximum values.
Standard 10k Thermistor or optional Pt-100 temperature sensor with CMP 21 and CMP 22.
Individual directional response and temperature dependence see data with CMP 21 and CMP 22.



Go to www.kippzonen.com for your local distributor

Sensor Calibration Certificates



CALIBRATION CERTIFICATE

CERTIFICATE NUMBER	008145830319
PYRANOMETER MODEL	CM 11
SERIAL NUMBER	830319
SENSITIVITY	4.67 $\mu\text{V}/\text{W}/\text{m}^2$ at normal incidence on horizontal pyranometer
IMPEDANCE	900 Ohm
TEMPERATURE	22 \pm 2 °C
REFERENCE PYRANOMETER	Kipp & Zonen CM 11 sn 892498 active from 01-01-2013
CALIBRATION DATE	31 January 2013 (recalibration is recommended every two years)
IN CHARGE OF TEST	P. van der Heijden

Calibration procedure

The indoor calibration procedure is based on a side-by-side comparison with a reference pyranometer under an artificial sun fed by an AC voltage stabiliser. It embodies a 150 W Metal-Halide high-pressure gas discharge lamp. Behind the lamp is a reflector with a diameter of 16 cm. The reflector is 1 m above the pyranometers producing a vertical beam. The reference and test pyranometers are mounted horizontally on a table, which can rotate. The irradiance at the pyranometers is approximately 500 W/m². During the calibration procedure the reference and test pyranometer are interchanged to correct for any non-homogeneity of the beam.

Hierarchy of traceability

The reference pyranometer was compared with the sun and sky radiation as source under mainly clear sky conditions using the "continuous sun-and-shade method". The measurements were performed in Davos (latitude: 46.8143°, longitude: -9.8458°, altitude: 1588 m above sea level). The readings are referred to the World Radiometric Reference (WRR) as stated in the WMO Technical Regulations. The originally estimated uncertainty of the WRR relative to SI is $\pm 0.3\%$.

The inclination of the receiver surface versus the true horizontal plane was set to 0.0 degrees, the instrument signal wire to the north. During the comparisons, the instrument received global radiation intensities from 629 to 1021 with a mean of 840 W/m². The angle between the solar beam and the normal of the receiver surface varied from 26.2 to 49.9 with a mean of 36.2 degrees. The ambient temperature ranged from +11.3 to +23.1 with a mean of +17.9 °C. The sensitivity calculation and the single measurements deviation (σ) are based on 381 individual measurements. The obtained sensitivity value and its expanded uncertainty (95% level of confidence) are valid for similar conditions and are: $4.44 \pm 0.06 \mu\text{V}/\text{W}/\text{m}^2$ (but is corrected by Kipp & Zonen to $4.43 \mu\text{V}/\text{W}/\text{m}^2$. See "correction applied" below.)
Dates of measurements: 2012, July 5, 9, 10, 18, 23, 24

Global radiation data were calculated from the direct solar radiation as measured with the absolute cavity pyrliometer PMO2 (member of the WSG, WRR-Factor: 0.998623, based on the last International Pyrliometer Comparison IPC-2010) and from the diffuse radiation as measured with a continuous disk shaded pyranometer CM 22 sn020059 with sensitivity 8.91 (ventilated with heated air, instrument-wire to the north).

Correction applied -0.2 %

This correction is necessary to compensate for the mean directional errors of the reference CM 11 in Davos. This error is estimated at Kipp & Zonen by measuring the directional error for the mean angle of incidence at azimuth S-30° and S+30°. The reference CM 11 now measures the vertical beam of the indoor calibration facility more correctly.

Justification of total instrument calibration uncertainty

The combined uncertainty of the result of the calibration is the positive "root sum square" of three uncertainties.

1. The expanded uncertainty due to random effects and instrumental errors during the calibration of the reference CM 11 as given by the World Radiation Center in Davos is $\pm 0.06/4.44 = \pm 1.4\%$. (See traceability text).
 2. The uncertainty in the correction for the systematic effect of a directional error (cosine error) during the calibration in Davos. Based on experience this cosine error can be estimated with an expanded uncertainty of $\pm 0.5\%$.
 3. Also based on experience the expanded uncertainty of the transfer procedure (calibration by comparison) is estimated to be $\pm 0.5\%$.
- The estimated combined expanded uncertainty is the positive "root sum square" of these three uncertainties: $\sqrt{(1.4^2 + 0.5^2 + 0.5^2)} = \pm 1.5\%$.

Notice

The calibration certificate supplied with the instrument is at the date of first use. Even though the calibration certificate is dated relative to manufacture, or recalibration, the instrument does not undergo any sensitivity changes when kept in the original packing. From the moment the instrument is taken from its packaging and exposed to irradiance the sensitivity may deviate with time. See the 'non-stability' value (% change in sensitivity per year) given in the radiometer specifications.

Page 1/1
Kipp & Zonen B.V.
Delftechpark 36, 2628 XH Delft
P.O. Box 507, 2600 AM Delft
The Netherlands

T: +31 (0) 15 2755 210
F: +31 (0) 15 2620 351
info@kippzonen.com
www.kippzonen.com

VAT no.: NLO055.74.857.B.01
Trade Register no.: 27239004
Member of HMEI

Product certificate

Pages: 1
Report date: 28 January 2013

Product code **PU22**
Product identification **serial number 160**
Product type heat flux sensor
Measurand heat flux

Calibration result

Sensitivity **$S = 56.4 \times 10^{-6} \text{ V}/(\text{W}/\text{m}^2)$**
Calibration uncertainty **$\pm 2.8 \times 10^{-6} \text{ V}/(\text{W}/\text{m}^2)$**

the number following the \pm symbol is the expanded uncertainty with a coverage factor $k = 2$, and defines an interval estimated to have a level of confidence of 95 percent

Measurement function $\Phi = U/S$
With Φ heat flux in $[\text{W}/\text{m}^2]$, U voltage output in [V]

Product specifications

1: resistance **534.9 Ω**

Sensitivity is calculated from the sensor response to an electrically generated heat flux that is forced through the sensor. Calibration is performed at room temperature. Traceability of calibration is to NPL.

Calibration performed by:
F. Warffemius

Date:
28 January 2013

Person authorising acceptance and release of product:
J. M. Konings

Date:
28 January 2013

Squirrel 2020 Technical Specifications

	SQ2020-1F8	SQ2020-2F8
Analogue Input Channel Options	Analogue to digital converters: 1 Differential: 8 Single Ended*: 16 3 or 4 wire: 0	Analogue to digital converters: 2 Differential: 8 Single Ended*: 16 3 or 4 wire: 4
Additional Channels	Pulse: (2 x fast-64kHz)& (2 x slow - 100Hz) Event/digital: 8 state inputs or 1 x 8 bit binary	Pulse: (2 x fast-64kHz)& (2 x slow - 100Hz) Event/digital: 8 state inputs or 1 x 8 bit binary
Logging Speed	20 readings / sec on 1 channel only	100 readings / sec on 2 channels only
Communication	Standard: RS232 (Auto bauding to 115200 baud) USB 1.1 & 2.0 compatible External options: GSM, Wifi and PSTN Modems	Standard: RS232 (Auto bauding to 115200 baud) USB 1.1 & 2.0 compatible Ethernet 10/100 base TCP/IP (Requires external power supply) External options: GSM, Wi-Fi and PSTN Modems
Analogue Inputs	Accuracy: (at 25°C) voltage and resistance ($\pm 0.05\%$ readings + 0.025% range) Common mode rejection: 100dB Linearity: 0.015% Input impedance: > 1M Ω Series mode line rejection: 50/60Hz 100dB	
Analogue - Digital Conversion	Type: Sigma - Delta Resolution: 24bit Sampling rate: up to 10, 20* or 100* readings per sec. per ADC. No 100Hz on 1F8 (* with mains rejection off)	
Thermistor Ranges	Y & U-type: - 50 to 150°C Pt100/ Pt1000: - 200 to - 850°C (2 wire only on 1F8) Customer specific thermistor range	
Thermocouple Ranges; Differential and Single Ended	K-type: - 200 to 1372°C T-type: - 200 to 400°C N-type: - 200 to 1300°C	R-type: - 50 to 1768°C S-type: - 50 to 1768°C J-type: -200 to 1200°C
Working Environment	- 30 to 65°C, RH up to 95% (non-condensing)	B-type: 250 to 1820°C C-type: 0 to 2320°C D-type: 0 to 2320°C
Voltage Ranges; Differential and Single Ended	- 0.075V to 0.075V, - 0.15V to 0.15V, - 0.3V to 0.3V, - 0.6V to 0.6V, 0.6V to 1.2V, 0.6V to 2.4V, - 3V to 3V, - 6V to 6V, -6V to 12V, - 6V to 25V	
High Voltage Input Range	4V to 20V, 4V to 4V, 4V to 60V (max 2 may be selected)	
Current Ranges, Differential (Requires external 10 Ω shunt)	-30 to 30mA, 4 to 20mA	
Resistance Ranges, all 2 wire	0 to 1250 Ω , 0 to 5000 Ω , 0 to 20000 Ω , 0 to 300000 Ω	
Resistance Range 3 and 4 wire (2F8)	0 to 500 Ω , 0 to 4000 Ω	
Digital/Alarm Outputs	4 open drain FET (18V 0.1A)	
Memory	Internal: up to 128Mb (up to 14 million readings) External: Up to 1Gb - removable MMC/ SD (for transferring internal memory and storing setups only)	
Internal Memory Modes	Stop when full or overwrite	
Calculated Channels	Up to 16 virtual channels derived from physical input channels	
Resolution	Up to 6 significant digits	
Display/Keypad	128*64 dot graphical display, 4 button keypad	
Power Supply	Internal: 6 x AA alkaline batteries External: 10-18VDC. Reverse and polarity and over-voltage protected	
Power Consumption @ 9V	Sleep mode: 600 μ A Logging: 40 - 80 mA	
Power Output for External Device	Regulated 5VDC at 50mA or logger supply voltage at 100mA	
Time and Date	In-built clock in 3 formats	
Programming / Logger setup	SquirrelView or SquirrelView Plus Software	
Dimensions (w x d x h), Weight	235 mm x 175 mm x 55 mm, 1.2 kg, enclosure material ABS	

Note: SQ2020 is supplied with software, manual, USB cable, wall bracket, batteries and 4 current shunt resistors.

Appendix C: VBA Code Transcripts

Solar Geometry

```
Private Function AST(time, xeot, xlong, lsm, mode)
'Function to display the apparent solar time, as decimal hour and full
time (depending on mode)
If mode = 0 Then
lct = decimalhour(time)
AST = lct + xeot + (lsm - xlong) / 15
Else
AST = time + (xeot + (lsm - xlong) / 15) / 24
End If
End Function
```

```
Private Function decimalhour(time)
'Simple function to convert time format to a decimal hour value
decimalhour = Hour(time) + Minute(time) / 60 + Second(time) / 3600
End Function
```

```
Private Function EOT(time, YRLNG)
'Function to calculate the equation of time, adapted from WiB software
' * indicates a line altered from the original code (for all subsequent
functions)
dtor = 3.14159 / 180 'radian conversion factor
xyr = Year(time) '* splitting of input variable into separate values
xmo = Month(time) xdy =
Day(time) xhr =
Hour(time) xs =
Second(time)
XLCT = decimalhour(time) '* derives hour as decimal value
UT = XLCT + YRLNG / 15 'something to do with the local meridian and
SHA, I think

'Need to convert values for formula: If xmo
> 2 Then
IYR1 = xyr
IMT1 = xmo - 3
Else
IYR1 = xyr - 1
IMT1 = xmo + 9
End If

'Implementation of Yallop formula: INTT1
= Int(30.6 * IMT1 + 0.5)
INTT2 = Int(365.25 * (IYR1 - 1976))
SMLT = ((UT / 24) + xdy + INTT1 + INTT2 - 8707.5) / 36525 'Why no
decimal point here?
EPSILN = 23.4393 - 0.013 * SMLT
CAPG = 357.528 + 35999.05 * SMLT

If CAPG > 360 Then 'Need to confine this to range 0-360
G360 = CAPG - Int(CAPG / 360) * 360 'clever piece of code... Else
G360 = CAPG
End If

CAPC = 1.915 * Sin(G360 * dtor) + 0.02 * Sin(2 * G360 * dtor)
```

```

CAPL = 280.46 + 36000.77 * SMLT + CAPC

If CAPL > 360 Then
XL360 = CAPL - Int(CAPL / 360) * 360
Else
XL360 = CAPL End If

alpha = XL360 - 2.466 * Sin(2 * XL360 * dtor) + 0.053 * Sin(4 * XL360
* dtor)
'final calculation of EoT
EOT = (XL360 - CAPC - alpha) / 15
End Function

Private Function DEC(time, YRLNG)
'Function to calculate the declination, adapted from WiB software
dtor = 3.14159 / 180
xyr = Year(time) '* splitting of input variable into seperate values
xmo = Month(time) xdy =
Day(time) xhr =
Hour(time) xs =
Second(time)
XLCT = decimalhour(time) '* UT =
XLCT + YRLNG / 15

If xmo > 2 Then
IYR1 = xyr
IMT1 = xmo - 3
Else
IYR1 = xyr - 1
IMT1 = xmo + 9
End If

INTT1 = Int(30.6 * IMT1 + 0.5)
INTT2 = Int(365.25 * (IYR1 - 1976))
SMLT = ((UT / 24) + xdy + INTT1 + INTT2 - 8707.5) / 36525
EPSILN = 23.4393 - 0.013 * SMLT CAPG =
357.528 + 35999.05 * SMLT

If CAPG > 360 Then 'constrain value to 0-360
G360 = CAPG - Int(CAPG / 360) * 360
Else
G360 = CAPG End If

CAPC = 1.915 * Sin(G360 * dtor) + 0.02 * Sin(2 * G360 * dtor) CAPL =
280.46 + 36000.77 * SMLT + CAPC

If CAPL > 360 Then 'constrain value to 0-360
XL360 = CAPL - Int(CAPL / 360) * 360
Else
XL360 = CAPL End If

alpha = XL360 - 2.466 * Sin(2 * XL360 * dtor) + 0.053 * Sin(4 * XL360
* dtor)
GHA = 15 * UT - 180 - CAPC + XL360 - alpha

If GHA > 360 Then 'constrain value to 0-360

```



```

GHA360 = GHA - Int(GHA / 360) * 360
Else
GHA360 = GHA End If

'final calculation of declination
DEC = Atn(Tan(EPSILN * dtor) * Sin(alpha * dtor)) / dtor
End Function

Private Function SOLALT(xlat, xdec, xast)
'Function to calculate the solar altitude, adapted from WiB software
dtor = 3.14159 / 180
sha = 15 * dtor * Abs(12 - xast) 'solar hour angle varies at 15
degrees per hour from solar noon
xdum1 = Sin(xlat * dtor) * Sin(xdec * dtor) + Cos(xlat * dtor) *
Cos(xdec * dtor) * Cos sha)
SOLALT = (Application.Asin(xdum1)) / dtor
End Function

Private Function SOLAZM(xlat, xdec, xast)
'Function to calculate the solar altitude, adapted from WiB software
dtor = 3.14159 / 180
xsolalt = SOLALT(xlat, xdec, xast) '* calculate solalt here, not from
the worksheet

sha = 15 * dtor * Abs(12 - xast)
xdum2 = Cos(xdec * dtor) * (Cos(xlat * dtor) * Tan(xdec * dtor) -
Sin(xlat * dtor) * Cos sha)) / Cos(dtor * xsolalt)
SOLAZM = (Application.Acos(xdum2)) / dtor
If (xast > 12) Then SOLAZM
= 360 - SOLAZM End If
End Function

Private Function daynum(time)
'Function to calculate the day number, adapted from WiB software, used
for ERAD calculation
IYR = Year(time) IMT =
Month(time) IDY =
Day(time)

If (IMT > 2) Then
IYR1 = IYR
IMT1 = IMT - 3
Else
IYR1 = IYR - 1
IMT1 = IMT + 9
End If

'Calculate first reference point
INTT1 = Int(30.6 * IMT1 + 0.5)
INTT2 = Int(365.25 * (IYR1 - 1976))
DN1 = (IDY + INTT1 + INTT2)

'Calculate 2nd reference point
IMT9 = 1
IYR1 = IYR - 1
IMT1 = IMT9 + 9
INTT1 = Int(30.6 * IMT1 + 0.5)
INTT2 = Int(365.25 * (IYR1 - 1976))

```

```
DN2 = (INTT1 + INTT2)
```

```
daynum = DN1 - DN2
```

```
End Function
```

```
Private Function ERAD(time, xsolalt)
```

```
'Function to calculate the extraterrestrial radiation, adapted from WiB software
```

```
dtor = 3.14159 / 180
```

```
DN = daynum(time) '* calculate daynum here
```

```
If (xsolalt > 0) Then
```

```
ERAD = 1367 * (1 + 0.033 * Cos(0.0172024 * DN)) * Sin(xsolalt * dtor)
```

```
Else
```

```
ERAD = 0
```

```
End If
```

```
End Function
```

DiffuseSlope

```
Private Function clearness(Ig, xerad)
```

```
'Simple function to calculate the clearness index
```

```
If Ig > 0 And xerad > 0 Then
```

```
clearness = Ig / xerad
```

```
Else
```

```
clearness = 0
```

```
End If
```

```
End Function
```

```
Private Function DiffuseCalc(Ig, Kt, a0, a1, a2, a3, a4, a5, lowlim, uplim)
```

```
'Function to calculate the horizontal diffuse irradiation from a regression formula
```

```
If IsNumeric(a0) Then 'use the Clarke limits
```

```
Select Case Kt
```

```
Case Is < lowlim
```

```
    K = a0
```

```
Case lowlim To uplim
```

```
K = a1 + a2 * Kt + a3 * Kt ^ 2 + a4 * Kt ^ 3
```

```
Case Is > uplim
```

```
    K = a5
```

```
End Select
```

```
Else 'use the quartic formula
```

```
K = a1 + a2 * Kt + a3 * Kt ^ 2 + a4 * Kt ^ 3 + a5 * Kt ^ 4
```

```
End If
```

```
DiffuseCalc = Ig * K End
```

```
Function
```

```
Private Function INC(xSOLAL, xSOLAZ, WAZ, TLT)
```

```
'Function to calculate the angle between the sun vector and the normal to the surface, adapted from WiB software
```

```
dtor = Application.Pi / 180 '* Changed to use excel's value for Pi xdum3
```

```
= Cos(xSOLAL * dtor) * Cos((xSOLAZ - WAZ) * dtor) * Sin(TLT * dtor)
```

```
+ Sin(xSOLAL * dtor) * Cos(TLT * dtor)
```

```
INC = (Application.Acos(xdum3)) / dtor
```

```
End Function
```

```
Private Function BSRAD(GRAD, DRAD, SOLALT, SOLINC)
```

'Function to determine the slope irradiation beam component, adapted from WiB software

```
dtor = Application.Pi / 180 '*
```

'If the sun is in view of the surface

```
If (SOLALT > 7) And (SOLINC < 90) Then '* Conditional terms combined
BSRAD = (GRAD - DRAD) * Cos(SOLINC * dtor) / Sin(SOLALT * dtor) Else
BSRAD = 0
```

```
End If
```

```
End Function
```

Private Function DSRAD(TLT, GRAD, DRAD, SOLALT, SOLINC, ERAD)

'Function to determine the slope irradiation sky diffuse component, adapted from WiB software

```
Pi = Application.Pi '*
```

```
dtor = Pi / 180
```

```
If (SOLALT <= 0) Then
```

```
DSRAD = 0
```

```
ElseIf (SOLALT > 0 And SOLALT <= 7) Then
```

```
CLRFRA = (GRAD - DRAD) / ERAD
```

```
DSRAD = DRAD * (Cos(TLT * dtor / 2) ^ 2) * (1 + CLRFRA * Sin(TLT * dtor / 2) ^ 3) *
```

```
(1 + CLRFRA * Cos(SOLINC * dtor) ^ 2) * Cos(SOLALT * dtor) ^ 3)
```

```
Else
```

```
If (SOLINC >= 90) Then
```

```
CAPB = 0.252
```

```
CLRFRA = 0
```

```
Else
```

```
' The user may select one of the following four models:
```

```
' CAPB= 0.003 33 -0.415 F -0.698 7 F**2 [for Northern Europe]
```

```
' CAPB= 0.002 63 -0.712 F -0.688 3 F**2 [for Southern Europe]
```

```
' CAPB= 0.080 00 -1.050 F -2.840 0 F**2 [for Japan]
```

```
' CAPB= 0.040 00 -0.820 F -2.026 0 F**2 [for the globe]
```

```
' Model for Northern Europe
```

```
CAPB = 0.00333 - 0.415 * CLRFRA - 0.6987 * CLRFRA ^ 2
```

```
' End of model for Northern Europe
```

```
CLRFRA = (GRAD - DRAD) / ERAD
```

```
End If
```

```
If ((GRAD - DRAD) < 6) Then
```

```
CAPB = 0.168
```

```
CLRFRA = 0
```

```
End If
```

```
TLTFAC = (Cos(TLT * dtor / 2) ^ 2) + CAPB * (Sin(TLT * dtor) - (TLT * dtor)
```

```
* Cos(TLT * dtor) - Pi * Sin(TLT * dtor / 2) ^ 2)
```

```
DSFAC = TLTFAC * (1 - CLRFRA) + CLRFRA * Cos(SOLINC * dtor) / Sin(SOLALT * dtor)
```

```
DSRAD = DSFAC * DRAD End If
```

```
End Function
```

Private Function GroundR(TLT, rho, GRAD)

'Function to calculate the ground-reflected component of the slope irradiation

```
dtor = Application.Pi / 180
```

```
GroundR = rho * GRAD * Sin(0.5 * TLT * dtor) ^ 2
End Function
```

```
Private Function GSRAD(slopebeam, skydiffuse, groundref)
'Simple function to sum the slope irradiation components
GSRAD = slopebeam + skydiffuse + groundref
End Function
```

9.3.3 CellTempEff

```
Private Function SimpleTemp(Islope, Inoct, Tair, Tcnoct, Tanoct, Effstc,
taualpha)
'Simplified cell temperature calculation based on static stc cell
efficiency
temp1 = Islope / Inoct
temp2 = Tcnoct - Tanoct
temp3 = 1 - Effstc / taualpha
SimpleTemp = temp1 * temp2 * temp3 + Tair
End Function
```

```
Private Function HOMERTemp(Islope, Inoct, Tair, Tcnoct, Tanoct, Tcstc,
Effstc, taualpha, alphap)
'More complex cell temperature calculation using linear equation for
cell efficiency, adapted from HOMER solar modelling software
kTcstc = Tcstc + 273 'Convert Tcstc to Kelvin, all other T are used
for differences
temp1 = Tcnoct - Tanoct
temp2 = Islope / Inoct
temp3 = Tair + temp1 * temp2 * (1 - Effstc * (1 - alphap * kTcstc) /
taualpha)
temp4 = 1 + temp1 * temp2 * alphap * Effstc / taualpha
HOMERTemp = temp3 / temp4
End Function
```

```
Private Function Cellefficiency(Effcellstc, alphap, Tcell, Tcstc)
'Simple function to calculate cell efficiency from cell temperature and
alpha, the temperature coefficient
Cellefficiency = Effcellstc + alphap * (Tcell - Tcstc)
End Function
```

```
Private Function CellEfficiency2(Effcellstc, Islope, gamma, alphap,
Tcell, Tcstc)
'Function using both cell temperature and slope irradiation to calculate
cell efficiency, from Mattei et al
beta = (-alphap) / Effcellstc
CellEfficiency2 = Effcellstc * (1 - beta * (Tcell - Tcstc) + gamma *
Application.WorksheetFunction.Log10(Islope))
End Function
```

ThermalModel

```
Private Function SkyTemp(airTemp)
'Equation to obtain the effective sky temperature for thermal radiation
SkyTemp = 0.0552 * airTemp ^ 1.5
End Function
```

```
Private Function HeatTransferAir(windSpeed)
'A range of equations to determine the coefficient of convective heat
```

```

transfer to the air
HeatTransferAir = 5.67 + 3.8 * windSpeed 'McAdams in Duffie &
Beckman
'HeatTransferAir = 5.82 + 4.07 * windSpeed 'Nolay
'HeatTransferAir = 0.5 * (11.4 + 5.7 + 5.7 * windSpeed) 'Cole &
Sturrock, adapted
'HeatTransferAir = 14.4 'Sadnes & Reckstad
'HeatTransferAir = 5 + 1 * windSpeed 'My Optimised Model
End Function

Private Function HeatTransferSky(phi, sigma, Tc, Tsky)
'Function to calculate the heat transfer coefficient to the sky
temp1 = phi * sigma * (Tc ^ 4 - Tsky ^ 4)
temp2 = Tc - Tsky
HeatTransferSky = temp1 / temp2
End Function

Private Function CellTemp(GSRAD, taualpha, cellEffSTC, Tsky, Ta, hcs,
hca)
'Implementation of energy balance equation to determine cell temperature
temp1 = GSRAD * taualpha * (1 - cellEffSTC) + hcs * Tsky + 2 * hca *
Ta
temp2 = hcs + 2 * hca
CellTemp = temp1 / temp2
End Function

Private Sub CellTempThermal()
'Macro to calculate the cell temperature via thermal model. Activated by
button click from spreadsheet.
Dim flag As Boolean

'read in constants
cellEffSTC = Cells(2, 9).Value
taualpha = Cells(3, 9).Value
sigma = Cells(4, 9).Value
phi = Cells(5, 9).Value

For i = 3 To 171 'set the range of calculation (time period)
'read in time-variant values
GSRAD = Cells(i, 2).Value
windSpeed = 4.75
windSpeed = Cells(i, 4).Value / 3
Ta = Cells(i, 3).Value + 273.15
Tc = Ta + 10 'set initial cell temp estimate
flag = False 'initialise flag

Tsky = SkyTemp(Ta)
hca = HeatTransferAir(windSpeed)

'Start the iterative calculation
Do
    hcs = HeatTransferSky(phi, sigma, Tc, Tsky)
    Tco = CellTemp(GSRAD, taualpha, cellEffSTC, Tsky, Ta, hcs,
hca)
    'Compare the newly-calculated value with the previous
    If Abs(Tc - Tco) < 0.01 Then
        flag = True
    Else
        Tc = Tco
    End If
Loop While flag = False 'Continue until stable value reached

```

```
'Write the result out to the spreadsheet
Cells(i, 5).Value = Tc - 273.15
Next i
End Sub
```

Sheet10 (Graphical Display Code)

```
Private Sub Worksheet_SelectionChange(ByVal Target As Excel.Range)
'This sub will select the correct data range for the chart based on the
day selected
'Runs whenever the correct cell is SELECTED
```

```
If Target.Address = "$B$5" Then
'Choose the correct range and write to the chart
ActiveSheet.ChartObjects("Chart 2").Activate Select Case
Range("B5").Value
Case "28/05/2013"
ActiveChart.SetSourceData Source:=Sheets("Graphical Display
Data").Range("A25:BL82")
Case "29/05/2013"
ActiveChart.SetSourceData Source:=Sheets("Graphical Display
Data").Range("A82:BL226")
Case "30/05/2013"
ActiveChart.SetSourceData Source:=Sheets("Graphical Display
Data").Range("A227:BL427")
Case "31/05/2013"
ActiveChart.SetSourceData Source:=Sheets("Graphical Display
Data").Range("A428:BL715")
Case "01/06/2013"
ActiveChart.SetSourceData Source:=Sheets("Graphical Display
Data").Range("A716:BL1003")
Case "02/06/2013"
ActiveChart.SetSourceData Source:=Sheets("Graphical Display
Data").Range("A1004:BL1295")
Case "03/06/2013"
ActiveChart.SetSourceData Source:=Sheets("Graphical Display
Data").Range("A1296:BL1580")
Case "04/06/2013"
ActiveChart.SetSourceData Source:=Sheets("Graphical Display
Data").Range("A1581:BL1868")
Case "05/06/2013"
ActiveChart.SetSourceData Source:=Sheets("Graphical Display
Data").Range("A1869:BL2156")
Case "06/06/2013"
ActiveChart.SetSourceData Source:=Sheets("Graphical Display
Data").Range("A2157:BL2444")
Case "07/06/2013"
ActiveChart.SetSourceData Source:=Sheets("Graphical Display
Data").Range("A2445:BL2600")
End Select
End If

End Sub
```

```
Private Sub Worksheet_Change(ByVal Target As Range)
'This sub will change 'Chart 3', the scatter plot, whenever an
appropriate cell is CHANGED.
If Target.Address = "$Q$5" Or Target.Address = "$S$5" Or
Target.Address = "$S$7" Or Target.Address = "$S$8" Then
```

```

'Delete the existing scatter plot, if any, and create a new one
based on the two data values selected
xValue = Range("Q5").Value yValue =
Range("S5").Value
If IsEmpty(xValue) = False And IsEmpty(yValue) = False Then
Dim cht As Chart
Dim chObj As ChartObject

'Delete all charts on the sheet bar 'Line Chart', the time- series
plot
For Each chtObj In Sheets("Graphical Display").ChartObjects
If Not (chtObj.Name = "Line Chart") Then
chtObj.Delete
End If
Next

startRow = Range("S7").Value endRow =
Range("S8").Value

With Sheets("Graphical Display Data 2")
'Determine the source of x data
xColumn = 2
Do
xColumn = xColumn + 1
Loop Until .Cells(24, xColumn) = xValue
'Determine the source of y data yColumn = 2
Do
yColumn = yColumn + 1
Loop Until .Cells(24, yColumn) = yValue
End With

'Create and position the new chart
Set cht = Worksheets("Graphical
Display").ChartObjects.Add(Left:=1320, Width:=600, Top:=180,
Height:=400).Chart
cht.ChartType = xlXYScatter
cht.SeriesCollection.NewSeries

'Set the source data for the chart
With Sheets("Graphical Display Data 2")
cht.FullSeriesCollection(1).XValues
= .Range(.Cells(startRow, xColumn), .Cells(endRow, xColumn))
cht.FullSeriesCollection(1).Values = .Range(.Cells(startRow, yColumn),
.Cells(endRow, yColumn))
End With

'Remove the legend and add a title cht.SetElement
(msoElementLegendNone) cht.SetElement
(msoElementChartTitleAboveChart) cht.ChartTitle.Text =
"X-Y Comparison"

'Add individual axis titles
cht.SetElement
(msoElementPrimaryCategoryAxisTitleAdjacentToAxis)
cht.SetElement (msoElementPrimaryValueAxisTitleAdjacentToAxis)
'Doesn't work
'cht.Axes(xlValue, xlPrimary).AxisTitle.Text = yValue
cht.Axes(xlCategory, xlPrimary).AxisTitle.Text = xValue
cht.Axes(xlCategory).HasMajorGridlines = True

```

```
'Add a trendline
With cht.FullSeriesCollection(1)
.Trendlines.Add
.Trendlines(1).DisplayEquation = True
.Trendlines(1).DisplayRSquared = True
End With
End If
End If
End Sub
```

Sub Checkbox_Click()

```
'Ensure the data table is updated correctly when a checkbox is changed
Sheets("Graphical Display Data").Calculate
End Sub
```

ThisWorkbook (Code applying to the workbook as a whole.)

Private Sub Workbook_SheetChange(ByVal Sh As Object, ByVal Target As Range)

```
'This sub runs a calculate on any sheet whose data is changed by the
user, overriding the application
''manual' mode while still speeding up spreadsheet operation.
'Special consideration is given to Graphical Display Data, which must be
updated when the Graphical
'Display sheet is changed (This now superseded by table control code.)
```

```
Select Case Sh.Name
Case "Graphical Display"
Sheets("Graphical Display Data").Calculate
Case Else
Sh.Calculate
End Select
```

```
End Sub
```


Appendix D: SSE System Documents

Project Title: Jewel & Esk Ground Mount

Item	Description		
1.00	Panels Total	£	331,788.80
2.00	Inverter Total	£	103,040.00
3.00	Mounting System Total	£	180,908.80
4.00	Meters Total	£	897.00
5.00	Accessories Total	£	33,466.38
6.00	Cabling Total	£	67,666.00
7.00	Installation Total	£	36,680.40
8.00	Groundswork Total	£	6,458.40
9.00	Miscellaneous Total	£	12,075.00
10.00	Transformer Total	£	106,375.00
	Total	£	879,355.78

SSE System Pricing, Source: (SSE, 2013)

Project Name: Variant Reference: Designer: **Jewel & Esk College** 11/05/2012
 Option 8 CSun 245 & Siemens inverter
 SP



Location: Climate Data Record: PV Output: **Edinburgh**
 Gross/Active PV Surface Area: **Edinburgh (1981-2000)**
 627.20 kWp
 4,156.42 / 4,154.07 m²

PV Array Irradiation: Energy Produced by PV Array (AC): Grid Feed-In: **4,376,046 kWh**
568,611 kWh
568,611 kWh

System Efficiency: Performance Ratio: Inverter Efficiency: PV Array Efficiency: **13.0 %**
86.1 %
 Specific Annual Yield: **95.6 %**
 CO2 Emissions Avoided: **13.6 %**
906.5 kWh/kWp
322,954 kg/a

The results are determined by a national model calculation. The actual yields of the photovoltaic system can differ from these values due to fluctuations in the weather, the efficiency modules and inverters, and other factors. The System Diagram above does not represent and cannot replace a full technical drawing of the PV system.

SAP 2005
 Customer Name: Jewel and Esk College
 Project Reference: 627 kWp Solar PV system
 Date: 06/05/2012

SAP Calculator:

System Size (kWp)	627.20		
Orientation	0		
Module pitch	31		
Radiation from Orientation (S)	1042		
Shading factor (Zpv)	1		
SAP 2005:	522833.92 kWh		

Total output 522833.92 kWh

S = annual solar radiation from table H2					
Tilt of collector	Orientation of collector				
	South	SE/SW	E/W	NE/NW	North
Horizontal	933				
30°	1042	997	886	762	709
45°	1023	968	829	666	621
60°	960	900	753	580	485
Vertical	724	684	565	427	360

Zpv = overshadowing factor from table H4		
Overshading	% of sky blocked by obstacles	Overshading factor
Heavy	>80%	0.5
Significant	>60% - 80%	0.65
Modest	20% - 60%	0.8
None or very little	<20%	1

Based on SAP 2005 Edition revision 2.
 System power output (kwh per annum) as per SAP calc = 0.8 X kWp x S x Zpv

SSE Shading Analysis (note Zpv value of 1) , Source: (SSE, 2013)

Appendix E – Solar Farm Blockage Data

First Row-Left	Angel (degrees°)		Degrees	Minutes	Seconds	Degrees	Inclination
	0°(east)	76°05'20"	76	5	20	76.089	13.911
	30°	74°15'20"	74	15	20	74.256	15.744
	60°	80°03'40"	80	3	40	80.061	9.939
	90°	74°33'00"	74	33	0	74.550	15.450
	120°	67°19'40"	67	19	40	67.328	22.672
	150°	76°34'40"	76	34	40	76.578	13.422
	180°	-	-			-	-
First Row-Centre	0°(east)	80°33'00"	80	33	0	80.550	9.450
	30°	77°52'40"	77	52	40	77.878	12.122
	60°	77°36'00"	77	36	0	77.600	12.400
	90°	80°38'20"	80	38	20	80.639	9.361
	120°	69°59'00"	69	59	0	69.983	20.017
	150°	64°50'10"	64	50	10	64.836	25.164
	180°	72°49'30"	72	49	30	72.825	17.175
First Row- Right	0°(east)	85°58'10"	85	58	10	85.969	4.031
	30°	78°59'40"	78	59	40	78.994	11.006
	60°	81°19'50"	81	19	50	81.331	8.669
	90°	69°02'20"	69	2	20	69.039	20.961
	120°	61°24'20"	61	24	20	61.406	28.594
	150°	63°47'10"	63	47	10	63.786	26.214
	180°	73°16'50"	73	16	50	73.281	16.719
Second Row- Right	0°(east)	82°59'40"	82	59	40	82.994	7.006
	30°	80°09'20"	80	9	20	80.156	9.844
	60°	81°55'10"	81	55	10	81.919	8.081
	90°	72°47'50"	72	47	50	72.797	17.203
	120°	58°59'10"	58	59	10	58.986	31.014
	150°	68°59'40"	68	59	40	68.994	21.006
	180°	72°23'40"	72	23	40	72.394	17.606
Third Row- Right	0°(east)	85°02'10"	85	2	10	85.036	4.964
	30°	81°25'10"	81	25	10	81.419	8.581
	60°	82°14'40"	82	14	40	82.244	7.756
	90°	71°24'50"	71	24	50	71.414	18.586
	120°	60°42'00"	60	42	0	60.700	29.300
	150°	62°47'00"	62	47	0	62.783	27.217
	180°	72°23'40"	72	23	40	72.394	17.606
Fourth Row- Left	0°(east)	81°13'30"	81	13	30	81.225	8.775
	30°	78°25'10"	78	25	10	78.419	11.581
	60°	76°02'30"	76	2	30	76.042	13.958
	90°	80°49'50"	80	49	50	80.831	9.169
	120°	78°03'40"	78	3	40	78.061	11.939
	150°	75°43'00"	75	43	0	75.717	14.283
	180°	81°41'50"	81	41	50	81.697	8.303

Fourth Row- Centre	0°(east)	82°59'00"	82	59	0	82.983	7.017
	30°	81°01'30"	81	1	30	81.025	8.975
	60°	79°39'40"	79	39	40	79.661	10.339
	90°	75°06'20"	75	6	20	75.106	14.894
	120°	62°33'30"	62	33	30	62.558	27.442
	150°	72°13'30"	72	13	30	72.225	17.775
	180°	84°02'00"	84	2	0	84.033	5.967
Fourth Row- Right	0°(east)	84°13'30"	84	13	30	84.225	5.775
	30°	82°53'20"	82	53	20	82.889	7.111
	60°	81°51'20"	81	51	20	81.856	8.144
	90°	75°37'10"	75	37	10	75.619	14.381
	120°	63°33'40"	63	33	40	63.561	26.439
	150°	63°40'50"	63	40	50	63.681	26.319
	180°	70°30'40"	70	30	40	70.511	19.489
Eight Row- Left	0°(east)	85°30'00"	85	30	0	85.500	4.500
	30°	84°15'10"	84	15	10	84.253	5.747
	60°	84°55'30"	84	55	30	84.925	5.075
	90°	73°31'50"	73	31	50	73.531	16.469
	120°	71°00'50"	71	0	50	71.014	18.986
	150°	72°34'10"	72	34	10	72.569	17.431
	180°	-	-			-	-
Eight Row- Centre	0°(east)	85°36'10"	85	36	10	85.603	4.397
	30°	83°07'30"	83	7	30	83.125	6.875
	60°	79°04'30"	79	4	30	79.075	10.925
	90°	74°04'30"	74	4	30	74.075	15.925
	120°	76°55'40"	76	55	40	76.928	13.072
	150°	71°55'30"	71	55	30	71.925	18.075
	180°	-	-			-	-
Eight Row- Right	0°(east)	74°26'20"	74	26	20	74.439	15.561
	30°	76°27'00"	76	27	0	76.450	13.550
	60°	70°40'10"	70	40	10	70.669	19.331
	90°	84°50'00"	84	50	0	84.833	5.167
	120°	82°06'10"	82	6	10	82.103	7.897
	150°	82°24'50"	82	24	50	82.414	7.586
	180°	-	-			-	-
17th Row- Left	0°(east)	67°14'00"	67	14	0	67.233	22.767
	30°	73°36'20"	73	36	20	73.606	16.394
	60°	67°12'40"	67	12	40	67.211	22.789
	90°	83°61'10"	83	61	10	84.019	5.981
	120°	76°55'40"	76	55	40	76.928	13.072
	150°	71°55'30"	71	55	30	71.925	18.075
	180°	-	-			-	-

Appendix F: MATLAB codes

Reading data from excel primary data

```
alldata=xlsread('primarydata.xlsx');
%%all the data from excel sheet is imported to matlab environment.
month=alldata(:,1);
%%first column of the transfered data is dedicated to month
day=alldata(:,2);
%%second column of the transfered data is dedicated to day
hours=alldata(:,3);
%%third column of the transfered data is dedicated to month
LSM=alldata(:,4);
year=alldata(:,5);
ut=hours+(LSM/60);
%% Exact hour where LSM is minuets
```

Yallop's algorithm to calculate sun declination and equation of time

```
if month>2
%% Yallop's algorithm to calculate solar declination and equation of time,
it has been implemented trough three if function to check the conditions.
year=year;
month=month-3;
t=((ut/24)+day+floor(30.6*month+0.5)+floor(365.25*(year-1976))-
8707.5)/36525;
else
year=year-1;
month=month+9;
t=((ut/24)+day+floor(30.6*month+0.5)+floor(365.25*(year-1976))-
8707.5)/36525;
end
d2r=3.14159/180;
g=357.528+(35999.05*t);
if g>360
g360=g-(floor(g/360)*360);
else
g360=g;
end
c=(1.915*sin(g360*d2r))+(0.02*sin(2*g360*d2r));
l=280.46+(36000.77*t)+c;
if l>360
l360=l-(floor(l/360)*360);
else
l360=l;
end
alpha=l360-(2.466*sin(2*l360*d2r))+(0.053*sin(4*l360*d2r));
epsilon=23.4393-(0.013*t);
dec=atan(tan(epsilon*d2r).*sin(alpha*d2r))/d2r;
eot=(l360-c-alpha)/15;
```

Greenwich hour angle

```
lat=55.95;
horang=15*d2r*abs(12-(1*hours-0.5));
trml2=(-tan(lat*d2r))*(tan(dec*d2r));
hafday=(1/15)*acos(trml2)/d2r;
srt=12-hafday;
sst=12+hafday;
minhour=(hours-1);
if minhour==floor(srt)
horang=15*d2r*abs(12-0.5*(hours+srt));
end
if minhour==floor(sst)
horang=15*d2r*abs(12-0.5*(hours-1+sst));
```

```
end
```

Solar geometry

```
%solalt
x1=(sin(lat*d2r)*sin(dec*d2r)+(cos(lat*d2r)*cos(dec*d2r).*cos(horang));
solalt=asin(x1)/d2r;
%solazm
x2=(cos(dec*d2r).*((cos(lat*d2r)*tan(dec*d2r))-
(sin(lat*d2r).*cos(horang))))./(cos(solalt*d2r));

solazm=acos(x2)/d2r;
%sun inclination (for loop has been used to constrain the values between 0-
360)
```

```
for n=1:1357;
```

```
if hours(n,1)>12
solazm(n,1)=360-solazm(n,1);
else
solazm(n,1)=solazm(n,1);
end
end
tilt=30;
aspect=180;
x3=(cos(solalt*d2r).*cos((solazm-
aspect)*d2r)*sin(tilt*d2r)+(sin(solalt*d2r)*cos(tilt*d2r));
inc=acos(x3)/d2r;
```

Hourly horizontal global irradiation

```
%ERAD (Exteraterrestrial radiation)
for n=1:1357;
if solalt(n,1)>0

erad(n,1)=1367*(1+0.033.*cos(0.0172024*daynumber(n,1))).*sin(solalt(n,1)*d2r);
else
erad(n,1)=0
end
end
% Ig (To read the measured horizontal global irradiation values)
ig=alldata(:,13);
% Kt (clearness index)
for n=1:1357;
if ig(n,1)>0 && erad(n,1)>0
kt(n,1)=ig(n,1)/erad(n,1);
else
kt(n,1)=0;
end
end
%Id (hourly horizontal diffuse radiation)
for n=1:1357;
if erad(n,1)>ig(n,1)
id(n,1)=ig(n,1)*(1.006-(0.317*kt(n,1))+(3.1241*(kt(n,1))^2)-
(12.7616*(kt(n,1))^3)+(9.7166*(kt(n,1))^4));
else
id(n,1)=ig(n,1);
end
end
```

Hourly global slop irradiation

```
%slop beam irradiation
```

```

for n=1:1357;
if solalt(n,1)>7 && inc(n,1)<90
bsrad(n,1)=((ig(n,1)-id(n,1))*cos(inc(n,1)*d2r))/sin(solalt(n,1)*d2r);
else
bsrad(n,1)=0;
end
end

```

```

%Diffuse irradiation on a tilted surface
for n=1:1357;
if solalt(n,1)<=0
dsrad(n,1)=0;
else
dsrad(n,1)=id(n,1)*(cos(tilt*d2r/2)^2);
end
end

```

```

%Ground reflection
for n=1:1357;
if ig(n,1)<=0
gref(n,1)=0
else
gref(n,1)=0.2.*ig(n,1)*(sin(0.5*tilt*d2r)^2);
end
end

```

Block dedication for specific azimuths (Block first row-left)

%first row left block (In this loop blocks related to different azimuths are dedicated)

```

myaz=alldata(:,11);
solal=alldata(:,8);

```

```

for n=1:1357;
if myaz(n,1)>=0 && myaz(n,1)<=15
bfrl(n,1)=13.911;
end
if myaz(n,1)>=16 && myaz(n,1)<=45
bfrl(n,1)=15.744;
end
if myaz(n,1)>=46 && myaz(n,1)<=75
bfrl(n,1)=9.939;
end
if myaz(n,1)>=76 && myaz(n,1)<=105
bfrl(n,1)=15.45;
end
if myaz(n,1)>=106 && myaz(n,1)<=135
bfrl(n,1)=22.672;
end
if myaz(n,1)>=136 && myaz(n,1)<=165
bfrl(n,1)=13.422
end
if myaz(n,1)<0
bfrl(n,1)=0
end
end

```

Blocks modification

Shading analysis (this loop will check in which hours the point is in %shade)


```

for n=1:1357;
if solal(n,1)>bfrl(n,1)
mbfrl(n,1)=0;
else
mbfrl(n,1)=bfrl(n,1);
end
end

```

Sky view factor

```

for n=1:1357;
skyview1(n,1)=1-
((30*3.141592/180)*(mbfrl(n,1)*3.141592/180))/(cos(15)^2);
end

```

Global slop irradiation with consideration to shade

```

for n=1:1357;
if skyview1(n,1)==1;
shadingeffect1(n,1)=(bsrad(n,1)+(dsrad(n,1)+(gref(n,1)))/2;
else

```

```

shadingeffect1(n,1)=(dsrad(n,1)*skyview1(n,1)+(gref(n,1)*skyview1(n,1)))/
2;
end
end

```

Mean global horizontal irradiation (December)

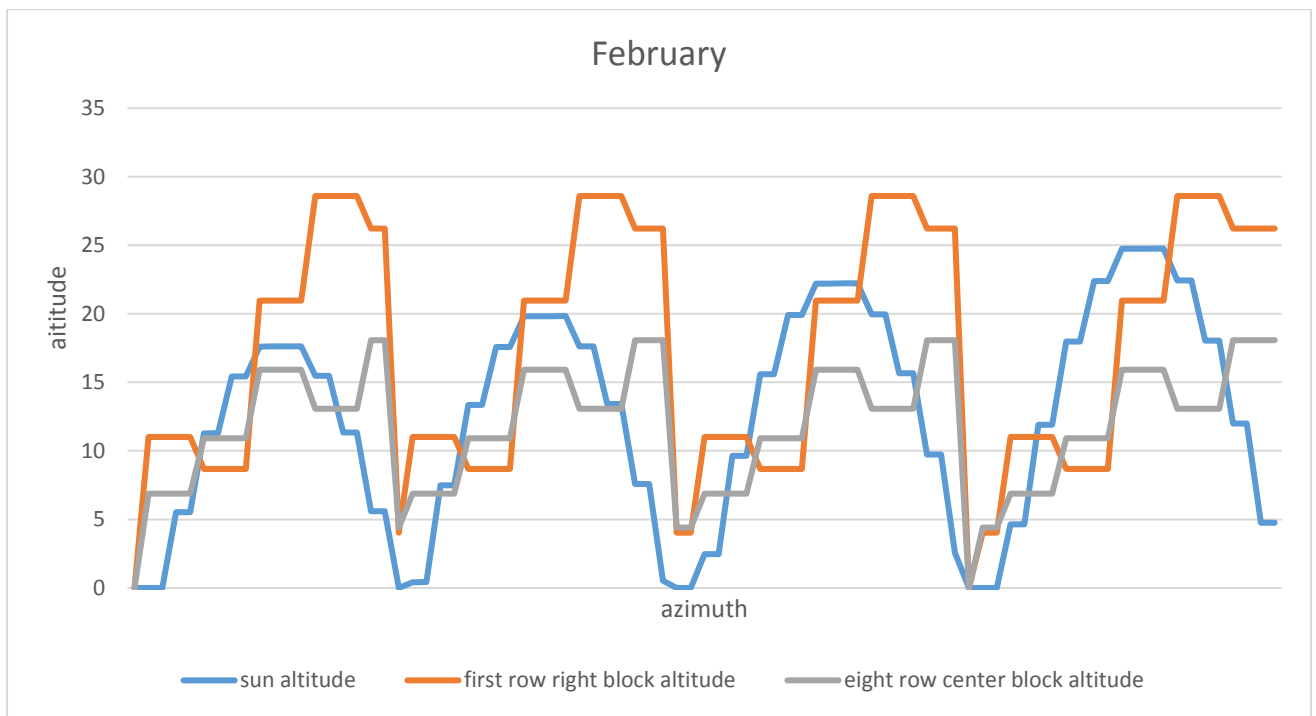
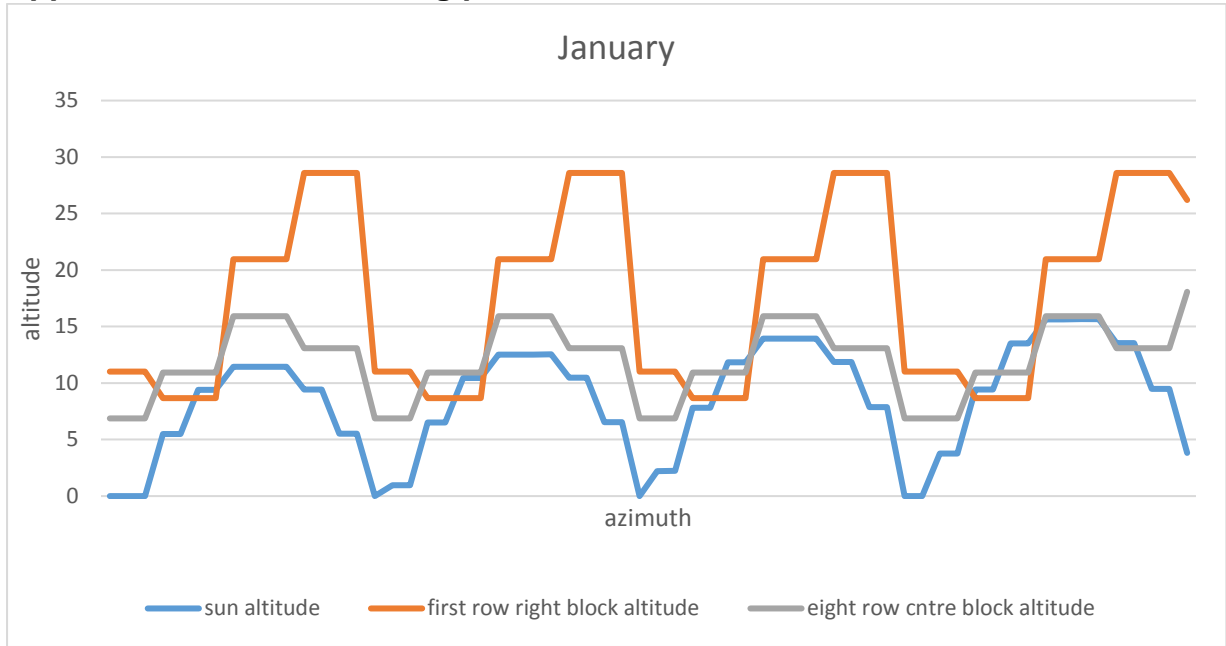
```

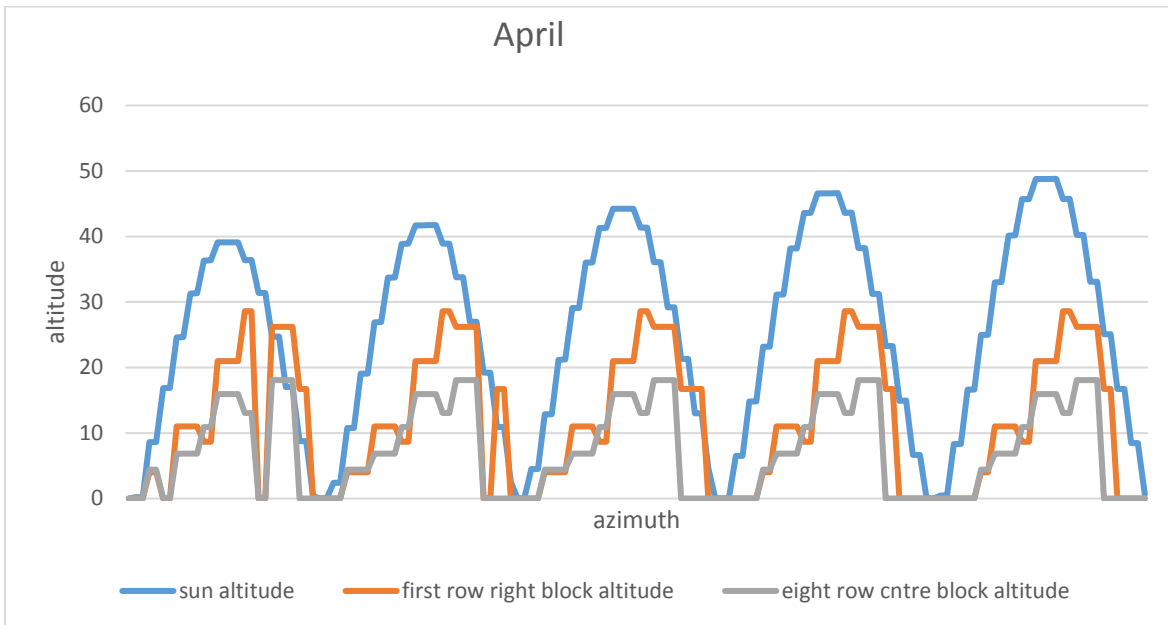
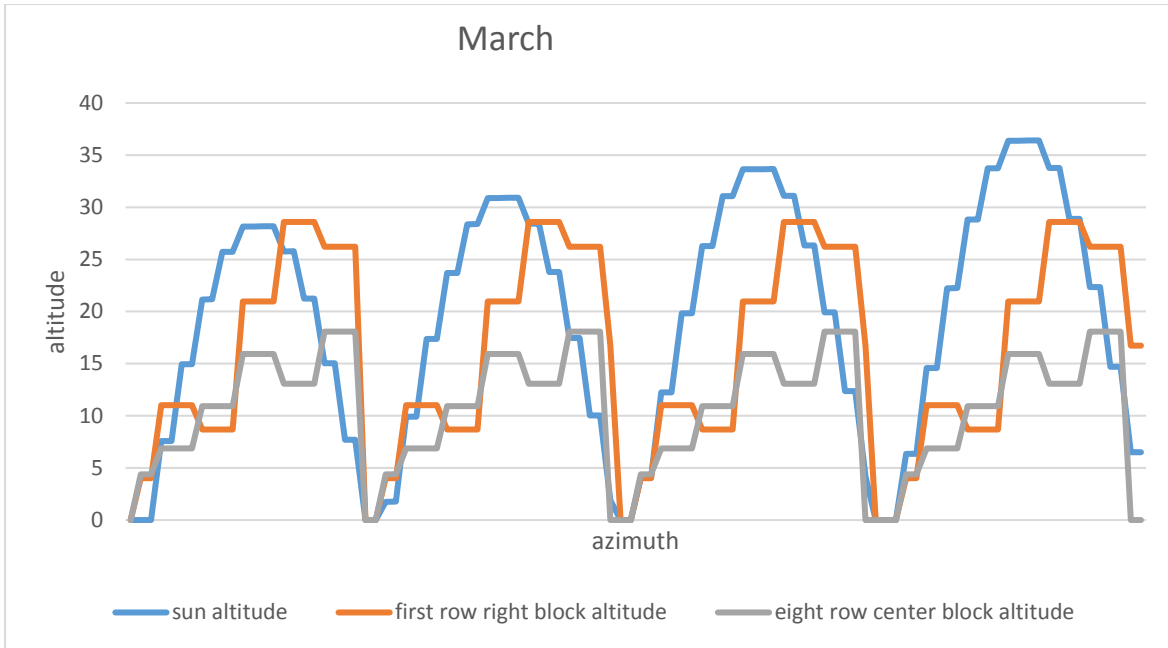
alldata=xlsread('december.xlsx');
N=1;
M=1;
index(1,1)=1;
while N<=length(alldata(:,2))
if alldata(N,1)==M
else
index(M+1,1)=N;
M=M+1;
end
N=N+1;
end
index(M+1,1)=N;
m=1;
for n=1:28
for x=index(n):(index(n+1)-1)
daily(m,n)=alldata(x,4);
m=m+1;
end
m=1;
end

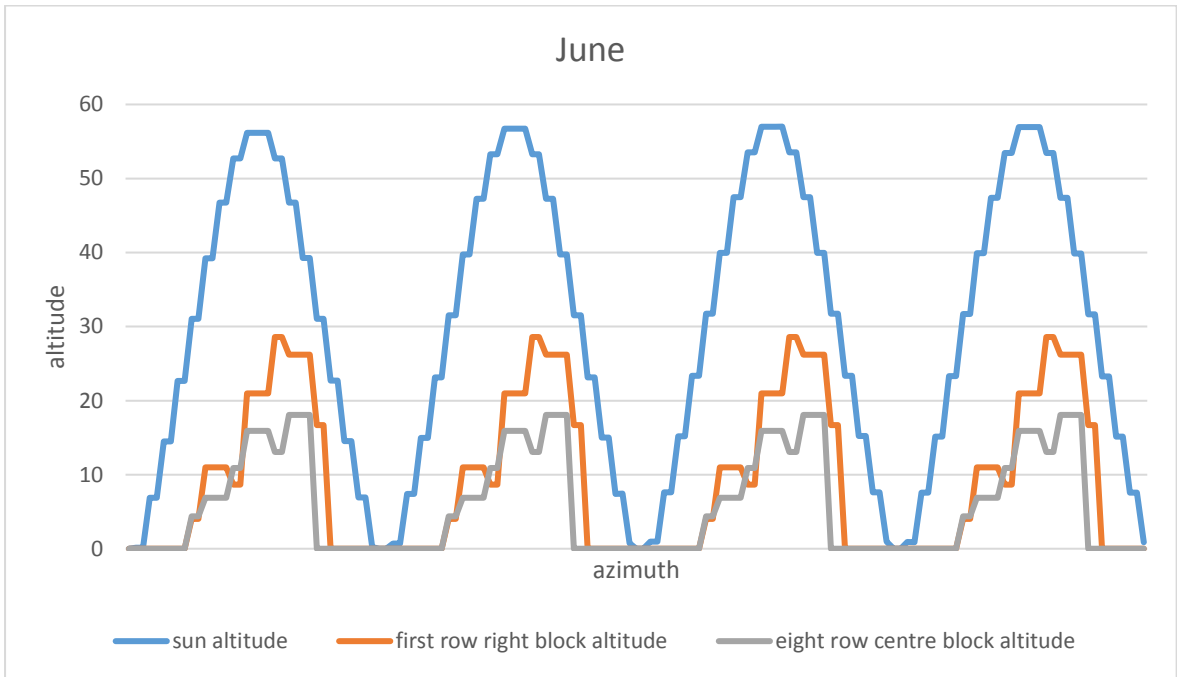
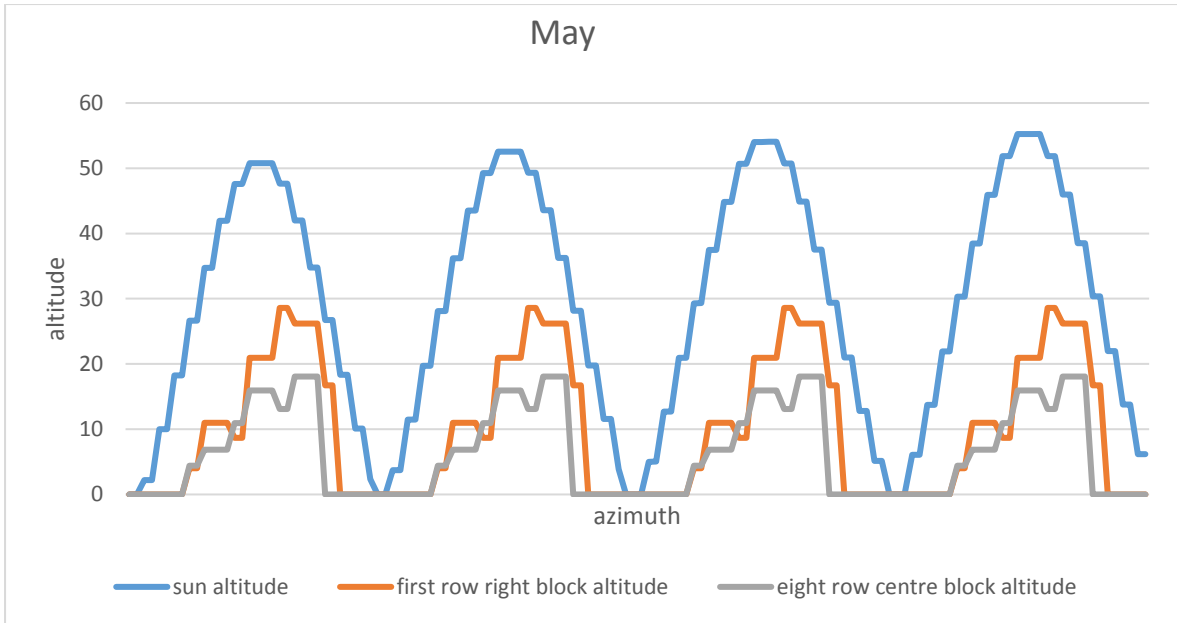
for i=1:24
meandaily(i,:)=mean(daily(i,:));
i=i+1;
end

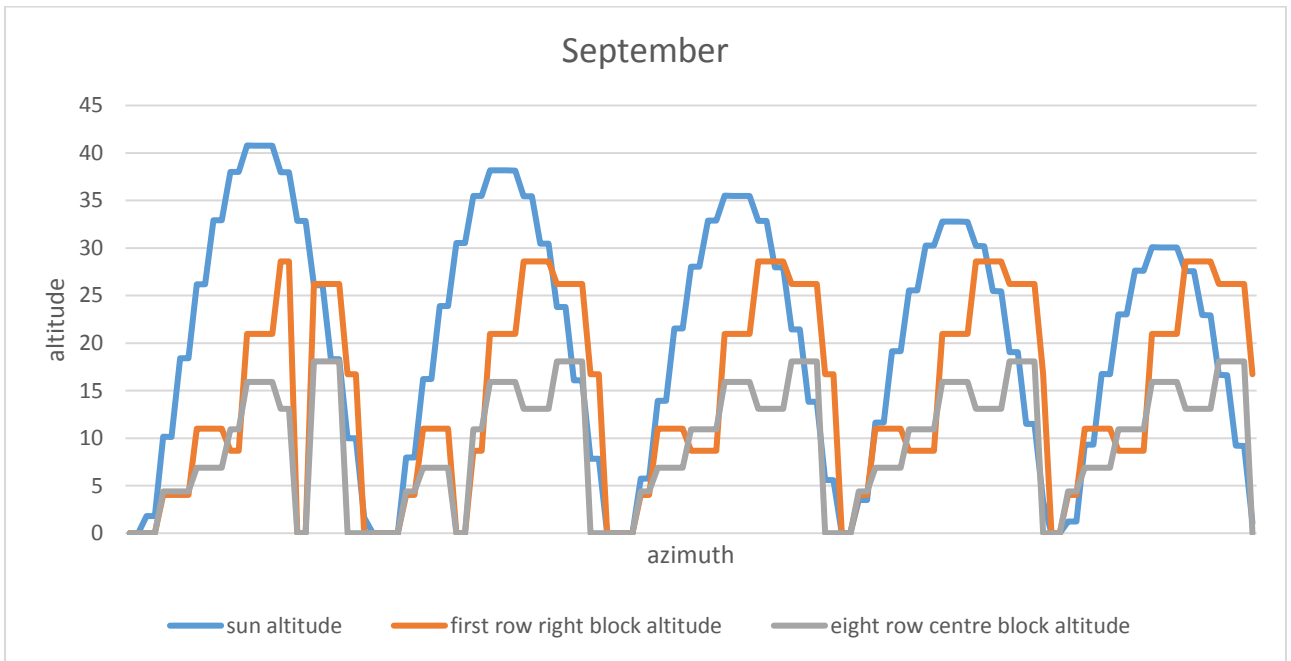
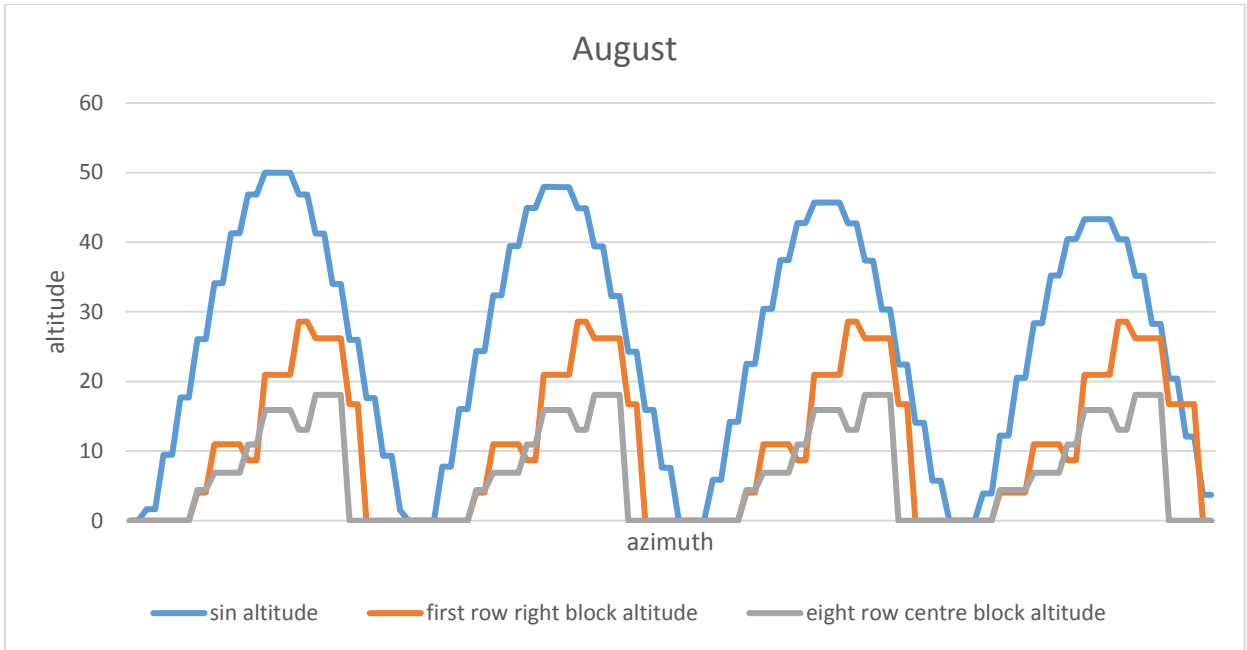
```

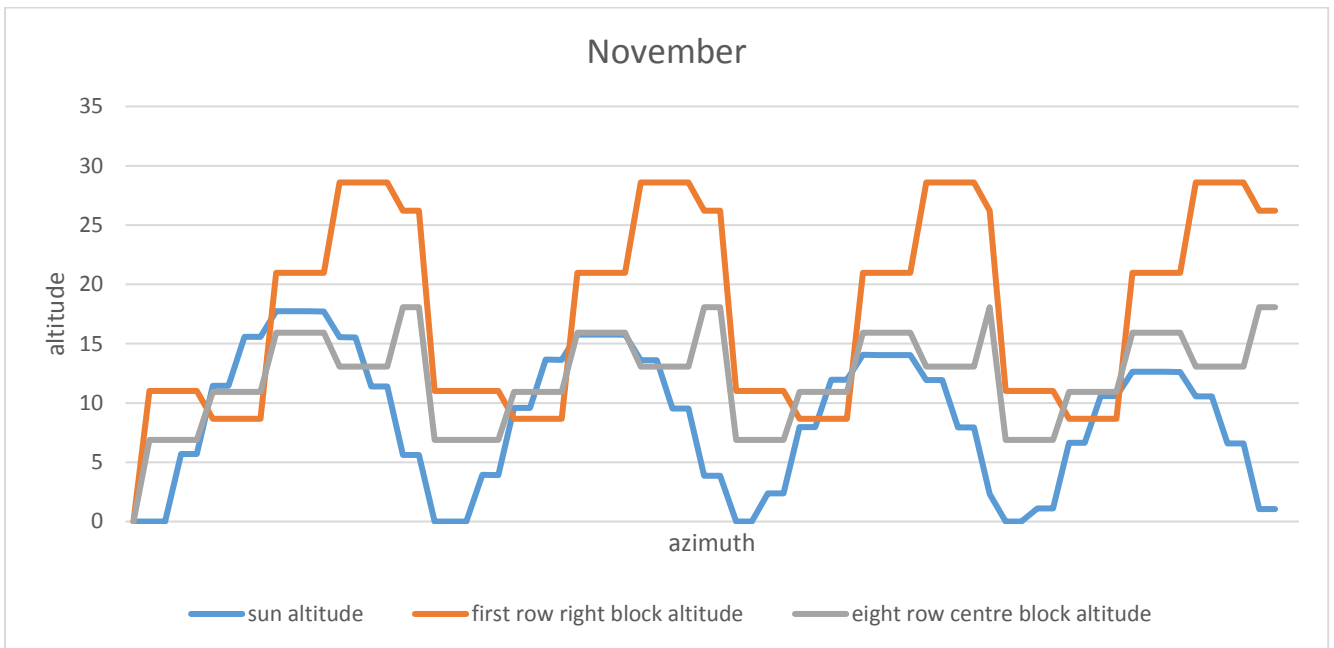
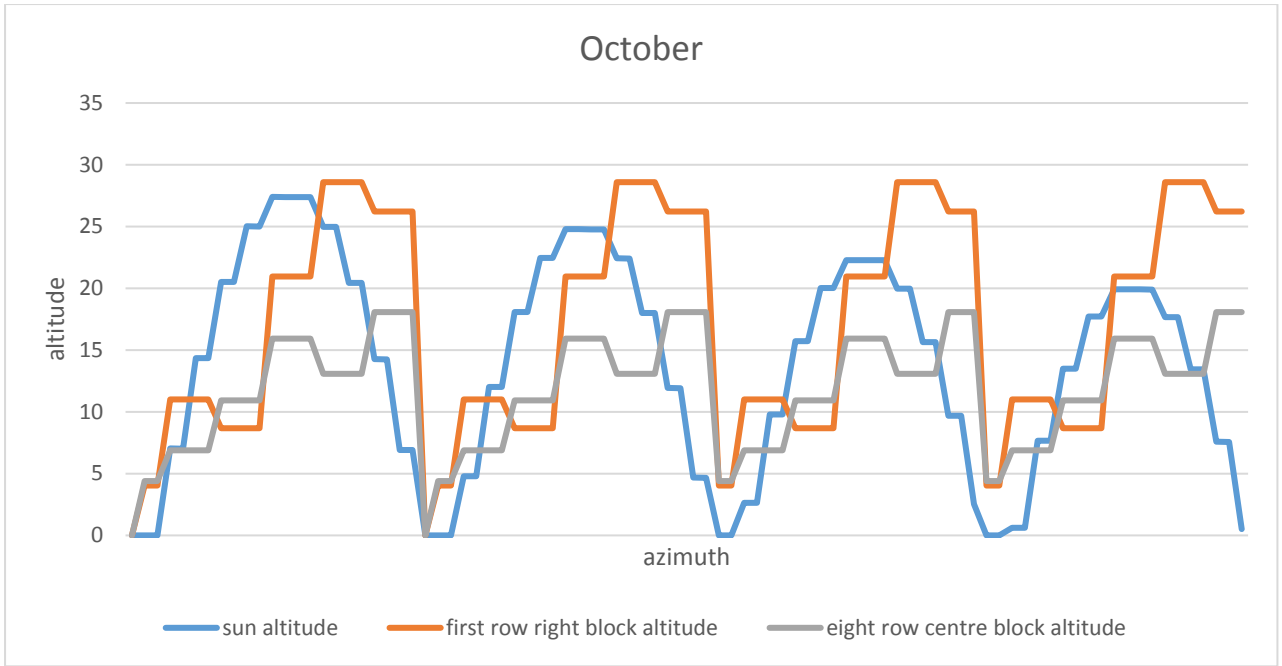
Appendix G – Linear Shading plots



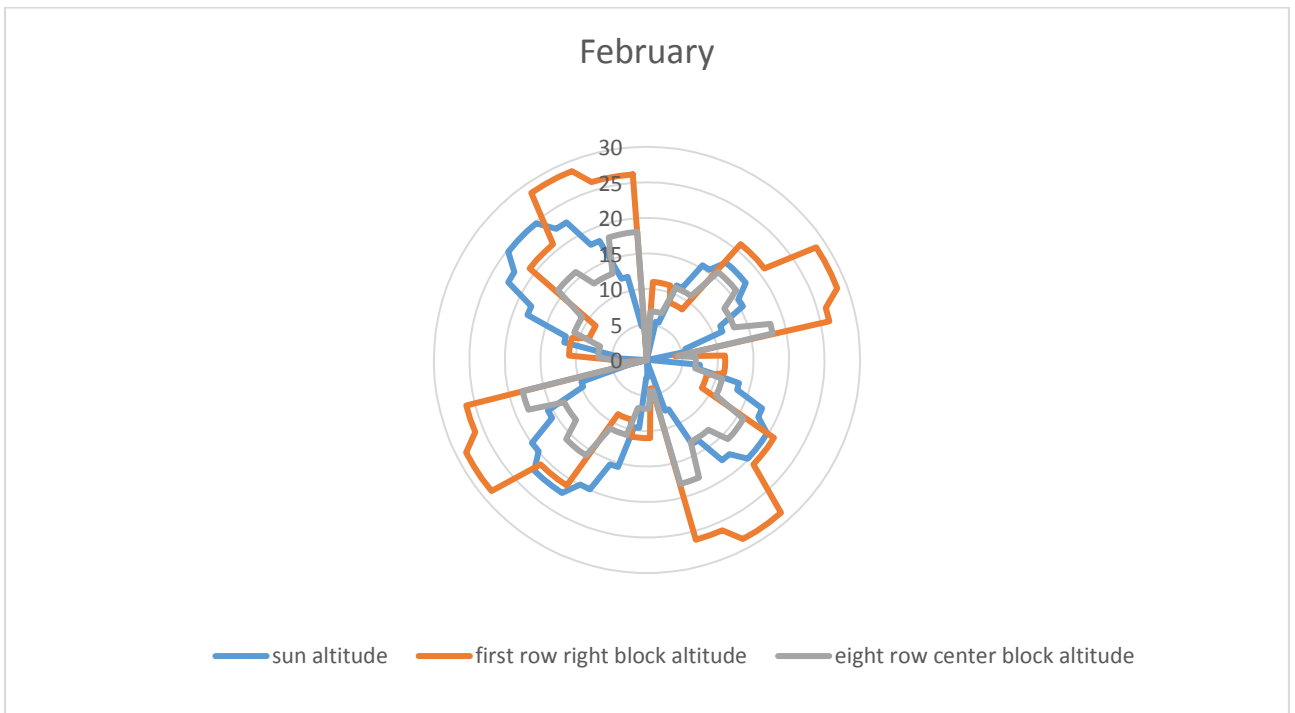
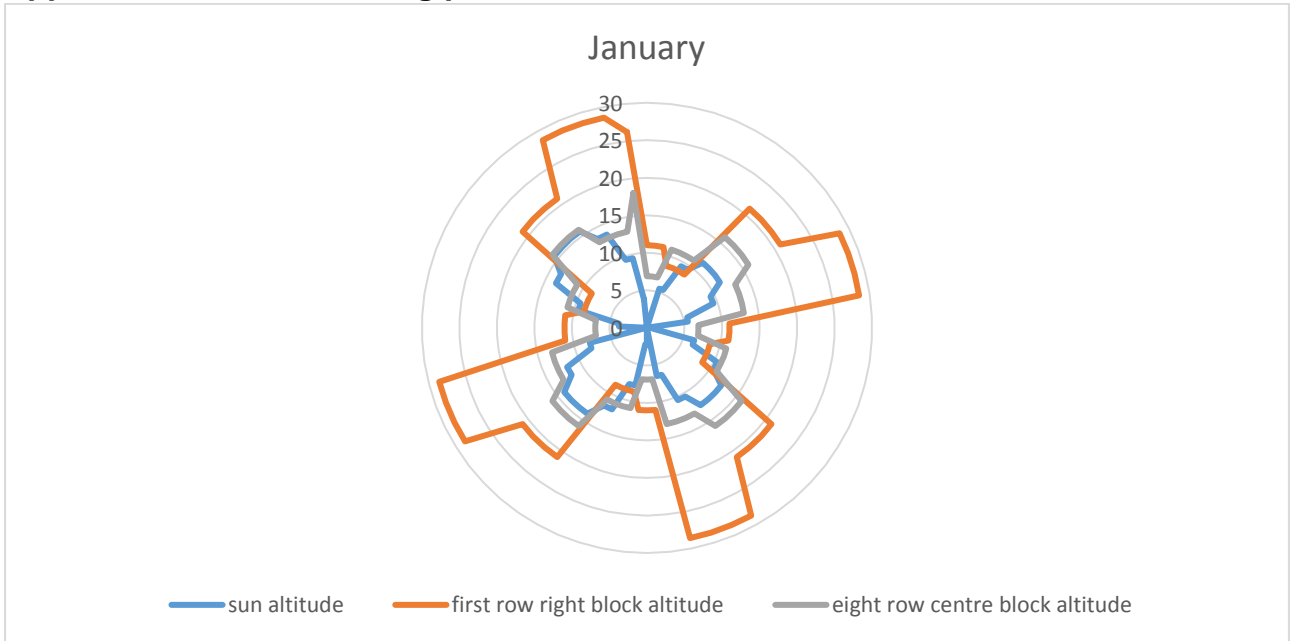




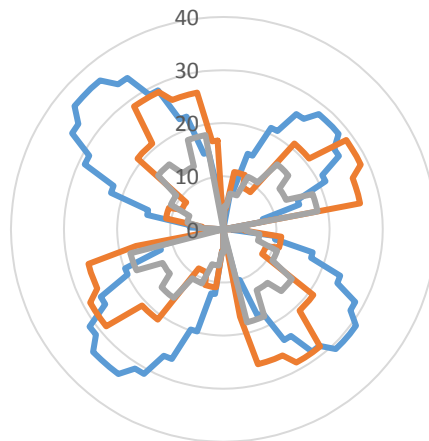




Appendix H– Radar Shading plots

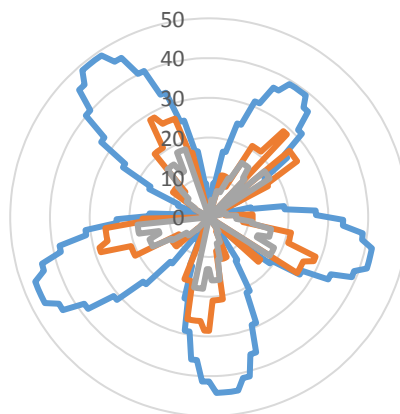


March



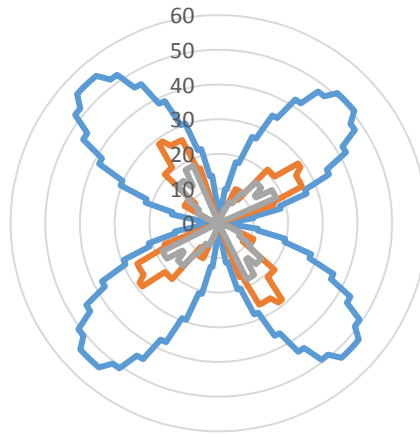
— sun altitude — first row right block altitude — eight row centre block altitude

April



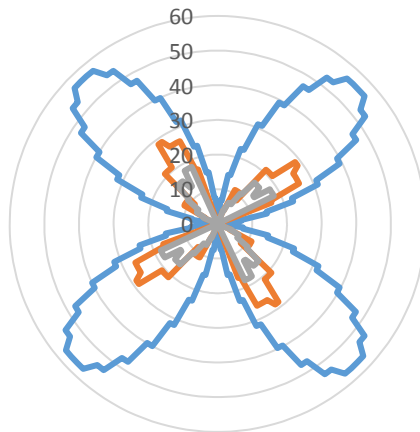
— sun altitude — first row right block altitude — eight row centre block altitude

May



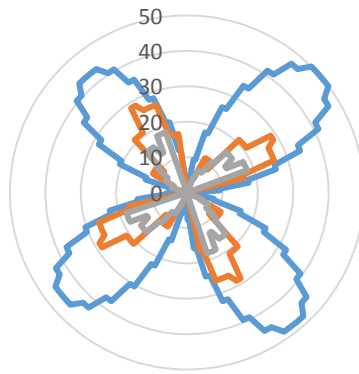
— sun altitude — first row right block altitude — eight row centre block altitude

June



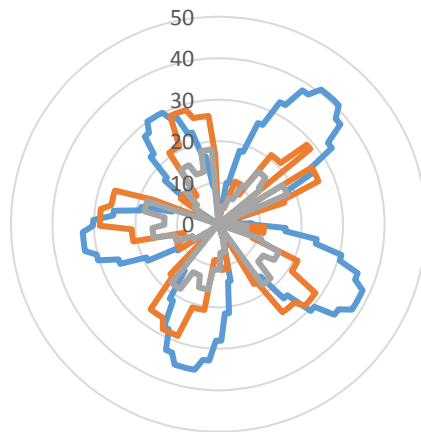
— sun altitude — first row right block altitude — eight row centre block altitude

August



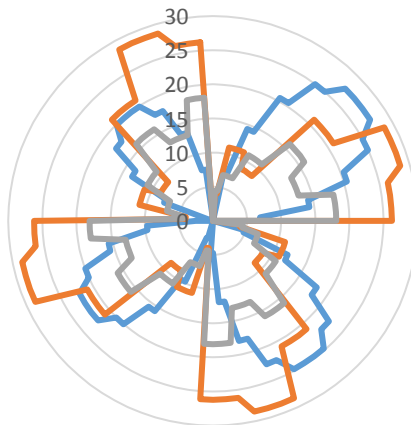
— sun altitude — first row right block altitude — eight row centre block altitude

September



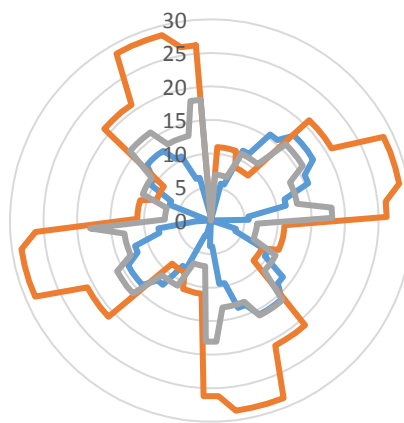
— sun altitude — first row right block altitude — eight row centre block altitude

October



— sun altitude — first row right block altitude — eight row centre block altitude

November



— sun altitude — first row right block altitude — eight row centre block altitude

Appendix I - Edinburgh College Midlothian Campus electricity consumption 2013-2017

DATA INPUT > ELECTRICITY - FINANCIAL YEAR (1st April - 31st March)		
Midlothian		
2013-14 Financial Year		
	kWh	% Change
April 2013	76,317.6	
May 2013	76,707.4	
June 2013	63,086.9	
July 2013	55,465.2	
August 2013	58,653.3	
Sept 2013	63,559.9	
Oct 2013	66,937.9	
Nov 2013	69,300.7	
Dec 2013	63,551.6	
Jan 2014	70,999.8	
Feb 2014	63,601.8	
Mar 2014	68,568.4	
TOTAL (by site)	796,750.5	
2014-15 Financial year		
	kWh	% Change
April 2014	58,637.2	-23%
May 2014	63,651.0	-17%
June 2014	57,376.4	-9%
July 2014	51,757.8	-7%
Aug 2014	51,184.5	-13%
Sept 2014	58,138.5	-9%
Oct 2014	60,025.3	-10%
Nov 2014	59,095.6	-15%
Dec 2014	53,576.9	-16%
Jan 2015	59,699.0	-16%
Feb 2015	55,262.5	-13%
Mar 2015	63,215.0	-8%
Total (by site)	691,619.7	-13%

2015-16 Financial year

	kWh	% Change
April 2015	52,044.2	-11%
May 2015	55,960.0	-12%
June 2015	48,986.3	-15%
July 2015	40,234.7	-22%
Aug 2015	42,388.4	-17%
Sept 2015	53,192.0	-9%
Oct 2015	52,041.2	-13%
Nov 2015	57,362.2	-3%
Dec 2015	59,840.9	12%
Jan 2016	62,317.0	4%
Feb 2016	66,150.0	20%
Mar 2016	68,444.4	8%
Total (by site)	658,961.3	-5%

2016-17 Financial year

	kWh	% Change
April 2016	59,063.4	13%
May 2016	57,063.6	2%
June 2016	54,762.8	12%
July 2016	44,925.8	12%
Aug 2016	51,596.3	22%
Sept 2016	61,009.7	15%
Oct 2016	61,768.4	19%
Nov 2016	71,358.0	24%
Dec 2016	62,847.0	5%
Jan 2017	64,992.0	4%
Feb 2017	63,553.4	-4%
Mar 2017	66,608.9	-3%
Total (by site)	719,549.2	9%

Appendix J – Edinburgh College Solar Array Cashflow only (SSE)

Input variables		Year0	Year1	Year2	Year3	Year4	Year5	Year6	Year7	Year8	Year9	Year10	Year11	Year12	Year13	Year14	Year15	Year16	Year17	Year18	Year19	Year20	
System size kWp	627.20																						
Price per Wp	£1.24																						
System price	£ 778,768.77																						
Yield in kWh per kWp	906.5																						
Degradation of PV pa	0.50%	938																					
Maintenance, insurance, admin /kWp pa	£0.00	£0.068	£0.068	£0.07	£0.07	£0.07	£0.08	£0.08	£0.08	£0.08	£0.09	£0.09	£0.09	£0.09	£0.10	£0.10	£0.10	£0.11	£0.11	£0.11	£0.11	£0.12	£0.12
Tariff	£0.03	£0.03	£0.03	£0.03	£0.03	£0.03	£0.03	£0.03	£0.03	£0.03	£0.03	£0.03	£0.03	£0.03	£0.03	£0.03	£0.03	£0.03	£0.03	£0.03	£0.03	£0.03	£0.03
Value of electricity sold	£0.08	£0.08	£0.08	£0.09	£0.09	£0.09	£0.10	£0.10	£0.11	£0.11	£0.12	£0.12	£0.13	£0.14	£0.14	£0.15	£0.16	£0.17	£0.17	£0.18	£0.19	£0.20	£0.20
Value of electricity saved																							
% generation used in building	100%																						
Inflation		1.00	1.03	1.06	1.09	1.13	1.16	1.19	1.23	1.27	1.30	1.34	1.38	1.43	1.47	1.51	1.56	1.60	1.65	1.70	1.75	1.81	1.81
Cash flow		Year0	Year1	Year2	Year3	Year4	Year5	Year6	Year7	Year8	Year9	Year10	Year11	Year12	Year13	Year14	Year15	Year16	Year17	Year18	Year19	Year20	
Cash flow		568,557	565,714	562,885	560,071	557,271	554,484	551,712	548,953	546,209	543,478	540,760	538,056	535,366	532,689	530,026	527,376	524,739	522,115	519,504	516,907	516,907	
kwh generated		37,536	37,348	37,161	36,976	36,791	36,607	36,424	36,242	36,060	35,880	35,701	35,522	35,345	35,168	34,992	34,817	34,643	34,470	34,297	34,126	34,126	
Cost of system		44,160	44,792	45,434	46,084	46,744	47,414	48,093	48,781	49,480	50,188	50,907	51,636	52,376	53,126	53,886	54,658	55,441	56,235	57,040	57,857	57,857	
Revenue from tariff		0	0	0	0	0	0	0	0	0	0	0	0	0	0	0	0	0	0	0	0	0	0
Value of electricity saved		0	0	0	0	0	0	0	0	0	0	0	0	0	0	0	0	0	0	0	0	0	0
Revenue from selling unused electricity		0	0	0	0	0	0	0	0	0	0	0	0	0	0	0	0	0	0	0	0	0	0
Maintenance		0	0	0	0	0	0	0	0	0	0	0	0	0	0	0	0	0	0	0	0	0	0
Total		81,696	82,140	82,595	83,060	83,535	84,020	84,516	85,023	85,540	86,068	86,608	87,158	87,720	88,293	88,878	89,475	90,084	90,704	91,337	91,983	91,983	
Unlevered IRR		8.96%																					
Yield on Year 1		10.49%																					
Income and savings over 25 years		£1,750,434																					
Profit		£951,666																					
Payback in years		9.3																					
Average income per annum		£86,522																					
Assumptions																							
A generation based tariff																							
£1 is index linked to RPI for the duration of the project life@2%																							
Tariff runs for 20 years																							
We have assumed you use all of the electricity																							
Maintenance is an estimate at this stage																							
All figures quoted above are on a pre-tax basis																							
We've assumed that 8p is price at which the client can currently buy electricity																							
Note there are savings after year 20 - a continuing growth in the line of £86,522 saved.																							